MICROBIAL EXOPOLYMERS: SOURCES, CHEMICO-PHYSIOLOGICAL PROPERTIES, AND ECOSYSTEM EFFECTS IN THE MARINE ENVIRONMENT

EDITED BY: Tony Gutierrez, Andreas Teske, Kai Ziervogel, Uta Passow and Antonietta Quigg

PUBLISHED IN: Frontiers in Microbiology and Frontiers in Marine Science

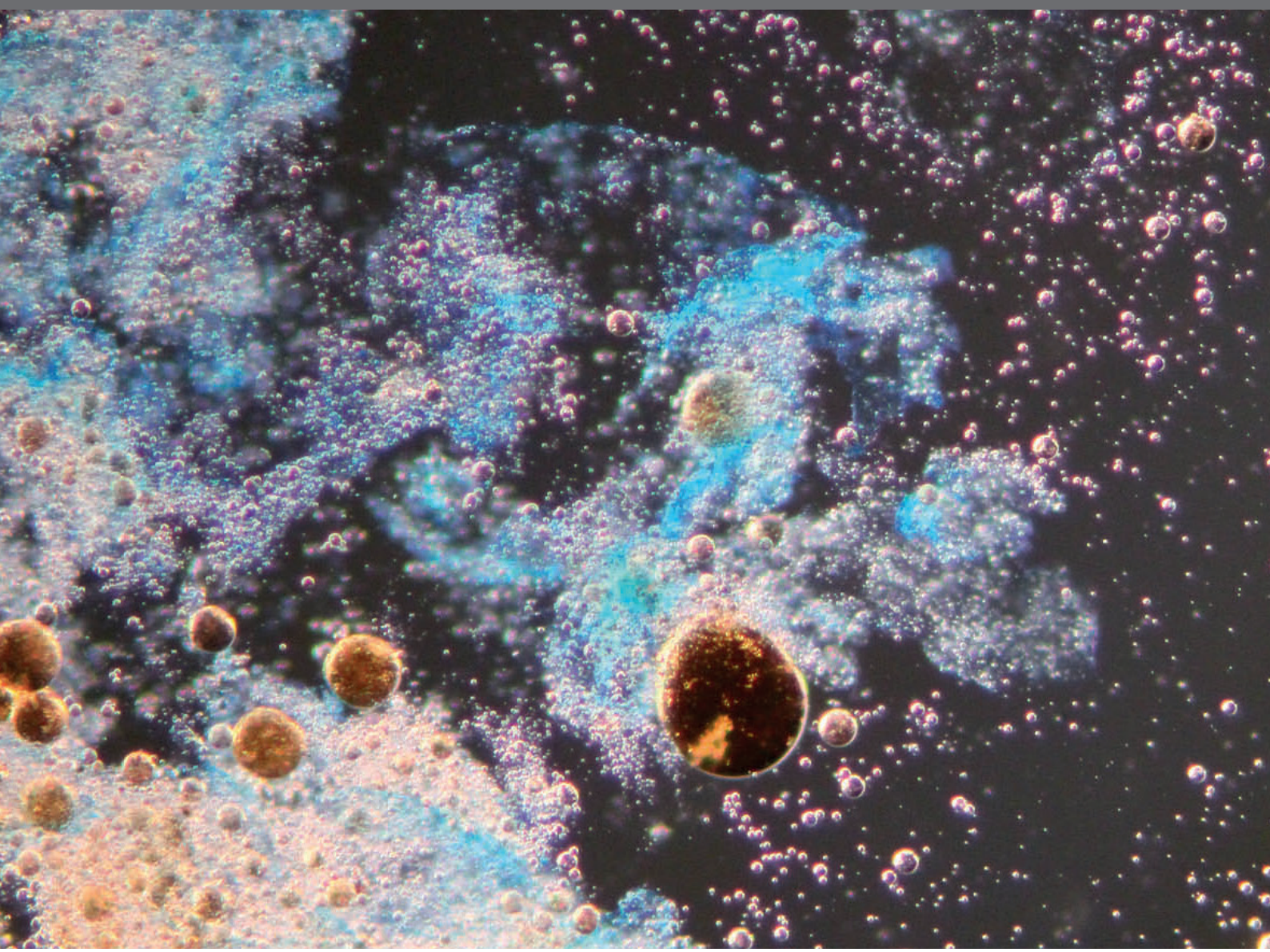

frontiers Research Topics

frontiers

ISSN 1664-8714
ISBN 978-2-88945-602-4
DOI 10.3389/978-2-88945-602-4

About Frontiers

Frontiers is more than just an open-access publisher of scholarly articles: it is a pioneering approach to the world of academia, radically improving the way scholarly research is managed. The grand vision of Frontiers is a world where all people have an equal opportunity to seek, share and generate knowledge. Frontiers provides immediate and permanent online open access to all its publications, but this alone is not enough to realize our grand goals.

Frontiers Journal Series

The Frontiers Journal Series is a multi-tier and interdisciplinary set of open-access, online journals, promising a paradigm shift from the current review, selection and dissemination processes in academic publishing. All Frontiers journals are driven by researchers for researchers; therefore, they constitute a service to the scholarly community. At the same time, the Frontiers Journal Series operates on a revolutionary invention, the tiered publishing system, initially addressing specific communities of scholars, and gradually climbing up to broader public understanding, thus serving the interests of the lay society, too.

Dedication to Quality

Each Frontiers article is a landmark of the highest quality, thanks to genuinely collaborative interactions between authors and review editors, who include some of the world's best academicians. Research must be certified by peers before entering a stream of knowledge that may eventually reach the public - and shape society; therefore, Frontiers only applies the most rigorous and unbiased reviews.
Frontiers revolutionizes research publishing by freely delivering the most outstanding research, evaluated with no bias from both the academic and social point of view. By applying the most advanced information technologies, Frontiers is catapulting scholarly publishing into a new generation.

What are Frontiers Research Topics?

Frontiers Research Topics are very popular trademarks of the Frontiers Journals Series: they are collections of at least ten articles, all centered on a particular subject. With their unique mix of varied contributions from Original Research to Review Articles, Frontiers Research Topics unify the most influential researchers, the latest key findings and historical advances in a hot research area! Find out more on how to host your own Frontiers Research Topic or contribute to one as an author by contacting the Frontiers Editorial Office: researchtopics@frontiersin.org

MICROBIAL EXOPOLYMERS: SOURCES, CHEMICO-PHYSIOLOGICAL PROPERTIES, AND ECOSYSTEM EFFECTS IN THE MARINE ENVIRONMENT

Topic Editors:
Tony Gutierrez, Heriot-Watt University, United Kingdom
Andreas Teske, University of North Carolina at Chapel Hill, United States
Kai Ziervogel, University of New Hampshire, United States
Uta Passow, University of California, United States; Memorial University of Newfoundland, Canada
Antonietta Quigg, Texas A&M University at Galveston, United States

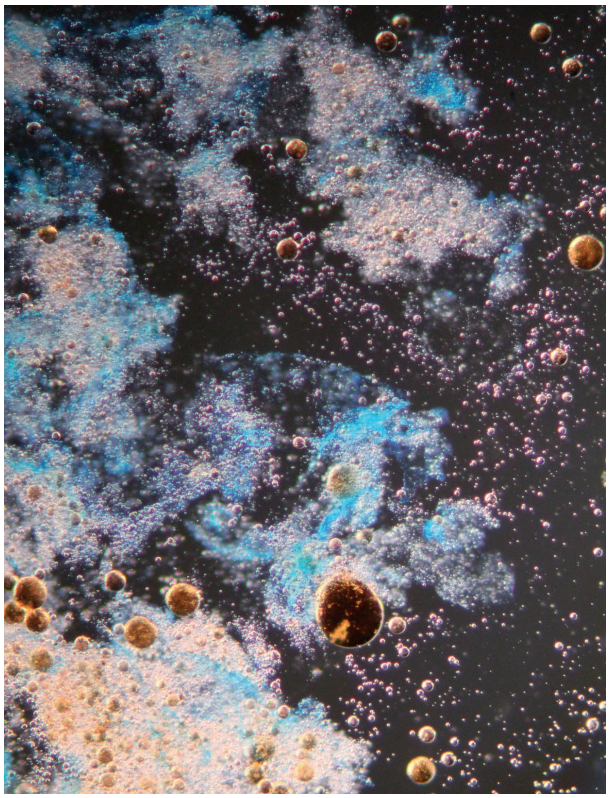

Formation of marine oil snow (MOS) by bacteria enriched on the sea surface during the Deepwater Horizon oil spill when incubated in a roller bottle with synthetic seawater and crude oil. This image shows the MOS particles (stained with Alcian Blue) viewed under the light microscope amongst a sea of oil droplets (brown spheres), of which many were observed embedded within the amorphous matrix of the MOS.
Image: Tony Gutierrez.

Microorganisms (bacteria, archaea, microeukaryotes) in marine environments secrete a diverse array of exopolymeric substances that facilitate attachment to surfaces, the formation of organic colloids and larger aggregations of cells (marine snow), and that can influence many ocean, as well as global, processes. The aim of this Research Topic is to highlight recent advances in the sources, chemistry and function of these microbial-produced macromolecules. We encouraged original research and

reviews on exopolymeric substances, from their sources, chemico-physiological properties, functions and ecosystem effects, and including their role in the Gulf of Mexico following the Deepwater Horizon oil spill disaster.

Citation: Gutierrez, T., Teske, A., Ziervogel, K., Passow, U., Quigg, A., eds (2018). Microbial Exopolymers: Sources, Chemico-Physiological Properties, and Ecosystem Effects in the Marine Environment. Lausanne: Frontiers Media.
doi: 10.3389/978-2-88945-602-4

Table of Contents

frontiers in Microbiology

EDITORIAL
published: 08 August 2018
doi: 10.3389/fmicb.2018.01822

Editorial: Microbial Exopolymers: Sources, Chemico-Physiological Properties, and Ecosystem Effects in the Marine Environment

Tony Gutierrez[1]*, *Andreas Teske*[2], *Kai Ziervogel*[3], *Uta Passow*[4,5] and *Antonietta Quigg*[6]

[1] School of Engineering and Physical Sciences, Heriot-Watt University, Edinburgh, United Kingdom, [2] UNC Marine Sciences, University of North Carolina at Chapel Hill, Chapel Hill, NC, United States, [3] Institute for the Study of Earth, Oceans, and Space, University of New Hampshire, Durham, NH, United States, [4] Marine Science Institute, University of California, Santa Barbara, Santa Barbara, CA, United States, [5] Ocean Sciences, Memorial University of Newfoundland, St. John's, NL, Canada, [6] Texas A&M University at Galveston, Galveston, TX, United States

Keywords: microbial exopolymers, phytoplankton, marine environment, marine snow, marine oil snow (MOS), Deepwater Horizon, exopolysaccharide (EPS)

OPEN ACCESS

Edited by:
Hongyue Dang,
Xiamen University, China

Reviewed by:
Angelina Lo Giudice,
Consiglio Nazionale Delle Ricerche (CNR), Italy
Brivaela Moriceau,
UMR6539 Laboratoire des Sciences de L'Environnement Marin (LEMAR), France

***Correspondence:**
Tony Gutierrez
tony.gutierrez@hw.ac.uk

Specialty section:
This article was submitted to Aquatic Microbiology, a section of the journal Frontiers in Microbiology

Received: *14 June 2018*
Accepted: *20 July 2018*
Published: *08 August 2018*

Citation:
Gutierrez T, Teske A, Ziervogel K, Passow U and Quigg A (2018) Editorial: Microbial Exopolymers: Sources, Chemico-Physiological Properties, and Ecosystem Effects in the Marine Environment. Front. Microbiol. 9:1822. doi: 10.3389/fmicb.2018.01822

Editorial on the Research Topic

Microbial Exopolymers: Sources, Chemico-Physiological Properties, and Ecosystem Effects in the Marine Environment

A large proportion of the total carbon in the World Ocean is in the form of dissolved organic matter (DOM), which is comparable in mass to the carbon in atmospheric CO_2 (Hansell and Carlson, 1998). A major source of this material derives from the synthesis and release of exopolymers, or extracellular polymeric substances (EPS), mainly by bacteria and eukaryotic phytoplankton (Verdugo, 1994; Aluwihare et al., 1997). An initial understanding on the secretion of EPS by microorganisms, and their potential stabilizing effects for microbial cells, emerged during the last century with the first report by ZoBell and Allen (1935). We now know that most bacteria, and other microorganisms, occur associated with biofilms, either attached to surfaces or as suspended-aggregates in the water column. Exopolymer secretions thus serve important functions in marine environments, where they may be involved in microbial adhesion to solid surfaces and biofilm formation (Thavasi and Banat, 2014). They have also been shown to be involved in emulsification of hydrocarbon oils to enhance biodegradation (Gutierrez et al., 2013), mediating the fate and mobility of heavy metals and trace metal nutrients (Bhaskar and Bhosle, 2005; Gutierrez et al., 2008, 2012), or interacting with dissolved and/or particulate organic matter (Long and Azam, 2001). This wide spectrum of functional activity is reflected not merely in the complex chemistry of these biopolymers, but also in the diversity of bacterial and phytoplankton genera found producing them.

In this special issue, nine articles highlight new findings on the sources, chemico-physiological properties, functions and ecosystem effects of microbial exopolymers, including their role in the Gulf of Mexico following the Deepwater Horizon oil spill disaster. To begin, the article by Decho and Gutierrez introduces this Research Topic with a comprehensive review on microbial-derived EPS, covering their wide chemical composition, their partitioning, turnover and roles within the marine water column and sediment, their provision of selective adaptations to the producing microorganisms and other organisms, including in animal-microbe interactions, and the broader influences of these diverse macromolecules upon ocean and planetary processes.

An important role of exopolymers is in forming marine snow—floating or suspended particles that harbor a community of microorganisms and drive the biological pump. They also play an essential role in marine oil snow (MOS) that forms as a consequence of oil spillage. The article by Sperling et al. reveals a correlation between the concentration of high-molecular-weight organic matter (HMW-OM) and the diversity of particle-associated bacteria during the development of a spring bloom in the southern North Sea, suggesting that the availability of carbohydrates contributes to the multifactorial control of marine bacterioplankton communities. The article by Suja et al. reports, for the first time, the use of Illumina MiSeq sequencing to analyse the bacterial communities associated with MOS. This study was conducted in subarctic waters of the northeast Atlantic, revealing the enrichment of oil-degrading and EPS-producing bacteria on MOS, and providing supporting evidence that MOS particles are "hotspots" of these organisms with potentially profound consequences to the oil biodegradation process in the water column. Since the seafloor is the final endpoint for MOS, the article by Yang et al. reports the distinct occurrence and patterns of oil-associated family- and genus-level bacterial groups over time in surficial sediments in the Gulf of Mexico following MOS sedimentation after the Deepwater Horizon oil spill, and suggest petrocarbon sedimentation and changing biogeochemical niches as factors that shape these bacterial communities in near-surface seafloor sediments.

A cluster of three articles (Nosaka et al.; Ortega-Retuerta et al.; Thornton et al.) focus on the origin, chemical composition, dynamics and distribution of transparent exopolymer particles (TEP), which are defined as >0.4-μm transparent particles and constitute an important component of EPS. TEP may promote marine snow formation, thereby influencing the efficiency of the biological pump. They serve as a labile source of carbon and energy to micro- and macro-heterotrophs, and are thus important in food webs. The article by Nosaka et al. (2017) focuses on TEP distribution and its potential correlation to diatom-derived chlorophyll-*a* biomass and DOC productivity during the spring bloom periods in 2010 and 2011 in surface waters of the Oyashio region of the western subarctic Pacific, where seasonal biological drawdown of the partial pressure of CO_2 is one of the greatest in the world's oceans. The article by Ortega-Retuerta et al. describes TEP distributions in the northwest Mediterranean Sea during late spring 2012, along perpendicular and parallel transects to the Catalan coast, and its correlation with chlorophyll-*a*, O_2 (as a proxy of primary production) and bacterial production. The paper by Thornton et al. focuses on the concentrations and potential correlation of TEP and Coomassie staining particles (CSP) in the sea surface microlayer and underlying water in the Pacific Ocean off the coast of Oregon (United States) during July 2011.

The production and utilization of fluorescent dissolved organic matter (DOM), and the influence of diatom-derived EPS in shaping microbial communities in marine waters are the research foci in the final two articles (Bohórquez et al.; Goto et al.), respectively. The paper by Goto et al. presents data linking bacterial growth and DOM production, of different recalcitrant characteristics, by the marine bacterial isolate *Alteromonas macleodii* as a model marine bacterium which is ubiquitously found from the sea surface to the deep waters of tropical and temperate oceans (López-Pérez et al., 2012). The article by Bohórquez et al. shows that fractions of EPS with different structural complexity (operationally termed colloidal and hot-bicarbonate extracted) in intertidal sediments are degraded at higher rates compared with those reported in previous studies, and contribute to the transfer of organic carbon from the microphytobenthos to heterotrophic bacteria.

In summary, these articles cover a range of roles and functions for microbial exopolymers in the marine environment. One challenge remains to develop methods that can accurately trace the production of exopolymers to their biological source in environmental samples. Such methods and approaches would be invaluable for understanding what type(s) of exopolymers participate in marine snow formation, as well as in the formation of MOS, and for consequently linking these exopolymers to their producing organism(s). We hope that this special issue stimulates more discussion and inspires new lines of research on the incredibly profound, and still largely enigmatic subject of microbial exopolymers.

AUTHOR CONTRIBUTIONS

All authors listed have made a substantial, direct and intellectual contribution to the work, and approved it for publication.

ACKNOWLEDGMENTS

Preparation of this manuscript were made possible by grants from OGIC-IBioIC, and the Gulf of Mexico Research Initiative to the ECOGIG and the ADDOMEx consortia.

REFERENCES

Aluwihare, L. I., Repeta, D. J., and Chen, R. F. (1997). A major biopolymeric component of dissolved organic carbon in surface seawater. *Nature* 387, 166–169. doi: 10.1038/387166a0

Bhaskar, P. V., and Bhosle, N. B. (2005). Microbial extracellular polymeric substances in marine biogeochemical processes. *Curr. Sci.* 88, 45–53. Available online at: www.jstor.org/stable/24110092

Gutierrez, T., Berry, D., Yang, T., Mishamandani, S., McKay, L., Teske, A., et al. (2013). Role of bacterial exopolysaccharides (EPS) in the fate of the oil released during the Deepwater Horizon oil spill. *PLoS ONE* 8:e67717. doi: 10.1371/journal.pone.0067717

Gutierrez, T., Biller, D. V., Shimmield, T., and Green, D. H. (2012). Metal binding properties of the EPS produced by *Halomonas* sp. TG39 and its potential in enhancing trace element bioavailability to eukaryotic phytoplankton. *Biometals* 25, 1185–1194. doi: 10.1007/s10534-012-9581-3

Gutierrez, T., Shimmield, T., Haidon, C., Black, K., and Green D. H. (2008). Emulsifying and metal ion binding activity of a glycoprotein exopolymer produced by *Pseudoalteromonas* sp. strain TG12. *Appl. Environ. Microbiol.* 74, 4867–4876. doi: 10.1128/AEM.00316-08

Hansell, D. A., and Carlson, C. A. (1998). Deep-ocean gradients in the concentration of dissolved organic carbon. *Nature* 395, 263–268. doi: 10.1038/26200

Long, R. A., and Azam, F. (2001). Microscale patchiness of bacterioplankton assemblage richness in seawater. *Aquat. Microb. Ecol.* 26, 103–113. doi: 10.3354/ame026103

López-Pérez, M., Gonzaga, A., Martin-Cuadrado, A.-B., Onyshchenko, O., Ghavidel, A., Ghai, R., et al. (2012). Genomes of surface isolates of *Alteromonas macleodii*: the life of a widespread marine opportunistic copiotroph. *Sci. Rep.* 2:696. doi: 10.1038/srep00696

Nosaka, Y., Yamashita, Y., and Suzuki, K. (2017). Dynamics and origin of transparent exopolymer particles in the oyashio region of the western subarctic pacific during the spring diatom bloom. *Front. Mar. Sci.* 4:79. doi: 10.3389/fmars.2017.00079

Thavasi, R., and Banat, I. M. (2014). "Biosurfactants and bioemulsifiers from marine sources," in *Biosurfactants: Research Trends and Applications*, Chap. 5, eds C. N. Mulligan, S. K. Sharma, and M. A. Hardback (Boca Raton, FL: CRC Press), 125–146.

Verdugo, P. (1994). Polymer gel phase transition in condensation-decondensation of secretory products. *Adv. Polymer Sci.* 110, 145–156. doi: 10.1007/BFb0021131

ZoBell, C. E., and Allen, E. C. (1935). The significance of marine bacteria in the fouling of submerged surfaces. *J. Bact.* 29, 239–251.

Conflict of Interest Statement: The authors declare that the research was conducted in the absence of any commercial or financial relationships that could be construed as a potential conflict of interest.

frontiers in Microbiology

REVIEW
published: 26 May 2017
doi: 10.3389/fmicb.2017.00922

Microbial Extracellular Polymeric Substances (EPSs) in Ocean Systems

Alan W. Decho[1]* *and Tony Gutierrez*[2]

[1] Department of Environmental Health Sciences, Arnold School of Public Health, University of South Carolina, Columbia, SC, United States, [2] School of Engineering and Physical Sciences, Heriot-Watt University, Edinburgh, United Kingdom

Microbial cells (i.e., bacteria, archaea, microeukaryotes) in oceans secrete a diverse array of large molecules, collectively called extracellular polymeric substances (EPSs) or simply *exopolymers*. These secretions facilitate attachment to surfaces that lead to the formation of structured '*biofilm*' communities. In open-water environments, they also lead to formation of organic colloids, and larger aggregations of cells, called '*marine snow.*' Secretion of EPS is now recognized as a fundamental microbial adaptation, occurring under many environmental conditions, and one that influences many ocean processes. This relatively recent realization has revolutionized our understanding of microbial impacts on ocean systems. EPS occur in a range of molecular sizes, conformations and physical/chemical properties, and polysaccharides, proteins, lipids, and even nucleic acids are actively secreted components. Interestingly, however, the physical ultrastructure of how individual EPS interact with each other is poorly understood. Together, the EPS matrix molecules form a three-dimensional architecture from which cells may localize extracellular activities and conduct cooperative/antagonistic interactions that cannot be accomplished efficiently by free-living cells. EPS alter optical signatures of sediments and seawater, and are involved in biogeomineral precipitation and the construction of microbial macrostructures, and horizontal-transfers of genetic information. In the water-column, they contribute to the formation of marine snow, transparent exopolymer particles (TEPs), sea-surface microlayer biofilm, and marine oil snow. Excessive production of EPS occurs during later-stages of phytoplankton blooms as an excess metabolic by product and releases a carbon pool that transitions among dissolved-, colloidal-, and gel-states. Some EPS are highly labile carbon forms, while other forms appear quite refractory to degradation. Emerging studies suggest that EPS contribute to efficient trophic-transfer of environmental contaminants, and may provide a protective refugia for pathogenic cells within marine systems; one that enhances their survival/persistence. Finally, these secretions are prominent in 'extreme' environments ranging from sea-ice communities to hypersaline systems to the high-temperatures/pressures of hydrothermal-vent systems. This overview summarizes some of the roles of exopolymer in oceans.

Keywords: EPS, biofilm, organic matter, oceans research, bacteria

OPEN ACCESS

Edited by:
Télesphore Sime-Ngando, Centre National de la Recherche Scientifique (CNRS), France

Reviewed by:
Varenyam Achal, East China Normal University, China
Eric D. van Hullebusch, UNESCO-IHE Institute for Water Education, Netherlands

***Correspondence:**
Alan W. Decho
awdecho@mailbox.sc.edu

Specialty section:
This article was submitted to Aquatic Microbiology, a section of the journal Frontiers in Microbiology

Received: *06 March 2017*
Accepted: *08 May 2017*
Published: *26 May 2017*

Citation:
Decho AW and Gutierrez T (2017) Microbial Extracellular Polymeric Substances (EPSs) in Ocean Systems. Front. Microbiol. 8:922. doi: 10.3389/fmicb.2017.00922

OVERVIEW

Microorganisms (e.g., bacteria, archaea, microeukaryotes) reside in ocean systems in an assortment of physical states ranging from free-living cells to complex communities attached to surfaces and to each other (Moran, 2015; Brussaard et al., 2016). Over the span of different ocean environments, microbial flora take up dissolved organics and ions, and then secrete polymeric organic compounds. These secretions, called *exopolymers* or extracellular polymeric substances (EPSs), are abundant and become mixed with other forms of organic matter within ocean systems. It was recognized early on, that under the fluctuating, and often less-predictable conditions of natural systems (compared to those of a laboratory culture flask), the attachment of microbes to surfaces, or to each other, offers a degree of environmental stability not experienced by free-living (non-attached) cells (ZoBell and Allen, 1935). An initial understanding of the purposeful secretion of EPS and their potential stabilizing effects for microbial cells initially emerged during the last century. It is now realized and mostly accepted that many bacteria and other microorganisms occur in a biofilm state; either attached to surfaces or as suspended-aggregates in the water column. EPS, the subject of this overview, consist of a wide range of molecules and provide selective adaptations for the cells that produce them, which in turn, influence broader ocean processes (**Figure 1**).

EPS: A MICROBIAL ADAPTATION FOR AGGREGATION AND ATTACHMENT

Extracellular polymeric substance are purposefully produced by microbes: (a) as secretions of biofilms that secure attachment and enhance their local environment, and/or (b) as metabolic-excess waste products. The differences between these two processes is easily discernable but becomes important when addressing the provenance of organic matter and the roles that EPS contribute to ocean systems. *It is important to point out that EPS are not an essential component to microbial life* (i.e., *cells can survive and grow without them), but rather their secretion strongly enhances the survival, metabolic efficiency and adaptation of cells.*

The Biofilm State

The term '*biofilm*' was coined long ago (Costerton et al., 1987), and refers to microbial cells that have attached to a surface or aggregated with each other, and have secreted a gelatinous matrix of EPS. The ability of a microbial cell, such as a bacterium, to attach, secrete EPS and form a biofilm under laboratory conditions, is well-established. The secretion of EPS (by cells) is a key emergent property of the biofilm (Flemming and Wingender, 2010; Flemming et al., 2016); the property that directly influences adaptations that cells utilize to enhance their efficiency and survival. The secretion of an EPS matrix

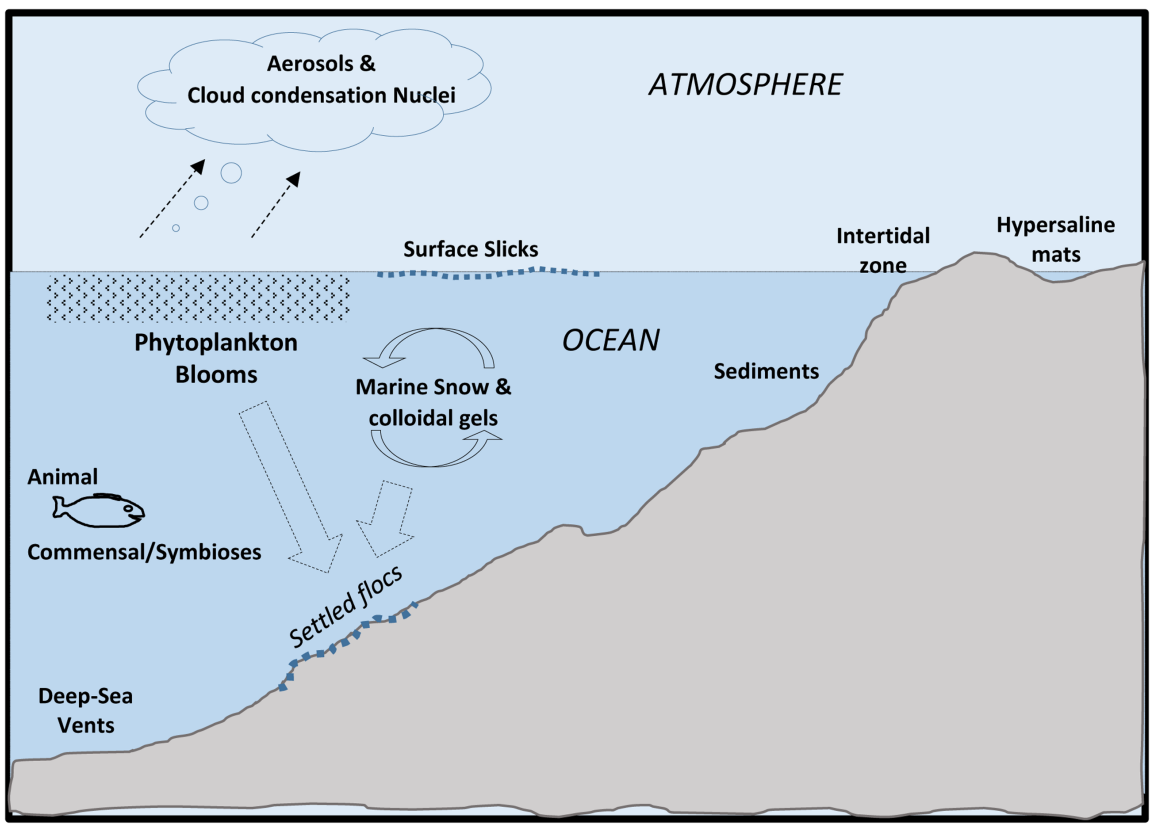

FIGURE 1 | Major locations of extracellular polymeric substances (EPSs) in Oceans.

represents, in the broadest sense, an extension of the cell. The presence of EPS facilitates the self-organization of cells into localized communities, and provides biofilm cells with an enhanced capability for: trapping other organics and localizing their digestion by extracellular enzymes, coordinating cell–cell chemical communication [quorum sensing (QS)], facilitating gene-exchange, and provides a degree of physical stability. The EPS often form a localization matrix for other molecules, keeping them in spatial proximity to cells where they can be efficiently utilized.

It is now generally recognized within microbiology that the 'biofilm state' is an omnipresent feature of microbial flora in most environments (Hall-Stoodley et al., 2004). Biofilms occur under a wide range of conditions and environments, and whose influences span aquatic, terrestrial, the epi- and endo-biont communities of plants and animals, which can be commensal, symbiotic or pathogenic. The cells within a biofilm can move, and periodically reorient themselves in relation to one another, and in doing so can resist invasion by other cells (Houry et al., 2012). The EPS matrix of biofilms provides a three-dimensional architecture framework that allows the arrangements of cells movements relative to other microbes as well as positioning among sharp geochemical gradients (Decho, 2000b). This will not be discussed further here, but directly contributes to the remarkable plasticity of biofilm cells. The EPS form a matrix of largely anionic molecules near cells, affording them with a proximal environment that is more stabilizing, and conducive to manipulation by the cell (**Table 1**), and one that contributes to broader ocean processes. However, in this overview we will not discuss biofilms as systems, except with regard to their secretion of EPS.

Finally, it is important to note that in ocean systems, the microbial communities of aggregates suspended in the water-column, and the sea-surface slick communities of oceans are also biofilms, since these communities contain EPS, and exhibit differing levels of organization. EPS are also secreted as a 'metabolic by product.' These are most apparent during the later stages of phytoplankton blooms, and will be discussed further below. Taken together, microbial extracellular secretions are now thought to comprise a large portion of the bioavailable carbon pool in oceans, especially in dissolved forms. The total amount of microbially produced EPS, although difficult to measure accurately and precisely, is likely to be very substantial.

DISSOLVED AND PARTICULATE ORGANIC CARBON IN THE OCEAN

Organic matter in seawater constitutes a complex mixture of compounds in a dissolved and particulate form – respectively, dissolved organic matter (DOM) and particulate organic matter (POM). Both forms serve a source of carbon and nutrients to heterotrophic microorganisms, including to mixotrophic eukaryotic phytoplankton and filter feeders. DOM is the dominant form of carbon in the oceans that can originate from any number of sources, much of which is produced *in situ* by marine microorganisms (largely eukaryotic phytoplankton and bacteria) and is derived from terrestrial inputs via transportation from river effluents and surface runoff. DOM comprises up to 700 Gt of carbon in the ocean, which is a staggering amount of dissolved organic carbon (DOC); so much so that 1% annual change of it in the ocean can produce as much CO_2 as that from fossil fuel combustion per annum (Hedges, 2002). Up to 70% of DOM in the oceans averages a molecular weight of <1 kDa and is defined as low-molecular-weight DOM (Benner, 2002), the bulk of which is refractory (Bauer et al., 2002) and difficult to chemically characterize down to the molecular level. The high-molecular-weight fraction of DOM (>1 kDa) in the oceans contributes about 30% of DOC. It is more labile and thus more readily degraded (Amon and Benner, 1994; Guo et al., 1994).

Depending on its physical state in seawater (gel, colloidal, or particulate form), DOC/POC can serve as a surface to which microorganisms attach. Marine snow, which comprises aggregates of >500 μm, is formed in the upper water-column when dead and dying phytoplankton cells come together with other planktonic microorganisms within a matrix of biopolymers (Alldredge et al., 1993; Tiselius and Kuylenstierna, 1996). Marine snow is one form of POC that is a key component of the biological pump in the ocean that participates in the redistribution of carbon in marine systems and principally in the flux of fixed carbon to the sea floor (Shanks and Trent, 1980; Shanks and Reeder, 1993; Long and Azam, 2001b). The processing of organic matter, such as marine snow, by bacteria in the ocean significantly affects its vertical flux from the upper water column to the ocean floor, and in turn impacting the global cycling of carbon and the planet's climate (Simon et al., 2002). The transport of organic carbon via sinking of POC from the sea surface to the seafloor is another major component of the "biological pump," which globally contributes in the exports of ca. 10 Gt C per year from the euphotic zone and accounts for 20% of ocean primary production (Treguer et al., 2003). However, at depths approaching 2000 m, this flux or organic carbon decreases to about 1% as the other 19% is mineralized and cycled by the "microbial loop."

In oceanography, organic matter in seawater is operationally defined as "dissolved" (i.e., DOM) if it passes through a 0.7 μm pore size filter; that which is retained on the filter is defined as POM. The diversity of dissolved organic carbon in seawater ranges from 'truly' dissolved molecules, such as glucose, to colloidal and transparent gel-like matter, and can also include microorganisms (e.g., micro-algae, bacteria, archaea, viruses) if they too pass through a 0.7 μm pore size filter. The introduction of sensitive analytical techniques for analyzing seawater, such as high-performance liquid chromatography (HPLC) (Mopper et al., 1992) have increased our understanding of the major classes of DOM in the ocean. Methods to recover and characterize DOM and POM are described by Wurl (2009).

Water Column

DOC and POC

The world's oceans contain a total DOC content that is comparable in mass to the carbon in atmospheric CO_2

TABLE 1 | Major EPS physical/chemical properties and functions and influence(s) on ocean processes.

EPS property	Influence on Ocean process	Reference*
Physical state		
Gel/solution state**:**	-Aggregation- formation of colloids, TEP, and marine snow; -Contribution to carbon flux;	-Alldredge et al., 1993; Verdugo, 1994; Passow, 2002; Simon et al., 2002; Verdugo and Santschi, 2010; -Long and Azam, 2001a; Engel et al., 2004; Wurl, 2009;
Amphiphilic:	-Dispersion of oil/ MOS and other hydrophobic contaminants; -Hydrophobic microdomains/contaminants; -Sea surface slicks and aerosols;	-Niu et al., 2011; Passow et al., 2012; Gutierrez et al., 2013; Valentine et al., 2014; Daly et al., 2016; -Decho, 2000b; Lawrence et al., 2007, 2016; -Kuznetsova et al., 2005; Facchini et al., 2008; Leck and Bigg, 2008; Wurl and Holmes, 2008; Fuentes et al., 2010
Chemical composition		
Degradability	-Consumer food source; -DOM/POM turnover/refractory OM pool;	-Decho and Moriarty, 1990; Decho and Lopez, 1993; Schlekat et al., 1998, 1999, 2000; Selck et al., 1999; -Ogawa et al., 2001; Benner, 2002; Decho et al., 2005; Repeta and Aluwihare, 2006; Walker et al., 2016;
Reactive groups	-Sorption of organic- /inorganic- ions; -Enhancement of iron bioavailability; -Biogeomineral precipitation;	-Bhaskar and Bhosle, 2006; Zhang et al., 2008; Braissant et al., 2009; Gutierrez et al., 2012; Deschatre et al., 2013; -Boyd et al., 2007; Hassler et al., 2011b; -Reid et al., 2000; Arp et al., 2001; Kawaguchi and Decho, 2002a; Dupraz et al., 2009; Obst et al., 2009
Excess metabolite	-Secretion by late-stage plankton blooms;	-Aluwihare et al., 1997; Bhaskar and Bhosle, 2005;
Protection/enhancement of microbial activities		
Diffusion-slowing/localization close to cells:	-*e*-Enzymes and hydrolysis products; -Quorum sensing signals; -Enhancement of microscale gradients; -Lipid vesicles and antibiotics;	-Smith et al., 1992; Stewart, 2002; Flemming and Wingender, 2010; Jatt et al., 2015; Sutherland, 2016; -Decho et al., 2009; Hmelo et al., 2011; Decho, 2015; - Visscher and Stolz, 2005; Vasconcelos et al., 2006; -Mashburn and Whiteley, 2005; Schooling et al., 2009; Biller et al., 2014;
Sorption/trapping:	-Concentration of viruses/phages; -Larval settlement cues;	- Drake et al., 2007; Dupuy et al., 2014; Guizien et al., 2014; -Holmström et al., 2002; Franks et al., 2006; Tran and Hadfield, 2011; Nielsen et al., 2015;
Stickiness/cohesiveness:	-Biofilm and microbial mat formation; -Sediment stabilization; -Biofouling and microbial metal corrosion;	- Rougeaux et al., 2001; Goh et al., 2009; Moppert et al., 2009; Benninghoff et al., 2016; Flemming et al., 2016; - Paterson et al., 2008; Gerbersdorf et al., 2009; Grabowski et al., 2011; Yang et al., 2016; -de Nys et al., 2009; Camacho-Chab et al., 2016;
Optical transparency	- Enhanced forward-scattering of photons;	-Decho et al., 2003;
Protection	-Hydrothermal vents; -Protection from grazing; -Antifreeze protection	-Rougeaux et al., 2001; Guezennec, 2002; -Plante, 2000; DePas et al., 2014; -Marx et al., 2009; Underwood et al., 2010; Liu et al., 2013; Ewert and Deming, 2014; Boetius et al., 2015;

*CNN, cloud condensation nuclei; e-enzymes, extracellular-enzymes; DOM/POM, dissolved/particulate organic matter; MOS, marine oil snow; TEP, transparent exopolymer particles; UV, ultraviolet; *references are examples and not all-inclusive.*

(Hansell and Carlson, 1998). The oceanic DOC pool comprises a wide spectrum of compounds, much of which is chemically uncharacterized – it could be regarded as a 'black hole' in terms of our relatively poor understanding of its chemical composition and from what biogenic sources this massive pool of organic carbon molecules originate. At least among the chemical constituents of oceanic DOC that have been characterized, three major compound classes have been identified: carbohydrates (mono- and polysaccharides or EPS), proteins, and lipids. Much of the DOC in the ocean water column exists as EPS biopolymers (ca. 10–25% of total oceanic DOM) that undergo reversible transition between colloidal and dissolved phases (Verdugo, 1994; Chin et al., 1998). Based on its predominance throughout the world ocean, it has important implications in microbial interactions and biogeochemical cycles.

Extracellular Polymeric Substance

The synthesis and extracellular release of EPS by eukaryotic phytoplankton and bacteria forms a major component to the total DOC pool in the ocean (Verdugo, 1994; Aluwihare et al., 1997).

EPS can serve a variety of functions, such as in the binding and fate of trace metal-nutrient species, the solubilisation of hydrophobic organic chemicals, and in biofilm formation (Decho, 1990; Santschi et al., 1998). Compared to EPS produced by marine eukaryotic phytoplankton (Bhaskar and Bhosle, 2005) and non-marine bacteria (Ford et al., 1991), EPS produced by marine bacteria generally contains higher levels of uronic acids, notably D-glucuronic and D-galacturonic acid (Kennedy and Sutherland, 1987). This renders these macromolecules highly polyanionic (negatively charged), which may be attributable to any number of anionic groups (e.g., COO^-, $C–O^-$, SO_4^-) and consequently quite reactive in their potential to interact with other chemical species (Kennedy and Sutherland, 1987). Nonetheless, the EPS released by some eukaryotic phytoplankton species can also be rich in uronic acids, such as that produced by the coccolithophore *Emiliania huxleyi,* which contains up to 20% galacturonic acids of total sugar content (De Jong et al., 1979).

The polyanionic nature of EPS serves important ecological functions in marine systems. These include microbial adhesion and biofilm formation (Thavasi and Banat, 2014), the emulsification of hydrocarbon oils and influencing their biodegradation (Gutierrez et al., 2013), or mediating the fate and mobility of heavy metals and trace metal nutrients (Bhaskar and Bhosle, 2005; Gutierrez et al., 2008, 2012). This wide spectrum of functional activity is reflected not merely in the complex chemistry of these molecules, but also in the diversity of bacterial genera producing them (Thavasi et al., 2011). Overall, the composition of marine EPS varies due to the producing species and physiological stage (Myklestad, 1977; Grossart et al., 2007).

A number of reports have described marine bacterial EPS binding heavy and toxic metal ions such as Cd, Cr, Pb, Ni, Cu, Al, and Ur (Zosim et al., 1983; Beech and Cheung, 1995; Schlekat et al., 1998; Iyer et al., 2005; Bhaskar and Bhosle, 2006; Gutierrez et al., 2008). Whilst the rationale to many of these studies was commercial, a few have addressed the ecological implications of marine EPS in biogeochemical cycles. In two studies by Loaec et al. (1997, 1998), the authors reported on the heavy metal-binding capacity of EPS produced by hydrothermal vent bacteria, and showed that this might represent a survival strategy for the bacteria by reducing their exposure to toxic metals released from the hydrothermal vents. Major elemental constituents of seawater, such as Na, Mg, Ca, K, Sr and Si, have been shown to be adsorbed by marine bacterial EPS (Gutierrez et al., 2008). What ecological implications this may have in marine systems, or indeed to the producing organisms, remains to be more-fully understood.

A key role of polyanionic EPS, particularly in the euphotic zone, is in its potential role in controlling soluble iron (Fe^{3+}) bioavailability. Studies in recent years have shown single anionic residues, such as glucuronic and galacturonic acids (Hassler and Schoemann, 2009; Hassler et al., 2011b), and purified marine bacterial EPS containing high levels of uronic acids (Gutierrez et al., 2008; Hassler et al., 2011a), can effectively bind Fe^{3+} and promote the uptake of this trace metal by eukaryotic phytoplankton (Hassler et al., 2011b; Gutierrez et al., 2012). The implications of this are significant because of the abundance of EPS in the ocean (Verdugo et al., 2004) and because Fe^{3+} is an essential trace metal that limits primary production in up to 40% of the open ocean (Martin et al., 1994; Boyd et al., 2007).

A large fraction of the EPS produced by bacteria in the ocean is of glycoprotein composition (Long and Azam, 1996; Verdugo et al., 2004). The amino acid and peptide components found associated with these glycoprotein biopolymers have been shown to confer amphiphilic characteristics to these macromolecules (Verdugo et al., 2004; Gutierrez et al., 2009), and which could explain, at least in part, their ability to interact with hydrophobic species, such as oil hydrocarbons.

Transparent Exopolymer Particle

A special class of EPS that are described as mucopolysaccharides is transparent exopolymer particles (TEPs). It is operational defined based on being retained by a filter with a pore size of >0.4 μm (Alldredge et al., 1993), and based on this, TEP are defined as gel particles. TEP exists in the water column suspended in colloidal form, likely formed via the aggregation of smaller EPS molecules (Engel et al., 2004). Aggregation may be mediated by the bridging of divalent cation (Ca^{2+}, Mg^{2+}) and half-ester sulfate (OSO_3^-) moieties of acidic monomers that constitute individual EPS molecules. TEP is transparent, but because these gel particles are rich in acidic sugars they can be observed under the light microscope after staining with the cationic copper phthalocyanine dye Alcian Blue at pH 2.5 (Alldredge et al., 1993).

The abundances of TEP in the ocean water column are on average in the order of 10^6 per L of seawater, and can reach as high as 10^8 per L (Passow, 2002; Bhaskar and Bhosle, 2005), particularly during periods of phytoplankton blooms. The contribution of TEP to the pool of POC in the upper water column in the Atlantic and Adriatic during certain periods of the year has been shown to be quite significant (Engel and Passow, 2001). A fraction of the TEP pool in the ocean is proteinaceous. It is referred to as Coomassie stainable particles (CSPs) because these gel particles can be stained with the amino acid-specific dye Coomassie Brilliant Blue and observed under the light microscope (Long and Azam, 1996). The abundances of CSP in coastal waters range between 10^6 and 10^8 per L of seawater (Long and Azam, 1996).

Transparent exopolymer particle contribute significantly to what is described as the marine gel phase. Verdugo et al. (2004) suggested this phase to span a large size spectrum, from colloids to particles of several 100s of micrometers. Its formation has been described to originate from the spontaneous aggregation of DOM molecules into POM within minutes in seawater (Chin et al., 1998) – a process that may involve crosslinks facilitated by cation bridging between DOM molecules.

Microbial Associates

Particulate organic matter can be described as a "hot spot" for microbial (esp. bacterial) activities in the water column, containing a rich microbial community with abundances reaching up to two orders of magnitude higher than in the surrounding seawater environment (Alldredge et al., 1986; Herndl, 1988). The establishment of a bacterial community within and surrounding (biofilm) POM leads to various levels of microbial interaction that include mutualism and

antagonism (Long and Azam, 2001a), as well as cooperative behavior such as QS (Gram et al., 2002). A study assessing the phylogenetic diversity of POM-associated versus free-living bacteria from a site ca. 5 km offshore the Santa Barbara coast revealed distinct differences between these communities, with primarily members of the *Cytophaga*, *Planctomyces,* and *Gammaproteobacteria* dominating aggregate particles, whereas *Alphaproteobacteria* dominated the free-living fraction (DeLong et al., 1993). Bacteria associated with POM have been shown to exhibit high activities for a range of extracellular enzymes (Hoppe et al., 2002; Simon et al., 2002), likely contributing to the hydrolysis of the POM aggregates. Whilst rich in microbial diversity and abundance, POM accounts for only <10% of total bacterial abundance and production in the marine water column, with the majority of bacterial cells occurring in a free-living state.

Studies using oxygen microelectrodes to measure dissolved oxygen in POM aggregates have shown that even the tiniest of marine snow particles can contain anoxic environments (Alldredge and Cohen, 1987; Alldredge and Silver, 1988; Ploug et al., 1997; Ploug, 2008). The high extracellular enzyme activities by bacteria associated with POM will deplete oxygen concentrations that create anoxic micro-niches within the aggregates, potentially supporting the growth of obligate anaerobic or microaerophilic microorganisms (Bianchi et al., 1992). It may therefore, be expected that diverse aerobic and anaerobic microorganisms associated with marine snow aggregates would colonize different niches of the aggregates. The formation of an oxygen gradient, which is increasingly more anoxic toward the interior of the aggregates, would pose a strong influence on the stratification of the microbial community. Essentially, the interior of aggregates will be enriched with obligate and/or facultative anaerobes.

Air–Water Interface

Surface Water Droplet Formation, Sea Spray, and Cloud Formation

Biological processes on the sea surface of the ocean can have a direct effect on atmospheric processes, such as modulating CO_2 exchange and release of cloud condensation nuclei (CCN), that in turn influence the Earth's climate. CCN are atmospheric particles that serve as nuclei for the formation of cloud droplets by taking up water vapor because they are sufficiently soluble. In the past decade there has been an increasing body of evidence supporting the hypothesis that atmospheric marine aerosols contain the same organic species that are found in oceanic DOM (Leck and Bigg, 2005; Bigg, 2007; Facchini et al., 2008). Seawater DOM, much of which comprises phytoplankton exudates and bacterial EPS, can be ejected into the atmosphere when bubbles at the sea surface burst (Bigg, 2007; Leck and Bigg, 2008). Bubbles can form by a number of physical forces at the sea surface, ranging from raindrops to breaking waves, which then burst and produce submicron droplets that disperse as aerosol into the atmosphere and carrying with it marine organic species such as microbial cells and DOM. A study by Kuznetsova et al. (2005) showed that TEP and CSP can accumulate in the sea surface microlayer and subsequently, through bubble bursting, become transported to the atmosphere as marine aerosol. The authors showed that the aerosols contained a large number of semitransparent gel-like particles, in addition to microorganisms, organic and inorganic matter. The semitransparent gel-like particles (primarily TEP and CSP) in the aerosols all contained amino acids, and based on D/L ratios of these acids it was suggested that they originated from phytoplankton exudates.

Several studies have shown that the organic species entrained within marine aerosols collected from various remote ocean sites are of a size range between 70 and 200 nm in diameter. The dominant size range between 50 and 100 nm (Tyree et al., 2007; Fuentes et al., 2010; Hultin et al., 2010), is reminiscent of EPS gels found on the sea surface (Bigg, 2007; Bigg and Leck, 2008; Leck and Bigg, 2008). In a review by Hawkins and Russell (2010) covering over 10 years of measurements of ocean-derived aerosol, the authors concluded that the organic species within marine aerosol is composed of EPS, proteins and amino acids, as well as microorganisms and their components. Facchini et al. (2008) suggested that the solubility continuum of phytoplankton exudates found in seawater is also reflected in marine aerosol, and there is a growing body of evidence supporting the hypothesis that phytoplankton exudates contribute to the formation of CNN (O'Dowd et al., 2004; Russell et al., 2010). Upon its entry into the atmosphere through bubble bursting, the entrained organic gel aggregates within the aerosol particles either directly contribute to the CCN pool in the marine boundary layer (MBL) or after they are degraded by ultraviolet light or acidification in the atmosphere.

Recent research by the DROPPS consortium, funded through the Gulf of Mexico Research Initiative (GOMRI) program, is carrying out experiments attempting to recreate the sea surface microlayer to investigate the potential for petrocarbon (crude oil) to enter the atmosphere. Initial results of this work reveal that crude oil droplets, formed by treatment with dispersants, can burst through physical forces and form aerosolized droplets containing crude oil. This oil-containing aerosol could be carried long distances by wind in the atmosphere and potentially pose health threats to humans and wildlife when inhaled or upon coming in contact with skin.

Marine Oil Snow

Marine oil snow (MOS) is essentially marine snow, with the exception that it distinctively contains oil hydrocarbons. Current knowledge recognizes its formation to be confined to the sea surface where oil slicks form in the event of an oil spill, but further work is needed to determine if MOS can also form in the subsurface. MOS can be described as a mucilaginous organic matter with a "fluffy" or gelatinous off-white appearance that contains oil droplets embedded within its amorphous matrix. Previous reports described evidence of MOS formation during the Ixtoc-I (Boehm and Fiest, 1980; Jernelöv and Lindén, 1981; Patton et al., 1981) and *Tsesis* (Johansson et al., 1980) oil spills (Teal and Howarth, 1984). However, MOS only recently received considerable attention when copious quantities of it, of macroscopic cm-size dimensions, were observed within 2 weeks

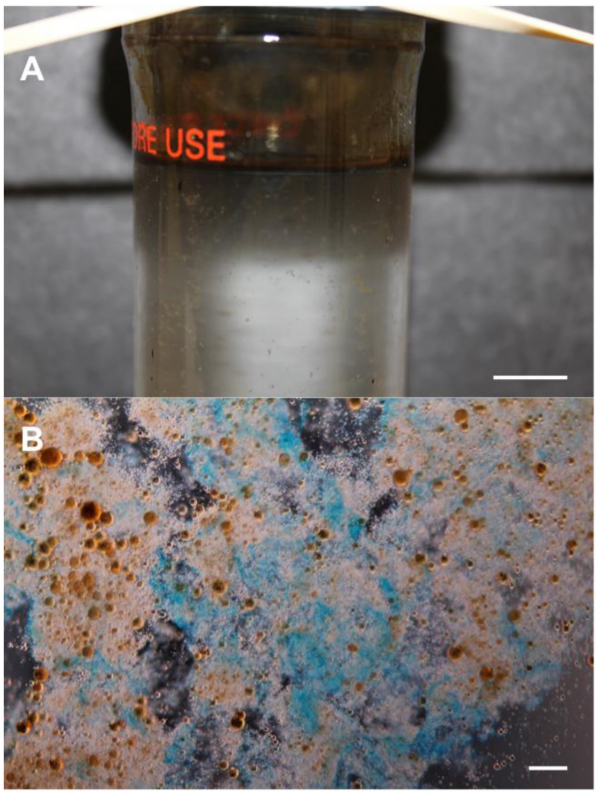

FIGURE 2 | Formation of marine oil snow (MOS). (A) A roller-bottle incubation showing the formation of MOS in synthetic seawater amended with crude oil and inoculated with the EPS-producing (and oil-degrading) bacterium *Alteromonas* sp. strain TK-46(2) that was isolated from sea-surface oil slicks during the Deepwater Horizon oil spill. **(B)** Light micrograph of MOS aggregates, after staining with the cationic copper phthalocyanine dye Alcian Blue showing that the aggregates are partially composed of polysaccharide. The orange-brown spheres in **(B)** are emulsified oil droplets embedded within and adsorbed to the amorphous matrix of the aggregates. Scale bars = 10 mm **(A)**, and = 10 μm **(B)**.

of the Deepwater Horizon (DWH) blowout in the Gulf of Mexico – a spill recorded as the worst oil spill disaster in US history. MOS was encountered frequently around the vicinity of surface oil slicks at DWH (Niu et al., 2011; Passow et al., 2012). It eventually sank to the seafloor in the Gulf of Mexico – a process described termed MOSSFA (Marine Oil Snow Sedimentation and Flocculent Accumulation), which contributed a significant role in the export of crude oil (ca. 14% of the oil released at DWH) to the sediment (Valentine et al., 2014).

Conjecture still surrounds MOS genesis at DWH and during the Ixtoc-I and *Tsesis* oil spills, but its formation and sedimentation appears to have been directly associated with the influx of crude oil. In roller-bottle experiments performed under conditions attempting to simulate sea surface oil slicks at the DWH spill, the presence of crude oil was shown to be an important factor in triggering MOS formation, and that MOS acted as hotspots for microorganism and oil-degrading enzyme activities (Ziervogel et al., 2012; Gutierrez et al., 2013). Bacterial and eukaryotic phytoplankton cells and/or their produced polymers (e.g., EPS) have been reported to induce MOS formation (Passow et al., 2012; Gutierrez et al., 2013; Passow, 2016), whilst there are reports describing conflicting results on the role of dispersants in this respect (Baelum et al., 2012; Fu et al., 2014; Kleindienst et al., 2015; Passow, 2016; Suja et al., 2017). **Figure 2A** shows MOS formation in a roller-bottle incubation containing synthetic seawater amended with crude oil and *Alteromonas* sp. strain TK-46(2) – an oil-degrading and EPS-producing bacterial strain that was found enriched in surface oil slicks in the Gulf of Mexico during the DWH spill (Gutierrez et al., 2013). Like TEP, MOS particles can be rich in acidic sugars of polysaccharides, such that may be produced by EPS-producing bacteria like strain TK-46(2) (**Figure 2B**).

Despite the interest in MOS formation as a product of spilled oil into the Gulf of Mexico, the microorganisms associated with MOS particles have received less attention. During incubations with uncontaminated deep-water samples collected during the active phase of the DWH oil spill and amended with the dispersant Corexit, Baelum et al. (2012) reported the formation of MOS, which was dominated by members of the genus *Colwellia*. In a more in-depth study of the bacterial community associated with MOS, Arnosti et al. (2015) showed that MOS particles contained a bacterial community that was distinctly different from that found freely living (i.e., not associated to MOS) in the surrounding seawater environment. The MOS-associated community was dominated by oil-degrading and EPS-producing members of the *Gammaproteobacteria*, principally *Cycloclasticus*, *Congregibacter*, *Haliela*, *Halomonas* and *Marinobacter*, and included diverse members of the *Alphaproteobacteria* (principally the *Roseobacter* clade) and some members within the *Bacteroidetes* and *Planctomycetes*. Using CARD-FISH (catalyzed reporter deposition – fluorescence *in situ* hybridization), MOS particles formed in incubations with Macondo crude oil and the dispersant Corexit were dominated by members of the class *Gammaproteobacteria*, including the order *Alteromonadales,* which comprises oil-degrading and EPS-producing taxa (Kleindienst et al., 2015). Using Illumina MiSeq sequencing, Suja et al. (2017) showed MOS particles formed in subarctic waters to be enrichment with oil-degrading (*Alcanivorax*, *Cycloclasticus*, *Thalassolituus*, *Marinobacter*) and EPS-producing (*Halomonas*, *Pseudoalteromonas*, *Alteromonas*) bacteria, and included major representation by *Psychrobacter* and *Cobetia* with putative oil-degrading/EPS-producing qualities. Collectively, these studies indicate that MOS are hotspots where oil-degrading and EPS-producing bacteria are enriched, and the latter may provide a clue on the role of these organisms in MOS formation through their synthesis and release of 'sticky' EPS.

Whilst significant knowledge gaps exist in our understanding on MOS formation and its subsequent sedimentation to the sea floor, the influx of crude oil and its interaction with planktonic microorganisms, as well as with dissolved and colloidal organic polymers, such as TEP, and with nutrient and suspended mineral discharges from river effluents, appear to be important factors that warrant further investigation (see Daly et al., 2016 for a review).

Turnover and Stability

Dissolved organic carbon in the ocean can be classified into three broadly defined pools of carbon based on their turnover times: labile, semilabile, and refractory. Collectively, the concentrations of these three DOC pools typically range from 60 to 90 μmol/L in the upper ocean water column, decreasing with depth to 40 μmol/L in the deep sea (Hansell, 2002). Fluctuations in the concentration of DOC in the water column occurs over certain periods of the year, due largely to periods of elevated photosynthetic production since this is the main source that fuels each of these three classes of DOC. The combined effect of biological and physical processes that alter the concentrations of these three pools of DOC is represented in the size-reactivity-continuum model (Amon and Benner, 1996; Benner and Amon, 2015), for which microbial processing of these molecules is the major mechanism that leads to rendering them progressively more recalcitrant (Jiao et al., 2010).

Labile DOC

Labile DOC in seawater comprises substrates with short residence times (minutes to days) since they are consumed almost as quickly as they are produced or released into the water column. An example of a common labile substrate in seawater is glucose, which is on average found at concentrations from 0.001 to 1.0 μmol/L, depending on the ocean region (Rich et al., 1996, 1997; Benner, 2002; Skoog et al., 2002). Other mono-sugar substrates (monosaccharides) also exist in the water column at concentrations typically ranging from 0.002 to 0.8 μmol C/L (Benner, 2002). On average across the oceans, glucose is the most abundant simple sugar, with concentrations as high as 187 nM measured in unfiltered water of the Gulf of Mexico, and 490 nM in high-molecular-weight DOM of the equatorial Pacific (Skoog and Benner, 1997). Glucose has been shown to contribute significantly in supporting a major fraction of bacterial growth in many ocean systems (Rich et al., 1996, 1997; Grossart and Simon, 2002), though other studies have shown glucose to play a less significant role in this respect (Keil and Kirchman, 1999; Skoog et al., 1999, 2002; Kirchman et al., 2001). Turnover rates for glucose can depend on the ocean environment, including the availability of certain nutrients, varying from rapid (hours to days) to relatively slow (100s of days). For example, surface waters limited by inorganic phosphorous can limit bacterial consumption of labile DOC, such as glucose, and result in a longer-than-average residence time of the endogenous pool of the labile DOC (Thingstad et al., 1997).

With respect to the chemical composition of POC in seawater, the abundance of glucose may be related to the major roles that this monosaccharide plays in phytoplankton biology – polymers of glucose (glucans) are major storage compounds in phytoplankton. Galactose is the second most abundant sugar in seawater, and polymers of it (galactans) are major structural components of phytoplankton cell walls (Romankevich, 1984).

Another simple carbohydrate that also contributes to the total pool of labile DOC in the ocean is mannitol. It is one of the most abundant sugar alcohol compounds in nature (Stoop et al., 1996); it is found in bacteria, fungi, algae and higher plants, where it often acts as a compatible solute, among conferring other functions. In ocean systems, mannitol is a major product of photosynthetic organisms, like algae, whereupon this polyol is released following cell lysis to join the pool of labile DOC in the ocean.

Carbohydrate concentrations in seawater can be as high as 10 μmol/L and contribute a significant fraction to the pool of labile substrates. Dissolved polysaccharides, such as EPS produced by bacteria and algae, form a major fraction of the total carbohydrates in the water column (Benner, 2002). Since concentrations of monosaccharides are typically 10-fold lower than dissolved polysaccharides, this suggests they are likely cycled more rapidly. Polysaccharides nonetheless contribute to fueling a major fraction of bacterial activity in some marine environments. On average, however, concentrations of labile DOC are very low (<1 μmol/L), constituting less than 1% of total organic carbon in the upper water column of the ocean. These substrates could potentially sustain oligotrophic microbial populations in regions of poor nutrient availability, such as in the open ocean. Nonetheless, the labile DOC pool is continuously replenished on a yearly basis by trophic (phytoplankton and bacterial excretion) and non-trophic (viral lysis, grazing) processes (Nagata, 2000).

Semilabile DOC

Approximately half of the total pool of DOC in the upper ocean water column is classed as semilabile, and comprises substrates that are consumed over weeks to months. Concentrations of semilabile DOC typically range from 20 to 30 μmol/L in the ocean water column, and because it is consumed over this median time scale, it assumes that this pool of DOC is important in supporting bacterial growth over seasonal to annual time scales (Carlson et al., 1994; Repeta and Aluwihare, 2006). In some ocean systems, such as the Sargasso Sea, the total semilabile DOC can account for as much as 89% of the total DOC (Carlson et al., 1994). In this study, up to 50% of this semilabile DOC was found to be more resistant to microbial degradation over weeks to months.

Interestingly, DOC produced in high-nutrient environments has been observed to be less susceptible to microbial degradation than that produced in low-nutrient environments. This may relate to the chemical qualities of the DOC produced in these contrasting environments – DOC produced in high-nutrient waters may be more nutrient rich than that produced in low-nutrient waters (Church, 2008). Semilabile DOC can accumulate as a result of inorganic nutrient limitation of bacterial growth (Thingstad et al., 1997), primarily from a limitation in PO_4^{3-} (Cotner et al., 1997; Rivkin and Anderson, 1997; Thingstad et al., 1998; Zohary and Robarts, 1998; Caron et al., 2000). Other studies, however, have not found evidence to support the hypothesis that inorganic nutrient limitation of bacterial growth leads to accumulation of semilabile DOC. Rather, the chemical nature of this DOC class, specifically acting as a poor substrate for bacterial degradation, likely contributes to its accumulation in the water column. This is especially the case in the upper water column where DOC concentrations are higher than in the mesopelagic. This could influence the microbial communities in these contrasting regions of the

water column where microbes in the upper water column have been found to degrade semilabile DOC less rapidly than those communities found in the mesopelagic (Carlson et al., 2004).

Refractory DOC

Much of the DOC in the ocean consists of low-molecular-weight solutes of <1000 Da, the majority of which comprises the refractory pool of DOC that is resistant to microbial degradation over time scales of 1000s of years – anywhere between 4000 and 6000 years (Williams and Druffel, 1987) – approaching or exceeding that of ocean circulation (Benner et al., 1992). Whilst concentrations of labile and semilabile DOC vary with depth, that of refractory DOC averages ca. 40 μmol/L throughout the water column with little to no variation with depth, and likely contributes insignificantly as a source of carbon and energy to bacterioplankton. However, a fraction of refractory DOC at the sea surface is destroyed by ultraviolet irradiation, which results in the release of labile DOC for heterotrophs to consume (Moran and Zepp, 2000). The refractory pool contributes to the sequestration of enormous quantities of carbon and acts as a carbon sink in the water column (Hedges, 2002). A recent study combining organic matter size, ^{14}C age and elemental composition of DOC estimated that small refractory molecules in the ocean are produced by microorganisms and at a rate of 0.24 PgC per year, which is on par in magnitude to the burial of organic carbon in sediments (Walker et al., 2016).

Major sources of this refractory DOC pool include complex cell fragments and other high-molecular-weight biopolymers produced by cells that are partially or almost totally recalcitrant to biodegradation. During viral lysis of eukaryotic phytoplankton cells, cellular components that are highly refractory to degradation are released into the water column. Similarly, phage-mediated lysis of bacterial cells leads to the release of outer-membrane proteins of the cell envelope, which also are very resistant to degradation. Conversely, highly labile cell components, such as nucleic acids and amino acids, are recycled in the photic zone.

A proportion of the DOC released through cell lysis, including that produced extracellularly by living cells, is converted by chemical mechanisms into humic substances. This complex material is quite resistant to biodegradative processes and contributes to the total pool of refractory organic matter in the water column. Either by agglomeration of these humic substances, or their attachment to other sinking particles, a proportion of this refractory material eventually sinks to the ocean floor and becomes buried. Not all refractory DOC in the marine water column, however, sinks to the seafloor. Rather, most of it remains suspended and circulating in the ocean for years to millennia. In fact, of the fixed organic carbon formed by primary production, only a very small fraction reaches the seafloor; much of it (>99%) is remineralized in the water column through microbial action.

Extracellular polymeric substance produced by marine bacteria, even that which is freshly produced, can be somewhat refractory to microbial degradation or chemical analysis (Ogawa et al., 2001). This is believed to be related to the presence of uronic acids (Anton et al., 1988; Bejar et al., 1996) or glycosidic linkages of hexosamines (Biermann, 1988). Such constituents can confer on EPS molecules a high resistance to degradation under acid hydrolysis conditions that are used to chemically analyze them. Some studies analyzing the chemical nature of EPS isolated from cultured marine bacterial strains have shown a major proportion of these macromolecules (up to 80%) can be unaccounted for by chemical analysis (Gutierrez et al., 2007a,b, 2008).

PHYSICAL/CHEMICAL PROPERTIES OF EPS

Extracellular polymeric substance comprise an expanding plethora of biochemical molecules that interact in many ways and that are, as yet, poorly understood. EPS consist of an array of molecules, ranging from quite large (e.g., >100 kDa) to much smaller (e.g., <10 kDa) polymers. Some of the molecules contribute to the structural stability, gel properties, and pliancy of the greater matrix (Flemming, 2016). We must determine how different types of molecules in this matrix interact with each other in order to provide the observed functional roles of the EPS matrix. An entire rethinking of the extracellular milieu of microorganisms will likely be required. An insightful examination is provided by Neu and Lawrence (2016).

Composition and Physical Properties

From the standpoint of microbial cells, the EPS, especially when in a gel state, form a three-dimensional matrix or scaffold within which cells can orient themselves relative to one another. The presence of certain polymers can afford the matrix physical stability. Polymers such as amyloids and/or eDNA (discussed below) can serve as an architectural framework for the EPS. Each type of EPS component can offer different physical properties (Chew et al., 2014). The physical ultrastructure of the EPS matrix has been very difficult to image in a fully hydrated state (Decho, 1999), owing to its delicate nature. Excellent pioneering efforts have been conducted by Dohnalkova et al. (2011) using a unique cryo-TEM approach. Recent developments in cryo-TEM and -SEM may provide further insights into this complex matrix.

Bacterial and microalgal EPS exist in nature in a range of different physical states, most of which are operationally defined. Capsules consist of polymers that closely surround individual or multiple cells and often serve a protective role (Whitfield, 2006). Further away from cells, EPS can exist as tight, dense-gels, to a continuum of physical states from looser-slime to truly dissolved forms. Dissolved forms, in the absence of cells, may condense to microgels in the open ocean (Chin et al., 1998; Verdugo et al., 2004; Verdugo and Santschi, 2010); a process that is of significant importance and has been well-summarized in a review (Verdugo, 2012). While differences in these physical states are relatively arbitrary, they likely serve very different functions to the microbial cells secreting them. The physical state of EPS results from a combination of the polymer concentrations, types and abundances of ions, composition, and steric availability of functional groups on polymers. Recently, this has been reviewed in greater detail (Neu and Lawrence, 2016).

Some microbial EPS can exhibit significant viscoelastic properties, being able to stretch and retract in response to an applied force such as intermittent water flow (Fabbri and Stoodley, 2016). This property offers the microbial cells contained within a biofilm with a certain degree of physical flexibility and mechanical resiliency (Peterson et al., 2015). This flexibility is important to the ability of cells to persist on a surface or as an aggregate in the water-column.

Compositional information is a useful starting point for investigating EPS. Strictly speaking, the term EPS is an operational designation that refers to the milieu of 'larger' molecules contained in the extracellular matrix in proximity to cells (Wotton, 2004). Many of the molecules contained in natural EPS cannot be conveniently characterized as either protein, lipid or carbohydrate. For this reason, it has been called the '*dark matter*' of biofilms (Flemming et al., 2007). It is now known that the EPS matrix can be quite heterogeneous, especially over small spatial scales (see Microdomains within EPS Matrices). It is for this reason that analyses of 'bulk' samples will not capture the smaller-scale variability that are critical to understanding the physical and chemical properties of the *in situ* matrix. When EPS from natural biofilms, for example, are extracted and then reconstituted, the physical (e.g., gel, viscocity, rheology, etc.) properties of the reconstituted EPS often do not readily resemble those of the original biofilm. (In much the same way, a cell cannot be taken apart via extractions, and then put back together as a functioning cell.) This suggests that the molecules within the matrix may have important molecular organization either by purposeful design or by result of the environment. *It is important from a functional standpoint, to determine which molecules and molecular interactions contribute to physical properties such as gel formation, rheology, and diffusion-slowing, and chemical properties, such as sorption.*

Finally, while matrix is actively secreted by cells, the properties of EPS may be changed post-secretion, modified by geochemical, enzymatic, and photochemical processes, and additionally contain trapped or sorbed molecules. These modifications may have dramatic effects on their physical properties. Thus, EPS under natural conditions exist in a 'continuum' of compositional and partial degradation states. Thus, it is imperative that future non-destructive approaches (e.g., Raman spectroscopy) are developed for characterizations of EPS *in situ*.

Laboratory studies of bacteria secreting EPS show that cells typically produce sugar monomers that are exported, then assembled to the existing polymer outside of the outer membrane (Whitfield, 2006; Sutherland, 2016). Polymers may consist of single sugar monomers, called homopolymers, or consist of several monomers linked together to form a repeating unit, called heteropolymers. Since several types of repeating units may be generated, this provides the cell with the capability to alter the physical chemical properties by mixing different amounts of repeating units. By changing the building blocks (i.e., repeating units), the polymer composition can be varied. This allows the polymer to have a variable composition and provides the cell the capability to modify its extracellular polymers in response to changing conditions.

At present, there are no specific biosignatures that can be assigned reliably for detection of EPS, simply because similar glycol-based compounds are produced throughout biological systems for many purposes. The secretion of carbohydrates and other glycosylated polymers is not unique to bacteria or even microorganisms; rather, it is a universal biological strategy employed by microalgae, fungi, invertebrate and vertebrate animals, and plants (Underwood and Paterson, 2003).

Extracellular polymeric substance have often been considered synonymous with 'exopolysaccharides' and acronym EPS. This was partially based on the carbohydrate-focus of investigators at the time, and additionally due to the artifact of carbon-rich culture conditions that were used to grow bacteria and obtain abundant quantities of EPS. Much has been learned regarding polysaccharide chemistry from these seminal studies. While polysaccharides are a major component of many natural EPS, they are only a component. The EPS matrix is now known to contain several different major groups of molecules, whose roles and involvement are still under study, and will be discussed briefly below. Hence, much discussion has evolved about what exactly constitutes the EPS matrix. Three points emerge as one studies the EPS of natural systems: (1) Many different types of molecules interact to provide the physical structure, impart chemical properties, and even actively manipulate EPS properties for the cell; (2) EPS-compositional studies should not be limited to culture-based systems; and (3) EPS under natural conditions will likely exist in a continuum of partial-degradation states.

Polysaccharides

The polysaccharide components of EPS are perhaps the best-studied to date. Common carbohydrate components that are often found in EPS include monomers such as D-glucose, D-galactose, D-mannose, L-fucose, L-rhamnose, D-glucuronic acid, D-galacturonic acid, L-guluronic acid, D-mannuronic acid, *N*-acetyl-D-glucosamine, and *N*-acetyl-D-galactosamine (Sutherland, 2001, 2016). Polysaccharides such as cellulose, alginic acid, dextran, xanthan, and *Vibrio* exopolysaccharide (VPS) are examples of polysaccharides produced by bacteria (for reviews see Decho, 1990; Wotton, 2004; Serra et al., 2013; Hobley et al., 2015).

The exopolysaccharide portion can exert significant net effects on physical and sorptive properties of EPS (Salek and Gutierrez, 2016). The presence of polar negative-charged groups such as carboxyls, phosphates and sulfate esters can provide negative charges (Thornton et al., 2007; Gutierrez et al., 2009). In certain microbial mat systems, highly sulfated exopolysaccharides have been isolated, and contained up to near 30% (wt/wt) in sulfate (Moppert et al., 2009).

In the presence of (positive) divalent cations (e.g., Ca^{2+}, Mg^{2+}) they can form cation bridges with adjacent polymers having also negative functional groups. EPS having abundant uronic acids often complex in this manner. Direct linkages between adjacent EPS can also occur. For example, linkages between a cationic polysaccharide and (anionic) extracellular-DNA has been shown to contribute to the physical stability of bacterial biofilms (Jennings et al., 2015). The abilities of EPS to link with each other is dependent, in part, on pH,

the presence of appropriate functional groups, and the steric availability of functional groups (Decho, 1990; Ulrich, 2009).

Microdomains within EPS Matrices

The natural EPS matrix is now known to be heterogeneous over small spatial scales (e.g., μm, even nm). In order to describe small, localized areas that exhibited different properties than the broader matrix, polysaccharide chemists long ago developed the term '*microdomain*.' The microdomain concept was extended to EPS (Decho, 2000a) to begin understanding why intact EPS exhibited very different properties than those of the extracted bulk EPS. Microdomains can result from localized concentrations of certain monomeric components of polymers, and/or differential binding of adjacent polymers to each other. Evidence for microdomains within *in situ* expolymer matrices has been evidenced by the careful combination of fluorescent lectin probes and confocal scanning laser microscopy (Lawrence et al., 2007, 2016; Aldeek et al., 2013). Microdomains are now realized to contribute to the smaller-scale heterogeneity that is observed within both suspended aggregate- and attached-biofilms. The presence of microdomains re-enforces the idea that the EPS matrix is not an amorphous, homogeneous entity, but rather can be structured at several different levels (Mayer et al., 1999; Decho, 2000a; Lawrence et al., 2003).

Proteins

Proteinacious moieties are common in natural EPS matrices and occur in a variety of molecular forms such as peptides, amino-sugars, glycoproteins, proteoglycans, and amyloid proteins (Gutierrez et al., 2007a,b; Fong and Yildiz, 2015; Zhang et al., 2015). They also can be grouped by their functions and properties such as extracellular enzymes (*e*-enzymes), membrane vesicle proteins, adhesins, amyloids, hydrophobins, and amphiphiles (Hobley et al., 2013). It is not well-understood yet, how proteins interact with other matrix molecules to accomplish these apparent functions.

While many proteins and peptides are easily hydrolyzed by microbial heterotrophy, certain proteins and peptides can be quite refractory to degradation. It is now realized that structured refractory complexes, called *amyloid* fibrils are a common component of EPS. These have not received much attention in oceanic environments but may contribute to a number of forms of refractory organic matter, and the refractory portions of EPS. Here, they may have important functions. Amyloids may form an important, refractory structural component of the EPS matrix (Gebbink et al., 2005; Larsen et al., 2007; Zheng et al., 2015).

Amyloids are loosely defined as any fibrillary polypeptide aggregate having a cross-β-quaternary structure (Fandrich, 2007), which self-assemble under the right environmental conditions. Amyloid fibrils consist of sets of 4–6 peptides linked together in a twisting, helical (i.e., rope-like) structure that is held together by non-covalent associations. A growing body of evidence supports the idea that amyloid fibrils, sometimes called curli fibers, may be formed from many different proteins (and peptides) and are a generic structure of peptide chain. While amyloid formation has been linked to many human disease processes (Barnhart and Chapman, 2006; van Gerven et al., 2015), they occur in natural microbial systems as a component of EPS. Their formation, at present, is thought to result from non-biological processes (Romero et al., 2010).

Extracellular *e*-DNA

A growing body of research now acknowledges the presence of extracellular forms of deoxyribonucleic acids (*e*DNA), and their role as an important structural component of the biofilm matrix (Böckelmann et al., 2005). Historically, *e*DNA was thought to result largely from the lysis of cells or release of plasmids. However, seminal studies by Whitchurch et al. (2002) showed the presence of *e*DNA as a part of the EPS. Concentrations of *e*DNA in sediments are often 3–4 orders of magnitude higher than those in the water-column, and suggest a role in the cycling of P in marine systems (Dell'Anno and Corinaldesi, 2004). Both *e*DNA and extracellular nucleases, together, may influence the physical consistency of biofilm EPS (Rice et al., 2007; Seper et al., 2011). Results of other studies indicated secretion by bacteria of *e*DNA is an active process (Nishimura et al., 2003; Steinberger and Holden, 2005; Suzuki et al., 2009; Gloag et al., 2013; Okshevsky and Meyer, 2013; Tang et al., 2013). The postulated roles suggest that *e*DNA may be a bacterial strategy that serves as an abundant structural scaffold within EPS. For example, in non-marine systems, the Gram-negative bacterium *Pseudomonas aeruginosa* uses *e*DNA bound to a specific cationic extracellular polysaccharide *pel* to provide structural stability to the EPS of biofilm (Jennings et al., 2015). Others have suggested an electron-transfer conduit, or substratum for the controlled movement of bound *e*-Enzymes (Flemming et al., 2007). Further studies await empirical testing of these ideas. However, an interesting caveat is that a recent study by Dell'Anno and Danovaro (2005) showed that DNA sorbed to sediments constituted an important source of phosphorus in normally P-limited deep-sea ecosystems. A review on *e*DNA pools in marine sediments summarizes many important aspects (Torti et al., 2015). Finally, DNA has been implicated in long-distance electron transfer processes (Giese, 2002). A pertinent question that warrants investigation is: does this offer the possibility for long-distance transfer of extracellular electrons through the EPS matrix?

Modifications Post-secretion

Extracellular polymeric substance, once-secreted by cells, are subjected to substantial environmental modifications, perhaps in predictable manners. Degradation of EPS may consist of a multi-step process. The steps likely represent the degradation of different components, ranging from highly labile to relatively refractory, which have different compositions and/or steric availabilities (to extracellular enzymes). A study of EPS produced within lithifying microbial mats showed that initial hydrolyses involved a rapid, and possibly selective, utilization by heterotrophs of certain sugar monomers, and LMW compounds. Certain components of the EPS, such as the uronic acids were highly labile to mat bacteria (Decho et al., 2005). Initial heterotrophic degradation of EPS was fueled by the large pool of LMW organics released by cyanobacteria during photosynthesis. This pool was consumed within 4–6 h post-daylight. The results indicated that a rapid, initial degradation occurred, followed by

a much slower decomposition, leaving behind a more "*refractory remnant*" that persist for extended periods. As alluded to above, specific components of EPS such as many polysaccharides should exhibit relatively rapid turnover rates, when compared to more refractory components such as amyloid proteins. Finally, degradation will be affected by the physical properties of the EPS such as their gel versus solution states.

Sorption, Trapping, and Diffusion-Slowing Properties

Diffusion is a key process in the design of the microbial cell, as it is the primary means by which small organic molecules and ions may be taken up by cells. Diffusion is also of relevance in the movement of signal molecules (i.e., autoinducers) involved in QS, extracellular enzymes, and antimicrobial agents. EPS can be broadly considered a sorptive sponge for the binding, trapping and concentration of organics and ions (Decho, 1990). Over the small spatial scales of biofilms, the EPS matrix influences the diffusion process. Diffusion is a multi-faceted process that is influenced by temperature, ionic concentrations, etc. A major driver in diffusion, of course, is the relative concentration gradient (Brogioli and Vailati, 2001). The density and properties of the EPS can influence diffusion rates (of ions or molecules) so they can range negligible (compared to diffusion in pure water at the same temperature) to having significantly slowed diffusivities (Decho, 2015).

Although bulk measurements of diffusivity may be estimated, it is difficult to determine how the smaller-scale variability in EPS densities influence diffusion at these scales. The natural matrix of EPS within aggregates or surface biofilms is often filled with channels, which by microbial design or by environmental influence, enhances mass transfer to/from cells.

A number of investigators have carefully measured diffusion rate constants by monitoring the movement of fluorescent molecules over time using confocal scanning laser microscopy and other approaches (Lawrence et al., 1994; Guiot et al., 2002; Stewart, 2002; De Beer et al., 2004; Waharte et al., 2010; Neu and Lawrence, 2014). Lawrence et al. (1994) initially used fluorescent molecules and confocal scanning laser microscopy to examine diffusivities and found them to be variable, ranging from those of pure water ($d = 1.0$) to extreme diffusion-slowing effects ($d = 0.02$) by the matrix. From a practical standpoint, one can assume there will be variability within an aggregate or attached biofilm. Collectively, these studies have shown that considerable changes occur in the movement of molecules and ions over microspatial distances (i.e., μms), which can relate to the observed heterogeneity that occurs within biofilms (Stewart and Franklin, 2008).

Physical trapping of organic and inorganic colloids, and nanoparticles also occurs in the EPS matrix. The viscoelastic nature and the dispersed arrangements of EPS at the surface-most fringes of biofilms make them ideal for the physical trapping of colloids, small particles, and/or sorption of ions and molecules. Sorption is influenced by a number of factors. These include pH, the forms and concentrations of ion(s), and the type(s) of ligands (binding sites) and associations (e.g., ionic- and covalent-bonds, van der Waals forces, etc.). The pH can have a strong effect on ionic binding, especially with regard to many EPS (Braissant et al., 2007, 2009; Gutierrez et al., 2008). In general, acidic pH tends to inhibit ion binding, while neutral or basic pH tend to promote binding. A caveat is that not all ions bind equally. A second caveat is that certain functional groups bind ions more efficiently at a given pH. For example, as the pH rises to near neutral, more complexation may occur to carboxyl sites. The increase in binding of divalent cations often results in a more cohesive polymeric gel structure.

This pH-dependent sorption process has practical importance in ocean systems (and biofilms) because the most abundant divalent ions in seawater are Ca^{2+} and Mg^{2+}. These ions often form suitable (bi-dentate) bridges between adjacent EPS molecules having carboxylic acid groups, and can contribute to gel formation or floc (marine snow) formation in the water column. However, other important ions (at a given pH) may 'outcompete' Ca^{2+} and Mg^{2+} for binding sites. The binding of transition and other metals, such as Th, Cd, Cu, Ag, Fe, and Se, to EPS isolated from different environments, such as hydrothermal vents, microbial mats, and other areas, has been described (Schlekat et al., 1998; Zhang et al., 2008; Moppert et al., 2009; Deschatre et al., 2013). Metal binding to EPS of surface floc material (i.e., marine snow) in the surface waters of oceans, and subsequent sinking of flocs may result in significant vertical transport (flux) of trace elements to ocean floor, a process of global biogeochemical significance (as mentioned above).

While ocean seawater is often pH 7.8–8.2, the range of pH over smaller spatial (and temporal) scales can be quite dramatic. In microbial mat systems, where highly active bacterial respiration and photosynthesis occur, the pH has been shown to vary from pH 6.0–10.0 over a 24 h (i.e., diel) cycle (Visscher et al., 2000; Des Marais, 2003; Baumgartner et al., 2006). This is due to net photosynthesis during daylight (which raise pH), and net respiration during darkness (which lowers pH). This can result in regular diel changes in the complexation of ions, and hence influence the physical stability of EPS over a 24 h cycle. The diffusion-slowing properties of EPS contribute to the sharp geochemical gradients often observed within aggregate and attached biofilms (Baumgartner et al., 2006).

Optical Properties

The biofilm is an organic gel coating (of EPS) on a surface (or within a suspended aggregate) with a collage of cells, and sorbed or localized molecules and ions, colloids, and particulates. All of these different components, individually or interactively, will influence the optical properties (i.e., refraction, scattering, and absorption of photons) of the broader surface (or water). The EPS can be thought of as a "semi-translucent" gel having different densities. Several processes act in concert to alter the optical properties of sediments. First, the polymers themselves appear to decrease the reflectance of the surface. In sediment systems, this can alter the amount of light entering the sediments. This is due to a combination of two processes. First, the gel polymers increase the spacing between sediment grains. This allows more light to enter in the spaces between grains, rather than being reflected from closely packed sediments. Second, the gel state of the polymer acts as a 'photon trap' because it mediates a

change in refractive index, relative to seawater. This enhances the forward-scattering of photons, relative to back-scattering. This has been termed the 'biofilm gel-effect' (Decho et al., 2003). The functional value is that light may be more homogenously scattered around photosynthetic cells, and allow cells to conduct photosynthesis deeper in sediments (or mats).

As light interacts with a surface, photons are either reflected, scattered, refracted and/or absorbed. Reflectance involves back-scattering of photons at a fixed angle (relative to incident direction of photon). Often photons are 'scattered' at many angles relative to the incident. Refraction involves continuing through the surface, but altering the angle (relative to the incident) resulting in a change in refractive index. Absorbance involves the capture of photon energy by surface molecules or atoms. Absorbed photons may be re-emitted, as fluorescence (within pico-sec to nano-secs after absorbance), or released as heat. However, the biofilm is not simply a translucent gel but rather a three-dimensional matrix harboring cells, sorbed, or localized molecules (e.g., scytonemins, amino acids, etc.), colloids, and particulates. Biological chromophores (molecules that absorb light near specific wavelengths) include the purines and pyrimidines of DNA, the 'ringed' amino acids (tyrosine, phenylalanine, etc.), and other molecules. The sea surface layer is known to harbor EPS gels (Wurl and Holmes, 2008). Of special interest will be how the sea-surface layers of EPS influence photon penetration into the underlying water.

LOCALIZATION OF MICROBIAL EXTRACELLULAR PROCESSES

Quorum Sensing

Do microbial communities communicate and coordinate activities? Classical microbiology during much of the past century has taught us to understand microbes simply as individual cells. Recently, however, a growing body of evidence supports the idea that bacteria often act in groups, rather than as individuals. When bacteria are attached, their proximity to each other results in the development of interactive relationships ranging from antagonistic to agonistic, and even altruistic. These interactions are often chemically mediated but are tempered by the ever-changing conditions of their local environment. The diffusion-slowing properties of the EPS matrix facilitates the development of such relationships among cells in a way that cannot be accomplished by free-living planktonic cells.

Quorum sensing is a type of bacterial cell–cell communication that involves the exchange of chemical signals among nearby cells to coordinate behaviors that are best conducted in groups (Fuqua et al., 1996). It involves the production, detection, and response by cells to diffusible signaling molecules (i.e., autoinducers). Autoinducers accumulate in the proximal environment as the bacterial population increases. When autoinducer concentration reaches a threshold-level, cells collectively alter gene expression. Many group activities such as bioluminescence, antibiotic production, and EPS secretion (Camilli and Bassler, 2006) are regulated by QS.

Quorum sensing can also be utilized by cells for '*diffusion-sensing*' (Redfield, 2002). This allows bacteria to sense the diffusional properties of its proximal environment, presumably to 'make decisions' whether to conduct more metabolically costly processes, such as production and release of extracellular enzymes, plasmids, antibiotics, etc. (Ruparell et al., 2016). Together, these two processes, quorum- and diffusion-sensing, have been termed '*efficiency sensing*' (Hense et al., 2007).

The foundation for cell–cell cooperative interactions originally was proposed for explaining the bioluminescence by a marine luminescent bacterium, previously *Photobacterium*, renamed *Vibrio fischeri*, and then *Aliivibrio fischeri*, which was isolated from a small Hawaiian squid (Ruby and Nealson, 1977; Nyholm et al., 2000). Studies progressively showed that autoinducer molecules, upon reaching a threshold concentration in the medium, triggered changes in gene expression that resulted in bacterial luminescence. Luminescence by populations of symbiotic bacteria, localized in the light organs of the squid, afforded it a selective advantage against predation. The ability to communicate, coordinate, and act as groups, however, does not relinquish the cells as an individual unit. Microbial cells can (and do) still act as individual cells. This amazing flexibility likely contributes to the tremendous success and resiliency of bacteria.

In open surface-water ocean environments, QS can have large-scale effects, especially when in overwhelming abundances. An obvious example of this was the 'milky ocean' that was observed at night by satellite off of Somalia, Africa (Nealson and Hastings, 2004; Miller et al., 2005). The milky ocean, which was 100s of square km in size, was due to QS-triggered bioluminescence in ocean surface populations of bacteria.

Several different classes of chemical signals exist. Most were described from the study of infection-causing bacteria. These include acylhomoserine lactones (AHL), unique oligopeptides, furanosyl borate diesters (Autoinducer-2), and gamma-butyrolactones (Waters and Bassler, 2005). The AHLs comprise a class of approximately 18 different types of signal molecules that are released into the surrounding environment, and eventually bind to an intracellular receptor protein, whose complex then triggers changes in gene expression (Churchill and Chen, 2011). AHLs in marine environments have been found in sponges (Taylor et al., 2004), microbial mats (McLean et al., 1997; Decho et al., 2009, 2010) and marine snow (Hmelo et al., 2011). Interestingly, signals such as AHLs are prone to inactivation under certain environmental conditions such as high pH (>8.0) (Decho et al., 2009; Hmelo and van Mooy, 2009). It is not known how fluctuating conditions (e.g., pH, oxidants, desiccation, photocatalytic degradation) in natural environments influence chemical signaling and coordination of microbial activities (Horswill et al., 2007; Decho et al., 2009, 2011; Frey et al., 2010). Signaling, however, will likely be localized and most pronounced within EPS matrices, and within planktonic aggregates (Gram et al., 2002; Wagner-Dobler et al., 2005; Hmelo et al., 2011; Amin et al., 2015; Jatt et al., 2015).

Signaling using AHLs, for example, is not limited to heterotrophic bacteria. Rather it has been found in photosynthetic cyanobacteria (Sharif et al., 2008) and Archaea (Zhang et al., 2012). Importantly, it is now realized that this

form of cell–cell communication can occur in single-species population, but may also be utilized by inter-Kingdom consortia, such as plant-microbe and animal–microbe associations. Contrastingly, molecules that may act as signals for some bacteria, may act as antibiotics against other bacteria (Kaufmann et al., 2005; Davies et al., 2006; Schertzer et al., 2009; Johnson et al., 2016). A final note is that currently only several classes of signaling molecules (e.g., AHLs, AI-2, and peptides, diffusible signal factors (DSFs), etc.) are known (Schaefer et al., 2008; Papenfort and Bassler, 2016, for review). However, QS and similar interactions via chemical signaling are likely to occur using a variety of signals; most of which may be unknown at present.

Extracellular Vesicles and Gene-Exchange

Bacteria possess the capability to bud-off portions of their cell membranes (Schooling et al., 2009; Biller et al., 2014), which are then released as extracellular vesicles. The vesicles provide bacteria with the ability to package molecules within a surrounding lipid membrane, and release them in their surrounding extracellular environment, and localize them within the EPS matrix. This can provide a protective 'minefield' against antibiotics, preserve extracellular signals and plasmids, and provide other functions as well. The presence of extracellular vesicles within biofilms, and specifically the EPS matrix, is now realized to be quite common (Mashburn and Whiteley, 2005; Biller et al., 2014). The vesicle composition is often similar to the plasma membrane (Gram-positives) or outer cell membrane (in Gram-negatives), but additionally contain specific proteins as part of the vesicle. The vesicles can package a wide range of molecules such as *e*DNA, RNA, *e*-enzymes, antibiotics, and signal molecules, and likely provide protective effects for the packaged molecules they carry (Mashburn-Warren et al., 2008; Schooling et al., 2009).

Gene exchange is an important process among bacteria. The EPS matrix can enhance gene exchange among cells for several reasons. First, conjugation (i.e., a uni-directional exchange of plasmids via a pilus connecting two cells) requires extended contact for a prolonged period of time (approximately 20 min). In open-water systems, this is difficult due to Brownian motion constraints. When localized in a three-dimensional EPS matrix, two cells can remain relatively stationary for prolonged periods of time, which can facilitate conjugative gene exchange. Second, extracellular DNA, used in transformation, can be rapidly degraded once outside of the cell, or strongly sorbed to sediment particles. When DNA is immobilized within EPS, its persistence can be enhanced, and thus increase chances for transformational exchange of DNA among cells. Direct measurements of these two processes, to our knowledge, are not yet available.

Extracellular Enzymes (e-Enzymes) and Hydrolysis products

Degradation of organic matter and its mineralization to CO_2 is a fundamental process of bacteria. In many ocean environments, bacteria produce *e*-enzymes to partially hydrolyze organic matter that becomes sorbed or trapped by the EPS (Hoppe et al., 2001). When conducted efficiently, with minimal loss to the surrounding water, the biofilm can be an efficient external digestion system for the microbial community (Flemming and Wingender, 2010).

The localization of *e*-enzymes is a process that is important in open water aggregate- as well as attached-biofilms. In order for efficient diffusional uptake, both enzymes and their hydrolysis products must remain localized in proximity to cells (e.g., approximately 30 μm). EPS provide a matrix to localize both enzymes and their hydrolysis products relatively close to cells. It is not known, however, how *e*-enzymes remain localized within the EPS matrix. Are they attached (bonded) to polymers with active sites exposed? In studies of other systems, bacteria are known to localize polysaccharases and other *e*-enzymes (Sutherland, 1999, 2016). *e*-Enzymes are also known to be contained within extracellular vesicles, localized within the expolymer matrix (Mashburn and Whiteley, 2005; Mashburn-Warren et al., 2008; Elhanawy et al., 2014), and e-DNA nucleases were found in *Vibrio cholerae* biofilms (Seper et al., 2011). Indeed, elevated microbial activities, such as enzymatic activities, have been reported in marine snow particles at higher-levels than those in surrounding sea water (Smith et al., 1992; Ploug et al., 1999; Grossart et al., 2003; Jatt et al., 2015), thus suggesting that marine snow are hotspots for remineralization of organic and inorganic materials (Azam and Long, 2001; Thornton et al., 2010).

Insight has been provided through studies of other systems (Tielen et al., 2013). They showed that extracellular lipase was protected against heat denaturation via complexation with the EPS alginate. Using molecular modeling they were able to show that *e*-enzymes can be physically bound to EPS, however, the enzyme/EPS bond must occur away from active sites on the enzyme. Finally, this bonding provides enhanced stability against denaturation. However, questions remain, such as: how are enzymatic activities maintained outside the cell? Empirical evidence has been relatively limited. Do the functional equivalents of extracellular chaperones help to maintain activities (i.e., prevent denaturation) of *e*-enzymes? It is also not known how extracellular enzymes may modify the EPS themselves.

EPS IN MICROBIAL MATS AND MINERAL PRECIPITATION

Microbialites are benthic microbial deposits (Burne and Moore, 1987). Microbial mats, a type of microbialite, are the longest-lived ecosystems that are known to have existed on Earth. Certain fossilized microbialites extend far back in the fossil record (Sprachta et al., 2001; for review, see Chagas et al., 2016). They are the earliest known macro-fossil evidence of life in the geological record, extending back an estimated 3.4–3.7 gy (Tice and Lowe, 2004; Nutman et al., 2016). They dominate the fossil record for 3 gy, which represents over 80% of the time life has existed on Earth (Allwood et al., 2007). Recently, the precipitation process has been studied at nanometer spatial scales (Benzerara et al., 2006).

Microbial mats typically exhibit a distinct vertical layering of microbial functional groups that is strongly

influenced by externally influenced gradients such as light and geochemical conditions (Des Marais, 2003; Vasconcelos et al., 2006; Franks and Stolz, 2009). In most cases, mats are examples of actively metabolizing, highly organized microbial communities, and constitute "high-yield" systems where resources are efficiently recycled amongst its members (Visscher and Stolz, 2005). These systems, therefore, offer excellent platforms from which to study how EPS may influence the precipitation of carbonate minerals. Thrombolites (Mobberley et al., 2015) and tufa deposits (Zippel and Neu, 2011; Dupraz et al., 2013) are other forms of microbialites.

Extracellular polymeric substances are abundantly present in microbialites, such as mats and contribute to the metabolic efficiency of mat communities (Neu, 1994). This occurs through their diffusion-slowing properties, light-attenuation, and abilities to influence 3D-architecture, chemical communication, extracellular enzymatic hydrolyses, and biogeochemical mineral precipitation. The details of how this relate to the molecular-scale interaction occurring between ions and the EPS are not, as yet, fully understood.

Carbonate Precipitation

Mats are well-known for their association with the biogeochemical precipitation of minerals such as carbonates (e.g., calcite, aragonite) (Decho, 2010). Present-day examples of precipitating mats include tufa mats, marine stromatolites, and marine thrombolites (see Dupraz et al., 2009, for review; Glunk et al., 2009; Tourney and Ngwenya, 2014). There are several different mechanisms known to directly or indirectly influence precipitation within mat environments (Visscher and Stolz, 2005). Microbial communities drive the basic alkalinity engine, which when coupled to the organic matrix of mats, results in biogeomineral precipitation (Dupraz and Visscher, 2005). Activities of several microbial groups, such as cyanobacteria, sulfate reducers, and anoxygenic phototrophs, can '*promote precipitation,*' while other groups (e.g., aerobic heterotrophs, sulfur oxidizers, and fermenters) can '*promote dissolution*' (Dupraz et al., 2009). Precipitation of $CaCO_3$ occurs in seawater that is near or exceeding supersaturation of carbonate ions, and has basic pH conditions (Arp et al., 2001, 2003). Cyanobacterial activities, for example, will raise the pH during daylight photosynthesis, which favors localized carbonate precipitation (Gautret et al., 2004; Ludwig et al., 2005). Specific moieties on EPS, such as acidic groups, can act as nuclei for subsequent $CaCO_3$ precipitation (Braissant et al., 2003; Bhaskar and Bhosle, 2005; Obst et al., 2009). Even bacterial cells themselves can serve as nucleation sites for precipitation (Varenyam et al., 2010). EPS can bind substantial amounts of free Ca^{2+} (Braissant et al., 2007) and other minerals such as phosphate and sulfate (Gallagher et al., 2013) from the surrounding water. This can result in precipitation of EPS-associated minerals such as apatite [$Ca_5(PO_4)_3(F,Cl,OH)$], struvite ($MgNH_4PO_4{\cdot}6H_2O$), dolomite [$CaMg(CO_3)_2$], and aragonite (Gallagher et al., 2012, 2013).

Under some conditions, however, EPS can inhibit precipitation, or even contribute to carbonate dissolution. Cation-binding by EPS removes free Ca^{2+} ions from solution, through depletion of carbonate minerals from the proximal surroundings. Acidic amino acids, such as aspartic or glutamic acids, and carboxylated polysaccharides (i.e., CO_3^{2-} groups of uronic acids) can act as strong inhibitors of $CaCO_3$ precipitation (Kawaguchi and Decho, 2002a,b; Dupraz et al., 2004; Gautret and Trichet, 2005). The functional groups and their steric availability (to bind ions) are key in this process (Rieger et al., 2007; Yang et al., 2008). The role(s) in carbonate precipitation of specific microbial clades such as sulfate reducers, however, remains controversial (Meister, 2013), but likely involves different types of community interactions under normal marine, hypersaline, and alkaline conditions (Gallagher et al., 2014).

Marine stromatolites are microbial mats having repeating layers of precipitated micritic laminae produced through interaction of the microbial communities and the environment (Krumbein, 1983). In present day, they occur in only a few limited marine environments such as the Bahamas (Reid et al., 2000; Paerl et al., 2001) and Shark Bay in Western Australia (Goh et al., 2009). Studies extending for over a decade have examined present-day open-water, subtidal, marine stromatolites at Highborne Cay (Bahamas) and showed the surface microbial community consisted of several distinct mat stages (i.e., termed Types 1, 2, and 3), each having very different phenotypic characteristics (Reid et al., 2000). The EPS produced during these stages had very different properties and influenced the microbial communities within. In the Type 1 stage, the community exhibited "high growth." It consisted of dense cyanobacteria with high EPS production that grew (upward) quickly, consuming resources (Decho et al., 2005). The abundant EPS resulted in a "sticky" surface that trapped ooid grains (i.e., sediment) washing over the mats during high wave actions; a process that propagated the continued upward growth of the mat. The EPS contained ligands to chelate much of the available free Ca^{2+} ions. The net result was that EPS in the Type 1 mat inhibited $CaCO_3$ precipitation (Visscher et al., 2000). When a Type 1 mat transitions to a Type 2 mat, sulfate-reducing bacteria (SRB) increase in their relative abundances. EPS, initially produced by the cyanobacteria, are consumed by SRBs, then re-secreted as different EPS, a process which enhances localized precipitation (Visscher et al., 2000; Decho et al., 2005). Infared (FT-IR) spectral analyses of EPS extracted from the precipitate closely resembles those extracted from SRB mat isolates (Braissant et al., 2009). Notably, the EPS properties change in the Type 2 mat, becoming "less sticky." These studies illustrated how the EPS properties of the different mat could influence their properties and growth. The Type 2 mat resembles a classic microbial mat, with less EPS production (or accumulation), and little/no upward growth. The cyanobacteria, SRB, sulfur-oxidizing bacteria (SOB), and aerobic heterotrophs become spatially organized, and exhibit a closer metabolically coupling.

With rising levels of atmospheric CO_2, efforts are beginning to examine if certain carbonate-precipitating bacteria can be used to sequester (and store) CO_2 (Paul et al., 2017) and understand how microbial mat processes influence C storage (Bouton et al., 2016).

Sediment Stabilization and Fossil Evidence of Mats

Sediment fluxes in marine systems are affected by many parameters, including sediment grain sizes, physically cohesive muds, and biologically cohesive microbial extracellular polymers (Gerbersdorf et al., 2009; Grabowski et al., 2011). EPS concentrations in marine sediments vary considerably (Underwood et al., 1995, 2004). EPS, especially those from microphytobenthos (e.g., diatomaceous mats), are important in cohesive sediment stability, and resistance against erosion and resuspension (Grant and Gust, 1987; Paterson, 1989; Smith and Underwood, 1998, 2000; Tolhurst et al., 2002; Underwood and Paterson, 2003; Hanlon et al., 2006). Levels of EPS present in sediments can be a crucial variable to sediment stability (Malarkey et al., 2015). However, more EPS isn't always better. Interesting experimental studies by Paterson et al. (2008) showed that lower levels of EPS were more efficient in increasing erosional thresholds than abundant EPS conditions. While is well-established that the cohesive properties of EPS contribute to sediment stability, it is however not well-understood how the molecular-scale interactions of EPS themselves contribute to their cohesiveness (Paterson et al., 2008). Sediment-inhabiting small animals may indirectly influence sediment stability. For example, increased EPS production was shown to occur in the presence of a grazing nematode (Hubas et al., 2010). Initial studies suggest that QS (see above) may be involved in biofilm formation in certain diatoms (Yang et al., 2016) and offers the possibility that QS may contribute to the sediment stabilization process.

Finally, the very same bedform patterns that contribute to sediment stability in present-day sediments (e.g., ripples) also are considered as fossil evidences of sediment stabilization. These include patterns such as microbially induced sedimentary structures (MISSs), which are considered to be indirect fossil remnants that illustrate the very earliest vestiges of microbial mat life through geologic time (Noffke et al., 2001, 2013; Noffke, 2010).

ANIMAL–MICROBIAL INTERACTIONS AND FOOD-WEBS

Feeding Studies

It was realized early on that biofilms, and more-specifically their EPS, can represent a potentially labile carbon source for animals ingesting microbial cells (Decho, 1990). Since many small animals, present in both the water column and sediments of ocean systems, ingest microbial flora as a food source, they will coincidently ingest the closely associated EPS during the feeding process. Many invertebrate taxa are filter-feeders (i.e., straining suspended particles from the water) or deposit-feeders (i.e., ingesting sediments and their organics), therefore will consume microbial flora and their associated EPS as a food. Initial feeding experiments addressing EPS utilization by marine animals were conducted using EPS that were isolated from bacterial cultures grown in the presence of radioactively labeled (^{14}C) substrates. Once the EPS were separated from cells and residual label, EPS were mixed with sediments and fed to animals. Results indicated that EPS comprised a highly labile carbon food source. Examples of such studies involved copepods (Decho and Moriarty, 1990), polychaete worms (Decho and Lopez, 1993), bivalves (Harvey and Luoma, 1985), and sea stars (Hoskins et al., 2003). Biofilms are even known to be grazed upon by benthic foraminifera (Bernhard and Bowser, 1992).

Extracellular polymeric substance can act as a 'sorptive sponge.' This is due to their ability to bind metals, other ions, and even relatively hydrophobic organic contaminants such as pesticides, which is attributed to the presence of charged moieties (i.e., positive or negatively charged functional groups) or hydrophobic moieties. This can result in the efficient trophic-transfer of metals and pesticides to consumer animals that are ingesting EPS. Together, these moieties serve to sorb and/or trap, and concentrate environmental contaminants. When animals ingest the matrix, coincidentally during their feeding on sediments, cells or flocs, they will consume the sorbed metals and organics as well. EPS have been shown to be an efficient trophic-transfer vehicle for sorbed metals in amphipods (Schlekat et al., 1998, 1999, 2000; Selck et al., 1999), and organic compounds such as pesticides, although most of the latter work has even been conducted in freshwater systems (Widenfalk et al., 2008; Lundqvist et al., 2010, 2012).

Binding of Nanoparticles to EPS and Biofilms

In ocean systems, both natural (e.g., geological) processes and anthropogenic processes result in the generation of extremely small particulates called nanoparticles. Nanoparticles measure 1–100 nm in at least one dimension, and have different physicochemical properties than larger particles. In oceans, nanoparticles occur in the form of metal contaminants, organics, and even degraded plastics and potentially may have long water-column residence times owing to their small sizes. A number of studies are indicating that nanoparticles are efficiently concentrated by biofilms, and more specifically their EPS (Battin et al., 2009; Ferry et al., 2009; Fabrega et al., 2011; Nevius et al., 2012; Ikuma et al., 2014, 2015). Further studies have shown that nanoparticles are taken up by protozoans (Holbrook et al., 2008; Werlin et al., 2011; Mortimer et al., 2016). Finally, the bioavailability and bioaccumulation of nanoparticles occurs in marine (and freshwater) animals such as snails, bivalves and oligochaetes (for review, see Luoma et al., 2014), all of which coincidently ingest EPS during feeding processes. Therefore, EPS can work as a trophic transfer vehicle for nanoparticles to enter food webs.

EPS Capsules, Survival of Digestion, and the Gut Microbiome

Bacteria often possess EPS capsules surrounding their cells. The presence of capsules is a protective measure for the cells. Studies conducted by Plante and colleagues showed that encapsulated bacteria were less susceptible to digestion during detritivore- and deposit-feeding (Plante et al., 1990; Plante and Schriver, 1998; Plante, 2000). DePas et al. (2014) showed that protection is

afforded to biofilm bacteria during grazing by the nematode *Caenorhabditis elegans*.

Finally, one understudied aspect of trophic interactions regarding biofilms that is gaining attention involves the roles of resident gut bacteria in consumer animals (including humans). The presence of these bacteria, whose densities and activities may be quite substantial, is often facilitated by EPS capsules and biofilms. Gut bacteria are a source of many new genes, and the diversity and ecological principles driving these microbiomes will be an interesting future area of study (Dorosz et al., 2016).

The Larval Settlement Process and Biofouling

Virtually any type of surface, when placed in seawater becomes fouled with organisms ranging from bacteria to animals and algae; a process known as biofouling (Lewin, 1984). Bacteria and other microbes are generally the initial colonizing organisms of a surface. The presence of a bacterial biofilm often sets the stage for subsequent larval settlement (Tran and Hadfield, 2011). Understanding how biofilms interact with larval settlement is important to the broader biofouling process, which constitutes a costly ocean-engineering problem.

Studies in marine systems suggest that larval settlement is also a multistep process, which involves initial sensing of specific chemical cues, initial settlement and "tasting" of the surface, and finally more-permanent settlement. The initial sensing step of waterborne cues is a concentration-dependent process.

Presently, data suggest that in many cases, the larval settlement cues are molecules that are produced by adult conspecifics and are concentrated within the surface biofilm matrix or, in some cases, may be produced by the biofilms themselves (Unabia and Hadfield, 1999; Bao et al., 2007). Cue(s) can be multifunctional, acting as agonists, antagonists, or toxins (Ferrer and Zimmer, 2012; Guezennec et al., 2012). Behaviors and responses of larvae to cues are often species-dependent.

Settlement cues may be localized within the biofilm, and more-specifically by the EPS matrix. Diatom biofilms and the possible involvement of heat-stable settlement cues are involved in the settlement of the polychaete *Hydroides elegans* (Lam et al., 2003). *Hydroides* sp. are examples of the initial colonizers of open surfaces in warmer water regions. Once they are set, the complexity of colonizing species increases. Settlement cues may be produced by the biofilm itself but has been challenging to verify. The beneficial effect of a specific epibiotic bacterial biofilm on marine animal or plant hosts has been suggested (Holmström et al., 1992; Tran and Hadfield, 2011). Coralline red algae, for example, are highly inductive surfaces for the settlement of marine invertebrates, and are now realized to be strongly influenced by the surface microbial flora and their cues (Nielsen et al., 2015).

In contrast, the inhibition of larval settlement seems to be influenced by waterborne or biofilm-associated molecules. This is important to the potential control of biofouling. Early studies noted that many marine animals and macroalgae exhibit reduced biofouling, and suggested that chemical defenses may be involved (Holmström et al., 2002; Rao et al., 2007). More recently, studies have shown that specific chemical inhibitors can be produced by either the host organism (e.g., algae, animal) or by biofilm bacteria growing on the surface of the host (Lau and Qian, 2000). These have included both large and small molecules. In tunicates, proteins produced by biofilm bacteria inhibit further colonization by bacteria (Holmström et al., 1992). In a series of landmark studies, de Nys et al. (2009) showed the macroalga *Delissia pulchra*, was not subject to biofouling. This inhibition (of biofouling) operates by jamming the cell–cell chemical communication pathways of bacteria. As mentioned above, many gram-negative bacteria use AHLs in chemical communication. Release of specific AHL analogs, which are similar in molecular design can "jam" the QS pathway(s) of AHLs. Small halogenated furanones, resembling AHLs, interfered with chemical signaling in bacteria. An ecological function of antifouling molecules produced by plants and animals was postulated (and was tested) by Kjelleberg and colleagues (Franks et al., 2006). Harder et al. (2002) found large (>100 kDa) polysaccharide-containing molecules, produced by both a host macroalga (*Ulva* sp.) and *Vibrio* sp. bacteria, to inhibit larval settlement. These molecules act as a broad-spectrum inhibitor for settlement. This has touched off substantial exploration for chemically based inhibitors of biofouling in both nature and medicine by many laboratories. This infers the complex interaction in biofouling among host organisms, bacterial biofilms, and chemical cues. Since the biofouling of marine surfaces has both positive and negative effects to hatcheries, this area has an emerging impact on aquaculture processes (Joyce and Utting, 2015; Camacho-Chab et al., 2016). Finally, work is in progress to understand how climate change may affect processes such as larval settlement (Whalan and Webster, 2014).

EXTREME OCEAN ENVIRONMENTS

In extreme and fluctuating conditions, microbes surround themselves with EPS in an effort to add stability to their extracellular environment. The physiological plasticity of microbial cells, combined with their EPS-based adaptations allow microbial life to succeed at the boundaries of where other forms of life can survive.

Low-temperature Sea-ice Communities

In polar regions, metabolic processes are slowed by relatively cold temperatures. It is here that microbes also employ EPS to their advantage. Earlier, pioneering studies in Antarctic systems showed the presence of specific 'anti-freeze proteins' (i.e., glycoproteins) within the blood plasma of fish (Devries, 1971). The proteins would bind to ice crystals as they formed and prevent further growth of damaging ice crystals in the blood. This realization launched many subsequent studies of other organisms, including bacteria.

In Arctic and Antarctic systems, the presence of EPS play key roles as cryoprotectants, for attachment to sea-ice interfaces, and to survive enclosure in ice (Underwood et al., 2010, 2013). Studies of bacterial isolates from sea-ice systems have demonstrated that certain glycoproteins and exopolysaccharides

act as cryoprotectants, which inhibit ice crystal nucleation, in addition to securing the attachment of cells to the ice surface (Nichols C. A. et al., 2005; Nichols C. M. et al., 2005; Marx et al., 2009; Ewert and Deming, 2014). EPS and TEP become routinely embedded in sea-ice (Meiners et al., 2003; Collins et al., 2008) and contribute to the survival of microbial cells in these environments (Krembs et al., 2002, 2011; Liu et al., 2013; Boetius et al., 2015). EPS, including TEP can account for the majority of the carbon pool in sea-ice, which is later released during melting (Miller et al., 2011; Wurl et al., 2011), and can even make their way into atmospheric ice (Wilson et al., 2015).

High-temperature Hydrothermal Vents

Since their initial discovery in 1977, ocean hydrothermal vent systems have received much scientific attention. They are located near specific regions of the ocean spreading centers of tectonic plates, where geothermally heated fluids, enriched in minerals, hydrogen sulfide, ammonia and methane are released and mix with much colder surrounding seawater. Mineral deposits form as chimneys, and are surrounded by islands of intense biological activity, where chemosynthetic bacteria and archaea form the base of a food web having a diversity of often unique animals (Tunnicliffe, 1991). For these reasons, they have been considered as a possible site for the origin of life on Earth, and as an analog for study in the exploration for possible life elsewhere.

Isolates of bacteria from vent systems demonstrate the capacity for abundant EPS production, perhaps to sequester dissolved minerals and other metals from the surrounding water (Raguénès et al., 1997a,b; Guezennec et al., 1998; Rougeaux et al., 1999, 2001; Guezennec, 2002). EPS, derived from isolate cultures, typically have uronic acid contents as high as 40%, and relatively high molecular masses (Guezennec, 2002). It is not yet understood, however, how the EPS may influence the microenvironment of the bacteria and archaea, in terms of *e*-enzymes, 3D-microspatial development of their communities, and microspatial acidification (to solubilize metal ions). It is not known if the EPS matrix facilitates these processes, and actually may serve to inhibit their precipitation, similarly to those in some shallow-water carbonate environments?

Hypersaline Environments and Desiccation

Hypersaline systems, such as salt ponds, salterns, and hypersaline lagoons, contain well-developed microbial mats. Many of these systems occur in proximity or directly connected to ocean systems, while others are inland. Examples of hypersaline systems are numerous and a few include Salt Pond, San Salvador, Bahamas (Pinckney and Paerl, 1997); Guerrero Negro, Baha California Sur, Mexico (Ley et al., 2006); Laguna Tebenquiche, Salar de Atama, Chile (Fernandez et al., 2016); Don Juan Pond [McMurdo Dry Valleys, Antarctica (Dickson et al., 2013)]; Dead Sea (Oren, 1994); Solar Lake, Sinai, Egypt (Teske et al., 1998); Hamelin Pool, Shark Bay, Western Australia (Goh et al., 2009); Polynesian islands (Rougeaux et al., 2001; Richert et al., 2005; Moppert et al., 2009).

The hypersaline environment presents unique challenges to microorganisms, especially in terms of fluctuations in ion concentrations and osmolarity. In addition, many hypersaline mats are exposed to intermittent and/or progressive desiccation. A lack of available water, during the desiccation process, can kill a bacterial cell, largely through denaturation of proteins and destabilization of cell membranes (see Potts, 1994, for review). EPS are an abundant component of such mats (Benninghoff et al., 2016), and likely provide a degree of protection to mat microbial flora against ion fluctuations and desiccation (Potts, 1994; Shaw et al., 2003; Decho, 2016). Interestingly, studies have shown that bacteria can survive in a desiccated state in salt crystal for 250 my (Vreeland et al., 2000).

In hypersaline mats, EPS occur in the form of capsules surrounding individual cells, or a larger EPS matrix surrounding many cells in a biofilm, which can buffer cells against either dessication or rapid changes in water potential. Salinities in hypersaline ponds are often >300 g/L (e.g., seawater is approximately 32 g/L), but can reach as high as 440 g/L, often with concentrations of individual ions not matching those observed for typical seawater. Here, mat communities often experience extended periods (i.e., days to months) of desiccation that often is followed by a rapid rehydration due to seasonal rain events.

Selective saltation also plays a role in the ability of mats to cope with increasing salinities. This allows less-soluble minerals to be removed from solution, as a function of concentration. The evaporation process that occurs throughout the dry season serves to increase ionic concentrations and promotes the selective precipitation of salts on the mat surface. As ionic concentrations increase, there is a sequential salting-out occurring of less-soluble minerals. For example, much of the Ca^{2+} is typically removed as gypsum ($CaSO_4$ $2H_2O$) or smaller amounts of calcite ($CaCO_3$). Gypsum begins to precipitate when salinity concentrations reach about 160 ppt. At very high ionic concentrations (>300 ppt) NaCl begins to precipitate.

Some EPS may condense with increasing salinity, and even form a hydrophobic barrier on the surface of the biofilm. This may result in enhanced protection during subsequent desiccation. It has been proposed that the exclusion of ions occurs via the EPS matrix in response to increasing salinity, which is designed to reduce osmotic stress and conserve water within the mat (Decho, 2016). Desiccation is a process occurring in many areas of marine environments. On the fringes of ocean systems, specifically on the upper reaches of rocky intertidal zones, intermittent desiccation is a common process. The roles of EPS in stabilizing microbial communities require further investigation.

SUMMARY: EPS RESEARCH LOOKING FORWARD

The growing awareness of microbial EPS and their influences on ocean processes are evidenced in this special issue and offers many avenues for future research. It is emphasized here that the

secretion of EPS is an adaptive response employed by microbes to enhance their metabolic efficiency and survival. An extensive literature on EPS and biofilms that is available in other areas of microbiology may have relevance to ocean studies.

Finally, there were many aspects of EPS that were not covered in this relatively short overview, but are important to understanding the dynamics of microbial extracellular biology. For example, we have not addressed: (1) EPS as electron-transfer vehicles; (2) the concentration of viruses; (3) molecular pathways of EPS secretion; and (4) the roles of biofilms in the search for life elsewhere. In addition, we anticipate that the roles of EPS in ocean systems will be integrated into the fundamental microbiology of the ocean, and into larger-scale topics such as global climate change, biotechnological applications of EPS, and the search for novel antibiotics and other medicinal compounds.

AUTHOR CONTRIBUTIONS

All authors listed, have made substantial, direct and intellectual contribution to the work, and approved it for publication.

ACKNOWLEDGMENTS

The authors wish to thank the many colleagues and collaborators, whose in-depth discussions have initially fueled, productively challenged and gradually refined many of the ideas put forth here. This work was supported, in part, by grants from the U.S. National Science Foundation to AD: Collaborative Research in Chemistry (CRC-0526821), Environmental Genomics (En-Gen-0723707) and BioMaterials (DMR-1608151) Programs.

REFERENCES

Aldeek, F., Schneider, R., Fontaine-Aupart, M. P., Mustin, C., Lécart, S., Merlin, C., et al. (2013). Patterned hydrophobic domains in the exopolymer matrix of *Shewanella oneidensis* MR-1 biofilms. *Appl. Environ. Microbiol.* 79, 1400–1402. doi: 10.1128/AEM.03054-12

Alldredge, A. L., and Cohen, Y. (1987). Can microscale chemical patches persist in the sea? Microelectrode study of marine snow, fecal pellets. *Science* 235, 689–691. doi: 10.1126/science.235.4789.689

Alldredge, A. L., Cole, J. J., and Caron, D. A. (1986). Production of heterotrophic bacteria inhabiting macroscopic organic aggregates (marine snow) from surface waters. *Limnol. Oceanogr.* 31, 68–78. doi: 10.4319/lo.1986.31.1.0068

Alldredge, A. L., Passow, U., and Logan, B. E. (1993). The abundance and significance of a class of large, transparent organic particles in the ocean. *Deep Sea Res.* 40, 1131–1140. doi: 10.1016/0967-0637(93)90129-Q

Alldredge, A. L., and Silver, M. W. (1988). Characteristics, dynamics and significance of marine snow. *Prog. Oceanogr.* 20, 41–82. doi: 10.1016/0079-6611(88)90053-5

Allwood, A. C., Walter, M. R., Burch, I. W., and Kamber, B. S. (2007). 3.43 billion-year-old stromatolite reef from the Pilbara Craton of Western Australia: ecosystem-scale insights to early life on Earth. *Precambr. Res.* 158, 198–227. doi: 10.1016/j.precamres.2007.04.013

Aluwihare, L. I., Repeta, D. J., and Chen, R. F. (1997). A major biopolymeric component of dissolved organic carbon in surface seawater. *Nature* 387, 166–169. doi: 10.1038/387166a0

Amin, S. A., Hmelo, L. R., van Tol, H. M., Durham, B. P., Carlson, L. T., Heal, K. R., et al. (2015). Interaction and signaling between a cosmopolitan phytoplankton and associated bacteria. *Nature* 522, 98–101. doi: 10.1038/nature14488

Amon, R. M. W., and Benner, R. (1994). Rapid cycling of high-molecular-weight dissolved organic matter in the ocean. *Nature* 369, 549–552. doi: 10.1038/369549a0

Amon, R. M. W., and Benner, R. (1996). Bacterial utilization of different size classes of dissolved organic matter. *Limnol. Oceanogr.* 41, 41–51. doi: 10.4319/lo.1996.41.1.0041

Anton, J., Meseguer, I., and Rodriguezvalera, F. (1988). Production of an extracellular polysaccharide by *Haloferax-mediterranei*. *Appl. Environ. Microbiol.* 54, 2381–2386.

Arnosti, C., Ziervogel, K., Yang, T., and Teske, A. (2015). Oil-derived marine aggregates – hot spots of polysaccharide degradation by specialized bacterial communities. *Deep Sea Res. II* 129, 179–186. doi: 10.1016/j.dsr2.2014.12.008

Arp, G., Reimer, A., and Reitner, J. (2001). Photosynthesis-induced biofilm calcification and calcium concentration in Phanerozoic oceans. *Science* 292, 1701–1704. doi: 10.1126/science.1057204

Arp, G., Reimer, A., and Reitner, J. (2003). Microbialite formation in seawater of increased alkalinity, Satonda Crater Lake, Indonesia. *J. Sed. Res.* 73, 105–127. doi: 10.1306/071002730105

Azam, F., and Long, R. A. (2001). Oceanography – Sea snow microcosms. *Nature* 414, 495–498. doi: 10.1038/35107174

Baelum, J., Borglin, S., Chakraborty, R., Fortney, J. L., Lamendella, R., Mason, O. U., et al. (2012). Deep-sea bacteria enriched by oil and dispersant from the Deepwater Horizon spill. *Environ. Microbiol.* 14, 2405–2416. doi: 10.1111/j.1462-2920.2012.02780.x

Bao, W.-Y., Satuito, C. G., Yang, J.-L., and Kitamura, H. (2007). Larval settlement and metamorphosis of the mussel *Mytilus galloprovincialis* in response to biofilms. *Mar. Biol.* 150, 565–574. doi: 10.1007/s00227-006-0383-4

Barnhart, M. M., and Chapman, M. R. (2006). Curli biogenesis and function. *Annu. Revs. Microbiol.* 60, 131–147. doi: 10.1146/annurev.micro.60.080805.142106

Battin, T. J., von der Kammer, F., Weilhartner, A., Ottofuelling, S., and Hofmann, T. (2009). Nanostructured TiO2: transport behavior and effects on aquatic microbial communities under environmental conditions. *Environ. Sci. Technol.* 43, 8098–8104. doi: 10.1021/es9017046

Bauer, J. E., Druffel, E. R. M., Wolgast, D. M., and Griffin, S. (2002). Temporal and regional variability in sources and cycling of DOC and POC in the northwest Atlantic continental shelf and slope. *Deep Sea Res. II* 49, 4387–4419. doi: 10.1016/S0967-0645(02)00123-6

Baumgartner, L. K., Reid, R. P., Dupraz, C., Decho, A. W., Buckley, D. H., Spear, J. R., et al. (2006). Sulfate reducing bacteria in microbial mats: changing paradigms, new discoveries. *Sed. Geol.* 185, 131–145. doi: 10.1016/j.sedgeo.2005.12.008

Beech, I. B., and Cheung, C. W. S. (1995). Interactions of EPS produced by sulphate-reducing bacteria with metal ions. *Int. Biodeter. Biodegrad.* 35, 59–72. doi: 10.1016/0964-8305(95)00082-G

Bejar, V., Calvo, C., Moliz, J., Diaz-Martinez, F., and Quesada, E. (1996). Effect of growth conditions on the rheological properties and chemical composition of *Volcaniella eurihalina* exopolysaccharide. *Appl. Biochem. Biotechnol.* 59, 77–86. doi: 10.1007/BF02787859

Benner, R. (2002). "Chemical composition and reactivity," in *Biogeochemistry of Marine Dissolved Organic Matter*, eds D. A. Hansell and C. A. Carslon (San Diego, CA: Academic Press), 59–90. doi: 10.1146/annurev-marine-010213-135126

Benner, R., and Amon, R. M. W. (2015). The size-reactivity continuum of major bioelements in the ocean. *Annu. Rev. Mar. Sci.* 7, 185–205. doi: 10.1146/annurev-marine-010213-135126

Benner, R., Pakulski, J. D., McCarthy, M., Hedges, J. I., and Hatcher, P. G. (1992). Bulk chemical characteristics of dissolved organic matter in the ocean. *Science* 255, 1561–1564. doi: 10.1126/science.255.5051.1561

Benninghoff, J. C., Wingender, J., Flemming, H.-C., and Siebers, B. (2016). "Biofilms X-treme: composition of extracellular polymeric substances in Archaea," in *The Perfect Slime -Microbial Extracellular Polymeric Substances (EPS)*, eds H.-C. Flemming, T. R. Neu, and J. Wingender (London: IWA Publishers), 301–317.

Benzerara, K., Menguy, N., Lopez-Garcia, P., Yoon, T.-H., Kazmierczak, J., Typiszczak, T., et al. (2006). Nanoscale detection of organic signatures

in carbonate microbialites. *Proc. Natl. Acad. Sci. U.S.A.* 103, 9440–9445. doi: 10.1073/pnas.0603255103

Bernhard, J. M., and Bowser, S. S. (1992). Bacterial biofilms as a trophic resource for certain benthic foraminifera. *Mar. Ecol. Prog. Ser.* 83, 263–272. doi: 10.3354/meps083263

Bhaskar, P. V., and Bhosle, N. B. (2005). Microbial extracellular polymeric substances in marine biogeochemical processes. *Curr. Sci.* 88, 45–53.

Bhaskar, P. V., and Bhosle, N. B. (2006). Bacterial extracellular poly- meric substances (EPS): a carrier of heavy metals in the marine food-chain. *Environ. Int.* 32, 191–198. doi: 10.1016/j.envint.2005.08.010

Bianchi, M., Marty, D., Teyssié, J. L., and Fowler, S. W. (1992). Strictly aerobic and anaerobic bacteria associated with sinking particulate matter and zooplankton fecal pellets. *Mar. Ecol. Prog. Ser.* 88, 55–60. doi: 10.3354/meps088055

Biermann, C. J. (1988). Hydrolysis and other cleavages of glycosidic linkages in polysaccharides. *Adv. Carbohydr. Chem. Biochem.* 46, 251–271. doi: 10.1016/S0065-2318(08)60168-7

Bigg, E. K. (2007). Sources, nature, and influence on climate of marine airborne particulates. *Environ. Chem.* 4, 155–161. doi: 10.1071/EN07001

Bigg, E. K., and Leck, C. (2008). The composition of fragments of bubbles bursting at the ocean surface. *J. Geophys. Res.* 113, D11209. doi: 10.1029/2007jd009078

Biller, S. J., Schubotz, F., Roggensack, S. E., Thompson, A. W., Summons, R. E., and Chisholm, S. W. (2014). Bacterial vesicles in marine ecosystems. *Science* 343, 183–186. doi: 10.1126/science.1243457

Böckelmann, U., Janke, A., Kuhn, R., Neu, T. R., Wecke, J., Lawrence, J. R., et al. (2005). Bacterial extracellular DNA forming a defined network-like structure. *FEMS Microbiol. Lett.* 262, 31–38. doi: 10.1111/j.1574-6968.2006.00361.x

Boehm, P. D., and Fiest, D. L. (1980). "Aspects of the transport of petroleum hydrocarbons to the offshore benthos during the Ixtoc-I blowout in the Bay of Campeche," in *Proceedings of the Symposium on the Preliminary Results from the September, 1979 Pierce/Research IXTOC-1Cruises*, (Boulder, CO: NOAA).

Boetius, A., Anesio, A. M., Deming, J. W., Mikucki, J. A., and Rapp, J. Z. (2015). Microbial ecology of the cryosphere: sea ice and glacial habitats. *Nat. Revs. Microbiol.* 13, 677–690. doi: 10.1038/nrmicro3522

Bouton, A., Vennin, E., Boulle, J., Pace, A., Bourillot, R., Thomazo, C., et al. (2016). Linking the distribution of microbial deposits from the Great Salt Lake (Utah, USA) to tectonic and climatic processes. *Biogeosciences* 13, 5511–5526. doi: 10.5194/bg-13-5511-2016

Boyd, P. W., Jickells, T., Law, C. S., Blain, S., Boyle, E. A., Buesseler, K. O., et al. (2007). Mesoscale iron enrichment experiments 1993–2005: synthesis and future directions. *Science* 315, 612–617. doi: 10.1126/science.1131669

Braissant, O., Cailleau, G., Dupraz, C., and Verrechia, E. P. (2003). Bacterially induced mineralization of calcium carbonate in terrestrial environments: the role of exopolysaccharides and amino acids. *J. Sed. Res.* 73, 485–490. doi: 10.1306/111302730485

Braissant, O., Decho, A. W., Dupraz, C., Glunk, C., Przekop, K. M., and Visscher, P. T. (2007). Exopolymeric substances of sulfate-reducing bacteria: Interactions with calcium at alkaline pH and implication for formation of carbonate minerals. *Geobiology* 5, 401–411. doi: 10.1111/j.1472-4669.2007.00117.x

Braissant, O., Decho, A. W., Przekop, K. M., Gallagher, K. L., Glunk, C., Dupraz, C., et al. (2009). Characteristics and turnover of exopolymeric substances in a hypersaline microbial mat. *FEMS Microbiol. Ecol.* 67, 293–307. doi: 10.1111/j.1574-6941.2008.00614.x

Brogioli, D., and Vailati, A. (2001). Diffusive mass transfer by non-equilibrium fluctuations: Fick's Law revisited. *Phys. Revs.* 63:012105. doi: 10.1103/PhysRevE.63.012105

Brussaard, C. P. D., Bidle, K. D., Pedrós-Alió, C., and Legrand, C. (2016). The interactive microbial ocean. *Nat. Microbiol.* 2:16255. doi: 10.1038/nmicrobiol.2016.255

Burne, R. V., and Moore, L. S. (1987). Microbialites: organosedimentary deposits of benthic microbial communities. *Palaios* 2, 241–254. doi: 10.2307/3514674

Camacho-Chab, J. C., Lango-Reynoso, F., del Refugio Castañeda-Chávez, M., Galaviz-Villa, I., Hinojosa-Garro, D., and Ortega-Morales, B. O. (2016). Implications of extracellular polymeric substance matrices of microbial habitats associated with coastal aquaculture systems. *Water* 8:369. doi: 10.3390/w8090369

Camilli, A., and Bassler, B. L. (2006). Bacterial small-molecule signaling pathways. *Science* 311, 1113–1116. doi: 10.1126/science.1121357

Carlson, C. A., Ducklow, H. W., and Michaels, A. F. (1994). Annual flux of dissolved organic carbon from the euphotic zone in the northwestern Sargasso Sea. *Nature* 371, 405–408. doi: 10.1038/371405a0

Carlson, C. A., Giovannoni, S. J., Hansell, D. A., Goldberg, S. J., Parsons, R., and Vergin, K. (2004). Interactions among dissolved organic carbon, microbial processes, and community structure in the mesopelagic zone of the northwestern Sargasso Sea. *Limnol. Oceanogr.* 49, 1073–1083. doi: 10.4319/lo.2004.49.4.1073

Caron, D. A., Lim, E. L., Sanders, R. W., Dennett, M. R., and Berninger, U. G. (2000). Responses of bacterioplankton and phytoplankton to organic carbon and inorganic nutrient additions in contrasting oceanic ecosystems. *Aquat. Microbiol. Ecol.* 22, 175–184. doi: 10.3354/ame022175

Chagas, A. A. P., Webb, G. E., Burne, R. V., and Southam, G. (2016). Modern lacustrine microbialites: toward a synthesis of aqueous and carbonate geochemistry and mineralogy. *Earth Sci. Revs.* 162, 338–363. doi: 10.1016/j.earscirev.2016.09.012

Chew, S. C., Kundukad, B., Seviour, T., van der Maarel, J. R. C., Yang, L., Rice, S. A., et al. (2014). Dynamic remodeling of microbial biofilms by functionally distinct exopolysaccharides. *MBio* 5:e1536-14. doi: 10.1128/mBio.01536-14

Chin, W.-C., Orellana, M. V., and Verdugo, P. (1998). Spontaneous assembly of marine dissolved organic matter into polymer gels. *Nature* 391, 568–572. doi: 10.1038/35345

Church, M. J. (2008). "Resource control of bacterial dynamics in the sea," in *Microbial Ecology of the Oceans*, 2nd Edn, ed. D. L. Kirchman (Hoboken, NJ: John Wiley & Sons, Inc).

Churchill, M. E. A., and Chen, L. (2011). Structural basis of acyl-homoserine lactone-dependent signaling. *Chem. Rev.* 111, 68–85. doi: 10.1021/cr1000817

Collins, R. E., Carpenter, S. D., and Deming, J. W. (2008). Spatial heterogeneity and temporal dynamics of particles, bacteria, and pEPS in Arctic winter sea ice. *J. Mar. Syst.* 74, 902–917. doi: 10.1016/j.jmarsys.2007.09.005

Costerton, J. W., Cheng, K. J., Geesey, G. G., Ladd, T. I., Nickel, J. C., Dasgupta, M., et al. (1987). Bacterial biofilms in nature and disease. *Annu. Rev. Microbiol.* 41, 435–464. doi: 10.1146/annurev.mi.41.100187.002251

Cotner, J. B., Ammerman, J. W., Peele, E. R., and Bentzen, E. (1997). Phosphorus-limited bacterioplankton growth in the Sargasso Sea. *Aquat. Microbiol. Ecol.* 13, 141–149. doi: 10.3354/ame013141

Daly, K. L., Passow, U., Chanton, J., and Hollander, D. (2016). Assessing the impacts of oil-associated marine snow formation and sedimentation during and after the Deepwater Horizon oil spill. *Anthropocene* 13, 18–33. doi: 10.1016/j.ancene.2016.01.006

Davies, J., Spiegelman, G. B., and Grace, Y. (2006). The world of subinhibitory antibiotic concentrations. *Curr. Opin. Microbiol.* 9, 445–453. doi: 10.1016/j.mib.2006.08.006

De Beer, D., Stoodley, P., Roe, F., and Lewandowski, Z. (2004). Effects of biofilm structure on oxygen distribution and mass transport. *Biotechnol. Bioeng.* 43, 1131–1133. doi: 10.1002/bit.260431118

De Jong, E., van Rens, L., Westbroek, P., and Bosch, L. (1979). Biocalcification by the marine alga *Emiliania huxleyi* (Lohmann) Kamptner. *Eur. J. Biochem.* 99, 559–567. doi: 10.1111/j.1432-1033.1979.tb13288.x

de Nys, R., Steinberg, P. D., Willemsen, P., Dworjanyn, S. A., Gabelish, C. L., and King, R. J. (2009). Broad spectrum effects of secondary metabolites from the red alga *Delisea pulchra* in antifouling assays. *Biofouling* 8, 259–271. doi: 10.1080/08927019509378279

Decho, A. W. (1990). Microbial exopolymer secretions in ocean environments: their role(s) in food webs and marine processes. *Oceanogr. Mar. Biol. Ann. Rev.* 28, 73–153.

Decho, A. W. (1999). Imaging an alginate polymer gel matrix using atomic force microscopy. *Carbohydr. Res.* 315, 330–333. doi: 10.1016/S0008-6215(99)00006-3

Decho, A. W. (2000a). "Exopolymer microdomains as a structuring agent for heterogeneity with microbial biofilms," in *Microbial Sediments*, eds R. E. Riding and S. M. Awramik (Berlin: Springer-Verlag Press), 9–15.

Decho, A. W. (2000b). Microbial biofilms in intertidal systems: an overview. *Cont. Shelf Res.* 20, 1257–1273. doi: 10.1016/S0278-4343(00)00022-4

Decho, A. W. (2010). Overview of biopolymer-induced mineralization: what goes on in biofilms? *Ecol. Eng.* 36, 137–144. doi: 10.1016/j.ecoleng.2009.01.003

Decho, A. W. (2015). "Localization of quorum sensing by extracellular polymeric substances (EPS): considerations of *in situ* signaling," in *The Physical Basis of Bacterial Quorum Communication*, ed. S. J. Hagen (New York, NY: Springer), doi: 10.1007/978-1-4939-1402-9_6

Decho, A. W. (2016). "Unique and baffling aspects of the matrix: EPS syneresis and glass formation during desiccation," in *The Perfect Slime*, eds H.-C. Flemming, T. R. Neu, and J. Wingender (London: IWA Publishing), 207–226. doi: 10.2166/9781780407418

Decho, A. W., Frey, R. L., and Ferry, J. L. (2011). Chemical challenges to bacterial AHL signaling in the environment. *Chem. Rev.* 111, 86–99. doi: 10.1021/cr100311q

Decho, A. W., Kawaguchi, T., Allison, M. A., Louchard, E. M., Reid, R. P., Stephens, C., et al. (2003). Sediment properties influencing upwelling spectral reflectance signatures: the "biofilm gel effect". *Limnol. Oceanogr.* 48, 431–443. doi: 10.4319/lo.2003.48.1_part_2.0431

Decho, A. W., and Lopez, G. R. (1993). Exopolymer microenvironments of microbial flora: multiple and interactive effects on trophic relationships. *Limnol. Oceanogr.* 38, 1633–1645. doi: 10.4319/lo.1993.38.8.1633

Decho, A. W., and Moriarty, D. J. W. (1990). Bacterial exopolymer utilization by a harpacticoid copepod: a methodology and results. *Limnol. Oceanogr.* 35, 1039–1049. doi: 10.4319/lo.1990.35.5.1039

Decho, A. W., Norman, R. S., and Visscher, P. T. (2010). Quorum sensing in natural environmental: emerging views from microbial mats. *Trends Microbiol.* 18, 73–80. doi: 10.1016/j.tim.2009.12.008

Decho, A. W., Visscher, P. T., Ferry, J., Kawaguchi, T., He, L., Przekop, K. M., et al. (2009). Autoinducers extracted from microbial mats reveal a surprising diversity of N-acylhomoserine lactones (AHLs) and abundance changes that may relate to diel pH. *Environ. Microbiol.* 11, 409–420. doi: 10.1111/j.1462-2920.2008.01780.x

Decho, A. W., Visscher, P. T., and Reid, R. P. (2005). Production and cycling of natural microbial EPS (EPS) within a marine stromatolite. *Palaeogeogr. Palaeoclimat. Palaeoecol.* 219, 71–86. doi: 10.1016/j.palaeo.2004.10.015

Dell'Anno, A., and Corinaldesi, C. (2004). Degradation and turnover of extracellular DNA in marine sediments: ecological and methodological considerations. *Appl. Environ. Microbiol.* 70, 4384–4386. doi: 10.1128/AEM.70.7.4384-4386.2004

Dell'Anno, A., and Danovaro, R. (2005). Extracellular DNA plays a role in deep-sea ecosystem functioning. *Science* 309, 2179. doi: 10.1126/science.1117475

DeLong, E. F., Franks, D. G., and Alldredge, A. L. (1993). Phylogenetic diversity of aggregate-attached vs. free-living marine bacterial assemblages. *Limnol. Oceanogr.* 38, 924–934. doi: 10.4319/lo.1993.38.5.0924

DePas, W. H., Syed, A. K., Sifuentes, M., Lee, J. S., Warshaw, D., Saggar, V., et al. (2014). Biofilm formation protects *Escherichia coli* against killing by *Caenorhabditis elegans* and *Myxococcus xanthus*. *Appl. Environ. Microb.* 80, 7079–7087. doi: 10.1128/AEM.02464-14

Des Marais, D. J. (2003). Biogeochemistry of hypersaline microbial mats illustrates the dynamics of modern microbial ecosystems and the early evolution of the biosphere. *Biol. Bull.* 204, 160–167. doi: 10.2307/1543552

Deschatre, M., Ghillebaert, F., Guezennec, J., and Colin, C. S. (2013). Sorption of copper(II) and silver(1) by four bacterial exopolysaccharides. *Appl. Biochem. Biotechnol.* 171, 1313–1327. doi: 10.1007/s12010-013-0343-7

Devries, A. L. (1971). Glycoproteins as biological antifreeze agents in antarctic fishes. *Science* 172, 1152–1155. doi: 10.1126/science.172.3988.1152

Dickson, J. L., Head, J. W., Levy, J. S., and Marchant, D. R. (2013). Don Juan Pond, Antarctica: near-surface CaCl2-brine feeding Earth's most saline lake and implications for Mars. *Sci. Rep.* 3:1166. doi: 10.1038/srep01166

Dohnalkova, A. C., Marshall, M. J., Arey, B. W., Williams, K. H., Buck, E. C., and Fredrickson, J. K. (2011). Imaging hydrated microbial extracellular polymers: comparative analysis by electron microscopy. *Appl. Environ. Microbiol.* 77, 1254–1262. doi: 10.1128/AEM.02001-10

Dorosz, J. N. A., Castro-Mejia, J. L., Hansen, L. H., Nielsen, D. S., and Skovgaard, A. (2016). Different microbiomes associated with the copepods *Acartia tonsa* and *Temora longicornis* from the same marine environment. *Aquat. Microb. Ecol.* 78, 1–9. doi: 10.3354/ame01799

Drake, L. A., Doblin, M. A., and Dobbs, F. C. (2007). Potential microbial bioinvasions via ships' ballast water, sediment, and biofilm. *Mar. Poll. Bull.* 55, 333–341. doi: 10.1016/j.marpolbul.2006.11.007

Dupraz, C., Fowler, A., Tobias, C., and Visscher, P. T. (2013). Stomatolitic knobs in Storr's Lake (San Salvador, Bahamas): a model system for formation and alteration of laminae. *Geobiology* 11, 527–548. doi: 10.1111/gbi.12063

Dupraz, C., Reid, R. P., Braissant, O., Decho, A. W., Norman, R. S., and Visscher, P. T. (2009). Processes of carbonate precipitation in modern microbial mats. *Earth Sci. Revs.* 96, 141–162. doi: 10.1016/j.earscirev.2008.10.005

Dupraz, C., and Visscher, P. T. (2005). Microbial lithification in marine stromatolites and hypersaline mats. *Trends Microbiol.* 13, 429–438. doi: 10.1016/j.tim.2005.07.008

Dupraz, C., Visscher, P. T., Baumgartner, L. K., and Reid, R. P. (2004). Microbe-mineral interactions: early carbonate precipitation in a hypersaline lake (Eleuthera Island, Bahamas). *Sedimentology* 51, 745–765. doi: 10.1111/j.1365-3091.2004.00649.x

Dupuy, C., Mallet, C., Guizien, K., Montanié, H., Bréret, M., Mornet, F., et al. (2014). Sequential resuspension of biofilm components (Viruses, prokaryotes and protists) as measured by erodimetry experiments in the Brouage mudflat (French Atlantic coast). *J. Sea Res.* 92, 56–65. doi: 10.1016/j.seares.2013.12.002

Elhanawy, W., Debelyy, M. O., and Feldman, M. F. (2014). Preferential packing of acidic glycosidases and proteases into bacteriodes outer membrane vesicles. *mBio* 5:e00909-14. doi: 10.1128/mBio.00909-14

Engel, A., and Passow, U. (2001). Carbon and nitrogen content of transparent exopolymer particles (TEP) in relation to their Alcian Blue adsorption. *Mar. Ecol. Progr. Ser.* 219, 1–10. doi: 10.3354/meps219001

Engel, A., Thoms, S., Riebesell, U., Rochelle-Newall, E., and Zondervan, I. (2004). Polysaccharide aggregation as a potential sink of marine dissolved organic carbon. *Nature* 428, 929–932. doi: 10.1038/nature02453

Ewert, M., and Deming, J. W. (2014). Bacterial responses to fluctuations and extremes in temperature and brine salinity at the surface of Arctic winter sea ice. *FEMS Microbiol. Ecol.* 89, 476–489. doi: 10.1111/1574-6941.12363

Fabbri, S., and Stoodley, P. (2016). "Mechanical properties of biofilms," in *The Perfect Slime*, eds H.-C. Flemming, T. R. Neu, and J. Wingender (London: IWA Publishing), 153–177. doi: 10.2166/9781780407418

Fabrega, J., Zhang, R., Renshaw, J. C., Liu, W.-T., and Lead, J. R. (2011). Impact of silver nanoparticles on natural marine biofilm bacteria. *Chemosphere* 85, 961–966. doi: 10.1016/j.chemosphere.2011.06.066

Facchini, M. C., Rinaldi, M., Decesari, S., Carbone, C., Finessi, E., Mircea, M., et al. (2008). Primary submicron marine aerosol dominated by insoluble organic colloids and aggregates. *Geophys. Res. Lett.* 35, L17814. doi: 10.1029/2008gl034210

Fandrich, M. (2007). On the structural definition of amyloid fibrils and other polypeptide aggregates. *Cell. Mol. Life Sci.* 64, 2066–2078. doi: 10.1007/s00018-007-7110-2

Fernandez, A. B., Rasuk, M. C., Visscher, P. T., Contreras, M., Novoa, F., Poire, D. G., et al. (2016). Microbial diversity in sediment ecosystems (evaporate domes, microbial mats and crusts) of hypersaline Laguna Tebenquiche, Salar de Atama, Chile. *Front. Microbiol.* 7:1284. doi: 10.3389/fmicb.2016.01284

Ferrer, R. P., and Zimmer, R. K. (2012). Community ecology and the evolution of molecules of keystone significance. *Biol. Bull.* 223, 167–177. doi: 10.1086/BBLv223n2p167

Ferry, J. L., Craig, P., Hexel, C., Sisco, P., Frey, R., Pennington, P. L., et al. (2009). Transfer of gold nanoparticles from the water column to the estuarine food web. *Nat. Nanotechnol.* 4, 441–444. doi: 10.1038/nnano.2009.157

Flemming, H.-C. (2016). "The perfect slime – and the 'dark matter' of biofilms," in *The Perfect Slime: Microbial Extracellular Polymeric Substances (EPS)*, eds H.-C. Flemming, T. R. Neu, and J. Wingender (London: IWA Publishers), 1–14. doi: 10.2166/9781780407418

Flemming, H. C., Neu, T. R., and Wozniak, D. (2007). The EPS matrix: The house of biofilm cells. *J. Bacteriol.* 189, 7945–7947. doi: 10.1128/JB.00858-07

Flemming, H. C., and Wingender, J. (2010). The biofilm matrix. *Nat. Rev. Microbiol.* 8, 623–633. doi: 10.1038/nrmicro2415

Flemming, H.-C., Wingender, J., Kjelleberg, S., Steinberg, P., Rice, S., and Szewzyk, U. (2016). Biofilms: an emergent form of microbial life. *Nat. Rev. Microbiol.* 14, 563–575. doi: 10.1038/nrmicro.2016.94

Fong, J. N. C., and Yildiz, F. H. (2015). Biofilm matrix proteins. *Microbiol. Spectr.* 3. doi: 10.1128/microbiolspec.MB-0004-2014

Ford, T., Sacco, E., Black, J., Kelley, T., Goodacre, R. C., and Berkeley, R. C. W. (1991). Characterization of EPS of aquatic bacteria by pyrolysis-mass spectrometry. *Appl. Environ. Microbiol.* 57, 1595–1601.

Franks, A., Egan, S., Holmstrom, C., James, S., Lappin-Scott, H., and Kjelleberg, S. (2006). Inhibition of fungal colonization by *Pseudoalteromonas tunicata* provides a competitive advantage during surface colonization. *Appl. Environ. Microbiol.* 72, 6079–6087. doi: 10.1128/AEM.00559-06

Franks, J., and Stolz, J. F. (2009). Flat laminated microbial mat communities. *Earth Sci. Rev.* 96, 163–172. doi: 10.1016/j.earscirev.2008.10.004

Frey, R. L., He, L., Cui, Y., Decho, A. W., Kawaguchi, T., Ferguson, P. L., et al. (2010). Reaction of N-acylhomoserine lactones with hydroxyl radicals: rates, products, and effects on signaling activity. *Environ. Sci. Technol.* 44, 7465–7469. doi: 10.1021/es100663e

Fu, J., Gong, Y., Zhao, X., O'Reilly, S. E., and Zhao, D. (2014). Effects of oil and dispersants on formation of marine oil snow and transport of oil hydrocarbons. *Environ. Sci. Technol.* 48, 14392–14399. doi: 10.1021/es5042157

Fuentes, E., Coe, H., Green, D., de Leeuw, G., and McFiggans, G. (2010). On the impacts of phytoplankton-derived organic matter on the production of marine aerosol – Part 1: source fluxes. *Atmos. Chem. Phys.* 10, 9295–9317. doi: 10.5194/acp-10-9295-2010

Fuqua, W. C., Winans, S. C., and Greenberg, E. P. (1996). Census and consensus in bacterial ecosystems: the *LuxR/Luxl* family of quorum sensing transcriptional regulators. *Annu. Rev. Microbiol.* 50, 727–751. doi: 10.1146/annurev.micro.50.1.727

Gallagher, K. L., Braissant, O., Kading, T. J., Dupraz, C., and Visscher, P. T. (2013). Phosphate-related artifacts in carbonate mineralization experiments. *J. Sed. Res.* 83, 37–49. doi: 10.2110/jsr.2013.9

Gallagher, K. L., Dupraz, C., and Visscher, P. T. (2014). Two opposing effects of sulfate reduction on carbonate precipitation in normal marine, hypersaline, and alkaline environments – Comment. *Geology* 42, e313–e314. doi: 10.1130/g34639c.1

Gallagher, K. L., Kading, T. J., Braissant, O., Dupraz, C., and Visscher, P. T. (2012). Inside the alkalinity engine: the role of electron donors in the organomineralization potential of sulfate-reducing bacteria. *Geobiology* 10, 518–530. doi: 10.1111/j.1472-4669.2012.00342.x

Gautret, P., Camoin, G., Golubic, S., and Sprachta, S. (2004). Biochemical control of calcium carbonate precipitation in modern lagoonal microbialites, Tikehau atoll, French Polynesia. *J. Sed. Res.* 74, 462–478. doi: 10.1306/012304740462

Gautret, P., and Trichet, J. (2005). Automicrites in modern cyanobacterial stromatolitic deposits of Rangiroa, Tuamotu Archipelago, French Polynesia: biochemical parameters underlaying their formation. *Sed. Geol.* 178, 55–73. doi: 10.1016/j.sedgeo.2005.03.012

Gebbink, M. F. B. G., Claessen, D., Bouma, B., Dijkhuizen, L., and Wösten, H. A. (2005). Amyloids – a functional coat for microorganisms. *Nat. Rev. Microbiol.* 3, 333–341. doi: 10.1038/nrmicro1127

Gerbersdorf, S. U., Bittner, R., Lubarsky, H., Manz, W., and Paterson, D. M. (2009). Microbial assemblages as ecosystem engineers of sediment stability. *J. Soils Sed.* 9, 640–652. doi: 10.1007/s11368-009-0142-5

Giese, B. (2002). Long-distance electron transfer through DNA. *Annu. Rev. Biochem.* 71, 51–70. doi: 10.1146/annurev.biochem.71.083101.134037

Gloag, E. S., Turnbull, L., Huang, A., Vallotton, P., Wang, H., Nolan, L. M., et al. (2013). Self-organization of bacterial biofilms is facilitated by extracellular DNA. *Proc. Natl. Acad. Sci. U.S.A.* 110, 11541–11546. doi: 10.1073/pnas.1218898110

Glunk, C., Dupraz, C., Braissant, O., Gallagher, K. L., Verrecchia, E. P., and Visscher, P. T. (2009). Microbially mediated carbonate precipitation in a hypersaline lake, Big Pond (Eleuthera, Bahamas). *Sedimentology* 58, 720–736. doi: 10.1111/j.1365-3091.2010.01180.x

Goh, F., Allen, M. A., Leuko, S., Kawaguchi, T., Decho, A. W., Burns, B. P., et al. (2009). Determining the specific microbial populations and their spatial distribution within the stromatolite ecosystem of Shark Bay. *ISME J.* 3, 383–396. doi: 10.1038/ismej.2008.114

Grabowski, R. C., Droppo, I. G., and Wharton, G. (2011). Erodibility of cohesive sediment: the importance of sediment properties. *Earth Sci. Rev.* 105, 101–120. doi: 10.1016/j.earscirev.2011.01.008

Gram, L., Grossart, H.-P., Schlingloff, A., and Kiorboe, T. (2002). Possible quorum sensing in marine snow bacteria: production of acylated homoserine lactones by *Roseobacter* strains isolated from marine snow. *Appl. Environ. Microbiol.* 68, 4111–4116. doi: 10.1128/AEM.68.8.4111-4116.2002

Grant, J., and Gust, G. (1987). Prediction of coastal sediment stability from photopigment content of mats of purple sulfur bacteria. *Nature* 330, 244–246. doi: 10.1038/330244a0

Grossart, H.-P., Engel, A., Arnosti, C., De La Rocha, C., Murray, A., and Passow, U. (2007). Microbial dynamics in autotrophic and heterotrophic seawater mesocosms. III. Organic matter fluxes. *Aquat. Microb. Ecol.* 49, 143–156. doi: 10.3354/ame01140

Grossart, H.-P., Kiørboe, T., Tang, K., and Ploug, H. (2003). Bacterial colonization of particles: growth and interactions. *Appl. Environ. Microbiol.* 69, 3500–3509. doi: 10.1128/AEM.69.6.3500-3509.2003

Grossart, H. P., and Simon, M. (2002). Bacterioplankton dynamics in the Gulf of Aqaba and the Northern Red Sea in early spring. *Mar. Ecol. Prog. Ser.* 239, 263–276. doi: 10.3354/meps239263

Guezennec, J. (2002). Deep-sea hydrothermal vents: a new source of innovative bacterial exopolysaccharides of biotechnological interests. *J. Indust. Microbiol. Biotechnol.* 29, 204–208. doi: 10.1038/sj.jim.7000298

Guezennec, J., Herry, J. M., Kouzayha, A., Bachere, E., Mittelman, M., and Fontaine, M. N. B. (2012). Exopolysaccharides from unusual marine environments inhibit early stages of biofouling. *Int. Biodeterior. Biodegrad.* 66, 1–7. doi: 10.1016/j.ibiod.2011.10.004

Guezennec, J., Pignet, P., Lijour, Y., Gentric, E., Ratiskol, J., and Colliec-Jouault, S. (1998). Sulfation and depolymerization of a bacterial exopolysaccharide of hydrothermal origin. *Carbohydr. Polymers* 37, 19–24. doi: 10.1016/S0144-8617(98)00006-X

Guiot, E., Georges, P., Brun, A., Fontaine-Aupart, M. P., Bellon-Fontaine, M. N., and Briandet, R. (2002). Heterogeneity of diffusion inside microbial biofilms determined by fluorescence correlation spectroscopy under two-photon excitation. *Photochem. Photobiol.* 75, 570–578. doi: 10.1562/0031-8655(2002)075<0570:HODIMB>2.0.CO;2

Guizien, K., Dupuy, C., Ory, P., Montainié, H., Hartmann, H., Chatelain, M., et al. (2014). Microorganism dynamics during a rising tide: disentangling effects of resuspension and mixing with offshore waters above an intertidal mudflat. *J. Mar. Syst.* 129, 178–188. doi: 10.1016/j.jmarsys.2013.05.010

Guo, L., Coleman, C. H. J., and Santschi, P. H. (1994). The distribution of colloidal and dissolved organic carbon in the Gulf of Mexico. *Mar. Chem.* 45, 105–119. doi: 10.1016/0304-4203(94)90095-7

Gutierrez, T., Berry, D., Yang, T., Mishamandani, S., McKay, L., Teske, A., et al. (2013). Role of bacterial exopolysaccharides (EPS) in the fate of the oil released during the Deepwater Horizon oil spill. *PLoS ONE* 8:e67717. doi: 10.1371/journal.pone.0067717

Gutierrez, T., Biller, D. V., Shimmield, T., and Green, D. H. (2012). Metal binding properties of the EPS produced by *Halomonas* sp. TG39 and its potential in enhancing trace element bioavailability to eukaryotic phytoplankton. *Biometals* 25, 1185–1194. doi: 10.1007/s10534-012-9581-3

Gutierrez, T., Morris, G., and Green, D. H. (2009). Yield and physicochemical properties of EPS from *Halomonas* sp. strain TG39 identifies a role for protein and anionic residues (sulfate and phosphate) in emulsification of *n*-hexadecane. *Biotechnol. Bioeng.* 103, 207–216. doi: 10.1002/bit.22218

Gutierrez, T., Mulloy, B., Bavington, C., Black, K., and Green, D. H. (2007a). Partial purification and chemical characterization of a glycoprotein (putative hydrocolloid) emulsifier produced by a marine Antarctobacter species. *Appl. Microbiol. Biotechnol.* 76, 1017–1026. doi: 10.1007/s00253-007-1091-9

Gutierrez, T., Shimmield, T., Haidon, C., Black, K., and Green, D. H. (2007b). Glycoprotein emulsifiers from two marine *Halomonas* species: chemical and physical characterization. *J. Appl. Microbiol.* 103, 1716–1727. doi: 10.1111/j.1365-2672.2007.03407.x

Gutierrez, T., Mulloy, B., Black, K., and Green, D. H. (2008). Emulsifying and metal ion binding activity of a glycoprotein exopolymer produced by *Pseudoalteromonas* sp strain TG12. *Appl. Environ. Microbiol.* 74, 4867–4876. doi: 10.1128/AEM.00316-08

Hall-Stoodley, L., Costerton, J. W., and Stoodley, P. (2004). Bacterial biofilms: from the natural environment to infectious diseases. *Nat. Rev. Microbiol.* 2, 95–108. doi: 10.1038/nrmicro821

Hanlon, A. R. M., Bellinger, B., Haynes, K., Xiao, G., Hofmann, T. A., Gretz, M. R., et al. (2006). Dynamics of extracellular polymeric substance (EPS) production

and loss in an estuarine, diatom-dominated, microalgal biofilm over a tidal emersion-immersion period. *Limnol. Oceanogr.* 51, 79–93. doi: 10.4319/lo.2006.51.1.0079

Hansell, D. A. (2002). "DOC in the global ocean carbon cycle," in *Biogeochemistry of Marine Dissolved Organic Matter*, eds D. A. Hansell and C. A. Carlson (San Diego, CA: Academic Press), 685–715. doi: 10.1016/B978-012323841-2/50017-8

Hansell, D. A., and Carlson, C. A. (1998). Deep-ocean gradients in the concentration of dissolved organic carbon. *Nature* 395, 263–268. doi: 10.1038/26200

Harder, T., Lam, C., and Qian, P. Y. (2002). Induction of larval settlement in the polychaete *Hydroides elegans* by marine bioWlms: an investigation of monospecifc diatom Wlms as settlement cues. *Mar. Ecol. Prog. Ser.* 229, 105–112. doi: 10.3354/meps229105

Harvey, R. W., and Luoma, S. N. (1985). Effect of adherent bacteria and bacterial cellular polymers upon assimilation by *Macoma balthica* of sediment bound Cd, Zn, and Ag. *Mar. Ecol. Prog. Ser.* 22, 281–289. doi: 10.3354/meps022281

Hassler, C. S., Alasonati, E., Mancuso-Nichols, C. A., and Slaveykova, V. I. (2011a). Exopolysaccharides produced by bacteria isolated from the pelagic Southern Ocean—role of Fe binding, chemical reactivity, and bioavailability. *Mar. Chem.* 123, 88–98. doi: 10.1016/j.marchem.2010.10.003

Hassler, C. S., Schoemann, V., Mancuso-Nichols, C., Butler, E. C. V., and Boyd, P. W. (2011b). Saccharides enhance iron bioavailability to Southern Ocean phytoplankton. *Proc. Natl. Acad. Sci. U.S.A.* 108, 1076–1081. doi: 10.1073/pnas.1010963108

Hassler, C. S., and Schoemann, V. (2009). Bioavailability of organically bound Fe to model phytoplankton of the Southern Ocean. *Biogeosciences* 6, 2281–2296. doi: 10.5194/bg-6-2281-2009

Hawkins, L. N., and Russell, L. M. (2010). Polysaccharides, proteins, and phytoplankton fragments: four chemically distinct types of marine primary organic aerosol classified by single particle spectromicroscopy. *Adv. Meteorol.* 2010, 612132. doi: 10.1155/2010/612132

Hedges, J. I. (2002). "Why dissolved organic matter," in *Biochemistry of Marine Dissolved Organic Matter*, eds D. A. Hansell and C. A. Carlson (San Diego, CA: Academic Press), 685–715.

Hense, B. A., Kuttler, C., Muller, J., Rothballer, M., Hartmann, A., and Kreft, J.-U. (2007). Does efficiency sensing unify diffusion and quorum sensing? *Nat. Rev. Microbiol.* 5, 230–239.

Herndl, G. (1988). Ecology of amorphous aggregations (marine snow) in the northern Adriatic Sea: 2. Microbial density and activity in marine snow and its implication to overall pelagic processes. *Mar. Ecol. Prog. Ser.* 48, 265–275. doi: 10.3354/meps048265

Hmelo, L., Mincer, T. J., and Van Mooy, B. A. S. (2011). Possible influence of bacterial quorum sensing on the hydrolysis of sinking particulate organic carbon in marine environments. *Environ. Microbiol. Rep.* 3, 682–688. doi: 10.1111/j.1758-2229.2011.00281.x

Hmelo, L., and van Mooy, B. A. S. (2009). Kinetic constraints on acylated homoserine lactone-based quorum sensing in marine environments. *Aquat. Microb. Ecol.* 54, 127–133. doi: 10.3354/ame01261

Hobley, L., Harkins, C., MacPhee, C. E., and Stanley-Wall, N. R. (2015). Giving structure to the biofilm matrix: and overview of individual strategies and emerging common themes. *FEMS Microbiol. Rev.* 39, 649–669. doi: 10.1093/femsre/fuv015

Hobley, L., Ostrowski, A., Rao, F. V., Bromley, K. M., Porter, M., Prescott, A. R., et al. (2013). BslA is a self-assembling bacterial hydrophobin that coats the *Bacillus subtilus* biofilm. *Proc. Natl. Acad. Sci. U.S.A.* 110, 13600–13605. doi: 10.1073/pnas.1306390110

Holbrook, R. D., Murphy, K. E., Morrow, J. B., and Cole, K. D. (2008). Trophic transfer of nanoparticles in a simplified invertebrate food web. *Nat. Nanotechnol.* 3, 352–355. doi: 10.1038/nnano.2008.110

Holmström, C., Egan, S., Franks, A., McCloy, S., and Kjelleberg, S. (2002). Antifouling activities expressed by marine surface associated *Pseudoalteromonas* species. *FEMS Microbiol. Ecol.* 41, 47–58. doi: 10.1111/j.1574-6941.2002.tb00965.x

Holmström, C., Rittschof, D., and Kjelleberg, S. (1992). Inhibition of settlement by larvae of *Balanus amphitrite* and *Ciona intestinalis* by a surface-colonizing marine bacterium. *Appl. Environ. Microbiol.* 58, 2111–2115.

Hoppe, H.-G., Arnosti, C., and Herndl, G. F. (2001). "Ecological significance of bacterial enzymes in the marine environment," in *Enzymes in the Environment*, eds R. G. Burns and R. P. Dick (Basel: Marcel Dekker), 73–107.

Hoppe, H.-G., Gocke, K., Koppe, R., and Begler, C. (2002). Bacterial growth and primary production along a north-south transect of the Atlantic Ocean. *Nature* 416, 168–171. doi: 10.1038/416168a

Horswill, A. R., Stoodley, P., Stewart, P. S., and Parsek, M. R. (2007). The effect of the chemical, biological, and physical environment on quorum sensing in structured microbial communities. *Anal. Bioanal. Chem.* 387, 371–380. doi: 10.1007/s00216-006-0720-y

Hoskins, D. L., Stancyk, S. E., and Decho, A. W. (2003). Utilization of algal and bacterial extracellular polymeric secretions (EPS) by the deposit-feeding brittlestar *Amphipholis gracillima* (Echinodermata). *Mar. Ecol. Prog. Ser.* 247, 93–101. doi: 10.3354/meps247093

Houry, A., Gohar, M., Deschamps, J., Tischendko, E., Aymerich, S., Gruss, A., et al. (2012). Bacterial swimmers that infiltrate and take over the biofilm matrix. *Proc. Natl. Acad. Sci. U.S.A.* 109, 13088–13093. doi: 10.1073/pnas.1200791109

Hubas, C., Sachidhanandam, C., Rybarcczyk, H., Lubarsky, H. V., Rigaux, A., Moens, T., et al. (2010). Bacterivorous nematodes stimulate microbial growth and exopolymer production in marine sediment microcosms. *Mar. Ecol. Prog. Ser.* 419, 85–94. doi: 10.3354/meps08851

Hultin, K. A. H., Nilsson, E. D., Krejci, R., Mårtensson, E. M., Ehn, M., and Hagström, Å. (2010). *In situ* laboratory sea spray production during the Marine Aerosol Production 2006 cruise on the northeastern Atlantic Ocean. *J. Geophys. Res.* 115, D06201. doi: 10.1029/2009jd012522

Ikuma, K., Decho, A. W., and Lau, B. L. T. (2015). When nanoparticles meet biofilms- interactions guiding the environmental fate and accumulation of nanoparticles. *Front. Microbiol.* 6:591. doi: 10.3389/fmicb.2015.00591

Ikuma, K., Madden, A. S., Decho, A. W., and Lau, B. L. T. (2014). Deposition of nanoparticles onto polysaccharide-coated surfaces: implications for nanoparticle–biofilm interactions. *Environ. Sci. Nano* 1, 117–122. doi: 10.1039/c3en00075c

Iyer, A., Mody, K., and Bhavanath, J. (2005). Biosorption of heavy metals by a marine bacterium. *Mar. Poll. Bull.* 50, 340–343. doi: 10.1016/j.marpolbul.2004.11.012

Jatt, A. N., Tang, K., Liu, J., Zhang, Z., and Zhang, X.-H. (2015). Quorum sensing in marine snow and its possible influence on production of extracellular hydrolytic enzymes in marine snow bacterium *Pantoea ananatis* B9. *FEMS Microbiol. Ecol.* 91, 1–13. doi: 10.1093/femsec/fiu030

Jennings, L. K., Storek, K. M., Ledvina, H. E., Coulon, C., Marmont, L. S., Sadovskaya, I., et al. (2015). Pel is a cationic exopolysaccharide that cross-links extracellular DNA in the *Pseudomonas aeruginosa* biofilm matrix. *Proc. Natl. Acad. Sci. U.S.A.* 112, 11353–11358. doi: 10.1073/pnas.1503058112

Jernelöv, A., and Lindén, O. (1981). Ixtoc I: a case study of the world's largest oil spill. *AMBIO* 10, 299–306.

Jiao, N., Herndl, G. J., Hansell, D. A., Benner, R., Kattner, G., Wilhelm, S. W., et al. (2010). Microbial production of recalcitrant dissolved organic matter: long-term carbon storage in the global ocean. *Nat. Rev. Microbiol.* 8, 593–599. doi: 10.1038/nrmicro2386

Johansson, S., Larsson, U., and Boehm, P. (1980). The Tsesis oil spill impact on the pelagic ecosystem. *Mar. Pollut. Bull.* 11, 284–293. doi: 10.1016/0025-326X(80)90166-6

Johnson, W. M., Soule, M. C. K., and Kujawinski, E. B. (2016). Evidence for quorum sensing and differential metabolite production by a marine bacterium in response to DMSP. *ISME J.* 10, 2304–2316. doi: 10.1038/ismej.2016.6

Joyce, A., and Utting, S. (2015). The role of exopolymers in hatcheries: an overlooked factor in hatchery hygiene and feed quality. *Aquaculture* 446, 122–131. doi: 10.1016/j.aquaculture.2015.04.037

Kaufmann, G. F., Sartorio, R., Lee, S.-H., Rogers, C. J., Meijler, M. M., Moss, J. A., et al. (2005). Revisiting quorum sensing: discovery of additional chemical and biological functions for 3-oxo-N-acylhomoserine lactones. *Proc. Natl. Acad. Sci. U.S.A.* 102, 309–314. doi: 10.1073/pnas.0408639102

Kawaguchi, T., and Decho, A. W. (2002a). A laboratory investigation of cyanobacterial extracellular polymeric secretions (EPS) in influencing CaCO3 polymorphism. *J. Cryst. Growth* 240, 230–235. doi: 10.1016/S0022-0248(02)00918-1

Kawaguchi, T., and Decho, A. W. (2002b). Characterization of extracellular polymeric secretions (EPS) from modern soft marine stromatolites (Bahamas)

and its inhibitory effect on CaCO3 precipitation Prep. *Biochem. Biotechnol.* 32, 51–63.

Keil, R. G., and Kirchman, D. L. (1999). Utilization of dissolved protein and amino acids in the northern Sargasso Sea. *Aquat. Microb. Ecol.* 18, 293–300. doi: 10.3354/ame018293

Kennedy, A. F. D., and Sutherland, I. W. (1987). Analysis of bacterial exopolysaccharides. *Biotechnol. Appl. Biochem.* 9, 12–19.

Kirchman, D. L., Meon, B., Ducklow, H. W., Carlson, C. A., Hansell, D. A., and Steward, G. F. (2001). Glucose fluxes and concentrations of dissolved combined neutral sugars (polysaccharides) in the Ross Sea and Polar Front Zone, Antarctica. *Deep Sea Res. II* 48, 4179–4197. doi: 10.1016/S0967-0645(01)00085-6

Kleindienst, S., Seidel, M., Ziervogel, K., Grim, S., Loftis, K., Harrison, S., et al. (2015). Chemical dispersants can suppress the activity of natural oil-degrading microorganisms. *Proc. Natl. Acad. Sci. U.S.A.* 112, 14900–14905. doi: 10.1073/pnas.1507380112

Krembs, C., Eicken, H., and Deming, J. W. (2011). Exopolymer alteration of physical properties of sea ice and implications for ice habitability and biogeochemistry in a warmer Arctic. *Proc. Natl. Acad. Sci. U.S.A.* 108, 3653–3658. doi: 10.1073/pnas.1100701108

Krembs, C., Eicken, H., Junge, K., and Deming, J. W. (2002). High concentrations of exopolymeric substances in Arctic winter sea ice: implication for the polar ocean carbon cycle and cryoprotection of diatoms. *Deep Sea Res. II* 49, 2163–2181. doi: 10.1016/S0967-0637(02)00122-X

Krumbein, W. E. (1983). Stromatolites – the challenge of a term in space and time. *Precambr. Res.* 20, 493–531. doi: 10.1016/0301-9268(83)90087-6

Kuznetsova, M., Lee, C., and Aller, J. (2005). Characterization of the proteinaceous matter in marine aerosols. *Mar. Chem.* 96, 359–377. doi: 10.1007/s00216-012-6363-2

Lam, C., Harder, T., and Qian, P. Y. (2003). Induction of larval settlement in the polychaete *Hydroides elegans* by surface-associated settlement cues of marine benthic diatoms. *Mar. Ecol. Prog. Ser.* 263, 83–92. doi: 10.3354/meps263083

Larsen, P., Nielsen, J. L., Dueholm, M., Wetzel, R., Otzen, D., and Nielsen, P. H. (2007). Amyloid adhesins are abundant in natural biofilms. *Environ. Microbiol.* 9, 3077–3090. doi: 10.1111/j.1462-2920.2007.01418.x

Lau, S. C. K., and Qian, P. Y. (2000). Inhibitory effect of phenolic compounds and marine bacteria on larval settlement of the barnacle *Balanus amphitrite* Darwin. *Biofouling* 16, 47–58. doi: 10.1080/08927010009378429

Lawrence, J. R., Swerhone, G. D. W., Kuhlicke, U., and Neu, T. R. (2007). In situ-evidence for microdomains in the polymer matrix of bacterial microcolonies. *Can. J. Microbiol.* 53, 450–458. doi: 10.1139/W06-146

Lawrence, J. R., Swerhone, G. D. W., Kuhlicke, U., and Neu, T. R. (2016). In situ evidence for metabolic and chemical microdomains in the structured polymer matrix of bacterial microcolonies. *FEMS Microbiol. Ecol.* 92:fiw183. doi: 10.1093/femsec/fiw183

Lawrence, J. R., Swerhone, G. D. W., Leppard, G. G., Araki, T., Zhang, X., West, M. M., et al. (2003). Scanning transmission X-ray, laser scanning and transmission electron microscopy mapping of the exopolymeric matrix of microbial biofilms. *Appl. Environ. Microbiol.* 69, 5543–5554. doi: 10.1128/AEM.69.9.5543-5554.2003

Lawrence, J. R., Wolfaardt, G. M., and Korber, D. R. (1994). Determination of diffusion coefficients in biofilms by confocal laser microscopy. *Appl. Environ. Microbiol.* 60, 1166–1173.

Leck, C., and Bigg, E. K. (2005). Evolution of the marine aerosol – a new perspective. *Geophys. Res. Lett.* 32, L19803. doi: 10.1029/2005GL023651

Leck, C., and Bigg, E. K. (2008). Comparison of sources and nature of the tropical aerosol with the summer high Arctic aerosol. *Tellus* 60B, 118–126. doi: 10.1111/j.1600-0889.2007.00315.x

Lewin, R. (1984). Microbial adhesion is a sticky problem. *Science* 224, 375–377. doi: 10.1126/science.6143401

Ley, R. E., Harris, J. K., Wilcox, J., Spear, J. R., Miller, S. R., Bebout, B. M., et al. (2006). Unexpected diversity and complexity from the Guerrero Negro hypersaline microbial mat. *Appl. Environ. Microbiol.* 72, 3685–3695. doi: 10.1128/AEM.72.5.3685-3695.2006

Liu, S.-B., Chen, X.-L., He, H.-L., Zhang, X.-Y., Xie, B.-B., Yu, Y., et al. (2013). Structure and ecological roles of a novel exopolysaccharide from the Arctic sea ice bacterium *Pseudoalteromonas* sp. Strain SM20310. *Appl. Environ. Microbiol.* 79, 224–230. doi: 10.1128/AEM.01801-12

Loaec, M., Olier, R., and Guezennec, J. (1997). Uptake of lead, cadmium and zinc by a novel bacterial exopolysaccharide. *Water Res.* 31, 1171–1179. doi: 10.1016/S0043-1354(96)00375-2

Loaec, M., Olier, R., and Guezennec, J. (1998). Chelating properties of bacterial exopolysaccharides from deep-sea hydrothermal vents. *Carbohydr. Polymers* 35, 65–70. doi: 10.1016/S0144-8617(97)00109-4

Long, R. A., and Azam, F. (1996). Abundant protein-containing particles in the sea. *Aquat. Microb. Ecol.* 10, 213–221. doi: 10.3354/ame010213

Long, R. A., and Azam, F. (2001a). Antagonistic interactions among marine pelagic bacteria. *Appl. Environ. Microbiol.* 67, 4975–4983.

Long, R. A., and Azam, F. (2001b). Microscale patchiness of bacterioplankton assemblage richness in seawater. *Aquat. Microb. Ecol.* 26, 103–113. doi: 10.3354/ame026103

Ludwig, R., Al-Horani, F. A., de Beer, D., and Jonkers, H. M. (2005). Photosynthesis controlled calcification in a hypersaline microbial mat. *Limnol. Oceanogr.* 50, 1836–1843. doi: 10.4319/lo.2005.50.6.1836

Lundqvist, A., Bertilsson, S., and Goedkoop, W. (2010). Effects of extracellular polymeric and humic substances on chlorpyrifos bioavailability to *Chironomus riparius*. *Ecotoxicology* 19, 614–622. doi: 10.1007/s10646-009-0430-2

Lundqvist, A., Bertilsson, S., and Goedkoop, W. (2012). Interactions with DOM and biofilms affect the fate and bioavailability of insecticides to invertebrate grazers. *Ecotoxicology* 21, 2398–2408. doi: 10.1007/s10646-012-0995-z

Luoma, S. N., Khan, F. R., and Croteau, M.-N. (2014). Bioavailability and bioaccumulation of metal-based engineered nanomaterials in aquatic environments: concepts and processes. *Nanosci. Environ.* 7, 157–193. doi: 10.1016/b978-0-08-099408-6.00005-0

Malarkey, J., Baas, J. H., Hope, J. A., Aspden, R. J., Parsons, D. R., Peakall, J., et al. (2015). The pervasive role of biological cohesion in bedform development. *Nat. Commun.* 6:6257. doi: 10.1038/ncomms7257

Martin, J. H., Coale, K. H., Johnson, K. S., Fitzwater, S. E., Gordon, R. M., Tanner, S. J., et al. (1994). Testing the iron hypothesis in ecosystems of the equatorial Pacific-Ocean. *Nature* 371, 123–129. doi: 10.1038/371123a0

Marx, J. G., Carpenter, S. D., and Deming, J. W. (2009). Production of cryoprotectant extracellular polymeric substances (EPS) by the marine psychrophilic bacterium *Colwellia psychrerythraea* strain 34H under extreme conditions. *Can. J. Microbiol.* 55, 63–72. doi: 10.1139/W08-130

Mashburn, L. M., and Whiteley, M. (2005). Membrane vesicles traffic signals and facilitate group activities in a prokaryote. *Nature* 437, 422–425. doi: 10.1038/nature03925

Mashburn-Warren, L., McLean, R. J. C., and Whiteley, M. (2008). Gram-negative outer membrane vesicles: beyond the cell surface. *Geobiology* 6, 214–219. doi: 10.1111/j.1472-4669.2008.00157.x

Mayer, C., Moritz, R., Kirschner, C., Borchard, W., Maibaum, R., Wingender, J., et al. (1999). The role of intermolecular interaction: studies on model systems for bacterial biofilms. *Int. J. Biol. Macromol.* 26, 3–16. doi: 10.1016/S0141-8130(99)00057-4

McLean, R. J. C., Whiteley, M., Stickler, D. J., and Fuqua, W. C. (1997). Evidence of autoinducer activity in naturally occurring biofilms. *FEMS Microbiol. Lett.* 154, 259–263. doi: 10.1111/j.1574-6968.1997.tb12653.x

Meiners, K., Gradinger, R., Fehling, J., Civitarese, G., and Spindler, M. (2003). Vertical distribution of exopolymer particles in sea ice of the Fram Strait (Arctic) during autumn. *Mar. Ecol. Prog. Ser.* 248, 1–13. doi: 10.3354/meps248001

Meister, P. (2013). Two opposing effects of sulfate reduction on carbonate precipitation in normal marine, hypersaline, and alkaline environments. *Geology* 41, 499–502. doi: 10.1130/G34185.1

Miller, L. A., Papkyriakow, T. N., Collins, R. E., Deming, J. W., Ehn, J. K., MacDonald, R. W., et al. (2011). Carbon dynamics in sea ice: a winter flux time series. *J. Geophys. Res.* 116:C02028. doi: 10.1029/2009jc006058

Miller, S. D., Haddock, S. H. D., Elvidge, C. D., and Lee, T. F. (2005). Detection of a bioluminescent milky sea from space. *Proc. Natl. Acad. Sci. U.S.A.* 102, 14181–14184. doi: 10.1073/pnas.0507253102

Mobberley, J. M., Khodadad, C. L. M., Visscher, P. T., Reid, R. P., Hagan, P., and Foster, J. S. (2015). Inner workings of thrombolites: spatial gradients of metabolic activity as revealed by metatranscriptome profiling. *Sci. Rep.* 5:12601. doi: 10.1038/srep12601

Mopper, K., Schultz, C. A., Chevolot, L., Germain, C., Revuelta, R., and Dawson, R. (1992). Determination of sugars in unconcentrated seawater and other natural waters by liquid chromatography and pulsed amperometric detection. *Environ. Sci. Technol.* 26, 133–138. doi: 10.1021/es00025a014

Moppert, X., Le Costaouec, T., Raguénès, G., Simon-Colin, C., Crassous, P., Costa, B., et al. (2009). Investigations into the uptake of copper, iron and selenium by a highly-sulphated bacterial exopolysaccharide isolated from microbial mats. *J. Indust. Microbiol. Biotechnol.* 36, 599–604. doi: 10.1007/s10295-009-0529-8

Moran, M. A. (2015). Microbiome: the global ocean microbiome. *Science* 350:aac8455. doi: 10.1126/science.aac8455

Moran, M. A., and Zepp, R. G. (2000). "UV radiation effects on microbes and microbial processes," in *Microbial Ecology of the Oceans*, 1st Edn, ed. D. L. Kirchman (Hoboken, NJ: Wile-Liss), 201–228.

Mortimer, M., Petersen, E. J., Buchholz, B. A., Orias, E., and Holden, P. A. (2016). Bioaccumulation of multiwall Carbon nanotubes in *Tetrahymena thermophila* by direct feeding or trophic transfer. *Environ. Sci. Technol.* 50, 8876–8885. doi: 10.1021/acs.est.6b01916

Myklestad, S. (1977). Production of carbohydrates by marine planktonic diatoms. II. Influence of the N/P ratio in the growth medium on the assimilation ratio, growth rate and production of cellular and extracellular carbohydrates by *Chaetoceros affinis* var Willei (Gran) Hustedt and *Skeletonema costatum* (Grev) Cleve. *J. Exp. Mar. Biol. Ecol.* 29, 161–179. doi: 10.1016/0022-0981(77)90046-6

Nagata, T. (2000). "Production mechanisms of dissolved organic matter," in *Microbial Ecology of the Oceans*, 1st Edn, ed. D. L. Kirchman (Hoboken, NJ: Wiley-Liss), 121–152.

Nealson, K. H., and Hastings, J. W. (2004). Quorum sensing on a global scale: massive numbers of bioluminsescent bacteria make milky seas. *Appl. Environ. Microbiol.* 72, 2295–2297. doi: 10.1128/AEM.72.4.2295-2297.2006

Neu, T. R. (1994). "Biofilms and microbial mats," in *Biostabilization of Sediments*, eds W. E. Krumbein, D. M. Paterson, and L. J. Stal (Oldenburg: BIS-Verlag), 9–17.

Neu, T. R., and Lawrence, J. R. (2014). Advanced techniques for in situ analysis of the biofilm matrix (structure, composition, dynamics) by means of laser scanning microscopy. *Methods Mol. Biol.* 1147, 43–64. doi: 10.1007/978-1-4939-0467-9_4

Neu, T. R., and Lawrence, J. R. (2016). "The extracellular matrix – an intractable part of biofilm systems," in *The Perfect Slime -Microbial Extracellular Polymeric Substances (EPS)*, eds H.-C. Flemming, T. R. Neu, and J. Wingender (London: IWA Publishers), 25–60.

Nevius, B. A., Chen, Y. P., Chen Ferry, J. L., and Decho, A. W. (2012). Surface-functionalization effects on uptake of fluorescent polystyrene nanoparticles by model biofilms. *Ecotoxicology* 21, 2205–2213. doi: 10.1007/s10646-012-0975-3

Nichols, C. A., Guezennec, J., and Bowman, J. P. (2005). Bacterial exopolysaccharides from extreme marine environments with special consideration of the Southern Ocean, sea ice, and deep-sea hydrothermal vents: a review. *Mar. Biotechnol.* 7, 253–271. doi: 10.1007/s10126-004-5118-2

Nichols, C. M., Lardière, S. G., Bowman, J. P., Nichols, P. D., Gibson, J. A. E., and Guézennec, J. (2005). Chemical characterization of exopolysaccharide for Antarctic marine bacteria. *Microb. Ecol.* 49, 578–589. doi: 10.1007/s00248-004-0093-8

Nielsen, S. J., Harder, T., and Steinberg, P. D. (2015). Sea urchin larvae decipher the epiphytic bacterial community composition when selecting sites for attachment and metamorphosis. *FEMS Microbiol. Ecol.* 91, 1–9. doi: 10.1093/femsec/fiu011

Nishimura, S., Tanaka, T., Fujita, K., Itaya, M., Hiraishi, A., and Kikuchi, Y. (2003). Extracellular DNA and RNA produced by a marine photosynthetic bacterium *Rhodovulum sulfidophilum*. *Nucleic Acids Res.* 3(Suppl.), 279–280. doi: 10.1093/nass/3.1.279

Niu, H., Li, Z., Lee, K., Kepkay, P., and Mullin, J. V. (2011). Modelling the transport of oil-mineral-aggregates (OMAs) in the marine environment and assessment of their potential risks. *Environ. Model Assess.* 16, 61–75. doi: 10.1007/s10666-010-9228-0

Noffke, N. (2010). *Microbial Mats in Sandy Deposits from the Archean to Today*. Heidelberg: Springer, 196.

Noffke, N., Christian, D., Wacey, D., and Hazen, R. M. (2013). Microbially induced sedimentary structures recording an ancient ecosystem in the *ca*. 3.48 billion-year-old dresser formation, Pilbara, Western Australia. *Astrobiology* 13, 1103–1124. doi: 10.1089/ast.2013.1030

Noffke, N., Gerdes, G., Klenke, T., and Krumbein, W. E. (2001). Microbially induced sedimentary structures- A new category within the classification of primary sedimentary structures. *J. Sed. Res.* 71, 649–656. doi: 10.1306/2DC4095D-0E47-11D7-8643000102C1865D

Nutman, A. P., Bennett, V. C., Friend, C. R. L., van Kranendonk, M. J., and Chivas, A. R. (2016). Rapid emergence of life shown by discovery of 3,700-million-year-old microbial structures. *Nature* 537, 535–538. doi: 10.1038/nature19355

Nyholm, S. V., Stabb, E. V., Ruby, E. G., and McFall-Ngai, M. J. (2000). Establishment of an animal bacterial association: recruiting symbiotic vibrios from the environment. *Proc. Natl. Acad. Sci. U.S.A.* 97, 10231–10235. doi: 10.1073/pnas.97.18.10231

Obst, M., Dynes, J. J., Lawrence, J. R., Swerhone, G. D. W., Benzerara, K., Karunakaran, C., et al. (2009). Precipitation of amorphous CaCO3 (aragonite-like) by cyanobacteria: a STXM study of the influence of EPS on the nucleation process. *Geochim. Cosmchim. Acta* 73, 4180–4198. doi: 10.1016/j.gca.2009.04.013

O'Dowd, C. D., Facchini, M. C., Cavalli, F., Ceburnis, D., Mircea, M., Decesari, S., et al. (2004). Biogenically-driven organic contribution to marine aerosol. *Nature* 431, 676–680. doi: 10.1038/nature02959

Ogawa, H., Amagai, Y., Koike, I., Kaiser, K., and Benner, R. (2001). Production of refractory dissolved organic matter by bacteria. *Science* 292, 917–920. doi: 10.1126/science.1057627

Okshevsky, M., and Meyer, R. L. (2013). The role of extracellular DNA in the establishment, maintenance and perpetuation of bacterial biofilms. *Crit. Revs. Microbiol.* 41, 341–352. doi: 10.3109/1040841X.2013.841639

Oren, A. (1994). The ecology of extremely halophilic archaea. *FEMS Microbiol. Rev.* 13, 415–439. doi: 10.1111/j.1574-6976.1994.tb00060.x

Paerl, H. W., Steppe, T. F., and Reid, R. P. (2001). Bacterially-mediated precipitation in marine Stromatolites. *Environ. Microbiol.* 3, 123–130. doi: 10.1046/j.1462-2920.2001.00168.x

Papenfort, K., and Bassler, B. L. (2016). Quorum sensing signal-response systems in Gram-negative bacteria. *Nat. Revs. Microbiol.* 14, 576–588. doi: 10.1038/nrmicro.2016.89

Passow, U. (2002). Transparent exopolymer particles (TEP) in aquatic environments. *Progr. Oceanogr.* 55, 287–333. doi: 10.1016/S0079-6611(02)00138-6

Passow, U. (2016). Formation of rapidly-sinking, oil-associated marine snow. *Deep Sea Res. II Top. Stud. Oceanogr.* 129, 232–240. doi: 10.1016/j.dsr2.2014.10.001

Passow, U., Ziervogel, K., Asper, V., and Diercks, A. (2012). Marine snow formation in the aftermath of the deepwater horizon oil spill in the Gulf of Mexico. *Environ. Res. Lett.* 7, 1–11. doi: 10.1088/1748-9326/7/3/035301

Paterson, D. M. (1989). Short-term changes in the erodibility of intertidal cohesive sediments related to the migratory behavior of epipelic diatoms. *Limnol. Oceanogr.* 34, 223–234. doi: 10.4319/lo.1989.34.1.0223

Paterson, D. M., Aspden, R. J., Visscher, P. T., Consalvey, M., Andres, M. S., Decho, A. W., et al. (2008). Light dependent biostabilisation of sediments by stromatolite assemblages. *PLoS ONE* 3:e3176. doi: 10.1371/journal.pone.0003176

Patton, J. S., Rigler, M. W., Boehm, P. D., and Fiest, D. L. (1981). Ixtoc I oil spill: flaking of surface mousse in the Gulf of Mexico. *Nature* 290, 235–238. doi: 10.1038/290235a0

Paul, V., Mormile, M. R., and Wronkiewicz, D. J. (2017). Impact of elevated CO2 concentrations on carbonate mineral precipitation ability of sulfate-reducing bacteria and implications for CO2 sequestration. *Appl. Geochem.* 78, 250–271. doi: 10.1016/j.apgeochem.2017.01.010

Peterson, B. W., He, Y., Ren, Y., Zerdoum, A., Libera, M. R., Sharma, P. K., et al. (2015). Viscoelasticity of biofilms and their recalcitrance to mechanical and chemical challenges. *FEMS Microbiol. Rev.* 39, 234–245. doi: 10.1093/femsre/fuu008

Pinckney, J. L., and Paerl, H. W. (1997). Anoxygenic photosynthesis and nitrogen fixation by a microbial mat community in a *Bahamian* hypersaline lagoon. *Appl. Environ. Microbiol.* 63, 420–426.

Plante, C. (2000). Role of bacterial exopolymeric capsules in protection from deposit feeder ingestion. *Aquat. Microb. Ecol.* 21, 211–219. doi: 10.3354/ame021211

Plante, C. J., Jumars, P. A., and Baross, J. A. (1990). Digestive associations between marine detritivores and bacteria. *Ann. Rev. Ecol. Syst.* 21, 29–44. doi: 10.1146/annurev.es.21.110190.000521

Plante, C. J., and Schriver, A. G. (1998). Differential lysis of sedimentary bacteria by *Arenicola marina* L.: examination of cell wall structure and exopolymeric capsules as correlates. *J. Exp. Mar. Biol. Ecol.* 229, 35–52. doi: 10.1016/S0022-0981(98)00039-2

Ploug, H. (2008). Cyanobacterial surface blooms formed by *Aphanizomenon* sp. and *Nodularia spumigena* in the Baltic Sea: small-scale fluxes, pH, and oxygen micro-environments. *Limnol. Oceanogr.* 53, 914–921. doi: 10.4319/lo.2008.53.3.0914

Ploug, H., Grossart, H. P., Azam, F., and Jørgensen, B. B. (1999). Photosynthesis, respiration, and carbon turnover in sinking marine snow from surface waters of the Southern California Bight: implications for the carbon cycle in the ocean. *Mar. Ecol. Prog. Ser.* 179, 1–11. doi: 10.3354/meps179001

Ploug, H., Kühl, M., Buchholz-Cleven, B., and Jørgensen, B. B. (1997). Anoxic aggregates - an ephemeral phenomenon in the pelagic environment? *Aquat. Microb. Ecol.* 13, 285–294. doi: 10.3354/ame013285

Potts, M. (1994). Desiccation tolerance or prokaryotes. *Microbiol. Rev.* 58, 755–805.

Raguénès, G., Christen, R., Guézennec, J., Pignet, P., and Barbier, G. (1997a). *Vibrio diabolicus* sp.nov., a new polysaccharide-secreting organism isolated from a deep-sea vent polychaete annelid, Alvinella pompejana. *Int. J. Syst. Bacteriol.* 47, 989–995.

Raguénès, G., Ruimy, R., Pignet, P., Christen, R., Loaec, M., Rougeaux, H., et al. (1997b). *Alteromonas* infernus sp. nov., a new polysaccharide producing bacterium isolated from a deep-sea hydrothermal vent. *J. Appl. Bacteriol.* 82, 422–430.

Rao, D., Webb, J. S., Holmstrom, C., Case, R., Low, A., Steinberg, P., et al. (2007). Low densities of epiphytic bacteria from the marine alga Ulva australis inhibit settlement of fouling organisms. *Appl. Environ. Microbiol.* 73, 7844–7852. doi: 10.1128/AEM.01543-07

Redfield, R. J. (2002). Is quorum sensing a side effect of diffusion sensing? *Trends Microbiol.* 10, 365–370.

Reid, R. P., Visscher, P. T., Decho, A. W., Stolz, J. F., Bebout, B. M., Dupraz, C., et al. (2000). The role of microbes in accretion, lamination and early lithication of modern marine stromatolites. *Nature* 406, 989–992. doi: 10.1038/35023158

Repeta, D. J., and Aluwihare, L. I. (2006). Radiocarbon analysis of neutral sugars in high-molecular-weight dissolved organic carbon: implications for organic carbon cycling. *Limnol. Oceanogr.* 51, 1045–1053. doi: 10.4319/lo.2006.51.2.1045

Rice, K. C., Mann, E. E., Endres, J. L., Weiss, E. C., Cassat, J. E., Smeltzer, M. S., et al. (2007). The *cidA* murein hydrolase regulator contributes to DNA release and biofilm development in *Staphylococcus aureus*. *Proc. Natl. Acad. Sci., U.S.A.* 104, 8113–8118. doi: 10.1073/pnas.0610226104

Rich, J., Gosselin, M., Sherr, E., Sherr, B., and Kirchman, D. L. (1997). High bacterial production, uptake and concentrations of dissolved organic matter in the Central Arctic Ocean. *Deep-Sea Res. II* 44, 1645–1663. doi: 10.1016/S0967-0645(97)00058-1

Rich, J. H., Ducklow, H. W., and Kirchman, D. L. (1996). Concentrations and uptake of neutral monosaccharides along 140°W in the Equatorial Pacific: contribution of glucose to heterotrophic bacterial activity and the POM flux. *Limnol. Oceanogr.* 41, 595–604. doi: 10.4319/lo.1996.41.4.0595

Richert, L., Golubic, S., Le Guédès, R., Ratiskol, J., Payri, C., and Guezennec, J. (2005). Characterization of exopolysaccharides produced by cyanobacteria isolated from polynesian microbial mats. *Curr. Microbiol.* 51, 379–384. doi: 10.1007/s00284-005-0069-z

Rieger, J., Frechen, T., Cox, G., Heckmann, W., Schmidt, C., and Thieme, J. (2007). Precursor structures in the crystallization/precipitation processes of CaCO3 and control of particle formation by polyelectrolytes. *Faraday Discuss.* 136, 265–277. doi: 10.1039/b701450c

Rivkin, R. B., and Anderson, M. R. (1997). Inorganic nutrient limitation of oceanic bacterioplankton. *Limnol. Oceanogr.* 42, 730–740. doi: 10.1038/nature07236

Romankevich, E. A. (1984). *Geochemistry of Organic Matter in the Ocean*. Berlin: Springer-Verlag. doi: 10.1007/978-3-642-49964-7

Romero, D., Aguilar, C., Losick, R., and Kolter, R. (2010). Amyloid fibers provide structural integrity to *Bacillus subtilus* biofilms. *Proc. Natl. Acad. Sci. U.S.A.* 107, 2230–2234. doi: 10.1073/pnas.0910560107

Rougeaux, H., Guezennec, M., Mao Che, L., Payri, C., Deslandes, E., and Guezennec, J. (2001). Microbial communities and exopolysaccharides from Polynesian mats. *Mar. Biotechnol.* 3, 181–187. doi: 10.1007/s101260000063

Rougeaux, H., Kervarec, N., Pichon, R., and Guezennec, J. (1999). Structure of the exopolysaccharide of *Vibrio diabolicus* isolated from a deep-sea hydrothermal vent. *Carbohydr. Res.* 322, 40–45. doi: 10.1016/S0008-6215(99)00214-1

Ruby, E. G., and Nealson, K. H. (1977). Luminous bacterium that emits yellow light. *Science* 196, 432–434. doi: 10.1126/science.850787

Ruparell, A., Dubern, J. F., Ortori, C. A., Harrison, F., Halliday, N. M., and Emtage, A. (2016). The fitness burden imposed by synthesizing quorum sensing signals. *Sci. Rep.* 6:33101. doi: 10.1038/srep33101

Russell, L. M., Hawkins, L. N., Frossard, A. A., Quinn, P. K., and Bates, T. S. (2010). Carbohydrate-like composition of submicron atmospheric particles and their production from ocean bubble bursting. *Proc. Natl. Acad. Sci. U.S.A.* 107, 6652–6657. doi: 10.1073/pnas.0908905107

Salek, K., and Gutierrez, T. (2016). Surface-active biopolymers from marine bacteria for potential biotechnological applications. *AIMS Microbiol.* 2, 92–107. doi: 10.3934/microbiol.2016.2.92

Santschi, P. H., Guo, L., Means, J. C., and Ravichandran, M. (1998). "Natural organic matter binding of trace metal and trace organic contaminants in estuaries," in *Biogeochemistry of Gulf of Mexico Estuaries*, eds T. S. Bianchi, J. R. Pennock, and R. Twilley (New York, NY: Wiley), 347–380.

Schaefer, A. L., Greenberg, E. P., Oliver, C. M., Oda, Y., Huang, J. J., Bittan-Banin, G., et al. (2008). A new class of homoserine lactone quorum sensing signals. *Nature* 454, 595–596. doi: 10.1038/nature07088

Schertzer, J. W., Boulette, M. L., and Whiteley, M. (2009). More than a signal: non-signaling properties of quorum sensingmolecules. *Trends Microbiol.* 17, 189–195. doi: 10.1016/j.tim.2009.02.001

Schlekat, C. E., Decho, A. W., and Chandler, G. T. (1998). Sorption of cadmium to bacterial extracellular polymeric sediment coatings under estuarine conditions. *Environ. Toxicol. Chem.* 17, 1867–1874. doi: 10.1002/etc.5620170930

Schlekat, C. E., Decho, A. W., and Chandler, G. T. (1999). Dietary assimilation of cadmium associated with bacterial exopolymer sediment coatings by the estuarine amphipod *Leptocheirus pluinulosus*: effects of Cd concentration and salinity. *Mar. Ecol. Prog. Ser.* 183, 205–216. doi: 10.3354/meps183205

Schlekat, C. E., Decho, A. W., and Chandler, G. T. (2000). Bioavailability of particle-associated Ag, Cd, and Zn to the estuarine amphipod, Leptocheirus plumulosus, through dietary ingestion. *Limnol. Oceanogr.* 45, 11–21. doi: 10.1371/journal.pone.0064060

Schooling, S. R., Hubley, A., and Beveridge, T. J. (2009). Interaction of DNA with biofilm-derived membrane vesicles. *J. Bacteriol.* 191, 4097–4102. doi: 10.1128/JB.00717-08

Selck, H., Decho, A. W., and Forbes, V. E. (1999). Effects of chronic metal exposure and sediment organic matter on digestive absorption efficiencies of cadmium by the deposit-feeding polychaete *Capitella* species I. *Environ. Toxicol. Chem.* 18, 1289–1297. doi: 10.1002/etc.5620180631

Seper, A., Fengler, V. H. I., Roier, S., Wolinski, H., Kohlwein, S. D., Bishop, A. L., et al. (2011). Extracellular nucleases and extracellular DNA play important roles in *Vibrio cholera* biofilm formation. *Mol. Microbiol.* 82, 1015–1037. doi: 10.1111/j.1365-2958.2011.07867.x

Serra, D. O., Richter, A. M., and Hengge, R. (2013). Cellulose as an architectural element in spatially structured *Escherichia coli* biofilms. *J. Bact.* 195, 5540–5554. doi: 10.1128/JB.00946-13

Shanks, A. L., and Reeder, M. L. (1993). Reducing microzones and sulfide production in marine snow. *Mar. Ecol. Prog. Ser.* 96, 43–47. doi: 10.3354/meps096043

Shanks, A. L., and Trent, J. D. (1980). Marine snow: sinking rates and potential role in vertical flux. *Deep Sea Res. Part A. Oceanogr. Res. Papers* 27, 137–143. doi: 10.1016/0198-0149(80)90092-8

Sharif, D. I., Gallon, J., Smith, C. J., and Dudley, E. (2008). Quorum sensing in cyanobacteria: *N*-octanoyl-homoserine lactone release and response, by the epilithic colonial cyanobacterium *Gloeotheca* PCC6909. *ISME J.* 2, 1171–1182. doi: 10.1038/ismej.2008.68

Shaw, E., Hill, D. R., Brittain, N., Wright, D. J., Täuber, U., Marand, H., et al. (2003). Unusual water flux in the extracellular polysaccharide of the cyanobacterium *Nostoc commune*. *Appl Environ. Microbiol.* 69, 5679–5684. doi: 10.1128/AEM.69.9.5679

Simon, M., Grossart, H.-P., Schweitzer, B., and Ploug, H. (2002). Microbial ecology of organic aggregates in aquatic ecosystems. *Aquat. Microb. Ecol.* 28, 175–211. doi: 10.3354/ame028175

Skoog, A., and Benner, R. (1997). Aldoses in various size fractions of marine organic matter: implications for carbon cycling. *Limnol. Oceanogr.* 42, 1803–1813. doi: 10.4319/lo.1997.42.8.1803

Skoog, A., Biddanda, B., and Benner, R. (1999). Bacterial utilization of dissolved glucose in the upper water column of the Gulf of Mexico. *Limnol. Oceanogr.* 44, 1625–1633. doi: 10.3389/fmicb.2013.00318

Skoog, A., Whitehead, K., Sperling, F., and Junge, K. (2002). Microbial glucose uptake and growth along a horizontal nutrient gradient in the North Pacific. *Limnol. Oceanogr.* 47, 1676–1683. doi: 10.4319/lo.2002.47.6.1676

Smith, D. C., Simon, M., Alldredge, A. L., and Azam, F. (1992). Intense hydrolytic enzyme activity on marine aggregates and implications for rapid particle dissolution. *Nature* 359, 139–142. doi: 10.1038/359139a0

Smith, D. J., and Underwood, G. J. C. (1998). Exopolymer production by intertidal epipelic diatoms. *Limnol. Oceanogr.* 43, 1578–1591. doi: 10.4319/lo.1998.43.7.1578

Smith, D. J., and Underwood, G. J. C. (2000). The production of extracellular carbohydrates by estuarine benthic diatoms: the effects of growth phase and light and dark treatment. *J. Phycol.* 36, 321–333. doi: 10.1046/j.1529-8817.2000.99148.x

Sprachta, S., Camoin, G., Golubic, S., and Le Campion, T. (2001). Microbialites in a modern lagoonal environment: nature and distribution, Tikehau atoll (French Polynesia). *Palaeogeogr. Palaeoclimatol. Palaeoecol.* 175, 103–124. doi: 10.1016/S0031-0182(01)00388-1

Steinberger, R. E., and Holden, P. A. (2005). Extracellular DNA in single and multiple-species unsaturated biofilms. *Appl. Environ. Microbiol.* 71, 5404–5410. doi: 10.1128/AEM.71.9.5404-5410.2005

Stewart, P. S. (2002). Diffusion in biofilms. *J. Bacteriol.* 185, 1485–1491. doi: 10.1128/JB.185.5.1485-1491.2003

Stewart, P. S., and Franklin, M. J. (2008). Physiological heterogeneity in biofilms. *Nat. Revs. Microbiol.* 6, 199–210. doi: 10.1038/nrmicro1838

Stoop, J. M. H., Williamson, J. D., and Pharr, D. M. (1996). Mannitol metabolism in plants: a method for coping with stress. *Trends Plant Sci.* 1, 139–144. doi: 10.1016/S1360-1385(96)80048-3

Suja, L. D., Summers, S., and Gutierrez, T. (2017). Role of EPS, dispersant and nutrients on the microbial response and MOS formation in the Subarctic Northeast Atlantic. *Front. Microbiol.* 8:676. doi: 10.3389/fmicb.2017.00676

Sutherland, I. W. (1999). "Polysaccharases in biofilms – sources – action – consequences," in *Microbial Extracellular Polymeric Substances*, eds J. Wingender, T. R. Neu, and H.-C. Flemming (Berlin: Springer Press), 201–216. doi: 10.1007/978-3-642-60147-7_11

Sutherland, I. W. (2001). The biofilm matrix – an immobilized but dynamic microbial environment. *Trends Microbiol.* 9, 222–227. doi: 10.1016/S0966-842X(01)02012-1

Sutherland, I. W. (2016). "EPS – a complex mixture," in *The Perfect Slime – Microbial Extracellular Polymeric Substances*, eds H.-C. Flemming, J. Wingender, and T. R. Neu (London: IWA Publishers), 15–24.

Suzuki, H., Daimon, M., Awano, T., Umekage, S., Tanaka, T., and Kikuchi, Y. (2009). Characterization of extracellular DNA production and flocculation of the marine photosynthetic bacterium *Rhodovulum sulfidophilum*. *Appl. Microbiol. Biotechnol.* 84, 349–356. doi: 10.1007/s00253-009-2031-7

Tang, L., Schramm, A., Neu, T. R., Revsbech, N. P., and Meyer, R. L. (2013). Extracellular DNA in adhesion and biofilm formation of four environmental isolates: a quantitative study. *FEMS Microbiol. Ecol.* 86, 394–403. doi: 10.1111/1574-6941.12168

Taylor, M. W., Schupp, P. J., Baillie, H. J., Charlton, T. S., de Nys, R., Kjelleberg, S., et al. (2004). Evidence for acyl homoserine lactone signal production in bacteria associated with marine sponges. *Appl. Environ. Microbiol.* 70, 4387–4389. doi: 10.1128/AEM.70.7.4387-4389.2004

Teal, J. M., and Howarth, R. W. (1984). Oil spill studies: a review of ecological effects. *Environ. Manag.* 8, 27–44. doi: 10.1007/BF01867871

Teske, A., Ramsing, N. B., Habicht, K., Fukul, M., Küver, J., Jørgensen, B. B., et al. (1998). Sulfate-reducing bacteria and their activities in cyanobacterial mats of Solar lake (Sinai. Egypt). *Appl. Environ. Microbiol.* 64, 2943–2951.

Thavasi, R., and Banat, I. M. (2014). "Biosurfactant and bioemulsifiers from marine sources-," in *Biosurfactants: Research Trends and Applications*, Chap. 5, eds C. N. Mulligan, S. K. Sharma, and M. A. Hardback (Boca Raton, FL: CRC Press), 125–146. doi: 10.1201/b16383-6

Thavasi, R., Jayalakshmi, S., and Banat, I. M. (2011). "Biosurfactant from marine bacterial isolates," in *current Research Technology and Education Topics in Applied Microbiology and Microbial Biotechnology Book Series* –, Vol. 2, ed. A. Mendez-Vilas (Badajoz: Formatex Research Center), 1367–1373.

Thingstad, T. F., Hagström, Å, and Rassoulzadegan, F. (1997). Accumulation of degradable DOC in surface waters: is it caused by a malfunctioning microbial loop? *Limnol. Oceanogr.* 42, 398–404. doi: 10.4319/lo.1997.42.2.0398

Thingstad, T. F., Li Zweifel, U., and Rassoulzadegan, F. (1998). P limitation of heterotrophic bacteria and phytoplankton in the northwest Mediterranean. *Limnol. Oceanogr.* 43, 88–94. doi: 10.4319/lo.1998.43.1.0088

Thornton, D. C. O., Fejes, E. M., Dimarco, S. F., and Clancy, K. M. (2007). Measurement of acid polysaccharides in marine and freshwater samples using alcian blue. *Limnol. Oceanogr. Method.* 5, 73–87. doi: 10.4319/lom.2007.5.73

Thornton, D. C. O., Kopac, S. M., and Long, R. A. (2010). Production and enzymatic hydrolysis of carbohydrates in intertidal sediments. *Aquat. Microb. Ecol.* 60, 109–125. doi: 10.3354/ame01403

Tice, M. M., and Lowe, D. R. (2004). Photosynthetic microbial mats in the 3,416-Myr-old ocean. *Nature* 431, 522–523. doi: 10.1038/nature02888

Tielen, P., Rosenau, F., Wilhelm, S., Jaeger, K.-C., Flemming, H.-C., and Wingender, J. (2013). Extracellular enzymes affect biofilm formation in mucoid *Pseudomonas aeruginosa*. *BMC Microbiol.* 159:221–228.

Tiselius, P., and Kuylenstierna, B. (1996). Growth and decline of a diatom spring bloom phytoplankton species composition, formation of marine snow and the role of heterotrophic dinoflagellates. *J. Plank. Res.* 18, 133–155. doi: 10.1093/plankt/18.2.133

Tolhurst, T. J., Gust, G., and Paterson, D. M. (2002). The influence of an extracellular polymeric substance (EPS) on cohesive sediment stability. *Proc. Marine Sci.* 5, 409–425. doi: 10.1016/S1568-2692(02)80030-4

Torti, A., Lever, M. A., and Jorgensen, B. B. (2015). Origin, dynamics and implications of extracellular DNA pools in marine sediments. *Mar. Genom.* 24, 185–196. doi: 10.1016/j.margen.2015.08.007

Tourney, J., and Ngwenya, B. T. (2014). The role of bacterial extracellular polymeric substances in geomicrobiology. *Chem. Geol.* 386, 115–132. doi: 10.1128/AEM.06568-11

Tran, C., and Hadfield, M. G. (2011). Larvae of *Pocillopora damicornis* (Anthozoa) settle and metamorphose in response to surface-biofilm bacteria. *Mar. Ecol. Prog. Ser.* 433, 85–96. doi: 10.3354/meps09192

Treguer, P., Legendre, L., Rivkin, R. T., Ragueneau, O., and Dittert, N. (2003). "Water column biogeochemistry below the euphotic zone," in *Ocean Biogeochemistry: A Synthesis of the Joint Global Ocean Flux Study (JGOFS)*, ed. J. R. M. Fasham (Berlin: Springer-Verlag), 145–156.

Tunnicliffe, V. (1991). The biology of hydrothermal vents: ecology and evolution. *Oceanogr. Mar. Biol. Ann. Rev.* 29, 319–408.

Tyree, C. A., Hellion, V. M., Alexandrova, O. A., and Allen, J. O. (2007). Foam droplets generated from natural and artificial seawaters. *J. Geophys. Res.* 112:D12204. doi: 10.1029/2006jd007729

Ulrich, M. (2009). *Bacterial Polysaccharides: Current Innovations and Future Trends*. Norwich: Caister Academic Press.

Unabia, C. R. C., and Hadfield, M. G. (1999). Role of bacteria in larval settlement and metamorphosis of the polychaete *Hydroides elegans*. *Mar. Biol.* 133, 55–64. doi: 10.1007/s002270050442

Underwood, G. J. C., Aslam, S. N., Niemi, A., Norman, L., Meiners, K. M., Laybourn-Parry, J., et al. (2013). Broad-scale predictability of carbohydrates and EPS in Antarctic and Arctic sea ice. *Proc. Natl. Acad. Sci. U.S.A.* 110, 15734–15739. doi: 10.1073/pnas.1302870110

Underwood, G. J. C., Boulcott, M., Raines, C. A., and Waldron, K. (2004). Environmental effects on exopolymer production by marine benthic diatoms – dynamics, changes in composition and pathways of production. *J. Phycol.* 40, 293–304. doi: 10.1111/j.1529-8817.2004.03076.x

Underwood, G. J. C., Fietz, S., Papadimitriou, S., Thomas, D. N., and Dieckmann, G. S. (2010). Distribution and composition of dissolved extracellular polymeric substances (EPS) in Antarctic sea ice. *Mar. Ecol. Prog. Ser.* 404, 1–19. doi: 10.3354/meps08557

Underwood, G. J. C., and Paterson, D. M. (2003). The importance of extracellular carbohydrate production by marine epipelic diatoms. *Adv. Bot. Res.* 40, 184–240. doi: 10.1016/S0065-2296(05)40005-1

Underwood, G. J. C., Paterson, D. M., and Parkes, R. J. (1995). The measurement of microbial carbohydrate EPS from intertidal sediments. *Limnol. Oceanogr.* 40, 1243–1253. doi: 10.4319/lo.1995.40.7.1243

Valentine, D. L., Fisher, G. B., Bagby, S. C., Nelson, R. K., Reddy, C. M., Sylva, S. P., et al. (2014). Fallout plume of submerged oil from Deepwater Horizon. *Proc. Natl. Acad. Sci. U.S.A* 111, 15906–15911. doi: 10.1073/pnas.1414873111

van Gerven, N., Klein, R. D., Hultgren, S. J., and Remaut, H. (2015). Bacterial amyloid formation: structural insights into curli biogenesis. *Trends Microbiol.* 23, 693–706. doi: 10.1016/j.tim.2015.07.010

Varenyam, A., Mukherjee, A., and Reddy, M. S. (2010). Characterization of two urease-producing and calcifying *Bacillus* spp. Isolated from cement. *J. Microbiol. Biotechnol.* 20, 1571–1576. doi: 10.4014/jmb.1006.06032

Vasconcelos, C., Warthmann, R., McKenzie, J., Visscher, P. T., Bittermann, A. G., and van Lith, Y. (2006). Lithifying microbial mats in lagoa vermelha, brazil: modern precambrian relics? *Sed. Geol.* 185, 175–183. doi: 10.1016/j.sedgeo.2005.12.022

Verdugo, P. (1994). Polymer gel phase transition in condensation-decondensation of secretory products. *Adv. Polymer Sci.* 110, 145–156. doi: 10.1007/BFb0021131

Verdugo, P. (2012). Marine microgels. *Ann. Rev. Marine Sci.* 4, 375–400. doi: 10.1146/annurev-marine-120709-142759

Verdugo, P., Alldredge, A. L., Azam, F., Kirchman, D. L., Passow, U., and Santschi, P. (2004). The oceanic gel phase: a bridge in the DOM-POM continuum. *Mar. Chem.* 92, 67–85. doi: 10.1016/j.marchem.2004.06.017

Verdugo, P., and Santschi, P. (2010). Polymer dynamics of DOC networks and gel formation in seawater. *Deep-Sea Res. II.* 57, 1486–1493. doi: 10.1016/j.dsr2.2010.03.002

Visscher, P. T., Reid, R. P., and Bebout, B. M. (2000). Microscale observations of sulfate reduction: evidence of microbial activity forming lithified micritic laminae in modern marine stromatolites. *Geology* 28, 919–922. doi: 10.1130/0091-7613(2000)28<919:MOOSRC>2.0.CO;2

Visscher, P. T., and Stolz, J. F. (2005). Microbial mats as bioreactors: populations, processes, and products. *Palaeogeo. Palaeoclim. Palaeoecol.* 219, 87–100. doi: 10.1016/j.palaeo.2004.10.016

Vreeland, R. H., Rosenzweig, W. D., and Powers, D. W. (2000). Isolation of a 250 million-year-old halotolerant bacterium from a primary salt crystal. *Nature* 407, 897–900. doi: 10.1038/35038060

Wagner-Dobler, I., Thiel, V., Eberl, L., Allgaier, M., Bodor, A., Meyer, S., et al. (2005). Discovery of complex mixtures of novel long-chain quorum sensing signals in free-living and host-associated marine alphaproteobacteria. *Chembiochem* 6, 2195–2206. doi: 10.1002/cbic.200500189

Waharte, F., Steenkeste, K., Briandet, R., and Fontaine-Aupart, M. P. (2010). Diffusion measurements inside biofilms by image-based fluorescence recovery after photobleaching (FRAP) analysis with a commercial confocal laser scanning microscope. *Appl. Environ. Microbiol.* 76, 5860–5869. doi: 10.1128/AEM.00754-10

Walker, B. D., Beaupré, S. R., Guilderson, T. P., McCarthy, M. D., and Druffel, E. R. M. (2016). Pacific carbon cycling constrained by organic matter size, age and composition relationships. *Nat. Geosci.* 9, 888–891. doi: 10.1038/ngeo2830

Waters, C. M., and Bassler, B. L. (2005). Quorum sensing: cell-to-cell communication in bacteria. *Annu. Revs. Cell Dev. Biol.* 21, 319–346. doi: 10.1146/annurev.cellbio.21.012704.131001

Werlin, R., Priester, J. H., Mielke, R. E., Kramer, S., Jackson, S., Stoimenov, P. K., et al. (2011). Biomagnification of cadmium selenide quantum dots in a simple experimental microbial food chain. *Nat. Nanotechnol.* 6, 65–71. doi: 10.1038/nnano.2010.251

Whalan, S., and Webster, N. S. (2014). Sponge larval settlement cues: the role of microbial biofilms in a warming ocean. *Sci. Rep.* 4:4072. doi: 10.1038/srep04072

Whitchurch, C. B., Tolker-Nielsen, T., Ragas, P. C., and Mattick, J. S. (2002). Extracellular DNA required for bacterial biofilm formation. *Science* 295:1487. doi: 10.1126/science.295.5559.1487

Whitfield, C. (2006). Biosynthesis and assembly of capsular polysaccharides in *Escherichia coli*. *Annu. Rev. Biochem.* 75, 39–68. doi: 10.1146/annurev.biochem.75.103004.142545

Widenfalk, A., Lundqvist, A., and Goedkoop, W. (2008). Sediment microbes and biofilms increase the bioavailability of chlorpyrifos in *Chironomus riparius* (Chironomidae, Diptera). *Ecotox. Environ. Saf.* 71, 490–497. doi: 10.1016/j.ecoenv.2007.10.028

Williams, P. M., and Druffel, E. R. M. (1987). Radiocarbon in dissolved organic matter in the central North Pacific Ocean. *Nature* 330, 246–248. doi: 10.1038/330246a0

Wilson, T. W., Ladino, L. A., Alpert, P. A., Breckels, M. N., Brooks, I. M., Browse, J., et al. (2015). A marine biogenic source of atmospheric ice-nucleating particles. *Nature* 525, 234–238. doi: 10.1038/nature14986

Wotton, R. S. (2004). The ubiquity and many roles of EPS (EPS) in aquatic systems. *Oceanogr. Mar. Biol. Annu. Revs.* 42, 57–94. doi: 10.1201/9780203507810.ch3

Wurl, O. (2009). *Practical Guidelines for the Analysis of Seawater*. Boca Raton, FL: CRC Press. doi: 10.1201/9781420073072

Wurl, O., and Holmes, M. (2008). The gelatinous nature of the sea-surface microlayer. *Mar. Chem.* 110, 89–97. doi: 10.1016/j.marchem.2008.02.009

Wurl, O., Miller, L., and Vagle, S. (2011). Production and fate of transparent exopolymer particles in the ocean. *J. Geophys. Res.* 116:C00H13. doi: 10.1111/j.1462-2920.2012.02873.x

Yang, C., Fang, S., Chen, D., Wang, J., Liu, F., and Xia, C. (2016). The possible role of bacterial signal molecules N-acyl homoserine lactones in the formation of diatom-biofilm (*Cylindrotheca* sp.). *Mar. Poll. Bull.* 107, 118–124. doi: 10.1016/j.marpolbul.2016.04.010

Yang, M., Stipp, S. L. S., and Harding, J. (2008). Biological control on calcite crystallization by polysaccharides. *Cryst. Growth Des.* 8, 4066–4074. doi: 10.1016/j.jsb.2015.03.007

Zhang, G., Zhang, F., Ding, G., Li, J., Guo, X., Zhu, J., et al. (2012). Acyl homoserine lactone-based quorum sensing in a methanogenic archaeon. *ISME J.* 6, 1336–1344. doi: 10.1038/ismej.2011.203

Zhang, S., Xu, C., and Santschi, P. H. (2008). Chemical composition and Thorium-234 (IV) binding of extracellular polymeric substances (EPS) by the marine diatom *Amphora* sp. *Mar. Chem.* 106, 967–976.

Zhang, W., Sun, J., Ding, W., Lin, J., Tian, R., Lu, L., et al. (2015). Extracellular matrix-associated proteins form an integral and dynamic system during *Pseudomonas aeruginosa* biofilm development. *Front. Cell. Infect. Microbiol.* 5:40. doi: 10.3389/fcimb.2015.00040

Zheng, G., Vad, B. S., Dueholm, M. S., Christiansen, G., Nilsson, M., Tolker-Nielsen, T., et al. (2015). Functional bacterial amyloid increases *Pseudomonas* biofilm hydrophobicity and stiffness. *Front. Microbiol.* 6:1099. doi: 10.3389/fmicb.2015.01099

Ziervogel, K., McKay, L., Rhodes, B., Osburn, C. L., Dickson-Brown, J., Arnosti, C., et al. (2012). Microbial activities and dissolved organic matter dynamics in oil-contaminated surface seawater from the Deepwater Horizon oil spill site. *PLoS ONE* 7:e34816. doi: 10.1371/journal.pone.0034816

Zippel, B., and Neu, T. R. (2011). Characterization of glycoconjugates of extracellular polymeric substances in Tufa-associated biofilms by using fluorescence lectin-binding analysis. *Appl. Environ. Microbiol.* 77, 505–516. doi: 10.1128/AEM.01660-10

ZoBell, C. E., and Allen, E. C. (1935). The significance of marine bacteria in the fouling of submerged surfaces. *J. Bact.* 29, 239–251.

Zohary, T., and Robarts, R. D. (1998). Experimental study of microbial P limitation in the eastern Mediterranean. *Limnol. Oceanogr.* 43, 387–395. doi: 10.1007/s00248-015-0713-5

Zosim, Z., Gutnick, D., and Rosenberg, E. (1983). Uranium binding by emulsan and emulsanosols. *Biotechnol. Bioeng.* 25, 1725–1735. doi: 10.1002/bit.260250704

Conflict of Interest Statement: The authors declare that the research was conducted in the absence of any commercial or financial relationships that could be construed as a potential conflict of interest.

frontiers in Microbiology

ORIGINAL RESEARCH
published: 31 January 2017
doi: 10.3389/fmicb.2017.00065

Combined Carbohydrates Support Rich Communities of Particle-Associated Marine Bacterioplankton

Martin Sperling[1,2,3], Judith Piontek[1,3], Anja Engel[3], Karen H. Wiltshire[2], Jutta Niggemann[4], Gunnar Gerdts[2] and Antje Wichels[2]*

[1] Alfred-Wegener-Institute Helmholtz Centre for Polar and Marine Research, Bremerhaven, Germany, [2] Biologische Anstalt Helgoland, Alfred-Wegener-Institute Helmholtz-Center for Polar and Marine Research, Helgoland, Germany, [3] Biological Oceanography, Marine Biogeochemistry, GEOMAR Helmholtz Centre for Ocean Research Kiel, Kiel, Germany, [4] Research Group for Marine Geochemistry (ICBM-MPI Bridging Group), Institute for Chemistry and Biology of the Marine Environment, University of Oldenburg, Oldenburg, Germany

Carbohydrates represent an important fraction of labile and semi-labile marine organic matter that is mainly comprised of exopolymeric substances derived from phytoplankton exudation and decay. This study investigates the composition of total combined carbohydrates (tCCHO; >1 kDa) and the community development of free-living (0.2–3 μm) and particle-associated (PA) (3–10 μm) bacterioplankton during a spring phytoplankton bloom in the southern North Sea. Furthermore, rates were determined for the extracellular enzymatic hydrolysis that catalyzes the initial step in bacterial organic matter remineralization. Concentrations of tCCHO greatly increased during bloom development, while the composition showed only minor changes over time. The combined concentration of glucose, galactose, fucose, rhamnose, galactosamine, glucosamine, and glucuronic acid in tCCHO was a significant factor shaping the community composition of the PA bacteria. The richness of PA bacteria greatly increased in the post-bloom phase. At the same time, the increase in extracellular β-glucosidase activity was sufficient to explain the observed decrease in tCCHO, indicating the efficient utilization of carbohydrates by the bacterioplankton community during the post-bloom phase. Our results suggest that carbohydrate concentration and composition are important factors in the multifactorial environmental control of bacterioplankton succession and the enzymatic hydrolysis of organic matter during phytoplankton blooms.

Keywords: bacterioplankton community, remineralization, extracellular enzymes, phytoplankton bloom, North Sea, Helgoland Roads, organic matter, spring bloom

OPEN ACCESS

Edited by:
Tony Gutierrez, Heriot-Watt University, UK

Reviewed by:
Guang Gao, Nanjing Institute of Geography and Limnology (CAS), China
Jeremy Andre Fonvielle, Leibniz Institute of Freshwater Ecology and Inland Fisheriess (LG), Germany

****Correspondence:***
Martin Sperling
msperling@geomar.de

Specialty section:
This article was submitted to Aquatic Microbiology, a section of the journal Frontiers in Microbiology

Received: *14 September 2016*
Accepted: *10 January 2017*
Published: *31 January 2017*

Citation:
Sperling M, Piontek J, Engel A, Wiltshire KH, Niggemann J, Gerdts G and Wichels A (2017) Combined Carbohydrates Support Rich Communities of Particle-Associated Marine Bacterioplankton. Front. Microbiol. 8:65. doi: 10.3389/fmicb.2017.00065

INTRODUCTION

It is well established that marine bacterioplankton communities maintain high genetic diversity. As for phytoplankton (Hutchinson, 1961), little is understood, however, how such high diversities are maintained or what determines the community composition *in situ*. In seasonal seas, phytoplankton development and temperature have repeatedly been reported to structure

bacterioplankton communities (Pinhassi et al., 2004; Rooney-Varga et al., 2005; Sapp et al., 2007; Rink et al., 2011). However, these two factors are not sufficient to explain the high diversity of marine bacterioplankton.

Reactive organic matter is released by phytoplankton and bacteria, often upon viral lysis and grazing, and is a major energy and carbon source for marine bacterioplankton communities. How structure and composition of bacterioplankton communities are influenced by spatial and temporal differences in organic matter (OM) composition is only poorly resolved. Numerous compounds in the vast pool of marine OM may support species-rich bacterioplankton communities, which are, in turn, able to efficiently remineralize large portions of the OM. In laboratory experiments, bacterioplankton exhibit specific OM uptake at a class and clade level (Pernthaler et al., 2002; Elifantz et al., 2005; Alonso-Sáez and Gasol, 2007). Single low molecular weight (LMW) compounds have been shown to structure bacterial communities (Gómez-Consarnau et al., 2012). The *in situ* structuring of bacterial communities is thought to be more complicated, involving a combination of available substrates, inorganic nutrients, physical factors and competition among bacteria (Gómez-Consarnau et al., 2012).

While large portions of marine OM are still chemically uncharacterized, carbohydrates have been identified as the largest fraction of characterized marine OM (Pakulski and Benner, 1994; Amon and Benner, 2003). Recent studies of the transcriptomic activity of marine bacterioplankton suggest that bacterial community composition and diversity are related to the genus-specific expression of metabolic genes (Teeling et al., 2012; Gifford et al., 2013), in particular those for carbohydrate-active enzymes. This allows for a succession of diverse bacterial strains that thrive on various forms of algal-derived OM during the spring phytoplankton bloom in the North Sea (Teeling et al., 2012).

Bacteria can take up LMW compounds as large as 0.6–0.8 kDa through porins and slightly larger compounds via TonB-dependent transporters (Weiss et al., 1991; Teeling et al., 2012) to meet their energy and carbon demands. Compounds with higher molecular weight must be hydrolyzed into smaller subunits by extracellular enzymes, prior to uptake. These are released by bacteria into the environment or attached to the outer cell membrane (Chróst, 1991). Heterotrophic bacteria have been found to favor HMW- over LMW-dissolved organic carbon (DOC), likely because HMW-DOC is less diagenetically altered and therefore more reactive and more usable (Amon and Benner, 1996). This underpins the importance of enzymatic hydrolysis as the first step in the bacterial degradation of complex carbohydrates. In addition to control through substrate availability, there is a close link between bacterioplankton species richness and diversity of β-glucosidase (β-Glcase) isoenzymes (Arrieta and Herndl, 2002), which likely influences the effectiveness of substrate utilization.

Understanding the interaction between bacterioplankton and diverse OM is important for our understanding of biogeochemistry (Azam et al., 1983). It is also an urgent matter, as there is growing evidence for the high potential of ocean acidification to alter phytoplankton OM production (Borchard and Engel, 2012; Engel et al., 2014), combined with changes in bacterial community composition (Allgaier et al., 2008; Krause et al., 2012; Sperling et al., 2013) and bacterial degradation activity (Grossart et al., 2006a; Tanaka et al., 2008; Piontek et al., 2013).

This field study aims to fill the gap between laboratory studies of single bacterial groups or carbohydrates and results inferred from *in situ* meta-transcriptomics. It investigates the influence of carbohydrate composition and concentration in seawater on the community structure of free-living (FL) and particle-associated (PA) bacteria by combining, for the first time, a detailed analysis of the composition of total combined carbohydrates (tCCHO; >1 kDa) using high-performance anion-exchange chromatography coupled with pulsed amperometric detection (HPAEC-PAD) and bacterial community analysis using Automated Ribosomal Intergenic Spacer Analysis (ARISA) and Catalyzed Reporter Deposition-Fluorescence *In Situ* Hybridization (CARD-FISH). Furthermore, it investigates the extracellular enzymatic activity of the bacterial community in relation to carbohydrates and the wide range of physicochemical and biological factors at the transition from winter to spring in the temperate North Sea.

MATERIALS AND METHODS

Sampling

Surface water (∼1 m depth) was collected in a 10-L plastic carboy in the morning twice a week from February 2nd to May 18th 2010 from a research vessel at the long-term North Sea monitoring station "Helgoland Roads" between the islands of Helgoland (54° 11′03″N, 7° 54′00″E) in the German Bight, North Sea (see Wiltshire and Manly, 2004; Wiltshire et al., 2008).

DNA Collection and Extraction

After pre-filtration through 10 μm-pore size filters, PA bacteria were collected by filtering 2 L of seawater through 3-μm filters (TCTP and TSTP, 47 mm, Millipore, Billerica, MA, USA). To collect FL bacteria, 500 mL of the resulting filtrate was filtered through a 0.2-μm filter (GTTP, 47 mm, Millipore, Billerica, MA, USA). All filters were cut into three equal pieces using sterilized pincers and scalpel and stored in a 2 mL-reaction tube at −20°C until processing.

The DNA from all three filter pieces was extracted simultaneously using lysozyme followed by phenol-chloroform-isoamylalcohol purification (as described in Sapp et al., 2007) with the addition of 0.002 mg of sterile Polyvinylpolypyrrolidone (PVPP) to bind larger contaminants. The DNA was re-diluted in 20 μL of PCR-grade water and the concentration measured using a NanoQuant Plate and an infinite M200 plate reader (both Tecan, Switzerland).

Bacterial Community Analyses

Automated Ribosomal Intergenic Spacer Analysis (ARISA), as described in Sperling et al. (2013) was used to investigate PA (3–10 μm) and FL (0.2–3 μm) bacterial communities. In brief, the Intergenic Spacer (IGS)-region was amplified using

the forward primer L-D-Bact-132-a-A-18 (5′-CCG GGT TTC CCC ATT CGG-3′) and the fluorescence-labeled reverse primer S-D-Bact-1522-b-S-20 (5′-TGC GGC TGG ATC CCC TCC TT-3′) described by Ranjard et al. (2000). Length separation was achieved in a 4300 DNA analyzer (Li-Cor, Bad Homburg, Germany) using polyacrylamide gels (5.5% ready to use matrix, Li-Cor Biosciences, Bad Homburg, Germany). The PCR products were amended with Blue Stop Solution (Li-Cor, Bad Homburg, Germany) in a 1:1 ratio, and the size standard IRDye®700, 50–1500 bp (Li-Cor, Bad Homburg, Germany), was applied. The wells were loaded with 0.25 or 0.5 μL of samples, depending on the amount needed to visualize bands clearly. Values obtained from the application of a 0.5 μL sample were divided by two prior to data analysis. The volume of applied sample was confirmed to have no significant effect on Sørensen-similarities in the PA- (ANOSIM, $R = 0.12$, $p = 0.20$) and FL- (ANOSIM, $R = -0.15$, $p = 0.72$) fractions. The software package BioNumerics (Applied Math, Sint-Martens-Latem, Belgium) was used to analyze the gel images. The bands with a length between 300 and 1500 bp were binned into size classes (termed "ARISA-band-classes") to correct for minor length variations of the IGS regions between lineages with almost identical 16S rDNA-sequences. Bins of 3 bp were used for fragments up to 700 bp in length, bins of 5 bp were used for fragments between 700 and 1,000 bp, and bins of 10 bp were used for fragments larger than 1,000 bp (Brown et al., 2005; Kovacs et al., 2010). In this way, the total number of bands, i.e., community richness, was reduced by approximately 4.5 and 1% for the PA and FL bacterial data, respectively.

Values for Catalyzed Reporter Deposition Fluorescence *In Situ* Hybridization (CARD-FISH) of non-prefiltered samples on 0.2-μm filters were taken from Teeling et al. (2016).

Analysis of Physicochemical and Phytoplankton Parameters

Physicochemical and phytoplankton parameters were investigated on a weekday basis (Monday–Friday) as part of the Helgoland Roads LTER time series, which is also accessible via the open database PANGEA[1] (Wiltshire and Manly, 2004; Wiltshire et al., 2008). Surface water samples were investigated using standard colorimetric methods (Grasshoff et al., 1999). Salinity was measured by converting conduction, as measured with an inductive salinometer (GDTAutosal8400B Salinometer, Guildline, ON, Canada), to salinity using UNESCO tables (Cox and Culkin, 1976; Wiltshire et al., 2008). A fluorometer (bbe Moldaenke, Kiel-Kronshagen, Germany) was used to measure Chl *a* concentrations (Wiltshire et al., 2009). Inorganic nutrients (phosphate, silicate, ammonium, nitrate, and nitrite) were measured in the laboratory using the methods of Grasshoff et al. (1999) and Knefelkamp et al. (2007). Measurement of pH according to the National Bureau of Standards (NBS) scale was performed after samples were brought back to the laboratory. The pH difference due to the difference between *in situ* temperature and measurement temperature in the lab was corrected after the method of Gieskes (1969) using the following equation:

$$\mathrm{pH}_{\text{in situ}} = \mathrm{pH}_{\text{measured}} + 0.0114\,(t_{\text{measured}} - t_{\text{in situ}})$$

where t_{measured} is the temperature in °C, measured simultaneously with pH using a combined electrode (ProLab 3000 pH meter, IoLine pH combination electrode with temperature sensor) calibrated with standard buffer solutions (all materials: SI Analytics, Mainz, Germany).

Particulate and Dissolved and Total Organic Carbon

Particulate carbon was collected on pre-combusted GF/F filters (25 mm, Whatman Nuclepore), which were stored at −20°C until analysis. The filtration volume (80–380 mL) was adjusted to the particle loading of the seawater. Filters were treated with 200 μL of carbon-free HCl (0.2 N) to remove inorganic carbon and dried at 60°C for approximately 48 h. After drying, filters were packed into small Zn-cartridges and analyzed using an elemental analyzer (Euro EA 3000, EuroVector Instruments & Software, Italy).

For analysis of DOC concentration, seawater was filtered through combusted (400°C, 4 h) GF/F filters (0.7 μm, Whatman), and 15 mL was sealed in combusted glass ampoules. Samples were stored at −80°C in the dark. Some of the ampoules were damaged during transport to the mainland, resulting in reduced temporal resolution. Acidified samples (pH 2, HCl) were analyzed using high-temperature catalytic oxidation (Sugimura and Suzuki, 1988) on a Shimadzu total organic carbon (TOC)-VCPH instrument with analytical precision better than 5% for three replicate samples. Accuracy was tested in each run against deep Atlantic seawater reference material (D.A. Hansell, University of Miami, FL, USA) and was better than 5%.

Total organic carbon (TOC) was calculated as the sum of particulate organic carbon (POC) and DOC.

Carbohydrate Analysis

Analysis of total combined carbohydrates (tCCHO; >1 kDa), which are a portion of high molecular weight organic matter (HMW-OM), was performed according to Engel and Händel (2011). In brief, two replicate seawater samples (20 mL each) were transferred to pre-combusted glass vials using pre-rinsed disposable syringes and immediately stored at −20°C until processing of the samples. Samples were desalinated using membrane dialysis (1 kDa MWCO, Spectra Por). Carbohydrate monomers that were produced from acid hydrolysis (1 M HCl) and subsequent acid evaporation (N_2), were analyzed on a Dionex ICS3000 system combining high performance anion exchange chromatography (HPAEC) and pulsed amperometric detection (PAD) using a Dionex CarboPac PA10 analytical column (2 × 250 mm) coupled to a Dionex CarboPac PA10 guard column (2 × 50 mm). The autosampler (Dionex AS50) was maintained at 8°C, and 17.5μL of sample was injected for each analysis. After every second sample, 17.5 μL of a mixed sugar solution was injected for standardization. Blanks (ultrapure water; Milli-Q) were analyzed using the same procedure used

[1]http://www.pangea.de

for the samples and subtracted from sample concentration. We identified 12 carbohydrate monomers (**Supplementary Table S1**). The neutral sugars arabinose (Ara), fucose (Fuc), galactose (Gal), glucose (Glc), and rhamnose (Rha) were investigated, as well as the co-eluting sugars mannose and xylose (Man/Xyl). The acidic sugars galacturonic acid (GalUA), gluconic acid (GlcA), glucuronic acid (GlcUA) and muramic acid (Mur) were measured. In addition, the concentrations of the two amino sugars galactosamine (GalN) and glucosamine (GlcN) were determined. The detection limit for the method was 1 nmol L^{-1}. Values for all sugar components and standard deviations can be found in **Supplementary Table S2**.

Extracellular Enzyme Activity

The activity of extracellular enzymes was determined by the use of fluorogenic substrate analogs (Hoppe, 1983). The rates of β-glucosidase, leucine (leu)-aminopeptidase, and alkaline phosphatase were assessed from the hydrolysis of 4-methylumbelliferyl-β-glucopyranoside, L-leucyl-4-methylcoumarinylamid-hydrochlorid and 4-methylumbelliferyl-phosphate, respectively. The substrate analogs were added to seawater samples at final concentrations of 1, 5, 10, 20, 50, 80, 100, and 200 μmol L^{-1} to determine enzyme kinetics. To measure fluorescence, the infinite M200 plate reader (Tecan, Männedorf, Switzerland) was used. The fluorescence emitted by 4-methylumbelliferone (MUF) was detected at 365 nm excitation and 440 nm emission wavelengths, and that of 7-amino-4-methyl-coumarine (AMC) was detected at 380 nm excitation and 440 nm emission wavelengths. Fluorescence units were converted into concentrations of MUF or AMC after calibration with standard solutions. Enzymatic rates were calculated from the increase in MUF or AMC concentration, over time. An initial fluorescence measurement was conducted immediately after the addition of the substrate analog, followed by two measurements within 4 h of incubation in the dark at the approximate *in situ* temperature for the sampling day (1–8°C). The initial fluorescence was subtracted as background fluorescence from the fluorescence measured at each time point. The slope of the linear regression between incubation time and the concentration of the fluorescent marker was applied for rate calculations. Experimental data were fitted using the Michaelis–Menten equation to determine the maximum velocity (V_{max}) of the enzymatic reactions. To estimate the amount of substrate hydrolyzed by β-glucosidase (β-Glcase) during the post-bloom phase, we calculated the enzymatic rate for each day using a mean post-bloom concentration of 2.13 μmol L^{-1} Glc. The resulting mean rate (83.05 nmol L^{-1} d^{-1}) was multiplied by the number of days (26) in the post-bloom phase.

Statistical Analysis

For multivariate statistical analyses, the software package PRIMER v.6 and the add-on PERMANOVA+ (both PRIMER-E, Auckland, New Zealand) were used. The analyses were performed using Sørensen-similarity-matrices generated from square-root transformed ARISA-band-class data. To test for community assemblage differences between phytoplankton bloom phases, permutational multivariate analysis of variance (PERMANOVA) was applied. Distance-based multivariate multiple regression (DistLM) was used to calculate correlations of community composition to environmental factors, and distance-based redundancy analysis (dbRDA) was used to visualize these correlations. For this analysis, the highly collinear combined carbohydrates (colCHO, Pearson $r > 0.8$) Fuc, Rha, Gal, Glc, GalN, GlcN, and GlcUA were pooled.

RESULTS

Phytoplankton Bloom Development

Chlorophyll *a* (Chl *a*) was used to determine the state of the phytoplankton bloom. After low Chl *a* concentrations (<1 μg L^{-1}) in February, a diatom-dominated spring phytoplankton bloom developed at the long-term monitoring station "Helgoland Roads" (54° 11′03″N, 7° 54′00″E). Bloom development started in mid-March and reached Chl *a* values of up to 12 μg L^{-1} in April (**Figure 1A**). The onset of the bloom coincided with a strong peak in dissolved inorganic phosphate (DIP) concentration and a slight increase in sea surface temperature (**Figures 1C,D**). The bloom development was accompanied by rising seawater pH. Salinity decreased from approximately 34 in February to approximately 31 at the end of April (**Figure 1B**). The phytoplankton bloom terminated in late April, likely due to the depletion of DIP and silicate (SiO_2) (**Figure 1D**).

Organic Carbon and Carbohydrate Composition

During the bloom, POC increased with diatom abundance, reaching a maximum of 54 μmol L^{-1} (**Figure 1B**), while DOC showed a maximum value of 151 μmol L^{-1} at the peak of the bloom. TOC values were calculated as the sum of POC and DOC and reached maximum values of 135 and 187 μmol L^{-1} before and after the phytoplankton bloom, respectively. Bloom development resulted in the accumulation of tCCHO, which contributed up to 14% of TOC in the post-bloom phase (**Figure 2A**). The subsequent decline in tCCHO and POC lagged behind the decrease in diatom cell numbers and Chl *a* (**Figures 1A,B** and **2A**). The carbon contribution of tCCHO to TOC strongly increased during the bloom (**Figure 2A**). Several carbohydrates in HMW-OM showed very similar temporal dynamics (Pearson $r > 0.8$) during spring 2010. Therefore, for the statistical analysis, glucose, galactose, fucose, rhamnose, galactosamine, glucosamine, and glucuronic acid were pooled into a single factor and designated as collinear CHO (colCHO). Its concentration strongly increased toward the end of the phytoplankton boom and maintained high values during the early post-bloom phase (**Figures 2B–D**). In contrast, Ara showed concentrations near the detection limit during the entire study, while GalUA revealed strong dynamics unrelated to the phytoplankton bloom. Throughout the bloom, the composition of tCCHO was dominated by neutral sugars (60–90 mol%). Glc alone contributed an average 53 mol%, with maximum concentrations of 3 μmol monomer

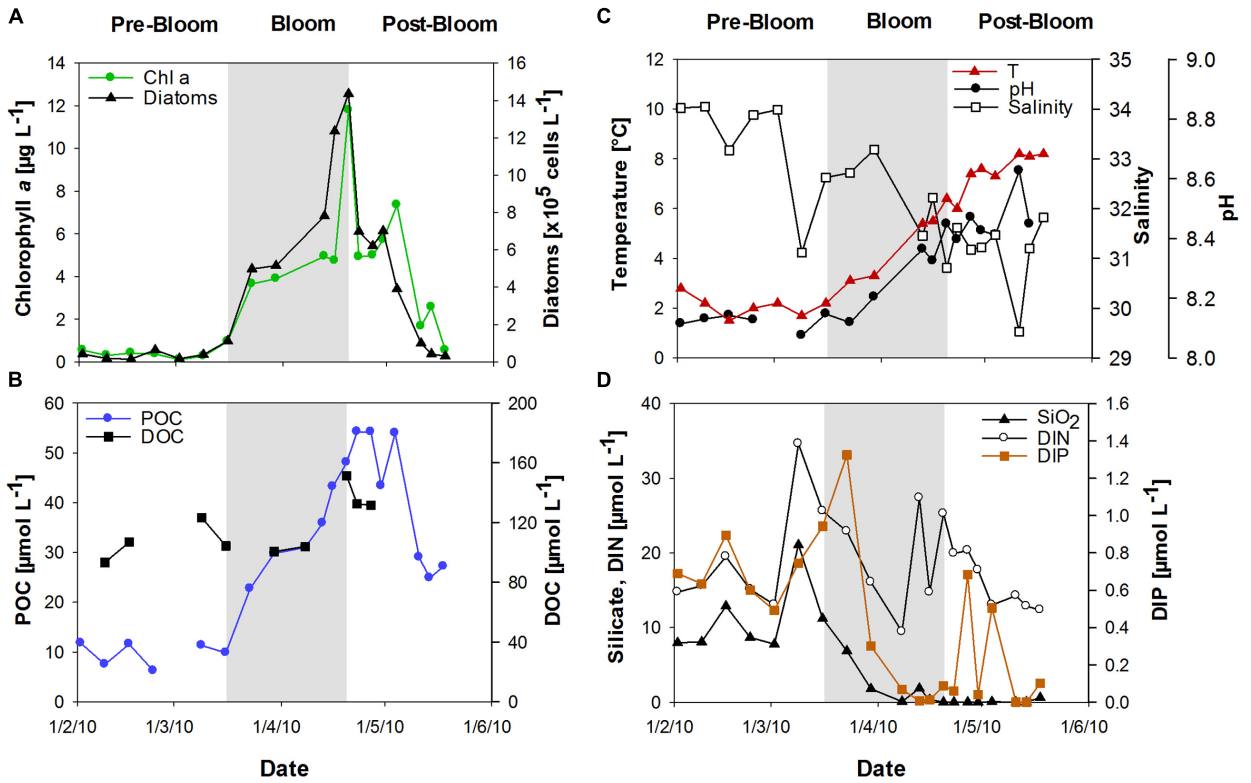

FIGURE 1 | Development of the spring bloom at Helgoland Roads in 2010. (A) Chlorophyll *a* (Chl *a*) concentrations and diatom abundance, **(B)** Temperature, salinity and seawater pH, **(C)** Particulate organic carbon (POC) and dissolved organic carbon (DOC), **(D)** Inorganic nutrients comprising silicate (SiO_2), dissolved inorganic nitrogen (DIN) and dissolved inorganic phosphorous (DIP).

equivalent L^{-1} in the late bloom and post-bloom phase (**Figure 2A**). Concentrations of Man/Xyl, Fuc and Gal increased with the onset of the phytoplankton bloom and maintained high values during the post-bloom phase, though maximum concentrations of 0.2–0.4 µmol L^{-1} were approximately an order of magnitude lower than that of Glc (**Figure 2B**). Man/Xyl and Fuc showed similar mean concentrations of 0.13 and 0.16 µmol monomer equivalent L^{-1}, respectively. In the late post-bloom period, Man/Xyl strongly increased, while Fuc decreased rapidly. Rha and Ara showed comparatively low concentrations $\leq$ 0.1 µmol L^{-1} throughout the investigation period.

The acidic sugar GalUA was a major component of tCCHO before the onset of the bloom in February, followed by strongly declining concentrations in March (**Figure 2C**). Concentrations increased again until the end of the phytoplankton bloom, reaching values of 0.2–0.3 µmol L^{-1}, comparable to the concentrations of most neutral sugars, in April (**Figure 2C**). The other acidic sugars GlcA, Mur, and GlcUA were only present in very low concentrations (below 0.02 µmol L^{-1}). Of those, only GlcUA increased slightly in concentration toward the end of the bloom and maintained an elevated level during the post-bloom. Amino sugars were only present at low concentrations (below 0.1 µmol L^{-1}) (**Figure 2D**). However, both, GalN and GlcN concentrations increased toward the end of the bloom, with GlcN reaching values of up to 0.07–0.08 µmol L^{-1}, higher than the concentrations of most acidic sugars during the late bloom and post-bloom phases.

Bacterial Community Composition

Particle-associated and FL bacterial communities were significantly different during the post-bloom phase (PERMANOVA; $p = 0.008$, 400 permutations) but were similar during the pre-bloom (PERMANOVA; $p = 0.092$, 10 permutations) and bloom phases (PERMANOVA; $p = 0.141$, 414 permutations). Both, PA and FL bacterial community significantly changed between phytoplankton bloom phases (PERMANOVA; $p = 0.003$, 992 permutations and $p < 0.001$; 999 permutations, respectively), revealing distinct temporal successions. DistLM shows that the development of PA communities is significantly related to three environmental variables. Apart from an abrupt change along a POC gradient (explaining ~31% of total community variability) at the onset of the phytoplankton bloom, PA bacteria showed the strongest community development during the post-bloom phase, following a gradient of temperature (explaining ~20%) and carbohydrates (colCHO, explaining ~9%) (**Table 1**, **Figure 3**). The FL bacterial community composition strongly changed during the ongoing phytoplankton bloom and during the post-bloom phase, mainly tracking with diatom abundance

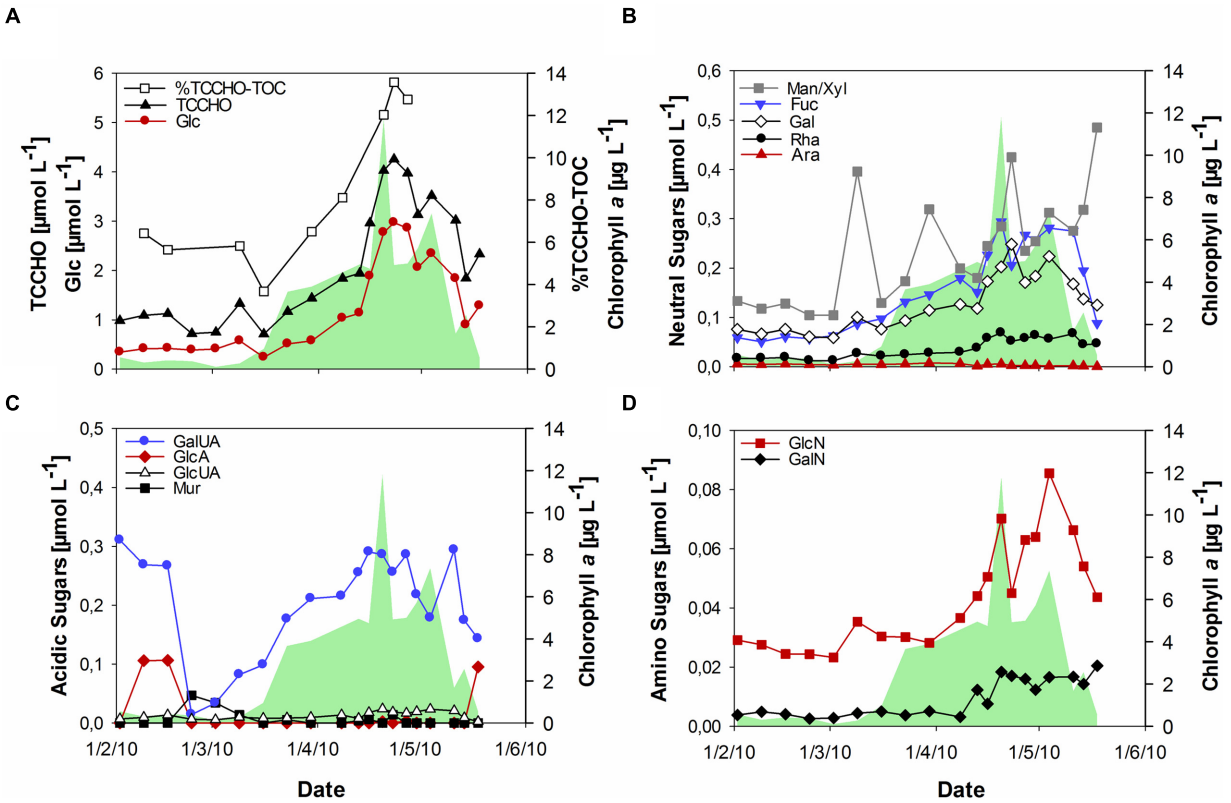

FIGURE 2 | Concentrations of combined carbohydrates >1 kDa (TCCHO) during the spring bloom. (A) Concentrations of TCCHO and combined glucose (Glc) and share of TCCHO in TOC (% TCCHO-TOC, TOC = POC + DOC) **(B)** Concentrations of neutral sugars including mannose/xylose (Man/Xyl), fucose (Fuc), galactose (Gal), rhamnose (Rha), and arabinose (Ara) **(C)** Concentrations of acidic sugars including gluconic acid (GlcA), glucuronic acid (GlcUA), galacturonic acid (GalUA), and muramic acid (Mur) **(D)** Amino sugars including glucosamine (GlcN) and galactosamine (GalN). The green shaded area represents concentrations of chlorophyll *a*.

(∼14%) and temperature (∼34%), respectively (**Table 1**, **Figure 3**). In total, significant environmental factors explained ∼60 and ∼48% of the variability in PA and FL communities, respectively. The richness of PA bacteria increased with rising Chl *a* and tCCHO concentrations, revealing a linear correlation (R^2 = 0.3779, p = 0.0093) between colCHO concentration and PA bacterial richness (**Supplementary Figure S1**). The PA richness reached a maximum approximately 1.5 weeks after the breakdown of the bloom at persistently high concentrations of tCCHO and was followed by a steep decrease in both richness and tCCHO thereafter (**Figures 2A** and **4**). In contrast, the richness of FL bacteria did not resemble the temporal development of Chl *a* or diatom cell numbers during the bloom (**Figure 4**).

Of the investigated microbial clades (CARD-FISH), only GAM42 (*Gammaproteobacteria*) showed a direct positive correlation to colCHO and to GalUA (**Supplementary Table S3**). Notably, these also correlated to temperature and pH, as well as POC and Chl *a*. Furthermore, they were correlated positively to all investigated extracellular enzymes. Although in total, *Roseobacter* did not correlate to any investigated parameter, the SAR11 subgroup correlated to pH and silicate. Bacteroidetes correlated to Chl *a*.

Extracellular Enzyme Activity

The activity of extracellular enzymes was near the detection limit from February to mid-March (**Figure 5**). With the onset of the phytoplankton bloom, leucine-aminopeptidase (LAPase) activity increased and maintained high levels during the bloom, reaching a maximum of 0.95 µmol L^{-1} h^{-1} in the post-bloom phase. The activity of β-glucosidase (β-Glcase) increased toward the end of the bloom, concurrent with a strong increase in tCCHO concentrations (**Figure 2A**). A maximum rate of 0.08 µmol L^{-1} h^{-1} was determined on May 11th. The amount of substrate hydrolyzed by β-Glcase during the post-bloom phase was estimated as approximately 2.16 µmol L^{-1}, equivalent to approximately 72% of the total combined glucose that accumulated during the bloom (**Figure 2A**). The rates of extracellular phosphatase (phos), increased rapidly after phosphate depletion (**Figures 1D** and **5**) at the end of the bloom, indicating the enhanced use of organic phosphorous by bacteria and phosphatase-releasing phytoplankton groups. The co-incidence of phosphate depletion with a pronounced increase in phosphatase activity correlates well with the increase in phosphate transporters, as reported in Teeling et al. (2012) for the year 2009. This implies that the enzymatic degradation

TABLE 1 | DistLM showing the correlation of ARISA-band-diversity (Sørensen) to environmental factors (sequential addition to the model).

Variable	Adj. R^2	Pseudo-*F*	*P*	Prop. %	Cumul. %
Particle-associated					
POC	0.26115	59.48	**0.001**	31.39	31.39
Temp	0.42877	48.15	**0.006**	19.65	51.04
colCHO	0.49407	25.49	**0.009**	9.21	60.25
pH	0.52738	17.76	0.075	5.99	66.24
Diatoms	0.55793	1.69	0.104	5.34	71.58
Sal	0.58148	15.06	0.169	4.50	76.08
DIN	0.60484	1.47	0.200	4.16	80.24
Ara	0.63418	15.61	0.194	4.08	84.32
Mur-A	0.66667	1.59	0.213	3.77	88.10
Chl	0.70459	16.42	0.221	3.46	91.56
Free-living					
Temp	0.29753	82.00	**0.001**	33.89	33.89
Diatoms	0.40907	40.20	**0.001**	13.98	47.86
PO4	0.42655	14.57	0.181	4.92	52.78
Chl	0.46659	2.05	0.073	6.44	59.21
Sal	0.47932	13.18	0.27	4.04	63.25
colCHO	0.5011	15.24	0.175	4.47	67.72
POC	0.53377	17.71	0.13	4.86	72.58

Significant variables ($p < 0.05$) are given in bold.

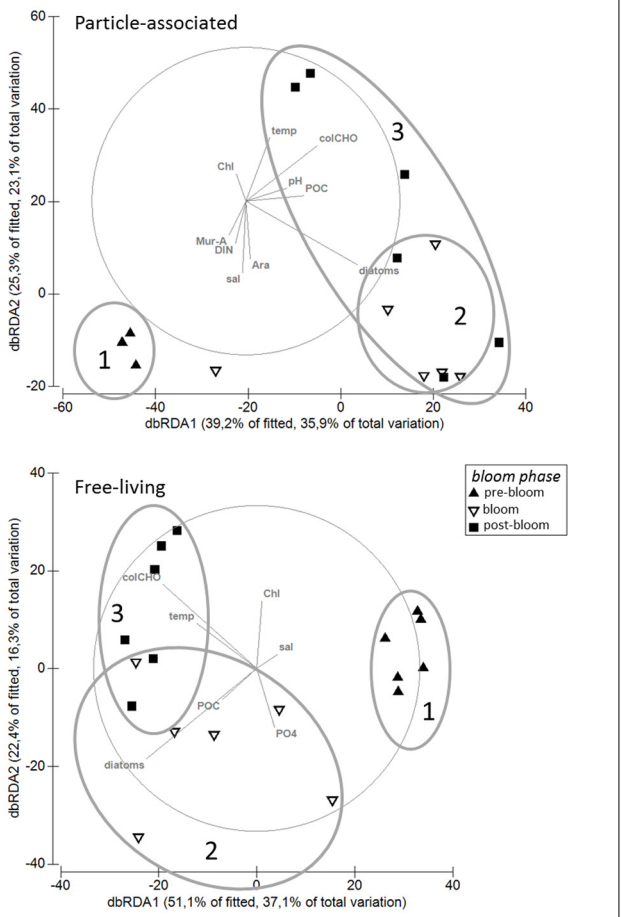

FIGURE 3 | Distance-based Redundancy Analysis (dbRDA) of the relationship between environmental parameters and (A) particle-associated and **(B)** free-living bacterial communities. The analysis is based on Sørensen-similarity-matrices of square root-transformed data. Ovals (1–3) illustrate community dynamics during the different phytoplankton bloom phases.

of organic phosphorous was repressed by the accumulation of its end product.

All enzyme activities were positively correlated with seawater pH, temperature and POC but were negatively correlated to nutrients (**Table 2**). Phos was positively correlated to DOC. In general, all neutral tCCHO except Ara and Man/Xyl showed strong ($r_s > 0.7$) to very strong ($r_s > 0.9$) positive correlations with LAPase, Glcase, and phos. Furthermore, amino sugars correlated well with enzyme activities. β-Glcase and LAPase activity were very strongly ($r_s > 0.9$) correlated with Fuc, while LAPase was correlated very strongly ($r_s > 0.9$) with Gal. Man/Xyl correlated with only amino-peptidase and phos, but not β-Glcase. The amino-sugars correlated well with enzyme activities. Glc-URA was the only acidic sugar showing a significant correlation with enzyme activities.

DISCUSSION

The present study is the first field study combining a detailed analysis of the monomeric composition of polysaccharides in seawater with an investigation of bacterial community composition and the activity of hydrolytic extracellular enzymes. Multivariate statistics were applied to investigate the relationship between the temporal development of the bacterioplankton community and environmental parameters during the spring bloom. Correlations cannot prove or disprove functional relationships but are a valuable measure of the relevance of certain environmental controls on communities and activities. The discussion addresses the temporal development of carbohydrate composition, bacterioplankton community composition and enzyme activities. Furthermore, it aims to reveal potential links between the succession of bacterioplankton and major abiotic and biotic factors during the spring bloom at Helgoland Roads.

The Contribution of Combined Carbohydrates to Organic Matter during Phytoplankton Bloom Development

Phytoplankton spring blooms are events of high OM input into marine systems. The diatom spring bloom investigated at Helgoland Roads in 2010 showed a maximum Chl *a* concentration of approximately 12 μg L^{-1}, similar to concentrations reported for the southern North Sea (Veldhuis et al., 1986) but twofold lower than at Helgoland Roads in 2009 (Teeling et al., 2012). The investigated bloom sustained an average POC concentration of 29 μmol C L^{-1}, well within the range observed previously in the German Bight (Rink

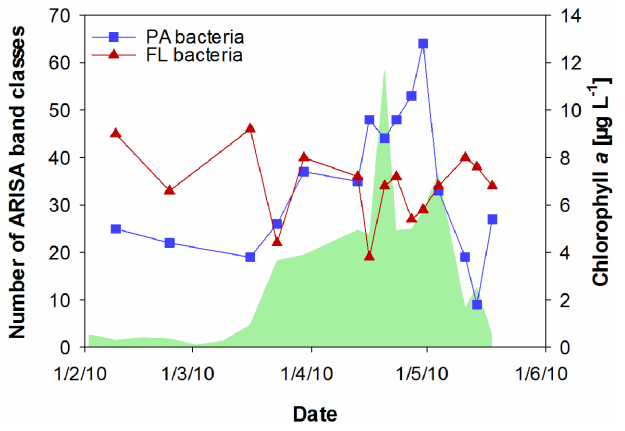

FIGURE 4 | Temporal changes in the richness of particle-associated (PA) bacteria and free-living (FL) bacteria at Helgoland Roads, derived from ARISA band classes. The green shaded area represents concentrations of chlorophyll *a*.

et al., 2011) and comparable to values found in springtime in the eastern North Atlantic (Engel et al., 2012). Average DOC concentrations of 116 µmol C L^{-1} and tCCHO concentrations of 2 µmol monomer equivalent L^{-1} determined in our study are approximately 30% higher than in the eastern North Atlantic Ocean (Engel et al., 2012). The contribution of tCCHO to TOC at Helgoland Roads averaged 8.3%, similar to the percentage of neutral sugars in the TOC of the NW-Mediterranean Sea in April (Jones et al., 2013) but approximately fourfold higher than at the oligotrophic Bermuda Atlantic Time-Series station (BATS) in June (Kaiser and Benner, 2009). The results of this study reveal collinear temporal dynamics of most monomeric components in combined carbohydrates (colCHO) during the growth and decline of the diatom spring bloom at Helgoland Roads. The carbohydrate composition was dominated by high shares of combined glucose. The molar percentages of the individual neutral sugars in tCCHO are more similar to the carbohydrate composition in Oregon inshore waters and Arctic waters than to the carbohydrate composition in the equatorial Pacific Ocean or the Sargasso Sea (Borch and Kirchman, 1997; Rich et al., 1997; Kirchman et al., 2001).

The contribution of tCCHO to TOC increased strongly during the late bloom phase. The coincidence of increasing tCCHO concentrations and the depletion of dissolved inorganic phosphorous and dissolved silicate suggests that enhanced phytoplankton exudation substantially contributed to the production of carbohydrate-rich OM. Laboratory studies have shown that large diatom species, in particular, release high amounts of carbohydrate-rich exudates when grown under nutrient-limited conditions (Engel et al., 2002; Passow, 2002). Diatom exudates are important precursors for the formation of marine particles. Exuded polysaccharidic gels, like transparent exopolymeric particles (TEP), provide surfaces for bacterial colonization and subsequent degradation. Furthermore, TEP play a decisive role in the formation of macroscopic aggregates that promote flocculation and sinking of biogenic material at the end of bloom events (Passow et al., 1994). Acidic sugars represent a substantial fraction of carbohydrates in TEP (Alldredge et al., 1993; Mopper et al., 1995; Passow, 2002). GalUA and GlcUA, the two acidic sugars analyzed in this study, showed very different temporal developments. While concentrations of GlcUA increased only slightly in the post-bloom phase, strong increases in GalUA coincided with rising Chl *a* concentrations. This accumulation of GalUA during the bloom supports the assumption of a high proportion of exudates derived from phytoplankton at Helgoland Roads. In addition to exudation, grazing has potentially contributed to the release of dissolved carbohydrates. The relatively low Chl *a* concentrations recorded in our study indicate a top-down control of phytoplankton by

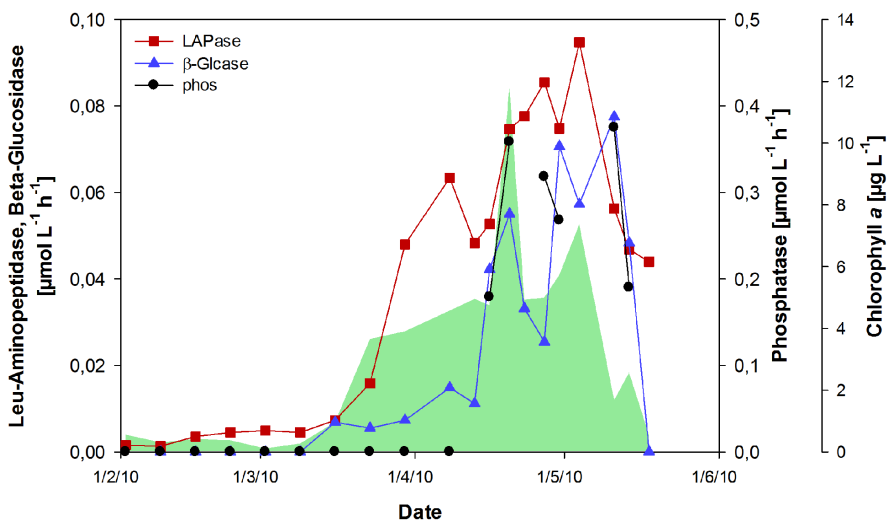

FIGURE 5 | Activity of hydrolytic extracellular enzymes during the spring bloom. Rates for leucine (Leu)-aminopeptidase (LAPase), β-glucosidase (β-Glcase), and phosphatase (phos) are shown. The green shaded area represents concentrations of chlorophyll *a*.

TABLE 2 | Spearman correlation ($p < 0.05$) of different carbohydrates and environmental factors to extracellular enzyme activity of β-glucosidase (β-Glcase), leucine amino peptidase (LAPase), and phosphatase (phos).

	β-Glcase	LAPase	phos
Carbohydrates			
Ara	ø	ø	−
Fuc	+++	+++	++
Gal	++	+++	++
Glc	++	++	++
Man/Xyl	ø	+	+
Rha	++	++	++
GalAM	+	+	++
GlcAM	++	++	++
GlcA	ø	ø	ø
MurA	ø	ø	ø
GalURA	ø	ø	ø
GlcURA	+	+	+
Environmental parameters			
pH	++	++	++
SECCI	−	ø	ø
Temp	++	++	++
Sal	−	−	−−
SiO_2	−−	−−	−−
PO_4	−	−	−
NO_2	−−	−−	−−
Diatoms	+	++	ø
Chl *a*	++	++	+
DOC	ø	ø	++
POC	+++	+++	++

Ø = no significant correlation; + = modest positive correlation ($r_s > 0.4$), ++ = strong positive correlation ($r_s > 0.7$), +++ = very strong positive correlation ($r_s > 0.9$), − = modest negative correlation ($r_s < -0.4$), −− = strong negative correlation ($r_s < -0.7$).

zooplankton (Lohmann and Wiltshire, 2012) that tends to lead to a release of complex carbohydrates from sloppy feeding (Storm et al., 1997).

The complex DOM released from phytoplankton is highly strain specific (Becker et al., 2014) and likely explains most of the associations of specific plankton bacteria with particular phytoplankton strains (e.g., Hahnke et al., 2013). Phytoplankton-derived polysaccharides have been shown to support clade-specific proliferation of bacterioplankton (Taylor et al., 2014). However, the species richness of heterotrophic bacteria is higher than that of autotrophs, suggesting a complex but not strictly species-related interaction between phytoplankton-derived OM and heterotrophic bacterioplankton. This is supported by the finding that relatively few strains of heterotrophic bacteria are associated with distinct phytoplankton communities (Teeling et al., 2016) and that most OM is used by generalists (Rink et al., 2007).

Succession of Bacterioplankton

A strong increase in almost all sugars in tCCHO toward the end of the bloom suggests an increase in ecological niches available to heterotrophic bacteria (Alonso-Sáez and Gasol, 2007; Teeling et al., 2012; Gifford et al., 2013). Indeed, a rapid increase in the richness of the PA bacterial community (approximately 50%) was observed within the 14 days after diatom cell numbers peaked. In that period, the concentration of colCHO (the combined concentration of collinear sugars) was a significant factor impacting the succession of the PA bacterial community. Our results suggest that the influence of carbohydrate concentration on bacterial growth and activity observed earlier (e.g., Borch and Kirchman, 1997; Rich et al., 1997; Piontek et al., 2011) might be induced by not only increasing metabolic rates at the cellular level but also changes in bacterial communities toward efficient carbohydrate degradation. A previous study conducted during the spring bloom at Helgoland Roads showed the taxonomically distinct expression of TonB-dependent transporters, implying the specialization of populations for the successional degradation of carbohydrates in different size ranges (Teeling et al., 2012). Recruitment of FL bacteria to particles cannot explain the rise in PA richness during the post-bloom phase, as PA and FL communities were very similar throughout the phytoplankton bloom. Hence, organic particles rich in carbohydrates provide beneficial niches for a distinct and diverse PA bacterial community that sustains high rates of hydrolytic enzyme activity. Furthermore, approximately three times more new ARISA band classes were detected during the post-bloom phase than tCCHO components rise in concentration. This suggests that only part of the rise in richness could be explained by specialists growing on specific monomeric carbohydrates. It seems likely that several bacterial taxa thrive on the same component or use a specific combination of different components.

Our CARD-FISH analysis, which did not distinguish between PA and FL fractions, revealed that *Gammaproteobacteria* (GAM42) were positively correlated to colCHO and showed higher abundances toward the end of the bloom. Further correlations of *Gammaproteobacteria* with POC and Chl *a* underline the importance of fresh OM derived from phytoplankton production for the growth of this group, which is a prominent member of bacterial communities associated with marine particles (Bižić-Ionescu et al., 2014). For the first time, this study shows that the abundance of *Gammaproteobacteria* is not only related to bulk OM but also to a specific OM component. TCCHO are considered a labile to semi-labile source of organic carbon, with turnover times ranging from days to months depending on molecular weight and structure. GAM42 is also correlated positively to β-Glcase, LAPase, and Phos in our study, indicating an active role in the enzymatic hydrolysis of organic particles and thereby in the transfer of carbon from the particulate to the dissolved pool.

Changes in community composition related to the concentrations of combined carbohydrates and POC during the post-bloom phase strongly suggest a partially substrate-controlled succession. Overall, the investigated factors in our study explain approximately 60 and 48% of the community variability in PA and FL bacterioplankton, respectively. Interestingly, the carbohydrate composition determined in this study does not explain the succession of bacterial communities, inferred from ARISA and CARD-FISH analysis, during the period of strongly rising Chl *a* concentrations (March 16th–April 20th, 2010). In addition, approximately 75% of PA ARISA band classes did not correlate with the development of carbohydrate

concentrations in any bloom phase. This might be explained by the fact that carbohydrates analyzed in this study are >1 kDa and thus part of the HMW-OM. The most labile fraction of freshly produced OM includes LMW compounds, which were shown to strongly affect bacterial community composition in *in vitro* experiments (Gómez-Consarnau et al., 2012). It can be suggested that freshly produced LMW-OM, which is not included in our analysis, had a stronger influence on bacterial community structure during earlier bloom phases before HMW-OM began to accumulate. In addition to the factors POC, colCHO and diatom abundance (related to phytoplankton productivity), temperature had a significant effect on the composition of bacterioplankton, indicating a multifactorial environmental control of bacterioplankton by seasonal changes. In line with previous findings, FL bacteria, which are more directly exposed to conditions in the water body, were found to be susceptible to temperature changes during spring bloom development (Sapp et al., 2007). Accordingly, the FL bacterial community richness is less dynamic than the PA community, and no correlation to the composition or concentration of tCCHO was observed. Furthermore, the hydrographic history of the water mass should be considered as an important factor in shaping bacterioplankton communities. The abundance of SAR11, which constituted up to 40% of total bacterial cells in this study, is related to salinity changes in the southern North Sea that track with the dynamics of water masses (Sperling et al., 2012). Hence, the origin and trajectories of water masses can affect temporal developments observed in time series studies, if complex current patterns, such as those in the shallow southern North Sea prevail.

Activity of Hydrolytic Extracellular Enzymes

Extracellular enzyme activities were dependent on the phytoplankton bloom phase and were correlated to Chl *a*, POC, pH and temperature. Enzymatic rates show positive correlations to the fluorescence intensity of many PA ARISA band classes that can serve as a semi-quantitative measure of the abundances of individual bands (**Supplementary Figure S2**). In addition, the high activity of extracellular β-Glcase was observed well after the Chl *a* and tCCHO peaks, when PA bacterial richness was high. This indicates that for β-Glcase, high PA bacterial richness facilitates the enzymatic turnover of tCCHO. It is likely that the richer PA bacterial community produces not only high amounts of β-Glcase but also a high diversity of β-Glcase isoenzymes (Arrieta and Herndl, 2002), thereby further enhancing the efficiency of carbohydrate hydrolysis. A study analyzing annotated prokaryotic genomes revealed that the capacity to produce extracellular enzymes varies at fine-scale phylogenetic resolution (Zimmerman et al., 2013). In line with previous studies, it can be suggested that PA bacteria are the main producers of extracellular enzymes, as they are closer to their substrates or even reside in semi-enclosed environments where they profit from the effort of producing extracellular enzymes. In contrast, FL bacteria do not appear to invest as much in extracellular enzymes, but preferentially consume carbohydrates that are suitable for direct uptake and, in some cases, subsequent hydrolysis (Teeling et al., 2016).

The rates of β-Glcase determined in the post-bloom phase are sufficiently high to drive the observed loss of tCCHO during this late bloom stage. In late April, a maximum tCCHO amount of approximately 4 μmol L^{-1} accumulated and was subsequently reduced by 2 μmol L^{-1} during the post-bloom phase. This loss of tCCHO matches well with β-Glcase activity integrated over the post-bloom phase, which could sustain the hydrolytic release of 2.16 μmol Glc L^{-1} within the 26 days of the post-bloom phase. In accordance with an earlier study (Arrieta and Herndl, 2002), high rates of extracellular β-Glcase were maintained even after the decline in bacterial richness. This can be explained by prolonged half-lives for excreted enzymes, in the range of days–weeks (Steen and Arnosti, 2011). The decay of the phytoplankton bloom did not result in increased FL bacterial richness, and only a few correlations of FL ARISA band classes to extracellular enzymes were found. This is in accordance with an earlier study that found no increased abundance of carbohydrate-active enzymes during post-phytoplankton spring blooms in FL bacteria at the same sampling site (Teeling et al., 2016). Therefore, it can be suggested that PA and FL bacteria mainly thrive on different forms of carbohydrates, and FL bacteria potentially profit from the pre-hydrolyzed substrates released from particles.

Little is known about the bioavailability of specific carbohydrates in seawater for heterotrophic marine bacterioplankton *in situ*. In our study, high concentrations of Glc, Fuc and Gal were associated with high PA bacterial diversity. Concentrations of these sugars in tCCHO clearly decreased during the post-bloom phase, suggesting preferential degradation via bacterial activity. This observation partly corroborates findings from the Bay of Biscay, which also indicated Fuc and Gal to be actively consumed CHO. In contrast, Glc appears to be very actively processed during our study, but less dynamic in the Bay of Biscay (Engel et al., 2012). The availability of monomeric and oligomeric sugars for bacterioplankton consumption is, to a large extent, dependent on the degradability of preceding polymers. A *Bacteroidetes* isolate from North Sea surface waters, *Gramella forsetii* KT0803, showed polymer-specific transcription of polysaccharide utilization loci (PULs) for laminarin and alginate that comprised genes of surface-exposed proteins such as oligomer transporters, substrate-binding proteins, and carbohydrate-active enzymes (Kabisch et al., 2014). In particular, laminarin is a widespread polymer in the ocean that is found as a storage glucan in diatoms and brown algae, among others. It consists of glucose monomers linked by β-glycosidic bonds that can be hydrolyzed by β-Glcase. Its homopolysaccharidic structure (i.e., consisting of only one type of monomer) further facilitates efficient hydrolysis by exo-enzymes. Homopolysaccharides have been found to be preferentially utilized over heteropolysaccharides (Amon and Benner, 2003). Heteropolysaccharides consisting of Rha, Fuc, Xyl, Man, and Gal are mainly part of the cell wall (Alderkamp et al., 2007) and are excreted as extracellular polymeric substances (Hama and Yanagi, 2001). Both glucanes and heteropolysaccharides appear to contribute to the rise in carbohydrates observed during the bloom in

our study. Apart from Glc in glucanes, Fuc and Gal appear to be part of labile polymers. In addition to the monomeric composition of polysaccharides, also the molecule structure of the substrate has been shown to co-determine the accessibility to extracellular enzymes (Pantoja and Lee, 1999; Arnosti, 2000, 2004). Laminarinase enzymes, for example, showed minimal activity on substrates, with similar glucosidic bonds to those of laminarin, but different sizes and secondary and/or tertiary structures, revealing that the hydrolysis rates among substrates of similar sizes but differing structures can vary considerably (Alderkamp et al., 2006). Overall, it can be assumed that the metabolic capacities of the bacterial community adapted to the chemical properties of available polysaccharides, resulting in efficient polysaccharide degradation during the spring bloom at Helgoland Roads.

CONCLUSION

The present study shows a correlation between the concentration of combined carbohydrates in HMW-OM and the diversity of PA bacteria during the development of a spring bloom, suggesting that the availability of carbohydrates contributes to the multifactorial control of marine bacterioplankton communities. Our study is in line with earlier findings demonstrating the importance of PA bacteria for total community activity (Alldredge and Silver, 1988; Herndl, 1988; Grossart et al., 2006b; Lyons and Dobbs, 2012). This highlights the additional value of analyzing bacterioplankton community composition in size-fractionated samples. As inferred from decreasing concentrations during the post-bloom phase, glucose, fucose, and galactose were preferentially utilized sugars in HMW-OM. There is growing evidence that phytoplankton primary production and OM release is susceptible to ocean change. Climate models project the shoaling of upper mixed layer depth as a consequence of sea-surface warming. Changes in the mixed layer depth can affect primary production and the timing of spring blooms and thus the pool of OM that is subject to bacterial remineralization. A mesocosm study further showed that phytoplankton growth under increasing temperature accelerates carbohydrate accumulation (Engel et al., 2011). In addition to warming, the dissolution of increasing anthropogenic CO_2 in seawater, referred to as ocean acidification, can significantly affect phytoplankton productivity. A mesocosm experiment revealed that elevated pCO_2 increased primary production in Arctic plankton communities (Engel et al., 2013). In the same experiment, the PA bacterial community richness was shown to be higher in mesocosms at elevated pCO_2 (Sperling et al., 2013). Increasing exudation has been suggested as a physiological strategy for *Emiliania huxleyi*, a bloom-forming coccolithophore, to grow under a condition of elevated pCO_2 and low nutrient availability (Borchard and Engel, 2012). Combining results from fieldwork and experiments, it can be suggested that carbohydrates, the primary product of photosynthesis, have high potential to mediate the effects of ocean change on bacterioplankton community structure and function (**Supplementary Figure S3**).

AUTHOR CONTRIBUTIONS

MS developed the study concept and conducted the sampling as well as most of the sample- and data analysis. He also wrote the manuscript. JP helped develop the study concept, provided methodological support, especially with acquisition and analysis of extracellular enzyme data, and contributed to the manuscript. AE and AW provided lab space and financial and methodological support, helped develop the study concept and contributed to the manuscript. KW provided phytoplankton- and physicochemical data and contributed to the manuscript. JN provided data on dissolved organic carbon and contributed to the manuscript. GG provided lab space and financial and methodological support, helped develop the study concept, supported the statistical analysis and contributed to the manuscript.

FUNDING

The German Federal Ministry of Education and Research (BMBF) supported this study by funding the Microbial Interactions in Marine Systems project (MIMAS, project 03F0480A, http://mimas-project.de). Financial support for MS was provided through a stipend by the Helmholtz Graduate School for Polar and Marine Research (POLMAR).

ACKNOWLEDGMENTS

The authors would like to thank the crews of the research vessels "Aade" and "Diker" at the Biological Institute Helgoland. We also like to thank Hilke Döpke and Mirja Meiners for help with sample preparation and laboratory work. We thank Niels Moritz for the dialysis/hydrolysis of the carbohydrate samples, Jon Roa for the analyses, Christiane Lorenzen for the POC analysis and Matthias Friebe for the DOC analysis. We thank Bernhard M. Fuchs for valuable contributions to the manuscript. We also thank the reviewers GG and JF for improvements to the manuscript.

SUPPLEMENTARY MATERIAL

The Supplementary Material for this article can be found online at: http://journal.frontiersin.org/article/10.3389/fmicb.2017.00065/full#supplementary-material

FIGURE S1 | Richness of particle-associated (3–10 μm) bacterioplankton vs. the concentration of colCHO ($R^2 = 0.3779$, $p = 0.0093$).

FIGURE S2 | Percent of particle-associated and free-living ARISA band classes (fluorescence intensity) correlating (Spearman Rank Correlation; $r_s > 0.5$, $p < 0.05$) to the maximum velocity (V_{max}) of the extracellular enzymes β-glucosidase (β-Glcase), leucine aminopeptidase (LAPase) and phosphatase (phos) during spring 2010 at the Helgoland Roads sampling station.

FIGURE S3 | Schematic representation of a mechanism for secondary effects of ocean change on bacterioplankton community and activity.

TABLE S1 | Analyzed carbohydrates and abbreviations.

TABLE S2 | Concentrations of tCCHO components in nmol L^{-1}.

TABLE S3 | Spearman correlation ($p < 0.05$) of FISH-counts to environmental factors (abiotic and biotic), concentrations of selected carbohydrates, and extracellular enzyme activities of β-glucosidase (β-Glcase), leucine amino peptidase (LAPases) and phosphatase (phos).

Ø = no significant correlation; + = modest positive correlation ($r_S > 0.4$), ++ = strong positive correlation ($r_S > 0.7$), +++ = very strong positive correlation ($r_S > 0.9$), − = modest negative correlation ($r_S < -0.4$), −− = strong negative correlation ($r_S < -0.7$).

REFERENCES

Alderkamp, A.-C., Buma, A. G. J., and van Rijssel, M. (2007). The carbohydrates offf *Phaeocystis* and their degradation in the microbial food web. *Biogeochemistry* 83, 99–118. doi: 10.1007/s10533-007-9078-2

Alderkamp, A.-C., Sintes, E., and Herndl, G. J. (2006). Abundance and activity of major groups of prokaryotic plankton in the coastal North Sea during spring and summer. *Aquat. Microb. Ecol.* 45, 237–246. doi: 10.3354/ame045237

Alldredge, A. L., Pasow, U., and Logan, B. E. (1993). The abundance and significance of a class of large, transparent organic particles in the ocean. *Deep Sea Res.* 40, 1131–1140. doi: 10.1016/0967-0637(93)90129-Q

Alldredge, A. L., and Silver, M. W. (1988). Characteristics, dynamics and significance of marine snow. *Prog. Oceanogr.* 20, 41–82. doi: 10.1016/0079-6611(88)90053-5

Allgaier, M., Riebesell, U., Vogt, M., Thyrhaug, R., and Grossart, H.-P. (2008). Coupling of heterotrophic bacteria to phytoplankton bloom development at different pCO2 levels: a mesocosm study. *Biogeosciences* 5, 1007–1022. doi: 10.5194/bg-5-1007-2008

Alonso-Sáez, L., and Gasol, J. M. (2007). Seasonal variations in the contributions of different bacterial groups to the uptake of low-molecular-weight compounds in Northwestern mediterranean coastal waters. *Appl. Environ. Microbiol.* 73, 3528–3535. doi: 10.1128/AEM.02627-06

Amon, R. M. W., and Benner, R. (1996). Bacterial utilization of different size classes of dissolved organic matter. *Limnol. Oceanogr.* 41, 41–51. doi: 10.4319/lo.1996.41.1.0041

Amon, R. M. W., and Benner, R. (2003). Combined neutral sugars as indicators of the diagenetic state of dissolved organic matter in the Arctic Ocean. *Deep Sea Res. Part I* 50, 151–169. doi: 10.1016/S0967-0637(02)00130-9

Arnosti, C. (2000). Substrate specificity in polysaccharide hydrolysis: contrasts between bottom water and sediments. *Limnol. Oceanogr.* 45, 1112–1119.

Arnosti, C. (2004). Speed bumps and barricades in the carbon cycle: substrate structural effects on carbon cycling. *Mar. Chem.* 92, 263–273. doi: 10.1016/j.marchem.2004.06.030

Arrieta, J. M., and Herndl, G. J. (2002). Changes in bacterial β-Glcase cosidase diversity during a coastal phytoplankton bloom. *Limnol. Oceanogr.* 47, 594–599. doi: 10.4319/lo.2002.47.2.0594

Azam, F., Fenchel, T., Field, J. G., Gray, J. S., Meyer-Reil, L. A., and Thingstad, T. F. (1983). The ecological role of water-column microbes in the sea. *Mar. Ecol. Prog. Ser.* 10, 257–263.

Becker, J. W., Berube, P. M., Follett, C. L., Waterbury, J. B., Chisholm, S. W., DeLong, E. F., et al. (2014). Closely related phytoplankton species produce similar suites of dissolved organic matter. *Front. Microbiol.* 5:111. doi: 10.3389/fmicb.2014.00111

Bižić-Ionescu, M., Zeder, M., Ionescu, D., Orlić, S., Fuchs, B. M., Grossart, H.-P., et al. (2014). Comparison of bacterial communities on limnic versus coastal marine particles reveals profound differences in colonization. *Environ. Microbiol.* 17, 3500–3514. doi: 10.1111/1462-2920.12466

Borch, N. H., and Kirchman, D. L. (1997). Concentration and composition of dissolved combined neutral sugars (polysaccharides) in sewater determined by HPLC-PAD. *Mar. Chem.* 57, 85–95. doi: 10.1016/S0304-4203(97)00002-9

Borchard, C., and Engel, A. (2012). Organic matter exudation by *Emiliania huxleyi* under simulated future ocean conditions. *Biogeosciences* 9, 3405–3423. doi: 10.5194/bg-9-3405-2012

Brown, M. V., Schwalbach, M. S., Hewson, I., and Fuhrman, J. A. (2005). Coupling 16S-ITS rDNA clone libraries and automated ribosomal intergenic spacer analysis to show marine microbial diversity: development and application to a time series. *Environ. Microbiol.* 7, 1466–1479. doi: 10.1111/j.1462-2920.2005.00835.x

Chróst, R. J. (ed.). (1991). *Microbial Enzymes in Aquatic Environments*. New York, NY: Springer.

Cox, R., and Culkin, F. (1976). Sodium, potassium, magnesium, calcium and strontium in sea water. *Deep Sea Res.* 13, 789–804.

Elifantz, H., Malmstrom, R. R., Cottrell, M. T., and Kirchmann, D. L. (2005). Assimilation of polysaccharides and glucose by major bacterial groups in the delaware estuary. *Appl. Environ. Microbiol.* 71, 7799–7805. doi: 10.1128/AEM.71.12.7799-7805.2005

Engel, A., Borchard, C., Piontek, J., Schulz, K. G., Riebesell, U., and Bellerby, R. (2013). CO2 Increases 14C primary production in an Arctic plankton community. *Biogeosciences* 10, 1291–1308. doi: 10.5194/bg-10-1291-2013

Engel, A., Goldthwait, S., Passow, U., and Alldredge, A. (2002). Temporal decoupling of carbon and nitrogen dynamics in a mesocosm diatom bloom. *Limnol. Oceanogr.* 47, 753–761. doi: 10.4319/lo.2002.47.3.0753

Engel, A., and Händel, N. (2011). A novel protocol for determining the concentration and composition of sugars in particulate and in high molecular weight dissolved organic matter (HMW-DOM) in seawater. *Mar. Chem.* 127, 180–191. doi: 10.1016/j.marchem.2011.09.004

Engel, A., Händel, N., Wohlers, J., Lunau, M., Grossart, H.-P., Sommer, U., et al. (2011). Effects of sea surface warming on the production and composition of dissolved organic matter during phytoplankton blooms: results from a mesocosm study. *J. Plankton Res.* 33, 357–372. doi: 10.1093/plankt/fbq122

Engel, A., Harlay, J., Piontek, J., and Chou, L. (2012). Contribution of combined carbohydrates to dissolved and particulate organic carbon after the spring bloom in the northern Bay of Biscay (North-Eastern Atlantic Ocean). *Cont. Shelf Res.* 45, 42–53. doi: 10.1016/j.csr.2012.05.016

Engel, A., Piontek, J., Grossart, H.-P., Riebesell, U., Schulz, K. G., and Sperling, M. (2014). Impact of CO2 enrichment on organic matter dynamics during nutrient induced coastal phytoplankton blooms. *J. Plankton Res.* 36, 641–657. doi: 10.1093/plankt/fbt125

Gieskes, J. M. (1969). Effect of temperature on the pH of seawater. *Limnol. Oceanogr.* 14, 679–685. doi: 10.4319/lo.1969.14.5.0679

Gifford, S. M., Sharma, S., Booth, M., and Moran, M. A. (2013). Expression patterns reveal niche diversification in a marine microbial assemblage. *ISME J.* 7, 281–298. doi: 10.1038/ismej.2012.96

Gómez-Consarnau, L., Lindh, M. V., Gasol, J. M., and Pinhassi, J. (2012). Structuring of bacterioplankton communities by specific dissolved organic carbon compounds. *Environ. Microbiol.* 14, 2361–2378. doi: 10.1111/j.1462-2920.2012.02804.x

Grasshoff, K., Kremling, K., and Ehrhardt, M. (1999). *Methods of Seawater Analysis*. Weinheim: Wiley-VCH.

Grossart, H. P., Allgaier, M., Passow, U., and Riebesell, U. (2006a). Testing the effect of CO2 concentration on the dynamics of marine heterotrophic bacterioplankton. *Limnol. Oceanogr.* 51, 1–11. doi: 10.4319/lo.2006.51.1.0001

Grossart, H. P., Kiørboe, T., Tang, K. W., Allgaier, M., Yam, E. M., and Ploug, H. (2006b). Interactions between marine snow and heterotrophic bacteria: aggregate formation and microbial dynamics. *Aquat. Microb. Ecol.* 42, 19–26. doi: 10.3354/ame042019

Hahnke, S., Sperling, M., Langer, T., Wichels, A., Gerdts, G., Beardsley, C., et al. (2013). Distinct seasonal growth patterns of the bacterium *Planktotalea fisia* in the North Sea and specific interaction with phytoplankton algae. *FEMS Microbiol. Ecol.* 86, 185–199. doi: 10.1111/1574-6941.12151

Hama, T., and Yanagi, K. (2001). Production and neutral aldose composition of dissolved carbohydrates excreted by natural marine phytoplankton populations. *Limnol. Oceanogr.* 46, 1945–1955. doi: 10.4319/lo.2001.46.8.1945

Herndl, G. J. (1988). Ecology of amorphous aggregations (marine snow) in the Northern Adriatic Sea. 2. Microbial density and activity in marine snow and its implications to the overall pelagic processes. *Mar. Ecol. Prog. Ser.* 48, 265–275.

Hoppe, H.-G. (1983). Significance of exoenzymatic activities in the ecology of brackish water: measurements by means of methylumbelliferyl-substrates. *Mar. Ecol. Prog. Ser.* 11, 299–308.

Hutchinson, G. E. (1961). The paradox of the plankton. *Am. Nat.* 95, 137–145. doi: 10.1086/282171

Jones, V., Meador, T. B., Gogou, A., Migon, C., Penkman, K. E. H., Collins, M. J., et al. (2013). Characterisation and dynamics of dissolved organic matter in the Northwestern Mediterranean Sea. *Prog. Oceanogr.* 119, 78–89.

Kabisch, A., Otto, A., König, S., Becher, D., Albrecht, D., Schüler, M., et al. (2014). Functional characterization of polysaccharide utilization loci in the marine Bacteroidetes '*Gramella forsetii*' KT0803. *ISME J.* 8, 1492–1502. doi: 10.1038/ismej.2014.4

Kaiser, K., and Benner, R. (2009). Biochemical composition and size distribution of organic matter at the Pacific and Atlantic time-series stations. *Mar. Chem.* 113, 63–77. doi: 10.1016/j.marchem.2008.12.004

Kirchman, D. L., Meon, B., Ducklow, H. W., Carlson, C. A., Hansell, D. A., and Steward, G. F. (2001). Glucose fluxes and concentrations of dissolved combined neutral sugars (polysaccharides) in the Ross Sea and Polar Front Zone, Antarctica. *Deep Sea Res. Partt II* 48, 4179–4197. doi: 10.1016/S0967-0645(01)00085-6

Knefelkamp, B., Carstens, K., and Wiltshire, K. H. (2007). Comparison of different filter types onchlorophyll-a retention and nutrient measurements. *J. Exp. Mar. Biol. Ecol.* 345, 61–70. doi: 10.1016/j.jembe.2007.01.008

Kovacs, A., Yacoby, K., and Gophna, U. (2010). A systematic assessment of automated ribosomal intergenic spacer analysis (ARISA) as a tool for estimating bacterial richness. *Res. Microbiol.* 161, 192–197. doi: 10.1016/j.resmic.2010.01.006

Krause, E., Wichels, A., Giménez, L., Lunau, M., Schilhabel, M. B., and Gerdts, G. (2012). Small changes in pH have direct effects on marine bacterial community composition: a microcosm approach. *PLoS ONE* 7:e47035. doi: 10.1371/journal.pone.0047035

Lohmann, G., and Wiltshire, K. H. (2012). Winter atmospheric circulation signature for the timing of the spring bloom of diatoms in the North Sea. *Mar. Biol.* 159, 2573–2581. doi: 10.1007/s00227-012-1993-7

Lyons, M. M., and Dobbs, F. C. (2012). Differential utilization of carbon substrates by aggregate-associated and water-associated heterotrophic bacterial communities. *Hydrobiologia* 686, 181–193. doi: 10.1007/s10750-012-1010-7

Mopper, K., Zhou, J., Sri Ramana, K., Passow, U., Dam, H. G., and Drapeau, D. T. (1995). The role of surface-active carbohydrates in the flocculation of adiatom bloom in a mesocosm. *Deap Sea Res. II* 42, 47–73.

Pakulski, J. D., and Benner, R. (1994). Abundance and distribution of carbohydrates in the ocean. *Limnol. Oceanogr.* 39, 930–940. doi: 10.4319/lo.1994.39.4.0930

Pantoja, S., and Lee, C. (1999). Molecular weight distribution of proteinaceous material in Long Island Sound sediments. *Limnol. Oceanogr.* 44, 1323–1330. doi: 10.4319/lo.1999.44.5.1323

Passow, U. (2002). Production of transparent exopolymer particles (TEP) by phyto- and bacterioplankton. *Mar. Ecol. Prog. Ser.* 236, 1–12. doi: 10.3354/meps236001

Passow, U., Alldredge, A. L., and Logan, B. E. (1994). The role of particulate carbohydrate exudates in the flocculationof diatom blooms. *Deep Sea Res.* 41, 335–357. doi: 10.1016/0967-0637(94)90007-8

Pernthaler, A., Pernthaler, J., Schattenhofer, M., and Amann, R. (2002). Identification of DNA-synthesising bacterial cells in coastal North Sea Plankton. *Appl. Environ. Microbiol.* 68, 5728–5736. doi: 10.1128/AEM.68.11.5728-5736.2002

Pinhassi, J., Sala, M. M., Havskum, H., Peters, F., Guadayol, O., Malits, A., et al. (2004). Changes in bacterioplankton composition under different phytoplankton regimens. *Appl. Environ. Microbiol.* 70, 6753–6766. doi: 10.1128/AEM.70.11.6753-6766.2004

Piontek, J., Borchard, C., Sperling, M., Schulz, K. G., Riebesell, U., and Engel, A. (2013). Response of bacterioplankton activity in an Arctic fjord system to elevated pCO2: results from a mesocosm study. *Biogesciences* 10, 297–314. doi: 10.5194/bg-10-297-2013

Piontek, J., Händel, N., de Bodt, C., Harlay, J., Chou, L., and Engel, A. (2011). The utilization of polysaccharides by heterotrophic bacterioplankton in the Bay of Biscay (North Atlantic Ocean). *J. Plankton Res.* 33, 1719–1735. doi: 10.1093/plankt/fbr069

Ranjard, L., Brothier, E., and Nazaret, S. (2000). Sequencing bands of ribosomal intergenic spacer analysis fingerprints for characterization and microscale distribution of soil bacterium populations responding to mercury spiking. *Appl. Environ. Microbiol.* 66, 5334–5339. doi: 10.1128/AEM.66.12.5334-5339.2000

Rich, J., Gosselin, M., Sherr, E., Sherr, B., and Kirchman, D. L. (1997). High bacterial production, uptake and concentrations of dissolved organic matter in the central Arctic Ocean. *Deep Sea Res. Part II* 44, 1645–1663. doi: 10.1016/S0967-0645(97)00058-1

Rink, B., Grüner, N., Brinkhoff, T., Ziegelmüller, K., and Simon, M. (2011). Regional patterns of bacterial community composition and biogeochemical properties in the southern North Sea. *Aquat. Microb. Ecol.* 63, 207–222. doi: 10.3354/ame01493

Rink, B., Seeberger, S., Martens, T., Duerselen, C.-D., Simon, M., and Brinkhoff, T. (2007). Effects of phytoplankton bloom in a coastal ecosystem on the composition of bacterial communities. *Auquat. Microb. Ecol.* 48, 47–60. doi: 10.3354/ame048047

Rooney-Varga, J. N., Giewat, M. W., Savin, M. C., Sood, S., LeGresley, M., and Martin, J. L. (2005). Links between phytoplankton and bacterial community dynamicsin a coastal marine environment. *Microb. Ecol.* 49, 163–175. doi: 10.1007/s00248-003-1057-0

Sapp, M., Wichels, A., Wiltshire, K. H., and Gerdts, G. (2007). Bacterial community dynamics during the winter-spring transition in the North Sea. *FEMS Microbiol. Ecol.* 59, 622–637. doi: 10.1111/j.1574-6941.2006.00238.x

Sperling, M., Giebel, H.-A., Rink, B., Grayek, S., Staneva, J., Stanev, E., et al. (2012). Differential effect of hydrographic and biogeochemical properties on SAR11 and *Roseobacter* RCA populations in the southern North Sea. *Aquat. Microb. Ecol.* 67, 25–34. doi: 10.3354/ame01580

Sperling, M., Piontek, J., Gerdts, G., Wichels, A., Schunck, H., Roy, A.-S., et al. (2013). Effect of elevated CO2 on the dynamics of particle attached and free-living bacterioplankton communities in an Arctic fjord. *Biogeosciences* 10, 181–191. doi: 10.5194/bg-10-181-2013

Steen, A. D., and Arnosti, C. (2011). Long lifetimes of β-glucosidase, leucine aminopeptidase, and phosphatase in Arctic seawater. *Mar. Chem.* 123, 127–132. doi: 10.1016/j.marchem.2010.10.006

Storm, S. L., Benner, R., Ziegler, S., and Dagg, M. J. (1997). Planktonic grazers are a potentially important source of marine dissolved organic carbon. *Limnol. Oceanogr.* 42, 1364–1374. doi: 10.4319/lo.1997.42.6.1364

Sugimura, Y., and Suzuki, Y. (1988). A high-temperature catalytic oxidation method for the determination of non-volatile dissolved organic carbon in seawater by direct injection of a liquid sample. *Mar. Chem.* 24, 105–131. doi: 10.1016/0304-4203(88)90043-6

Tanaka, T., Thingstad, T. F., Løvdal, T., Grossart, H.-P., Larsen, A., Allgaier, M., et al. (2008). Availability of phosphate for phytoplankton and bacteria and of glucose for bacteria at different pCO2 levels in a mesocosm study. *Biogeosciences* 5, 669–678. doi: 10.5194/bg-5-669-2008

Taylor, J. D., Cottingham, S. D., Billinge, J., and Cunliffe, M. (2014). Seasonal microbial community dynamics correlate with phytoplankton-derived polysaccharides in surface coastal waters. *ISME J.* 8, 245–248. doi: 10.1038/ismej.2013.178

Teeling, H., Fuchs, B. M., Becher, D., Klockow, C., Gardebrecht, A., Bennke, C. M., et al. (2012). Substrate-controlled succession of marine bacterioplankton populations induced by a phytoplankton bloom. *Science* 336, 608–611. doi: 10.1126/science.1218344

Teeling, H., Fuchs, B. M., Bennke, C. B., Krüger, K., Chafee, M., Kappelmann, L., et al. (2016). Recurring patterns in bacterioplankton dynamics during coastal spring algae blooms. *Elife* 5:e1188. doi: 10.7554/eLife.11888

Veldhuis, M. J. W., Admiraal, W., and Colijn, F. (1986). Chemical and physiological changes of phytoplankton during the spring bloom, dominated by *Phaeocystis pouchetii* (Haptophyceae): observations in dutch coastal waters of the North Sea. *Neth. J. Sea Res.* 20, 49–60. doi: 10.1016/0077-7579(86)90060-8

Weiss, M. S., Abele, U., Weckesser, J., Welte, W., Schiltz, E., and Schulz, G. E. (1991). Molecular architecture and electrostatic properties of a bacterial porin. *Science* 254, 1627–1630. doi: 10.1126/science.1721242

Wiltshire, K. H., Kraberg, A., Bartsch, I., Boersma, M., Franke, H.-D., Freund, J., et al. (2009). Helgoland Roads, North Sea: 45 years of change. *Estuaries Coasts* 33, 295–310.

Wiltshire, K. H., Malzahn, A. M., Wirtz, K., Greve, W., Janisch, S., Mangelsdorf, P., et al. (2008). Resilience of North Sea phytoplankton spring bloom dynamics: an analysis of long-term data at Helgoland Roads. *Limnol. Oceanogr.* 53, 1294–1302. doi: 10.4319/lo.2008.53.4.1294

Wiltshire, K. H., and Manly, B. F. J. (2004). The warming trend at Helgoland Roads, North Sea: phytoplankton response. *Helgol. Mar. Res.* 58, 269–273.

Zimmerman, A. E., Martiny, A. C., Allison, S. D. (2013). Microdiversity of extracellular enzyme genes among sequenced prokaryotic genomes. *ISME J.* 7, 1187–1199. doi: 10.1038/ismej.2012.176

Conflict of Interest Statement: The authors declare that the research was conducted in the absence of any commercial or financial relationships that could be construed as a potential conflict of interest.

frontiers in Microbiology

ORIGINAL RESEARCH
published: 21 April 2017
doi: 10.3389/fmicb.2017.00676

Role of EPS, Dispersant and Nutrients on the Microbial Response and MOS Formation in the Subarctic Northeast Atlantic

*Laura Duran Suja, Stephen Summers and Tony Gutierrez**

Institute of Mechanical, Process and Energy Engineering, School of Engineering and Physical Sciences, Heriot-Watt University, Edinburgh, UK

In this study we report the formation of marine oil snow (MOS), its associated microbial community, the factors influencing its formation, and the microbial response to crude oil in surface waters of the Faroe-Shetland Channel (FSC). The FSC is a subarctic region that is hydrodynamically complex located in the northeast Atlantic where oil extraction is currently occurring and where exploration is likely to expand into its deeper waters (>500 m). A major oil spill in this region may mirror the aftermath that ensued following the Deepwater Horizon (DWH) blowout in the Gulf of Mexico, where the massive influx of Macondo crude oil triggered the formation of copious quantities of rapidly sinking MOS and successional blooms of opportunistic oil-degrading bacteria. In laboratory experiments, we simulated environmental conditions in sea surface waters of the FSC using water collected from this site during the winter of 2015. We demonstrated that the presence of dispersant triggers the formation of MOS, and that nutrient amendments magnify this. Illumina MiSeq sequencing revealed the enrichment on MOS of associated oil-degrading (*Cycloclasticus*, *Thalassolituus*, *Marinobacter*) and EPS-producing (*Halomonas*, *Pseudoalteromonas*, *Alteromonas*) bacteria, and included major representation by *Psychrobacter* and *Cobetia* with putative oil-degrading/EPS-producing qualities. The formation of marine snow, in the absence of crude oil and dispersant, in seawater amended with nutrients alone indicated that the *de novo* synthesis of bacterial EPS is a key factor in MOS formation, and the glycoprotein composition of the MOS aggregates confirmed that its amorphous biopolymeric matrix was of microbial (likely bacterial) origin. The presence of dispersants and crude oil with/without nutrients resulted in distinct microbial responses marked by intermittent, and in some cases short-lived, blooms of opportunistic heterotrophs, principally obligate hydrocarbonoclastic (*Alcanivorax*, *Cycloclasticus*, *Thalassolituus*, *Marinobacter*) and EPS-producing (*Halomonas*, *Alteromonas*, *Pseudoalteromonas*) bacteria. Interestingly, members of the *Vibrionales* (principally the genus *Vibrio*) were strongly enriched by crude oil (with/without dispersant or nutrients), highlighting a putative importance for these organisms in crude oil biodegradation in the FSC. Our findings mirror those observed at DWH and hence underscore their broad relevance.

Keywords: marine oil snow (MOS), Faroe-shetland channel, hydrocarbon-degrading bacteria, Deepwater Horizon, crude oil, marine environment

OPEN ACCESS

Edited by:
Raquel Peixoto,
Federal University of Rio de Janeiro, Brazil

Reviewed by:
Meinhard Simon,
University of Oldenburg, Germany
Ian M. Head,
Newcastle University, UK

****Correspondence:***
Tony Gutierrez
tony.gutierrez@hw.ac.uk

Specialty section:
This article was submitted to Aquatic Microbiology, a section of the journal Frontiers in Microbiology

Received: *20 October 2016*
Accepted: *03 April 2017*
Published: *21 April 2017*

Citation:
Suja LD, Summers S and Gutierrez T (2017) Role of EPS, Dispersant and Nutrients on the Microbial Response and MOS Formation in the Subarctic Northeast Atlantic. Front. Microbiol. 8:676. doi: 10.3389/fmicb.2017.00676

INTRODUCTION

A distinctive feature of the Deepwater Horizon (DWH) oil spill was the formation of large quantities of marine oil snow (MOS) that were observed in profuse quantities on the sea surface near and around the blowout (Passow et al., 2012). MOS was observed by scientists on the first research cruise that reached the spill site within 2 weeks from the onset of the spill on April 20 of 2010, and it sparked intense interest to understand the factors that triggered and influenced its genesis and evolution. MOS can be described as mucilaginous floating organic particles of >0.5 mm in diameter containing oil droplets embedded within its amorphous matrix. By June 2010, a little over a month after the onset of the spill, MOS was no longer visible at DWH and it is now understood that it had rapidly sedimented – a process termed MOSSFA (Marine Oil Snow Sedimentation and Flocculent Accumulation) – taking with it a significant fraction (ca. 14%) of the Macondo oil to the seafloor (Valentine et al., 2014) – it was found deposited east of the DWH spill site in the DeSoto Canyon region (Brooks et al., 2015) and further afield in the Gulf of Mexico (Valentine et al., 2014; Chanton et al., 2015; Romero et al., 2015).

It has been suggested that MOS formation may be a consequence of the interaction between oil and suspended organic matter, including dispersants (Fu et al., 2014; Kleindienst et al., 2015a) and eukaryotic phytoplankton cells (Passow, 2016). In roller-bottle experiments performed under conditions simulating sea surface conditions during the DWH spill, EPS produced by oil-degrading bacteria enriched in sea surface oil slicks was shown to trigger MOS formation (Gutierrez et al., 2013), and similar results were observed with EPS produced by axenic cultures of eukaryotic phytoplankton (van Eenennaam et al., 2016). Furthermore, Ziervogel et al. (2012) demonstrated that the suspended MOS particles acted as 'hotspots' for microbial oil-degrading activity, and Arnosti et al. (2016) showed MOS particles contained an associated bacterial community that was distinctly different from the free-living community in the surrounding seawater. Whilst the underlying mechanism(s) affecting the formation of MOS have yet to be properly understood, various factors, such as hydrodynamic conditions, collision rate of suspended particles, particle coagulation and flocculation and interaction of oil components with microorganism may be important in this process (Passow et al., 2012).

Considering that one of the largest reservoirs of organic matter on the Earth is found in the oceans, existing in the form of dissolved organic matter (DOM) – ca. 6.9×10^{17} g C, which is comparable in mass to the carbon in atmospheric CO_2 (Hansell and Carlson, 2001) – its role in MOS formation has been a focus of many recent reports. DOM can play various functions and important roles in chemical, biological and physical oceanography, and is involved in fueling the microbial loop and in generating gasses (CO, CO_2) and nutrients (Pomeroy, 1974; Azam et al., 1983). Much of this marine DOM is produced and released by bacteria and eukaryotic phytoplankton as extracellular polymeric substances (EPS) (Decho, 1990; Santschi et al., 1999). These are high molecular-weight polymers that are mainly composed of monosaccharides, but can also contain non-carbohydrate substituents (e.g., amino acid groups). A number of studies have reported large quantities of EPS in sea surface and deep-sea environments, including Antarctic marine waters (Mancuso Nichols et al., 2004 and references therein). Marine bacteria can contribute large quantities of EPS to the total DOM pool in the ocean (Azam, 1998), a large fraction of which exists as glycoproteins (Long and Azam, 1996; Verdugo et al., 2004). Since EPS, in particular those produced by marine bacteria, are endowed with an overall negative charge that is largely conferred by carboxyl groups of uronic acids (Kennedy and Sutherland, 1987), these acids have been implicated in the capacity of EPS to complex with metals (Gyurcsik and Nagy, 2000; Bhaskar and Bhosle, 2005). For example, at hydrothermal vents where these polymers are found, they can participate in complexing metal ions or radionuclides and contribute to their mobility and entry into the food web (Mancuso Nichols et al., 2004 and references therein). Some studies have also shown that uronic acids can confer EPS with an ability to interact with and increase the dissolution of hydrophobic organic chemicals, such as oil hydrocarbons (Janecka et al., 2002; Gutierrez et al., 2008, 2009). Amino acids and peptides, which are also often found associated with marine bacterial EPS, can also confer amphiphilic characteristics to these polymers and hence ability to interact with oils (Decho, 1990; Wolfaardt et al., 1999; Gutierrez et al., 2009).

Following a deep water oil spill, there are multiple stages of evolution for the oil, the first stage of which is rapid and concerns a non-hydrostatic release and adjustment of a buoyant plume from the wellhead. Uncontrolled and without intervention, the oil rapidly rises to become a surface slick in a matter of hours. Intervention with dispersants, however, can effectively emulsify a proportion of the oil and reduce its buoyancy, reminiscent to that during the DWH spill, which led to the formation of a massive subsurface oil plume at 1000–1300 m depth. With oil exploration expanding into more challenging environments, such as the Arctic and in deeper waters, it is necessary to instigate studies that aim to understand the fate of oil in these types of environments. One region of interest is the Faroe-Shetland Channel (FSC), which is located between the Faroe Islands (Faroese plateau) and the Shetland Islands (Scottish continental shelf) located ca. 100–150 miles north of Scotland's most northerly mainland point. The FSC is a subarctic region defined by a dynamically complex confluence of different water masses, defined by active water mixing zones, variable physical conditions and large water masses flowing in opposite directions (Berx et al., 2013); it is the 'spaghetti junction' of Icelandic, Norwegian and Atlantic currents. Current oil extraction in the FSC occurs at depths down to ca. 500 m, though oil exploration may expand in the future to depths down to 1500 m. In the event of an oil spill in the FSC, the formation of MOS and its subsequent sedimentation to the seafloor by the process of MOSSFA could cause significant impacts to sensitive benthic ecosystems in these waters, such as rich communities of sponge fauna, the scleractinian coral *Lophelia pertusa*, polychaetes and anemones (Frederiksen et al., 1992; Howell, 2010).

Since the formation of MOS and how oil-degrading communities respond to oil contamination can differ substantially both in space and time in the global ocean, here we investigate MOS formation and the microbial community response to crude oil in surface waters of the FSC, and compare and contrast this to the Gulf of Mexico. We explore this using a deep-sequencing approach with the surface seawater treated with and without nutrient and dispersant amendments, and discuss the role of natural seawater EPS, dispersants and nutrients in influencing MOS formation in the FSC, and of the MOS-associated bacterial community. The findings of this work are anticipated to provide a greater level of understanding on MOS formation and the microbial community response in the FSC as a reference of a contrasting Atlantic water body to the Gulf of Mexico, and to help predict where the oil could end up on the seafloor in the event of an oil spill in this region.

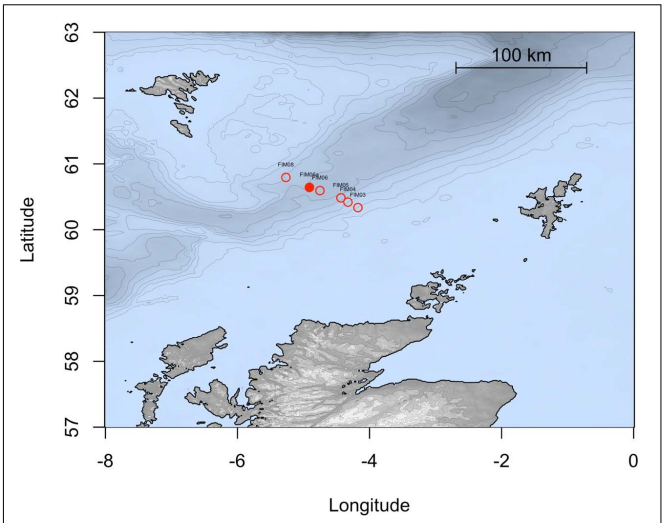

FIGURE 1 | Map representing the stations studied along the FIM section of the Faroe Shetland channel. The solid point shows the station sampled in this study.

MATERIALS AND METHODS

Field Samples

During a research cruise on the MRV *Scotia* on 15 December 2015, sea surface water samples were collected from a depth of 5 m in the FSC (60°38.12′ N, 4°54.03′ W; temp. 8.7°C) at approximately 10 km from the Schiehallion oilfield. Sampling was conducted along the Fair Isle-Munken (FIM) line, which is a sampling transect that runs between the Faroe and Shetland Isles. The water samples fall within a water mass defined as Modified North Atlantic Water (MNAW) which originates from the Faroe Islands and travels in a south to south-westerly direction through the FSC before diverging at the south end of the FSC (**Figure 1**). MNAW is a warm and saltier Atlantic water mass compared to the underlying Arctic/Icelandic cold-water masses that are found at depths from 400 to 1500 m in the FSC (Berx et al., 2013). The water samples were immediately stored at 4°C aboard the ship in 10 L carboys and used within 1 week for the preparation of water-accommodated fractions (WAFs) and in enrichment experiments with crude oil, dispersant and/or nutrient amendment.

Water-accommodated Fractions

A WAF is defined as a laboratory-prepared medium containing dispersed and solubilized crude oil hydrocarbons/droplets by mixing a bulk liquid (e.g., seawater) with crude oil, and subsequent removal of the non-dispersed/solubilised oil. Here, WAF was prepared following the method of Kleindienst et al. (2015b). Briefly, seawater collected from the FSC was first passaged through 0.22 μm filters to remove microbial cells, with the exception that the filtrate was not pasteurized as described in the method of Kleindienst et al. (2015b). Heat treatment could alter seawater chemistry, in particular the molecular integrity of DOM, such as bacterial EPS which was found to play a direct role in MOS formation during the DWH oil spill (Gutierrez et al., 2013). A 100-mL volume of the filter-sterilized seawater was amended with 17.6 mL of pre-filtered (0.22 μm) Schiehallion crude oil (provided by BP) from the offshore Schiehallion oilfield located approximately 175 km west of the Shetland Isles. Seawater amended with only dispersant comprised 100 mL of the filter-sterile seawater and 1.76 mL of Superdispersant-25, which is a UK-approved dispersant. The effective dilution of the dispersant in seawater (dispersant-to-seawater ratio, v/v) was 1:10, which is a dilution that is recommended by the oil and gas industry (Approved oil spill treatment products, Government UK, July 2016). Chemically enhanced WAF (CEWAF) medium was prepared with 100 mL of sterile seawater amended with 17.6 mL of filtered Schiehallion crude oil and 1.76 mL of Superdispersant-25 – the effective dilution of the dispersant in this treatment was also 1:10.

The various mixtures of sterile seawater (SW) amended with oil (WAF), oil+dispersant (CEWAF) and solely dispersant (SW+D) were mixed on a rotary magnetic stirrer at 140 rpm for 48 h at 7°C in the dark in clean sterile (acid-washed) 500-mL glass bottles. The mixtures were allowed to stand for 1 h and then the aqueous phases (avoiding non-dispersed/solubilized oil or dispersant) were sub-sampled into clean (autoclaved and acid-washed with 5% nitric acid) screw-capped glass tubes with Teflon caps. These WAF, CEWAF and SW+D solutions were stored at 4°C and used within 48 h for the various microcosm experiments. Treatments containing nutrients – i.e., seawater+nutrients (SW+N) and CEWAF+nutrients (CEWAF+N) – were amended with 10 μM ammonium chloride, 10 μM sodium nitrate and 1 μM potassium phosphate (final concentrations).

Microcosm Setup and Sampling

To examine the microbial response and formation of MOS in sea surface waters of the FSC when exposed to crude oil, dispersant and/or nutrients, a roller-bottle design was used as previously described (Gutierrez et al., 2013). For this, four microcosm experimental treatments were setup, each prepared using 250-ml

Pyrex© glass bottles (38 × 265 mm) that were maintained in constant and gentle motion in order to simulate pelagic seawater conditions (Jackson, 1994). Each treatment was run in duplicate and comprised of 42.75 ml of filter-sterile WAF, dispersant-only, or CEWAF (with/without nutrients) added to 150 ml of unfiltered natural seawater from the FSC. In addition, two oil-dispersant untreated controls were setup and run in parallel: one comprised seawater alone with no other additions (SW), and the second of seawater with only nutrients added (SW+N). Treatments and controls were each established in duplicates and incubated at 7°C (approx. sea surface temp. in the FSC at the time of sampling) and in the dark at a rotation speed of 15 rpm. The treatments and controls were sampled at five time points over the course of 6 weeks: T_0 at day 0, T_1 after 1 week, T_2 after 2.5 weeks, T_4 after 4 weeks, and T_6 after 6 weeks. At each sampling time, the bottles were placed in an upright position to capture a photographic record of MOS formation. Sub-samples of water were also withdrawn for DNA extraction and DAPI cell counts (see below); care was taken not to capture MOS particles in order to quantify bacterial abundance in the free-living fraction.

Visible aggregates were carefully withdrawn using glass Pasteur pipettes and transferred to 1.5-ml microcentrifuge tubes for staining with the cationic copper phthalocyanine dye alcian blue (AB) at pH 2.5 (Alldredge et al., 1993) or the amino acid-specific dye coomassie brilliant blue G (CBBG) at pH 7.4 (Long and Azam, 1996). AB is used for staining acidic sugars of EPS or transparent exopolymer particles (TEP) in seawater, whereas CBBG is used for staining the proteinaceous component of these polymeric substances. Following staining, the aggregates were washed by transferring them through several droplets of sterile water prior to their examination under the light microscope. To directly examine the prokaryotic community under the microscope, MOS particles were also stained with acridine orange (AO) (Francisc et al., 1973) for imaging with a FITC filter on a Zeiss Axioscope epifluorescence microscopy (Carl Zeiss, Germany). Moreover, the treatments and controls were observed daily over the course of the experiment for detection of any visual change, such as turbidity, emulsion and/or MOS formation.

Genomic DNA Extraction

DNA was extracted from the original natural seawater collected from the FSC and from subsamples taken from each of the treatments and controls of the 6-week roller-bottle experiment. For this, ten milliliter samples were filtered using a glass column filtration system (Millipore) with 45 mm polycarbonate membrane filters (0.22 μm pore size; Isopore) and the filters stored at −20°C. The membrane filters were cut into three equal parts, and then each part placed into 1.5-mL microcentrifuge tubes and ground up with liquid nitrogen. The liquid nitrogen was allowed to completely evaporate from each tube and the contents extracted according to the method of Tillett and Neilan (2000). Purified DNA was stored at −20°C for subsequent molecular analysis.

Barcoded Amplicon Metagenomic Sequencing and Analysis

Barcoded 16S rRNA gene MiSeq sequencing, targeting the V3-V4 hypervariable region, was employed to analyze the bacterial community over the 6-weeks duration of the experiments at time points T_0, T_2, T_4 and T_6. We amplified the 16S rRNA gene in duplicate 50 μl reactions. Each reaction comprised 32 μl molecular biology grade water, 10 μl 5x MyTaq polymerase reaction buffer, 2.5 μl 4 uM primer mix, 0.5 μl MyTaq Enzyme (2.5U; BioLine), 3 μl DMSO (6%), and 2 μl gDNA. The primers used were 341f-CCTACGGGNGGCWGCAG and 785r-GGACTACHVGGGTWTCTAAT. Both primers also had Illumina MiSeq overhangs attached to their 5′ ends. Barcodes were not added at this point of PCR. Thermocycler conditions for this first round of PCR were an initial denaturation of 96°C for 1 min, 32 cycles of 96°C for 15 sec, 55°C for 15 sec, and 72°C for 30s, and a final extension at 72°C for 3 min. PCR clean-up was performed using 20 μl of the PCR product, and adding 1 μl FastAP (1U), 0.5 μl Exonuclease I (10U; both Thermofisher) and 3.5 μl molecular grade water. Conditions for the PCR clean-up reaction were 45 min at 37°C followed by 15 min enzyme denaturation step at 85°C. The purified PCR amplicons were then subjected to a second-step PCR at the sequencing facility for the addition of the Golay barcodes, which were unique to each treatment.

All samples were sequenced via the Illumina MiSeq platform (Illumina 2 × 250 V.2 kit) at the University of Liverpool Centre for Genomic Research[1]; sequences were demultiplexed prior to receipt at our laboratory. Subsequent processing was conducted using the MiSeq SOP (accessed: September 2016) cited within the MOTHUR program (Kozich et al., 2013). In brief, single end reads were examined using MOTHUR (v1.36.1). Contiguous sequences were constructed from paired end sample reads. All sequences with any ambiguities or homopolymers longer than eight bases were excluded from further analysis. All remaining sequences were aligned against a SILVA compatible database. All sequences were trimmed to a maximum length of 465 bases before chimeric sequences were identified and removed using UCHIME (Edgar et al., 2011). The taxonomic identity of sequences was determined by comparison to a MOTHUR formatted RDP database (v.14). Any sequence returned as unknown, chloroplast or mitochondrial were removed from further downstream analysis. Operational taxonomic units (OTUs) were clustered based on 97% sequence identity and subsampled to 35,000 sequences per sample to eliminate sampling bias during subsequent diversity examination. All sequences were deposited in SRA repository under accession number SAMN06246901.

Prokaryotic Cell Counts

To quantify prokaryotic (bacteria and archaea) cell counts, we used the DAPI (4′6-diamidino-2-phenylindole) staining technique. For this, sub-samples of water from each treatment and control of the roller-bottle incubations were fixed with 3.7%

[1]https://www.liverpool.ac.uk/genomic-research

formaldehyde and stored at 4°C for a maximum of 2 weeks. The collection of MOS particles, as part of these water samples, was avoided here, as the accurate enumeration of cells associated with MOS was not feasible due to oil autofluorescence and obscured visualization of cells due to the agglomerate matrix. For each fixed water sample, 5 ml was filtered (0.22 μm) onto gridded (3 mm × 3 mm) polycarbonate filters – this volume was adjusted in order to achieve 10–150 cells per grid. The filters were mounted onto glass slides and the cells stained with DAPI (1 μg/ml) for 20 min and then counted under the Zeiss Axioscope epifluorescence microscope (Carl Zeiss, Germany). A minimum of 10 grids were randomly selected and photographed for counting of cells. The number of cells counted was calculated using the formula: $N = (n_b/n_{Sq}) \times V_f \times (A/A_{Sq})$, where N is the total number of bacteria per mL, n_b is the number of bacteria counted, n_{Sq} is the number of squares counted, V_f is the volume of sea water filtered, A is the effective filter area, and A_{Sq} is the area of one square of the grid.

Statistical Analyses

Relative abundances of sequences obtained using MiSeq were compared using an NMDS plot to visualize β-diversities of each sample for both treatment and time point. An ANOSIM analysis was conducted to determine if there was any significant difference between treatments employed. Further examination of the α-diversity was achieved by generation of rarefaction curves, based on 97% sequence similarity. Moreover, Shannon-Weiner diversity indices of H' were generated and compared using an analysis of variance to determine significant differences between diversity of treatments and time points sampled. All data was log transformed to meet the assumptions of parametric analysis.

RESULTS

MOS Formation

In the roller-bottle microcosm incubations, a rapid formation of MOS was observed within 5 days in the CEWAF+N treatment, and within 7 days in the CEWAF treatment. In both treatments the MOS particles appeared brownish, round and of 'fluffy' texture (**Figures 2A,B**). Initially, the aggregates were small (<3 mm in diameter) and exhibiting amorphous definition. With the naked eye, small oil droplets could be seen associated within the amorphous matrix of the MOS aggregates from these treatments. Over the course of these roller-bottle incubations, the aggregates were observed to become progressively less buoyant, and by week 6 they settled to the bottom of the glass tubes when held in an upright position. The size of the MOS aggregates in these incubations (CEWAF and CEWAF+N) also increased over time (from initially 2–3 mm to ∼2 cm after 4 weeks) and we posit that smaller aggregates had merged together since we observed that the absolute abundance of MOS particles (i.e., that could be counted by visual observation) had decreased over time. By week 4, aggregate size appeared to stabilize (1–2 cm average aggregate size) and remained unchanged thereafter.

In the treatment of seawater with only dispersant (SW+D), however, the formation of large (size range 0.5–3 cm) white aggregates occurred within 3 days (**Figure 2C**), for which we propose to define hereafter as 'marine dispersant snow' (MDS). Aggregates of MDS were approximately 2–3 times larger in size compared to MOS aggregates that formed in the CEWAF and CEWAF+N treatments. As similarly observed for MOS particles in these treatments, MDS aggregates progressively lost their buoyancy and eventually, by week 2, settled to the bottom of the glass tubes when held in an upright position (**Figure 2C**). Manipulation of selected MDS aggregates on a microscope slide revealed they exhibited quite viscous/gelatinous characteristics.

In contrast, the formation of MOS was not observed in the WAF treatment, and no marine snow particles formed in the SW control incubations. However, in the SW+N treatment the formation of marine snow (no oil) was observed and these particles were comparatively small (1–2 mm) and remained so for the duration of these experiments. They were also observed to be extremely fragile and disintegrate when the incubation chamber was gently shaken.

When viewed under the epifluorescence microscope with AO staining, MOS aggregates from the CEWAF and CEWAF+N treatments appeared as amorphous 'fluffy' particles with associated oil droplets (large green blobs; average size range 5 to >20 μm diameter) and represented foci for the attachment of prokaryotic cells (**Figure 3A**). Similarly, MDS aggregates also showed the presence of associated prokaryotic cells (results not shown). Marine snow particles (without oil) that formed in the SW+N treatment, however, were observed to contain markedly fewer prokaryotic cells (**Figure 3B**). When viewed under the light microscope with the aid of dark field illumination, MOS aggregates partially stained with CBBG (**Figure 3C**) and AB (**Figure 3D**).

Bacterial Community Composition of MOS

Barcoded 16S rRNA Illumina MiSeq technology was used to analyze the bacterial community associated with MOS and of that in the surrounding (not associated with MOS) seawater. We were limited to performing this with only the CEWAF+N treatment because MOS aggregates that formed in this treatment maintained there structural integrity and did not disintegrate when handled; MOS aggregates from the other treatments were found to be quite fragile and handling them during the initial processing steps for MiSeq sequencing resulted in them breaking up and completely disintegrating.

Figure 4 shows the bacterial community structure – at family-level classification – of MOS formed in the CEWAF+N treatment at weeks 2.5–4, presented here alongside the community of the surrounding seawater from the same roller-bottle incubation. Of a total of up to 448,754 high quality partial 16S rRNA gene sequences, the MOS bacterial community at the 2.5-week time point showed a clear dominance of members within the *Alcanivoracaceae*, *Alteromonadaceae* and *Pseudoalteromonadaceae* – respectively, on average 38.0, 25.5 and 22.4% of the total MOS-associated community. Minor representation (of >1%) included phyla within the *Rhodobacteraceae* (2.9%), *Rhodospirillaceae* (2.3%),

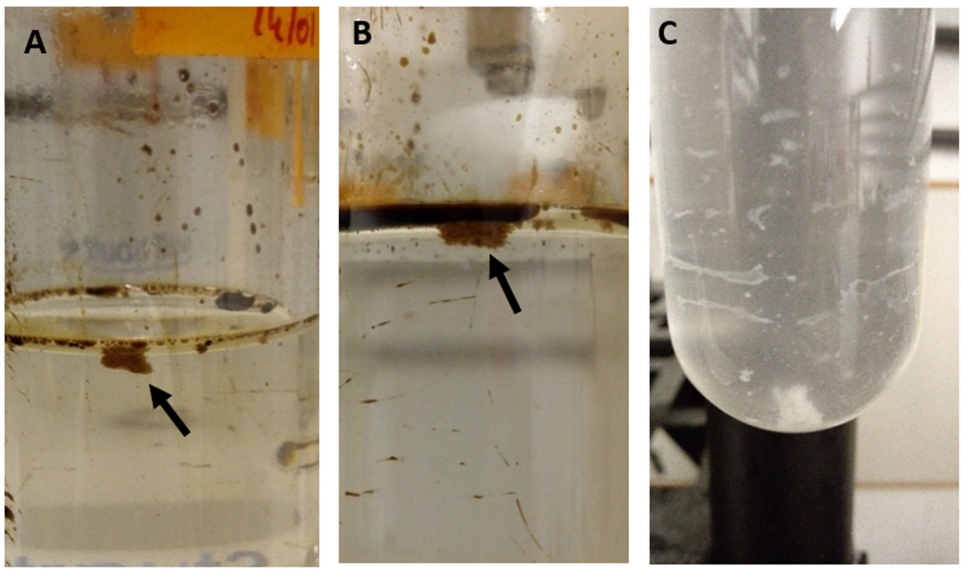

FIGURE 2 | Marine oil snow aggregates shown floating at the surface of the CEWAF (A) and CEWAF+N **(B)** roller-bottle incubations, and Marine Dispersant Snow (MDS) aggregates shown settled at the bottom of the bottles in the SW+D treatments **(C)**.

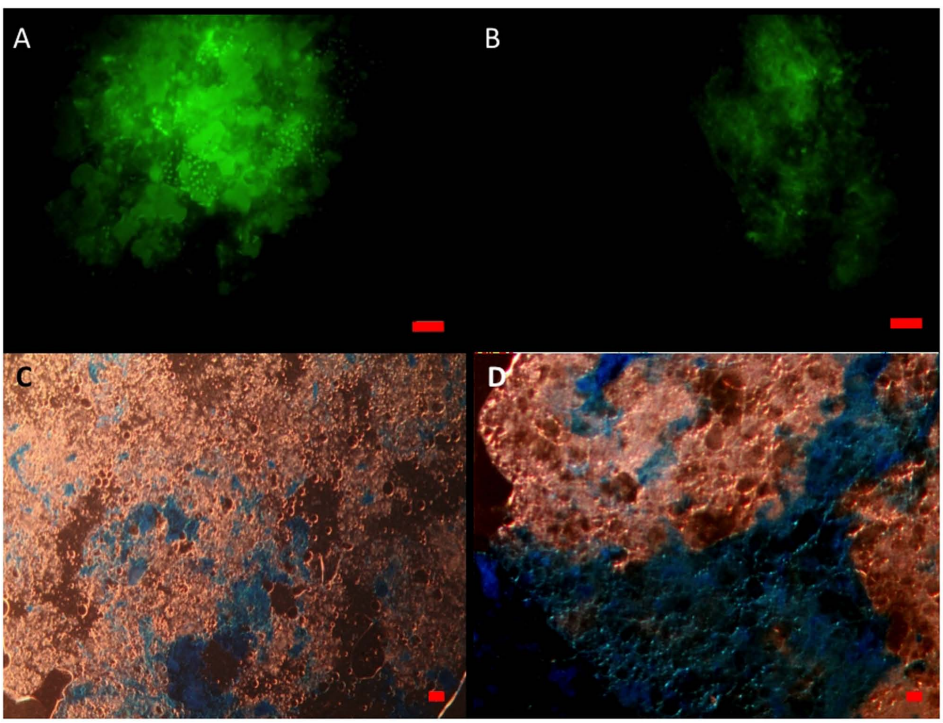

FIGURE 3 | Formation of MOS and marine snow in the roller bottle incubations. Under the epifluorenscence microscope after staining with acridine orange, MOS **(A)** which formed in the CEWAF (±nutrients) treatments was populated with associated prokaryotic cells (small green dots) and oil droplets (larger green spherical/irregular blobs). Marine snow **(B)** that formed in the SW+N treatments contained few associated prokaryotic cells. Under the light microscope, MOS stained with coomassie brilliant blue G **(C)** and Alcian Blue **(D)**. Bar, 10 μm.

Vibrionaceae (2.1%) and *Piscirickettsiaceae* (1.2%). In contrast, the bacterial community of the seawater surrounding the MOS aggregates from this same CEWAF+N treatment at week 2.5 was dominated by phyla within the *Vibrionaceae* (46.1%), with high contributions also by *Pseudoalteromonadaceae* (13.4%), *Rhodobacteraceae* (10.0%), *Alteromonadaceae* (9.0%),

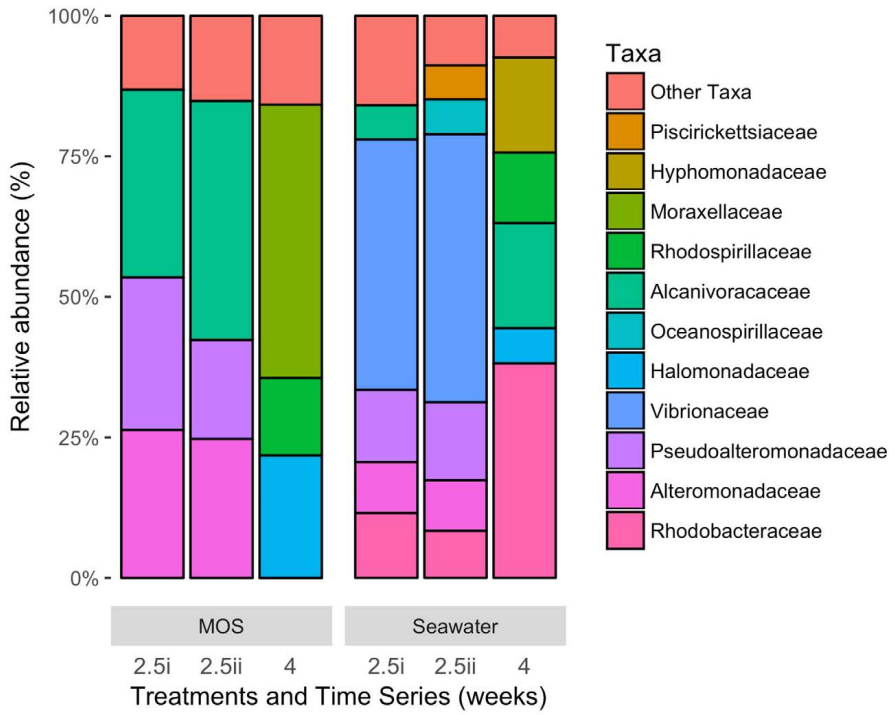

FIGURE 4 | Bacterial community composition at family-level classification of MOS compared to that in the surrounding seawater in the CEWAF+N treatment at weeks 2.5 and 4.

Oceanospirillaceae (5.6%), *Piscirickettsiaceae* (5.5%) and *Alcanivoracaceae* (5.3%).

An analysis of the major orders at the level of genus revealed some interesting groups that dominated the community associated with MOS in the CEWAF+N treatment when analyzed at the T_2 and T_4 time points compared to that in the surrounding seawater (**Supplementary Table S1**). At T_2, MOS was dominated by members of the genera *Alcanivorax* (33–42%), *Pseudoalteromonas* (17–27% of total sequence reads), *Alteromonas* (25%), with minor representation by *Sulfitobacter*, *Vibrio*, *Thalassospira*, *Cycloclasticus* and *Mesonia* (collectively contributing < 10% of total reads). At the T_4 time point, MOS was dominated by members of the genera *Psychrobacter* (48.4% of total sequence reads), *Cobetia* (21.6%), *Thalassospira* (13.8%), with minor representation by *Pseudoalteromonas* (4.4%), *Alcanivorax* (2.7%), *Cycloclasticus* (1.6%) and *Marinobacter* (1.2%). In terms of the number of 16S rRNA reads that were found enriched on MOS compared to their abundance in the surrounding seawater at the T_4 time point, *Psychrobacter* was 970-fold higher in abundance, *Marinobacter* 20-fold higher, *Halomonas* 8.5-fold higher, *Pseudoalteromonas* 7.5-fold higher, *Cobetia*, *Cycloclasticus* and *Vibrio* 3.5-fold higher, *Alteromonas* 3-fold and *Thalassolituus* 1.5-fold higher.

Bacterial Community Dynamics in the Various Treatments

To assess the free-living (not associated with MOS) prokaryotic community dynamics in the different treatments amended with and without nutrients, dispersant or crude oil, DAPI counts were determined over the 6-week duration of these experiments at time-points T_0 (start day of the experiment), T_1 (after 1 week), T_2 (after 2.5 weeks), T_4 (after 4 weeks) and T_6 (after 6 weeks). As shown in **Figure 5**, prokaryotic cell abundance across all six treatments at the start of the experiment (T_0)

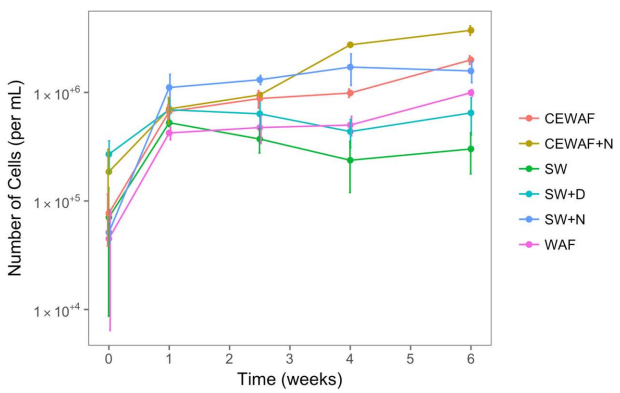

FIGURE 5 | Prokaryotic (bacterial and archaeal) cell numbers from roller-bottle incubations of the different treatments with sea surface water from the FSC amended with or without nutrients, dispersant and/or crude oil (as WAF). SW, seawater; SW+N, seawater with nutrients; SW+D, seawater with dispersant; WAF, water-accomodated fraction; CEWAF, chemically enhanced WAF; CEWAF+N, chemically enhanced WAF with nutrients.

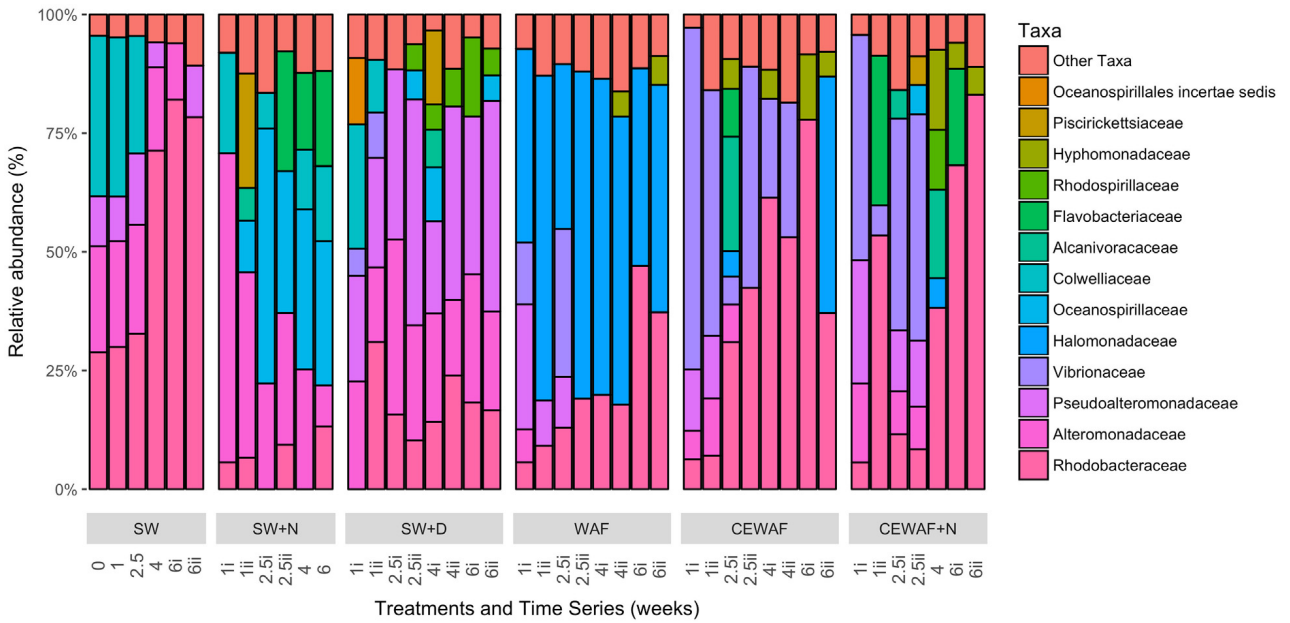

FIGURE 6 | Bacterial community composition at family level classification for each of the different treatments over the 6 week incubation period that the roller-bottle experiments were run. SW, seawater; SW+N, seawater with nutrients; SW+D, seawater with dispersant; WAF, water-accomodated fraction; CEWAF, chemically enhanced WAF; CEWAF+N, chemically enhanced WAF with nutrients.

was 0.8–15.0 $\times$ 10^4 cells/ml, and as expected cell abundance in the untreated control (SW) remained low relative to the other treatments throughout the 6-week duration of these experiments. Similarly, low prokaryotic cell abundances were achieved in the SW+D and WAF treatments (6.9 $\times$ 10^5 and 9.9 $\times$ 10^5 cells/ml, respectively). In the SW+N treatment, however, cell numbers showed the highest increase within the 1st week, and then slowing down to a steady increase over the proceeding 3 weeks, and reaching maximal abundances by week 4 (1.7 $\times$ 10^6 cells/ml). Prokaryotic cell abundances in the CEWAF and CEWAF+N treatments followed a similar increasing trend initially, and their dynamics diverged after about 2 weeks. Cell abundances in the CEWAF+N treatment showed the most notable increase compared to the other treatments, reaching 3.7 $\times$ 10^6 cells/ml by week 6.

We note that although our DAPI counts demonstrated an expected pattern for prokaryotic dynamics in these treatments, the counts are likely to be somewhat underestimated with particularly the treatments where MOS had formed due to the high numbers of DAPI-stained prokaryotic cells associated with MOS particles (**Figure 3**). The enumeration of the cells was practically impossible to count accurately because of their density and localization within and on the surface of the MOS aggregates.

The diversity of the bacterial communities in the surface seawater of the FSC and their response to and dynamics in the various treatments (SW, SW+N, SW+D, WAF, CEWAF, CEWAF+N) was assessed using Illumina MiSeq technology and shown at family-level classification in **Figure 6**. At the commencement of these experiments (denoted by time point T_0), the community was initially dominated by groups within the *Alteromonadales* and *Rhodobacterales* – collectively 96% of total sequence reads. The major genera of this T_0 community constituted *Colwellia* (33.7%), *Sulfitobacter* (28.2%), *Pseudoalteromonas* (10.5%), *Alteromonas* (2.7%) and other members of the family *Alteromonadaceae* (22.4%) (**Supplementary Table S1**). Other phyla, such as the hydrocarbonoclastic bacteria *Alcanivorax*, *Cycloclasticus*, *Marinobacter* and *Thalassolituus*, as well as *Halomonas* that, like *Alteromonas* and *Pseudoalteromonas*, are recognized producers of EPS, were also present though in low abundance ($\leq$0.5% for each; **Supplementary Table S1**). This bacterial community of the FSC sea surface in the untreated control (SW) maintained a relatively consistent structure throughout the 6-week duration of these experiments. Rarefaction analysis of a sub-set (35,000 sequences) of the 16S rRNA gene sequences showed that for no treatment was saturation of sequencing reached (**Supplementary Figure S1**). The OTU richness of each treatment ranged between 520 and 1,010 of identified OTUs at T_1, and upon the termination of the experiment (T_6) all the treatments exhibited, with the exception of SW+N and CEWAF+N, a reduction in the number of OTUs. Overall the α-diversity indices (Shannon-Weiner H') for each treatment indicated that only SW+D and SW+N had higher diversities than were measured for the SW controls (**Supplementary Figure S2A**; ANOVA, $F_5 = 0.05326$, $p < 0.01$). Moreover, diversity also declined overall during the period of the experiment (**Supplementary Figure S2B**; ANOVA, $F_1 = 0.1192$, $p < 0.01$). The similarity between treatments and samples therein can be visualized in **Figure 7**. This indicated the similarity of each sample to all other samples examined and confirmed that there was significant dissimilarity between the bacterial communities

within the treatments (ANOSIM, $R = 0.6624$, $p < 0.001$). Here it can be observed that the β-diversity most prominently differs between water types and not time points measured. Most distinct is the SW+N and SW+D treatments.

Within the first week, this complex community of the FSC surface seawater became overlayed by opportunistic bacteria that were stimulated by the presence of either nutrients, dispersant and/or crude oil. The community in the SW+N control treatment showed a rapid enrichment of members within the order *Alteromonadales*, mainly of the genus *Alteromonas*, which remained as a dominant group (21–60%) until the termination of the experiment when their abundance decreased to ca. 8% at week 6. To a lesser extent, *Neptuniibacter* within the order *Oceanospirillales* and members of the family *Flavobacteriaceae* were also dominant groups that bloomed by week 2 and collectively persisted as the most dominant groups for the remaining duration of these incubations. Furthermore, a progressive enrichment of members within the *Rhodobacteraceae* occurred by week 1 and reached 13% of the total community by week 6. Similarly in the SW+D treatment, members of the *Alteromonadales* dominated the community, though this time contributed by the genera *Pseudoalteromonas* and *Alteromonas*, and their dominance persisted for the remaining duration of the experiment. However, the community showed clear, though lower, representation of groups within the *Rhodospirillales*, mainly contributed by the genus *Thalassospira*, and by members of the *Rhodobacterales* and *Oceanospirillales*, and by phyla of the class *Gammaproteobacteria* that included the genus *Vibrio*, although it bloomed (up to 10%) in only the first week. Compared to the SW and SW+N controls, the presence of dispersant in the SW+D treatment effected a clear reduction (to <1%) in the abundance of *Colwellia* by week 2.

In the WAF treatment, where the FSC seawater was amended with crude oil in the form of a WAF, the microbial response was distinctly different compared to the SW, SW+N and SW+D treatment. Within 1 week the community of the WAF treatment became strongly dominated by members of the *Oceanospirillales*, largely of the genus *Halomonas* (34–65%) that persisted as the major group for the remaining duration of the experiment. Other major groups included members of the *Alteromonodales*, largely of the genus *Pseudoalteromonas* but that bloomed in week 1 (up to 25%) and progressively decreased in abundance thereafter. Members of the family *Rhodobacteraceae* increased in abundance from week 1, reaching maximal levels (42.2%) by week 6, and a short-lived bloom of *Vibrio* occurred within weeks 1–2. As observed in the SW+D treatment, the abundance of *Colwellia* dramatically decreased in abundance, this time within week 1, in the WAF treatment.

The bacterial community response in the CEWAF and CEWAF+N treatments contrasted substantially to the controls and other treatments. Here, the bacterial community response to the oil and dispersant (in the presence or absence of nutrients) revealed a more complex pattern of microbial succession, especially when viewed at the genus-level classification, over the 6-week duration of these incubations. Within the first week, both treatments showed a strong bloom for members of the *Vibrionales*, principally the genus *Vibrio*, that then decreased in abundance by week 3 in the CEWAF+N treatment, and by week 4 in the CEWAF treatment. In parallel, a progressive decrease in the abundance for members of the order *Alteromonadales* occurred within the first few weeks, principally contributed by the genera *Colwellia*. As similarly observed in the SW+D and WAF treatments, the abundance of *Colwellia* in these CEWAF and CEWAF+N treatments dramatically decreased within week 1 and remained in very low abundance (<0.4%) for the remaining duration of these experiments. On the other hand, *Pseudoalteromonas*, also a member of the order *Alteromonadales*, remained at relatively high abundance for the first week in the CEWAF treatment (13.2%) and second week in the CEWAF+N treatment (13.4–14.1%) before decreasing thereafter, whereas *Marinobacter* bloomed intermittently at weeks 1–2 in, respectively, the CEWAF (6.5%) and CEWAF+N (6.2%) treatments. Other phyla that became strongly selected for in these oil-dispersant treatments were members of the order *Rhodobacterales* within the class *Alphaproteobacteria*, principally contributed by *Sulfitobacter* in only the CEWAF treatment, and other members of the family *Rhodobacteraceae* in both treatments, with minor representation by *Hyphomonas* at week 6 in the CEWAF treatment and in weeks 4–6 in the CEWAF+N treatment. Other enriched groups of *Rhodobacterales* included *Oceanicaulis* and *Oceanicola* in only the CEWAF treatment at weeks 2–6. Short-lived blooms of *Mesonia*, of the class *Bacteroidetes*, occurred at week 2 and in weeks 4–6 in, respectively, the CEWAF and CEWAF+N treatments.

Notably, the enrichment of the obligate alkane-degrader *Alcanivorax* occurred in the CEWAF treatment during the

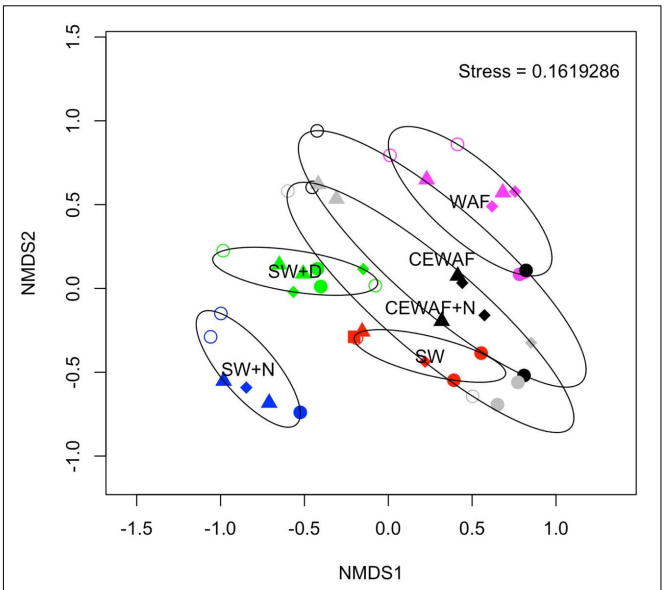

FIGURE 7 | Non-metric multidimensional scaling (NMDS) plot showing the similarity of each sample. The stress achieved is indicated in the top right of the plot. Symbol colors signify the original treatment: SW (red); SW+N (blue); SW+D (green); WAF (purple); CEWAF (black); CEWAF+N (gray). Each time point is represented by a different symbol: T_0 (square); T_1 (open circle); T_2 (triangle); T_4 (diamond); T_6 (closed circle). Ellipses shown surrounding symbols represent grouping the treatment types with 95% confidence interval.

first 2 weeks and which was prolonged into week 4 in the CEWAF+N treatment before the abundance of these organisms dissipated thereafter in both of these treatments to background levels. Members of another alkane-degrader, *Thalassolituus*, and of the PAH-degrader *Cycloclasticus* were also enriched in only the CEWAF+N treatment, occurring during week 2. A less pronounced enrichment of members within the genus *Thalassospira*, for which some species have been described to degrade hydrocarbons, occurred in both these treatments and only toward the end of these incubations.

DISCUSSION

To our knowledge this is the first study examining the formation of MOS in northeast Atlantic waters. We specifically focused on the FSC where subsurface oil extraction is currently occurring and where exploration for oil in deeper waters (>1000 m depth) within this channel may expand in the near future. This is important given that an oil spill in the deep waters of the FSC could produce a similar oil spill as occurred during the DWH blowout in the Gulf of Mexico, and one that could be considerably more complex and difficult to combat given how much more hydrodynamic the FSC water column is compared to the Gulf of Mexico. Our findings showed that crude oil alone does not act as an inducer for MOS formation in surface waters of the FSC, and that the addition of dispersant in the presence of oil appeared to be an important factor in triggering MOS formation, as observed in the CEWAF and CEWAF+N treatments. Even in the absence of crude oil, however, aggregates formed in the SW+D treatment and resembled those observed in the experiments of Kleindienst et al. (2015b) who used water from the Gulf of Mexico supplemented with the dispersant Corexit – a dispersant that was profusely used by BP on sea surface oil slicks and pumped directly at the leaky Macondo well-head during the DWH spill (National-Commission on the BP Deepwater Horizon Oil Spill and Offshore Drilling, 2011). In both studies, these dispersant aggregates appeared white, gelatinous and viscous when handled. These findings suggest that contrasting waters – i.e., the Gulf of Mexico and FSC – can lead to the formation of dispersant-induced aggregates displaying similar macroscopic characteristics. Since the use of dispersants in a marine setting is mainly as a contingency to combat oil spills, the SW+D treatment acted as a semi-control to test the effects of the dispersant on the microbial community in our experiments and is discussed below.

The formation of MOS is likened to marine snow particles that are a crucial component of the biological pump in the ocean and defined as 'hot spots' for microbial activity (Long and Azam, 2001; Daly et al., 2016) where their exists a heightened level of enzyme activity and degradation rates compared to that in the seawater environment immediately surrounding these particles (Smith et al., 1992). As reported by Giani et al. (2005), the formation of marine snow correlates with specific physical conditions (water column stratification, low mixing) and biological production patterns in the water column, such as nutrient concentrations, microbial production of TEP and EPS. Furthermore, the formation and evolution of marine snow particles can vary considerably in terms of their size and content of mucilaginous matter, such as TEP and EPS (Giani et al., 2005; Passow et al., 2012) which are a matrix for marine snow formation (Passow, 2016). Our results showed that the presence of dispersant and crude oil (CEWAF treatment) yields MOS, but that oil alone (WAF treatment) does not. Furthermore, the addition of nutrients alone to seawater (SW+N treatment) triggers the formation of marine snow in surface waters of the FSC. Notably, nutrients amplified the abundance and size of MOS particles, as observed in the CEWAF+N treatment, and the structural integrity of these nutrient-aided MOS particles was more robust compared to that of their counterparts formed in the CEWAF treatment without added nutrients. van Eenennaam et al. (2016) also described the formation of fragile MOS that easily falls apart when agitated, and that the bacteria associated with eukaryotic phytoplankton, principally through their production and release of EPS, enhances MOS formation. These findings indicate that microorganisms, in particular EPS-producing bacteria, play a key role in MOS formation, and that nutrients enhanced the activities of these organisms and yielded higher concentrations of EPS in the CEWAF+N. We hypothesize that EPS then interacted with crude oil and/or dispersant to form MOS, as previously observed (Gutierrez et al., 2013). Other reports have also shown nutrient additions to seawater in influencing the formation of MOS (Kleindienst et al., 2015b; Daly et al., 2016 and references therein).

We used MiSeq sequencing to examine the bacterial taxa that were influenced by nutrients and potentially induced or upregulated the release of EPS and effected MOS formation in the CEWAF+N treatment. Hitherto, the only published study to have examined this type of community analysis for MOS was reported by Arnosti et al. (2016) who used Sanger sequencing of clone libraries to analyze the bacterial community associated with MOS that formed in roller-bottle experiments with sea surface waters from the Gulf of Mexico. As in our present study, Arnosti et al. (2016) showed their MOS aggregates harbored a bacterial community composition that was distinctly different from that in the surrounding seawater. The MOS aggregates from the Gulf of Mexico were primarily composed of oil-degrading (*Cycloclasticus*, *Marinobacter*) and EPS-producing (*Halomonas*) bacteria, including diverse members of the order *Rhodobacterales* (principally within the family *Rhodobacteraceae*). This corroborates our results with FSC surface waters where we identified the enrichment of these taxa on MOS formed in the CEWAF+N treatment, as well as other taxa with recognized oil-degrading (*Alcanivorax*, *Thalassolituus*, *Thalassospira*) and EPS-producing (*Pseudoalteromonas*, *Alteromonas*, *Vibrio*, *Cobetia*) qualities. This enrichment of bacterial taxa which specialize in oil-degradation and EPS production is consistent with the reduction in α-diversity observed in the water fractions of this study over the course of the incubations (**Supplementary Figure S2B**). Kleindienst et al. (2015b) used catalyzed reporter deposition in combination with fluorescence *in situ* hybridization (CARD–FISH) to analyze MOS aggregates from their CEWAF+N treatments with Gulf of Mexico seawater and found the aggregates were dominated

by members of the class *Gammaproteobacteria*, including the order *Alteromonadales*, and in particular members of the genus *Colwellia*, hence suggesting that *Colwellia* may play an important role in MOS formation in the presence of dispersants. During incubations with uncontaminated deep water samples collected during the active phase of the Gulf oil spill, Baelum et al. (2012) also reported the formation of MOS which was also dominated by members most closely related to *Colwellia*. Conversely, *Colwellia* contributed 0.01% abundance to MOS that formed in our CEWAF+N treatments by week 4 (T_4), and the abundance of these organisms decreased sharply within week 1 in all the treatments amended with dispersant and/or crude oil. Hence, these contrasting water bodies of the Atlantic region (i.e., the Gulf of Mexico vs FSC) differ with respect to the bacterial taxa associated with MOS, and potentially also its formation and fate.

Interestingly, the most dominant organisms associated with MOS were members of the genus *Psychrobacter* (48.5% of total community reads from T_4 samples), which is a genus recognized for cold-tolerance – some have been isolated from permafrost and Antarctic waters – and reported to produce EPS (Leiye et al., 2016). These organisms have also been found in waters contaminated with crude oil in the Arctic (Deppe et al., 2005) and Antarctic Sea (Prabagaran et al., 2007), hence suggesting putative hydrocarbon-degrading qualities. *Psychrobacter* has not previously been reported associated with MOS, and based on its dominant abundance of the total MOS-associated bacterial community these organisms may be an important contributor to MOS formation in surface waters of the FSC and/or the degradation of oil droplets associated with these aggregates. Although, further work will be needed to better elucidate this. We posit that the collective community of opportunistic heterotrophs associated with MOS contributes two key roles. The first is in the formation of MOS, which we hypothesize is mediated by EPS of organisms such as *Pseudoalteromonas* and *Alteromonas* that were abundant taxa associated with MOS at the initial stages of its formation (T_2) in our experiments. The second is to the degradation of hydrocarbons within crude oil droplets entrained within the amorphous 'net-like' scaffolding of MOS. We hypothesize that hydrocarbon-degradation rates are markedly higher on MOS aggregates compared to in the surrounding seawater medium. This is supported by high rates of lipase hydrolysis acitivity detected on MOS aggregates formed in roller bottle experiments with surface seawater collected from the Gulf fo Mexico during the DWH oil spill (Ziervogel et al., 2012). The enrichment of obligate hydrocarbonoclastic bacteria on MOS, such as members of the genus *Alcanivorax* (33–42% relative abundance of the total MOS community) identified in our experiments, indicates MOS as a niche environment where oil biodegradation activities may be significantly elevated compared to that in the surrounding seawater environment. By week 4 the *Alcanivorax* population associated with MOS had decreased to <3% of the total community, suggesting that the bulk of the *n*-alkane hydrocarbons, which these organisms preferentially use as carbon substrates, had become sufficiently depleted on the MOS aggregates. This assumes these organisms had detached from the MOS aggregates to find new sources of utilizable hydrocarbons, which corroborates with the observed increase in their relative abundance in the seawater environment surrounding these aggregates.

Considering that MOS had already been observed on surface waters of the Gulf of Mexico during the DWH oil spill before BP had begun their operation of spraying tons of dispersants (Passow et al., 2012), and laboratory roller-bottle experiments without added dispersants showed the rapid formation of MOS (Ziervogel et al., 2012; Gutierrez et al., 2013), MOS formation is very likely a biologically driven process. Halomonads, in particular, are commonly linked with the production of large quantities of EPS (Quesada et al., 1994; Béjar et al., 1998; Calvo et al., 1998, 2002; Arias et al., 2003; Gutierrez et al., 2007), and like for many other EPS-producing marine bacteria (e.g., *Alteromonas*, *Pseudoalteromonas*), they can contribute large quantities of EPS to the total DOM pool in the ocean (Azam, 1998). In fact, a large fraction of the DOM in the ocean is of glycoprotein in composition (Long and Azam, 1996; Verdugo et al., 2004), which is consistent with the composition of marine bacterial EPS (Mancuso Nichols et al., 2004; Gutierrez et al., 2007; Hassler et al., 2011). This concurs with our observation of MOS aggregates under the microscope after staining with AB or CBBG, which revealed marine snow formed in the SW+N treatments and MOS formed in the CEWAF and CEWAF+N treatments is largely composed of glycoprotein, and is evidence that it is of biogenic (likely bacterial) origin.

It has been suggested that MOS formation is initiated via the physicochemical interaction between oil droplets, microbial cells and biopolymer – the latter likely of microbial origin (Passow et al., 2012). Our results showed that the presence of a dispersant (Superdispersant-25) enhances MOS formation, as observed in the CEWAF treatment and reported elsewhere using the dispersant Corexit that was used at DWH (Fu et al., 2014). Nutrients were, however, found to amplify the abundance and size of MOS, as observed in the CEWAF+N treatment. However, the fact that marine snow was formed in the SW+N treatment, without any added dispersant, suggests that MOS formation is indeed a biologically driven process that likely involves endogenous DOM in seawater (in the form of TEP and EPS) and which is likely enhanced by the *de novo* synthesis of EPS by EPS-producing bacteria. This is supported by the diversity of EPS-producing taxa we identified enriched on MOS that formed in the CEWAF+N treatment. Correlating this to the Gulf of Mexico environment where profuse quantities of MOS were observed during the DWH oil spill, Lin and Guo (2015) found elevated levels of dilute-HCL-resistant polysaccharides (HR-PCHO) abundance and total dissolved carbohydrates-to-dissolved organic carbon (TCHO/DOC) ratio at some sampling stations. This likely resulted from enhanced microbial production of EPS due to the presence of oil components and nutrient inputs from the Mississippi river (Muschenheim and Lee, 2002; Khelifa et al., 2005).

The CEWAF and CEWAF+N treatments simulated the application of a UK-approved dispersant (Superdispersant-25) and of nutrients – approaches that are often used as a bioremediation strategy for combatting marine oil spills – to investigate the microbial response in surface waters of

the FSC. Although we did not conduct measurements for nutrient concentrations, the observed increase in prokaryotic cell abundance, as well as significantly greater α- and β-diversities, in the SW+N treatments is indicative that nutrients are a significant limiting factor in surface waters of the FSC. In support of this, experimental studies in the North Atlantic have shown that bacterial growth can be restricted by the availability of PO_4^{3-} (Cotner et al., 1997; Rivkin and Anderson, 1997; Caron et al., 2000). Interestingly, Kleindienst et al. (2015b) observed highest prokaryotic cell abundances in WAF treatments by the end of their experiments, whereas we reported highest abundances in the CEWAF+N treatments. This difference across these two studies may be explained by differences in endogenous concentrations of nutrients in the Gulf of Mexico compared to in the FSC that could support growth without addition of an exogenous carbon source (e.g., crude oil or dispersant). Differences in crude oil constituents and their solubility, as well as concentrations of labile/semi-labile DOM between these studies should also be considered. We also measured higher cell abundances in the CEWAF treatments compared to in the WAF treatments. Taken collectively, these results suggest that the presence of dispersant, and particularly added nutrients, stimulate microbial growth in FSC surface waters when contaminated with crude oil. Whether any microbial group was able to degrade and grow on the dispersant used in this study (Superdispersant-25) remains to be investigated.

Our microbial community analysis of FSC surface waters indicated that members of the order *Alteromonadales* and *Rhodobacterales* constituted the dominant proportion (96%) of total sequence reads – lineages which are consistently found and often in high relative abundance in surface waters of the Gulf of Mexico (Yang et al., 2016) and open-ocean Atlantic (Swan et al., 2011). However, the exception was a lack of representation by the SAR11 clade, which is a major group that is commonly found in pelagic waters (Morris et al., 2002) and, quite possibly, because this group has been shown to be susceptible to oil pollution (Lanfranconi et al., 2010; Chronopoulou et al., 2015). Whilst we are planning to analyze whether the surface waters of the FSC are contaminated with hydrocarbons, as might be likely due to the prevalent oil extraction activities occurring in these waters and in those of the adjacent North Sea, the presence of hydrocarbon contaminants could explain the undetectable presence of these organisms in our sequencing libraries. *Colwellia* is a genus of psychrophilic marine heterotrophic generalists, which expectedly was found in the cold surface waters of the FSC, but atypically in quite high relative abundance. Unlike the rapid colonization of these organisms in sea surface oil slicks and subsurface oil plume in the Gulf of Mexico during the DWH spill (Redmond and Valentine, 2012; Yang et al., 2016), the dramatic decline of *Colwellia* in our experiments amended with dispersant, crude oil or both suggests that these organisms may too be susceptible to hydrocarbons in FSC surface waters and to synthetic dispersants, such as Superdispersant-25. Their rapid reduction in the SW+N treatment, however, suggests that these organisms may also suffer a competitive disadvantage to other members of the community during periods of spiked nutrient influxes. *Colwellia* in the surface waters of the FSC may be physiologically inclined as strict oligotrophs. This in contrast to certain oligotypes of *Colwellia* that were identified in the Gulf of Mexico with a predilection for degrading and growing on the dispersant Corexit and crude oil (Kleindienst et al., 2015b). Of further interest, surface waters of the FSC contained a dominance of *Sulfitobacter* (up to 28%), which is a sulfite-oxidizing member of the *Alphaproteobacteria* within the *Roseobacter* clade (Buchan et al., 2005). The abundance of these organisms dramatically fell and was sustained at low levels (often < 2%) by the presence of either exogenous nutrients or crude oil. However, in the presence of dispersant (+/− crude oil and nutrients), an initial dramatic reduction in their abundance was followed by their recovery to abundances >5% and as high as 50%. Since Superdispersant-25 is a sulfur-containing dispersant, it is likely that certain members of the *Sulfitobacter* community sustained a relative high abundance in these dispersant-amended treatments because they were capable of feeding on the sulfur constituent as an energy source.

The presence, albeit in relative low abundances (<0.6%), of obligate hydrocarbonoclastic bacteria (*Alcanivorax*, *Cycloclasticus*, *Oleispira*, *Thalassolituus*) – organisms that are recognized as key players in the biodegradation of crude oil and its refined petrochemical products in the marine environment (Yakimov et al., 2007) – was not unexpected, and included representation of the 'generalist' oil-degrader *Marinobacter*. These organisms are typically found at background levels in the global ocean (Yakimov et al., 2007). With the exception of *Oleispira*, the intermittent (1 week) or sustained (over several weeks) bloom of these organisms in the CEWAF and/or CEWAF+N treatments is reminiscent of their strong enrichment in oil-impacted environments where they can be expected to increase in numbers from near undetectable levels. Other taxa that were also strongly selected for in these treatments included *Halomonas*, *Alteromonas* and *Pseudoalteromonas* – genera that contain members with reported hydrocarbon-degrading capabilities, though are more commonly associated with producing EPS (Béjar et al., 1998; Calvo et al., 1998, 2002; Arias et al., 2003; Mancuso Nichols et al., 2004; Bhaskar and Bhosle, 2005; Gutierrez et al., 2007, 2008, 2009, 2013). Interestingly, a study that investigated the response of pelagic bacterial communities to crude oil in the North Sea showed that the most dominant responder was *Pseudoalteromonas* (10-fold enrichment), with practically no detection for any of the obligate hydrocarbonoclastic taxa; however, denaturing gradient gel electrophoresis (DGGE) of the bacterial 16S rRNA gene was used for analyzing microbial community profiles in this study which, based on its limited coverage for capturing near total diversity, will likely have missed less abundant taxa (Chronopoulou et al., 2015). Nonetheless, this highlights how different water bodies, even those adjacent to each other at the same or proximal latitude, can yield differential microbial community responses to crude oil contamination, which may be attributed to, though not always entirely, to a predilection of certain taxa to hydrocarbons.

Interestingly, a short, but strong enrichment in the CEWAF and CEWAF+N treatments for members of the *Vibrionales* – principally the genus *Vibrio* – revealed that these organisms may

participate in the degradation of crude oil in FSC surface waters. The enrichment of these organisms is not frequently observed at contaminated sites in the marine environment, although there are snippets in the literature reporting on the enrichment of these organisms by crude oil. For example, members of the *Vibrionales* were found enriched in beach sands of the Gulf coast that had become contaminated with Macondo oil from the DWH spill, and several oil-degrading *Vibrio* spp. were isolated and found to degrade hydrocarbons (Kostka et al., 2011). Also, a 91-fold increase in the relative abundance of *Vibrionales* was detected in oil contaminated sea surface oil-slick water samples from DWH when incubated to develop anaerobically (Gutierrez et al., 2016). An analysis of the genomes of several *Vibrio* species found these organism capable of metabolizing hydrocarbons, including PAHs (Grimes et al., 2009). Further work will be needed to fully understand the hydrocarbon-degrading potential and role of these organisms in the FSC.

This study highlights the importance for the application of dispersants and/or nutrient-amendments in MOS formation in the event of an oil spill in the FSC. We also identified oil-degrading and EPS-producing bacteria associated with MOS, and that crude oil alone does not yield MOS in these waters. We note that the seawater used in this study was obtained from one seasonal period of the year (the winter of 2015) and that further work would be needed to explore MOS formation in waters collected during other seasons in order to provide a more conceptual understanding of this process given the unpredictability of when an oil spill might occur in the FSC. We also demonstrate that surface waters of the FSC harbor communities of hydrocarbonoclastic bacteria that positively respond to crude oil contamination, and that amending these waters with dispersant and/or nutrients could stimulate microbial community activities. Based on our findings, such approaches should be considered in bioremediation strategies in the event of a major oil spill in this region of the northeast Atlantic, although further instigative work to assess this is warranted. Essentially, the influence of dispersants on oil-degrading bacteria remains poorly understood and requires further investigation using different types of dispersants and evaluation across different water bodies. Our findings on MOS formation and the microbial response to oil in FSC surface waters mirror those observed at DWH and hence underscore their broad relevance.

CONCLUSION

Marine oil snow is possibly the most important mechanism by which oil reaches the seafloor in the event of a spill at sea. Our study shows that in the event of an oil spill in the FSC, the use of dispersants would likely lead to the formation of MOS and trigger a subsurface "dirty blizzard," reminiscent to that during the DWH oil spill where a large proportion of sea surface oil ended up on the sea floor. In the absence of dispersant applications, the majority of surface oil is likely to remain at the sea surface. Hence, any research conducted to evaluate crude oil impacts to benthic ecosystems in the FSC would need to take into account the physicochemical state of the oil presented in the form of MOS aggregates – direct exposure of sediment samples or cores to crude oil for such investigations would be unrealistic. Our study also showed that MOS particles formed with FSC surface seawater harbor rich communities of prokaryotes, including oil-degrading bacteria, potentially acting as 'hot spots' where a heightened level of oil biodegradation occurs.

AUTHOR CONTRIBUTIONS

LDS and TG contributed to the design of the work and its interpretation. LDS and SS produced all of the data and, together with TG, wrote the manuscript.

FUNDING

This manuscript contains work conducted during a Ph.D. study undertaken as part of the Natural Environment Research Council (NERC) Centre for Doctoral Training (CDT) in Oil and Gas. It is sponsored by Heriot-Watt University via their James-Watt Scholarship Scheme to LDS and whose support is gratefully acknowledged. Partial support was also provided through a Royal Society Research Grant (RG140180) and a Society for Applied Microbiology grant to TG.

ACKNOWLEDGMENTS

We thank chief scientist Alejandro Gallego of Marine Scotland Science, and the ship and scientific crew of MRV *Scotia* for their hard work, facilities and support to accommodate our research needs during a research cruise to the FSC. We also thank Angelina Angelova for assistance with the preparation of the DNA for MiSeq analysis, Paul Smith at Oil Slick Dispersants Ltd. for Superdispersant-25, and BP for the Schiehallion crude oil. We would also like to thank the two reviewers for their valuable comments during the preparation of the manuscript.

SUPPLEMENTARY MATERIAL

The Supplementary Material for this article can be found online at: http://journal.frontiersin.org/article/10.3389/fmicb.2017.00676/full#supplementary-material

FIGURE S1 | Rarefaction curves signify the α-diversity of all treatments across all sampling times. OTUs are identified based on similiarity of the 16S rRNA gene (97%). SW, seawater; SW+N, seawater with nutrients; SW+D, seawater with dispersant; WAF, water-accomodated fraction; CEWAF, chemically enhanced WAF; CEWAF+N, chemically enhanced WAF with nutrients. Sample points are: T_1, **(A)**; T_2, **(B)**; T_4, **(C)**; T_6 **(D)**.

FIGURE S2 | The Shannon-Weiner diversity indices are presented here as a boxplot comparing the α-diversity between water treatments (A) and time points **(B)** measured in this study.

Table S1 | Composition of MiSeq sequenced 16S rRNA gene reads, analyzed in genus-, family-, and order-level resolution for each of the different treatments.

REFERENCES

Alldredge, A. L., Passow, U., and Logan, B. E. (1993). The abundance and significance of a class of large, transparent organic particles in the ocean. *Deep Sea Res.* 40, 1131–1140. doi: 10.1016/0967-0637(93)90129-Q

Arias, S., Del Moral, A., Ferrer, M. R., Tallon, R., Quesada, E., and Bejar, V. (2003). Mauran, an exopolysaccharide produced by the halophilic bacterium *Halomonas maura*, with a novel composition and interesting properties for biotechnology. *Extremophiles* 7, 319–326. doi: 10.1007/s00792-003-0325-8

Arnosti, C., Ziervogel, K., Yang, T., and Teske, A. (2016). Oil-derived marine aggregates–hot spots of polysaccharide degradation by specialized bacterial communities. *Deep Sea Res. Part 2 Top. Stud. Oceanogr.* 129, 179–186. doi: 10.1016/j.dsr2.2014.12.008

Azam, F. (1998). Microbial control of oceanic carbon flux: the plot thickens. *Science* 280, 694–696. doi: 10.1126/science.280.5364.694

Azam, F., Fenchel, T., Field, J. G., Gray, J., Meyer-Reil, L., and Thingstad, F. (1983). The ecological role of water-column microbes in the sea. *Estuaries* 50, 257–263. doi: 10.3354/meps010257

Baelum, J., Borglin, S., Chakraborty, R., Fortney, J. L., Lamendella, R., Mason, O. U., et al. (2012). Deep-sea bacteria enriched by oil and dispersant from the Deepwater Horizon spill. *Environ. Microbiol.* 14, 2405–2416. doi: 10.1111/j.1462-2920.2012.02780.x

Béjar, V., Llamas, I., Calvo, C., and Quesada, E. (1998). Characterization of exopolysaccharides produced by 19 halophilic strains of the species *Halomonas eurihalina*. *J. Biotechnol.* 61, 135–141. doi: 10.1016/S0168-1656(98)00024-8

Berx, B., Hansen, B., Østerhus, S., Larsen, K., Sherwin, T., and Jochumsen, K. (2013). Combining in situ measurements and altimetry to estimate volume, heat and salt transport variability through the Faroe–Shetland Channel. *Ocean Sci. J.* 9, 639–654. doi: 10.5194/os-9-639-2013

Bhaskar, P., and Bhosle, N. B. (2005). Microbial extracellular polymeric substances in marine biogeochemical processes. *Curr. Sci.* 88, 45–53.

Brooks, G. R., Larson, R. A., Schwing, P. T., Romero, I., Moore, C., Reichart, G.-J., et al. (2015). Sedimentation pulse in the NE Gulf of Mexico following the 2010 DWH blowout. *PLoS ONE* 10:e0132341. doi: 10.1371/journal.pone.0132341

Buchan, A., González, J. M., and Moran, M. A. (2005). Overview of the marine *Roseobacter* lineage. *Appl. Environ. Microb.* 71, 5665–5677. doi: 10.1128/AEM.71.10.5665-5677.2005

Calvo, C., Martinez-Checa, F., Mota, A., Bejar, V., and Quesada, E. (1998). Effect of cations, pH and sulfate content on the viscosity and emulsifying activity of the *Halomonas eurihalina* exopolysaccharide. *J. Ind. Microbiol. Biotechnol.* 20, 205–209. doi: 10.1038/sj.jim.2900513

Calvo, C., Martínez-Checa, F., Toledo, F., Porcel, J., and Quesada, E. (2002). Characteristics of bioemulsifiers synthesised in crude oil media by *Halomonas eurihalina* and their effectiveness in the isolation of bacteria able to grow in the presence of hydrocarbons. *Appl. Microbiol. Biotechnol.* 60, 347–351. doi: 10.1007/s00253-002-1115-4

Caron, D. A., Lim, E. L., Sanders, R. W., Dennett, M. R., and Berninger, U. G. (2000). Responses of bacterioplankton and phytoplankton to organic carbon and inorganic nutrient additions in contrasting oceanic ecosystems. *Aquat. Microbiol. Ecol.* 22, 175–184. doi: 10.3354/ame022175

Chanton, J., Zhao, T., Rosenheim, B. E., Joye, S., Bosman, S., Brunner, C., et al. (2015). Using natural abundance radiocarbon to trace the flux of petrocarbon to the seafloor following the Deepwater Horizon oil spill. *Environ. Sci. Technol.* 49, 847–854.

Chronopoulou, P. M., Sanni, G. O., Silas-Olu, D. I., Meer, J. R., Timmis, K. N., Brussaard, C. P., et al. (2015). Generalist hydrocarbon-degrading bacterial communities in the oil-polluted water column of the North Sea. *Microb. Biotechnol.* 8, 434–447. doi: 10.1111/1751-7915.12176

Cotner, J. B., Ammerman, J. W., Peele, E. R., and Bentzen, E. (1997). Phosphorus-limited bacterioplankton growth in the Sargasso Sea. *Aquat. Microbiol. Ecol.* 13, 141–149. doi: 10.3354/ame013141

Daly, K. L., Passow, U., Chanton, J., and Hollander, D. (2016). Assessing the impacts of oil-associated marine snow formation and sedimentation during and after the Deepwater Horizon oil spill. *Anthropocene* 13, 18–33. doi: 10.1016/j.ancene.2016.01.006

Decho, A. W. (1990). "Microbial exopolymer secretions in ocean environments: their role (s) in food webs and marine processes," in *Oceanography Marine Biology Annual Review*, ed. M. Barnes (Aberdeen: Aberdeen University Press), 73–153.

Deppe, U., Richnow, H.-H., Michaelis, W., and Antranikian, G. (2005). Degradation of crude oil by an arctic microbial consortium. *Extremophiles* 9, 461–470. doi: 10.1007/s00792-005-0463-2

Edgar, R. C., Haas, B. J., Clemente, J. C., Quince, C., and Knight, R. (2011). UCHIME improves sensitivity and speed of chimera detection. *Bioinformatics* 27, 2194–2200. doi: 10.1093/bioinformatics/btr381

Francisc, D. E., Mah, R. A., and Rabin, A. C. (1973). Acridine orange-epifluorescence technique for counting bacteria in natural waters. *Trans. Am. Microsc. Soc.* 92, 416–421. doi: 10.2307/3225245

Frederiksen, R., Jensen, A., and Westerberg, H. (1992). The distribution of the scleractinian coral *Lophelia pertusa* around the Faroe Islands and the relation to internal tidal mixing. *Sarsia* 77, 157–171. doi: 10.1080/00364827.1992.10413502

Fu, J., Gong, Y., Zhao, X., O'reilly, S., and Zhao, D. (2014). Effects of oil and dispersant on formation of marine oil snow and transport of oil hydrocarbons. *Environ. Sci. Technol.* 48, 14392–14399. doi: 10.1021/es5042157

Giani, M., Berto, D., Zangrando, V., Castelli, S., Sist, P., and Urbani, R. (2005). Chemical characterization of different typologies of mucilaginous aggregates in the Northern Adriatic Sea. *Sci. Total Environ.* 353, 232–246. doi: 10.1016/j.scitotenv.2005.09.027

Grimes, D. J., Johnson, C. N., Dillon, K. S., Flowers, A. R., Noriea Iii, N. F., and Berutti, T. (2009). What genomic sequence information has revealed about *Vibrio* ecology in the ocean—a review. *Microb. Ecol.* 58, 447–460. doi: 10.1007/s00248-009-9578-9

Gutierrez, T., Berry, D., Teske, A., and Aitken, M. D. (2016). Enrichment of *Fusobacteria* in sea surface oil slicks from the Deepwater Horizon oil spill. *Microorganisms* 4:24. doi: 10.3390/microorganisms4030024

Gutierrez, T., Berry, D., Yang, T., Mishamandani, S., McKay, L., Teske, A., et al. (2013). Role of bacterial exopolysaccharides (EPS) in the fate of the oil released during the *Deepwater Horizon* oil spill. *PLoS ONE* 8:e67717. doi: 10.1371/journal.pone.0067717

Gutierrez, T., Morris, G., and Green, D. H. (2009). Yield and physicochemical properties of EPS from *Halomonas* sp. strain TG39 identifies a role for protein and anionic residues (sulfate and phosphate) in emulsification of n-hexadecane. *Biotechnol. Bioeng.* 103, 207–216. doi: 10.1002/bit.22218

Gutierrez, T., Mulloy, B., Black, K., and Green, D. (2007). Glycoprotein emulsifiers from two marine *Halomonas* species: chemical and physical characterization. *J. Appl. Microbiol.* 103, 1716–1727. doi: 10.1111/j.1365-2672.2007.03407.x

Gutierrez, T., Shimmield, T., Haidon, C., Black, K., and Green, D. H. (2008). Emulsifying and metal ion binding activity of a glycoprotein exopolymer produced by *Pseudoalteromonas* sp. strain TG12. *Appl. Environ. Microbiol.* 74, 4867–4876. doi: 10.1128/AEM.00316-08

Gyurcsik, B., and Nagy, L. (2000). Carbohydrates as ligands: coordination equilibria and structure of the metal complexes. *Coord. Chem. Rev.* 203, 81–149. doi: 10.1016/S0010-8545(99)00183-6

Hansell, D. A., and Carlson, C. A. (2001). Marine dissolved organic matter and the carbon cycle. *Oceanography* 14, 41–49. doi: 10.5670/oceanog.2001.05

Hassler, C. S., Schoemann, V., Nichols, C. M., Butler, E. C., and Boyd, P. W. (2011). Saccharides enhance iron bioavailability to Southern Ocean phytoplankton. *Proc. Natl. Acad. Sci. U.S.A.* 108, 1076–1081. doi: 10.1073/pnas.1010963108

Howell, K. L. (2010). A benthic classification system to aid in the implementation of marine protected area networks in the deep/high seas of the NE Atlantic. *Biol. Conserv.* 143, 1041–1056. doi: 10.1016/j.biocon.2010.02.001

Jackson, G. A. (1994). Particle trajectories in a rotating cylinder: implications for aggregation incubations. *Deep Sea Res. Part I Top. Stud. Oceanogr.* 41, 429–437.

Janecka, J., Jenkins, M., Brackett, N., Lion, L., and Ghiorse, W. (2002). Characterization of a *Sinorhizobium* isolate and its extracellular polymer implicated in pollutant transport in soil. *Appl. Environ. Microbiol.* 68, 423–426. doi: 10.1128/AEM.68.1.423-426.2002

Kennedy, A., and Sutherland, I. (1987). Analysis of bacterial exopolysaccharides. *Biotechnol. Appl. Biochem.* 9, 12–19.

Khelifa, A., Moulay, S., and Naceur, A. (2005). Treatment of metal finishing effluents by the electroflotation technique. *Desalination* 181, 27–33. doi: 10.1016/j.desal.2005.01.011

Kleindienst, S., Paul, J. H., and Joye, S. B. (2015a). Using dispersants after oil spills: impacts on the composition and activity of microbial communities. *Nat. Rev. Microbiol.* 13, 388–396. doi: 10.1038/nrmicro3452

Kleindienst, S., Seidel, M., Ziervogel, K., Grim, S., Loftis, K., Harrison, S., et al. (2015b). Chemical dispersants can suppress the activity of natural oil-degrading microorganisms. *Proc. Natl. Acad. Sci. U.S.A.* 112, 14900–14905. doi: 10.1073/pnas.1507380112

Kostka, J. E., Prakash, O., Overholt, W. A., Green, S. J., Freyer, G., Canion, A., et al. (2011). Hydrocarbon-degrading bacteria and the bacterial community response in Gulf of Mexico beach sands impacted by the Deepwater Horizon oil spill. *Appl. Environ. Microbiol.* 77, 7962–7974. doi: 10.1128/AEM.05402-11

Kozich, J. J., Westcott, S. L., Baxter, N. T., Highlander, S. K., and Schloss, P. D. (2013). Development of a dual-index sequencing strategy and curation pipeline for analyzing amplicon sequence data on the MiSeq Illumina sequencing platform. *Appl. Environ. Microbiol.* 79, 5112–5120. doi: 10.1128/AEM.01043-13

Lanfranconi, M. P., Bosch, R., and Nogales, B. (2010). Short-term changes in the composition of active marine bacterial assemblages in response to diesel oil pollution. *Microb. Biotechnol.* 3, 607–621. doi: 10.1111/j.1751-7915.2010.00192.x

Leiye, Y., Guojie, S., Jingfang, W., Yingze, W., Chao, D., and Jiang, L. (2016). Activation of macrophages by an exopolysaccharide isolated from Antarctic *Psychrobacter* sp. B-3. *Chin. J. Oceanol. Limnol.* 34, 1064–1071. doi: 10.1007/s00343-016-4393-x

Lin, P., and Guo, L. (2015). Spatial and vertical variability of dissolved carbohydrate species in the northern Gulf of Mexico following the Deepwater Horizon oil spill, 2010–2011. *Mar. Chem.* 174, 13–25. doi: 10.1016/j.marchem.2015.04.001

Long, R. A., and Azam, F. (1996). Abundant protein-containing particles in the sea. *Aquat. Microb. Ecol.* 10, 213–221. doi: 10.3354/ame010213

Long, R. A., and Azam, F. (2001). Microscale patchiness of bacterioplankton assemblage richness in seawater. *Aquat. Microb. Ecol.* 26, 103–113. doi: 10.3354/ame026103

Mancuso Nichols, C., Garon, S., Bowman, J., Raguénès, G., and Guezennec, J. (2004). Production of exopolysaccharides by Antarctic marine bacterial isolates. *Appl. Environ. Microbio.* 96, 1057–1066. doi: 10.1111/j.1365-2672.2004.02216.x

Morris, R. M., Rappé, M. S., Connon, S. A., Vergin, K. L., Siebold, W. A., Carlson, C. A., et al. (2002). SAR11 clade dominates ocean surface bacterioplankton communities. *Nature* 420, 806–810. doi: 10.1038/nature01240

Muschenheim, D., and Lee, K. (2002). Removal of oil from the sea surface through particulate interactions: review and prospectus. *Spill Sci. Technol. Bull.* 8, 9–18. doi: 10.1016/S1353-2561(02)00129-9

National-Commission on the BP Deepwater Horizon Oil Spill and Offshore Drilling (2011). National Commission on the BP Deepwater Horizon Oil Spill and Offshore Drilling: The Use of Surface and Subsea Dispersants during the BP Deepwater Horizon oil Spill [Online]. GPO. Available at: https://permanent.access.gpo.gov/gpo184/working%20Paper.Dispersants.For%20Release.pdf [accessed September 2016].

Passow, U. (2016). Formation of rapidly-sinking, oil-associated marine snow. *Deep Sea Res. Part II Top. Stud. Oceanogr.* 129, 232–240. doi: 10.1016/j.dsr2.2014.10.001

Passow, U., Ziervogel, K., Asper, V., and Diercks, A. (2012). Marine snow formation in the aftermath of the Deepwater Horizon oil spill in the Gulf of Mexico. *Environ. Res. Lett.* 7:035301. doi: 10.1088/1748-9326/7/3/035301

Pomeroy, L. R. (1974). The ocean's food web, a changing paradigm. *Bioscience* 24, 499–504. doi: 10.2307/1296885

Prabagaran, S. R., Manorama, R., Delille, D., and Shivaji, S. (2007). Predominance of *Roseobacter*, *Sulfitobacter*, *Glaciecola* and *Psychrobacter* in seawater collected off Ushuaia, Argentina, Sub-Antarctica. *FEMS Microb. Ecol.* 59, 342–355. doi: 10.1111/j.1574-6941.2006.00213.x

Quesada, E., Del Moral, A., and Béjar, V. (1994). Comparative methods for isolation of *Volcaniella eurihalina* exopolysaccharide. *Biotechnol. Tech.* 8, 701–706. doi: 10.1007/BF00151472

Redmond, M. C., and Valentine, D. L. (2012). Natural gas and temperature structured a microbial community response to the Deepwater Horizon oil spill. *Proc. Natl. Acad. Sci. U.S.A.* 109, 20292–20297. doi: 10.1073/pnas.1108756108

Rivkin, R. B., and Anderson, M. R. (1997). Inorganic nutrient limitation of oceanic bacterioplankton. *Limnol. Oceanogr.* 42, 730–740. doi: 10.1038/nature07236

Romero, I. C., Schwing, P. T., Brooks, G. R., Larson, R. A., Hastings, D. W., Ellis, G., et al. (2015). Hydrocarbons in deep-sea sediments following the 2010 Deepwater Horizon blowout in the northeast Gulf of Mexico. *PLoS ONE* 10:e0128371. doi: 10.1371/journal.pone.0128371

Santschi, P. H., Guo, L., Means, J. C., and Ravichandran, M. (1999). "Natural organic matter binding of trace metals and trace organic contaminants in estuaries," in *Biogeochemistry of Gulf of Mexico Estuaries*, eds T. S. Bianchi, J. R. Pennock, and R. R. Twilley (New York, NY: John Wiley), 347–380.

Smith, D. C., Simon, M., Alldredge, A. L., and Azam, F. (1992). Intense hydrolytic enzyme activity on marine aggregates and implications for rapid particle dissolution. *Nature* 359, 139–142. doi: 10.1038/359139a0

Swan, B. K., Martinez-Garcia, M., Preston, C. M., Sczyrba, A., Woyke, T., Lamy, D., et al. (2011). Potential for chemolithoautotrophy among ubiquitous bacteria lineages in the dark ocean. *Science* 333, 1296–1300. doi: 10.1126/science.1203690

Tillett, D., and Neilan, B. A. (2000). Xanthogenate nucleic acid isolation from cultured and environmental cyanobacteria. *J. Phycol.* 36, 251–258. doi: 10.1046/j.1529-8817.2000.99079.x

Valentine, D. L., Fisher, G. B., Bagby, S. C., Nelson, R. K., Reddy, C. M., Sylva, S. P., et al. (2014). Fallout plume of submerged oil from Deepwater Horizon. *Proc. Natl. Acad. Sci. U.S.A.* 111, 15906–15911. doi: 10.1073/pnas.1414873111

van Eenennaam, J. S., Wei, Y., Grolle, K. C., Foekema, E. M., and Murk, A. J. (2016). Oil spill dispersants induce formation of marine snow by phytoplankton-associated bacteria. *Mar. Pol. Bull.* 104, 294–302. doi: 10.1016/j.marpolbul.2016.01.005

Verdugo, P., Alldredge, A. L., Azam, F., Kirchman, D. L., Passow, U., and Santschi, P. H. (2004). The oceanic gel phase: a bridge in the DOM–POM continuum. *Mar. Chem.* 92, 67–85. doi: 10.1016/j.marchem.2004.06.017

Wolfaardt, G. M., Lawrence, J. R., and Korber, D. R. (1999). "Function of EPS," in *Microbial Extracellular Polymeric Substances*, eds J. Wingender, T. R. Neu, and H.-C. Flemming (Berlin: Springer), 171–200.

Yakimov, M. M., Timmis, K. N., and Golyshin, P. N. (2007). Obligate oil-degrading marine bacteria. *Curr. Opin. Biotechnol.* 18, 257–266. doi: 10.1016/j.copbio.2007.04.006

Yang, T., Nigro, L. M., Gutierrez, T., Joye, S. B., Highsmith, R., and Teske, A. (2016). Pulsed blooms and persistent oil-degrading bacterial populations in the water column during and after the Deepwater Horizon blowout. *Deep Sea Res. Part II Top. Stud. Oceanogr.* 129, 282–291. doi: 10.1016/j.dsr2.2014.01.014

Ziervogel, K., Mckay, L., Rhodes, B., Osburn, C. L., Dickson-Brown, J., Arnosti, C., et al. (2012). Microbial activities and dissolved organic matter dynamics in oil-contaminated surface seawater from the Deepwater Horizon oil spill site. *PLoS ONE* 7:e34816. doi: 10.1371/journal.pone.0034816

Conflict of Interest Statement: The authors declare that the research was conducted in the absence of any commercial or financial relationships that could be construed as a potential conflict of interest.

frontiers in Microbiology

ORIGINAL RESEARCH
published: 13 September 2016
doi: 10.3389/fmicb.2016.01384

Distinct Bacterial Communities in Surficial Seafloor Sediments Following the 2010 Deepwater Horizon Blowout

Tingting Yang[1†], Kelly Speare[1†], Luke McKay[1†], Barbara J. MacGregor[1], Samantha B. Joye[2] and Andreas Teske[1]*

[1] Department of Marine Sciences, University of North Carolina, Chapel Hill, NC, USA, [2] Department of Marine Sciences, University of Georgia, Athens, GA, USA

OPEN ACCESS

Edited by:
Hongyue Dang,
Xiamen University, China

Reviewed by:
Zhanfei Liu,
University of Texas at Austin, USA
Bin-Bin Xie,
Shandong University, China

***Correspondence:**
Andreas Teske
teske@email.unc.edu

†Present address:
Tingting Yang,
Section for Microbiology & Center for Geomicrobiology, Department of Bioscience, Aarhus University, Aarhus, Denmark
Kelly Speare,
Department of Ecology, Evolution and Marine Biology, University of California at Santa Barbara, Santa Barbara, CA, USA
Luke McKay,
Center for Biofilm Engineering, Montana State University, Bozeman, MT, USA

Specialty section:
This article was submitted to Aquatic Microbiology, a section of the journal Frontiers in Microbiology

Received: *12 June 2016*
Accepted: *22 August 2016*
Published: *13 September 2016*

Citation:
Yang T, Speare K, McKay L, MacGregor BJ, Joye SB and Teske A (2016) Distinct Bacterial Communities in Surficial Seafloor Sediments Following the 2010 Deepwater Horizon Blowout. Front. Microbiol. 7:1384. doi: 10.3389/fmicb.2016.01384

A major fraction of the petroleum hydrocarbons discharged during the 2010 Macondo oil spill became associated with and sank to the seafloor as marine snow flocs. This sedimentation pulse induced the development of distinct bacterial communities. Between May 2010 and July 2011, full-length 16S rRNA gene clone libraries demonstrated bacterial community succession in oil-polluted sediment samples near the wellhead area. Libraries from early May 2010, before the sedimentation event, served as the baseline control. Freshly deposited oil-derived marine snow was collected on the surface of sediment cores in September 2010, and was characterized by abundantly detected members of the marine *Roseobacter* cluster within the *Alphaproteobacteria*. Samples collected in mid-October 2010 closest to the wellhead contained members of the sulfate-reducing, anaerobic bacterial families *Desulfobacteraceae* and *Desulfobulbaceae* within the *Deltaproteobacteria*, suggesting that the oil-derived sedimentation pulse triggered bacterial oxygen consumption and created patchy anaerobic microniches that favored sulfate-reducing bacteria. Phylotypes of the polycyclic aromatic hydrocarbon-degrading genus *Cycloclasticus*, previously found both in surface oil slicks and the deep hydrocarbon plume, were also found in oil-derived marine snow flocs sedimenting on the seafloor in September 2010, and in surficial sediments collected in October and November 2010, but not in any of the control samples. Due to the relative recalcitrance and stability of polycyclic aromatic compounds, *Cycloclasticus* represents the most persistent microbial marker of seafloor hydrocarbon deposition that we could identify in this dataset. The bacterial imprint of the DWH oil spill had diminished in late November 2010, when the bacterial communities in oil-impacted sediment samples collected near the Macondo wellhead began to resemble their pre-spill counterparts and spatial controls. Samples collected in summer of 2011 did not show a consistent bacterial community signature, suggesting that the bacterial community was no longer shaped by the DWH fallout of oil-derived marine snow, but instead by location-specific and seasonal factors.

Keywords: Deepwater Horizon, marine sediment, MOSSFA, marine snow, bacterial populations, *Cycloclasticus*

INTRODUCTION

The Deepwater Horizon (DWH) oil spill released more than 4.9 million barrels of crude oil into the Gulf of Mexico (McNutt et al., 2012). Available oil budgets indicated that in total about 25% of the spilled oil was recovered or skimmed and burned, between 28 and 34% were consumed via biological oxidation in deep waters (Joye et al., 2016), 2–15% sedimented to the seafloor (Valentine et al., 2014; Chanton et al., 2015), and the remaining 32–39% did not have a clear environmental fate (Joye et al., 2016). Large amounts of marine oil-derived snow formed at the sea surface within a few days of the wellhead explosion (Dell'Amore, 2010; Passow et al., 2012). As demonstrated in lab studies, these floating oil aggregates gradually lose their buoyancy due to increasing aggregation of phyto- and zooplankton debris, fecal pellets, oily particles and droplets into a sticky matrix of microbially produced extracellular polymeric substances (Passow et al., 2012; Passow, 2016). Oil uptake by zooplankton (Mitra et al., 2012) and subsequent packaging into fecal pellets may interact with aggregate formation, or shuttle petrocarbon to the seafloor directly (Muschenheim and Lee, 2002). In addition to particle-associated transport, the dynamic deepwater hydrocarbon plume, containing an estimated 50% of the discharged oil (Joye, 2015), is likely to have impacted the slope sediments of the northern Gulf of Mexico (reviewed in Daly et al., 2016). These modes of oil transport to the seafloor are effective, as shown by several lines of geochemical evidence: the chemical composition of the sedimented hydrocarbons was congruent with Macondo oil as its source (Mason et al., 2014); widespread sedimentation of large amounts of fossil petrocarbon, equivalent to approximately 3–5% of the total carbon emitted during the Deepwater Horizon blowout, was demonstrated by analysis of C-isotopic composition ($\delta^{13}C$ and $\Delta^{14}C$) in seafloor hydrocarbon deposits (Chanton et al., 2015); sedimentation rates accelerated by two orders of magnitude during summer and early fall of 2010, as determined by analyzing the ^{234}Th inventories of surficial sediment cores (Brooks et al., 2015); coinciding with the sedimentation pulse, redox conditions in the sediment changed, and showed biogeochemical signatures of microbial metal reduction in the upper sediments (Hastings et al., 2016).

The microbial communities in the surficial seafloor sediments respond and adapt to the availability of hydrocarbon-derived substrates, and gradual depletion of electron acceptors. Oil-impacted seafloor sediments (1.5–3 cm depth) from October 2010 harbored sulfate-reducing *Deltaproteobacteria* with genes indicating degradation of aromatic hydrocarbons (Kimes et al., 2013). Sediments collected in 2011 near the wellhead area have yielded sequence libraries suggesting members of the methylotrophic genera *Methylobacter* and *Methylococcus* and the phyla *Actinobacteria*, *Firmicutes,* and *Chloroflexi* as the most abundant groups (Liu and Liu, 2013). A large-scale metagenomic survey found that in sediments near the wellhead with peak concentrations of total petroleum hydrocarbons, microbial populations were structured by the concentrations of total petroleum hydrocarbons and bioavailable nitrogen ($NH_3 + NO_3$; Mason et al., 2014), suggesting links to anaerobic denitrification (supported by recovery of the functional genes of this pathway) but also to aerobic ammonia oxidation, the first step of nitrification.

Since these studies rely on sample sets collected at one time point or within short time frames, for example during a single cruise, we complement these investigations with a longterm timeline survey of bacterial sedimentary communities from May 2010 to July 2011, using nearly full length 16S rRNA gene clone libraries for maximum taxonomic specificity. We document the distinct occurrence patterns of oil-associated family- and genus-level bacterial groups over time, and suggest petrocarbon sedimentation and changing biogeochemical niches as factors that shape these bacterial communities in near-surface seafloor sediments.

MATERIALS AND METHODS

Sampling

Our sediment samples were obtained from five different cruises (**Table 1**). The May 2010 samples were collected by boxcoring and subcoring on the first R/V *Pelican* oil spill cruise, 2 weeks after the spill occurred (Diercks et al., 2010a,b). These uniformly ochre-colored sediments from the wellhead area showed no visible oil floc deposition, had no hydrocarbon or sulfide smell, shared the low DIC concentrations (3–4 mM) of northern Gulf slope sediments (McKay et al., 2013), and lacked the redox-sensitive metal signatures of the oil-derived sedimentation pulse (Hastings et al., 2016). Thus, they provided controls for the seafloor conditions before the impact of oil-derived sedimentation. Subsequently, samples were collected by multicorer. In September 2010, oil-contaminated sediment cores were collected on R/V *Oceanus*; the sediment surface was now covered with floc-like deposits smelling noticeably of petroleum (**Figures 1A,E**), and fluorescing green under UV light. Seafloor sediments from the wellhead area with a conspicuous red-brown coloration of the upper 3–4 cm layer (**Figure 1B**), and well-documented concentrations of petroleum polyaromatic compounds (Woodruff, 2014), were collected in mid-October 2010 on R/V *Cape Hatteras*. Later sediment sample sets collected near the wellhead in late November 2010 with R/V *Atlantis* (Ziervogel et al., 2016b) as well as in July 2011 with R/V *Endeavor* retained the red-brown surface layer (**Figures 1C,D**), but lacked the hydrocarbon smell. The red-brown coloration represents precipitated MnO_2 and ferric iron hydroxide; these metals were originally mobilized as reduced Fe^{2+} and Mn^{2+} after stimulation of microbial metal-reducing bacteria in oil-impacted sediment, and subsequently reoxidized and precipitated near the sediment surface as soon as oxidizing conditions returned; this redox signature was consistently absent in control cores (Hastings et al., 2016). All sediment cores were sectioned and stored immediately in −80°C freezers.

DNA and RNA Extraction from Sediments

The surface layer from each sediment sample was used for DNA and RNA extraction (**Table 1**). Total sediment DNA was extracted from 0.25 g of each sample by using the PowerSoil™

TABLE 1 | Samples collected on multiple research cruises near the Macondo wellhead with sampling dates, depths, and geographical coordinates.

Sample names	Ship	Date	Depth (m)	Latitude (N)	Longitude (W)	Oil-impacted	Sample layer
PE6	RV *Pelican*	5/5/2010	1380	28°46.557	88°24.293	Negative	0–3 cm
PE21	RV *Pelican*	5/8/2010	1605	28°42.150	88°21.729	Negative	0–3 cm
C40	RV *Oceanus*	9/7/2010	1496	28°47.282	88°10.020	Oil flocs	0–3 cm
C75	RV *Oceanus*	9/10/2010	1087	28°42.650	88°44.900	Oil flocs	0–1 cm
C82	RV *Oceanus*	9/11/2010	1372	28°32.950	88°40.760	Oil flocs	0–1 cm
GIP24	RV *Cape Hatteras*	10/17/2010	1418	28°46.235	88°22.874	Surface brown layer	0–1 cm
GIP16	RV *Cape Hatteras*	10/16/2010	1560	28°43.383	88°24.577	Surface brown layer	0–1 cm
GIP16 (RNA)	RV *Cape Hatteras*	10/16/2010	1560	28°43.383	88°24.577	Surface brown layer	0–1 cm
GIP16 3–4 cm	RV *Cape Hatteras*	10/16/2010	1560	28°43.383	88°24.577	Below brown layer	3–4 cm
GIP08	RV *Cape Hatteras*	10/13/2010	2360	27°54.370	88°27.001	Negative	0–1 cm
GIP08 (RNA)	RV *Cape Hatteras*	10/13/2010	2360	27°54.370	88°27.001	Negative	0–1 cm
MUC19	RV *Atlantis*	11/30/2010	1574	28°43.350	88°21.770	Surface brown layer	0–2.5 cm
MUC20	RV *Atlantis*	12/1/2010	1885	28°29.290	88°19.050	Negative	0–2.5 cm
E01801	RV *Endeavor*	7/25/2011	1630	28°42.382	88°21.815	Surface brown layer	0–2 cm
E01804	RV *Endeavor*	7/26/2011	1620	28°42.491	88°21.999	Surface brown layer	0–2 cm
E01402	RV *Endeavor*	7/21/2011	64	28°20.919	91°49.563	Negative	0–2 cm

DNA isolation kit (MoBio Laboratories, Carlsbad, CA, USA), according to the manufacturer's instruction manual. Sediment for RNA extraction was thawed in 4.5 M sodium trichloroacetic acid (TCA) lysis buffer (pH 7.0; McIlroy et al., 2008). The TCA lysis buffer and sample mixture was split between three baked shaking flasks that each contained 27 g 0.1 mm beads, 7 g 0.4 mm beads, 0.33 g polyvinylpolypyrrolidone, and 550 μL antifoam B. The contents of each flask were subjected to bead-beating in two intervals of 40 s at high speed in the bead beater machine (Miyatake et al., 2013). Samples were transferred to PPCO centrifuge tubes (Nalgene™, Oak Ridge, TN, USA) and centrifuged for 20 min at 2500 rpm, 4°C. The supernatant was transferred to 50 mL Falcon® tubes with a maximum of 30 mL per tube. Nucleic acids were precipitated in 0.6 volumes isopropanol overnight at −20°C, centrifuged for 30 min at 2500 rpm, 4°C, washed with 25 mL cold 70% ethanol, and then centrifuged again for 10 min at 2500 rpm, 4°C and air dried. Precipitated nucleic acid pellets were resuspended in 20 mL distilled nuclease-free water, split into two Teflon Oak Ridge centrifuge tubes, and extracted by multiple separations with low-pH (5.1) phenol, phenol–chloroform, and chloroform. For each extraction equal volume of either phenol, phenol–chloroform, or chloroform was added to the remaining aqueous RNA solution, vortexed for 30 s, and centrifuged for 10 min at 2500 rpm, 4°C. Following each extraction the aqueous layer was transferred to a new tube and the extraction was repeated until there was a clear interface. The final aqueous sample was transferred to a clean tube and precipitated overnight at −20°C in 0.7 by volume isopropanol and 0.5 by volume ammonium acetate (Lin and Stahl, 1995; MacGregor et al., 1997). Nucleic acid pellets were resuspended in 125 μL nuclease-free water, and purified with the RNeasy RNA cleanup kit (Qiagen, Germantown, MD, USA). One or more DNase treatments, using Turbo DNase I (Thermo Fisher Scientific, Waltham, MA, USA) either on the column during RNeasy cleanup or in solution or both, were necessary to eliminate PCR-detectable DNA.

PCR Amplification and Cloning

The resuspended rRNA was reverse transcribed to cDNA first by the SuperScript® III One-Step RT-PCR system with Platinum® Taq DNA Polymerase (Thermo Fisher Scientific, Waltham, MA, USA) according to the recommended reaction conditions. Then the cDNA and the extracted total DNA were amplified with Speedstar DNA polymerase (TaKaRa, Shiga, Japan) using the bacterial primers 8f and 1492r (Teske et al., 2002) and the manufacturer's recommended concentration for buffer, dNTPs and DNA polymerase. Each PCR reaction consisted of 2 μl DNA extract, 2.5 μl 10x FBI buffer (TaKaRa, Shiga, Japan), 2.0 μl dNTP mix, 2.0 μl 10 μM solution of primers 8F and 1492R, respectively (both primers from Invitrogen, Carlsbad, CA, USA), and 0.25 μl SpeedStar polymerase (TaKaRa), and was brought to 25 μl with sterile H_2O. Amplification was performed in a BioRad iCycler Thermal Cycler (BioRad, Hercules, CA, USA) as follows: initial denaturation at 95°C for 4 min, 25 cycles of 95°C (10 s), 55°C (15 s) and 72°C (20 s), and a final 10 min extension of 72°C. PCR and RT-PCR product aliquots, including positive and negative controls, were SYBR green stained and visualized using a 1.5% agarose gel. The products were purified using the MinElute® PCR Purification Kit according to the manufacturer's instructions (Qiagen, Valencia, CA, USA), and cloned into OneShot® TOP10 competent Cells using the TOPO TA Cloning® Kit for Sequencing (Invitrogen, Carlsbad, CA, USA) according to the manufacturer's instructions. Transformed cells were grown on LB/Xgal/Kanamycin plates. Individual white colonies were arbitrarily picked, re-plated and sanger-sequenced at Genewiz Corporation (South Plainfield, NJ, USA) using vector primers M13 F and M13 R.

Phylogenetic Analysis

Near-complete 16S rRNA gene sequences were analyzed using Sequencher (Gene Codes, Ann Arbor, MI, USA) and compared to other sequences via the Basic Local Alignment Search Tool

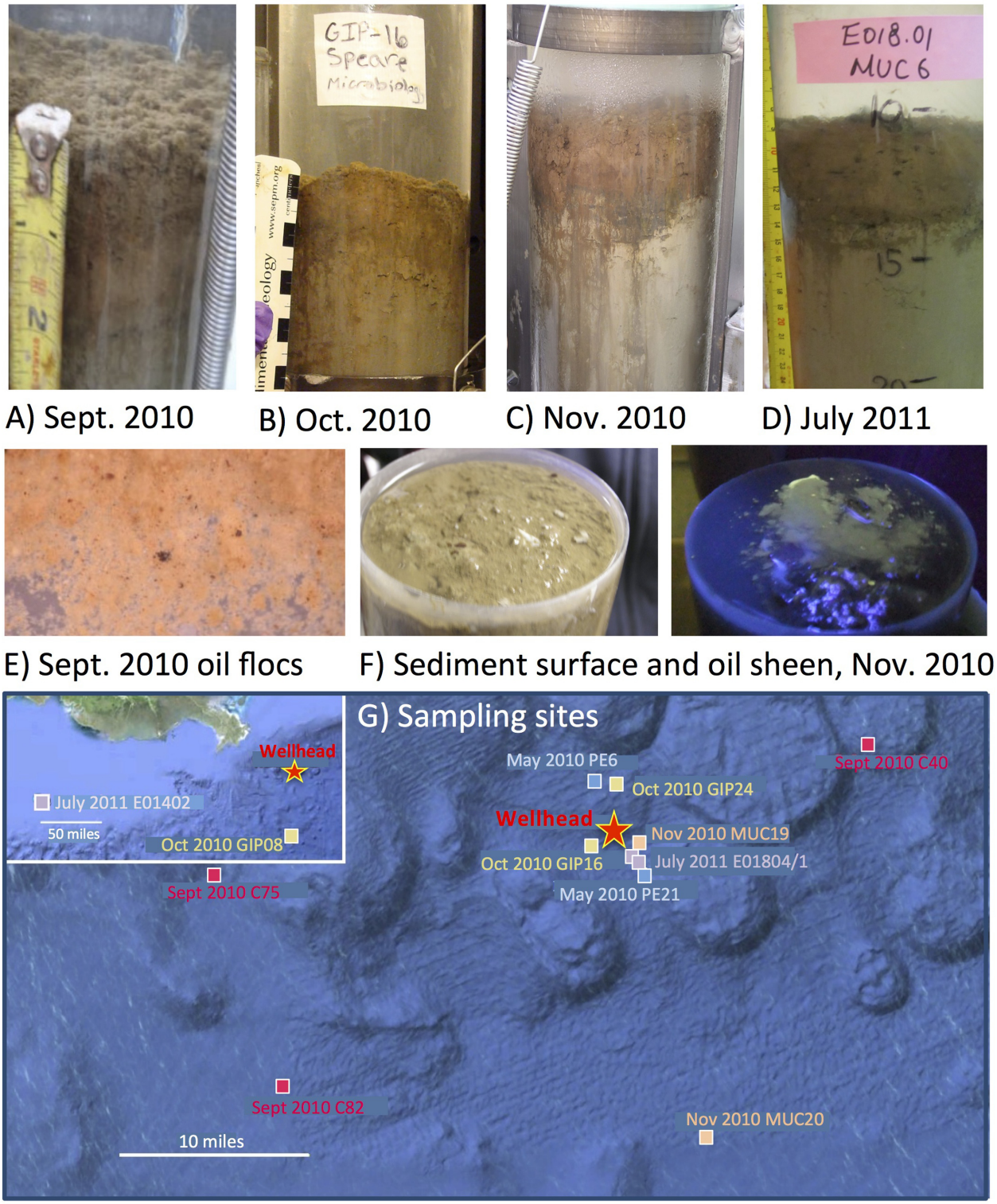

FIGURE 1 | Oil-contaminated sediment cores, characterized by a red-brown layer at the top of the gray sediment. The photos show a representative core from the RV Oceanus cruise in September 2010 **(A)**, core GIP16 collected in Mid-October 2010 **(B)**, core MUC19 collected at the end of November 2010 **(C)**, and core E01801 collected in July 2011 **(D)**. Close-up of oil-derived marine snow flocs collected from the surface of 2010 September sediment, and spread in a Petri dish, with small dark oil droplets in millimeter size **(E)**. Surface of MUC 19 without and with UV illumination, showing the bare surface of the sediments, and the green fluorescence sheen under UV, indicating petroleum hydrocarbons **(F)**. Seafloor map of sampling sites around the Macondo wellhead **(G)**.

(BLAST) of the National Center for Biotechnology Information[1] (Altschul et al., 1990). The sequences were examined for chimeras using Pintail 1.1 software (Ashelford et al., 2005). After construction of a general 16S rRNA alignment using the ARB phylogeny software package (Ludwig et al., 2004) and the SILVA 115 database (Pruesse et al., 2007), separate alignments for the *Gamma-* and *Alphaproteobacteria* were prepared with sequences for related *Gammaproteobacteria* and *Alphaproteobacteria*. Sequences of well-characterized pure cultures and described species were used for phylogenies whenever possible; otherwise, molecular phylotypes with an informative literature history were selected to anchor major phylogenetic branches of uncultured bacteria. The identifications were made based on a full-length, manually curated ARB alignment for all 2200 sequences. Phylogenetic trees were constructed and bootstrap checks (1000 reruns) of the tree topology were performed using ARB's neighbor-joining function with Jukes-Cantor correction.

Statistical Analysis

To compare the homogeneity of the sediment 16S rRNA and rDNA clone libraries, principal coordinates analysis (PCoA) hierarchical clustering was performed by using UniFrac online program http://bmf.colorado.edu/unifrac/ (Lozupone et al., 2011) using a NJ tree generated with ARB software. X-Fig[2] was used to edit image files obtained from the ARB software when necessary.

Database Access

The 16S rRNA gene sequences were submitted to GenBank and are accessible under GenBank Numbers KX172179–KX173285. Specifically, the GenBank numbers for sample C40 are KX172179–KX172328; sample C75, KX172329–KX172396; sample C82, KX172397–KX172514; sample E014, KX172515–KX172558; sample E01801, KX172559–KX172596; sample E01804, KX172597–KX172667; sample GIP08, KX172668–KX172718; sample GIP08RNA, KX172719–KX172771; sample GIP16-0-1 cm, KX172772–KX172892; sample GIP16-3-4 cm, KX172893–KX172944; sample GIP16RNA, KX172945–KX172993; sample GIP24, KX172994–KX173048; sample MUC19, KX173049–KX173105; sample MUC20, KX173106–KX173165, sample PE6, KX173166–KX173236; sample PE21, KX173237–KX173285.

[1]http://blast.ncbi.nlm.nih.gov/

[2]https://web.archive.org/web/20090116042509/http://www.xfig.org/

RESULTS

Bacterial Community Change at Phylum or Class Resolution

The earliest sediment samples of this dataset were collected during the first oil spill cruise on R/V *Pelican* on May 5 and 8, 2010, during the third week after the onset of the DWH blowout (**Table 1**). Sediment cores PE6 and PE21 were collected 3 miles northwest and 2.7 miles southeast of the wellhead, respectively (**Figure 1**). Neither hydrocarbon smell nor oily flocs were found on these sediments; cores collected on the same cruise that were examined for geochemical signatures of oil floc-derived sedimentation (including core PE6) also lacked the geochemical signature of hydrocarbon-induced microbial metal mobilization that characterizes oil-impacted sediments (Hastings et al., 2016). Therefore, these sediment samples are control sediments near the wellhead that represent the microbial community baseline of surficial sediments before oil deposition. Five bacterial phyla or sub-phyla were abundant in the bacterial 16S rRNA gene clone libraries of cores PE6 and PE21: *Gammaproteobacteria* (15.5,

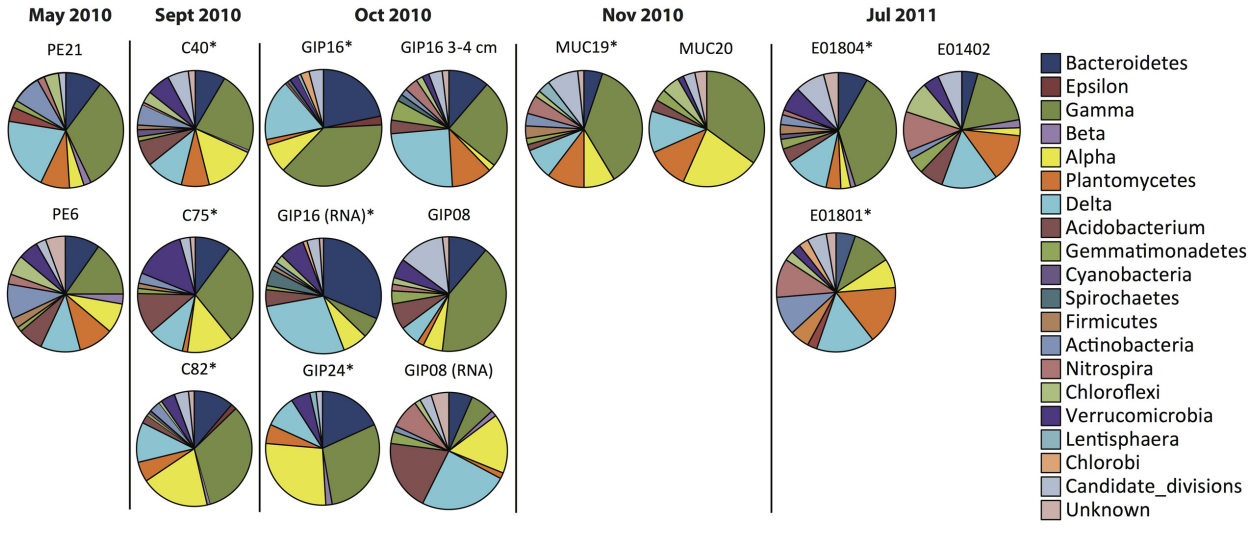

FIGURE 2 | Phylum-level resolution pie chart plots of bacterial 16S rRNA gene clone libraries and reverse-transcript 16S rRNA clone libraries from oil polluted sediment samples (labeled with *) and control sites.

32.7%), *Deltaproteobacteria* (11.3, 20.4%), *Bacteroidetes* (9.9, 10.2%), *Planctomycetes* (9.9, 8.2%), and *Actinobacteria* (9.9, 8.2%; **Figure 2**; **Table 2**). The PE6 and PE21 clone libraries also shared the minority groups *Betaproteobacteria*, *Alphaproteobacteria*, *Acidobacteria*, *Gemmatimonadetes*, *Nitrospira*, and *Chloroflexi*. Members of the phyla *Verrucomicrobia* and *Firmicutes* were only found in PE6 but not in PE21. In general, PE6 and PE21 shared the major bacterial groups of control surface sediment in a previous Gulf of Mexico bacterial community survey (Lloyd et al., 2010).

Recovered during the September 2010 R/V *Oceanus* cruise, the first oil-impacted sediment cores of this sample set were characterized by a brown, flocculent layer of marine snow-like deposits overlaying ochre-colored seafloor sediment. This overlying material contained small droplets and particles of weathered oil (**Figure 1E**) similar to oil droplets observed embedded in freshly formed, sinking marine snow (Passow et al., 2012); the samples were also characterized by strong petroleum smell. Three samples of oil-contaminated, recently deposited marine snow flocs from surficial sediments (C40, C75, and C82) were examined, from sampling sites 14 miles northeast, 21 miles west, and 22 miles southwest of the wellhead (**Figure 1**). While the *Gammaproteobacteria* dominated in the 16S rRNA gene clone libraries C40, C75, and C82 (23.2, 29.4, and 32.8%), the *Alphaproteobacteria* had become the second-most abundant group in all three samples (14.6, 13.2, 19.3%; **Figures 2** and **3**). This change is consistent with the alphaproteobacterial bloom detected in independent metagenomic analyses of seafloor sediments collected in September 2010 (Mason et al., 2014). *Deltaproteobacteria* and *Bacteroidetes* were still within the most frequently detected groups, but the *Actinobacteria* decreased to a similar level as other minority groups. The *Planctomycetes* contributed significantly to clone libraries of C40 and C82 (7.9 and 5.9%), but were barely found in C75 (1.5%; **Table 2**).

One month later, more oil-contaminated cores were recovered from the wellhead area during the October 2010 R/V *Cape Hatteras* cruise. At sites GIP16 (1.6 miles west-southwest to the wellhead), and GIP24 (2.4 miles north-northeast of the wellhead), the reddish surface sediment layers with UV-fluorescent oil spots and petroleum odor were recovered again (**Figure 1**). *Gammaproteobacteria* (37.7, 29.1%) contributed most abundantly to the 16S rRNA gene clone libraries of both GIP16 and GIP24; the contribution of the *Bacteroidetes* (22.1, 18.2%) almost doubled in October compared to the September samples (**Figure 2**). Interestingly, *Deltaproteobacteria* increased sharply (17.2%) while *Alphaproteobacteria* decreased (7.4%) in GIP16, whereas in GIP24 both groups persisted at similar levels (9.1% *Deltaproteobacteria*, 27.3% *Alphaproteobacteria*) as in September. The remaining minority bacterial groups in total accounted for 15.6 and 16.4% in both GIP samples.

Since the oil-derived sedimentation pulse covered the pre-spill sediment surface but did not appear to be mixed in, the pre-spill sediment microbial community could have remained intact in the underlying sediment. To check this possibility, the 3–4 cm sediment layer of core GIP16, right below the red-brown colored surface sediment, was sampled and sequenced. The 16S rRNA gene clone library results showed that this sample diverged from the immediately overlying surface sediment, but it resembled the pre-spill sediment samples PE6 and PE21 collected in May 2010. The 3–4 cm layer and the surficial sediment of GIP16 shared nine microbial groups, but 13 groups on phylum and sub-phylum level were shared between GIP16 3–4 cm, PE6, and PE21 (**Table 2**). These three samples also shared a low proportion of *Bacteroidetes* and a high percentage of *Planctomycetes*, in contrast to the GIP16 surface sample.

A spatial reference core (GIP08) without visible hydrocarbon pollution was taken 57 miles south of the wellhead (**Figure 1**). Its clone library demonstrated a distinct bacterial community dominated by the highest proportion of *Gammaproteobacteria* (43.1%) and of Candidate Divisions OD1/OP11 (11.8%) compared to all other samples. The *Bacteroidetes* accounted for 11.8% (**Figure 2**; **Table 2**). The GIP08 and GIP16 3–4 cm libraries shared 12 groups, seven of which were found at less than 8% each. The *Planctomycetes* and *Deltaproteobacteria* were found in lower percentages (2.0 and 5.9%) in GIP08, compared to 11.5 and 23.1% in GIP16 3–4 cm.

To identify active bacterial groups with increased rRNA content, we compared the reverse-transcribed 16S rRNA clone libraries of the oil-impacted core GIP16 and the reference core GIP08 to each other and to their corresponding 16S rRNA gene clone libraries. The two sediments showed distinct active phylum-level groups. In the GIP16 clone library of 16S rRNA transcripts, the *Bacteroidetes* (32.5%) and *Deltaproteobacteria* (28.9%) were the two most abundant groups; the remaining 11 groups accounted for less than 8% each (**Figure 2**). In contrast, in the 16S rRNA clone library of GIP08, *Deltaproteobacteria* (21.8%), *Acidobacteria* (21.8%) and *Alphaproteobacteria* (18.2%) predominated, while other groups contributed below 10%. The *Gammaproteobacteria*, the dominant group in DNA-based sediment clone libraries of these samples, contributed much less in the reverse-transcribed 16S rRNA gene clone libraries (6.0 and 7.3% in GIP16 and GIP08, respectively), suggesting that the *Gammaproteobacteria* contributed less to overall cellular activity and rRNA gene expression than to DNA presence.

The wellhead area was revisited and resampled in late November 2010 with R/V *Atlantis* and submersible *Alvin* (**Table 1**). The sediment core MUC19 was recovered from approximately 1.7 miles southeast of the wellhead (**Figure 1**); it showed a red-brownish surface layer about 4.5 cm thick but lacked noticeable petroleum smell (Ziervogel et al., 2016b). Under UV light, MUC19 showed fluorescent spots suggesting oil in the supernatant water (**Figure 1**), a possible consequence of residual leakage of fresh hydrocarbons around the DWH site. A reference core MUC20 was taken 17.4 miles south-southeast of the wellhead; the entire core was evenly ochre-gray colored, and lacked the red–brown surface layer. These sediments showed similar total organic carbon and total nitrogen content, microbial cell numbers and enzymatic activities (Ziervogel et al., 2016b). While the *Gammaproteobacteria* (36.8%) represented the most abundant clone library group of MUC19, the proportion of *Planctomycetes* increased compared to the September and October 2010 surface samples, and these sequences became the second-most dominant clone library group (8.8%). All other groups accounted for less than 10%

TABLE 2 | Percentage of main phyla in 16 sediment bacterial 16S rRNA and rRNA gene clone libraries from May 2010 to July 2011.

	May 2010 non-oily		September 2010 oily			October 2010 oily			October 2010 non-oily			November 2010 oily	November 2010 non-oily	July 2011 oily		July 2011 non-oily
	PE6	PE21	C40	C75	C82	GIP24	GIP16	GIP16 (RNA)	GIP16 3–4 cm	GIP08	GIP08 (RNA)	MUC19	MUC20	E01801	E01804	E014
Bacteroidetes	9.9%	10.2%	8.6%	10.3%	11.8%	18.2%	22.1%	32.5%	11.5%	11.8%	7.3%	5.3%	0.0%	5.3%	8.5%	4.5%
Epsilon	0.0%	0.0%	0.0%	0.0%	1.7%	0.0%	2.5%	0.0%	0.0%	0.0%	0.0%	0.0%	0.0%	0.0%	0.0%	0.0%
Gamma	15.5%	32.7%	23.2%	29.4%	32.8%	29.1%	37.7%	6.0%	25.0%	43.1%	7.3%	36.8%	35.0%	10.5%	38.0%	18.2%
Beta	2.8%	2.0%	0.7%	0.0%	0.8%	1.8%	0.0%	0.0%	0.0%	0.0%	1.8%	0.0%	0.0%	0.0%	1.4%	2.3%
Alpha	8.5%	4.1%	14.6%	13.2%	19.3%	27.3%	7.4%	7.2%	1.9%	5.9%	18.2%	8.8%	21.7%	7.9%	2.8%	2.3%
Plantomycetes	9.9%	8.2%	7.9%	1.5%	5.9%	5.5%	1.6%	0.0%	11.5%	2.0%	1.8%	8.8%	11.7%	15.8%	2.8%	11.4%
Delta	11.3%	20.4%	4.6%	4.4%	8.4%	9.1%	17.2%	28.9%	23.1%	5.9%	21.8%	8.8%	11.7%	15.8%	12.7%	15.9%
Acidobacterium	7.0%	4.1%	7.3%	11.8%	2.5%	0.0%	0.8%	4.8%	3.8%	7.8%	21.8%	1.8%	3.3%	2.6%	4.2%	6.8%
Gemmatimonadetes	1.4%	2.0%	1.3%	1.5%	0.8%	0.0%	0.0%	1.2%	5.8%	3.9%	3.6%	1.8%	3.3%	0.0%	2.8%	4.5%
Cyanobacteria	0.0%	0.0%	2.0%	0.0%	0.8%	0.0%	0.0%	0.0%	0.0%	0.0%	0.0%	0.0%	0.0%	0.0%	1.4%	0.0%
Spirochaetes	0.0%	0.0%	0.0%	0.0%	0.0%	0.0%	0.8%	4.8%	1.9%	0.0%	0.0%	0.0%	0.0%	0.0%	0.0%	0.0%
Firmicutes	2.8%	0.0%	1.3%	1.5%	0.0%	0.0%	0.0%	1.2%	0.0%	0.0%	0.0%	3.5%	0.0%	5.3%	2.8%	0.0%
Actinobacteria	9.9%	8.2%	6.0%	2.9%	3.4%	0.0%	0.0%	1.2%	1.9%	0.0%	1.8%	3.5%	0.0%	10.5%	2.8%	2.3%
Nitrospira	2.8%	2.0%	0.7%	0.0%	0.0%	0.0%	0.0%	0.0%	3.8%	2.0%	9.1%	5.3%	0.0%	10.5%	1.4%	11.4%
Chloroflexi	5.6%	4.1%	3.3%	0.0%	0.8%	0.0%	0.0%	2.4%	1.9%	2.0%	0.0%	1.8%	5.0%	2.6%	0.0%	9.1%
Verrucomicrobia	5.6%	0.0%	6.6%	14.7%	4.2%	5.5%	2.5%	6.0%	1.9%	3.9%	0.0%	0.0%	1.7%	2.6%	7.0%	4.5%
Lentisphaera	0.0%	0.0%	0.0%	0.0%	0.0%	1.8%	0.8%	0.0%	0.0%	0.0%	0.0%	3.5%	0.0%	0.0%	0.0%	0.0%
Chlorobi	0.0%	0.0%	0.0%	0.0%	0.0%	0.0%	2.5%	1.2%	0.0%	0.0%	0.0%	0.0%	0.0%	2.6%	0.0%	0.0%
Candidate_divisions	2.8%	2.0%	10.6%	8.8%	5.0%	1.8%	4.1%	2.4%	3.8%	11.8%	3.6%	8.8%	3.3%	5.3%	7.0%	6.8%
Unknown	4.2%	0.0%	1.3%	0.0%	1.7%	0.0%	0.0%	0.0%	1.9%	0.0%	1.8%	1.8%	3.3%	2.6%	4.2%	0.0%

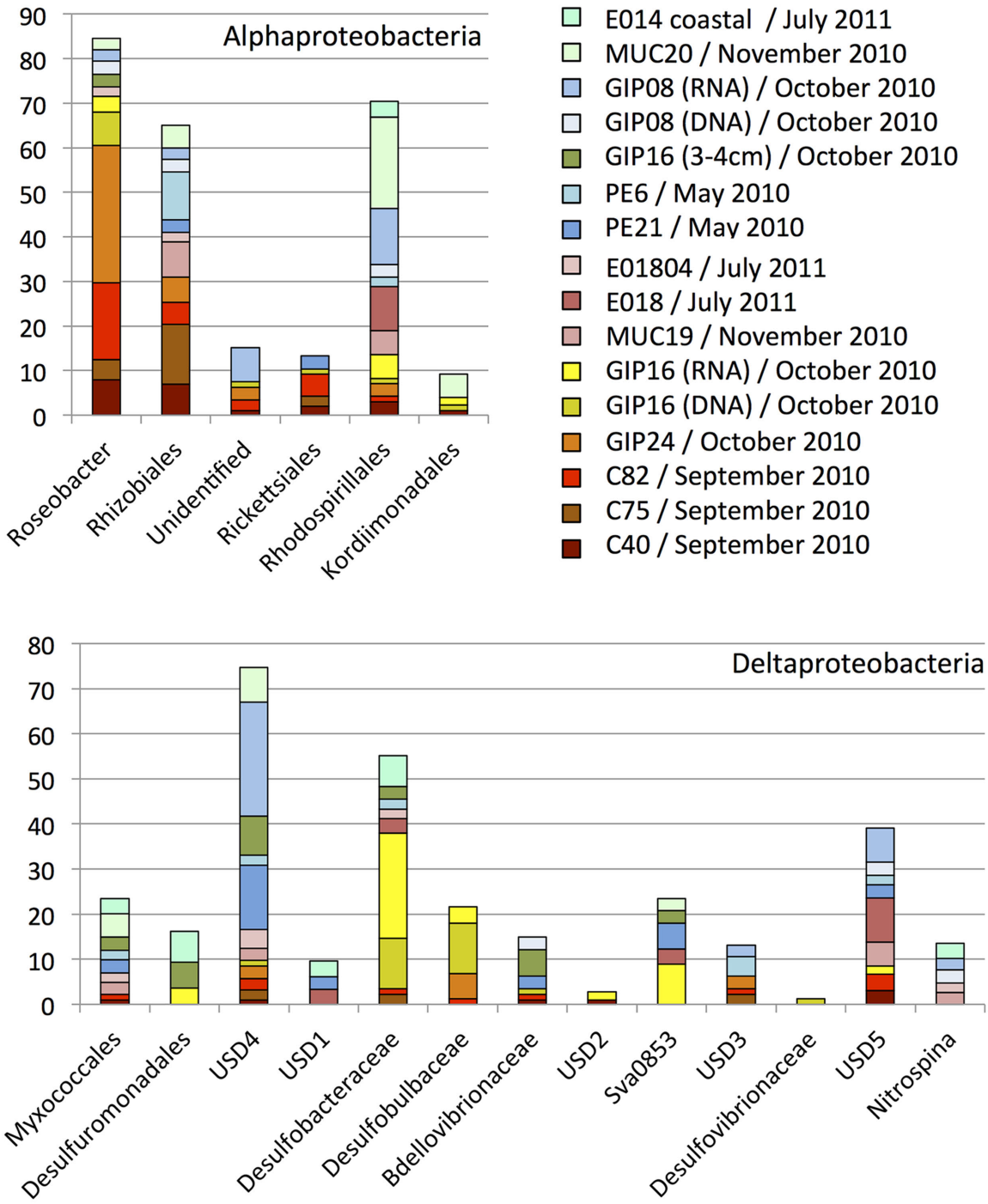

FIGURE 3 | Order, family- and genus-level identification of 16S rRNA clones representing the *Alphaproteobacteria* and *Deltaproteobacteria* in the sequence dataset shown in Figure 2 at phylum-level resolution. The y-axis shows the total number of sequences. The color key identifies the 16S rRNA gene contributions for every sediment sample. Yellow, orange, red and brown colors were chosen for oil-contaminated samples, and green and blue colors were chosen for control samples lacking visible oil impact.

individually. In MUC20, members of the *Gammaproteobacteria* (35%), *Alphaproteobacteria* (21.7%), *Planctomycetes* (11.7%), and *Deltaproteobacteria* (11.7%) in total accounted for more than 80% of the clone library (**Figure 2**; **Table 2**).

In July 2011, 1 year after the wellhead was capped, two cores E01801 and E01804 were taken 0.26 miles from each other, ca. 2 miles south-east to the DWH site, close to the May 2010 sampling site of core PE21 (**Figure 1**). The cores showed the red-brown

surface layer known from the 2010 oil-impacted cores. Members of the *Planctomycetes*, especially of the *Phycisphaera mikurensis* group, dominated the clone library (15.8%, the *P. mikurensis* group counts for 10.5%) in the surface sediment of core E01801; the *Deltaproteobacteria* were found in the same proportion (15.8%), followed by the *Gammaproteobacteria*, *Actinobacteria,* and *Nitrospira* (10.5% each), and the other nine minority groups (<8% each; **Figure 2**). In the replicate core E01804, the *Planctomycetes* accounted for only 2.8% and represented one of the 13 microbial groups that were represented in smaller proportions, whereas *Gammaproteobacteria* (38.0%) and *Deltaproteobacteria* (12.7%) dominated the library, as previously seen in PE21. Such strongly divergent bacterial communities in cores from the same marine area suggest patchily distributed seafloor communities, possibly impacted by episodic particle resuspension at the sediment/seawater interface (Ziervogel et al., 2016a). The *Gammaproteobacteria*, *Deltaproteobacteria,* and *Planctomycetes* appeared again as the most frequently detected phyla in the shallow-water reference core E01402 (depth 64 m) 211 miles west of the wellhead, with higher proportions of *Nitrospira* and *Chloroflexi* than in deepwater cores (**Figure 2**).

Bacterial Community Changes at Order, Family, and Genus-Level Resolution

In general, *Alphaproteobacteria*, *Deltaproteobacteria*, *Gammaproteobacteria*, *Bacteroidetes*, *Planctomycetes,* and *Verrucomicrobia* occurred in high proportions in most sediment clone libraries, but their role in oil degradation remained hard to infer since the classification at phylum or sub-phylum level is not precise enough for functional or ecological inferences. Therefore, we fine-tuned our results by further analyzing the 16S rRNA sequences at the level of order, family or genus of these dominant groups.

Alphaproteobacteria

The *Alphaproteobacteria* in the sediments represented six family- or order-level subgroups (**Figure 3**), mostly the monophyletic marine *Roseobacter* clade. This clade is physiologically highly diversified and includes genera and species capable of aerobic or nitrate-reducing heterotrophic degradation of dissolved and particular organic substrates, oxidation of inorganic and organic sulfur compounds (Lenk et al., 2012) or carbon monoxide as auxiliary electron and energy sources, anoxygenic photosynthetic sulfur oxidation, or aromatic hydrocarbon degradation (Wagner-Döbler and Biebl, 2006). *Roseobacter* genome studies revealed its potential for numerous biogeochemically relevant activities, including carbon monoxide oxidation, sulfur oxidation, dimethylsulfoniopropionate demethylation, aromatic compound degradation, denitrification, and phosphonate utilization (Buchan and González, 2010). While the marine *Roseobacter* clade was not found in sediment clone libraries before the oil fallout had settled on the seafloor (PE6 and PE21), it dominated the *Alphaproteobacteria* in the 2010 September samples C40, C75, and C82. The *Roseobacter* clones remained conspicuous in the October sample GIP24, where they contributed 20% of the clone library (the GIP24 *Roseobacter* accounted for 36% of the total *Roseobacter* sequences derived from all samples). The *Roseobacter* group was still detectable in GIP16 at lower abundance (9% of total *Roseobacter* sequences). Reference sediments without visible oil-derived sedimentation and red-brown coloration yielded *Roseobacter* sequences only in small numbers or not at all. These results suggest that *Roseobacter* are enriched in oil-derived marine aggregates, likely in response to the availability of substituted aromatic compounds, polysaccharides and other high-molecular weight substrates derived from decaying algae, as in a typical late-stage algal bloom (Dang and Lovell, 2016). Considering that members of the *Roseobacter* clade were detected frequently in laboratory-generated marine flocs growing on weathered Macondo crude oil collected from the sea surface (Arnosti et al., 2016), enrichment, transport and seafloor accumulation of *Roseobacter* clade members in marine oil snow is plausible.

Several studies suggested that members of the marine *Roseobacter* cluster play an important role in alkane and PAH degradation. Culture-independent studies suggested that members of the marine *Roseobacter* cluster were enriched in decane, hexadecane and other alkane-degrading seawater microcosms, but may be inhibited by some components of crude oil (McKew et al., 2007). Cultured representatives of the *Roseobacter* cluster were isolated from mangrove sediment and seawater by using media amended with pyrene, naphthalene, fluoranthrene, or phenanthrene (Brito et al., 2006; Pinyakong et al., 2012). Aromatics degradation pathways were identified in several *Roseobacter* cluster genomes (Buchan and González, 2010), including in a recently described new species and genus, *Tritonibacter horizontis*, from DWH surface oil flocs that can utilize substituted aromatics as sole carbon source (Klotz, 2016). The decline of *Roseobacter* cluster phylotypes in GIP16 and after October 2010 could be linked to increasing substrate limitation, as the available substrates transitioned from short hydrocarbons to more recalcitrant ones such as PAHs. Also, the cold *in situ* temperatures on the seafloor of deep Gulf of Mexico slope (ca. 4–5°C; Yang et al., 2016) may inhibit the physiological activity of surface-derived *Roseobacter* clade populations and select against them. While *Roseobacter* populations native to cool environments persist in oil enrichment studies at 4°C (Coulon et al., 2007), the *Roseobacter* clade isolate *Tritonibacter horizontis* from surface oil slicks has an optimal growth temperature of 30°C, close to the sea surface temperature of 26°C at the time of sampling, and a growth temperature range of 4–45°C (Klotz, 2016). In consequence, cold-adapted sediment bacteria with otherwise similar growth requirements and ecophysiological preferences for particle attachment – for instance, members of the *Bacteroidetes* that were detected frequently in the October samples – could outcompete the warm-water *Roseobacter* clade arrivals from the sea surface (Dang and Lovell, 2016).

Deltaproteobacteria

The numerous natural hydrocarbon seeps in the Gulf of Mexico provide suitable permanent habitats for sulfate-reducing

hydrocarbon-oxidizing bacteria (Lloyd et al., 2006, 2010; Teske, 2010; Kleindienst et al., 2012; Ruff et al., 2015). Here, members of the sulfate-reducing bacterial (SRB) family *Desulfobacteraceae* including the *Desulfosarcina*/*Desulfococcus* (DSS) clade, the *Desulfobulbaceae*, and two uncultured clusters (called here "uncultured sediment dwellers," USD4 and USD5) constituted the principal deltaproteobacterial groups in these sediment samples (**Figure 3**). Some members of the DSS group can degrade short chain alkanes under strict anoxic conditions in coastal as well as deep seafloor sediments (Kniemeyer et al., 2007; Jaekel et al., 2013; Kleindienst et al., 2014). The *Desulfobacteraceae* and *Desulfobulbaceae* clades included sequences from the oil-polluted surficial sediments GIP24 and GIP16 (both 16S rRNA gene sequences and the reverse-transcript 16S rRNA cDNA sequences), and few sequences from non-polluted surface sediments (**Figure 4**).

Members of *Desulfobacteraceae* and *Desulfobulbaceae* were previously identified at natural seeps, mud volcanoes, and gas hydrates in the Gulf of Mexico (Lloyd et al., 2010; Orcutt et al., 2010), but also from the oil spills, such as the Prestige oil spill on the coast of northern Spain (Acosta-Gonzalez et al., 2013). In this case, the evidence linked the clones in GIP16 and GIP24 to the Deepwater Horizon oil spill, not to natural seepage: the GIP16 and GIP24 cores lacked methane gas pockets, gas hydrate or porewater sulfide accumulation. In contrast to seep sediments (Lloyd et al., 2006, 2010), the *Desulfobacteraceae* and *Desulfobulbaceae* clones were limited to the surface sediment layers, except for a single *Desulfobacteraceae* clone from the 3–4 cm layer of the GIP16 core. Secondly, the surficial fluffy sediment showed much smaller grain sizes than the sediments below this layer, indicating a specific depositional event (Brooks et al., 2015). Furthermore, isotopic analysis using Th234 as a

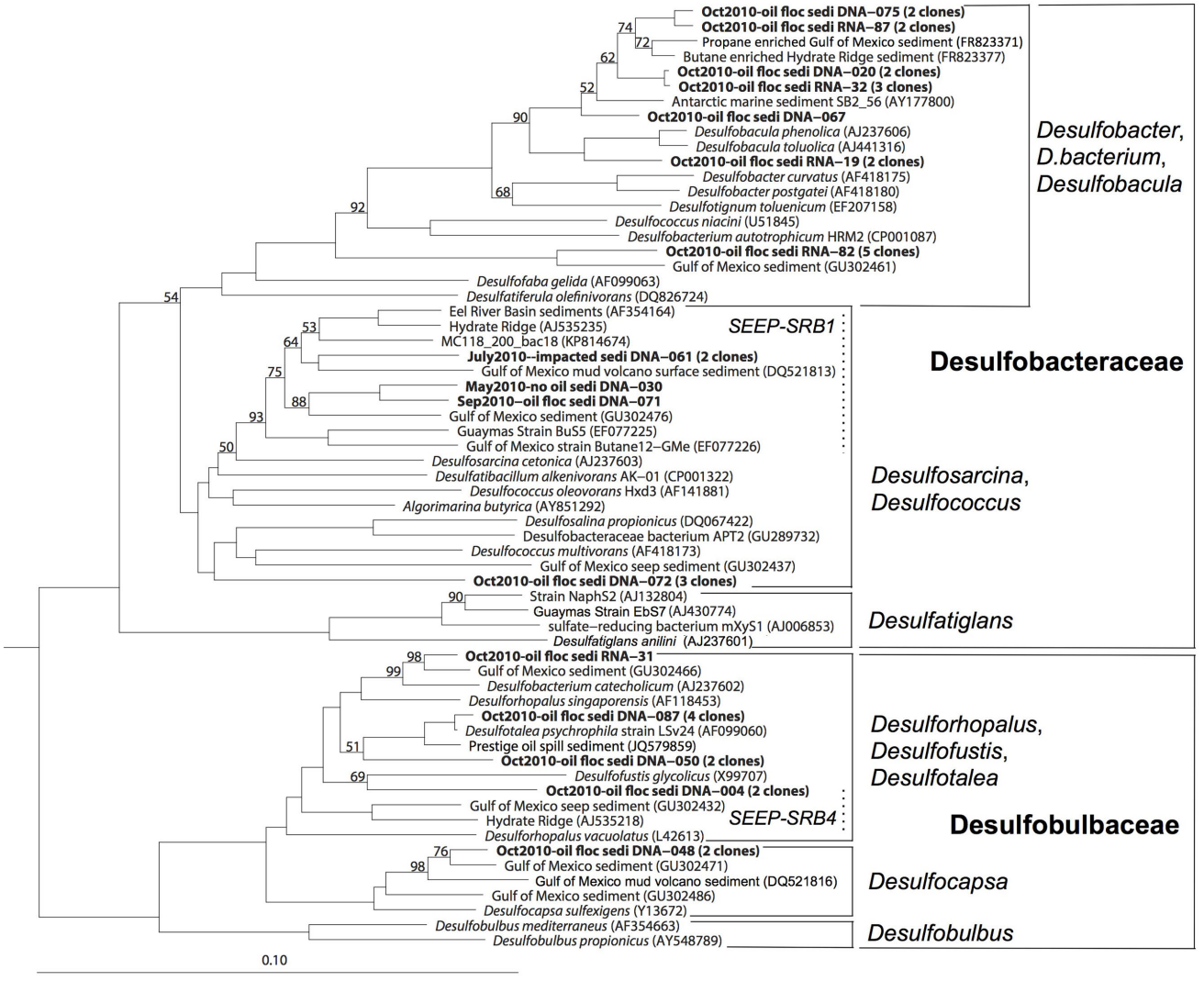

FIGURE 4 | 16S rRNA gene phylogenetic tree of the deltaproteobacterial families *Desulfobacteraceae* and *Desulfobulbaceae*. The scale bar corresponds to 10% sequence distance (Jukes-Cantor). The phylogeny was rooted with the Gammaproteobacterium *Colwellia psychrerythraea*.

short-lived marker (half-life time 24 days) for fast sedimentation pulses showed this layer was deposited within a few months, which is congruent with the timeline of the oil spill (Brooks et al., 2015; Chanton et al., 2015). Finally, the phylogenetic analysis of SRB groups demonstrated that the majority of the SRB sequences from October 2010 formed distinct clades that differed from the SRB clades (SEEP-SRB1 to SEEP-SRB4; Knittel et al., 2003) that are frequently found in natural cold seeps. Most phylotypes formed sister lineages to cultured aromatics-degrading *Desulfobacula* and alkane enrichments within the Desulfobacteraceae, or the psychrophilic genus *Desulfotalea* within the *Desulfobulbaceae*; phylogenetic overlap of the October sediment clones with potentially seep-dwelling SRB was limited to the SEEP-SRB-1 clade (**Figure 4**).

The *Desulfobacteraceae* and *Desulfobacteraceae* are anaerobes, and oxic surface sediments are by no means their favorite natural habitat. The appearance of these obligate anaerobes indicates changing, increasingly reducing redox conditions within the surficial oily sediment, a conclusion supported by the proliferation of nitrate-reducing genes detected in sediment metagenomes (Mason et al., 2014), and by the geochemical imprint of microbial metal reduction and mobilization pulses in oil-impacted surficial sediments (Hastings et al., 2016). Possibly, anoxic and reducing conditions that favor the development of SRB in surficial sediment result from oxygen consumption by *Roseobacter* clade members and *Bacteroidetes* that grow on suitable hydrocarbons and organic matter of planktonic origin as carbon source. Following this scenario, heterotrophic activity could sharply lower the oxygen concentration toward the center of the oil aggregates, and generate micro-scale anoxic niches. The anaerobic SRBs could then thrive in these anoxic particles and degrade remaining recalcitrant high-molecular weight aromatic hydrocarbons. Other deltaproteobacterial subgroups, such as the *Myxococcales* which accumulated in oil polluted sediment after the Prestige oil spill (Acosta-Gonzalez et al., 2013), were not detected forming temporary blooms in the Gulf of Mexico sediment.

Gammaproteobacteria

Members of the *Gammaproteobacteria* constituting 15 subgroups were found in high proportions in all clone libraries except the sample E01801 from July 2011 (**Figure 5**). The most abundant group, designated JTB255, was previously found in deep cold seep sediments of the Japan Trench (Li et al., 1999), and in diverse marine seafloor environments (Teske et al., 2011). Oil input apparently did not influence the occurrence pattern of the JTB255 group (**Figure 5**). A polyphyletic assemblage of sulfur-oxidizer-related bacteria, and a cluster including members of the *Legionellales*, *Coxiella* and *Rickettsiella*, constituted the next-most abundant gammaproteobacterial groups after JTB255. Sequences of the *Oceanospirillales* were found in small numbers in the sediments, but they did not fall into the DWH *Oceanospirillales* group recovered from the hydrocarbon plume (Yang et al., 2016). The remaining minor groups include the genera *Congregibacter*/*Haliea*/*Dasania*, *Fangia*, a *Kangiella*-related group, *Alteromonas*/*Pseudoalteromonas*, a *Balneatrix* sister group, the E01-9C-26 group, a SAR156 sister group and the *Thiotrichales*. The genera *Cycloclasticus* and *Colwellia* accounted for small portions of the gammaproteobacterial phylotypes.

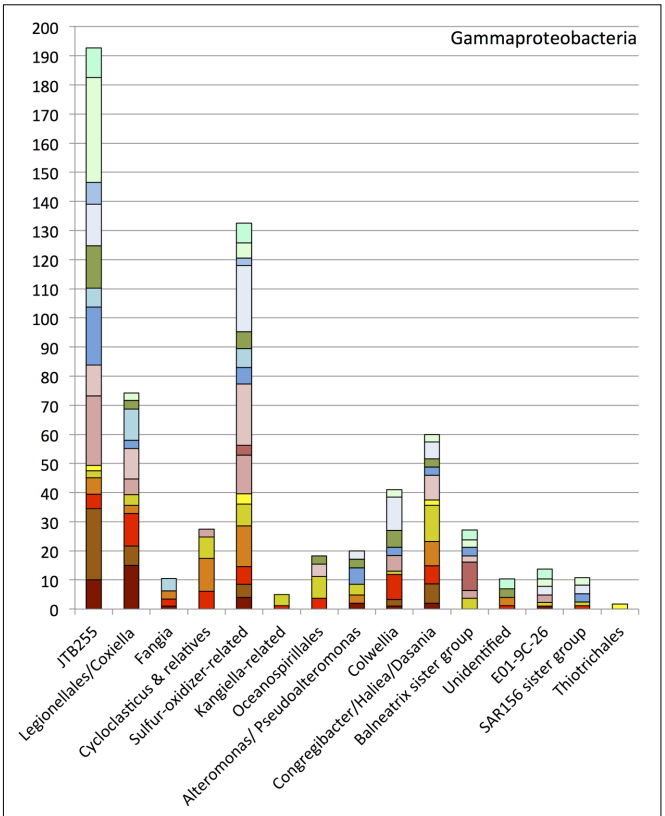

FIGURE 5 | Order, family- and genus-level identification of 16S rRNA clones representing the *Gammaproteobacteria* in the sequence dataset shown in Figure 2 at phylum-level resolution.

Cycloclasticus

The obligately polyaromatic hydrocarbon-degrading genus *Cycloclasticus*, previously cultured from Gulf of Mexico sediments amended with phenanthrene or naphthalene (Geiselbrecht et al., 1998), was repeatedly detected in oil polluted surficial sediments from September, October, and November 2010 (**Figure 5**). *Cycloclasticus* was consistently present in surface oil slick collected in May 2010 (Yang et al., 2016), in the deep hydrocarbon plume in June 2010 (Redmond and Valentine, 2012), and in post-plume deep water in September 2010 (Yang et al., 2016). *Cycloclasticus* phylotypes were also enriched from marine snow grown on weathered Macondo oil (Arnosti et al., 2016), in stable-isotope probing enrichments on phenanthrene (Gutierrez et al., 2013), and in sediment incubations with weathered oil slick in the lab (Yang, 2014); a pure-culture isolate from weathered surface oil slick (*Cycloclasticus* sp. TK-8) is now available for detailed study (Gutierrez et al., 2013). These *Cycloclasticus* phylotypes formed phylogenetically tight clusters; three of them consisted exclusively or predominantly of uncultured sequences from the water column and the sediment, and a fourth cluster included the previously described species

and the new isolates and enrichments from Deepwater Horizon samples (**Figure 6**). Interestingly, these clusters obtained by full-length 16S rRNA gene sequencing also matched clusters obtained independently by high-resolution oligotyping (Kleindienst et al., 2016). Cluster 2, containing phylotypes from the sediment and water column sampled in September, October and November 2010, corresponded to *Cycloclasticus* ecotypes termed type 02 and 07 that accounted for the majority of *Cycloclasticus* phylotypes in post-plume water column samples (Kleindienst et al., 2016). Cluster 3, which contained phylotypes from sediment and water column sampled in September and October 2010, corresponded to *Cycloclasticus* ecotype 4, a plume population sampled in May and June 2010 (Kleindienst et al., 2016). These mixed seawater and sediment *Cycloclasticus* clusters indicate transportation by sinking particle flux and habitat connectivity: their members followed the continuous sedimentation of oil-derived marine snow, containing oil particles and oil-degrading bacteria, to the seafloor. Since *Cycloclasticus* spp. are obligate aromatic hydrocarbon degraders, the weathered oil-derived aggregates on the seafloor most likely sustained populations of *Cycloclasticus* spp. that had originally arrived on sinking particles. Phylotypes of *Cycloclasticus* persisted into the November 2010 sediments, but were no longer detected in the sediments collected in July 2011 (**Figure 5**).

Colwellia

Members of the heterotrophic bacterial genus *Colwellia* were continuously detected in deep hydrocarbon plumes and post-plume seawater (Valentine et al., 2010; Redmond and Valentine, 2012; Yang et al., 2016), as well as in seafloor sediments with high concentrations of total hydrocarbon petroleum (Mason et al., 2014); a new *Colwellia* strain was isolated from Gulf of Mexico seawater enrichments supplied with Macondo oil and dispersant Corexit (Baelum et al., 2012). In contrast to *Cycloclasticus*, *Colwellia* was found in both oily and non-oily sediments in September, October and November 2010. Although the *Colwellia* bloom was initially triggered during the late stage of the deepwater hydrocarbon plume (Valentine et al., 2010), the growth of *Colwellia* spp. does not solely depend on external hydrocarbon supply. This heterotrophic group was previously found in organic-rich sediments ranging from fish farm sediments (Bissett et al., 2006) to Antarctic continental shelf sediment (Bowman and McCuaig, 2003). Since *Colwellia* spp. could be autochthonous to the seafloor surficial sediment, it cannot be unambiguously linked to the oil fallout.

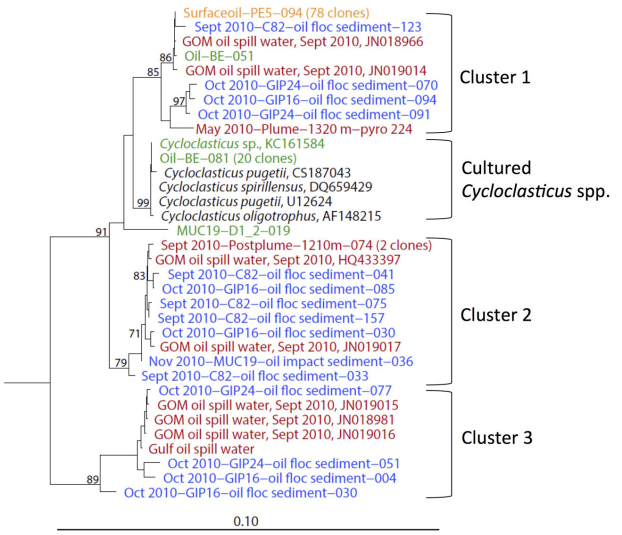

FIGURE 6 | 16S rRNA gene phylogenetic tree of *Cycloclasticus* sequences derived from both water column and the surficial sediment of the Gulf of Mexico at various time points. The orange-colored clone is from May 2010 surface oil slick; red clones are from post-plume water (Valentine et al., 2010; Redmond and Valentine, 2012; Yang et al., 2016); blue clones are from surficial sediments of September, October and November 2010; green clones represent phylotypes and a new strain from oil slick incubations (Gutierrez et al., 2013) and 4°C enrichments (Yang, 2014).

Bacteroidetes

Two major family level groups, the *Flavobacteriaceae* and the *Marinifilum/Cytophaga* group, increased the contribution of the phylum *Bacteroidetes* to the October 2010 oil-impacted samples; the rRNA survey also confirmed their high activity at that time (**Figure 7**). The *Flavobacteriaceae* increased already in the oil-contaminated sediments of September 2010, whereas the *Marinifilum/Cytophaga* group was not detected in the September 2010 sediments and peaked 1 month later in the October oily sediments. Here, the reverse-transcribed 16S rRNA clone library implied high activity of an uncultured *Cytophaga* group; relatives of this group were enriched on crude oil at 5°C, similar to the temperature at the bottom of Gulf of Mexico (Brakstad and Bonaunet, 2006). Several studies indicated that members of the *Flavobacteriaceae* and *Cytophaga* respond to the presence of hydrocarbons. In beach sediments polluted by

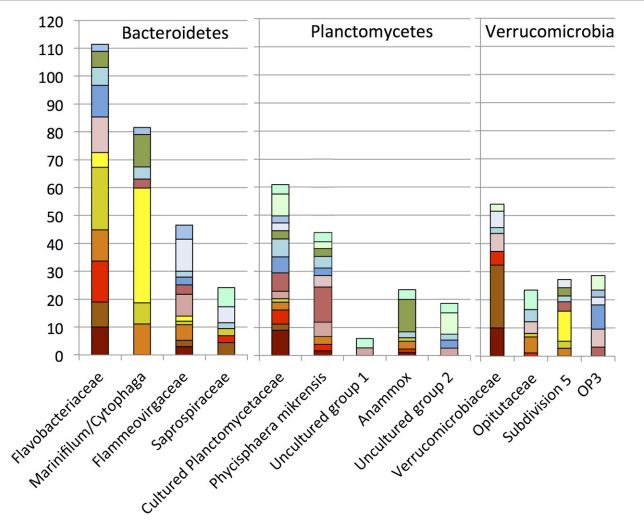

FIGURE 7 | Order, family- and genus-level identification of 16S rRNA clones representing the phyla *Bacteroidetes, Planctomycetes,* and *Verrucomicrobia* in the sequence dataset shown in Figure 2.

the 2002 Prestige oil spill in northwestern Spain, members of the *Bacteroidetes* – mostly *Flavobacteria* and *Sphingobacteria* – accounted for up to a quarter of the bacterial clone libraries in samples that were taken 5 years later (Acosta-Gonzalez et al., 2013). Several *Bacteroidetes* isolates are known to participate in the biodegradation of polyaromatic compounds. For example, *Yeosuana aromativorans,* from estuarine sediment and seawater, is capable of degrading PAHs such as pyrene (Kwon et al., 2006; Sheppard et al., 2012), and strains of *Flavobacterium* sp. isolated from sewage were able to grow on biphenyl (Stucki and Alexander, 1987).

Planctomycetes

Within oil-impacted sediments, the phylum *Planctomycetes* was mostly represented by clades of cultured *Planctomycetes* and by the largely uncultured clade represented by *P. mikurensis* (Fukunaga et al., 2009), originally isolated from algae (**Figure 7**). Many *Planctomycetes* sequences were closely related to those derived from marine seafloor habitats, such as sediments in the South China Sea (Hu et al., 2010), deep sea sediment underlying two whale falls (Goffredi and Orphan, 2010), and seafloor lavas from the East Pacific Rise (Santelli et al., 2008). Their association with marine snow particles (Delong et al., 1993) and the high numbers of sulfatases in marine *Planctomycetes* characterize them as specialists for the initial breakdown of sulfated heteropolysaccharides in marine snow and indicate their importance for recycling carbon from these compounds (Woebken et al., 2007). In the seafloor clone libraries, *Planctomycetes* occur abundantly in individual samples (E01801, E01402) but do not show a preference for oil-impacted sediments; in this regard they contrast with other bacterial groups that are stimulated by fresh oil sedimentation. Clones of the Anammox clade (in marine environments, genus *Scalindua*) were mostly obtained from the GIP3-4 cm sample, indicating a potential enrichment in sediments below the oil-impacted surface layer.

Verrucomicrobia

Phylotypes of the *Verrucomicrobia* occurred in intermediate abundance in most sediment samples. Our family-and genus-level resolution analysis demonstrated divergent dynamics of the *Verrucomicrobia* subgroups (**Figure 7**). The phylum *Verrucomicrobia* contains a total of seven subdivisions that are not all represented by cultured strains (Hugenholtz et al., 1998; Freitas et al., 2012). The family *Verrucomicrobiaceae*, previously defined as subdivision 1 (Hugenholtz et al., 1998), and containing the methanotrophic genus *Acidomethylosilex* (Freitas et al., 2012), responded to the oil input in early September 2010, whereas members of the uncultured subdivision 5 were appeared only in mid-October 2010 (**Figure 6**). The representative sequences of subdivision 5 were originally cloned from the methanogenic layer of an aquifer contaminated with hydrocarbons and chlorinated solvents (Dojka et al., 1998). Therefore, members of subdivision 5 may be capable of hydrocarbon bioremediation in anoxic environments, consistent with the hypothesis of micro-scale anoxic niches at the seafloor in October 2010.

PCoA Analysis of Sediment Samples

Weighted UniFrac analysis was applied to explore control factors that shaped the clone library structure of the DWH samples using PCoA, based on the phylogenetic affiliations obtained with ARB (Ludwig et al., 2004; Lozupone et al., 2006). Principal components P1 and P2 could explain 32.42% of the variation in bacterial community composition (**Figure 8**). Oil-derived sedimentation was one of the major controls on bacterial community composition, as the principal component P1 clearly separated most oil-impacted samples (P1 value > 0) from the non-impacted control samples. The 2010 September oil floc samples and a 2011 July sample close to the wellhead area (E01804) grouped together, indicating high similarity between these samples. The two contaminated samples GIP16 and GIP24 collected in October 2010 clustered adjacent to, but separately from the September 2010 samples, indicating that their DNA-based bacterial community structures diverged. It is possible to view the September and October clusters as a continuum that could be linked across the two least-distant members of the two clusters, the adjacent September sample C82 and the October sample GIP24 (**Figure 8**). In this view, the bacterial community in the oily sediments is gradually changing over time, potentially in sync with microbially accessible substrate pools or geochemical characteristics of the surficial sediments.

The non-oily samples have P1 and P2 values near or below zero (**Figure 8**). Non-oily samples from May 2010 (PE6 and PE21) and October 2010 (GIP08 and GIP16 3–4 cm), and also the November samples MUC19 and MUC20, formed three clusters that grouped closely to each other, and separately from the oil-impacted September and October samples. The bacterial community of GIP16 3–4 cm shared high similarity with the May 2010 samples, but differed from its oily surface layer (GIP16), consistent with the hypothesis that much of the bacterial community that is usually found in non-oily sediment surface samples persists underneath the layer of oil-derived fallout. Somewhat unexpectedly, the oil-impacted sample MUC19, characterized by the red-brown redox signature of oil-induced metal mobilization (Hastings et al., 2016), groups closely with the distant background sample MUC20. Even more remarkably, this pair is the closest neighbor of the two pre-sedimentation May 2010 samples (**Figure 8**). This result suggests that in late November 2010, specific groups of oil-degrading or oil-responding bacteria no longer determine the overall microbial community composition. The successive enrichments of *Roseobacter*, *Desulfobacteraceae*/*Desulfobulbaceae*, *Bacteroidetes,* and *Verrucomicrobia* that structured benthic bacterial communities in oil-impacted samples collected in September and October of 2010 do not last into the late November 2010 samples; instead, the benthic bacterial communities of these samples are reverting to resemble the pre-spill baseline. This does not mean that the oil-derived sedimentation pulse has left no imprint on these samples, but that it is no longer conspicuous on the whole-community level. The July 2011 samples do not show any consistent clustering with each other or other groups of oil- or non-oil impacted sediment samples; it is possible that the microbial communities of these samples from

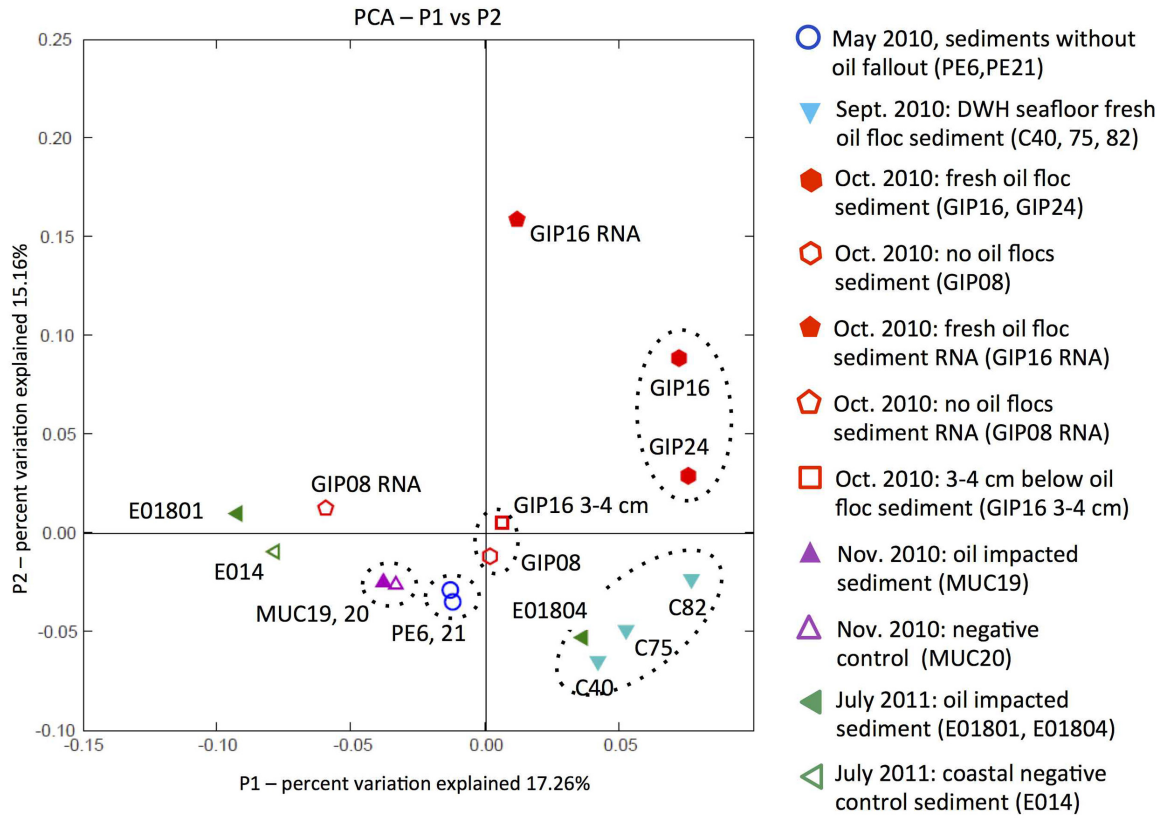

FIGURE 8 | Principal coordinates analysis (PCoA) of 16S rRNA gene distances between phylotypes in all sediment samples. Solid symbols stand for the DWH-impacted sediments; open symbols represent the control sediments without visible imprint of oil-derived sedimentation, or samples below the oil-impacted sediment surface, as in the case of GIP16 3–4 cm.

different locations are subject to divergent ecosystem trajectories (seasonal phytoplankton and bacterioplankton blooms; sediment resuspension and oxidative processing; long-term processing of oil-derived substrates) that no longer tie them unambiguously to the DWH oil spill. Interestingly, the 2011 July sample E01804 clusters with the oil floc samples C40, C75, and C82 collected in September 2010, suggesting that close analogs of these oil floc communities may – under specific circumstances – recur in benthic sediments.

The reverse-transcribed RNA samples GIP16 and GIP08 RNA of October 2010 diverge generally from their DNA counterparts, suggesting that the bacterial community patterns of gene expression are different from those based DNA and gene presence. The clustering that is observed on the DNA level might turn out differently if the entire study was replicated on the RNA level.

DISCUSSION AND OUTLOOK

A large proportion of the oil that escaped earlier budgeting efforts (McNutt et al., 2012; Joye et al., 2016) reached the seafloor on the continental slope of the northern Gulf of Mexico by sedimentation of oily marine snow (Passow et al., 2012; Ziervogel et al., 2012), as recently substantiated by comprehensive stable carbon isotopic analyses of seafloor hydrocarbon deposits (Chanton et al., 2015). This deposition event took place in summer and early fall 2010, as dated by ^{234}Th decay in surficial sediment cores (Brooks et al., 2015), and it appears to have triggered consecutive microbial population changes that were detected in this clone library survey. In our scenario, the rapid consumption of easily accessible hydrocarbons (short chain alkanes or polar substituted aromatics) or extracellular polymeric substrates in oil-derived marine snow by aerobic heterotrophic bacteria such as *Roseobacter*, *Verrucomicrobiaceae,* and *Bacteroidetes* in September and October 2010, could lead to localized oxygen depletion close to the sediment-seawater interface, or favor the formation of anoxic zones at micro-scale on the surface of the sediment. Anoxic microniches would provide suitable habitats and substrates for a wide range of anaerobes, such as denitrifying (Mason et al., 2014), metal-reducing (Hastings et al., 2016), or SRB (Kimes et al., 2013) that continue to degrade recalcitrant petroleum hydrocarbons at the seafloor *in situ*. This scenario explains the conspicuous appearance of *Desulfobacteraceae* and *Desulfobulbaceae* in the surficial sediment samples collected in October 2010. The microbial degradation cascade triggered by oil snow deposition on the seafloor seems to have slowed down in late November 2010, in the sense that the

overall bacterial community structure is no longer controlled by the oil sedimentation response but resembles again the pre-spill community. The microbial response to petrocarbon deposition remains detectable on finer taxonomic scales when specialized oil-degrading bacterial populations are considered. For example, the obligate polycyclic aromatics degrader *Cycloclasticus* could be traced into the November 2010 sediment sample set.

To link microbial community signatures and hydrocarbon content of the sediment, the literature and databases were searched for chemical analyses performed on the same sediment samples, obtained with the same multicorer deployment. Concentrations of total polyaromatic hydrocarbons (TPAH) and compound-specific results are published for oil-impacted sediment cores collected with R/V Cape Hatteras in Mid-October 2010 near the Macondo wellhead (Woodruff, 2014), including core GIP16 with TPAH concentrations of 2192, 309 and 272 ng/g at 0–1, 1–2, and 2–3 cm depth, respectively, and core GIP24 with TPAH concentrations of 819, 287, and 262 ng/g in 0–1, 1–2, and 2–3 cm depth, respectively. These elevated TPAH concentrations demonstrate the arrival of a sedimentation pulse of petroleum-derived aromatic compounds on the seafloor. At 3 cm sediment depth, the TPAH concentrations approach the average pre-spill TPAH concentrations in sediments of the northern Gulf of Mexico, near 140 ng/g (Wade et al., 2008). Thus, the impact of polyaromatic hydrocarbon availability on microbial community structure should diminish with sediment depth, as indeed observed in the GIP16 3–4 cm sample (**Figure 8**). In general, TPAH concentrations of surficial sediments (0–1 cm layer) sampled in mid-October 2010 around the Macondo wellhead increased to above 400 ng/g, with an average near 1100 ng/g and localized peaks near 17,000 ng/g (Woodruff, 2014). Specific classes of polyaromatic compounds (fluorenes, phenanthrenes, anthracenes, chrysenes, pyrenes) decreased in concentration over the upper three centimeters, consistent with recent deposition from the water column (Woodruff, 2014). On resampling in 2011, TPAH concentrations in surficial sediments had decreased to 200–300 ng/g, with an average of 220 ng/g (Woodruff, 2014); specific polyaromatic compounds had also decreased in concentration by approximately an order of magnitude, presumably reflecting microbial degradation of these substrates (Woodruff, 2014).

As a distinguishing characteristic, the microbial community of the seafloor sediments changed on longer time scales than the oil-impacted community in the water column. The seafloor sediments received the oil-derived sedimentation pulse and its associated microbial communities after the onset of marine oil snow formation in the surface water in early May 2010, and the development of the deepwater hydrocarbon plume in May and June 2010 (Yang et al., 2016). Once the oil-derived marine snow and its embedded hydrocarbon particles started to settle on the seafloor sediment surface, the seafloor acted as an integrator of the microbial and chemical fallout, collecting the oil-derived sedimentation pulse continuously throughout the summer and fall of 2010. The microbial responses of oil-degrading sediment bacteria, or opportunistic heterotrophs that took advantage of other oil snow components, were reflected in conspicuous whole-community changes in September and October 2010. At this time, the bacterial communities in the overlying water column were reverting to pre-spill conditions (Yang et al., 2016) and the prevailing transport direction, toward the west and southwest, moved the oil-impacted water masses and their residual oxygen minima and microbial populations from the study area (Diercks et al., 2010b; Joye et al., 2016). The seafloor sediment integrates the changeable water column input over time, and retains the permanent geochemical archive of the oil-derived sedimentation pulse in the same manner as other events that have impacted the quaternary sedimentation regime in the northern Gulf of Mexico (Ingram et al., 2013). As the increasingly recalcitrant oil-derived fallout is buried by ongoing sedimentation under increasingly anaerobic conditions, slow microbial degradation and assimilation of recalcitrant hydrocarbons should remain detectable with molecular assays and enrichments, for example by ^{13}C-analysis of hydrocarbons that are gradually assimilated into the resident bacterial rRNA (Pearson et al., 2008).

AUTHOR CONTRIBUTIONS

TY and AT designed the study; TY, AT, LM, and KS collected and recorded sediment samples on research cruises in the Gulf of Mexico. KS also extracted and reverse-transcribed RNA from samples GIP08 and GIP16. BM designed the modified RNA extraction method for marine sediments. SJ served as chief scientist on cruise AT18-02 (November/December 2010), provided additional samples from RV Oceanus cruise in August/September 2010 (OC486) and served as PI on the ECOGIG consortium that subsequently funded TY's graduate study. TY performed the 16S rRNA gene sequencing, the phylogenetic analyses, and calculated the PCoA plots; AT and TY wrote the manuscript with input from the other authors.

ACKNOWLEDGMENTS

We would like to thank the chief scientists, shipboard, and science crews of our cruises for successful sediment sampling operations on tight schedules. AT and TY were initially supported by NSF (RAPID Response: the microbial response to the Deepwater Horizon Oil Spill; NSF- OCE 1045115). This work was in part made possible by a grant from the BP/The Gulf of Mexico Research Initiative to support the consortium research entitled "Ecosystem Impacts of Oil and Gas Inputs to the Gulf (ECOGIG)" administered by the University of Mississippi. Data are publicly available through the Gulf of Mexico Research Initiative Information and Data Cooperative (GRIIDC) at https://data.gulfresearchinitiative.org (doi: 10.7266/N7GH9FZ8).

REFERENCES

Acosta-Gonzalez, A., Rossello-Mora, R., and Marques, S. (2013). Characterization of the anaerobic microbial community in oil-polluted subtidal sediments: aromatic biodegradation potential after the Prestige oil spill. *Environ. Microbiol.* 15, 77–92. doi: 10.1111/j.1462-2920.2012.02782.x

Altschul, S. F., Gish, W., Miller, W., Myers, E. W., and Lipman, D. J. (1990). Basic local alignment search tool. *J. Mol. Biol.* 215, 403–410. doi: 10.1016/S0022-2836(05)80360-2

Arnosti, C., Ziervogel, K., Yang, T., and Teske, A. (2016). Oil-derived marine aggregates - hot spots of polysaccharide degradation by specialized bacterial communities. *Deep Sea Res. Part II* 129, 179–186. doi: 10.1016/j.dsr2.2014.12.008

Ashelford, K. E., Chuzhanova, N. A., Fry, J. C., Jones, A. J., and Weightman, A. J. (2005). At least 1 in 20 16S rRNA sequence records currently held in public repositories is estimated to contain substantial anomalies. *Appl. Environ. Microbiol.* 71, 7724–7736. doi: 10.1128/AEM.71.12.7724-7736.2005

Baelum, J., Borglin, S., Chakraborty, R., Fortney, J. L., Lamendella, R., Mason, O. U., et al. (2012). Deep-sea bacteria enriched by oil and dispersant from the Deepwater Horizon spill. *Environ. Microbiol.* 14, 2405–2416. doi: 10.1111/j.1462-2920.2012.02780.x

Bissett, A., Bowman, J., and Burke, C. (2006). Bacterial diversity in organically-enriched fish farm sediments. *FEMS Microbiol. Ecol.* 55, 48–56. doi: 10.1111/j.1574-6941.2005.00012.x

Bowman, J. P., and McCuaig, R. D. (2003). Biodiversity, community structural shifts, and biogeography of prokaryotes within Antarctic continental shelf sediment. *Appl. Environ. Microbiol.* 69, 2463–2483. doi: 10.1128/AEM.69.5.2463-2483.2003

Brakstad, O. G., and Bonaunet, K. (2006). Biodegradation of petroleum hydrocarbons in seawater at low temperatures (0-5 degrees C) and bacterial communities associated with degradation. *Biodegradation* 17, 71–82. doi: 10.1007/s10532-005-3342-8

Brito, E. M., Guyoneaud, R., Goni-Urriza, M., Ranchou-Peyruse, A., Verbaere, A., Crapez, M. A. C., et al. (2006). Characterization of hydro-carbonoclastic bacterial communities from mangrove sediments in Guanabara Bay, Brazil. *Res. Microbiol.* 157, 752–762. doi: 10.1016/j.resmic.2006.03.005

Brooks, G. R., Larson, R. A., Flower, B., Hollander, D., Schwing, P. T., Robero, I., et al. (2015). Sedimentation pulse in the NE Gulf of Mexico following the 2010 DWH blowout. *PLoS ONE* 10:e0132341. doi: 10.1371/journal.pone.0132341

Buchan, A., and González, J. M. (2010). "Roseobacter," in *Handbook of hydrocarbon and lipid microbiology*, ed. K. N. Timmis (Berlin: Springer-Verlag), 1335–1343.

Chanton, J. P., Zhao, T., Rosenheim, B., Joye, S. B., Bosman, S., Brunner, C., et al. (2015). Radiocarbon tracing of the flux of petrocarbon to the sea floor associated with the Deepwater Horizon event. *Environ. Sci. Technol.* 49, 847–854. doi: 10.1012/es5046524

Coulon, F., McKew, B. A., Osborn, A. M., McGenity, T. J., and Timmis, K. N. (2007). Effects of temperature and biostimulation on oil-degrading microbial communities in temperate estuarine waters. *Environ. Microbiol.* 9, 177–186. doi: 10.1111/j.1462-2920.2006.01126.x

Daly, K., Passow, U., Chanton, J., and Hollander, D. (2016). Assessing the impacts of oil-associated marine snow formation and sedimentation during and after the Deepwater Horizon oil spill. *Anthropocene* 13, 18–33. doi: 10.1016/j.ancene.2016.01.006

Dang, H., and Lovell, C. R. (2016). Microbial surface colonization and biofilm development in marine environments. *Microbiol. Mol. Biol. Rev.* 80, 91–138. doi: 10.1128/MMBR.00037-15

Dell'Amore, C. (2010). *"Sea Snot" Explosion Caused by Gulf Oil Spill? National Geographic*. Available at: http://news.nationalgeographic.com/news/2010/09/100916-sea-snot-gulf-bp-oil-spill-marine-snow-science-environment

Delong, E. F., Franks, D. G., and Alldredge, A. L. (1993). Phylogenetic diversity of aggregate-attached vs free-living marine bacterial assemblages. *Limnol. Oceanogr.* 38, 924–934. doi: 10.4319/lo.1993.38.5.0924

Diercks, A.-R., Asper, V. L., Highsmith, R., Woolsey, M., Lohrenz, S., McLetchie, K., et al. (2010a). "NIUST – Deepwater horizon oil spill response cruise," in *Proceedings of the OCEANS 2010, in OCEANS-IEEE Series*, (Piscataway, NJ: IEEE), 1–7.

Diercks, A.-R., Highsmith, R. C., Asper, V. L., Joung, D., Zhou, Z., Guo, L., et al. (2010b). Characterization of subsurface polycyclic aromatic hydrocarbons at the Deepwater Horizon site. *Geophys. Res. Lett.* 37:L20602. doi: 10.1029/2010GL045046

Dojka, M. A., Hugenholtz, P., Haack, S. K., and Pace, N. R. (1998). Microbial diversity in a hydrocarbon- and chlorinated-solvent-contaminated aquifer undergoing intrinsic bioremediation. *Appl. Environ. Microbiol.* 64, 3869–3877.

Freitas, S., Hatosy, S., Fuhrman, J. A., Huse, S. M., Welch, D. B. M., Sogin, M. L., et al. (2012). Global distribution and diversity of marine Verrucomicrobia. *ISME J.* 6, 1499–1505. doi: 10.1038/ismej.2012.3

Fukunaga, Y., Kurahashi, M., Sakiyama, Y., Ohuchi, M., Yokota, A., and Harayama, S. (2009). Phycisphaera mikurensis gen. nov., sp nov., isolated from a marine alga, and proposal of Phycisphaeraceae fam. nov., Phycisphaerales ord. nov. and Phycisphaerae classis nov. in the phylum Planctomycetes. *J. Gen. Appl. Microbiol.* 55, 267–275. doi: 10.2323/jgam.55.267

Geiselbrecht, A. D., Hedlund, B. P., Tichi, M. A., and Staley, J. T. (1998). Isolation of marine polycyclic aromatic hydrocarbon (PAH)-degrading Cycloclasticus strains from the Gulf of Mexico and comparison of their PAH degradation ability with that of Puget Sound *Cycloclasticus* strains. *Appl. Environ. Microbiol.* 64, 4703–4710.

Goffredi, S. K., and Orphan, V. J. (2010). Bacterial community shifts in taxa and diversity in response to localized organic loading in the deep sea. *Environ. Microbiol.* 12, 344–363. doi: 10.1111/j.1462-2920.2009.02072.x

Gutierrez, T., Singleton, D. R., Berry, D., Yang, T., Aitken, M. D., and Teske, A. (2013). Hydrocarbon-degrading bacteria enriched by the Deepwater Horizon oil spill identified by cultivation and DNA-SIP. *ISME J.* 7, 2091–2104. doi: 10.1038/ismej.2013.98

Hastings, D. W., Schwing, P. T., Brooks, G. R., Larson, R. A., Morford, J. L., Roeder, T., et al. (2016). Changes in sediment redox conditions following the BP DWH blowout event. *Deep Sea Res. Part II Top. Stud. Oceanogr.* 129, 167–178. doi: 10.1016/j.dsr2.2014.12.009

Hu, Y. F., Fu, C. Z., Yin, Y. S., Cheng, G., Lei, F., Yang, X., et al. (2010). Construction and preliminary analysis of a deep-Sea sediment metagenomic fosmid Library from Qiongdongnan Basin, South China Sea. *Mar. Biotechnol.* 12, 719–727. doi: 10.1007/s10126-010-9259-1

Hugenholtz, P., Goebel, B. M., and Pace, N. R. (1998). Impact of culture-independent studies on the emerging phylogenetic view of bacterial diversity. *J. Bacteriol.* 180, 4765–4774.

Ingram, W. C., Myers, S. R., and Martens, C. S. (2013). Chemostratigraphy of deep-sea quaternary sediments along the Northern Gulf of Mexico slope: quantifying the source and burial of sediments and organic carbon at Mississippi Canyon 118. *Mar. Petrol. Geol.* 46, 190–200. doi: 10.1016/j.marpetgeo.2013.05.004

Jaekel, U., Musat, N., Adam, B., Kuypers, M., Grundmann, O., and Musat, F. (2013). Anaerobic degradation of propane and butane by sulfate-reducing bacteria enriched from marine hydrocarbon cold seeps. *ISME J.* 7, 885–895. doi: 10.1038/ismej.2012.159

Joye, S. B. (2015). Deepwater Horizon, 5 years on. *Science* 349, 592–593. doi: 10.1126/science.aab4133

Joye, S. B., Braco, A., Özgökmen, T. M., Chanton, J. P., Grosell, M., MacDonald, I. R., et al. (2016). The Gulf of Mexico ecosystem, six years after the Macondo oil well blowout. *Deep Sea Res. Part II Top. Stud. Oceanogr.* 129, 4–19. doi: 10.1016/j.dsr2.2016.04.018

Kimes, N. E., Callaghan, A. V., Aktas, D. F., Smith, W. L., Sunner, J., Golding, B. T., et al. (2013). Genomic analysis and metabolite profiling of deep-sea sediments from the Gulf of Mexico following the Deepwater Horizon oil spill. *Front. Microbiol.* 4:50. doi: 10.3389/fmicb.2013.00050

Kleindienst, S., Grim, S., Sogin, M., Bracco, A., Crespo-Medina, M., and Joye, S. B. (2016). Diverse, rare microbial taxa responded to the Deepwater Horizon deep-sea hydrocarbon plume. *ISME J.* 10, 400–415.

Kleindienst, S., Herbst, F.-A., Stagars, M., von Netzer, F., von Bergen, M., Seifert, J., et al. (2014). Diverse sulfate-reducing bacteria of the *Desulfosarcina/Desulfococcus* clade are the key alkane degraders at marine seeps. *ISME J.* 8, 2029–2044. doi: 10.1038/ismej.2014.51

Kleindienst, S., Ramette, A., Amann, R., and Knittel, K. (2012). Distribution and in situ abundance of sulfate-reducing bacteria in diverse marine hydrocarbon seep sediments. *Environ. Microbiol.* 14, 2689–2710. doi: 10.1111/j.1462-2920.2012.02832.x

Klotz, F. M. (2016). *Characterization of Tritonibacter horizontis, Isolated from Seawater after the Deepwater Horizon Oil Spill*. Masters thesis, Institute for the Chemistry and Biology of the Marine Environment, Oldenburg University, Oldenburg.

Kniemeyer, O., Musat, F., Sievert, S. M., Knittel, K., Wilkes, H., Blumenberg, M., et al. (2007). Anaerobic oxidation of short-chain hydrocarbons by marine sulphate-reducing bacteria. *Nature* 449, 898–901. doi: 10.1038/nature06200

Knittel, K., Boetius, A., Lemke, A., Eilers, K., Lochte, K., Pfannkuche, O., et al. (2003). Activity, distribution, and diversity of sulfate reducers and other bacteria in sediments above gas hydrate (Cascadia Margin, OR). *Geomicrobiol. J.* 20, 269–294. doi: 10.1080/01490450303896

Kwon, K. K., Lee, H. S., Jung, H. B., Kang, J. H., and Kim, S. J. (2006). *Yeosuana aromativorans* gen. nov., sp nov., a mesophilic marine bacterium belonging to the family Flavobacteriaceae, isolated from estuarine sediment of the South Sea, Korea. *Int. J. Syst. Evol. Microbiol.* 56, 727–732. doi: 10.1099/ijs.0.64073-0

Lenk, S., Moraru, C., Hahnke, S., Arnds, J., Richter, M., Kube, M., et al. (2012). *Roseobacter* clade bacteria are abundant in coastal sediments and encode a novel combination of sulfur oxidation genes. *ISME J.* 6, 2178–2187. doi: 10.1038/ismej.2012.66

Li, L., Kato, C., and Horikoshi, K. (1999). Microbial diversity in sediments collected from the deepest cold-seep area, the Japan Trench. *Mar. Biotechnol.* 1, 391–400. doi: 10.1007/PL00011793

Lin, C., and Stahl, D. A. (1995). Taxon-specific probes for the cellulolytic genus Fibrobacter reveal abundant and novel equine-associated populations. *Appl. Environ. Microbiol.* 61, 1348–1351.

Liu, Z., and Liu, J. (2013). Evaluating bacterial community structures in oil collected from the sea surface and sediment in the northern Gulf of Mexico after the Deepwater Horizon oil spill. *Microbiologyopen* 2, 492–504. doi: 10.1002/mbo3.89

Lloyd, K. G., Albert, D. B., Biddle, J. F., Chanton, J. P., Pizarro, O., and Teske, A. (2010). Spatial structure and activity of sedimentary microbial communities underlying a *Beggiatoa* spp. mat in a Gulf of Mexico hydrocarbon seep. *PLoS ONE* 5:e8738. doi: 10.1371/journal.pone.0008738

Lloyd, K. G., Lapham, L., and Teske, A. (2006). An anaerobic methane-oxidizing community of ANME-1 archaea in hypersaline Gulf of Mexico sediments. *Appl. Environ. Microbiol.* 72, 7218–7230. doi: 10.1128/AEM.00886-06

Lozupone, C., Hamady, M., and Knight, R. (2006). UniFrac - An online tool for comparing microbial community diversity in a phylogenetic context. *BMC Bioinformatics* 7:371. doi: 10.1186/1471-2105-7-371

Lozupone, C., Lladser, M. E., Knights, D., Stombaugh, J., and Knight, R. (2011). UniFrac: an effective distance metric for microbial community comparison. *ISME J.* 5, 169–172. doi: 10.1038/ismej.2010.133

Ludwig, W., Strunk, O., Westram, R., Richter, L., Meier, H., Yadhukumar, et al. (2004). ARB: a software environment for sequence data. *Nucleic Acids Res.* 32, 1363–1371. doi: 10.1093/nar/gkh293

MacGregor, B. J., Moser, D. P., Alm, E. W., Nealson, K. H., and Stahl, D. A. (1997). Crenarcheota in Lake Michigan sediment. *Appl. Environ. Microbiol.* 63, 1178–1181.

Mason, O. U., Scott, N. M., Gonzalez, A., Robbins-Pianka, A., Bælum, J., Kimbrel, J., et al. (2014). Metagenomics reveals sediment microbial community response to Deepwater Horizon oil spill. *ISME J.* 8, 1464–1475. doi: 10.1038/ismej.2013.254

McIlroy, S., Porter, K., Seviour, R. J., and Tillett, D. (2008). Simple and safe method for simultaneous isolation of microbial RNA and DNA from problematic populations. *Appl. Environ. Microbiol.* 74, 6806–6807. doi: 10.1128/AEM.01047-08

McKay, L., Speare, K., Mendlovitz, H., Hale, A., Yang, T., Nigro, L., et al. (2013). "Pre- and post-spill porewater DIC concentrations and δ13C-DIC signatures of Gulf of Mexico sediments," in *Proceedings of the Abstract and Talk at Gulf of Mexico Ecosystem Conference*, New Orleans, LA, USA.

McKew, B. A., Coulon, F., Osborn, A. M., Timmis, K. N., and McGenity, T. J. (2007). Determining the identity and roles of oil-metabolizing marine bacteria from the Thames estuary, UK. *Environ. Microbiol.* 9, 165–176. doi: 10.1111/j.1462-2920.2006.01125.x

McNutt, M. K., Chu, S., Lubchenco, J., Hunter, T., Dreyfus, G., Murawski, S. A., et al. (2012). Applications of science and engineering to quantify and control the Deepwater Horizon oil spill. *Proc. Natl. Acad. Sci. U.S.A.* 109, 20222–20228. doi: 10.1073/pnas.1214389109

Mitra, S., Kimmel, D. G., Snyder, J., Scalise, K., McGlaughon, B. D., Roman, M. R., et al. (2012). Macondo-1 well oil-derived polycyclic aromatic hydrocarbons in mesozooplankton from the northern Gulf of Mexico. *Geophys. Res. Lett.* 39, 1–7. doi: 10.1029/2011GL049505

Miyatake, T., MacGregor, B. J., and Boschker, H. T. S. (2013). Depth-related differences in organic substrate utilization by major microbial groups in intertidal marine sediment. *Appl. Environ. Microbiol.* 79, 389–392. doi: 10.1128/AEM.02027-12

Muschenheim, D. K., and Lee, K. (2002). Removal of oil from the sea surface through particulate interactions: review and prospectus. *Spill Sci. Technol. Bull.* 8, 9–18. doi: 10.1016/S1353-2561(02)00129-9

Orcutt, B. N., Joye, S. B., Kleindienst, S., Knittel, K., Ramette, A., Reitz, A., et al. (2010). Impact of natural oil and higher hydrocarbons on microbial diversity, distribution, and activity in Gulf of Mexico cold-seep sediments. *Deep Sea Res. Part II Top. Stud. Oceanogr.* 57, 2008–2021. doi: 10.1016/j.dsr2.2010.05.014

Passow, U. (2016). Formation of rapidly-sinking, oil-associated marine snow. *Deep Sea Res. Part II Top. Stud. Oceanogr.* 129, 232–240. doi: 10.1016/j.dsr2.2014.10.001

Passow, U., Ziervogel, K., Asper, V., and Diercks, A. (2012). Marine snow formation in the aftermath of the Deepwater Horizon oil spill in the Gulf of Mexico. *Environ. Res. Lett.* 7:035031. doi: 10.1088/1748-9326/7/3/035301

Pearson, A., Kraunz, K. S., Sessions, A. L., Dekas, A. E., Leavitt, W. D., and Edwards, K. J. (2008). Quantifying microbial utilization of petroleum hydrocarbons in salt marsh sediments by using the 13C content of bacterial DNA. *Appl. Environ. Microbiol.* 74, 1157–1166. doi: 10.1128/AEM.01014-07

Pinyakong, O., Tiangda, K., Iwata, K., and Omori, T. (2012). Isolation of novel phenanthrene-degrading bacteria from seawater and the influence of its physical factors on the degradation of phenanthrene. *Scienceasia* 38, 36–43. doi: 10.2306/scienceasia1513-1874.2012.38.036

Pruesse, E., Quast, C., Knittel, K., Fuchs, B. M., Ludwig, W. G., Peplies, J., et al. (2007). SILVA: a comprehensive online resource for quality checked and aligned ribosomal RNA sequence data compatible with ARB. *Nucleic Acids Res.* 35, 7188–7196. doi: 10.1093/nar/gkm864

Redmond, M. C., and Valentine, D. L. (2012). Natural gas and temperature structured a microbial community response to the Deepwater Horizon oil spill. *Proc. Natl. Acad. Sci. U.S.A.* 109, 20292–20297. doi: 10.1073/pnas.1108756108

Ruff, E., Biddle, J. F., Teske, A., Knittel, K., Boetius, A., and Ramette, A. (2015). Global dispersion and local diversification of the methane seep microbiome. *Proc. Natl. Acad. Sci. U.S.A.* 112, 4015–4020. doi: 10.1073/pnas.1421865112

Santelli, C. M., Orcutt, B. N., Banning, E., Bach, W., Moyer, C. L., Sogin, M. L., et al. (2008). Abundance and diversity of microbial life in ocean crust. *Nature* 453, 653–656. doi: 10.1038/nature06899

Sheppard, P. J., Simons, K. L., Kadali, K. K., Patil, S. S., and Ball, A. S. (2012). The importance of weathered crude oil as a source of hydrocarbonoclastic microorganisms in contaminated seawater. *J. Microbiol. Biotechnol.* 22, 1185–1192. doi: 10.4014/jmb.1201.01049

Stucki, G., and Alexander, M. (1987). Role of dissolution rate and solubility in biodegradation of aromatic compounds. *Appl. Environ. Microbiol.* 53, 292–297.

Teske, A. (2010). "Sulfate-reducing and methanogenic hydrocarbon-oxidizing microbial communities in the marine environment. Part 21: Microbial communities based on hydrocarbons, oils and fats: natural habitats," in *Handbook of Hydrocarbon and Lipid Microbiology*, ed. K. Timmis (Berlin: Springer), 2203–2223. doi: 10.1007/978-3-540-77587-4_160

Teske, A., Durbin, A., Ziervogel, K., Cox, C., and Arnosti, C. (2011). Microbial community composition and function in permanently cold seawater and sediments from an Arctic Fjord of Svalbard. *Appl. Environ. Microbiol.* 77, 2008–2018. doi: 10.1128/AEM.01507-10

Teske, A., Hinrichs, K.-U., Edgcomb, V., de Vera Gomez, A., Kysela, D., Sylva, S. P., et al. (2002). Microbial diversity in hydrothermal sediments in the Guaymas Basin: evidence for anaerobic methanotrophic communities. *Appl. Environ. Microbiol.* 68, 1994–2007. doi: 10.1128/AEM.68.4.1994-2007.2002

Valentine, D. L., Fisher, G. B., Bagby, S. C., Nelson, R. K., Reddy, C. M., Sylva, S. P., et al. (2014). Fallout plume of submerged oil from *Deepwater Horizon*. *Proc. Natl. Acad. Sci. U.S.A.* 111, 15906–15911. doi: 10.1073/pnas.1414873111

Valentine, D. L., Kessler, J. D., Redmond, M. C., Mendes, S. D., Heintz, M. B., Farwell, C., et al. (2010). Propane respiration jump-starts microbial response to a deep oil spill. *Science* 330, 208–211. doi: 10.1126/science.1196830

Wade, T. L., Soliman, Y., Sweet, S. T., Wolff, G. A., and Presley, B. J. (2008). Trace elements and polycyclic aromatic hydrocarbons (PAHs) concentrations in deep Gulf of Mexico sediments. *Deep Sea Res. Part II Top. Stud. Oceanogr.* 55, 2585–2593. doi: 10.1016/j.dsr2.2008.07.006

Wagner-Döbler, I., and Biebl, H. (2006). Environmental biology of the marine *Roseobacter* lineage. *Ann. Rev. Microbiol.* 60, 255–280. doi: 10.1146/annurev.micro.60.080805.142115

Woebken, D., Teeling, H., Wecker, P., Dumitriu, A., Kostadinov, I., DeLong, E. F., et al. (2007). Fosmids of novel marine Planctomycetes from the Namibian and Oregon coast upwelling systems and their cross-comparison with planctomycete genomes. *ISME J.* 1, 419–435. doi: 10.1038/ismej.2007.63

Woodruff, O. P. (2014). *Temporal and Spatial Characterization of Macondo 252 Signatures in Gulf of Mexico Shelf and Slope Sediments*. Master Thesis, Department of Earth and Environmental Sciences, University of Kentucky, Louisville, KT, USA.

Yang, T. (2014). *Microbial Community Dynamics of the Deepwater Horizon Oil Spill*. Ph.D. thesis, Department of Marine Sciences, University of North Carolina at Chapel Hill, Chapel Hill, NC, USA.

Yang, T., Nigro, L. M., Gutierrez, T., D'Ambrosio, L., Joye, S. B., Highsmith, R., et al. (2016). Pulsed blooms and persistent oil-degrading bacterial populations in the water column during and after the Deepwater Horizon blowout. *Deep Sea Res. Part II Top. Stud. Oceanogr.* 129, 282–291. doi: 10.1016/j.dsr2.2014.01.014

Ziervogel, K., Dike, C., Asper, V., Montoya, J., Battles, J., D'Souza, N., et al. (2016a). Enhanced particle flux and heterotrophic bacterial activities in Gulf of Mexico bottom waters following storm-induced sediment resuspension. *Deep Sea Res. Part II Top. Stud. Oceanogr.* 129, 77–88. doi: 10.1016/j.dsr2.2015.06.017

Ziervogel, K., Joye, S. B., and Arnosti, C. (2016b). Microbial enzymatic activity and secondary production in sediments affected by the sedimentation pulse following the Deepwater Horizon oil spill. *Deep Sea Res. Part II Top. Stud. Oceanogr.* 129, 241–248. doi: 10.1016/j.dsr2.2014.04.003

Ziervogel, K., McKay, L., Rhodes, B., Osburn, C. L., Dickson-Brown, J., Arnosti, C., et al. (2012). Microbial activities and dissolved organic matter dynamics in oil-contaminated surface seawater from the Deepwater Horizon oil spill site. *PLoS ONE* 7:e34816. doi: 10.1371/journal.pone.0034816

Conflict of Interest Statement: The authors declare that the research was conducted in the absence of any commercial or financial relationships that could be construed as a potential conflict of interest.

frontiers in Marine Science

ORIGINAL RESEARCH
published: 30 March 2017
doi: 10.3389/fmars.2017.00079

Dynamics and Origin of Transparent Exopolymer Particles in the Oyashio Region of the Western Subarctic Pacific during the Spring Diatom Bloom

Yuichi Nosaka[1*†], *Youhei Yamashita*[1, 2] *and Koji Suzuki*[1, 2, 3]

[1] Graduate School of Environmental Science, Hokkaido University, Sapporo, Japan, [2] Faculty of Environmental Earth Science, Hokkaido University, Sapporo, Japan, [3] JST-CREST, Sapporo, Japan

OPEN ACCESS

Edited by:
Uta Passow,
University of California, Santa Barbara, USA

Reviewed by:
Eva Ortega-Retuerta,
Consejo Superior de Investigaciones Científicas, Spain
Luca Zoccarato,
University of Trieste, Italy

***Correspondence:**
Yuichi Nosaka
yuichi.nosaka@gmail.com

†Present Address:
Yuichi Nosaka,
Research Center for Creative Partnerships, Ishinomaki Senshu University, Ishinomaki, Japan

Specialty section:
This article was submitted to Aquatic Microbiology, a section of the journal Frontiers in Marine Science

Received: *05 October 2016*
Accepted: *07 March 2017*
Published: *30 March 2017*

Citation:
Nosaka Y, Yamashita Y and Suzuki K (2017) Dynamics and Origin of Transparent Exopolymer Particles in the Oyashio Region of the Western Subarctic Pacific during the Spring Diatom Bloom. Front. Mar. Sci. 4:79. doi: 10.3389/fmars.2017.00079

The seasonal biological drawdown of the partial pressure of CO_2 (pCO_2) in the surface waters of the Oyashio region of the western subarctic Pacific is one of the greatest among the world's oceans. This is attributable to spring diatom blooms. Transparent exopolymer particles (TEPs) are known to affect efficiency of the biological carbon pump, and higher TEP levels are frequently associated with massive diatom blooms. However, TEP dynamics in the Oyashio region remain unclear. We investigated the TEP distribution from three cruises during the spring diatom bloom periods in 2010 and 2011. TEP concentrations varied from $<$ 15 to 196 $\pm$ 71 μg xanthan gum equiv. L^{-1} above 300 m and generally declined with depth. Vertical TEP concentrations were significantly related not only to chlorophyll *a* concentrations but also to bacterial abundance. Average TEP concentrations within the mixed layer ($>$ 30 m) were significantly higher during the bloom (155 $\pm$ 12 μg xanthan gum equiv. L^{-1}) than in the post-bloom phase (90 $\pm$ 32 μg xanthan gum equiv. L^{-1}). In contrast, bacteria abundance within the mixed layer changed little during the bloom to post-bloom phases. These results suggest that the abundance of phytoplankton greatly contributed to dynamics of the TEP distribution. To evaluate the ability of the phytoplankton to produce TEP, an axenic strain of the diatom *Thalassiosira nordenskioeldii*, which is a representative species of Oyashio blooms, was examined within a batch culture system. Cell abundance-normalized TEP and dissolved organic carbon (DOC) production rates changed simultaneously with growth of the strain. Although these production rates were significantly higher in the stationary phase than in the exponential growth period, values of the TEP/DOC ratio changed little throughout incubation. These findings suggest that TEP production in the Oyashio region may be enhanced by an increase in DOC production from spring diatoms.

Keywords: transparent exopolymer particles, primary production, dissolved organic carbon, diatom bloom, *Thalassiosira nordenskioeldii*, subarctic Pacific

INTRODUCTION

Transparent exopolymer particles (TEPs) are defined as > 0.4-μm transparent particles that consist of acidic polysaccharides, and are stainable with the dye Alcian blue (Alldredge et al., 1993). These particles are very sticky, so that they can facilitate the aggregation of particles in seawater (e.g., Passow, 2002a; Wurl et al., 2011; Mari et al., 2017). Generally, the presence of TEP may increase the efficiency of the biological carbon pump, because TEP-attached particles sink readily (e.g., Passow, 2002a; Wurl et al., 2011). In contrast, TEPs can decrease the sinking rates of aggregates, because the density of TEPs is lower than that of seawater (Azetsu-Scott and Passow, 2004; Mari et al., 2017). TEPs also can be consumed by heterotrophic organisms, such as bacteria, zooplankton, and fish (e.g., Grossart et al., 1998, 2006; Prieto et al., 2001), indicating that the particles are important in marine food webs. It is known that many marine organisms, including phytoplankton and bacteria, can generate extracellular polysaccharides such as TEPs (Passow, 2002a). However, TEPs and their precursors in seawater can be utilized as organic substrates by heterotrophic organisms (Passow, 2002a). TEP levels in the world's oceans are highly variable (0–14,800 μg xanthan gum equivalent L^{-1}; e.g., Hong et al., 1997; Radić et al., 2005). Higher TEP levels are sometimes associated with blooms of phytoplankton, such as diatoms (e.g., Passow et al., 1995), *Phaeocystis* spp. (e.g., Hong et al., 1997), dinoflagellates (e.g., Berman and Viner-Mozzini, 2001), cryptophytes (e.g., Passow et al., 1995), and cyanobacteria (e.g., Grossart and Simon, 1997). In particular, diatoms are known to excrete large amounts of polysaccharides, which can form TEPs during their actively growing and/or senescent phases (Mari and Burd, 1998; Passow, 2002b). Using batch cultures, Passow (2002b) reported that TEP production varied widely among phytoplankton species. Fukao et al. (2010) showed that TEP productivity of the diatom *Coscinodiscus granii* was greater in the exponential growth phase than in stationary and decline periods, whereas those of diatoms *Eucampia zodiacus*, *Rhizosolenia setigera,* and *Skeletonema* sp. were greater in the stationary growth and decline phases than in the exponential growth period. To our knowledge, the relationship between the physiology of diatoms and TEP production remains poorly understood.

In the Oyashio region of the Northwest Pacific, massive diatom blooms occur during spring (e.g., Kasai et al., 1998; Saito et al., 2002; Suzuki et al., 2011). These blooms are generally triggered by water-column stratification during the transition from winter to spring (Kasai et al., 1997). The chlorophyll (Chl) *a* concentration and primary production integrated within the water column can reach 500 mg Chl *a* m^{-2} (Kasai et al., 1998) and 3,200 mg C m^{-2} d^{-1} (Isada et al., 2010), respectively. The enormous spring blooms cause an increase in meso- and macro-zooplankton biomass and fishery production in the Northwest Pacific (Sakurai, 2007; Ikeda et al., 2008). Takahashi et al. (2002) reported that the Northwest Pacific including the Oyashio is one of the regions where the seasonal drawdown effect of pCO_2 by marine organisms is maximized. This is mainly caused by spring diatom blooms (Midorikawa et al., 2003; Ayers and Lozier, 2012). Honda (2003) reported that among the world's oceans, efficiency of the biological carbon pump was relatively high in the Northwest Pacific. Hence, it can be inferred that the relatively high flux of settling particles in the Northwest Pacific is caused by vigorous primary production of diatoms that aggregate and sink. However, TEP dynamics in the Oyashio region during the spring diatom blooms are still poorly understood, even though they are pivotal in biogeochemical and ecological processes.

The main aims of this study were to understand TEP dynamics in the Oyashio region during the spring diatom bloom periods of 2010 and 2011 and to evaluate the relationship between TEP and other parameters. Those parameters include particulate organic carbon (POC) and dissolved organic carbon (DOC) concentrations, POC and DOC production, and phytoplankton and bacterial abundance. In addition, to understand TEP productivity in greater detail, we examined the characteristics of TEP production of an axenic strain of the Oyashio diatom *Thalassiosira nordenskioeldii*, which is a representative species of spring blooms (Chiba et al., 2004; Suzuki et al., 2011). This was grown in a batch culture system. The importance of TEP production by this strain was assessed.

MATERIALS AND METHODS

Research Cruises

Three field campaigns were conducted, 13–23 April 2010, 7–16 June 2010, and 5–13 May 2011 (**Figure 1**). The FR/V *Wakataka-Maru* (Fisheries Research Agency of Japan) and R/V *Tansei-Maru* (JAMSTEC/AORI, University of Tokyo) were used for two cruises in 2010 and a single cruise in 2011, respectively. In April, June, and May, two (A1 and A2), four (J1, J2, J3, and J4) and three (M1, M2, and M3) sampling stations were visited, respectively. In all cruises, incident photosynthetic available radiation (PAR) above the sea surface was continuously measured on deck with a PAR sensor (ML-020P, EKO Instruments Co., Ltd., Japan) every 10 min on average, and values were recorded with a data logger. Seawater sampling at all stations was accomplished using a CTD-CMS equipped with acid-clean Niskin bottles. The samples were corrected from 5, 10, 20, 40, 60, 80, 100, 200, and 300 m depths in April 2010, and from the those depths plus 30, 50, and 150 m layers in June 2010 and May 2011. Nutrients (nitrite plus nitrate, hereafter referred to as nitrate, phosphate, and silicate) were determined with a BRAN + LUEBBE auto-analyzer following manufacturer protocol. Basal depth of the mixed layer was defined as a threshold value of temperature or density from a near-surface value at 10-m depth ($\Delta T = 0.2^{\circ}$C or $\Delta\sigma_\theta = 0.03$ kg m^{-3}; Montégut et al., 2004).

Phytoplankton Pigments and CHEMTAX Processing

Phytoplankton pigments were analyzed using high-performance liquid chromatography (HPLC). Water samples (500 mL) collected from 5 to 300 m depths were filtered on 25-mm Whatman GF/F filters under a gentle vacuum (< 0.013 MPa). The filter samples were folded, blotted with filter paper, and stored at −80°C. Phytoplankton pigments were extracted with sonication in *N, N*-dimethylformamide (DMF) according to the protocol of Suzuki et al. (2005). HPLC pigment was analyzed according to

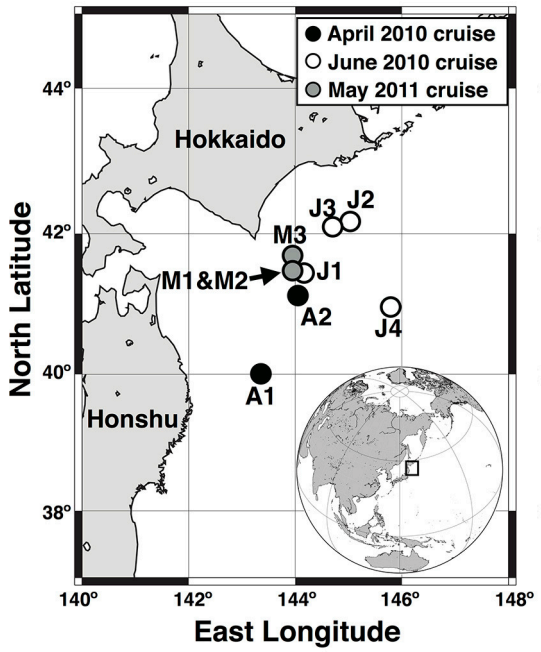

FIGURE 1 | Sampling stations during cruises of April and June 2010 and May 2011, in Oyashio region of western subarctic Pacific.

the method of Van Heukelem and Thomas (2001), except that the flow rate was 1.2 mL min^{-1}. Details of the analysis method are in Suzuki et al. (2014).

To estimate the contribution of each algal group in the two layers (5–20 and 30–50 m depths) to total Chl *a* biomass, the pigment data were interpreted by factorization using the CHEMTAX program (Mackey et al., 1996). The initial and final pigment ratios were calculated following the method of Latasa (2007) (Supplementary Table 1). Initial ratios were based on Suzuki et al. (2002, 2005, 2009), who estimated the community composition of phytoplankton in the northwestern Pacific. Prymnesiophytes, pelagophytes, and prasinophytes in our CHEMTAX analysis are synonymous with type 3 haptophytes, type 2 chrysophytes, and type 3 prasinophytes according to Mackey et al. (1996), respectively. Chl *a* biomass of each algal group was calculated by multiplying *in situ* Chl *a* concentrations by the CHEMTAX outputs.

To confirm the development and decline in Chl *a* concentration from spring to summer, we also examined monthly satellite images of that concentration as observed by a MODIS/Aqua satellite sensor. MODIS/Aqua monthly Chl *a* data (4-km resolution, OC3M algorithm) for the period February–July 2010 and 2011 were obtained from the Distributed Active Archive Center (DAAC)/Goddard Space Flight Center (GSFC), NASA (http://oceancolor.gsfc.nasa.gov/cgi/l3).

Identification and Cell Abundance of Phytoplankton

Water samples (500 mL) were taken at 5-m depth to count diatoms and coccolithophores, and these samples were fixed with buffered formalin (pH 7.8, 1% final concentration). An aliquot (3–11 mL) of the sample was filtered onto a Nuclepore membrane (1-μm pore size) filter set in a glass funnel (3-mm in diameter at the base) in a vacuum (0.013–0.026 MPa). The filter membrane was rinsed with Milli-Q water to remove salts and immediately dried for 3 h in an oven at 60°C. To identify and count the algal cells, the entire area of the membrane (∼7 mm^2) was examined by a scanning electron microscope (SEM, VE-8800, Keyence Corp., Japan) at magnification approximately 2,000×. Phytoplankton species were identified according to Fukuyo et al. (1990); Tomas et al. (1997), Young et al. (2003), Scott and Marchant (2005), and Round et al. (2007). In our study, the dominant diatom species were defined such that they contributed > 25% to total diatom abundance.

Abundance of Heterotrophic Bacteria

Duplicate water samples (each 2 mL) from 5 to 300 m depths were preserved with paraformaldehyde (0.2% final concentration) and stored at −80°C until analysis on land. An EPICS flow cytometer (XL ADC system, Beckman Coulter, Inc., USA) equipped with a 15-mW air-cooled argon laser exciting at 488 nm and a standard filter setup were used for enumeration of heterotrophic bacteria. Prior to analysis, samples were thawed and drawn through a 35-μm, nylon-mesh-capped Falcon cell strainer (Becton-Dickinson) to remove larger cells. Cells were stained with the nucleic acid stain SYBR Gold solution (Invitrogen). The stock SYBR Gold stain (10^4-fold concentrations in the commercial solution) was diluted to 10-fold concentrations with Milli-Q water. Twenty-five microliters of the 10-fold SYBR Gold stain was added to the 225-μL bacteria sub-sample and incubated in the dark at room temperature (25°C) for 30 min prior to analysis. The incubated samples were mixed with 250 μL of Flow-Count fluorophores (Beckman Coulter) and then analyzed. Details of the flow cytometric analysis are given in Suzuki et al. (2005).

Particulate Organic Carbon (POC) Concentration

The POC concentration was determined only for the 5-m depth. The 300-mL water sample was filtered onto pre-combusted Whatman GF/F filters (25-mm in diameter, 450°C for 5 h) under a gentle vacuum (< 0.013 MPa) and stored at −20°C until analysis. On land, the samples were thawed at room temperature, exposed to HCl fumes to remove inorganic carbon, and completely dried in a vacuum desiccator for > 24 h. The POC concentrations on the filters were determined with an online elemental analyzer (FlashEA1112, Thermo Fisher Scientific, Inc., USA).

Dissolved Organic Carbon (DOC) Concentration

Samples of DOC were collected from 12 depths between 5 and 300 m. Inline filter holders (PP-47, Advantec MFS, Inc., USA) and tubes (Tygon R-3603, United States Plastic Corp., USA) were pre-cleaned by soaking in 1 M HCl and then rinsed with Milli-Q water. Before sampling, pre-combusted Whatman GF/F filters (47 mm diameter) were set in the inline filter holders, and the tubes were mounted. The water samples were taken by connecting the tube with the spigot of the Niskin bottle. At the start of sampling, filtrates were well drained to pre-wash the tubing, filter holder and filter.

Afterward, triplicate samples were collected in pre-combusted 24-mL screw vials with acid-cleaned PTFE septum caps. The samples were immediately stored at −20°C until analysis on land. The frozen samples were thawed and well mixed. DOC concentrations were determined with a total organic carbon analyzer (TOC-V CSH, Shimadzu Corp., Japan). The accuracy and variance of the measured DOC concentrations were checked by analyzing deep seawater reference material provided from the consensus reference material (CRM) program (Prof. Dennis Hansell, University of Miami).

Daily POC and DOC Production

Daily POC and DOC production were estimated using a simulated *in situ* incubation technique at 5-m depth, except at Station M3 during the May 2011 field campaign. The samples were dispensed into three 300-mL, acid-cleaned polycarbonate bottles (two light and one dark) and inoculated with a solution of $NaH^{13}CO_3$ (99 atom% ^{13}C), equivalent to ∼10% of total inorganic carbon (TIC) in the seawater. All bottles were incubated for ∼24 h. The incubated POC samples were filtered onto pre-combusted Whatman GF/F filters (25 mm in diameter, 450°C for 5 h) with a gentle vacuum (< 0.013 MPa), and the filtrate was collected in pre-combusted, 500-mL glass bottles (450°C for 5 h). The filter and water samples were stored at −20°C until analysis.

The filter samples of POC production were thawed at room temperature, exposed to HCl fumes to remove inorganic carbon, and then completely dried in a vacuum desiccator for > 24 h. POC concentrations on the filters and ^{13}C abundance were determined using a mass spectrometer (DELTA V, Thermo Fisher Scientific, Inc., USA) with online elemental analyzer (FlashEA1112, Thermo Fisher Scientific). Daily primary production was calculated according to Equation (1) (Hama et al., 1983):

$$\text{POC production} = \frac{(a_{is} - a_{ns})}{(a_{ic} - a_{ns})} \times \frac{[C_p]}{t} \times f, \quad (1)$$

where a_{is} is the ^{13}C atom% in an incubated sample, a_{ns} is the ^{13}C atom% in a natural (i.e., non-incubated) sample, a_{ic} is the ^{13}C atom% in inorganic carbon, $[C_p]$ is the concentration of POC in the incubated sample, t is the incubation duration (day), and f is the discrimination factor of ^{13}C (i.e., 1.025). In our study, TIC concentrations were determined with a total alkalinity analyzer (ATT-05, Kimoto Electric Co., Ltd., Japan).

DOC production was estimated according to Hama and Yanagi (2001) with a few modifications. The frozen samples were thawed at room temperature (25°C) and were desalinated using an electro dialyzer (Micro Acilyzer S3, ASTOM Corp., Japan) equipped with AC-220-550 cartridge (CMX-SB/AMX-SB, ASTOM Corp., Japan). Conductivity of the water samples decreased from ∼53 to 3.0 mS cm^{-1} within 2–3 h. Before and after desalination, the DOC concentrations were examined. The recovery percentage of those concentrations ranged from 62 to 96%, whereas the conductivity decreased to 6% of the initial value (Supplementary Table 2). The desalinated seawater samples were concentrated to ∼5 mL with a rotary evaporator at 45°C using a pre-combusted 500-mL eggplant-shaped flask. HCl was added to the concentrated 5-mL samples to reduce the pH to 2. The low-pH concentrates were purged with N_2 gas for ∼9 min to remove dissolved inorganic ^{13}C. Thereafter, the samples were further concentrated to ∼0.5–1 mL with a rotary evaporator at 45°C using a pre-combusted 10-mL pear-shaped flask. The ^{13}C atom% of DOC absorbed onto the Whatman GF/F filters combusted in a muffle furnace (450°C, 5 h) were determined using a mass spectrometer (DELTA V, Thermo Fisher Scientific) with an online elemental analyzer (FlashEA1112, Thermo Fisher Scientific). Daily DOC production was calculated according to Equation (2) (Hama and Yanagi, 2001):

$$\text{DOC production} = \frac{(a_{is} - a_{ns})}{(a_{ic} - a_{ns})} \times \frac{[C_d]}{t}, \quad (2)$$

where $[C_d]$ is the DOC concentration (mg m^{-3}).

Furthermore, we estimated the ratio (PER) of DOC production/total production by phytoplankton according to

$$\text{PER (\%)} = \frac{\text{DOC production}}{(\text{POC} + \text{DOC production})} \times 100, \quad (3)$$

Transparent Exopolymer Particle (TEP) Analysis

Water samples of TEP were taken from depths 5–300 m. Triplicate water samples of 250 mL were filtered using Whatman 0.4-μm Nuclepore filters, applying a gentle vacuum (< 0.013 MPa). TEPs captured by the filter were stained with Alcian blue solution (Passow and Alldredge, 1995). The stained filters were immediately rinsed with Milli-Q water and then stored at −20°C until analysis on land.

For the standard TEP curve, the method of Claquin et al. (2008) was modified. As reported by Claquin et al. (2008), the standard curve described in Passow and Alldredge (1995) is applicable only for low concentrations of TEP (i.e., calibration standard weight of xanthan gum ranging between 0 and 40 μg). One milligram of xanthan gum was put into a 15-mL centrifugal tube and added to 10 mL of the Alcian blue stain. The tube was shaken well for ∼1 h to combine the xanthan gum and Alcian blue. Thereafter, it was centrifuged at 3,200 × g for 20 min, and the supernatant liquid was carefully removed using micro pipets. Ethanol (99.5%) was added to the tube, which was then centrifuged, and the supernatant liquid was removed via the ethanol precipitation method. The ethanol precipitation was repeated at least five times until the solution became transparent. Finally, as much of the ethanol in the tube as possible was removed. To dry the blue-stained xanthan gum, N_2 gas was gently sprayed into the tube. Subsequently, the xanthan gum was completely dried in a desiccator under vacuum for more than 24 h. The blue-stained xanthan gum was dissolved with 6 mL of 80% H_2SO_4 using a volumetric pipette (stock solution of 1 mg xanthan gum 6-mL^{-1}). The stock solution was diluted with 80% H_2SO_4, to make a dilution series with five concentrations (10, 50, 100, 150, and 200 μg xanthan gum 6-mL^{-1}). Absorption at 787 nm was measured with a Shimadzu spectrophotometer (MPS-2400) in 1-cm cuvettes, with

reference to Milli-Q water. Four slopes of the TEP standard curve were compared with those of Passow and Alldredge (1995) and Claquin et al. (2008) (Supplementary Table 3). Also we conducted a comparison between the standard curves made with this centrifugation and conventional filtration (Passow and Alldredge, 1995) methods. The comparison revealed that the slope (136) of the centrifugation method was lower than that (207) of the conventional method (Supplementary Figure 1). Hence, all TEP concentrations in this study were corrected by multiplying a factor of 1.52. Passow and Alldredge reported that average absorption of the filter blank with 0.4-μm polycarbonate filters was between 0.07 and 0.09. In our study, the filter blank (average ± standard deviation) was 0.081 ± 0.003 ($n = 4$).

The natural filter samples were transferred into 20-mL vials. Six milliliters of 80% H_2SO_4 was added to the vials, and the filters were soaked for 2 h. The vials were gently agitated five times over this period. Absorption at 787 nm was measured with the spectrophotometer in 1-cm cuvettes against Milli-Q water as reference. The TEP levels (μg xanthan gum equivalent L^{-1}) were determined according to Passow and Alldredge (1995).

TEP Production by the Oyashio Diatom *Thalassiosira nordenskioeldii*

A single cell of *T. nordenskioeldii* Cleve was isolated from Oyashio waters during the May 2011 field campaign. The strain was sterilized in f/2 medium (Guillard and Ryther, 1962; Guillard, 1975) with penicillin and streptomycin (25 U mL^{-1} of penicillin and 25 μg mL^{-1} of streptomycin, 17-603E, Lonza Group Ltd., Switzerland) following the methods of Sugimoto et al. (2007). For the culture experiment, salinity of the medium was adjusted to 33.0, which is a typical value of surface Oyasho waters in spring (e.g., Hattori-Saito et al., 2010). Initial nutrient levels in the medium were also modified from f/2 medium to mimic Oyashio water: 20 μM $NaNO_3$, 35 μM $Na_2SiO_3 \cdot 9H_2O$, 2.0 μM $NaH_2PO_4 \cdot H_2O$, 600 nM $FeCl_3 \cdot 6H_2O$, 600 μM $Na_2EDTA \cdot 2H_2O$, 46.7 nM $MnCl \cdot 4H_2O$, 3.9 nM $ZnSO_4 \cdot 7H_2O$, 2.2 nM $CoCl_2 \cdot 6H_2O$, 2.0 nM $CuCO_4 \cdot 5H_2O$, 1.3 nM $Na_2MoO_4 \cdot 2H_2O$, 15 nM Thiamine · HCl, 100 pM Biotin, 19 pM Cyanocobalamin. The axenic strain was inoculated in the medium and grown for ∼30 generations in an incubator (MIR-554, Sanyo Electric Co., Ltd., Japan) at 5°C, under 100 μmol photons m^{-2} s^{-1} from white fluorescent lamps (FL20SS · BRN/18, Toshiba) with a light-dark cycle of 12 h. At the start of this experiment, the well-acclimated axenic strain was inoculated in Oyashio-simulated medium (17 L) in two acid-cleaned 20-L culture vessels (P/N 2600-0012, Thermo Fisher Scientific) and cultured for 40 days.

Nutrient, Cell Abundance, and Chl *a* Measurements in the Culture Experiment

Nutrients were sampled every other day. Duplicate water samples per culture vessel were dispensed into acrylic tubes with screw caps, and the samples were immediately stored at −20°C. The frozen samples were thawed at room temperature and well mixed. The nutrient concentrations (nitrate, phosphate, and silicate) were determined with an auto-analyzer (QuAAtro 2-HR, BLTEC Corp., Japan) as described above. Sampling of cell abundance was done every other day. Ten to fifty milliliters of the water samples were transferred into 15 or 50-mL centrifuge tubes. During days 0–14, *T. nordenskioeldii* was filtered using a 25-mm Whatman Nuclepore membrane filter of 1.0-μm pore size and was immediately resuspended in the non-concentrated water samples. One point five milliliters of the concentrated sample (days 0–14) or non-concentrated sample (days 16–40) was transferred to a micro-slide glass chamber of thickness 1.1 mm (S109502, Matsunami Glass Ind., Ltd., Japan), and covered with a cover glass. To estimate cell abundance, duplicate samples were observed per culture vessel using an epifluorescence microscope (BZ-9000, Keyence Corp., Japan) equipped with a GFP optical filter (OP-66835 BZ filter GFP, Keyence Corp., Japan). The Chl *a*-derived fluorescence in *T. nordenskioeldii* was automatically photographed with 28 photos and 4× magnification, and the fluorescence was summed using image analysis software (Keyence Corp., Japan). Therefore, cell abundance was estimated by dividing the observed volume (mL) by the total value of fluorescence. The specific daily growth rate (μ, d^{-1}) during the culture experiment was estimated by the method of Guillard (1973):

$$\mu = \frac{(\ln N_t - \ln N_0)}{t_t - t_0}, \quad (4)$$

where N_0 is initial cell abundance (cells mL^{-1}), N_t the abundance after t days, t_0 the initial time (d), and t_t the time after t days.

Chl *a* concentrations were determined in the mid-exponential phase. Triplicate samples per vessel (each 200 mL) were filtered onto Whatman GF/F filters with a gentle vacuum (< 0.013 MPa). The filters were folded, blotted with filter paper, and stored at −80°C. The pigment analysis is described in Section Phytoplankton Pigments and CHEMTAX Processing.

TEP Measurement in the Culture Experiment

TEP was sampled once every 4 days between days 0 and 36. Triplicate water samples (1–20 mL) per culture vessel were filtered using Whatman 0.4-μm Nuclepore membrane filters in a gentle vacuum (< 0.013 MPa). Post-treatment used the same method described in Section Transparent Exopolymer Particle (TEP) Analysis.

DOC Determination in the Culture Experiment

DOC was sampled once every 4 days between days 0 and 36. A filter funnel (25-mm in diameter, PN 4203, PALL Corp., USA) was pre-cleaned by soaking in 1 M HCl, and then rinsed with Milli-Q water. Pre-combusted Whatman GF/F filters were placed in the filter funnel, which was equipped with a suction vessel. The water sample was filtrated in a gentle vacuum (< 0.013 MPa). At the start of sampling, a few milliliters of the filtrates were drained to prewash the GF/F filter and filter funnel. Then, duplicate samples were collected in pre-combusted 24-mL screw vials with acid-cleaned PTFE septum caps. The samples were immediately stored at −20°C until analysis. The analysis method was described in Section Dissolved Organic Carbon (DOC) Concentration.

Daily TEP and DOC Productivities

Based on TEP or DOC concentration in the culture vessels, cellular TEP productivity [pg xanthan gum equiv. (cell)$^{-1}$ d^{-1}] and DOC productivity [pg C (cell)$^{-1}$ d^{-1}] averaged during the exponential growth and stationary phases (initial and final) using two data points of those phases were estimated via

$$\text{Cellular TEP or DOC productivity} = \frac{(C_t - C_0)}{(t_t - t_0) \times (N_t - N_0)}, \quad (5)$$

where C_0 is TEP concentration (pg xanthan gum equiv. mL^{-1}) or DOC concentration (pg C mL^{-1}) at the initial time of the exponential growth phase or stationary phase, C_t is concentration of the TEP or DOC at the final time after t days, t_0 is the initial time (d) of the exponential growth phase or stationary phase, t_t is the final time after t days, N_0 is initial cell abundance (cells mL^{-1}) of the exponential growth or stationary phase, and N_t is cell abundance at the final time after t days. Carbon-based TEP productivity was estimated by multiplying TEP productivity by a factor of 0.75 (Engel and Passow, 2001).

RESULTS

TEP Observations during the Oyashio Spring Diatom Bloom

Hydrography

Seawater temperatures at 5 m increased from April through June 2010 (**Table 1**). By contrast, salinity only changed slightly throughout the cruises (32.8–33.3). Relatively high nutrient levels were found in April 2010, which declined in June. The surface mixed layer was above 30 m at stations A2, M1, and M2, whereas it was shallower than 10 m at the other stations.

Chlorophyll *a* Concentrations and Community Composition as Estimated from the CHEMTAX Program

Chl *a* concentrations generally decreased from April through June 2010 and from 5 to 300 m depths (**Figures 2A–C**). Satellite surface Chl *a* images also indicated that decreases in the algal pigment concentration from April to June in 2010 and 2011 (Supplementary Figure 2). The highest Chl *a* concentration at 5-m depth was observed at station A1 in April 2010 (8.8 μg L^{-1}), whereas the lowest was at station J2 in June 2010 (0.4 μg L^{-1}) (**Table 1**). Chl *a* within the mixed layer significantly decreased from April to June (Kruskal-Wallis ANOVA, $p < 0.01$, Steel-Dwass test, April vs. May: $p < 0.01$; April vs. June: $p < 0.01$; May vs. June: $p < 0.01$).

The final ratio matrix in the 5–20 m layer estimated with the CHEMTAX program (Supplementary Table 1B) was within the range of Mackey et al. (1996), except for the alloxanthin:Chl *a* ratio (0.25), which was slightly larger than that of the maximum (0.23) of Mackey et al. The final ratio matrix in the 30–50 m layer (Supplementary Table 1D) was within the range of Mackey et al. The contributions of each phytoplankton group to Chl *a* biomass from 5 to 50 m depths are shown in **Figure 3**. Diatoms dominated in both April 2010 (average ± standard deviation: 94

TABLE 1 | Hydrographic conditions and phytoplankton productivity at 5 m depth during Oyashio spring diatom blooms in April and June 2010 and May 2011.

Cruise	Station	Temperature (°C)		Salinity	Nitrate (μM)	Silicate (μM)	Phosphate (μM)	Chl *a* (μg L^{-1})	Diatom abundance (×10^3 cells L^{-1})	Heterotrophic bacteria abundance (×10^5 cells mL^{-1})	TEP (μg xanthan gum equivalent L^{-1})	POC (μg C L^{-1})	DOC (μg C L^{-1})	POC production (mg C m^{-3} d^{-1})	DOC production (mg C m^{-3} d^{-1})	PER (%)
		5 m	100 m													
April, 2010	A1	3.1	3.1	32.9	8	20	0.9	8.8	382	4.2 ± 0.3	167 ± 33	503	704 ± 18	290 ± 17	1.6 ± 0.04	0.5
April, 2010	A2	4.5	3.9	33.3	11	24	1.0	4.2	288	5.4 ± 0.4	166 ± 40	404	688 ± 14	100 ± 1	4.2 ± 0.1	4.1
June, 2010	J1	7.0	1.3	32.9	8	8	1.0	0.6	11	3.5 ± 0.1	79 ± 8	143	736 ± 12	25 ± 1	1.9 ± 0.02	7.1
June, 2010	J2	7.0	0.6	32.9	8	8	1.0	0.4	4	2.2 ± 0.1	52 ± 23	137	715 ± 8	28 ± 0.3	1.7 ± 0.4	5.8
June, 2010	J3	9.0	1.3	32.8	4	9	0.8	0.7	1	4.1 ± 0.3	108 ± 18	139	753 ± 10	43 ± 2	2.6 ± 0.2	5.7
June, 2010	J4	7.8	0.8	32.9	8	13	1.0	0.8	3	3.6 ± 0.1	105 ± 17	154	749 ± 17	36 ± 1	1.3 ± 0.02	3.5
May, 2011	M1	5.0	1.7	33.1	13	11	1.1	1.0	23	2.2 ± 0.03	50 ± 9	163	685 ± 14	43 ± 0.4	2.3 ± 0.9	5.1
May, 2011	M2	4.3	2.9	33.0	9	6	0.7	2.0	247	5.4 ± 0.02	184 ± 52	213	704 ± 10	100 ± 5	4.2 ± 0.4	4.0
May, 2011	M3	4.4	2.0	32.9	7	2	0.6	1.7	320	N.D.	132 ± 73	235	728 ± 8	N.D.	N.D.	N.D.

N.D., No data.

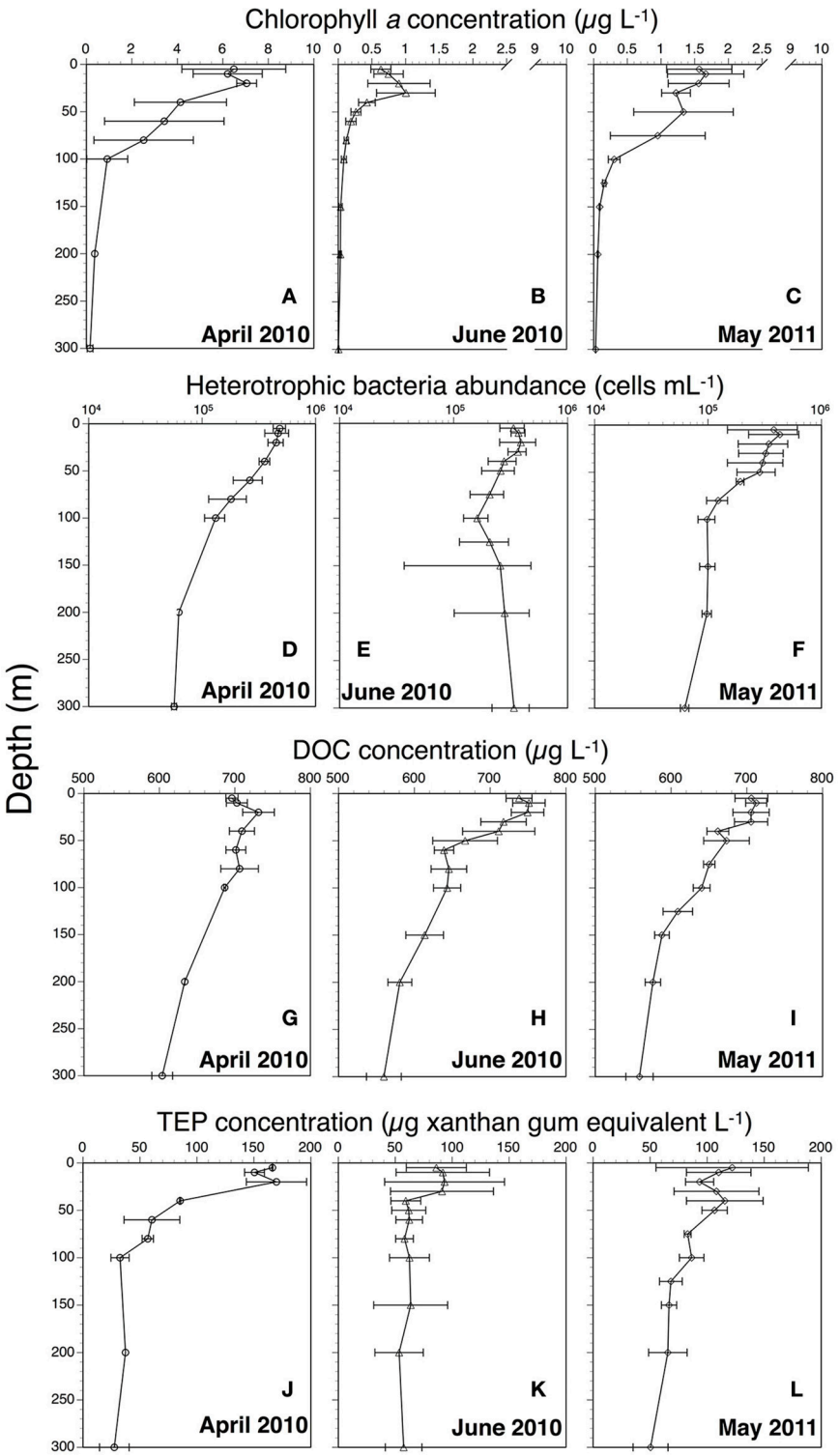

FIGURE 2 | Vertical profiles of chlorophyll *a* (**A**: April 2010; **B**: June 2010; **C**: May 2011), heterotrophic bacteria abundance (**D**: April 2010; **E**: June 2010; **F**: May 2011), dissolved organic carbon (DOC) (**G**: April 2010; **H**: June 2010; **I**: May 2011), and transparent exopolymer particles (TEP) (**J**: April 2010; **K**: June 2010; **L**: May 2011). All profiles show average values. Error bars represent range for April 2010 ($n = 2$) and standard deviation for June 2010 ($n = 4$) and May 2011 ($n = 3$).

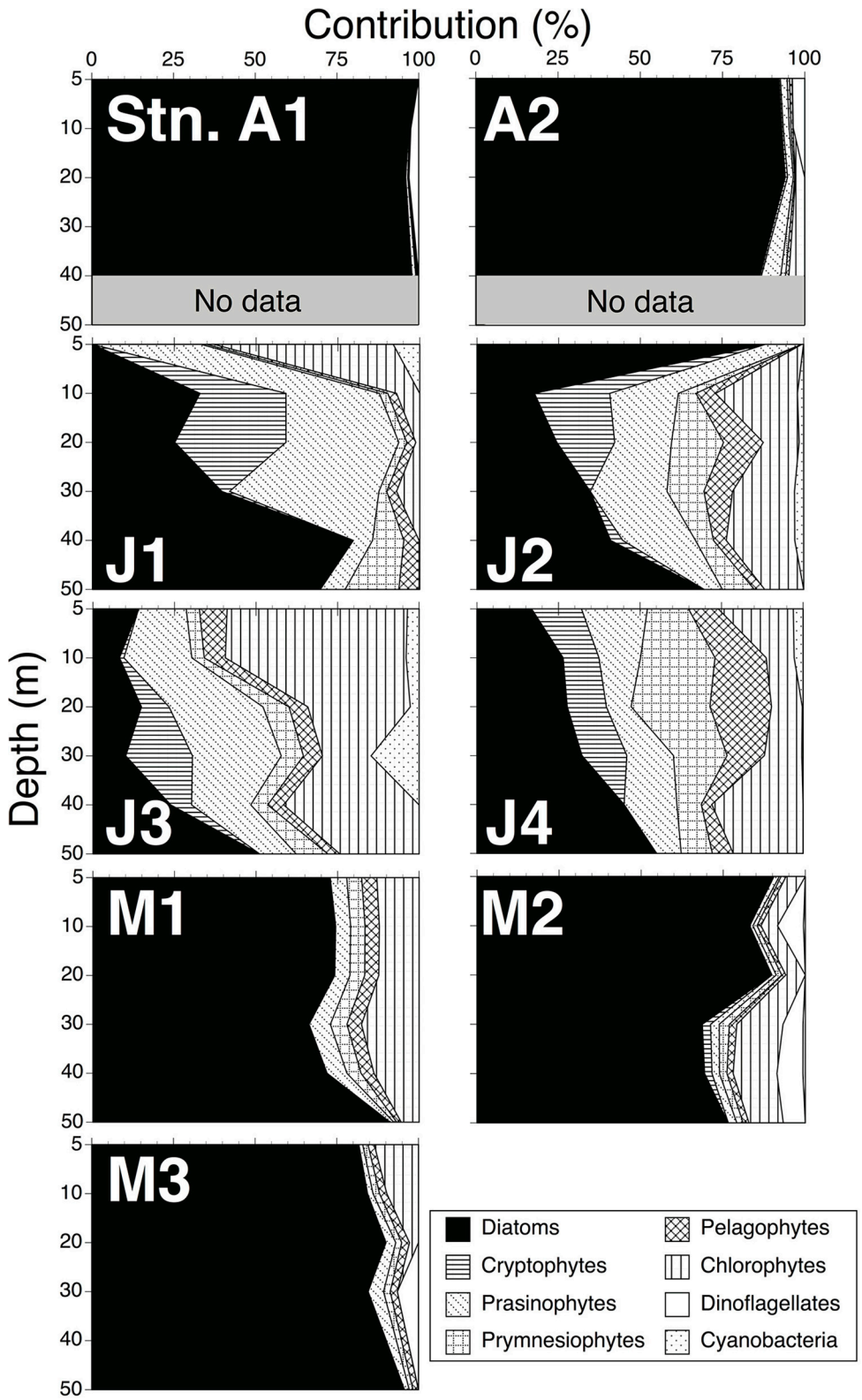

FIGURE 3 | Contributions of each phytoplankton group to chlorophyll *a* biomass within 0–50 m depths, estimated by CHEMTAX.

± 4%) and May 2011 (80 ± 9%). By contrast, the contributions in June 2010 (35 ± 23%) were relatively small. The contributions of the other phytoplankton groups, such as cryptophytes (20 ± 17%), prasinophytes (19 ± 10%) and prymnesiophytes (9 ± 6%), were larger than those in April 2010 (cryptophytes: 1 ± 2%; prasinophytes: 2 ± 2%; prymnesiophytes: 0.4 ± 0.5%) and May 2011 (cryptophytes: 9 ± 5%; prasinophytes: 3 ± 2%; prymnesiophytes: 3 ± 1%).

Cell Abundance and Composition of Diatoms and Coccolithophores

Cell abundances of diatoms at 5-m depth were relatively high in April 2010 (335 × 10^3 cells L^{-1} on average) and low in June 2010 (5 ± 4 × 10^3 cells L^{-1}) (**Table 1**). Diatom abundance in May 2011 was highly variable (150 ± 115 × 10^3 cells L^{-1}). Using SEM, we identified 34 centric diatom species, 13 pennate diatom species, and 3 coccolithophore species, including a holococolith species (**Table 2**). The dominant diatom species in April 2010 were *Thalassiosiara nordenskioeldii* and *Chaetoceros* spp. In June 2010, *Fragilariopsis pseudonana* and *Neodenticula seminae* were predominant in the diatom community. In May 2011, *Ch. atlanticus* and *Chaetoceros* spp. dominated the diatom assemblages. Chl *a* concentrations were significantly correlated with the cell abundance of centric diatoms (Spearman's rank correlation $\rho = 0.90$, $p < 0.005$, $n = 9$), but only weakly correlated with that of pennate diatoms ($\rho = 0.45$, $p = 0.17$, $n = 9$). The cell abundance of coccolithophores was relatively low throughout the surveys (0–3.6 × 10^3 cells L^{-1}).

Heterotrophic Bacterial Abundance Estimated by Flow Cytometry

Bacterial abundances in April 2010 and May 2011 were higher in the surface waters than at depth (**Figures 2D,F**, **Table 1**). However, in June 2011, little difference was observed from 5 to 300 m (**Figure 2E**, **Table 1**). Bacterial abundance within the mixed layer changed only slightly between April 2010 (4.8 ± 0.9 × 10^5 cells mL^{-1}), June 2010 (3.5 ± 0.9 × 10^5 cells mL^{-1}), and May 2011 (3.8 ± 1.7 × 10^5 cells mL^{-1}) (Kruskal-Wallis ANOVA, $p = 0.15$). Bacteria abundances from 5 to 300 m depths were significantly correlated with those of Chl *a* concentrations (Spearman's rank correlation, $\rho = 0.65$, $p < 0.001$, $n = 94$). Significant relationships between these were also observed on each cruise (Spearman's rank correlation, April: $\rho = 0.75$, $p < 0.001$, $n = 16$; June: $\rho = 0.49$, $p < 0.005$, $n = 45$; May: $\rho = 0.94$, $p < 0.001$, $n = 33$). Furthermore, there was a significant relationship between bacterial abundance and Chl *a* within the mixed layer (Spearman's rank correlation, $\rho = 0.57$, $p < 0.01$, $n = 22$). Values of bacteria abundance/Chl *a* concentration within the mixed layer increased significantly over time, e.g., April 2010 [85 ± 40 cells (pg Chl $a)^{-1}$], May 2011 [242 ± 68 cells (pg Chl $a)^{-1}$] and June 2010 [524 ± 70 cells (pg Chl $a)^{-1}$] (Kruskal-Wallis ANOVA, $p < 0.01$, Steel-Dwass test, April vs. May: $p < 0.01$; April vs. June: $p < 0.01$; May vs. June: $p < 0.01$).

POC Concentration

The POC concentration at 5-m depth decreased from April through June 2010 (**Table 1**; April 2010: 454 μg L^{-1} on average; June 2010: 143 ± 8 μg L^{-1}), and that of May 2011 was 203 ± 37 μg L^{-1}. The ratio of POC/Chl *a* increased from April through June 2010 (April: 77 on average; June: 237 ± 58), and that in May 2011 was 134 ± 25.

DOC Concentration

DOC concentrations generally decreased from 5 to 300 m depths (**Table 1**, **Figures 2G–I**). The highest concentration (∼768 μg L^{-1}) was found at 10 and 20 m depths at station J2 and at 10 m at station J3. The lowest concentration (∼540 μg L^{-1}) was observed at 300 m depth at stations M2, J3, and J4. The DOC concentration within the mixed layer in June 2010 (744 ± 24 μg L^{-1}) was significantly higher than that in April 2010 (696 ± 12 μg L^{-1}) and May 2011 (708 ± 12 μg L^{-1}) (Kruskal-Wallis ANOVA, $p < 0.01$, Steel-Dwass test, April vs. May: $p = 0.99$; April vs. June: $p < 0.05$; May vs. June: $p < 0.01$).

POC and DOC Production

POC production at 5 m depth was between 25 mg C m^{-3} d^{-1} at the J1 station and 290 mg C m^{-3} d^{-1} at the A1 station (**Table 1**). Average productivity in April and June 2010 and May 2011 decreased from April to June (195 ± 95 mg C m^{-3} d^{-1} in April 2010, 72 ± 29 mg C m^{-3} d^{-1} in May 2011, and 33 ± 8 mg C m^{-3} d^{-1} in June 2010). The average DOC production at 5 m depth in April and June 2010 and May 2011 was 2.9 ± 1.3 mg C m^{-3} d^{-1}, 1.9 ± 0.5 mg C m^{-3} d^{-1}, and 3.2 ± 1.0 mg C m^{-3} d^{-1}, respectively (**Table 1**). PER ratios were estimated. The average ratios increased slightly from April to June (2.3 ± 1.8% in April 2010, 4.6 ± 0.6% in May 2011, and 5.5 ± 1.5% in June 2010) (**Table 1**).

TEP Concentration

Minimum and maximum TEP concentrations in our surveys were observed at station A1, at 300 m (< 15 μg xanthan gum equiv. L^{-1}) and 20 m (196 ± 71 μg xanthan gum equiv. L^{-1}) respectively (**Figures 2K–L**, **Table 1**). TEP concentrations from 5 to 300 m depths were significantly correlated with those of Chl *a* concentrations throughout the observation period (Spearman's rank correlation, $\rho = 0.65$, $p < 0.001$, $n = 98$) and on each cruise (Spearman's rank correlation, April: $\rho = 0.85$, $p < 0.001$, $n = 17$; June: $\rho = 0.52$, $p < 0.001$, $n = 47$; May: $\rho = 0.78$, $p < 0.001$, $n = 34$). The TEP concentrations were also significantly correlated with bacteria abundance throughout the observation period (Spearman's rank correlation, $\rho = 0.65$, $p < 0.001$, $n = 98$). Additionally, there were significant relationships between the two on each cruise (Spearman's rank correlation, April: $\rho = 0.86$, $p < 0.001$, $n = 17$; June: $\rho = 0.36$, $p < 0.05$, $n = 48$; May: $\rho = 0.58$, $p < 0.001$, $n = 33$).

Average TEP concentrations within the mixed layer in April and June 2010 and May 2011 were 155 ± 12, 90 ± 32, and 112 ± 38 μg xanthan gum equiv. L^{-1}, respectively. TEP levels within the mixed layer in April 2010 were significantly higher than those in June 2010, whereas those in May 2011 were not significantly different from those in April and June 2010 (Kruskal-Wallis ANOVA, $p < 0.01$, Steel-Dwass test, April 2010 vs. June 2010: $p < 0.01$, April 2010 vs. May 2011: $p = 0.07$; May vs. June: $p = 0.48$). TEP concentrations within the mixed layer in April and

TABLE 2 | List of phytoplankton species identified in Oyashio diatom bloom surveys.

April 2010	June 2010	May 2011
Centric diatoms	**Centric diatoms**	**Centric diatoms**
Actinocyclus curvatulus	*Asteromphalus hyalinus*	*Actinocyclus* spp.
Actinocyclus spp.	*Chaetoceros atlanticus*	*Asteromphalus hyalinus*
Asteromphalus hyalinus	*Ch. concavicornis*	***Chaetoceros atlanticus***
Chaetoceros atlanticus	*Ch. neglectus*	*Ch. concavicornis*
Ch. concavicornis	*Corethron criophilum*	*Ch. radicans*
Ch. decipience	*Co. inerme*	***Chaetoceros* spp.**
Ch. debilis	*Coscinodiscus* spp.	*Rhizosolenia* spp.
Ch. diadema	*Rhizosolenia* spp.	*Thalassiosira eccentrica*
Ch. neglectus	*Thalassiosira lineata*	*T. lineata*
Ch. pseudocurvisetus	*T. nordenskioeldii*	*T. nordenskioeldii*
Ch. radicans	*T. oestrupii*	*T. pacifica*
***Chaetoceros* spp.**	*T. pacifica*	*T. trifulta*
Corethron criophilum	*Thalassiosira* spp.	*Thalassiosira* spp.
Co. inerme	**Pennate diatoms**	**Pennate diatoms**
Odontella aurita	*Fragilariopsis atlantica*	*Fragilariopsis atlantica*
Rhizosolenia spp.	*F. cylindriformis*	*F. oceanica*
Stephanopyxis turris	*F. cylindrus*	*F. pseudonana*
Thalassiosira allenii	*F. oceanica*	*Fragilariopsis* spp.
T. angulata	***F. pseudonana***	*Neodenticula seminae*
T. eccentrica	*Fragilariopsis* spp.	*Thalassionema nitzchioides*
T. hyalina	***Neodenticula seminae***	**Coccolithophores**
T. lineata	*Thalassionema nitzchioides*	*Emiliania huxleyi*
T. lineoides	*Thalassiothrix longissima*	
T. mala	**Coccolithophores**	
T. nordenskioeldii	*Coccolithus pelagicus* ssp. *Pelagicus*	
T. oceanica	*Emiliania huxleyi*	
T. pacifica	*Coccolithus pelagicus* ssp. *Pelagicus HOL**	
T. leptopus		
T. trifulta		
Thalassiosira spp.		
Pennate diatoms		
Fragilariopsis atlantica		
F. cylindrus		
Navicula directa		
Navicula spp.		
Neodenticula seminae		
Nizschia spp.		
Pseudonizschia spp.		
Thalassionema nitzchioides		
Coccolithophores		
Coccolithus pelagicus ssp. *Pelagicus*		

*Genus and species names are arranged alphabetically, not systematically. Dominant species in April, May and June are shown in bold. *HOL, holococcolith.*

June 2010 and May 2011 were also significantly higher than those below the mixed layer in April (64 ± 49 μg xanthan gum equiv. L^{-1}) and June 2010 (67 ± 27 μg xanthan gum equiv. L^{-1}), and May 2011 (81 ± 23 μg xanthan gum equiv. L^{-1}) (Wilcoxon rank-sum test, April: $p < 0.01$, $n = 17$; May: $p < 0.05$, $n = 34$; June: $p < 0.05$, $n = 48$). TEP values were significantly correlated not only with Chl *a* concentrations but also diatom-derived Chl *a* biomass (Spearman's rank correlation, TEP vs. Chl *a*: $\rho = 0.70$, $p < 0.001$, $n = 23$; TEP vs. diatom-derived Chl *a*: $\rho = 0.66$, $p < 0.001$, $n = 23$). However, no significant relationship was found between TEP levels and Chl *a* biomass of other phytoplankton groups (Spearman's rank correlation, TEP vs. cryptophytes-Chl *a*: $\rho = -0.22$, $p = 0.31$, $n = 23$; TEP vs. prasinophyte-derived Chl *a*: $\rho = -0.27$, $p = 0.22$, $n = 23$; TEP vs. prymnesiophyte-derived Chl *a*: $\rho = -0.28$, $p = 0.19$, $n = 23$). The TEP/Chl *a* ratio increased significantly from April to June (26 ± 10 in April 2010,

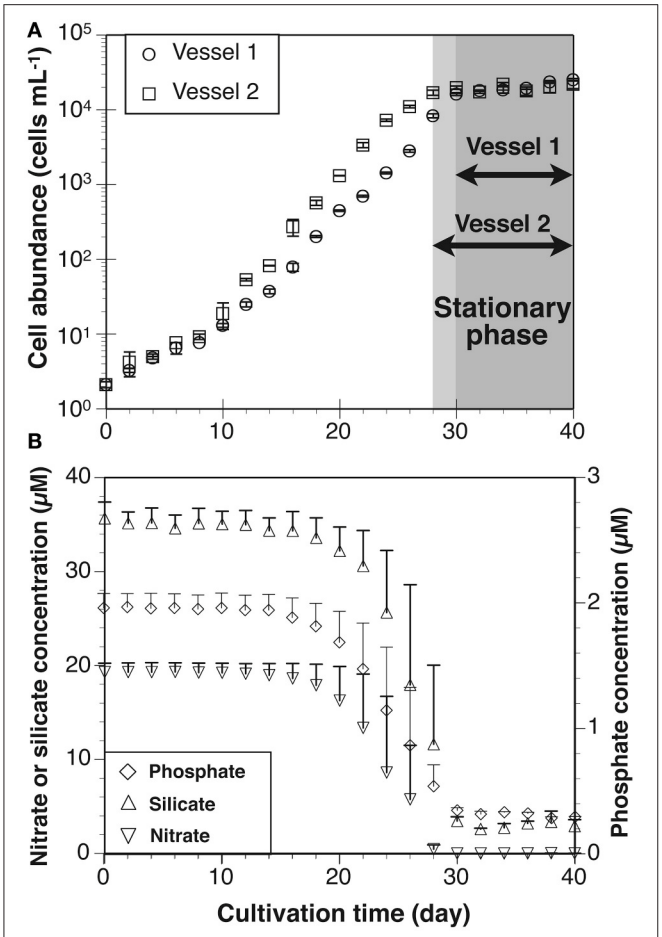

FIGURE 4 | (A) Growth curves of *Thalassiosira nordenskioeldii* in laboratory cultivation experiment. Each stationary phase in cultivation vessels 1 and 2 is indicated by gray color. **(B)** Average nitrate, silicate and phosphate concentrations in vessels 1 and 2. Error bars in growth curve and nitrate concentration represent ranges ($n = 2$).

76 ± 24 in May 2011, and 128 ± 31 in June 2010) (Kruskal-Wallis ANOVA, $p < 0.01$, Steel-Dwass test, April vs. May: $p < 0.01$; April vs. June: $p < 0.01$; May vs. June: $p < 0.05$). In contrast, values of TEP concentration/bacteria abundance changed little from April and June [0.33 ± 0.06 μg xanthan gum ($\times 10^6$ bacterial cells)$^{-1}$ in April 2010, 0.34 ± 0.16 μg xanthan gum ($\times 10^6$ bacterial cells)$^{-1}$ in May 2011, and 0.25 ± 0.07 μg xanthan gum ($\times 10^6$ bacterial cells)$^{-1}$ in June 2010] (Kruskal-Wallis ANOVA, $p < 0.01$, Steel-Dwass test, April vs. May: $p < 0.01$; April vs. June: $p < 0.01$; May vs. June: $p < 0.05$).

Laboratory Experiments

Growth Curves, Nutrient Levels, and Chl *a* Concentrations

Cell abundances in vessels 1 and 2 increased from 2 to ~20,000 cells mL^{-1} (**Figure 4A**). As estimated from the specific growth rate, the exponential growth phase was between days 0 and 30 in Vessel 1 and days 0 and 28 in Vessel 2. The stationary phase was observed between days 30 and 40 in Vessel 1 and days 28 and 40 in Vessel 2. The average specific growth rate in both vessels during the exponential growth and stationary phases was 0.31 ± 0.14 d^{-1} and 0.03 ± 0.07 d^{-1}, respectively (**Table 3**). The average nitrate, silicate and phosphate levels in both vessels are shown in **Figure 4B**. During the exponential growth phase, these levels decreased with time. In the stationary phase, nitrate depleted (< 0.1 μM), whereas silicate and phosphate concentrations maintained values of 3.1 ± 0.7 μM and 0.3 ± 0.03 μM. Chlorophyll *a* concentrations in Vessel 1 (day 20) and 2 (day 18) in the mid-exponential growth phase were 6.1 ± 0.1 μg L^{-1} and 7.1 ± 0.1 μg L^{-1}, respectively. Ratios calculated from the Chl *a* concentrations and cell abundance sampled at the same time were 14 pg cell^{-1} in Vessel 1 and 13 pg cell^{-1} in Vessel 2 (average 13 ± 1 pg cell^{-1}).

TEP and DOC Concentrations

The initial (day 0) TEP concentration in Vessel 1 was undetectable, so this concentration was assumed to be 0 μg xanthan gum equiv. L^{-1}. The average TEP concentration in both vessels increased with time (**Figure 5**). The concentrations ranged from 12 ± 12 μg xanthan gum equiv. L^{-1} to $1{,}488 \pm 93$ μg xanthan gum equiv. L^{-1}. Average DOC concentration also generally increased with time (**Figure 5**). The concentrations were between $1{,}148 \pm 62$ μg C L^{-1} and $1{,}647 \pm 10$ μg C L^{-1}. TEP concentrations in the vessels increased with DOC concentrations ($\rho = 0.91$, $p < 0.001$, $n = 21$).

Cellular TEP and DOC Productivities

Cellular TEP production rates during the exponential and stationary phases were 2.7 ± 0.5 pg xanthan gum equiv. [cell]$^{-1}$ d^{-1} and 8.1 ± 0.9 pg xanthan gum equiv. [cell]$^{-1}$ d^{-1}, respectively (**Table 3**). Cellular DOC productivity was 1.0 ± 0.2 pg C [cell]$^{-1}$ d^{-1} and 4.0 ± 2.2 pg C [cell]$^{-1}$ d^{-1} during the exponential and stationary phases, respectively. The cellular TEP and DOC productivities during the exponential growth phase were also converted to a Chl *a*-normalized TEP production rate (0.21 μg xanthan gum [μg Chl *a*]$^{-1}$ d^{-1}) and DOC production rate [0.07 μg C (μg Chl *a*)$^{-1}$ d^{-1}], using the factor of Chl *a* concentration per cell. The cellular TEP and DOC productivities were 2.9 and 4.0-fold greater in the stationary than exponential growth phase, respectively. Ratios of carbon-based TEP/DOC productivities were 2.2 ± 0.02 in the exponential growth phase and 2.0 ± 0.9 in the stationary phase.

DISCUSSION

Factors Controlling TEP Levels in Oyashio Region

According to Kawai (1972), the Oyashio was defined as the water mass where temperatures at 100 m were < 5°C. Therefore, all stations in this study were in the Oyashio (**Table 1**). However, hydrographic conditions were variable throughout the observation period (**Table 1**). In the Oyashio region, it is known that spring diatom blooms occur during April and May, and decline toward summer every year (e.g., Saito et al., 2002). Indeed, decreases in Chl *a* concentration were observed from April to June in both 2010 and 2011 as estimated from the satellite images (Supplementary Figure 2).

TABLE 3 | Summary of results in exponential growth and stationary phases, obtained from laboratory cultivation experiments.

Parameters	Exponential growth phase		Stationary phase	
	Vessel 1	Vessel 2	Vessel 1	Vessel 2
Term (day)	0–30	0–28	30–36	28–40
Specific growth rate ± S.D. (d^{-1})	0.30 ± 0.12	0.32 ± 0.16	0.03 ± 0.02	0.02 ± 0.09
Cellular TEP productivity (pg xanthan gum equiv. [cell]$^{-1}$ d^{-1})	3.2	2.3	7.1	9.0
Cellular DOC productivity (pg C [cell]$^{-1}$ d^{-1})	1.1	0.8	1.8	6.2
Ratio of cellular carbon-based TEP/DOC productivities	2.2	2.1	3.0	1.1

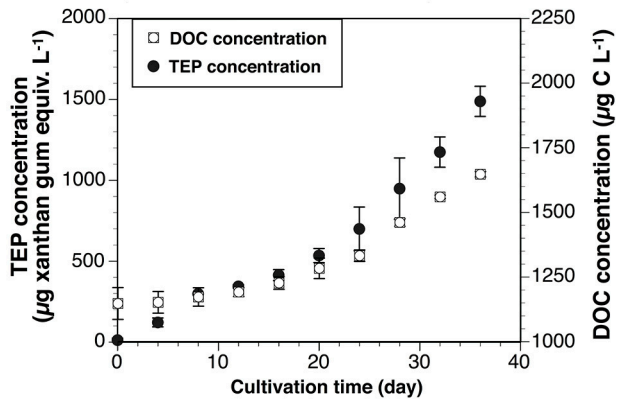

FIGURE 5 | Average TEP and DOC concentrations in vessels 1 and 2 during cultivation experiment.

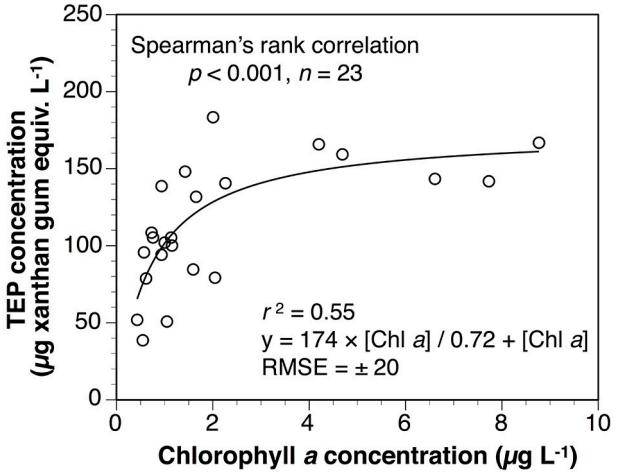

FIGURE 6 | Relationship between TEP and Chl *a* concentrations within surface mixed layer, revealing significant relationship.

TEP concentrations from 5 to 300 m depths were significantly correlated with those of Chl *a* concentrations and with bacteria abundances. Similarly, the TEP concentrations were higher in the mixed layer than in the layer below. These results indicate that TEP was derived from these microorganisms. The Chl *a* concentrations within the mixed layer decreased significantly from April to June 2010, whereas bacterial cell abundances changed little in that period. The difference in temporal variation between the Chl *a* concentrations and bacteria abundances within the mixed layer suggest that the main TEP producer was phytoplankton. We used the following Michaelis-Menten-type equation for estimating TEP levels within the surface mixed layer, using Chl *a* concentration during the spring Oyashio diatom blooms (**Figure 6** and Equation 6).

$$[\mathrm{TEP}]_{\mathrm{SML}} = \frac{174 \times [\mathrm{Chl}\,a]}{0.72 + [\mathrm{Chl}\,a]}, \quad (6)$$

where $[\mathrm{TEP}]_{\mathrm{SML}}$ is TEP concentration within the surface mixed layer (μg xanthan gum equiv. L^{-1}) and [Chl *a*] is Chl *a* concentration within the mixed layer (μg L^{-1}). The root mean square error (RMSE) of this curve was estimated at ± 20 μg xanthan gum equiv. L^{-1}. These findings also suggest that TEP within the surface mixed layer was mainly from phytoplankton.

Assuming that TEP was largely produced by phytoplankton, data of each phytoplankton group to Chl *a* biomass estimated from the CHEMTAX program were useful to discover which group contributed predominately to TEP concentrations. These data showed that diatom-derived Chl *a* concentrations were dominant in April 2010 (94 ± 4%) and May 2011 (80 ± 9%) (**Figure 3**). This suggests that the diatoms contributed to the relatively high TEP concentration in our study. In addition, data of phytoplankton species composition by SEM showed that *T. nordenskioeldii* and *Chaetoceros* spp. dominated phytoplankton assemblages in April 2010, and *C. atlanticus* and *Chaetoceros* spp. were dominant in May 2011 (**Table 2**). The relatively high TEP levels may have been caused by these diatom species. Compared to April 2010 and May 2011, the dominant phytoplankton groups in June 2010 were diatoms (35 ± 23%), cryptophytes (20 ± 17%), prasinophytes (19 ± 10%), and prymnesiophytes (9 ± 6%) (**Figure 3**). It has been reported that cryptophytes and prymnesiophytes contribute to high TEP concentrations (Passow et al., 1995; Hong et al., 1997). These phytoplankton groups may have also affected the TEP concentration in June 2010.

Data on TEPs are very limited for the Northwest Pacific. Ramaiah et al. (2005) investigated changes in TEP levels in the Western Subarctic Gyre (WSG) of the North Pacific during an *in situ* iron fertilization experiment. According to that work, the centric diatom *Ch. debilis* bloomed in the WSG after iron enrichment, and TEP levels (∼50–190 μg xanthan gum equiv. L^{-1}) in an iron-enriched patch increased with Chl *a*

concentration (∼1–19 μg L^{-1}) at 5 and 10 m depths. TEP levels found by Ramaiah et al. were similar to those observed in our study. However, Passow (2002a) reported that TEP concentration during diatom blooms can reach > 1,000 μg xanthan gum equiv. L^{-1} in various regions (Engel, 2000; Prieto et al., 2002). Environmental factors such as temperature, nutrient concentrations, and UV intensity may modulate the TEP production rate of phytoplankton (Mari et al., 2017). An increase of water temperature can raise the TEP production rate (Claquin et al., 2008; Fukao et al., 2012). Seawater temperatures in April 2010 and those in Ramaiah et al. (2005) were relatively low, at 3.1–4.5 and 7.5–9.5°C, respectively. The depletion of nutrients can also increase the TEP concentration because of enhanced release of extracellular polysaccharides (Myklestad, 1995). It has been reported that the ratio of silicate and nitrate concentrations during diatom blooms is relatively constant (approximately 1:1; Brzezinski, 1985; Kudo et al., 2000), and the half-saturation constants of uptake kinetics were ∼3 μM in silicate and ∼1 μM in nitrate (e.g., Kanda et al., 1985; Nelson and Tréguer, 1992). In April 2010, nutrient concentrations were abundant (> 20 μM in silicate and > 8 μM in nitrate). These results suggest that the lower temperatures and higher nutrients in April 2010 did not increase the TEP levels in seawater much. Recently, Annane et al. (2015) reported lower TEP levels (< 200 μg xanthan gum equiv. L^{-1}) during the centric diatom bloom (> 20 μg L^{-1} in terms of Chl *a* level, mainly consisting of *T. nordenskioeldii*) in the lower St. Lawrence Estuary of Canada. The temperature and nitrate concentrations in Annane et al. were similar to those in our study. Therefore, TEP productivity can vary with diatom species and can be relatively low during Oyashio spring diatom blooms when *T. nordenskioeldii* becomes dominant (Chiba et al., 2004; Suzuki et al., 2011).

Heterotrophic organisms such as eubacteria can also be important in production (e.g., Passow, 2002b; Sugimoto et al., 2007), decomposition (e.g., Passow et al., 2001), and transformation (e.g., Gärdes et al., 2011; Yamada et al., 2013) processes of TEP. Although the present study suggests that the main TEP producer was likely phytoplankton as described above, bacteria abundance was significantly correlated with not only TEP concentration but also Chl *a* concentration. This indicates close interaction between these microorganisms and TEP. Values of bacteria abundance/Chl *a* concentration within the mixed layer increased significantly from April 2010 to June 2010, suggesting that relative abundance of bacteria to phytoplankton was low in April 2010. In contrast, TEP levels within the mixed layer were significantly higher in April 2010 than in June 2010. It has been suggested that TEP produced by phytoplankton may serve as protection against hydrolases of attached bacteria (Azam and Smith, 1991; Smith et al., 1995). Hence, the relatively lower Chl *a* normalized TEP concentrations in April 2010 may have partially contributed to the relative abundance of bacteria to phytoplankton. The lower TEP concentrations may also mean that bacteria had colonized and degraded TEPs. Indeed, the TEPs and their precursors produced by diatoms can be utilized by bacteria. Recently, Cisternas-Novoa et al. (2015) stated that bacterial abundance affected TEP production by *T. weissflogii*. However, interactions between TEPs and bacteria in nature are complex because of combinations of various environmental factors, as reviewed by Passow (2002b).

Relationship between TEP Production and Phytoplankton Physiology

The TEP levels appeared to decrease from April to June, together with the decline of diatom blooms in the Oyashio region. In contrast, the TEP/Chl *a* ratio increased significantly from April to June. If the main source of TEP is phytoplankton assemblages, the increase in ratios of TEP/Chl *a* concentrations from April to June may show that the ability to produce TEP was weaker in diatoms than in other phytoplankton groups, such as cryptophytes, prasinophytes and prymnesiophytes. In our laboratory experimentation, the TEP production rate of the axenic strain of *T. nordneskioeldii* was estimated at 0.21 μg xanthan gum equiv. [μg Chl *a*]$^{-1}$ d^{-1} during the exponential growth phase. Hong et al. (1997) showed that Chl *a*-normalized TEP production rates of *Phaeocystis antarctica* were >500 μg xanthan gum equiv. [μg Chl *a*]$^{-1}$ h^{-1} at photon flux density ∼100 μmol photons m^{-2} s^{-1}. These findings suggest that *T. nordenskioeldii* was a weaker TEP producer than *P. antarctica*. In this study, although the sampling from each culture vessel was performed very carefully on a clean bench to avoid any contamination, perhaps bacteria could be slightly contaminated during incubation, and that might underestimate the TEP productivity by *T. nordenskioeldii* due to its utilization by bacteria. On the other hand, TEP decomposition by bacteria could increase the refractory form of gel particles, because it has been reported that microbial processes can alter the molecular structure of dissolved organic matter (Ogawa et al., 2001). This would contribute to increase in the TEP/Chl *a* ratio between the bloom and post-bloom phases.

Although diatom species composition possibly affects TEP productivity as mentioned above, the incubation experiment using *T. nordenskioeldii* revealed that cellular TEP productivity during the stationary phase was 2.9-fold greater than that during the exponential growth phase (**Table 3**). Changes in physiological state from the exponential to stationary growth phases in this batch culture experiment were likely caused by nitrate depletion (**Figure 4B**). Therefore, we speculate that nitrate availability probably influences TEP levels during spring diatom blooms in the Oyashio region.

TEP precursors have been considered to be dissolved acid polysaccharides (Thornton et al., 2007; Wurl et al., 2011), which may mainly be from DOC excreted by phytoplankton (Passow, 2002a). Hence, we examined the relationship between TEP levels and DOC production at 5 m depth, but this was not significant (Spearman's rank correlation, $p = 0.42$, $n = 8$). In addition, the relationship was evaluated using the axenic strain of *T. nordenskioeldii* (Chiba et al., 2004; Suzuki et al., 2011). Productivities of cellular TEP and DOC generally varied simultaneously with growth of the diatom strain. These results suggest that TEP production was linked to DOC in the experiment. The *in situ* DOC production was clearly lower than POC production (**Table 1**) and was comparable to those (<0.5–1.2 mg C m^{-3} d^{-1}) in the Mediterranean Sea between June and

July (Lopez-Sandval et al., 2011). However, the PER values were smaller than those (30–41%) in the Mediterranean. In general, relatively low PER values can be found in eutrophic waters (e.g., Hama and Yanagi, 2001; Marañón et al., 2004) and relatively high values were observed in oligotrophic regions (e.g., Alonso-Sáez et al., 2008; Lopez-Sandval et al., 2011). The relatively low PER possibly weaken the relationship between TEP levels and DOC production.

Interestingly, however, the averaged ratio (2.2 ± 0.02) of carbon-based TEP/DOC rates for *T. nordenskioeldii* in the exponential growth phase was nearly the same as the stationary growth phases (2.0 ± 0.9) (**Table 3**). If all TEP were formed from DOC released by *T. nordenskioeldii*, the carbon-based TEP/DOC production ratio would be < 1. Our laboratory experiment also found that TEP was rich at the cell surface of *T. nordneskioeldii* (Supplemental Figure 3). This indicates that some of the DOC excreted by *T. nordenskioeldii* were trapped on the cell surfaces. Therefore, the carbon-based TEP/DOC production rate > 1 suggests that the TEP was partly formed at cell surfaces. Moreover, the similar carbon-based TEP/DOC production ratios in the exponential and stationary growth phases imply that the formation rate of TEP to DOC was not significantly different between the two phases. The results of our field observations and laboratory experiments imply that high primary production by diatoms leads to relatively strong DOC production, and that subsequently, the excretion of acid polysaccharides (a type of DOC) can generate higher TEP levels in seawater. This was even though the activity of heterotrophic organisms possibly masked the relationship between TEP concentrations and DOC productivity, together with decay of the diatom bloom. Thus, TEP production in the Oyashio region may be enhanced with the increase in DOC production from spring diatoms.

CONCLUSIONS

This study revealed TEP dynamics and DOC productivity in the Oyashio region of the Northwest Pacific during spring diatom blooms. Our results showed that TEP levels within the mixed layer were correlated with diatom-derived Chl *a* biomass, suggesting that diatoms were the main TEP producers. However, TEP levels were not correlated with DOC productivity in the Oyashio region. In contrast, we found that the average TEP and DOC productivities of *T. nordenskioedlii* varied simultaneously with growth of the strain and that the carbon-based TEP/DOC ratio changed little between the growth phases. These results suggest that TEP productivity in the Oyashio region increases with DOC productivity during spring diatom periods and that TEP removal (e.g., through consumption by heterotrophic organisms) must be considered in evaluating the relationship between TEP levels and DOC productivity. Further laboratory experiments using isolated diatom and bacteria strains should be made to clarify these issues.

AUTHOR CONTRIBUTIONS

YN and KS designed this research. All authors performed the field observations. The laboratory cultivation experiment was executed by YN. YN analyzed the samples and wrote the paper with KS and YY.

ACKNOWLEDGMENTS

We thank the captain, crew, and scientists of the FR/V *Wakataka-Maru* (Tohoku National Fisheries Research Institute, Japan) and R/V *Tansei-Maru* (JAMSTEC/Atmospheric and Ocean Research Institute, University Tokyo) for their valuable help. We are also grateful to Dr. A. Sugimoto and Ms. Y. Hoshino for ^{13}C analyses of POC and DOC production. Dr. S. Takao is acknowledged for the satellite images. This study was partly supported by the JSPS Grant-in-Aid for Scientific Research (B) (22310002) and Grant-in-Aid for Scientific Research on Innovative Areas (24121004) to KS, and the Sasagawa Scientific Research Grant from the Japan Science Society (24–744) to YN.

SUPPLEMENTARY MATERIAL

The Supplementary Material for this article can be found online at: http://journal.frontiersin.org/article/10.3389/fmars.2017.00079/full#supplementary-material

REFERENCES

Alldredge, A. L., Passow, U., and Logan, B. E. (1993). The abundance and significance of a class of large, transparent organic particles in the ocean. *Deep Sea Res. I* 40, 1131–1140. doi: 10.1016/0967-0637(93)90129-q

Alonso-Sáez, L., Vázquez-Domínguez, E., Cardelús, C., Pinhassi, J., Sala, M., Lekunberri, I., et al. (2008). Factors controlling the year-round variability in carbon flux through bacteria in a costal marine system. *J. Geophys. Res.* 11, 397–409. doi: 10.1007/s10021-008-9129-0

Annane, S., St-Amand, L., Starr, M., Pelletier, E., and Ferreyra, G. A. (2015). Contribution of transparent exopolymeric particles (TEP) to estuarine particulate organic carbon pool. *Mar. Ecol. Prog. Ser.* 529, 17–34. doi: 10.3354/meps11294

Ayers, J. M., and Lozier, M. S. (2012). Unraveling dynamical controls on the North Pacific carbon sink. *J. Geophys. Res.* 117, C01017. doi: 10.1029/2011JC007368

Azam, F., and Smith, D. C. (1991). "Bacterial influence on the variability in the ocean's biochemical state: a mechanistic view," in *Particle Analysis in Oceanography,* ed S. Demers (San Diego, CA: NATO ASI Series), 213–236.

Azetsu-Scott, K., and Passow, U. (2004). Ascending marine particles: significance of transparent exopolymer particles (TEP) in the upper ocean. *Limnol. Oceanogr.* 49, 741–748. doi: 10.4319/lo.2004.49.3.0741

Berman, T., and Viner-Mozzini, Y. (2001). Abundance and characteristics of polysaccharide and proteinaceous particles in Lake Kinneret. *Aquat. Microb. Ecol.* 24, 255–264. doi: 10.3354/ame024255

Brzezinski, M. A. (1985). The Si:C:N ratio of marine diatoms: interspecific variability and the effect of some environmental variables. *J. Phycol.* 21, 347–357. doi: 10.1111/j.0022-3646.1985.00347.x

Chiba, S., Ono, T., Tadokoro, K., Midorikawa, T., and Saino, T. (2004). Increased stratification and decreased lower trophic level productivity in the Oyashio region of the North Pacific: a 30-year retrospective study. *J. Oceanogr.* 60, 149–162. doi: 10.1023/b:joce.0000038324.14054.cf

Cisternas-Novoa, C., Lee, C., and Engel, A. (2015). Transparent exopolymer particles (TEP) and Coomassie stainable particles (CSP): differences between their origin and vertical distributions in the ocean. *Mar. Chem.* 175, 56–71. doi: 10.1016/j.marchem.2015.03.009

Claquin, P., Probert, I., Lefebvre, S., and Veron, B. (2008). Effects of temperature on photosynthetic parameters and TEP production in eight species of marine microalgae. *Aquat. Microb. Ecol.* 51, 1–11. doi: 10.3354/ame001187

Engel, A. (2000). The role of transparent exopolymer particles (TEP) in the increase in apparent particle stickiness (α) during the decline of a diatom bloom. *J. Plankton Res.* 22, 485–497. doi: 10.1093/plank/22.3.485

Engel, A., and Passow, U. (2001). Carbon and nitrogen content of transparent exopolymer particles (TEP) in relation to their Alcian Blue adsorption. *Mar. Ecol. Prog. Ser.* 219, 1–10. doi: 10.3354/meps219001

Fukao, T., Kimono, K., and Kotani, Y. (2010). Production of transparent exopolymer particles by four diatom species. *Fish. Sci.* 76, 755–760. doi: 10.1007/s12562-010-0265-z

Fukao, T., Kimoto, K., and Kotani, Y. (2012). Effect of temperature on cell growth and production of transparent exopolymer particles by the diatom *Coscinodiscus granii* isolated from marine mucilage. *J. Appl. Phycol.* 24, 181–186. doi: 10.1007/s10811-011-9666-3

Fukuyo, Y., Takano, H., Chihara, M., and Matsuoka, K. (1990). *Red Tide Organisms in Japan—An Illustrated Taxonomic Guide.* Tokyo: Uchida Rokakuho Publishing.

Gärdes, A., Iversen, M. H., Grossart, H.-P., and Passow, U. (2011). Diatom-associated bacteria are required for aggregation of *Thalassiosira weissflogii*. *ISME J.* 5, 436–445. doi: 10.1038/ismej.2010.145

Grossart, H.-P., Berman, T., Simon, M., and Pohlmann, K. (1998). Occurrence and microbial dynamics of macroscopic organic aggregates (lake snow) in Lake Kinneret, Israel, in fall. *Aquat. Microb. Ecol.* 14, 59–67. doi: 10.3354/ame014059

Grossart, H.-P., Czub, G., and Simon, M. (2006). Algae–bacteria interactions and their effects on aggregation and organic matter flux in the sea. *Environ. Microbiol.* 8, 1074–1084. doi: 10.111/j.1462-2920.2006.00999.x

Grossart, H.-P., and Simon, M. (1997). Formation of macroscopic organic aggregates (lake snow) in a large lake: the significance of transparent exopolymer particles, phytoplankton, and zooplankton. *Limnol. Oceanogr.* 42, 1651–1659. doi: 10.4319/lo.1997.42.8.1651

Guillard, R. R. L. (1973). "Division rates," in *Handbook of Phycological Methods: Culture Methods and Growth Measurements*, ed J. R. Stein (Cambridge: Cambridge University Press), 289–312.

Guillard, R. R. L. (1975). "Culture of phytoplankton for feeding marine invertebrates" in *Culture of Marine Invertebrate Animals,* eds W. L. Smith and M. H. Chanley (New York, NY: Plenum Press), 26–60.

Guillard, R. R., and Ryther, J. H. (1962). Studies of marine planktonic diatoms. I. Cyclotella nana Hustedt and Detonula confervacea Cleve. *Can. J. Microbiol.* 8, 229–239. doi: 10.1139/m62-029

Hama, T., Miyazaki, T., Ogawa, Y., Iwakuma, T., Takahashi, M., Otsuki, A., et al. (1983). Measurement of photosynthetic production of a marine phytoplankton population using a stable ^{13}C isotope. *Mar. Biol.* 73, 31–36. doi: 10.1007/bf00396282

Hama, T., and Yanagi, K. (2001). Production and neutral aldose composition of dissolved carbohydrates excreted by natural marine phytoplankton populations. *Limol. Oceanogr.* 46, 1945–1955. doi: 10.4319/lo.2001.46.8.1945

Hattori-Saito, A., Nishioka, J., Ono, T., Michael, R., McKay, L., and Suzuki, K. (2010). Iron deficiency in micro-sized diatoms in the Oyashio region of the western subarctic Pacific during spring. *J. Oceanogr.* 66, 105–115. doi: 10.1007/s10872-010-0009-9

Honda, M. C. (2003). Biological pump in the northwestern north Pacific. *J. Oceanogr.* 59, 671–684. doi: 10.1023/b:joce.0000009596.57705.0c

Hong, Y., Smith, W. O. Jr., and White, A.-M. (1997). Studies on transparent exopolymer particles (TEP) production in the Ross Sea (Antarctica) and by *Phaeocystis antarctica* (prymnesiophyceae). *J. Phycol.* 33, 368–376. doi: 10.1111/j.0022-3646.1997.00368.x

Ikeda, T., Shiga, N., and Yamaguchi, A. (2008). Structure, biomass, distribution and trophodynamics of the pelagic ecosystem in the Oyashio region, western subarctic Pacific. *J. Oceanogr.* 64, 339–354. doi: 10.1007/s10872-008-0027-z

Isada, T., Hattori-Saito, A., Saito, H., Ikeda, T., and Suzuki, K. (2010). Primary productivity and its bio-optical modeling in the Oyashio region, NW Pacific during the spring bloom 2007. *Deep Sea Res. II* 57, 1653–1664. doi: 10.1016/j.dsr2.2010.03.009

Kanda, J., Saino, T., and Hattori, A. (1985). Nitrogen uptake by natural populations of phytoplankton and primary production in the Pacific Ocean: regional variability of uptake capacity. *Limnol. Oceanogr.* 30, 987–999. doi: 10.4319/lo.1985.30.5.0987

Kasai, H., Saito, H., and Tsuda, A. (1998). Estimation of standing stock of chlorophyll a and primary production from remote-sensed ocean color in the Oyashio region, the western subarctic Pacific, during the spring bloom in 1997. *J. Oceanogr.* 54, 527–537. doi: 10.1007/bf02742454

Kasai, H., Saito, H., Yoshimori, A., and Taniguchi, S. (1997). Variability in timing and magnitude of spring bloom in the Oyashio region, the western subarctic Pacific off Hokkaido, Japan. *Fish. Oceanogr.* 6, 118–129. doi: 10.1046/j.1365-2419.1997.00034.x

Kawai, H. (1972). "Hydrography of the Kuroshio and Oyashio," in *Physical Oceanography II: Fundamental Lectures of Oceanography*, ed J. Masuzawa (Kanagawa: Tokai University Press), 129–320.

Kudo, I., Yoshimura, T., Yanada, M., and Matsunaga, K. (2000). Exhaustion of nitrate terminates a phytoplankton bloom in Funka Bay, Japan: change in SiO_4:NO_3 consumption rate during the bloom. *Mar. Ecol. Prog. Ser.* 193, 45–51. doi: 10.3354/meps193045

Latasa, M. (2007). Improving estimation of phytoplankton class abundance using CHEMTAX. *Mar. Ecol. Prog. Ser.* 329, 13–21. doi: 10.3354/meps329013

Lopez-Sandval, D. C., Fernández, A., and Marañón, E. (2011). Dissolved and particulate primary production along a longitudinal gradient in the Mediterranean sea. *Biogeosciences* 8, 815–825. doi: 10.5194/bg-8-815-2011

Mackey, M. D., Mackey, D. J., Higgins, H. W., and Wright, S. W. (1996). CHEMTAX— a program for estimating class abundances from chemical markers: application to HPLC measurements of phytoplankton. *Mar. Ecol. Prog. Ser.* 144, 265–283. doi: 10.3354/meps144265

Marañón, E., Cermeño, P., and Fernández, E. (2004). Significance and mechanisms of photosynthetic production of dissolved organic carbon in a coastal eutrophic ecosystem. *Limnol. Oceanogr.* 49, 1652–1666. doi: 10.4319/lo.2004.49.5.1652

Mari, X., and Burd, A. (1998). Seasonal size spectra of transparent exopolymer particles (TEP) in a coastal sea and comparison with those predicted using coagulation theory. *Mar. Ecol. Prog. Ser.* 163, 63–76. doi: 10.3354/meps163063

Mari, X., Passow, U., Migon, C., Burd, B. A., and Legendre, L. (2017). Transparent exopolymer particles: effects on carbon cycling in the ocean. *Prog. Oceanogr.* 151, 13–37. doi: 10.1016/j.pocean.2016.11.002

Midorikawa, T., Iwano, S., Kazuhiro, S., Takano, H., Kamiya, H., Ishii, M., et al. (2003). Seasonal changes in oceanic pCO_2 in the Oyashio region from winter to spring. *J. Oceanogr.* 59, 871–882. doi: 10.1023/b.joce.0000009577.40878.d4

Montégut, C. B., Madec, G., Fischer, A. S., Lazar, A., and Indicone, D. (2004). Mixed layer depth over the global ocean: an examination profile data and a profile-based climatology. *J. Geophys. Res.* 109:C12003. doi: 10.1029/2004jc002378

Myklestad, S. M. (1995). Release of extracellular products by phytoplankton with special emphasis on polysaccharides. *Sci. Total Environ.* 165, 155–164. doi: 10.1016/0048-9697(95)04549-g

Nelson, D. L., and Tréguer, P. (1992). Role of *silicon* as a limiting nutrient to Antarctic diatoms: evidence from kinetic studies in the Ross Sea ice-edge zone. *Mar. Ecol. Prog. Ser.* 80, 255–264.

Ogawa, H., Amagai, Y., Koike, I., Kaiser, K., and Benner, R. (2001). Production of refractory dissolved organic carbon matter by bacteria. *Science* 292, 917–920. doi: 10.1126/science.1057627

Passow, U. (2002a). Transparent exopolymer particles (TEP) in aquatic environments. *Prog. Oceanogr.* 55, 287–333. doi: 10.1021/es5041738

Passow, U. (2002b). Production of transparent exopolymer particles (TEP) by phyto- and bacterioplankton. *Mar. Ecol. Prog. Ser.* 236, 1–12. doi: 10.3354/meps236001

Passow, U., and Alldredge, A. L. (1995). A dye-binding assay for the spectrophotometric measurement of transparent exopolymer particles (TEP). *Limnol. Oceanogr.* 40, 1326–1335. doi: 10.4319/lo.1995.40.7.1326

Passow, U., Kozlowski, W., and Vernet, M. (1995). Palmer LTER: temporal variability of transparent exopolymer particles in Arthur Harbor during the 1994–1995 growth season. *Antarct. J. Rev.* 1995, 265–266.

Passow, U., Shipe, R. F., Murray, A., Pak, D. K., Brzezinski, M. A., and Alldredge, A. L. (2001). The origin of transparent exopolymer particles (TEP) and their

role in the sedimentation of particulate matter. *Cont. Shelf Res.* 21, 327–346. doi: 10.1016/S0278-4343(00)00101-1

Prieto, L., Ruiz, J., Echevarría, F., García, C. M., Bartual, A., Gálvez, J. A., et al. (2002). Scales and processes in the aggregation of diatom blooms: high time resolution and wide size range records in a mesocosm study. *Deep Sea Res. II* 49, 1233–1253. doi: 10.1016/S0967-0637(02)00024-9

Prieto, L., Sommer, F., Stibor, H., and Koeve, W. (2001). Effects of planktonic copepods on transparent exopolymer particles (TEP) abundance and size spectra. *J. Plankton Res.* 23, 515–525. doi: 10.1098/plank/23.5.515

Radić, T., Kraus, R., Fuks, D., Radić, J., and Pećar, O. (2005). Transparent exopolymer particles distribution in the northern Adriatic and their relation to microphytoplankton biomass composition. *Sci. Total Environ.* 353, 151–161. doi: 10.1007/s12562-010-0265-z

Ramaiah, N., Takeda, S., Furuya, K., Yoshimura, T., Nishioka, J., Aono, T., et al. (2005). Effect of iron enrichment on the dynamics of transparent particles in the western subarctic Pacific. *Prog. Oceanogr.* 64, 253–261. doi: 10.1016/j.pocean.2005.02.012

Round, F. E., Crawford, R. M., and Mann, D. G. (2007). *The Diatoms Biology & Morphology of the Genera*. Cambridge: Cambridge University Press.

Saito, H., Tsuda, A., and Kasai, H. (2002). Nutrient and plankton dynamics in the Oyashio region of the western subarctic Pacific Ocean. *Deep Sea Res. II* 49, 5463–5486. doi: 10.1016/s0967-0645(02)00204-7

Sakurai, Y. (2007). An overview of the Oyashio ecosystem. *Deep Sea Res. II* 54, 2526–2542. doi: 10.1016/j.dsr2.2007.02.007

Scott, F. J., and Marchant, H. J. (2005). *Antarctic Marine Protists.* Canberra, ACT: Goanna Print.

Smith, D. C., Steward, G. F., Long, R. A., and Azam, F. (1995). Bacterial mediation of carbon fluxes during a diatom bloom in a mesocosm. *Deep Sea Res. II* 42, 75–97. doi: 10.1016/0967-0645(95)00005-B

Sugimoto, K., Fukuda, H., Baki, M. A., and Koike, I. (2007). Bacterial contribution to formation of transparent exopolymer particles (TEP) and seasonal trends in coastal waters of Sagami Bay, Japan. *Aquat. Microb. Ecol.* 46, 31–41. doi: 10.3354/ame046031

Suzuki, K., Hattori-Saito, A., Sekiguchi, Y., Nishioka, J., Shigemitsu, M., Isada, T., et al. (2014). Spatial variability in iron nutritional status of large diatoms in the Sea of Okhotsk with special reference to the Amur River discharge. *Biogeosciences* 11, 2503–2517. doi: 10.5194/bg-11-2503-2014

Suzuki, K., Hinuma, A., Saito, H., Kiyosawa, H., Liu, H., Saino, T., et al. (2005). Responses of phytoplankton and heterotrophic bacteria in the northwest subarctic Pacific to *in situ* iron fertilization as estimated by HPLC pigment analysis and flow cytometry. *Prog. Oceanogr.* 64, 167–187. doi: 10.1016/pocean.2005.02.007

Suzuki, K., Kuwata, A., Yoshie, N., Shibata, A., Kawanobe, K., and Saito, H. (2011). Population dynamics of phytoplankton, heterotrophic bacteria, and viruses during the spring bloom in the western subarctic Pacific. *Deep Sea Res. I* 58, 575–589. doi: 10.1016/j.dsr.2011.03003

Suzuki, K., Saito, H., Isada, T., Hattori-Saito, A., Kiyosawa, H., Nishioka, J., et al. (2009). Community structure and photosynthetic physiology of phytoplankton in the northwest subarctic Pacific during an *in situ* iron fertilization experiment (SEEDS-II). *Deep Sea Res. II* 56, 2733–2744. doi: 10.1016/j.dsr2.2009.06001

Suzuki, K., Tsuda, A., Kiyosawa, H., Takeda, S., Nishioka, J., Saino, T., et al. (2002). Grazing impact of microzooplankton on a diatom bloom in a mesocosm as estimated by pigment-specific dilution technique. *J. Exp. Mar. Biol. Ecol.* 271, 99–120. doi: 10.1016/s0022-0981(02)00038-2

Takahashi, T., Sutherland, S. C., Sweeney, C., Poisson, A., Metzl, N., Tilbrook, B., et al. (2002). Global sea-air CO_2 flux based on climatological surface ocean pCO_2, and seasonal biological and temperature effects. *Deep-Sea Res. II* 49, 1601–1622. doi: 10.1016/s0967-0645(02)00003-6

Thornton, D. C. O., Fejes, E. M., DiMarco, S. F., and Clancy, K. M. (2007). Measurement of acid polysaccharides in marine and freshwater samples using Alcian blue. *Limol. Oceanogr. Methods* 5, 73–87. doi: 10.4319/lom.2007.5.73

Tomas, C. R., Syvertsen, E. E., Steidinger, K. A., Tangen, K., Throndsen, J., and Heimdal, B. R. (1997). *Identifying Marine Phytoplankton.* London: Academic Press.

Van Heukelem, L., and Thomas, C. S. (2001). Computer-assisted high-performance liquid chromatography method development with applications to the isolation and analysis of phytoplankton pigments. *J. Chromatogr. A* 910, 31–49. doi: 10.1016/s0378-4347(00)00603-4

Wurl, O., Miller, L., and Vagle, S. (2011). Production and fate of transparent exopolymer particles in the ocean. *J. Geophys. Res.* 116:C00H13. doi: 10.1029/2011jc007342

Yamada, Y., Fukuda, H., Inoue, K., Kogure, K., and Nagata, T. (2013). Effects of attached bacteria on organic aggregate setting velocity in seawater. *Aquat. Microb. Ecol.* 70, 261–272. doi: 10.3354/ame01658

Young, J. R., Geisen, M., Cros, L., Kleijne, A., Sprengel, C., Probert, I., et al. (2003). *A Guide to Extant Coccolithophore Taxonomy*. Bremerhaven: Druckstudio Digital Concept.

Conflict of Interest Statement: The authors declare that the research was conducted in the absence of any commercial or financial relationships that could be construed as a potential conflict of interest.

frontiers in Microbiology

ORIGINAL RESEARCH
published: 31 January 2017
doi: 10.3389/fmicb.2016.02159

Horizontal and Vertical Distributions of Transparent Exopolymer Particles (TEP) in the NW Mediterranean Sea Are Linked to Chlorophyll *a* and O_2 Variability

*Eva Ortega-Retuerta *, Maria M. Sala, Encarna Borrull, Mireia Mestre, Fran L. Aparicio, Rachele Gallisai, Carolina Antequera, Cèlia Marrasé, Francesc Peters, Rafel Simó and Josep M. Gasol*

Biologia Marina i Oceanografia, Consejo Superior de Investigaciones Científicas, Institut de Ciències del Mar, Barcelona, Spain

OPEN ACCESS

Edited by:
Kai Ziervogel, University of New Hampshire, USA

Reviewed by:
Lars-Eric Heimbürger, Mediterranean Institute of Oceanography (CNRS), France
Daniel Conrad Ogilvie Thornton, Texas A&M University, USA
Astrid Anne-Marie Gärdes, Leibniz Center for Tropical Marine Ecology, Germany

***Correspondence:**
Eva Ortega-Retuerta
ortegaretuerta@icm.csic.es

Specialty section:
This article was submitted to Aquatic Microbiology, a section of the journal Frontiers in Microbiology

Received: *12 September 2016*
Accepted: *22 December 2016*
Published: *31 January 2017*

Citation:
Ortega-Retuerta E, Sala MM, Borrull E, Mestre M, Aparicio FL, Gallisai R, Antequera C, Marrasé C, Peters F, Simó R and Gasol JM (2017) Horizontal and Vertical Distributions of Transparent Exopolymer Particles (TEP) in the NW Mediterranean Sea Are Linked to Chlorophyll a and O_2 Variability. Front. Microbiol. 7:2159. doi: 10.3389/fmicb.2016.02159

Transparent Exopolymer Particles (TEP) are relevant in particle and carbon fluxes in the ocean, and have economic impact in the desalination industry affecting reverse osmosis membrane fouling. However, general models of their occurrence and dynamics are not yet possible because of the poorly known co-variations with other physical and biological variables. Here, we describe TEP distributions in the NW Mediterranean Sea during late spring 2012, along perpendicular and parallel transects to the Catalan coast. The stations in the parallel transect were sampled at the surface, while the stations in the perpendicular transect were sampled from the surface to the bathypelagic, including the bottom nepheloid layers. We also followed the short-term TEP dynamics along a 2-day cycle in offshore waters. TEP concentrations in the area ranged from 4.9 to 122.8 and averaged 31.4 ± 12.0 μg XG eq L^{-1}. The distribution of TEP measured in transects parallel to the Catalan Coast correlated those of chlorophyll *a* (Chla) in May but not in June, when higher TEP-values with respect to Chla were observed. TEP horizontal variability in epipelagic waters from the coast to the open sea also correlated to that of Chla, O_2 (that we interpret as a proxy of primary production) and bacterial production (BP). In contrast, the TEP vertical distributions in epipelagic waters were uncoupled from those of Chla, as TEP maxima were located above the deep chlorophyll maxima. The vertical distribution of TEP in the epipelagic zone was correlated with O_2 and BP, suggesting combined phytoplankton (through primary production) and bacterial (through carbon reprocessing) TEP sources. However, no clear temporal patterns arose during the 2-day cycle. In meso- and bathypelagic waters, where phytoplanktonic sources are minor, TEP concentrations (10.1 ± 4.3 μg XG eq l^{-1}) were half those in the epipelagic, but we observed relative TEP increments coinciding with the presence of nepheloid layers. These TEP increases were not paralleled by increases in particulate organic carbon, indicating that TEP are likely to act as aggregating agents of the mostly inorganic particles present in these bottom nepheloid layers.

Keywords: transparent exopolymer particles, chlorophyll *a*, bacteria, carbon, Mediterranean Sea

INTRODUCTION

Transparent Exopolymer Particles (TEP) are defined as a subclass of gel-like organic particles, mainly composed by acidic polysaccharides, that are stainable with Alcian Blue (Alldredge et al., 1993). These particles are widespread in aquatic ecosystems, and their study in the ocean has biogeochemical and applied interests. Due to their high stickiness, TEP act as gluing agents for other particles to form larger aggregates susceptible to sink in the water column, hence stimulating the biological carbon pump (Passow et al., 2001; Burd and Jackson, 2009). However, TEP themselves have low density, and when unballasted, they can ascend through the water column (Azetsu-Scott and Passow, 2004) and accumulate in the sea surface microlayer (Wurl et al., 2011) where they can constitute a major source of primary aerosols (Orellana et al., 2011). The study of TEP has also gained interest in the water desalination industry since they are major agents of reverse osmosis membrane fouling (Berman, 2013). Given the ecological and economic relevance of TEP, there is a need to improve the knowledge about how these substances are distributed in the field and what factors affect their dynamics.

TEP were first observed, and have mostly been described, associated with phytoplankton blooms, in the field (Alldredge et al., 1993; Van Oostende et al., 2012) or in mesocosms and controlled chambers (Engel et al., 2015). From these studies we know that phytoplankton are a major source of TEP and TEP precursors in the sea. However, the relationship between phytoplankton and TEP varies depending on phytoplankton composition and physiology (Passow, 2002; Klein et al., 2011), and environmental variables such as nutrient availability (Mari et al., 2001), turbulence (Pedrotti et al., 2010), or UV irradiation (Ortega-Retuerta et al., 2009a). Therefore, even when phytoplankton are the likely main source for TEP, this is not necessarily translated into predictable relationships in the field between TEP and chlorophyll *a* (Chla), the most used proxy for phytoplankton biomass or production. Elucidating the sources of variability in the TEP-Chla relationships would help predicting the occurrence and dynamics of TEP in the ocean.

In addition to the role of phytoplankton, there are other sources of TEP in the sea, such as macroalgae (Thornton, 2004) or zooplankton (Prieto et al., 2001). Also bacteria are known to modify TEP distributions in the sea in various ways: They colonize and degrade TEP that are released by other organisms (Bar-Zeev et al., 2011; Taylor et al., 2014), thus acting as TEP sinks. Bacteria can also directly release TEP (Ortega-Retuerta et al., 2010) so they constitute TEP sources themselves. Finally, bacterial interactions with phytoplankton mediate TEP release (Van Oostende et al., 2013) and induce changes on their formation rates and properties such as their stickiness (Rochelle-Newall et al., 2010). The relative importance of these mechanisms governing the TEP dynamics in aquatic habitats, specifically in the Mediterranean Sea, remains unexplored.

The published information on TEP distributions in the Mediterranean Sea is particularly scarce (Prieto et al., 2006; Ortega-Retuerta et al., 2010; Bar-Zeev et al., 2011). The few published studies, however, concur in that TEP stocks are high when compared to other oceans. For instance, maximum TEP concentrations (up to 11,000 μg Xeq. L^{-1} in surface waters) were observed in Adriatic Sea samples (Passow, 2002). Exceptionally high in the Mediterranean Sea are the relative TEP concentrations with respect to Chla concentrations; higher TEP/Chla ratios than in other ocean basins have been taken to suggest that TEP are an important fraction of the particulate organic matter pool, and likely important drivers of carbon and particle fluxes in this oligotrophic sea.

Here, we report for the first time TEP distributions in the Catalan Sea (NW Mediterranean). Our specific goals were: (1) to determine the potential drivers of TEP from a wide range of physicochemical and biological variables and (2) to examine the variability in the TEP-Chla relationship across multiple spatial and temporal scales.

MATERIALS AND METHODS

Study Site and Sampling

Samples were taken during the cruises NEMO1, NEMO2, and SUMMER2 in Mediterranean waters between the Catalan Coast and north of Majorca Island on board the Spanish RV "García del Cid" (**Figure 1**). Transects parallel to the Catalan coast (following the bathymetry line at 40 m bottom depth) between Barcelona and Blanes were conducted in May 10th (transect 1) and June 11th (transect 2, **Figure 1**). During these transects, surface (2 m) samples were taken every hour from the underway continuous flow with the ship moving at ∼7 knots, so that each sample was taken approximately at every 12 km. A coast-to-offshore transect was performed during NEMO1, from May 11th to 20th, including stations located in the shelf (Stations 1 and 2), slope (stations 3, 4, and 5) and basin (stations 6, 8, and 9). Station 7 was sampled during NEMO2, 1 month later (June 12th). Water samples in these transects were collected using a rosette (12 Niskin bottles with external spring, 12 L each) coupled to a Sea-Bird Conductivity-Temperature-Depth profiler, a WET Labs C-Star transmissometer and a SeaPoint optical backscatter sensor. Up to six depths were sampled from each station, from surface to bottom (down to 2300 m) waters including the surface, the O_2 maximum, the deep chlorophyll maximum (DCM) when present, mesopelagic waters, and bottom nepheloid layers.

The 2-day lagrangian study (SUMMER2 cruise) was conducted aboard R/V "García del Cid" from 22nd to 24th May at ca. 45 nautical miles from the coast, within the core of a cyclonic eddy over a water-column depth of ca. 2000 m. A Lagrangian drifter was deployed to track the movement of the upper 15-m water layer. Each drifter consisted of a spherical floatable enclosure that contained a GPS and an emitter, from which 10 m cylindrical drogues hanged 5 m below the sphere. The drifters sent their position every 30 min, and all ship operations were conducted next to them. Samples were taken with the rosette every 4 h at six depths from surface to 200 m.

Chemical and Biological Analyses

TEP were analyzed following the colorimetric method proposed by Passow and Alldredge (1995). Samples (250–500 mL) were filtered through 25 mm diameter 0.4 μm pore size Polycarbonate filters (DHI) at low pressure (100 mm Hg). The filters were

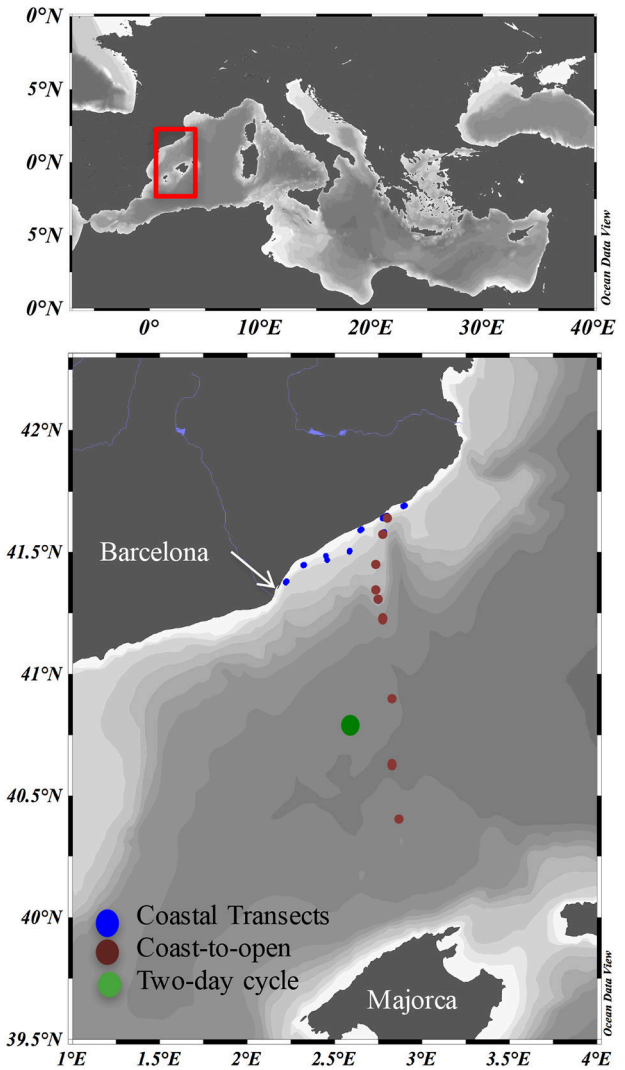

FIGURE 1 | Study area. Blue symbols, Coastal transects. symbols, Coast-to-open sea transect. Green symbol, 2-day cycle.

stained with 500 μL of Alcian Blue (0.02%, pH 2.5) for 5 s and rinsed with MilliQ water. The filters were soaked in 80% sulfuric acid for 3 h and the absorbance of the extract was determined at 787 nm in a Varian Cary spectrophotometer. Duplicates were taken for each sample. Previous analyses have shown a CV of 13% between TEP replicated measurements with this method (details not shown). We have calculated an average range of ±30.9% between duplicates in our dataset. Duplicate blanks (empty filters stained with alcian blue) were also taken at every station. The Alcian Blue dye solution was calibrated just before the cruise using a standard solution of xanthan gum processed with a tissue grinder and subsequently filtered through two sets of filters (five points in triplicate).

Chla concentration was determined by filtering 150 mL of seawater on GF/F filters (Whatman), extracting the pigment in acetone (90% v:v) in the dark at 4°C for 24 h, and measuring fluorescence with a Turner Designs fluorometer.

Analyses of dissolved inorganic nutrient concentrations [nitrate (NO_3), nitrite (NO_2), phosphate (PO_4), and silicate (SiO_2)], were done by standard segmented flow analyses with colorimetric detection (Hansen and Grasshoff, 1983) using an Seal Analytical AA3 High Resolution AutoAnalyzer.

Particulate organic carbon (POC) was measured by filtering 1000 mL of seawater on pre-combusted GF/F glass fiber filters (4 h, 450°C). The filters were frozen in liquid nitrogen and kept at −80°C until analysis. Prior to analysis, the filters were dried at 60°C for 24 h. Then the filters were dried again and analyzed with a C:H:N autoanalyser (Perkin-Elmer 240).

For bacterial abundance samples, 1.8 ml were preserved with 1% paraformaldehyde + 0.05% glutaraldehyde (final conc.) and frozen in liquid nitrogen until processed in the lab. Bacterial abundance (BA) was analyzed by flow cytometry (FACSCalibur cytometer, Becton and Dickinson) after staining with SYBRGreen I (Molecular probes). Bacteria were detected by their signature in a plot of side scatter vs. FL1 (green fluorescence) as explained in Gasol and del Giorgio (2000).

Bacterial Production (BP) was estimated using the ^{3}H-leucine incorporation method described by Kirchman et al. (1985). Three 1.2-mL aliquots and two trichloroacetic acid (TCA)-killed controls (5% final concentration) of each sample were incubated with 40 nmol $L^{-1,3}$H-leucine (epipelagic samples) or 80 nmol $L^{-1,3}$H-leucine (meso- and bathy-pelagic samples). The incubations were carried out in a water bath at *in situ* temperature in the dark. The incorporation was stopped by adding cold TCA (5% final concentration) to the vials, and samples were kept at −20°C until processing as described by Smith and Azam (1992). Radioactivity was then counted on a Beckman scintillation counter. Leucine incorporation rates were converted into carbon production using the conversion factor of 1.55 kg C produced per mole of leucine incorporated and considering no isotope dilution (Simon and Azam, 1989).

Given that TEP are frequently enriched in fucose (Zhou et al., 1998), we determined fucosidase activity using a fluorogenic substrate, as in Sala et al. (2016). Each sample (350 μl) was pipetted in quadriplicates into 96 black well-plates, with 50 μl of the substrate 4-methylumbelliferyl β-D-fucoside (Sigma-Aldrich) at a final concentration of 125 μM. Fluorescence was measured immediately after addition of the substrate and after incubations, at *in situ* temperature and in the dark, for 15, 30 min, 1, 3, and 5 h. The measurements were done with a Modulus Microplate (DISMED, Turner BioSystems) at 450 nm excitation and 365 nm emission wavelengths. The increase of fluorescence units during the period of incubation was converted into enzymatic activity with a standard curve prepared with 4-methylumbelliferone (MUF, Sigma-Aldrich).

Statistical Analyses

We used the Statistica 7.0 software package to test the potential drivers of TEP distributions across the different spatial and timescales. We performed pairwise Pearson correlations between TEP concentrations and the following physico-chemical and biological variables: Temperature, salinity, turbidity, O_2, nutrients (NO_3, PO_4, SiO_4), particulate organic carbon (POC) and nitrogen (PON), chlorophyll *a* (Chla), bacterial abundance

(BA), bacterial production (BP), and extracellular fucosidase activity. Data were log_{10}-transformed and Bonferroni-corrected when needed.

RESULTS

Horizontal TEP Distribution along the Catalan Coast

In the coastal transects, TEP concentrations ranged from 27.4 to 122.8 μg XG eq L^{-1}, and were overall higher in June (average 83.7 ± 23.9 μg XG eq L^{-1}) than in May (average 56.1 ± 25.8 μg XG eq L^{-1}; **Table 1**). In contrast, Chla concentrations were overall higher in May (0.65 ± 0.55 μg L^{-1}) than in June (0.24 ± 0.14 μg L^{-1}) and BP rates were similar in the two transects (0.18 ± 0.16 μg C L^{-1} h^{-1}, ranging from 0.91 to 10.97, in May, 0.14 ± 0.21 μg C L^{-1} h^{-1}, ranging from 0.50 to 14.79 in June). Dissolved inorganic nitrogen (DIN, nitrate+nitrite+ammonia) averaged 0.65 μM in May, ranging from 0.19 to 1.28 μM, and averaged 0.41 μM in June, ranging from 0.21 to 1.02 μM. Dissolved phosphate concentrations averaged 0.07 μM in May, ranging from 0.05 to 0.10 μM, and averaged 0.06 μM in June, ranging from 0.05 to 0.10 μM (**Supplementary Figure 2**). In May, TEP showed maxima in waters near Barcelona and north of the outflow of the Tordera River (**Figure 2A**). In these locations DIN concentration was 1.2 μM and phosphate concentration was 0.093 μM, two to eight-fold higher than in the rest of the stations. TEP-values were significantly correlated to Chla concentration ($r = 0.93$, $p = 0.0003$, $n = 7$) and marginally correlated to BP ($r = 0.72$, $p = 0.06$, $n = 7$, **Figure 3**). In June, TEP distributions showed maxima south of the outflow of the Tordera River, and were uncorrelated to Chla (**Figure 2B**) nor to BP. The TEP/Chla ratios were markedly higher in June (434.0 ± 197.5) than in May (136.7 ± 91.0, **Table 1**).

Horizontal TEP Distribution from Coastal to Open Sea Waters

The concentration of TEP in the studied coast-to-open sea transect ranged from 4.9 to 54.2 μg XG eq L^{-1} with a mean concentration of 18.7 ± 11.4 μg XG eq L^{-1}.

We calculated depth-averaged TEP concentrations in epipelagic waters (0–200 m) in an attempt to look at horizontal distribution patterns. Depth-averaged epipelagic TEP ranged from 9.9 to 24.9 μg XG eq L^{-1} (**Figure 4A**). TEP concentrations were highest near the coast and 60 km offshore, at the slope to basin transition (station 6, **Figure 4A**). The same horizontal patterns were observed for Chla, O_2, BP (**Figure 4B**), rendering significant correlations with TEP ($r = 0.7$, $p < 0.05$, $n = 9$). TEP were likewise related to POC ($r = 0.9$, $p < 0.01$, $n = 9$) and to the ratio between BP and O_2($r = 0.7$, $p < 0.05$, $n = 9$),

TABLE 1 | Ranges of TEP concentration and TEP/Chla ratios in the different transects, depth profiles and diel cycles presented here.

	TEP (μg XG eq L^{-1})	TEP/Chla	*n*
Coastal transect May	27.4–92.1	57.7–283.4	7
Coastal transect June	49.8–122.8	98.4–706.7	7
Epipelagic	4.9–54.2	18.1–316.8	36
Meso- and bathy-pelagic	5.2–19.0	–	23
2-day cycle	5.7–55.9	15.3–1217.6	78

n, number of samples.

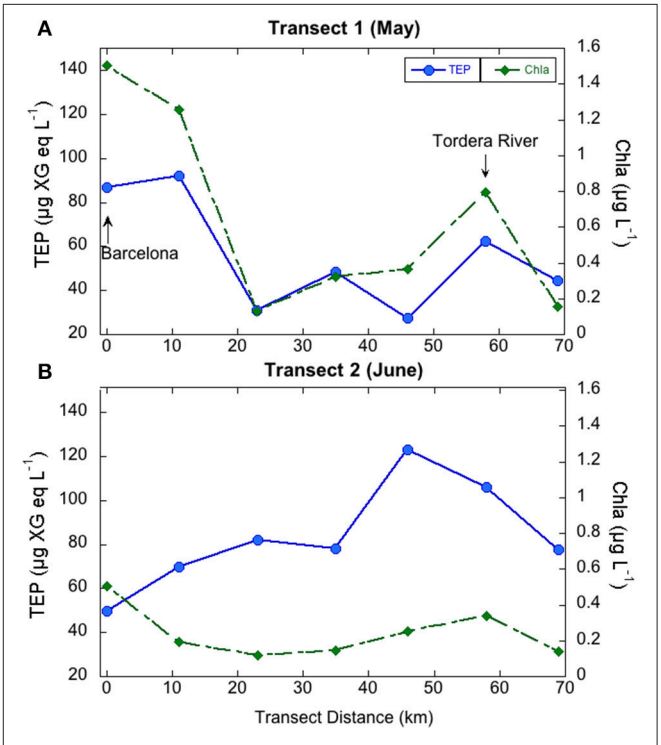

FIGURE 2 | Variations of TEP (blue symbols) and chlorophyll *a* (green symbols) concentration in the coastal transects performed in May (A) and June **(B)**.

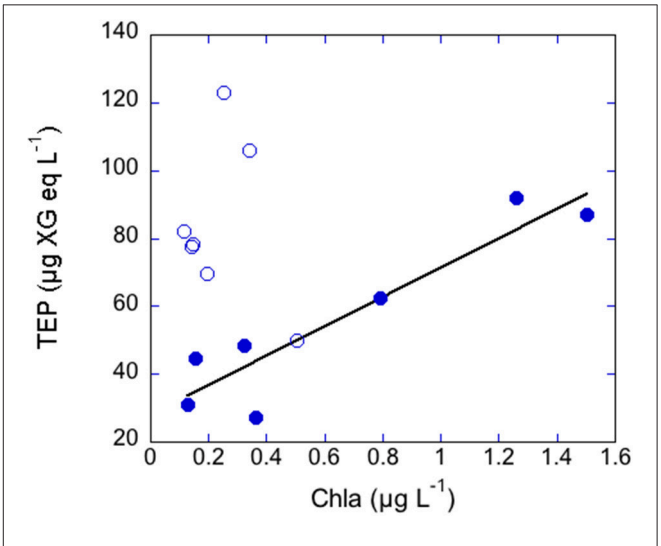

FIGURE 3 | Scatterplot between Chla and TEP concentrations in the coastal transects performed in May (filled symbols) and June (open symbols). TEP were related to Chla in May ($r = 0.93$, $p < 0.001$, $n = 7$).

which can be considered a proxy of bacterial reprocessing of photosynthetically fixed carbon.

TEP Vertical Distribution in Epipelagic Waters

TEP vertical distribution patterns were variable among stations. Shelf waters exhibited mixed temperature and salinity profiles (**Figure 5**) and other chemical and biological variables were also quite uniform in the vertical profile. In these stations, Chla ranged from 0.10 to 0.38 μg L^{-1}, BP ranged from 0.012 to 0.078 μg C L^{-1} h^{-1}, and POC ranged from 3.7 to 7.2 μM. TEP vertical distributions were also quite homogenous from surface to the bottom, averaging 24.9 ± 3.0 and 19.7 ± 2.5 μg XG eq L^{-1} in stations 1 and 2, respectively (**Figure 5**). Conversely, well-developed DCM were detected in slope and basin waters between 50 and 60 m, with Chla concentrations ranging from 0.41 (station 5, slope) to 1.73 (station 6, basin) μg L^{-1}. The TEP/Chla ratios ranged from 16.8 (station 6, DCM) to 316.0 (station 3, surface). They were generally higher at the surface and lower at the DCM. Bacterial production ranged from 0.005 to 0.065 μg C L^{-1} h^{-1} and the vertical distribution varied between stations: at the slope stations, BP was highest at the surface and subsurface, while in basin stations BP showed a bimodal profile, with peaks at the surface and at the DCM. POC concentrations, that ranged from 2.9 to 11.5 μM, showed similar distributions than TEP in the slope stations (with surface or subsurface peaks) but covaried with Chla, with maxima at the DCM, in the basin stations. TEP also showed marked vertical changes in slope and basin waters (**Figure 5**): they generally peaked at the surface (slope stations 3 and 5) or at the subsurface (slope station 4 and basin stations). These subsurface maxima were located between 25 and 55 m and showed values from 33.0 to 54.2 μg XG eq L^{-1} (mean concentration 39.6 ± 10.3 μg XG eq L^{-1}). TEP maxima were always located shallower than the DCM and coincided with O_2 maxima, and nutrient minima (**Figure 5**). At the slope, TEP maxima were also coincident with BP and POC maxima, while the Chla maximum was always deeper. By contrast, in the basin, BP and POC coincided with Chla while TEP and O_2 peaked at shallower depths.

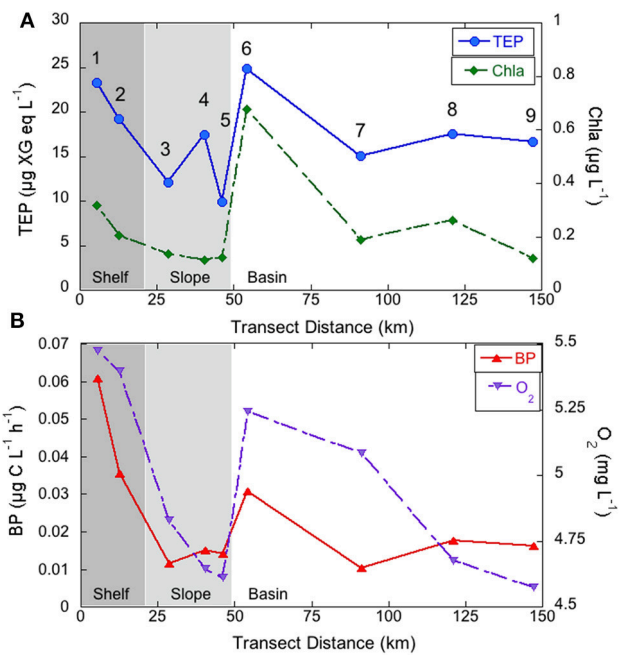

FIGURE 4 | Depth-averaged TEP concentration (μg XG eq L^{-1}) and Chla (μg L^{-1}) (A) and BP (μg C L^{-1} h^{-1}) and O_2 (mg L^{-1}) **(B)** in epipelagic waters of the coast to open sea transect.

Drivers of TEP Vertical Distribution

We assessed which were the environmental drivers of TEP vertical distributions in epipelagic waters performing Pearson correlation tests between TEP concentrations and a number of physical (temperature, salinity, turbulence), chemical (nutrients, O_2), and biological (Chla, BP, bacterial abundance, bacterial fucosidase activity) variables (**Table 2**). Since vertical distribution patterns of TEP and biological variables such as Chla and BP differed among shelf, slope and basin stations, we separated shelf stations from the others for the analysis. TEP was never significantly correlated to Chla. In shelf waters, TEP was not related to any other physicochemical or biological parameter. In slope and basin waters, TEP was significantly and positively correlated to O_2, BP and the ratio BP/O_2, and significantly negatively correlated to nutrients and N/P ratios (**Table 2**).

TEP Vertical Distribution in Mesopelagic and Bathypelagic Waters

TEP concentrations were half lower in meso- and bathypelagic waters with respect to the epipelagic, showing minima between

TABLE 2 | Results of Pearson correlations between TEP concentration and different physical, chemical, and biological variables measured in epipelagic waters during the NEMO cruises at the slope and basin stations.

Dependent variable	Independent variable	*r*	*p*
SLOPE AND BASIN STATIONS (*n* = 25)			
TEP	Temperature	0.55	0.004
	Turbidity	0.68	0.000
	O_2	0.83	0.000
	NO_3	−0.82	0.000
	PO_4	−0.58	0.005
	N/P	−0.56	0.008
	SiO_4	−0.73	0.003
	POC	0.79	0.000
	Chla	ns	
	Bact. Ab.	ns	
	Bact. Prod.	0.70	0.000
	Bact. Fuc.	ns	
	BP/O_2	0.68	0.000

r, correlation coefficient; p, level of significance.

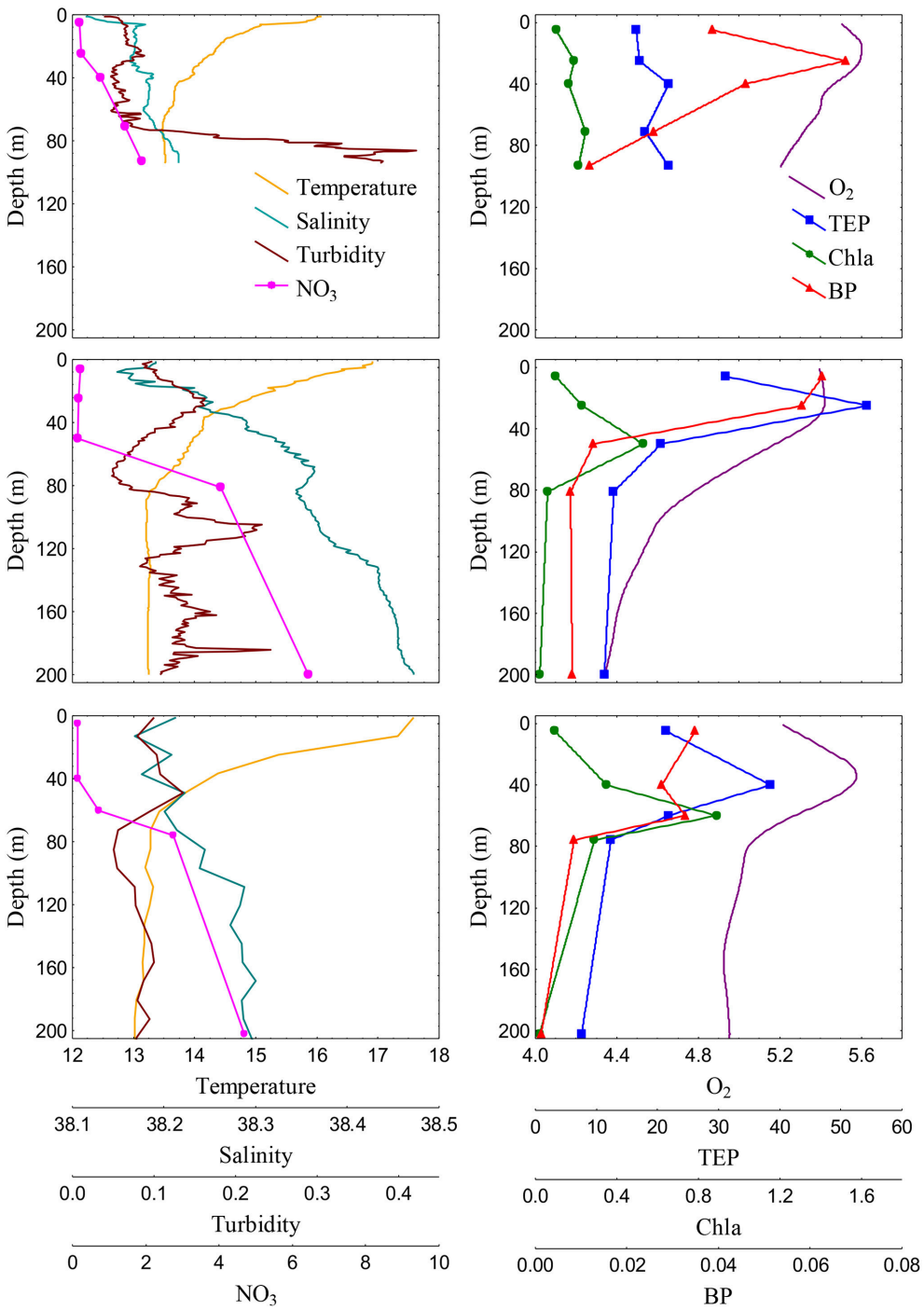

FIGURE 5 | Vertical profiles of Temperature (°C), salinity (practical salinity units), turbidity (FTU) and NO_3 (μM) (left panels) and O_2 (mg L^{-1}), TEP concentration (μg XG eq L^{-1}), Chla (μg L^{-1}) and BP (μg C L^{-1} h^{-1}) (right panels) in epipelagic waters of station 2 (shelf, upper panels), station 4 (slope, middle panels), and station 8 (basin, bottom panels).

4.9 and 11.2 μg XG eq L^{-1}. By contrast, relative TEP increases were observed in waters near the bottom in all slope and basin stations, parallel to increases in turbidity (proxy of total particle concentration).

TEP in meso- and bathypelagic waters were only significantly related to turbidity ($r = 0.54$, $p < 0.01$ $n = 23$), indicative of the relevance of bottom nepheloid layers (BNL). Remarkably, TEP were uncorrelated with POC in these layers. No significant

correlation was found between TEP and BP, but a correlation with bacterial fucosidase activity ($r = 0.45$, $p < 0.05$ $n = 23$) could be observed.

Diel TEP Variations

The same surface water mass was sampled over time during the 2-day lagrangian study in the SUMMER2 cruise, as confirmed by plotting depth-averaged temperature and salinity values of each CTD cast (**Supplementary Figure 1**), except for the last two casts were a warmer water mass was likely sampled. We did not detect a recurrent diel pattern of TEP or of any other biological variables such as Chla or BP (**Figure 6**), even though these variables varied highly during the cycle. Chla showed subsurface maxima of 0.75–1.33 μg L^{-1} between 40 and 54 m. TEP concentrations ranged ten-fold, from 5.7 to 55.9 μg XG eq L^{-1} (average 34.1 ± 5.7 μg XG eq L^{-1}). TEP maxima were situated between 25 and 47 m with highest values during the night (10 p.m. and 2 a.m.). These maxima were always shallower than the DCM, and were again vertically coincident with O_2 and BP maxima. TEP concentrations were not significantly correlated to Chla, but a significant correlation was observed with O_2 ($r = 0.70$, $p = 0.000$, $n = 78$), BP ($r = 0.48$ $p = 0.000$, $n = 78$), and the ratio BP/O_2 ($r = 0.44$, $p = 0.0001$, $n = 78$). We looked at temporal variations of TEP, Chla, O_2, and BP using depth-averaged values for all the epipelagic depths. Diel dynamics of TEP, Chla, O_2, and BP were not coupled, but we detected Chla and O_2 increases that were followed by a TEP increase after 4–12 h (**Figure 6**). However, lagged correlations between these variables, using either maxima or integrated values, were not significant.

DISCUSSION

TEP dynamics can affect particle aggregation rates because of stickiness, and particle sinking rates due to their low density. Thus, determining and predicting TEP dynamics is crucial if we want to accurately estimate carbon and particle fluxes. The TEP-values observed in this study are within the range of data published for Mediterranean Sea waters (Prieto et al., 2006; Ortega-Retuerta et al., 2010; Bar-Zeev et al., 2011) and at the lower range of other coastal ocean areas (Klein et al., 2011; Van Oostende et al., 2012). By contrast, the TEP/Chla ratios were in the upper range of those previously published for other ocean basins (Prieto et al., 2006), except for those measured in the Mediterranean Sea (Ortega-Retuerta et al., 2010; Bar-Zeev et al., 2011).

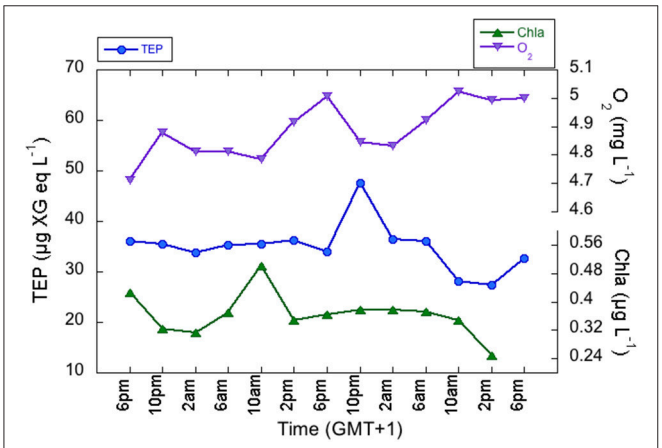

FIGURE 6 | Diel variations of depth-averaged TEP (blue circles), Chlorophyll a (green triangles), O_2 (purple triangles) concentration.

TEP Variation in the Coastal Transects

TEP maxima were observed near the city of Barcelona and near the outflow of the Tordera River, areas with higher nutrient concentrations. Coincidentally, there are two desalination plants located at the mouth of the Llobregat (next to Barcelona) and Tordera Rivers, whose feedwater intake pipes are located between 800 and 2200 m from the coast and at 30 m depth, although they are not always operative. Given that TEP are directly linked to membrane fouling, it is important to be able to predict TEP occurrence in these locations. In May, TEP variations in these coastal waters could be explained by variations in Chla, suggesting a direct linkage between phytoplankton and TEP at this geographical scale. However, this relationship was absent in June (**Figure 2**). The higher TEP/Chla ratios in June were due to both higher TEP concentrations than in May and lower Chla concentrations than in May. Indeed, primary productivity (PP) is on average two-fold higher in May than in June in coastal NW Mediterranean Sea waters (Gasol et al., 2016). Bacteria did not seem to be a significant TEP source in June as no significant correlations between TEP and BP or TEP and the BP/Chla ratios were observed. Hence, TEP may accumulate in the sea surface at the beginning of the stratification period, similar to other phytoplankton-derived organic matter (Avril, 2002; Vila-Reixach et al., 2012; Romera-Castillo et al., 2013). These substances may be not taken up immediately by bacterioplankton due to nutrient defficiency, which is common in summer (Sala et al., 2002; Pinhassi et al., 2006). What we could resolve in this analysis was that the distribution of TEP in coastal waters could be predicted from Chla, a variable that is frequently monitored, but only at certain periods of the year.

TEP Horizontal Distribution from Coastal to Offshore Waters

Our dataset also allowed concluding that Chla is a good predictor of TEP concentrations at the horizontal scale from the coast to the open sea, since significant positive relationships were observed between these two variables. This information is important because it would allow estimating TEP concentrations, for instance, using remote sensing Chla values. It is worthy to mention that, if we restrict the analysis to surface values only instead of depth-averaged values, TEP and Chla were also related ($r = 0.63$ $p = 0.06$, $n = 9$), while not remarkable covariations were found between TEP and other biological variables. This reinforces the possibility of using remote sensing Chla data to estimate the geographical distributions of TEP in the area.

At the horizontal scale, TEP was also positively related to O_2, POC, and BP. The covariance between all these variables

at the horizontal scale suggests physical forces that drive them all. We observed maxima of TEP in epipelagic waters near the coast and at the interface between slope and basin waters. In this area, which is located next to the Catalan front, a salinity doming is frequently observed (Font et al., 1988; Estrada and Salat, 1989), and relatively high Chla and PP values are found due to increased deep ocean nutrient availability at shallower depths (Estrada, 1996; Pedrós-Alió et al., 1999). This is, however, not evident in our dataset since some basin stations (i.e., stations 8 and 9) were sampled during stormy conditions that rendered more mixed temperature and salinity profiles, while the rest were sampled in sunny days and well-stratified profiles.

TEP Vertical Distribution in Epipelagic Waters

In contrast to horizontal TEP distributions, vertical TEP distributions could not be predicted from Chla at the vertical scale. In this case, TEP maxima were always located shallower than the DCM. TEP maxima above the DCM and near the surface have been reported in previous studies in the Alboran Sea (García et al., 2002), the Eastern Mediterranean Sea (Bar-Zeev et al., 2011), and along a West to East transect in the Mediterranean Sea (Ortega-Retuerta et al., 2010). Furthermore, in a recent study (Kodama et al., 2014), TEP maxima were associated to layers of maximum O_2 and nutrient minima, similar to what we observed in our study. Correlation analyses confirmed the Chla-TEP decoupling. From the whole set of variables, those that explained TEP distribution in both slope and basin waters were O_2 (positively related to TEP) and nitrate (negatively related to TEP, **Table 2**). This suggests that TEP are a direct product of PP, which is frequently decoupled from Chla concentration and whose highest rates are located at depths shallower than the DCM (Estrada et al., 1993). This suggests that Chla is not the best proxy of phytoplankton biomass or PP at the vertical scale. Indeed, increases in Chla concentration at the DCM reflect photoacclimation to low light levels through increases in the Chla/carbon ratio, and do not necessarily match highest phytoplankton biomass (Delgado et al., 1992; Gernez et al., 2011).

Given that we lacked direct PP estimates, in this study we consider O_2 as a proxy of PP in this area. We are aware, however, that O_2 concentration in the ocean is a result of biological processes as well as physical processes, such as ventilation in the upper mixed layer. But a non-significant correlation between O_2 and temperature indicates that O_2 distribution in the area majorly reflects biological processes. Furthermore, in surface waters of our study, TEP and O_2 were not significantly correlated, which supports our view that the O_2-TEP correlation is through PP with O_2 being a proxy of the latter. Similarly, the absence of negative correlations between O_2 and bacterial abundance or production suggests that respiration by heterotrophs is not the main driver of O_2 distributions.

The observed significant positive correlation with bacterial production would suggest one of the following mechanisms: (1) bacteria act as a source of TEP, (2) bacterial colonization and utilization of TEP, or (3) dependence of both TEP and bacteria on other factors, namely organic compounds released by phytoplankton during primary production. We performed multiple regression analyses with TEP as the dependent variable and O_2 and BP as independent variables. Both variables significantly explained TEP variability ($r^2 = 0.71$, $p = 0.000$, $n = 25$), with partial coefficients of 0.72 for O_2 and 0.46 for BP, respectively. Additionally, we correlated the raw residuals of the O_2-TEP regression against BP, resulting significant and positive ($r = 0.38$, $p < 0.05$, $n = 25$). Both analyses lead us to conclude that both PP (with O_2 as surrogate) and bacterial activity (with BP as surrogate) has a significant influence on vertical TEP distributions. Finally, the correlation between TEP and the BP/O_2 ratio was significant and positive. The positive correlation indicates that the higher the bacterial processing of organic matter originated in primary production, the higher TEP concentrations we observed, suggesting then a synergy between carbon fixation and bacterial reutilization of this fixed C to generate TEP.

Nutrients may also have an impact on TEP distributions as suggested by the negative correlations with NO_3, PO_4, and SiO_4. TEP are enriched in carbon respect to N and P (Mari et al., 2001), and different experimental studies have demonstrated a higher TEP release rate when nutrients are limiting (Mari et al., 2005; Pedrotti et al., 2010). Also, the N/P ratios are likely important in determining TEP production and degradation, as suggested by a significant correlation between the N/P ratio and TEP concentration in epipelagic waters. Although how nutrient stoichiometry affects TEP dynamics is unclear and probably dependent on the composition of the initial microbial community (Gärdes et al., 2012); our negative correlation suggests that the lower the relative proportion of P, the higher the TEP; which contrasts with previous experimental results (Engel et al., 2015). However, the likely limitation by phosphorus in our system (e.g., Sala et al., 2002; Pinhassi et al., 2006) in contrast to the Atlantic area studied by Engel et al. (2015) could differently affect TEP production. Indeed, it has been proposed that extracellular organic carbon production is highest under P limitation (Mauriac et al., 2011). TEP properties also vary depending on whether they are released during active growth or during bloom senescence (Mari et al., 2001), with implications for the fate of these particles in seawater (degradation vs. export). In the NW Mediterranean, PP usually peaks at the end of winter and spring (Gasol et al., 2016), so we sampled during the transition of spring to summer, which coincides with the beginning of nutrient depletion and associated decreases in PP. Thus, we expected TEP to accumulate and be prone to further export.

TEP Vertical Distribution in Meso- and Bathy-Pelagic Waters

In meso- and bathypelagic waters TEP distributions were only explained by turbidity changes. Specifically, we could detect TEP increases associated with near-bottom particle-rich layers (BNL). Surprisingly, these TEP increases were not paralleled by increases in POC. This suggests that these BNL were composed

TABLE 3 | Review of TEP-Chla relationships available in the literature.

Scale	Year	Season	Area	Depth	TEP range	Chl range	Correlation	*r*	References
Horizontal	1997	Spring	Gulf of Cadiz	10 m			+	0.60	Prieto et al., 2006
		Spring		25 m			+	0.33	
		Spring		Euphotic	63.8–202.4		+	0.29	
		Spring		Aphotic					
		Spring	NW Alboran Sea				+	0.92	
	2006	Spring	Bay of Biscay	0–160 m	1.41–31.7*[1]	0.8–2.1	+	0.61	Harlay et al., 2010
	2006–2008	Spring	Celtic Sea	0–80 m	22–1101	0.39-1.44	+	0.42	Van Oostende et al., 2012
	2012	Spring	NW Mediterranean Sea	0–200 m	9.9–24.9		+	0.75	This study
	1999–2002	All year	Adriatic Sea	Surface	4–14000	1–14	+		Radic et al., 2005
Vertical	2008–2009	Spring–summer	Eastern mediterranean Sea		51–290	0.02–0.99	–	–0.69	Bar-Zeev et al., 2011
	2009	Spring	North Pacific	Mixed layer	5.1–65.4	0.30–1.72	ns		Wurl et al., 2011
	2009	Summer	Hawaii	Mixed layer	<2.5–60.2	0.38–0.63	ns		
	2009	Fall	Arctic	Mixed layer	7.9–117.9	0.57–7.80	ns		
	2009-2010	Summer–winter	Pearl River Estuary		88.7–1586	na	ns		Sun et al., 2012
	2012	Spring	NW mediterranean Sea	0-2300	4.9–54.9	0–1.73	ns		This study
	2013	Spring	NW Pacific	Epipelagic	35.3–47.2	0.05–0.26	ns		Kodama et al., 2014
Hor-vert	2007	Spring	Mediterranean Sea	0–200 m	4.5–94.3	0–1.78	ns		Ortega-Retuerta et al., 2010
	2014	Spring	Mediterranean Sea	Surface-deep			ns		Mazuecos, 2015, thesis
	2005	Summer	Southern ocean	0-200 m	0–48.9	0.01–5.36	+	0.52	Ortega-Retuerta et al., 2009b
	2010–2011	All	Tropical and subtropical World oceans	Surface-deep			ns		Mazuecos, 2015, thesis
		Summer	Gibraltar Strait	0–75 m	169.3		+	0.73	Prieto et al., 2006
Temporal	1997–1998	All	Tokio Bay	0–10 m	14–1774	<5–30	+	0.65	Ramaiah and Furuya, 2002
	1998–2000	All	Dona Paula Bay	Surface	1.3–149.1	1.2–12.3	ns		Bhaskar and Bhosle, 2006
	1999–2000	All	NW Mediterranean Sea	Surface-DCM	Nd*[2]	0–2.8	+	0.71	Beauvais et al., 2003
	2012	Spring-summer	English channel	Surface and microlayer	254–1301	0.5–5.5	ns		Taylor et al., 2014
		Spring-summer	English channel	Surface	36.9–1735.1	9	+*[3]	0.87	Klein et al., 2011
	2002–2004	Summer–winter	Aegean Sea	Surface to 4 m (bottom)	101–259	0.1–7	+	0.19	Scoullos et al., 2006

Horizontal-vertical scales (hor-vert in the Table) are considered when analyses are made using data that covered wide geographical areas but also include deep vertical profiles. ns, not significant. na, not available.

**[1] Relative units (samples not calibrated).*

**[2] TEP analyzed by microscopic enumeration.*

**[3] Analysis only with chl >10 μm.*

mostly of mineral particles that could be coated or aggregated by TEP. A previous study in the NW Mediterranean (Puig et al., 2013) observed the presence of fine particles in the BNL. Via microscope visualizations, they showed that organic matter in the BNL was mainly composed by "amorphous aggregates," and suggested that these aggregates had lower sinking rates than phytoplankton cells or other solid organic particles. This is in line with our findings, where TEP, which are low density particles, may have a longer residence time in the BNL than the rest of POC compounds. In bathypelagic waters, TEP cannot have a direct phytoplanktonic source as light is absent. However, a bacterial source was not evident either since no significant correlations were observed between TEP and BA or BP. Interestingly, TEP concentrations in that layer were positively correlated to bacterial fucosidase activity. Since TEP are enriched in fucose (Zhou et al., 1998), this may reflect bacterial degradation of TEP in deep waters. Therefore, bacteria would act as a sink instead of a source for TEP, and a probable non-local TEP source must exist, material either sunk from epipelagic waters, resuspended from the sediment, or advected off the shelf.

TEP Diel Variations

To our knowledge this is the first time that high frequency (every 4 h) and short-term (i.e., 2-day) TEP changes have been monitored in the field during a lagrangian study. However, we did not find a recurrent pattern of any of the variables measured. In our case, this lack of diel patterns of microbial biomass/activity likely explained the absence of recurrent TEP diurnal or nocturnal maxima. Additionally, although we confirmed in this study the vertical decoupling between Chla and TEP and the better coincidence with O_2 concentrations, the results of short-term variations of these variables were less conclusive. We got some hints about short-term temporal decoupling, where TEP peaks followed Chla and O_2 peaks, but further work, with longer diel sampling, is needed to explore this issue.

CONCLUSIONS

We showed that the TEP-Chla relationship in the ocean is variable and mainly depends on the time and spatial scale studied. TEP can be predicted from Chla distributions at the horizontal scale, which opens the possibility to estimate surface TEP using remote sensing Chla; but this relationship is not evident at the vertical scale, nor at a short timescale, and also likely varies seasonally. Since our dataset is limited, in an attempt to compare our results to other areas, we compiled information on the various TEP-Chla relationships published in the literature (**Table 3**). The previous results mainly concur with our observations: TEP patterns mimic Chla patterns horizontally, but they are vertically decoupled, and TEP concentration maxima are frequently found at depths shallower than the DCM. Hence, we propose O_2 concentrations and bacterial production as predictive variables for vertical TEP distributions in the ocean. Further, we suggest looking at the spatial and temporal variations of TEP together with primary productivity measurements and orienting further work to elucidate what is the specific role of bacterioplankton at explaining geographical and vertical TEP distributions in the ocean.

AUTHOR CONTRIBUTIONS

EO, MS, FP, RS, CM, and JG designed the work. EO, CM, FA, CA, RG, EB, and MM sampled and performed laboratory analyses and processed the data. EO wrote the manuscript with the help and inputs of all co-authors.

ACKNOWLEDGMENTS

This work was funded by projects funded by the Spanish Ministry of Science STORM (CTM2009-09352/MAR), SUMMER (CTM2008-03309/MAR), DOREMI (CTM2012-34294), REMEI (CTM2015-70340-R), ANIMA (CTM2015-65720-R), PEGASO (CTM2012-37615), and Grup consolidat de Recerca de la Generalitat de Catalunya (2014SGR/1179). We thank the captain and crew of the R/V "García del Cid" and the Marine Technology Unit for their assistance in the field. We also thank the reviewers for helping improve the manuscript. EO was supported by Beatriu de Pinós (Generalitat de Catalunya) and Juan de la Cierva (Spanish Ministry of Economy) postdoctoral fellowships.

SUPPLEMENTARY MATERIAL

The Supplementary Material for this article can be found online at: http://journal.frontiersin.org/article/10.3389/fmicb.2016.02159/full#supplementary-material

Supplementary Figure 1 | Bivariate plot between depth-averaged (upper mixed layer) temperature (abscises) and salinity (ordinates) in the 13 sampling stations along the diel cycle.

Supplementary Figure 2 | Variations of dissolved inorganic nitrogen (DIN, orange circles), dissolved inorganic phosphorus (DIP, green-yellow triangles), and estimated bacterial production with factor 1.55 kgC mol leucine (BP, purple triangles) in the coastal transects in May (A) and June **(B)**.

REFERENCES

Alldredge, A. L., Passow, U., and Logan, B. E. (1993). The abundance and significance of a class of large, transparent organic particles in the ocean. *Deep Sea Res. I* 40, 1131–1140. doi: 10.1016/0967-0637(93)90129-Q

Avril, B. (2002). DOC dynamics in the northwestern Mediterranean Sea (DYFAMED site). *Deep Sea Res. II* 49, 2163–2182. doi: 10.1016/S0967-0645(02)00033-4

Azetsu-Scott, K., and Passow, U. (2004). Ascending marine particles: significance of transparent exopolymer particles (TEP) in the upper ocean. *Limnol. Oceanogr.* 49, 741–748. doi: 10.4319/lo.2004.49.3.0741

Bar-Zeev, E., Berman, T., Rahav, E., Dishon, G., Herut, B., Kress, N., et al. (2011). Transparent exopolymer particle (TEP) dynamics in the eastern Mediterranean Sea. *Mar. Ecol. Progr. Ser.* 431, 107–118. doi: 10.3354/meps09110

Beauvais, S., Pedrotti, M. L., Villa, E., and Lemée, R. (2003). Transparent exopolymer particle (TEP) dynamics in relation to trophic and hydrological

conditions in the NW Mediterranean Sea. *Mar. Ecol. Progr. Ser.* 262, 97–109. doi: 10.3354/meps262097

Berman, T. (2013). Transparent exopolymer particles as critical agents in aquatic biofilm formation: implications for desalination and water treatment. *Desal. Water Treat.* 51, 1014–1020. doi: 10.1080/19443994.2012.713585

Bhaskar, P. V., and Bhosle, N. B. (2006). Dynamics of transparent exopolymeric particles (TEP) and particle-associated carbohydrates in the Dona Paula bay, west coast of India. *J. Earth Sys. Sci.* 115, 403–413. doi: 10.1007/BF02702869

Burd, A. B., and Jackson, G. A. (2009). Particle aggregation. *Ann. Rev. Mar. Sci.* 1, 65–90. doi: 10.1146/annurev.marine.010908.163904

Delgado, M., Latasa, M., and Estrada, M. (1992). Variability in the size-fractionated distribution of the phytoplankton across the Catalan front of the north-west Mediterranean. *J. Plankton Res.* 14, 753–771. doi: 10.1093/plankt/14.5.753

Engel, A., Borchard, C., Loginova, A., Meyer, J., Hauss, H., and Kiko, R. (2015). Effects of varied nitrate and phosphate supply on polysaccharidic and proteinaceous gel particle production during tropical phytoplankton bloom experiments. *Biogeosciences* 12, 5647–5665. doi: 10.5194/bg-12-5647-2015

Estrada, M. (1996). Primary production in the northwestern Mediterranean. *Sci. Mar.* 60, 55–64.

Estrada, M., Marrasé, C., Latasa, M., Berdalet, E., Delgado, M., and Riera, T. (1993). Variability of deep chlorophyll maximum characteristics in the Northwestern Mediterranean. *Mar. Ecol. Prog Ser.* 92, 289–300. doi: 10.3354/meps092289

Estrada, M., and Salat, J. (1989). Phytoplankton assemblages of deep and surface water layers in a Mediterranean frontal zone. *Sci. Mar.* 53, 203–214.

Font, J., Salat, J., and Tintore, J. (1988). Permanent features of the circulation in the Catalan Sea. *Oceanol. Acta.* 51–57. Special issue.

García, C. M., Prieto, L., Vargas, M., Echevarría, F., García-Lafuente, J., Ruiz, J., et al. (2002). Hydrodynamics and the spatial distribution of plankton and TEP in the Gulf of Cádiz (SW Iberian Peninsula). *J. Plankton Res.* 24, 817–833. doi: 10.1093/plankt/24.8.817

Gärdes, A., Ramaye, Y., Grossart, H. P., Passow, U., and Ullrich, M. S. (2012). Effects of *Marinobacter adhaerens* HP15 on polymer exudation by *Thalassiosira weissflogii* at different N:P ratios. *Mar. Ecol. Prog. Ser.* 461, 1–14. doi: 10.3354/meps09894

Gasol, J., and del Giorgio, P. (2000). Using flow cytometry for counting natural planktonic bacteria and understanding the structure of planktonic bacterial communities. *Sci. Mar.* 64, 197–224. doi: 10.3989/scimar.2000.64n2197

Gasol, J. M., Cardelús, C., Morán, X. A. G., Balagué, V., Massana, R., Pedrós-Alió, C., et al. (2016). Seasonal patterns in phytoplankton photosynthetic parameters and primary production in a coastal NW Mediterranean site. *Sci. Mar.* 80, 63–77. doi: 10.3989/scimar.04480.06E

Gernez, P., Antoine, D., and Huot, Y. (2011). Diel cycles of the particulate beam attenuation coefficient under varying trophic conditions in the northwestern Mediterranean Sea: observations and modeling. *Limnol. Oceanogr.* 56, 17–36. doi: 10.4319/lo.2011.56.1.0017

Hansen, H. P., and Grasshoff, K. (1983). "Automatic chemical analysis," in *Methods of Seawater Analysis, 2nd Edn.,* eds K. Grassohoff, M. Ehrhardt, and K. Kremling (Weinheim: Verlag Chemie), 368–376.

Harlay, J., Borges, A. V., Van Der Zee, C., Delille, B., Godoi, R. H. M., Schiettecatte, L. S., et al. (2010). Biogeochemical study of a coccolithophore bloom in the northern Bay of Biscay (NE Atlantic Ocean) in June 2004. *Progr. Oceanogr.* 86, 317–336. doi: 10.1016/j.pocean.2010.04.029

Kirchman, D., Knees, E., and Hodson, R. (1985). Leucine incorporation and its potential as a measure of protein-synthesis by bacteria in natural aquatic systems. *Appl. Environ. Microbiol.* 49, 599–607.

Klein, C., Claquin, P., Pannard, A., Napoléon, C., Le Roy, B., and Véron, B. (2011). Dynamics of soluble extracellular polymeric substances and transparent exopolymer particle pools in coastal ecosystems. *Mar. Ecol. Progr. Ser.* 427, 13–27. doi: 10.3354/meps09049

Kodama, T., Kurogi, H., Okazaki, M., Jinbo, T., Chow, S., Tomoda, T., et al. (2014). Vertical distribution of transparent exopolymer particle (TEP) concentration in the oligotrophic western tropical North Pacific. *Mar. Ecol. Progr. Ser.* 513, 29–37. doi: 10.3354/meps10954

Mari, X., Beauvais, S., Lemée, R., and Pedrotti, M. L. (2001). Non-Redfield C: N ratio of transparent exopolymeric particles in the northwestern Mediterranean Sea. *Limnol. Oceanogr.* 46, 1831–1836. doi: 10.4319/lo.2001.46.7.1831

Mari, X., Rassoulzadegan, F., Brussaard, C. P. D., and Wassmann, P. (2005). Dynamics of transparent exopolymeric particles (TEP) production by Phaeocystis globosa under N- or P-limitation: a controlling factor of the retention/export balance. *Harmful Algae* 4, 895–914. doi: 10.1016/j.hal.2004.12.014

Mauriac, R., Moutin, T., and Baklouti, M. (2011). Accumulation of DOC in Low Phosphate Low Chlorophyll (LPLC) area: is it related to higher production under high N:P ratio? *Biogeosciences* 8, 933–950. doi: 10.5194/bg-8-933-2011

Mazuecos, I. P. (2015). *Exopolymer Particles in the Ocean: Production by Microorganisms, Carbon Export and Mesopelagic Respiration*. PhD, University of Granada, 281.

Orellana, M. V., Matrai, P. A., Leck, C., Rauschenberg, C. D., Lee, A. M., and Coz, E. (2011). Marine microgels as a source of cloud condensation nuclei in the high Arctic. *Proc. Natl. Acad. Sci.* 108, 13612–13617. doi: 10.1073/pnas.1102457108

Ortega-Retuerta, E., Duarte, C. M., and Reche, I. (2010). Significance of bacterial activity for the distribution and dynamics of transparent exopolymer particles in the Mediterranean Sea. *Microb. Ecol.* 59, 808–818. doi: 10.1007/s00248-010-9640-7

Ortega-Retuerta, E., Passow, U., Duarte, C. M., and Reche, I. (2009a). Effects of ultraviolet B radiation on (not so) transparent exopolymer particles. *Biogeosciences* 6, 3071–3080. doi: 10.5194/bg-6-3071-2009

Ortega-Retuerta, E., Reche, I., Pulido-Villena, E., Agustí, S., and Duarte, C. M. (2009b). Uncoupled distributions of transparent exopolymer particles (TEP) and dissolved carbohydrates in the Southern Ocean. *Mar. Chem.* 115, 59–65. doi: 10.1016/j.marchem.2009.06.004

Passow, U. (2002). Transparent exopolymer particles (TEP) in aquatic environments. *Progr. Oceanogr.* 55, 287–333. doi: 10.1016/S0079-6611(02)00138-6

Passow, U., and Alldredge, A. L. (1995). A dye-binding assay for the spectrophotometric measurement of transparent exopolymer particles (TEP). *Limnol. Oceanogr.* 40, 1326–1335. doi: 10.4319/lo.1995.40.7.1326

Passow, U., Shipe, R. F., Murray, A., Pak, D. K., Brzezinski, M. A., and Alldredge, A. L. (2001). The origin of transparent exopolymer particles (TEP) and their role in the sedimentation of particulate matter. *Cont. Shelf Res.* 21, 327–346. doi: 10.1016/S0278-4343(00)00101-1

Pedrós-Alió, C., Calderon-Paz, J. I., Guixa-Boixereu, N., Estrada, M., and Gasol, J. M. (1999). Bacterioplankton and phytoplankton biomass and production during summer stratification in the northwestern Mediterranean Sea. *Deep Sea Res. I* 46, 985–1019. doi: 10.1016/S0967-0637(98)00106-X

Pedrotti, M. L., Peters, F., Beauvais, S., Vidal, M., Egge, J., Jacobsen, A., et al. (2010). Effects of nutrients and turbulence on the production of transparent exopolymer particles: a mesocosm study. *Mar. Ecol. Progr. Ser.* 419, 57–69. doi: 10.3354/meps08840

Pinhassi, J., Gómez-Consarnau, L., Alonso-Sáez, L., Sala, M., Vidal, M., Pedrós-Alió, C., et al. (2006). Seasonal changes in bacterioplankton nutrient limitation and their effects on bacterial community composition in the NW Mediterranean Sea. *Aquat. Microb. Ecol.* 44, 241–252. doi: 10.3354/ame044241

Prieto, L., Navarro, G., Cózar, A., Echevarría, F., and García, C. M. (2006). Distribution of TEP in the euphotic and upper mesopelagic zones of the southern Iberian coasts. *Deep Sea Res. II* 53, 1314–1328. doi: 10.1016/j.dsr2.2006.03.009

Prieto, L., Sommer, F., Stibor, H. N., and Koeve, W. (2001). Effects of planktonic copepods on transparent exopolymeric particles (TEP) abundance and size spectra. *J. Plankton Res.* 23, 515–525. doi: 10.1093/plankt/23.5.515

Puig, P., Madron, X. D. D., Salat, J., Schroeder, K., Martín, J., Karageorgis, A. P., et al. (2013). Thick bottom nepheloid layers in the western Mediterranean generated by deep dense shelf water cascading. *Progr. Oceanogr.* 111, 1–23. doi: 10.1016/j.pocean.2012.10.003

Radic, T., Kraus, R., Fuks, D., Radic, J., and Pecar, O. (2005). Transparent exopolymeric particles' distribution in the northern Adriatic and their relation to microphytoplankton biomass and composition. *Sci. Total Environ.* 353, 151–161. doi: 10.1016/j.scitotenv.2005.09.013

Ramaiah, N., and Furuya, K. (2002). Seasonal variations in phytoplankton composition and transparent exopolymer particles in a eutrophicated coastal environment. *Aquat. Microb. Ecol.* 30, 69–82. doi: 10.3354/ame030069

Rochelle-Newall, E. J., Mari, X., and Pringault, O. (2010). Sticking properties of transparent exopolymeric particles (TEP) during aging and biodegradation. *J. Plankton Res.* 32, 1433–1442. doi: 10.1093/plankt/fbq060

Romera-Castillo, C., Álvarez-Salgado, X. A., Galí, M., Gasol, J. M., and Marrasé, C. (2013). Combined effect of light exposure and microbial activity on distinct

dissolved organic matter pools. A seasonal field study in an oligotrophic coastal system (Blanes Bay, NW Mediterranean). *Mar. Chem.* 148, 44–51. doi: 10.1016/j.marchem.2012.10.004

Sala, M. M., Aparicio, F., Balagué, V., Boras, J. A., Borrull, E., Cardelús, C., et al. (2016). Contrasting effects of ocean acidification on the microbial food web under different trophic conditions. *ICES J. Mar. Sci.* 73, 670–679. doi: 10.1093/icesjms/fsv130

Sala, M. M., Peters, F., Gasol, J. M., Pedrós-Alió C., Marrasé C., and Vaqué D. (2002). Seasonal and spatial variations in the nutrient limitation of bacterioplankton growth in the Northwestern Mediterranean. *Aquat. Microb. Ecol.* 27, 47–56. doi: 10.3354/ame027047

Scoullos, M., Plavšić, M., Karavoltsos, S., and Sakellari, A. (2006). Partitioning and distribution of dissolved copper, cadmium and organic matter in Mediterranean marine coastal areas: the case of a mucilage event. *Estuarine Coast. Shelf Sci.* 67, 484–490. doi: 10.1016/j.ecss.2005.12.007

Simon, M., and Azam, F. (1989). Protein content and protein synthesis rates of planktonic marine bacteria. *Mar. Ecol. Prog. Ser.* 51, 201–213. doi: 10.3354/meps051201

Smith, D. C., and Azam, F. (1992). A simple, economical method for measuring bacterial protein synthesis rates in seawater using 3H-leucine. *Mar. Microb. Food Webs* 6, 107–114.

Sun, C. C., Wang, Y. S., Li, Q. P., Yue, W. Z., Wang, Y. T., Sun, F. L., et al. (2012). Distribution characteristics of transparent exopolymer particles in the Pearl River estuary, China. *J. Geophys. Res. Biogeosci.* 117. doi: 10.1029/2012JG001951

Taylor, J. D., Cottingham, S. D., Billinge, J., and Cunliffe, M. (2014). Seasonal microbial community dynamics correlate with phytoplankton-derived polysaccharides in surface coastal waters. *ISME J.* 8, 245–248. doi: 10.1038/ismej.2013.178

Thornton, D. C. O. (2004). Formation of transparent exopolymeric particles (TEP) from macroalgal detritus. *Mar. Ecol. Prog. Ser.* 282, 1–12. doi: 10.3354/meps282001

Van Oostende, N., Harlay, J., Vanelslander, B., Chou, L., Vyverman, W., and Sabbe, K. (2012). Phytoplankton community dynamics during late spring coccolithophore blooms at the continental margin of the Celtic Sea (North East Atlantic, 2006–2008). *Progr. Oceanogr.* 104, 1–16. doi: 10.1016/j.pocean.2012.04.016

Van Oostende, N., Moerdijk-Poortvliet, T. C., Boschker, H. T., Vyverman, W., and Sabbe, K. (2013). Release of dissolved carbohydrates by Emiliania huxleyi and formation of transparent exopolymer particles depend on algal life cycle and bacterial activity. *Environ. Microbiol.* 15, 1514–1531. doi: 10.1111/j.1462-2920.2012.02873.x

Vila-Reixach, G., Gasol, J. M., Cardelús, C., and Vidal, M. (2012). Seasonal dynamics and net production of dissolved organic carbon in an oligotrophic coastal environment. *Mar. Ecol. Progr. Ser.* 456, 7–19. doi: 10.3354/meps09677

Wurl, O., Miller, L., and Vagle, S. (2011). Production and fate of transparent exopolymer particles in the ocean. *J. Geophys. Res. Oceans* 116. doi: 10.1029/2011JC007342

Zhou, J., Mopper, K., and Passow, U. (1998). The role of surface-active carbohydrates in the formation of transparent exopolymer particles by bubble adsorption of seawater. *Limnol. Oceanogr.* 43, 1860–1871. doi: 10.4319/lo.1998.43.8.1860

Conflict of Interest Statement: The authors declare that the research was conducted in the absence of any commercial or financial relationships that could be construed as a potential conflict of interest.

frontiers in Marine Science

ORIGINAL RESEARCH
published: 04 August 2016
doi: 10.3389/fmars.2016.00135

Protein and Carbohydrate Exopolymer Particles in the Sea Surface Microlayer (SML)

Daniel C. O. Thornton[1]*, *Sarah D. Brooks*[2] and *Jie Chen*[1†]

[1] Department of Oceanography, Texas A & M University, College Station, TX, USA, [2] Department of Atmospheric Sciences, Texas A & M University, College Station, TX, USA

Exchanges of matter and energy between ocean and atmosphere occur through the sea surface microlayer (SML). The SML is the thin surface layer of the ocean at the ocean-atmosphere interface that has distinctive physical, chemical and biological properties compared with the underlying water. We measured the concentration of two types of exopolymer particles in the SML and underlying water in the Pacific Ocean off the coast of Oregon (United States) during July 2011. Transparent exopolymer particles (TEP) are defined by their acidic polysaccharide content, whereas Coomassie staining particles (CSP) are composed of protein. TEP and CSP were ubiquitous in the SML. TEP were not significantly enriched in the SML compared with the underlying water. CSP were significantly enriched in the SML, with an enrichment factor (EF) of 1.4–2.4. The distribution of exopolymer particles in the water and microscopic imaging indicated that TEP and CSP are distinct populations of particles rather than different chemical components of the same particles. Dissolved polysaccharides were not enriched in the SML, whereas monosaccharides had an EF of 1.2–1.8. Sampling occurred during the collapse of a diatom bloom, and diatoms were found both in the water column and SML. While there were living diatoms in the samples, most of the diatoms were dead and there were abundant empty frustules covered in layer of TEP. The collapsing diatom bloom was probably the source of exopolymer particles to both the SML and underlying water. Exopolymer particles are a component of the SML that may play a significant role in the marine carbon and nitrogen cycles, and the exchange of material between ocean and atmosphere.

Keywords: coomassie staining particles (CSP), diatom, dissolved organic matter (DOM), exopolymers, Pacific Ocean, sea surface microlayer (SML), transparent exopolymer particles (TEP)

OPEN ACCESS

Edited by:
Tony Gutierrez,
Heriot-Watt University, Scotland

Reviewed by:
Gerhard J. Josef Herndl,
University of Vienna, Austria
Andrew Decker Steen,
University of Tennessee, USA

***Correspondence:**
Daniel C. O. Thornton
dthornton@ocean.tamu.edu

†Present Address:
Jie Chen,
South China Sea Marine Planning and Environmental Research Institute, SOA, Guangzhou, China

Specialty section:
This article was submitted to Aquatic Microbiology, a section of the journal Frontiers in Marine Science

Received: *15 April 2016*
Accepted: *21 July 2016*
Published: *04 August 2016*

Citation:
Thornton DCO, Brooks SD and Chen J (2016) Protein and Carbohydrate Exopolymer Particles in the Sea Surface Microlayer (SML). Front. Mar. Sci. 3:135. doi: 10.3389/fmars.2016.00135

INTRODUCTION

The sea surface microlayer (SML) is the thin skin that covers the ocean, and therefore the majority (71%) of the Earth's surface. Hunter (1997) defined the SML as "that microscopic portion of the surface ocean which is in contact with the atmosphere and which may have physical, chemical or biological properties that are measurably different from those of adjacent sub-surface waters." It is operationally defined as being 1–1000 μm thick (Liss and Duce, 1997). Many constituents of the SML occur at higher concentrations than in the underlying waters (Cunliffe et al., 2011). Enrichment factors (EF) are used to express the relative concentration of an analyte in the SML

relative to the underlying water and are simply the quotient of the concentration in the SML and bulk water. For example, the SML is frequently enriched (EF > 1) with dissolved organic carbon (DOC) (Sieburth et al., 1976; Hunter, 1997; Reinthaler et al., 2008). The SML is dynamic, and its composition and the enrichment in particular chemicals or organisms varies considerably in time and space (Karavoltsos et al., 2015).

Microorganisms are frequently more abundant in the SML compared with the underlying water. Aller et al. (2005) found that the EF for bacteria and virus abundances were 10 and 7, respectively. Protistan community composition in the SML is different from the underlying waters and is enriched in some taxa (Joux et al., 2006; Cunliffe and Murrell, 2010; Taylor and Cunliffe, 2014). Joux et al. (2006) proposed that buoyant particles and bubbles play a role in the enrichment of the SML with specific taxa. Research has shown differences in the bacterial community composition of the SML compared with the underlying water (Franklin et al., 2005; Cunliffe et al., 2009), whereas other work has shown no significant difference (Agogué et al., 2005; Obernosterer et al., 2008). While the SML is potentially enriched in substrates to support microbial growth, it is also a harsh environment due to exposure to high photon flux densities, including ultraviolet light. The burden of photoprotection may explain that while rates of bacterial respiration are high, growth efficiency is lower than the underlying water (Reinthaler et al., 2008).

The current model of the SML (Wurl and Holmes, 2008; Cunliffe and Murrell, 2009; Wurl et al., 2011) stems from the work of Sieburth (1983) who first proposed that the SML was a loose, hydrated gel of macromolecules and colloids. This "gelatinous film" is enriched with transparent exopolymer particles (TEP) compared with underlying waters (Wurl and Holmes, 2008; Cunliffe et al., 2011). TEP are rich in acid polysaccharides (Alldredge et al., 1993). Work over the last 20 years has shown that TEP are ubiquitous and play an important role in particle dynamics and carbon cycling in the ocean (see reviews by Passow, 2002a; Burd and Jackson, 2009; Verdugo, 2012). Ultraviolet light enhances TEP production by microorganisms (Ortega-Retuerta et al., 2009), indicating that the high concentrations of microorganisms in the SML may be a significant source of TEP. However, the effects of ultraviolet light are complex as it also causes TEP photolysis (Ortega-Retuerta et al., 2009). Another source of exopolymers to the SML is the accumulation of surface-active material on bubbles rising through the water column (Wurl and Holmes, 2008). TEP can be buoyant and rise up toward the ocean surface, particularly if there are relatively few solid particles embedded in it (Azetsu-Scott and Passow, 2004; Mari, 2008). Coomassie staining particles (CSP) are exopolymer particles that are detected based on their protein content (Long and Azam, 1996). Relatively few measurements of CSP have been made in the ocean. CSP deserve more attention, as they may be a significant pool of bioavailable nitrogen in aquatic systems, including in the SML.

The SML is biogeochemically important as all exchanges of material between ocean and atmosphere must occur through it. Several studies, using a variety of methods, have identified gel-like particles and exopolymers in aerosols collected over the Arctic Ocean (Bigg and Leck, 2008; Leck and Bigg, 2008; Orellana et al., 2011). Kuznetsova et al. (2005) measured both TEP and CSP in aerosols generated using Atlantic waters. There is a growing interest in the role of marine biogenic aerosol in atmospheric processes, including cloud formation and climate forcing (Russell et al., 2010; Orellana et al., 2011; Quinn et al., 2014; Wang et al., 2015; Wilson et al., 2015).

The primary objectives of this work were: (1) to determine if CSP and TEP are concentrated in the SML compared with underlying waters, and (2), to determine if there was a direct relationship between TEP and CSP concentrations in the SML and underlying waters. Our approach differs from recent work (Wurl and Holmes, 2008; Cunliffe et al., 2009; Wurl et al., 2009, 2011) as we measured TEP concentrations using microscopy and image analysis rather than the colorimetric technique. Because image analysis was used to enumerate both TEP and CSP particles, the data collected on these two types of exopolymer particle were directly comparable. CSP have been overlooked in the SML and have only been measured in two previous studies (Kuznetsova et al., 2005; Engel and Galgani, 2016). Image analysis also allowed us to qualitatively determine what other visible particles were associated with TEP and CSP in the SML and underlying water and thereby determine the associations between exopolymers (TEP and CSP) and other particles.

METHODS

Study Stations and Sampling

Samples were collected during a cruise onboard the R/V *Wecoma* in coastal waters of the Pacific Ocean off the state of Oregon (United States) during July 2011. The vessel left Newport (OR) on the 8 July 2011 and returned on 14 July 2011. Samples were collected along a seaward transect out from the mouth of the Columbia River (stations A, B, and C) and at two stations further south in deeper waters beyond the shelf break (stations D and E). **Figure 1** and **Table 1** shows the location of the stations at which exopolymer (TEP and CSP) and carbohydrate samples were taken. Prior to sampling, glassware was acid washed (5% HCl) overnight, rinsed at least three times in reverse osmosis water and a further two times using ultra high purity (UHP) water. Items were then individually wrapped in aluminum foil and combusted for 2 h at 150°C followed by 4 h at 500°C. GF/F filters (Whatman, nominal pore size of 0.7 μm) were used to filter sea water for dissolved carbohydrate analysis. Each filter was individually wrapped in aluminum foil and combusted at 150°C for 2 h followed by 500°C for 7 h.

It is challenging to collect samples of the SML in the ocean as the platform from which the samples are taken disrupts the SML during the sampling process (Wurl, 2009). To reduce these effects, samples of the SML and underlying water were collected from a rigid hulled inflatable boat (RHIB) launched from the R/V *Wecoma*. Samples were taken by going ahead of the R/V *Wecoma* in the RHIB to reduce the effects of the ship's wake on sample integrity. The wake of the RHIB will also disturb the SML, therefore samples were collected when the RHIB was drifting through the water rather than under power. The SML was sampled by repeatedly dipping a glass plate vertically into the

water over the side of the RHIB (Harvey and Burzell, 1972; Wurl, 2009). The glass plates were made from 0.2 cm thick window glass. An insulation foam handle was mounted onto the glass and the sampling area was 25 × 26 cm in size, which was a total area of 1300 cm^2 (0.13 m^2), including both sides of the plate. While larger plates would collect a larger sample of water with one dip, safety considerations limit the size of the plate to a size that can easily be handled at sea in the RHIB.

The plate was dipped into the water vertically and withdrawn at a rate of approximately 5 cm s^{-1}. Excess water was allowed to drain off the plate for a few seconds and the SML was scraped into a polyethylene funnel placed in a 500 ml glass bottle (medium bottle, VWR Scientific). The scrapers were 8′ (203 mm) polystyrene taping knives (Wal-Board Tools, Home Depot). Plasticware was soaked in 5% HCl for 48 h and rinsed multiple times in UHP water before the cruise. To get sufficient sample for analysis, two operators dipped plates simultaneously, one on each side of the bow of the RHIB, while a third person ensured that splashes and other extraneous water did not enter the sample bottle. The dips were pooled into one bottle and each dip recovered 3–5 ml. The process was continued until 350–500 ml of sample was collected. The R/V *Wecoma* was stationary during RHIB operations and CTD casts were made during this time. The CTD rosette included instruments to measure temperature, salinity, oxygen concentrations, and chlorophyll fluorescence. The position of the RHIB relative to the R/V *Wecoma* was generally within 500 m.

In addition to sampling the SML, water was collected using a portable peristaltic pump (Alexis pump, Pegasus Pump Company, Bradenton, Florida) at depths of 1, 5, and 10 m from the RHIB (**Table 1**). The peristaltic pump was set up for collecting water samples for trace metal analysis (Aaron Beck, personal communication). The tubing running through the pump was Masterflex C-flex tubing (Cole-Parmer) connected to the fluorinated ethylene propylene (FEP) tubing that was lowered into the ocean. Prior to the cruise, the tubing was soaked in 6 M HCl for 6 months and rinsed in UHP water. The tubing was lowered over the side of the boat using a weighted line, ensuring that it descended vertically to ensure that the correct depth was sampled. The pump was flushed for 5 min to push five times the volume of the tubing through the pump before the water was collected. Samples were collected into 500 ml medium bottles, which were rinsed 3 times with site water from the correct depth before the sample was collected. One bottle was filled per sample depth. All water samples were placed in a cooler and returned to the R/V *Wecoma*, where they were processed immediately.

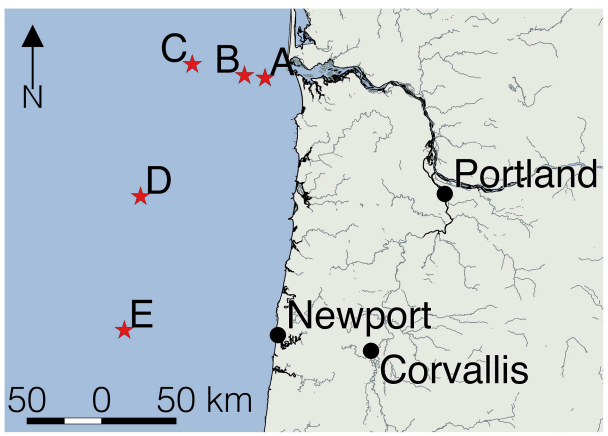

FIGURE 1 | Location of the five sampling sites in the eastern Pacific Ocean. Sampling stations (red stars) were located off Oregon (United States). Station A was located closest to the mouth of the Columbia River.

Preparation of TEP and CSP Samples

Both TEP and CSP were separated from the water sample by filtration onto 25 mm diameter 0.4 μm pore size polycarbonate filters (Nuclepore, Whatman). Low vacuum (<150 mm Hg) was used to ensure that the delicate exopolymer particles were retained on the filters (Alldredge et al., 1993; Passow and Alldredge, 1995). A glass fiber filter (GF/C, Whatman) was placed onto a drop of UHP water on top of the sintered glass filter bed. Another drop of UHP water was placed on top of the GF/C filter and the polycarbonate filter was floated on top of this drop and an extremely low vacuum was used to draw it down onto the GF/C filter, ensuring that no air bubbles were trapped between the filters. These steps were taken to ensure an even distribution of sample across the polycarbonate filter. The volume of water sampled was varied between sites (20–50 ml) with the objective of obtaining enough material to analyze without overloading the filter with sample. Once all the sample was drawn through the filter, then it was either stained for TEP using Alcian blue, or with Coomassie Brilliant Blue for CSP. Due to the similar blue color of the dyes it was not possible to stain for both TEP and CSP on the same filter.

TABLE 1 | Stations sampled in the eastern Pacific Ocean off the coast of Oregon (United States) in July 2011.

Station	Location	Date	Depths sampled (m)	Deepest CTD cast (m)
A	46°10′48.00″ N 124°15′54.00″ W	9 July 2011	SML, 1, 5, 10	88
B	46°11′21.30″ N 124°26′41.16″ W	9 July 2011	SML, 1	123
C	46°14′21.12″ N 124°54′11.40″ W	9 July 2011	SML, 1	781
D	45°25′34.92″ N 125°16′58.14″ W	10 July 2011	SML, 1, 5, 10	1657
E	44°36′58.74″ N 125°21′2.94″ W	12 July 2011	SML, 1	2863

The depths sampled indicate the depths at which exopolymer particles were collected. SML is the sea surface microlayer. The relative depths of the stations are indicated by the depth of the deepest CTD cast while on station.

TEP were stained with 1 ml of Alcian blue 8GX (Sigma-Aldrich) solution at pH 2.5 (0.02% (w/v) in 0.06% acetic acid (v/v); Passow and Alldredge, 1995). The dye was allowed to stain the TEP retained on the filter for 5 s and then it was drawn through the filter at low vacuum. Excess dye was rinsed through the filter with two 1 ml rinses of UHP water. The filter was placed in a drop of immersion oil on a Cyto-clear microscope slide (GE Water and Process Technologies; Logan et al., 1994). A second drop of oil was placed on top of the filter and it was covered with a glass coverslip. Prepared slides were stored frozen (−20°C) in the dark until analysis. CSP slides were prepared using the same protocol, except that the filters were stained with a solution of Coomassie Brilliant Blue G-250 (Sigma-Aldrich) (Long and Azam, 1996), a stain commonly used to quantify proteins in solutions (Bradford, 1976). Working Coomassie Brilliant Blue G-250 solutions were prepared each day by making a 1/25 dilution of the stock solution (1 g Coomassie Brilliant Blue G-250 in 100 ml of UHP water) with 0.2 μm filtered artificial seawater salts (Berges et al., 2001). This resulted in a 0.04 % (w/v) working solution with a pH of 7.4. Three TEP slides and three CSP slides were prepared per sample bottle.

Image Analysis of TEP and CSP

Microscope slides were photographed and analyzed on return to the laboratory at Texas A&M University. Images were captured using a AxioCam ERc 5 s color camera (Carl Zeiss MicroImaging) mounted on a Axioplan 2 microscope (Carl Zeiss MicroImaging) run from Axiovision 4.8 software (Carl Zeiss MicroImaging). To ensure that the images could be quantitatively analyzed it was important to standardize the imaging and therefore the setup of the microscope. Ten images were taken working across the diameter of the filtered area. Medium sized (1280 × 960 pixels) rather than large images (2560 × 1920) were taken to reduce vignetting.

Images were processed quantitatively in ImageJ (National Institutes of Health; Schneider et al., 2012) using a protocol based on Engel (2009). Images were analyzed from the JPEG format using a calibrated LCD monitor (MultiSync PA241W, NEC). Particles that did not stain blue were removed from the image for analysis. This was done using the brush and pencil tools in ImageJ to cover up the particles with the background color of that specific image. The image was then split into three color channels corresponding to the primary colors that make up the original color image (red, blue, and green). The blue and green images were discarded and further analysis was carried out on the grayscale representation of the red channel as this channel accentuated the exopolymer particles against the background. Quantitative analysis required a binary (black and white) image and therefore a threshold was selected along the 256 point grayscale to determine what were exopolymer particles (black pixels) and what was background (white). A constant threshold value could not be used as the filter itself absorbs dye and there is variation between filters. The triangle method (Zack et al., 1977) was used to determine the threshold within ImageJ and produce the final binary image.

The binary images were analyzed using protocols to determine the total area of exopolymer particles and the particle size distribution (PSD). Particles with an area $<10\ \mu m^2$ were not included in the analysis as many of these were noise caused by the uneven adsorption of dye to the filter giving it a slightly grainy appearance. The total area of exopolymer was determined automatically in ImageJ and included all particles $\geq 10\ \mu m^2$. Other data extracted from the images were the total number of particles and the sizes of individual particles. Particles overlapping the edges of the image were included in the measure of total TEP area per image and in the particle counts. The final data were total exopolymer particle area per unit volume, particle number per unit volume, and particle size distributions.

In addition to TEP and CSP, the samples contained numerous other microscopic particles and amorphous aggregates of organic matter. Qualitative notes were kept as a description of these particles and their relative abundance in the different samples. Separate images of representative non-exopolymer particles were captured. These images were not used in the quantitative analysis as they were set up to capture the best quality image of the objects in question (for example, objects of interest were centered in the field of view) rather than using the standardized protocols described above.

Measurement of Dissolved Carbohydrates

Three aliquots from each bottle were filtered under low vacuum through combusted GF/F filters and the filtrate was placed in glass vials with Teflon lined caps and frozen in the dark at −20°C until analysis. Samples were analyzed for carbohydrates from the SML and 1 m water depths. Samples for carbohydrate were analyzed using the 2,4,6-tripyridyl-s-triazine (TPTZ) method of Myklestad et al. (1997) calibrated with D-glucose as a standard over the range 0–2 mg l^{-1} (0–66.7 μmol l^{-1} C). Results are expressed as glucose carbon equivalents. Measurements were made by absorbance (595 nm) in a 1 cm path cuvette against an UHP water blank using a spectrophotometer (UV-mini 1240, Shimadzu). Dissolved monosaccharides were measured directly using 1 ml of thawed sample. Total dissolved carbohydrate was measured after hydrolysis into monosaccharides. Hydrolysis was carried out in 10 ml glass ampoules (Wheaton, Milleville, New Jersey) into which 4 ml of sample was placed with 0.4 ml of 1 M HCl. The ampoules were sealed in a flame and heated to 85°C for 24 h in a drying oven. After acid hydrolysis, the vials were opened and the contents was neutralized with 1 M NaOH and analyzed as before using the TPTZ method. Preliminary experiments were conducted to optimize hydrolysis conditions (Chen, 2014). The mean recovery rate of starch hydrolyzed for 24 h at 85°C with 0.09 M HCl was 79%.

Data Analysis

Data were plotted and analyzed using SigmaPlot 12.0 (Systat Software Inc.). Analysis of variance (ANOVA) was conducted on data that met the assumptions of normality and equality of variance. Data that did not meet these assumptions were transformed before analysis. If the transformed data did not meet these assumptions, then a non-parametric statistical test was used. One-tailed *t*-tests to determine whether the SML was significantly enriched compared with the underlying water were

calculated using a spreadsheet in Excel (Microsoft Corporation) following methods in Zar (1996).

RESULTS

Hydrographic Profiles and Distribution of Exopolymers (TEP and CSP)

Table 1 shows the location of the five sampling stations off the coast of Oregon, including the depths of the deepest hydrographic casts at each station. Station D and E were south of the Columbia River mouth and west of the shelf break over deeper waters (**Figure 1**). As we were interested in the SML, the depth profiles presented in this paper are to a relatively shallow depth of 25 m (**Figures 2**, **3**). Detailed depth profiles are presented for stations A and D, as these were the stations at which samples for exopolymer particles were taken at several depths (**Table 1**). Station A, which was over the continental shelf and closest to the mouth of the Columbia River (**Figure 1**), shows riverine influence (**Figure 2**). Surface waters were relatively warm, decreasing from 14.3°C at 1 m to 8.3°C at 25 m (**Figure 2A**). There was a distinct shallow halocline, with a salinity of 18.2 at 1 m and 30.8 at 5 m (**Figure 2A**). TEP and CSP concentrations were relatively constant with depth from 1 to 10 m, with TEP concentration higher than CSP concentration (**Figure 2B**). In the SML, CSP concentration was greater than TEP (**Figure 2B**). The chlorophyll maximum was located just below the halocline, with a peak chlorophyll concentration of 2.82 mg m^{-3} at 7 m (**Figure 2C**). Oxygen concentration peaked just below the chlorophyll maximum, with a concentration of 263 μmol O_2 kg^{-1} at 11 m (**Figure 2D**).

Figure 3 shows that there was a clear riverine influence further off shore and south of the Columbia River mouth at station D (**Figure 1**). Comparing the two stations, the surface waters at Station D (**Figure 3A**) were approximately 2°C warmer than those of station A (**Figure 2A**). The halocline was distinct between 5 and 10 m at station D, with a salinity of approximately 24 from the surface to 5 m, and a salinity of >31 below 10 m (**Figure 3A**). Although, there was a large change in salinity between 5 and 10 m, there was no change in TEP or CSP concentrations between these depths (**Figure 3B**). TEP and CSP concentrations were generally lower than at station A, though they followed the same general pattern, TEP concentrations were greater than CSP, except in the SML. Chlorophyll concentrations were lower at station D (<0.5 mg m^{-3}; **Figure 3C**) than at

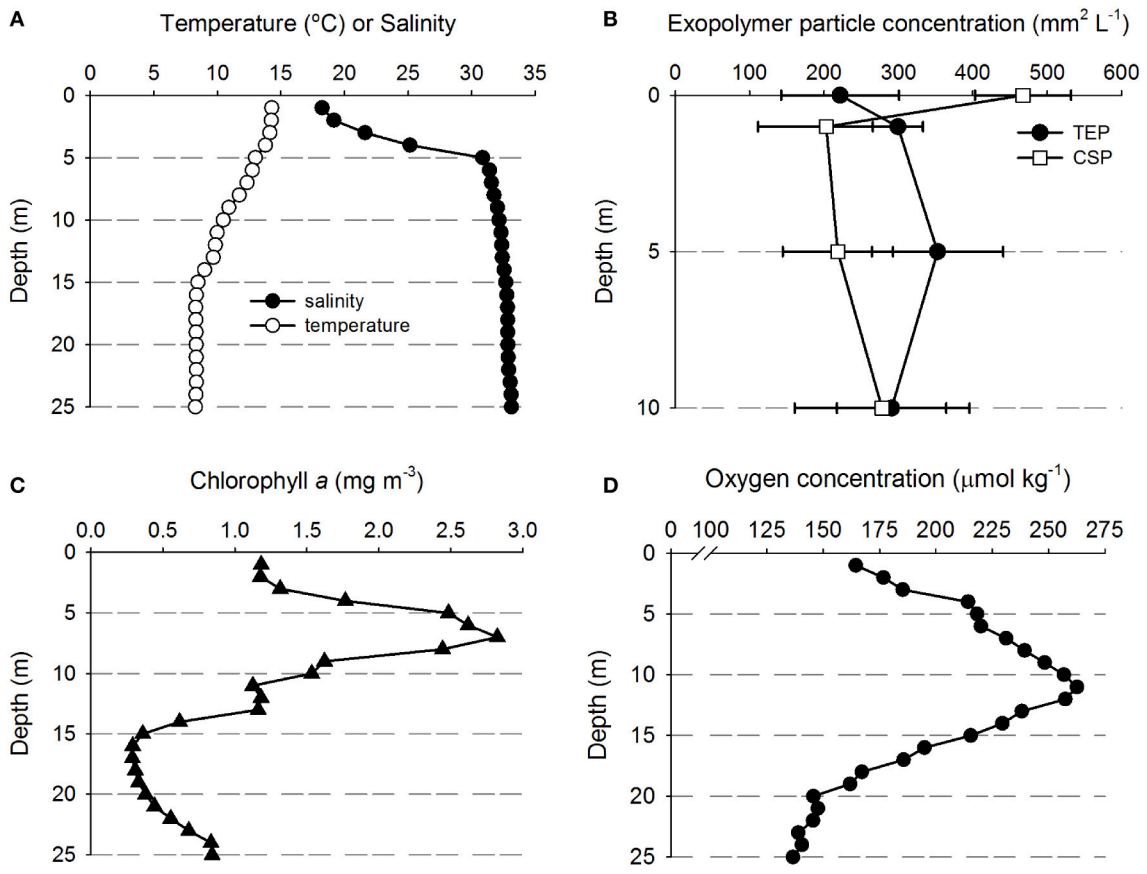

FIGURE 2 | Depth profiles of water properties and exopolymer particles at station A. (A) Temperature and salinity. **(B)** Transparent exopolymer particles (TEP) and Coomassie staining particles (CSP); data points show mean ± standard deviation ($n = 3$). **(C)** Chlorophyll concentration. **(D)** Oxygen concentration.

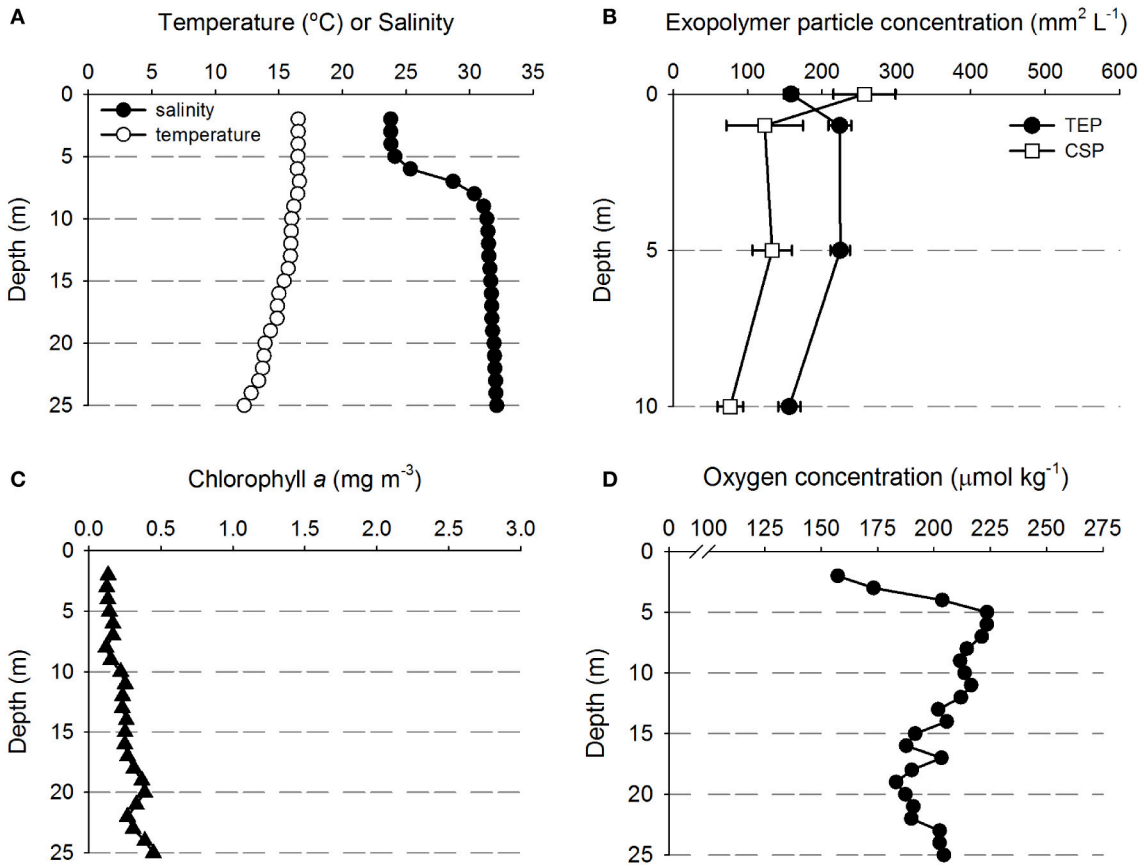

FIGURE 3 | Depth profiles of water properties and exopolymer particles at station D. (A) Temperature and salinity. **(B)** Transparent exopolymer particles (TEP) and Coomassie staining particles (CSP); data points show mean ± standard deviation ($n = 3$). **(C)** Chlorophyll concentration. **(D)** Oxygen concentration.

station A. Oxygen concentrations were relatively low above the pycnocline (**Figure 3D**) and increased to a maximum at the pycnocline of 224 μmol O_2 kg^{-1} at 5 m.

Figure 4 shows the concentrations of both TEP and CSP in the SML and at 1 m at the remaining stations (**Figures 4A,C,E**). At all stations, the influence of the Columbia River was apparent by the low salinity water in the upper 5 m (**Figures 4B,D,F**). This was most pronounced at Station B (**Figure 4B**) and least pronounced at station at Station E (**Figure 4F**), reflecting the relative distance of the two stations from the mouth of the river. Pooling the data from all stations to compare exopolymer particle concentrations in the SML and at 1 m depth, there was a significant difference in CSP concentration (Mann-Whitney; $U = 26.0$, $n = 30$, $P < 0.001$), but no significant difference in TEP concentration.

There was a significant difference between the concentration of TEP and CSP when the data for all stations and depths were pooled (Mann-Whitney; $U = 648$, $n = 42$, $P < 0.05$), indicating that the two dyes used to distinguish CSP and TEP were not staining the same material. This is further illustrated by **Figure 5**, in which CSP was plotted against TEP concentration and there was no linear relationship between the two. In addition, **Figure 5** shows that the SML was generally enriched in CSP relative to TEP, compared with the underlying water. There was no significant difference in particle concentrations of TEP and CSP, either in the SML or at 1 m depth.

Distribution of Dissolved Carbohydrates

Table 2 shows the distribution of dissolved carbohydrates in the SML and 1 m below the surface. In both the SML and at 1 m, the concentration of dissolved polysaccharides was generally higher than dissolved monosaccharides. Exceptions to this generalization were the two stations closest to the mouth of the Columbia River, where the monosaccharide concentration was approximately the same as polysaccharides. Two-way ANOVA showed that there was a significant difference in dissolved polysaccharides with depth [$F_{(1, 20)} = 8.173$, $p = 0.01$] and station [$F_{(4, 20)} = 38.997$, $p < 0.001$], and no significant interaction between depth and station [$F_{(1, 20)} = 2.734$, $p = 0.058$]. There was a significant difference in dissolved polysaccharide concentrations between all stations (Holm-Sidak method, $p < 0.05$), with the exceptions of between A and B, and Stations E and C. Two-way ANOVA indicated significant differences between monosaccharide and total carbohydrates with both station and depth. However, in both analyses there was a

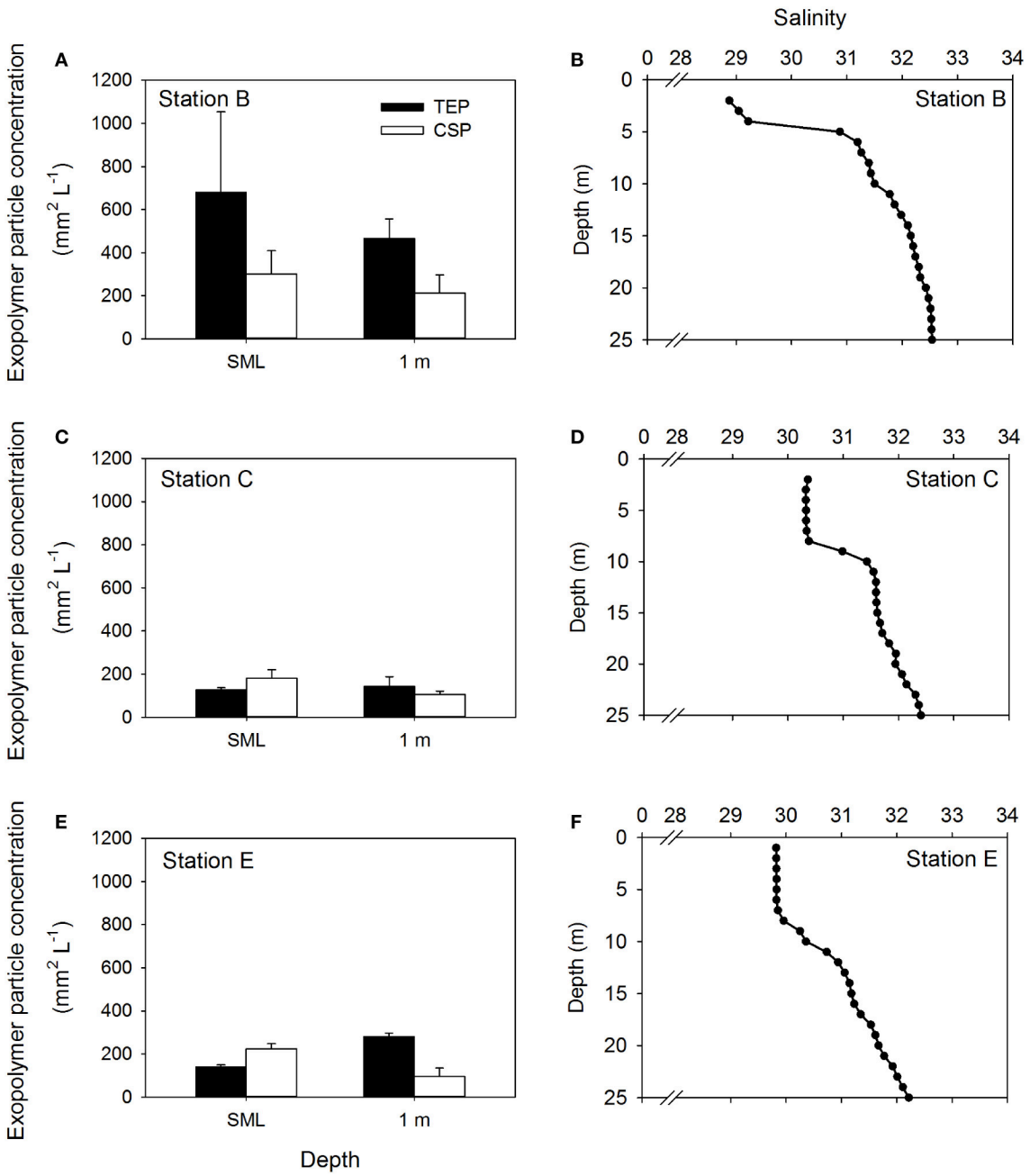

FIGURE 4 | Depth distribution of exopolymer particles at three stations. Concentrations of transparent exopolymer particles (TEP) and Coomassie staining particles (CSP) in the sea surface microlayer (SML) and at 1 m depth in the water column **(A,C,E)**. Bars show mean + standard deviation ($n = 3$). Profiles of salinity in the upper 25 m of the water column at each station are shown for reference **(B,D,F)**.

significant interaction ($p < 0.05$) between the fixed factors, precluding a simple interpretation of the effects of depth and station.

Enrichment Factors (EF)

There was no significant enrichment of TEP in the SML (**Table 3**). CSP were significantly enriched in the SML, with EF > 1 at each station. While there was significant enrichment of monosaccharides, there was no significant enrichment of polysaccharides in the SML (**Table 3**).

Description of Non-exopolymer Particles in the SML and Underlying Waters

An advantage of the imaging method for the measurement of exopolymer particles is that the association of exopolymers with other particles can be observed. Representative material from

the SML at Station A are shown in **Figures 6A,B**. In addition to the large amount of exopolymers (blue color in the images), there was evidence of biological and non-biological material in the SML. **Figure 6A** shows green material toward the upper left of the image, this was probably a fragment of terrestrial plant or green macroalga. In addition, **Figure 6A** shows a number of green algal cells which appear to be embedded in a matrix that has not stained with the Commassie brilliant blue dye (indicating that the matrix was not formed from protein). The abundant CSP (**Figure 6A**) are generally <50 μm across and are in the form of thin sheets of material, in contrast to TEP (**Figure 6B**), which appears more three-dimensional. Samples from the SML contained large numbers of small (<10 μm across) particles, which were black, brown, or red in color (**Figures 6A,B**). It is likely that these particles were from a range of origins (terrestrial, marine, and anthropogenic) and compositions such as mineral grains, biological particles, and microplastics. **Figures 6C,D** show examples of aggregates that occurred at all depths. Aggregates stained with alcian blue indicating that the components of the aggregates were embedded in a matrix of TEP (**Figure 6C**). CSP was less significant in the matrix of aggregates stained with Coomassie brilliant blue (**Figure 6D**).

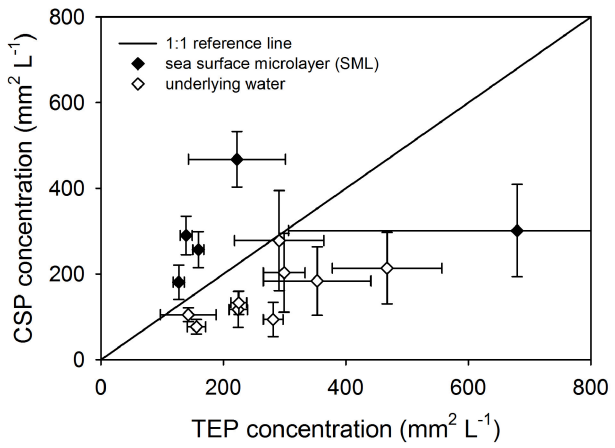

FIGURE 5 | Comparing exopolymer particle concentrations in the sea surface microlayer (SML) and underlying water. Pooled data for all stations showing the relationship between transparent exopolymer particle (TEP) and Coomassie staining particle (CSP) concentrations in the SML and underlying water. The reference lines shows where TEP and CSP concentrations would be equal. Data points show mean ± standard deviation ($n = 3$).

The large numbers of predominantly dead diatoms in the water column indicate that the samples were collected during the collapse of a diatom bloom (**Figure 7**). While empty diatom frustules are almost invisible under transmitted light, staining with alcian blue caused the dead diatoms to become visible as the exterior of the frustules were coated in TEP (**Figures 7A–C**). This may indicate that diatoms were directly producing TEP. However, cells that contained pigments, indicating that they were alive, were less stained, suggesting that a lot of the TEP material was sticking to frustules after death (**Figure 7C**). Diatom frustules coated in TEP and live diatoms were found in the SML (**Figure 7C**), as well as in the underlying water (**Figures 7A,B**).

TABLE 2 | Dissolved carbohydrate concentrations in the sea surface microlayer (SML) and underlying water (1 m depth).

Station	Monosaccharides		Polysaccharides		Total	
	SML	1 m	SML	1 m	SML	1 m
A	17.9 ± 3.0	9.7 ± 3.0	16.4 ± 2.9	17.7 ± 2.0	34.3 ± 0.4	27.4 ± 3.7
B	15.1 ± 2.5	10.2 ± 1.6	16.0 ± 3.1	11.2 ± 3.5	31.1 ± 0.7	21.4 ± 5.1
C	5.4 ± 1.4	3.0 ± 0.9	14.1 ± 5.3	14.9 ± 1.3	19.5 ± 4.0	17.9 ± 1.9
D	8.8 ± 1.9	7.6 ± 0.8	12.9 ± 3.5	14.3 ± 2.1	21.7 ± 5.2	21.9 ± 2.0
E	5.9 ± 1.8	3.9 ± 0.7	17.7 ± 2.6	11.9 ± 1.6	23.5 ± 2.7	15.8 ± 0.8

Data are expressed as glucose equivalents (μmol C L^{-1}). Values are the mean ± standard deviation (n = 3).

TABLE 3 | Enrichment factors (EF) in the sea surface microlayer (SML).

Station	TEP	CSP	Monosaccharides	Polysaccharides	Total carbohydrate
A	0.7	2.3	1.8	0.9	1.3
B	1.5	1.4	1.5	1.4	1.5
C	0.9	1.6	1.8	1.0	1.1
D	0.7	2.1	1.2	0.9	1.0
E	0.5	2.4	1.5	1.5	1.5
EF > 1?	No	Yes	Yes	No	Yes

EF for two classes of exopolymer particles: transparent exopolymer particles (TEP) and Coomassie staining particles (CSP). EF for three fractions of the dissolved carbohydrate pool (monosaccharides, polysaccharides and total). EFs were calculated based on concentrations in the SML and underlying water (1 m depth). Samples were collected at five stations in the eastern Pacific Ocean off the coast of Oregon (United States) in July 2011. A one-tailed t-test was used to determine whether the SML was enriched relative to the underlying water, which was occurred when the EF was significantly ($p < 0.05$) greater than 1. Results are shown in the final row of the table; a significant enrichment is indicated by "yes."

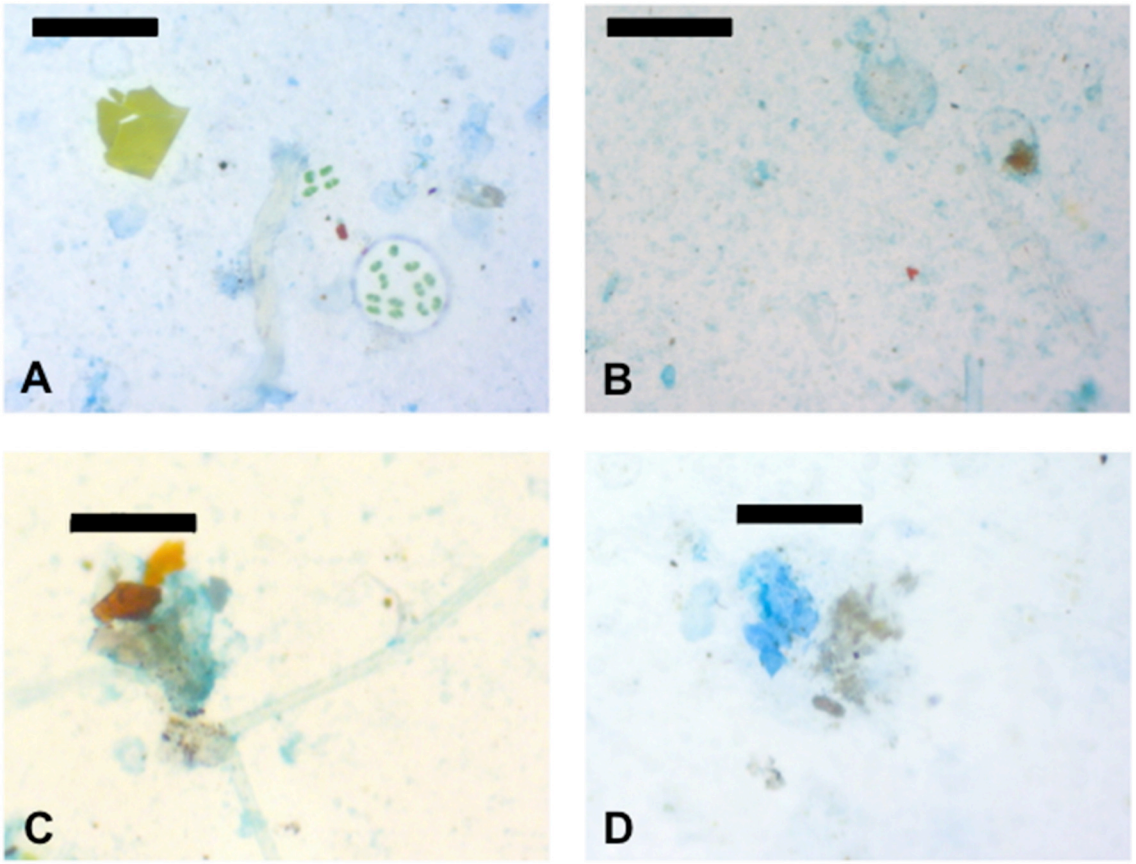

FIGURE 6 | Images of representative particles in the samples. (A) Coomassie staining particles (CSP) dyed blue and associated particles from the sea surface microlayer (SML) at station A. **(B)** Transparent exopolymer particles (TEP) dyed blue and associated particles from the sea surface microlayer (SML) at station A. **(C)** Amorphous aggregate stuck together with TEP from the SML at station B. **(D)** CSP and an amorphous aggregate from 5 m depth at station A. Scale bars are 100 μm (images **A,B,D**) and 50 μm long (image **C**).

Figure 7D shows two live *Pseudo-nitzschia* sp. diatoms stained with Commassie brilliant blue, indicating that the surface of the cells were coated in proteins. Other diatom genera which were abundant in the samples included *Rhizosolenia* spp. (**Figures 7A,B**), *Chaetoceros* spp. (**Figures 7A,B**), *Coscinodiscus* sp., and *Nitzschia* spp. At stations close to the Columbia River mouth there was evidence of freshwater phytoplankton as can be seen by the green algal cells in **Figure 6A**. Identifiable freshwater taxa at stations A and B were the green colonial alga *Pediastrum* sp. and the diatom *Asterionella* sp.

DISCUSSION

There are no standard methods for sampling the SML (Cunliffe et al., 2013). This presents a challenge in comparing data as the differences between studies may be as dependent on sampling methods as environmental factors. Zhang et al. (2003) found that properties of the SML (such as pH, nutrient concentrations, density, particle counts, and chlorophyll concentrations) change rapidly between 40 and 60 μm depth, leading them to conclude that the SML is 50 ± 10 μm deep. However, in practice the SML is operationally defined as between 1 and 1000 μm (Liss and Duce, 1997). We used the glass plate method (Harvey and Burzell, 1972), which is considered to sample the upper 20–150 μm (Cunliffe et al., 2013) and therefore captured the SML as defined by Zhang et al. (2003), without substantial dilution with underlying water that occurs with some methods, such as mesh screens. Based on the number of dips, area of the glass plate, and volume of sample recovered (Wurl, 2009), we estimated that our application of the glass plate method sampled a depth of 30–80 μm.

Wurl et al. (2011) found that 10 ± 4% of the TEP in bulk seawater stuck to the inside of the inside of glass bottles. Similarly, Ortega-Retuerta et al. (2009) found that 11 ± 3% of TEP model compounds (using (alginic acid and gum xanthan) stuck to the inside of borosilicate glass bottles. Wurl et al. (2011) noted that TEP also sticks to the glass plates used to collect SML samples, but that the plates became "conditioned" once they have been dipped in the water a few times and did not take up any more TEP. It is unknown if CSP concentrations were effected by sticking to glass. These observations indicate that TEP concentrations may have

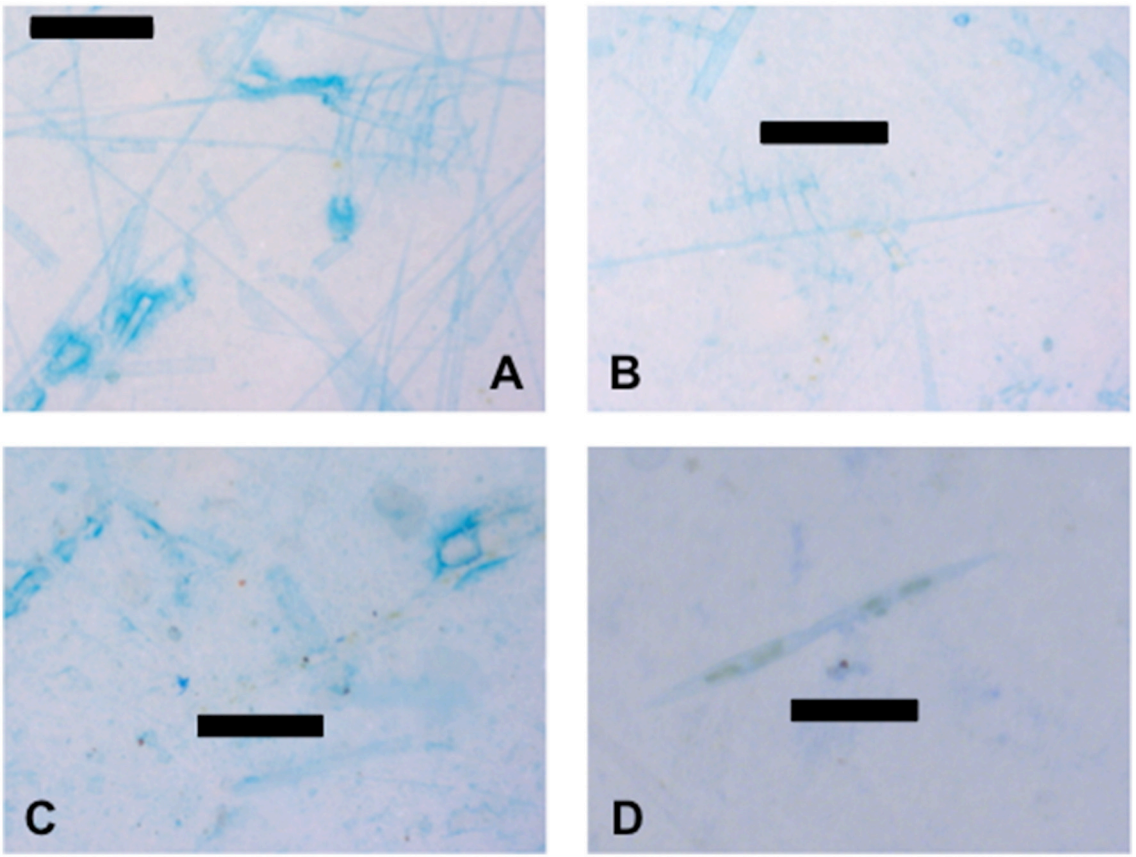

FIGURE 7 | TEP and CSP associated with diatoms. (A) Empty diatom frustules coated with transparent exopolymer particles (TEP) from 5 m at station D. **(B)** Empty diatom frustules coated with TEP and live diatoms from 10 m at station D. **(C)** Empty diatom frustules coated with TEP, live diatoms, and unidentified particles from the SML at station D. **(D)** Live diatoms and associated Coomassie staining particles (CSP) from station C at 1 m. Scale bars are 100 μm (images **A–C**) and 50 μm long (image **D**).

been underestimated in the SML and underlying water. However, as we rinsed both the plates and bottles in sample water prior to taking the samples, it is likely that this effect was negligible due to the conditioning effect.

Using image analysis, the amount of TEP and CSP can be presented as either concentrations ($mm^2\ L^{-1}$) or particle abundance (particles L^{-1}). We presented the amount of TEP and CSP in terms of concentration ($mm^2\ L^{-1}$) as concentrations can be compared between the SML and underlying water, and concentration does not imply anything about the number and size of individual exopolymer particles. Exopolymer particles retained on 0.4 μm pore size polycarbonate filters from water underlying the SML are likely to be discreet particles, which is unlikely to be the case for the SML. Sampling methods for collecting the SML will fragment a gelatinous biofilm. It is these fragments that are collected and stained on 0.4 μm filters for exopolymer particle analysis and therefore the size, and size distribution, of exopolymer particles in the SML using these methods is of little value. Ideally, concentrations of exopolymer particles would be expressed in terms of carbon (or nitrogen), as this would allow direct comparison of exopolymer particle concentrations with other pools of organic matter in the ocean, and the incorporation of exoplymer particles in the SML into biogeochemical models. Estimation of the carbon concentration associated with TEP can be obtained from the size of TEP particles (Mari, 1999; Engel, 2009). However, the carbon content of TEP varies considerably depending on the source of the TEP precursors (Mari, 1999; Engel and Passow, 2001; Engel et al., 2005). We did not convert TEP particle concentration and size to a carbon concentration as there was no way of determining whether the conversion was representative.

Sieburth (1983) proposed the formation of organic matter aggregates in the SML and their subsequent sinking as "snow flakes." The CSP in many of the samples appeared to be in the form of thin sheets, which suggests that these exopolymer particles formed on a surface or at an interface. A hypothetical mechanism for their formation is the transport and concentration of surface-active CSP precursors at the air-sea interface by rising bubbles (Wurl and Holmes, 2008). Aggregation of the concentrated CSP precursors at the air-sea interface would result in thin sheets of CSP forming. The hydrophobic properties of amino acids with aliphatic and aromatic side chains (Cunliffe et al., 2013) probably plays an important role in both the concentration of CSP precursors in

the SML by rising bubbles and their subsequent aggregation into CSP. Subsequent sinking of the thin sheets of CSP would explain their observation in the underlying water column during our research and in other studies (Long and Azam, 1996).

TEP was a component of the SML, but unlike previous work (Wurl and Holmes, 2008; Cunliffe et al., 2009; Wurl et al., 2009, 2011), we did not find significant enrichment of the SML with TEP. The relatively low EF observed in our work could be explained if the stations sampled off the Oregon coast represent a different environment from those sampled previously. The Columbia River was a dominant feature as a thin layer of relatively low salinity water was found throughout the region. However, TEP (Wetz et al., 2009) and TEP precursors (Thornton, 2009) have been measured in estuaries. Wurl and Holmes (2008) found that TEP were enriched in the surface microlayer of the estuarine Johar Strait (Singapore). Therefore, the lack of TEP enhancement in the SML was unlikely to be a feature associated with relatively low salinity waters. Previous work used the spectrophotometric method to quantify TEP, contrasting to the image analysis method used in this work. There is generally a linear relationship between data from the two methods (Passow, 2002a). However, the microscopic method does not account for the smallest TEP particles, which are too small to be resolved by light microscopy (Passow, 2002a). This could also lead to an underestimation of TEP concentration in the SML. Engel and Galgani (2016) measured TEP concentrations in the SML off the coast of Peru, a location similar to waters off the coast of Oregon as both areas are upwelling regimes associated with an eastern boundary current in the Pacific Ocean. Engel and Galgani (2016) also used imaging to determine the concentration of TEP, therefore their results are directly comparable. They found that the EF for TEP ranged between 0.2 and 12, depending on wind speed and location. TEP concentrations in the SML off Peru were 100 ± 106 mm^2 L^{-1} (mean $\pm$ SD), which were similar to our values of 265 ± 261 mm^2 L^{-1} off Oregon.

We found CSP in the SML and all other depths surveyed. CSP were found in higher concentrations in the SML than TEP and their concentration was enriched (**Table 3**) relative to the underlying water. CSP have been under-sampled compared with TEP, and data for their distribution in the SML is limited to measurements in the Atlantic (Kuznetsova et al., 2005) and the Pacific Ocean (Engel and Galgani, 2016). Engel and Galgani (2016) found that CSP was enriched in the SML by a factor of 0.4–4.8, which is comparable to our EFs of 1.4–2.4. CSP concentrations in the SML were generally higher in coastal waters off Peru (1024 ± 728 mm^2 L^{-1}, Engel and Galgani, 2016) compared with our measurements off the coast of Oregon (286 ± 115 mm^2 L^{-1}; mean $\pm$ SD). Research in the Atlantic Ocean and Mediterranean Sea has shown that dissolved organic matter (DOM) in the SML is enriched with nitrogen; Reinthaler et al. (2008) found a mean C:N ratio of 8.9 ± 6.2 in the SML compared with 18.2 ± 9.3 for the underlying water. The enrichment of the SML with nitrogen fits with our observation of enrichment of the SML with CSP. However, other factors could account for nitrogen enrichment in the SML; Several studies have shown that the SML is highly enriched with dissolved amino acids (Kuznetsova et al., 2004; Reinthaler et al., 2008; van Pinxteren et al., 2012; Engel and Galgani, 2016), which would pass through the filters used for CSP analysis. The concentration of dissolved free amino acids in the SML is generally an order of magnitude greater than the underlying water (Kuznetsova et al., 2004; Reinthaler et al., 2008). Higher rates of peptide hydrolysis in the SML, compared with the underlying water, indicate that the proteins and amino acids are rapidly turning over (Kuznetsova and Lee, 2001). Kuznetsova et al. (2005) conducted experiments in which natural seawater from the coastal North Atlantic was bubbled to induce aerosol formation. CSP were found in the underlying water, SML, and aerosol during these experiments. Estimates of CSP EF relative to the underlying water were 5.3 ± 2.7 and 57 ± 29 for the SML and aerosol, respectively. These EF were based on crude estimates of particle volume, and therefore were considered to be approximations (Kuznetsova et al., 2005). Nonetheless, they illustrate the potential significance of proteins both in the SML and the potential of the SML to supply the atmosphere with proteins of marine origin.

TEP and CSP may be separate populations of particles or they may be the same particles that are composed from a mixture of acid polysaccharides and protein. Based on the data and qualitative observations of the exopolymer particles in this study, TEP and CSP are different particles. Qualitative evidence for the difference between TEP and CSP was evident in the visual images. Firstly, CSP was often found in thin sheets of material, whereas TEP was more amorphous in shape. While it is hard to predict three dimensional shape from particles retained on a two-dimensional surface, the sheet-like nature of much of the CSP is apparent from its apparent thinness and in places where it has been folded back on itself. Secondly, TEP was associated with other types of particle more than CSP, indicating that it is more sticky than CSP. This is apparent from aggregates in which TEP appeared to be the glue holding the aggregate together (**Figure 6C**) and from acid polysaccharides adhered to the surface of empty diatom frustules (**Figure 7A**). Finally, quantitative data indicates that TEP and CSP are not the same; **Figure 5** shows no relationship between the concentration of CSP and TEP. The selective concentration of CSP relative to TEP in the SML is further evidence that these two types of exopolymer particles are not the same. Cisternas-Novoa et al. (2015) also concluded that TEP and CSP are different populations of particles. They conducted mesocosm experiments and found that phytoplankton produced both TEP and CSP, but that the peak concentrations of TEP and CSP occurred at different stages of the bloom. In agreement with our results, they also found that TEP were more likely to be associated with other particles, such as diatoms (Cisternas-Novoa et al., 2015).

Our data show enrichment of dissolved monosaccharides and no significant enrichment of dissolved polysaccharides in the SML. The enrichment of monosaccharides may indicate high degradation rates of polysaccharides through processes such as photolysis and hydrolysis. Total dissolved carbohydrates had an EF of 1.0–1.5, mainly due to the enrichment of monosaccharides. van Pinxteren et al. (2012) found a similar EF for dissolved carbohydrates, ranging from 0.7 to 1.2 in the Baltic Sea. Relatively high EF values of 3.5–12.1 have been measured for dissolved polysaccharides in the SML of the Arctic, with bubble scavenging

from the underlying water proposed as the mechanism of enrichment from water containing extracellular carbohydrates produced by both phytoplankton and sea ice algae (Gao et al., 2012).

All the stations were sampled during a diatom bloom. The bloom was in the process of collapsing as most of the diatom frustules were empty (**Figure 7A**). There were also live diatoms in the samples, such as the pigmented *Pseudo-nitzschia* sp. cells in **Figure 7D**. *Pseudo-nitzschia* is significant as it is a harmful algal bloom species that is known to bloom along the Oregon coast (McKibben et al., 2015). Phytoplankton, and to a lesser extent bacteria, are considered to be the source of TEP and the polysaccharide precursors that form TEP (Passow, 2002a,b; Thornton, 2014). It is likely that the collapsing diatom bloom was the major source of exopolymers that produced the TEP and CSP found in both water column and SML. Diatoms release a significant proportion of the carbon that they fix through photosynthesis as exudates, including as TEP and CSP, or their precursors (Engel et al., 2002; Passow, 2002b; Thornton, 2014; Chen and Thornton, 2015). TEP accumulate in cultures of diatoms (Corzo et al., 2000; Claquin et al., 2008; Fukao et al., 2010; Chen and Thornton, 2015) and in diatom-dominated blooms within mesocosm experiments using natural waters (Engel et al., 2002). Less work has been done on CSP production by diatoms; Thornton (2014) found that CSP are generally abundant in batch cultures of several different diatom species. Galgani and Engel (2013) showed that both TEP and CSP accumulated in the water column and SML in cultures of *Thalassiosira weissflogii*. The accumulation of diatom frustules and organic matter in the SML (**Figure 7C**) indicates that diatoms may make a contribution to marine aerosols. Recent work has shown that diatoms may play an important role in generating atmospheric ice nuclei (IN) and potentially affecting the formation of mixed phase and ice clouds over remote regions of the ocean (Knopf et al., 2011; Wilson et al., 2015).

The coloration and shape of many of the relatively small ($<10\,\mu m$ across) particles indicated that they were not exopolymer particles and were probably non-biological in origin. This was particularly apparent in samples from the SML (e.g. dark red particles in **Figures 7A,B**). Many of these particles may have been mineral grains blown onto the SML from the terrestrial environment or buoyant particles carried into the ocean by the Columbia River. Anthropogenic particles may have been a significant contributor as many were brightly colored, which suggests that they were composed of plastics or paints. Microplastics composed of a variety of polymers have been sampled from the SML in coastal waters off South Korea (Song et al., 2014, 2015).

These data confirm previous work showing that TEP are found in the SML. In addition, we showed that CSP are enriched in the SML compared with the underlying water. TEP and CSP are not components of the same exopolymer particles as the two pools of exopolymers behaved differently. Our samples were collected during the collapse of a diatom bloom, suggesting that diatoms were the source of the organic matter in the water column and SML. Diatom blooms vary in time and space depending on the season (Alvain et al., 2008), but are a regular occurrence in many areas of the ocean, such as in the eastern boundary current upwelling system observed in this study, the spring bloom in the North Atlantic, and the Southern Ocean during austral summer. The accumulation of diatom-derived material (TEP, CSP, empty frustules etc.) in the SML indicates that diatoms may be major contributors to the SML and on a regional scale during bloom periods.

AUTHOR CONTRIBUTIONS

DT, SB conceived the work and collected the samples during the cruise. JC undertook the carbohydrate analysis. DT took the images, conducted the image analysis, and analyzed the data. DT, SB wrote the manuscript with input from JC.

FUNDING

SB, DT were supported by the National Science Foundation (United States) under Grant No. AGS 1026804. Financial support for the cruise was provided by the National Science Foundation (United States) under Grant No. OCE 1125396 to Dr. Clare Reimers (Oregon State University). Any opinions, findings, and conclusions or recommendations expressed in this material are those of the authors and do not necessarily reflect the views of the National Science Foundation. JC acknowledges financial support through a scholarship from the government of the People's Republic of China.

ACKNOWLEDGMENTS

We thank the Captain, crew, marine technicians and the Science Party aboard the *R/V Wecoma* on cruise W1106A, especially the colleagues that assisted us in sampling the sea surface microlayer. We thank Dr. Clare Reimers for the opportunity to participate in the cruise. Dr. Alyson Santoro (University of Maryland Center for Environmental Science) generously provided us with processed data from the CTD casts. Dr. Aaron Beck (Virginia Institute of Marine Science) assisted with sampling and provided a pump to collect water from below the surface. Elise Wilbourn made the map used in **Figure 1**.

REFERENCES

Agogué, H., Casamayor, E. O., Bourrain, M., Obernosterer, I., Joux, F., Herndl, G. J., et al. (2005). A survey on bacteria inhabiting the sea surface microlayer of coastal ecosystems. *FEMS Microbiol. Ecol.* 54, 269–280. doi: 10.1016/j.femsec.2005.04.002

Alldredge, A. L., Passow, U., and Logan, B. E. (1993). The abundance and significance of a class of large, transparent organic particles in the ocean. *Deep Sea Res.* 40, 1131–1140. doi: 10.1016/0967-0637(93)90129-q

Aller, J. Y., Kuznetsova, M. R., Jahns, C. J., and Kemp, P. F. (2005). The sea surface microlayer as a source of viral and bacterial enrichment in marine aerosols. *J. Aerosol. Sci.* 36, 801–812. doi: 10.1016/j.jaerosci.2004.10.012

Alvain, S., Moulin, C., Dandonneau, Y., and Loisel, H. (2008). Seasonal distribution and succession of dominant phytoplankton groups in the global ocean: a satellite view. *Glob. Biogeochem. Cycles* 22, GB3001. doi: 10.1029/2007gb003154

Azetsu-Scott, K., and Passow, U. (2004). Ascending marine particles: significance of transparent exopolymer particles (TEP) in the upper ocean. *Limnol. Oceanogr.* 49, 741–748. doi: 10.4319/lo.2004.49.3.0741

Berges, J. A., Franklin, D. J., and Harrison, P. J. (2001). Evolution of an artificial seawater medium: improvements in enriched seawater, artificial water over the last two decades. *J. Phycol.* 37, 1138–1145. doi: 10.1046/j.1529-8817.2001.01052.x

Bigg, E. K., and Leck, C. (2008). The composition of fragments of bubbles bursting at the ocean surface. *J. Geophys. Res. Atmos.* 113, D11209. doi: 10.1029/2007jd009078

Bradford, M. M. (1976). Rapid and sensitive method for quantitation of microgram quantities of protein utilizing principle of protein-dye binding. *Anal. Biochem.* 72, 248–254. doi: 10.1006/abio.1976.9999

Burd, A. B., and Jackson, G. A. (2009). Particle Aggregation. *Annu. Rev. Mar. Sci.* 1, 65–90. doi: 10.1146/annurev.marine.010908.163904

Chen, J. (2014). *Factors Affecting Carbohydrate Production and the Formation of Transparent Exopolymer Particles (TEP) by Diatoms*. Dissertation, Texas A&M University, College Station, TX.

Chen, J., and Thornton, D. C. O. (2015). Transparent exopolymer particle production and aggregation by a marine planktonic diatom (*Thalassiosira weissflogii*) at different growth rates. *J. Phycol.* 51, 381–393. doi: 10.1111/jpy.12285

Cisternas-Novoa, C., Lee, C., and Engel, A. (2015). Transparent exopolymer particles (TEP) and Coomassie stainable particles (CSP): differences between their origin and vertical distributions in the ocean. *Mar. Chem.* 175, 56–71. doi: 10.1016/j.marchem.2015.03.009

Claquin, P., Probert, I., Lefebvre, S., and Veron, B. (2008). Effects of temperature on photosynthetic parameters and TEP production in eight species of marine microalgae. *Aquat. Microb. Ecol.* 51, 1–11. doi: 10.3354/ame01187

Corzo, A., Morillo, J. A., and Rodriguez, S. (2000). Production of transparent exopolymer particles (TEP) in cultures of Chaetoceros calcitrans under nitrogen limitation. *Aquat. Microb. Ecol.* 23, 63–72. doi: 10.3354/ame023063

Cunliffe, M., Engel, A., Frka, S., Gasparovic, B., Guitart, C., Murrell, J. C., et al. (2013). Sea surface microlayers: a unified physicochemical and biological perspective of the air-ocean interface. *Prog. Oceanogr.* 109, 104–116. doi: 10.1016/j.pocean.2012.08.004

Cunliffe, M., and Murrell, J. C. (2009). The sea-surface microlayer is a gelatinous biofilm. *ISME J.* 3, 1001–1003. doi: 10.1038/ismej.2009.69

Cunliffe, M., and Murrell, J. C. (2010). *Eukarya* 18S rRNA gene diversity in the sea surface microlayer: implications for the structure of the neustonic microbial loop. *ISME J.* 4, 455–458. doi: 10.1038/ismej.2009.133

Cunliffe, M., Salter, M., Mann, P. J., Whiteley, A. S., Upstill-Goddard, R. C., and Murrell, J. C. (2009). Dissolved organic carbon and bacterial populations in the gelatinous surface microlayer of a Norwegian fjord mesocosm. *FEMS Microb. Lett.* 299, 248–254. doi: 10.1111/j.1574-6968.2009.01751.x

Cunliffe, M., Upstill-Goddard, R. C., and Murrell, J. C. (2011). Microbiology of aquatic surface microlayers. *FEMS Microbiol. Rev.* 35, 233–246. doi: 10.1111/j.1574-6976.2010.00246.x

Engel, A. (2009). "Determination of marine gel particles," in *Practical Guidelines for the Analysis of Seawater,* ed O. Wurl (Boca Raton, FL: CRC Press), 125–142.

Engel, A., and Galgani, L. (2016). The organic sea-surface microlayer in the upwelling region off the coast of Peru and potential implications for air–sea exchange processes. *Biogeosciences* 13, 989–1007. doi: 10.5194/bg-13-989-2016

Engel, A., Goldthwait, S., Passow, U., and Alldredge, A. (2002). Temporal decoupling of carbon and nitrogen dynamics in a mesocosm diatom bloom. *Limnol. Oceanogr.* 47, 753–761. doi: 10.4319/lo.2002.47.3.0753

Engel, A., and Passow, U. (2001). Carbon and nitrogen content of transparent exopolymer particles (TEP) in relation to their Alcian Blue adsorption. *Mar. Ecol. Prog. Ser.* 219, 1–10. doi: 10.3354/meps219001

Engel, A., Zondervan, I., Aerts, K., Beaufort, L., Benthien, A., Chou, A., et al. (2005). Testing the direct effect of CO_2 concentration on a bloom of the coccolithophorid *Emiliania huxleyi* in mesocosm experiments. *Limnol. Oceanogr.* 50, 493–507. doi: 10.4319/lo.2005.50.2.0493

Franklin, M. P., McDonald, I. R., Bourne, D. G., Owens, N. J. P., Upstill-Goddard, R. C., and Murrell, J. C. (2005). Bacterial diversity in the bacterioneuston (sea surface microlayer): the bacterioneuston through the looking glass. *Environ. Microbiol.* 7, 723–736. doi: 10.1111/j.1462-2920.2004.00736.x

Fukao, T., Kimoto, K., and Kotani, Y. (2010). Production of transparent exopolymer particles by four diatom species. *Fish. Sci.* 76, 755–760. doi: 10.1007/s12562-010-0265-z

Galgani, L., and Engel, A. (2013). Accumulation of gel particles in the sea-surface microlayer during an experimental study with the diatom *Thalassiosira weissflogii*. *Int. J. Geosci.* 4, 129–145. doi: 10.4236/ijg.2013.41013

Gao, Q., Leck, C., Rauschenberg, C., and Matrai, P. A. (2012). On the chemical dynamics of extracellular polysaccharides in the high Arctic surface microlayer. *Ocean Sci.* 8, 401–418. doi: 10.5194/os-8-401-2012

Harvey, G. W., and Burzell, L. A. (1972). Simple microlayer method for small samples. *Limnol. Oceanogr.* 17, 156–157.

Hunter, K. A. (1997). "Chemistry of the sea-surface microlayer," in *The Sea Surface and Global Change,* ed P. Liss and R. A. Duce (Cambridge: Cambridge University Press), 287–320.

Joux, F., Agogué, H., Obernosterer, I., Dupuy, C., Reinthaler, T., Herndl, G. J., et al. (2006). Microbial community structure in the sea surface microlayer at two contrasting coastal sites in the northwestern Mediterranean Sea. *Aquat. Microbiol. Ecol.* 42, 91–104. doi: 10.3354/ame042091

Karavoltsos, S., Kalambokis, E., Sakellari, A., Plavšić, M., Dotsika, M., Karalis, P., et al. (2015). Organic matter characterization and copper complexing capacity in the sea surface microlayer of coastal areas of the Eastern Mediterranean. *Mar. Chem.* 173, 234–243. doi: 10.1016/j.marchem.2014.12.004

Knopf, D. A., Alpert, P. A., Wang, B., and Aller, J. Y. (2011). Stimulation of ice nucleation by marine diatoms. *Nat. Geosci.* 4, 88–90. doi: 10.1038/ngeo1037

Kuznetsova, M., and Lee, C. (2001). Enhanced extracellular enzymatic peptide hydrolysis in the sea-surface microlayer. *Mar. Chem.* 73, 319–332. doi: 10.1016/s0304-4203(00)00116-x

Kuznetsova, M., Lee, C., and Aller, J. (2005). Characterization of the proteinaceous matter in marine aerosols. *Mar. Chem.* 96, 359–377. doi: 10.1016/j.marchem.2005.03.007

Kuznetsova, M., Lee, C., Aller, J., and Frew, N. (2004). Enrichment of amino acids in the sea surface microlayer at coastal and open ocean sites in the North Atlantic Ocean. *Limnol. Oceanogr.* 49, 1605–1619. doi: 10.4319/lo.2004.49.5.1605

Leck, C., and Bigg, E. K. (2008). Comparison of sources and nature of the tropical aerosol with the summer high Arctic aerosol. *Tellus B.* 60, 118–126. doi: 10.1111/j.1600-0889.2007.00315.x

Liss, P. S., and Duce, R. A. (1997). "Preface," in *The Sea Surface and Global Change,* eds P. Liss and R. A. Duce (Cambridge: Cambridge University Press), xiii–xvi.

Logan, B. E., Grossart, H. P., and Simon, M. (1994). Direct observation of phytoplankton, TEP and aggregates on polycarbonate filters using brightfield microscopy. *J. Plankton Res.* 16, 1811–1815. doi: 10.1093/plankt/16.12.1811

Long, R. A., and Azam, F. (1996). Abundant protein-containing particles in the sea. *Aquat. Microb. Ecol.* 10, 213–221. doi: 10.3354/ame010213

Mari, X. (1999). Carbon content and C:N ratio of transparent exopolymeric particles (TEP) produced by bubbling exudates of diatoms. *Mar. Ecol. Prog. Ser.* 183, 59–71. doi: 10.3354/meps183059

Mari, X. (2008). Does ocean acidification induce an upward flux of marine aggregates? *Biogeosciences* 5, 1023–1031. doi: 10.5194/bg-5-1023-2008

McKibben, S. M., Watkins-Brandt, K. S., Wood, A. M., Hunter, M., Forster, Z., Hopkins, A., et al. (2015). Monitoring oregon coastal harmful algae: observations and implications of a harmful algal bloom-monitoring project. *Harmful Algae* 50, 32–44. doi: 10.1016/j.hal.2015.10.004

Myklestad, S. M., Skanoy, E., and Hestmann, S. (1997). A sensitive and rapid method for analysis of dissolved mono- and polysaccharides in seawater. *Mar. Chem.* 56, 279–286. doi: 10.1016/s0304-4203(96)00074-6

Obernosterer, I., Catala, P., Lami, R., Caparros, J., Ras, J., Bricaud, A., et al. Lebaron, P. (2008). Biochemical characteristics and bacterial community structure of the sea surface microlayer in the South Pacific Ocean. *Biogeosciences* 5, 693–705. doi: 10.5194/bg-5-693-2008

Orellana, M. V., Matrai, P. A., Leck, C., Rauschenberg, C. D., Lee, A. M., and Coz, E. (2011). Marine microgels as a source of cloud condensation nuclei in the high Arctic. *Proc. Natl. Acad. Sci. U.S.A.* 108, 13612–13617. doi: 10.1073/pnas.1102457108

Ortega-Retuerta, E., Passow, U., Duarte, C. M., and Reche, I. (2009). Effects of ultraviolet B radiation on (not so) transparent exopolymer particles. *Biogeosciences* 6, 3071–3080. doi: 10.5194/bg-6-3071-2009

Passow, U. (2002a). Transparent exopolymer particles (TEP) in aquatic environments. *Prog. Oceanogr.* 55, 287–333. doi: 10.1016/s0079-6611(02)00138-6

Passow, U. (2002b). Production of transparent exopolymer particles (TEP) by phyto- and bacterioplankton. *Mar. Ecol. Prog. Ser.* 236, 1–12. doi: 10.3354/meps236001

Passow, U., and Alldredge, A. L. (1995). A dye-binding assay for the spectrophotometric measurement of transparent exopolymer particles (TEP). *Limnol. Oceanogr.* 40, 1326–1335.

Quinn, P. K., Bates, T. S., Schulz, K. S., Coffman, D. J., Frossard, A. A., Russell, L. M., et al. (2014). Contribution of sea surface carbon pool to organic matter enrichment in sea spray aerosol. *Nat. Geosci.* 7, 228–232. doi: 10.1038/ngeo2092

Reinthaler, T., Sintes, E., and Herndl, G. J. (2008). Dissolved organic matter and bacterial production and respiration in the sea-surface microlayer of the open Atlantic and the western Mediterranean Sea. *Limnol. Oceanogr.* 53, 122–136. doi: 10.4319/lo.2008.53.1.0122

Russell, L. M., Hawkins, L. N., Frossard, A. A., Quinn, P. K., and Bates, T. S. (2010). Carbohydrate-like composition of submicron atmospheric particles and their production from ocean bubble bursting. *Proc. Natl. Acad. Sci. U.S.A.* 107, 6652–6657. doi: 10.1073/pnas.0908905107

Schneider, C. A., Rasband, W. S., and Eliceiri, K. W. (2012). NIH Image to ImageJ: 25 years of image analysis. *Nat. Methods* 9, 671–675. doi: 10.1038/nmeth.2089

Sieburth, J. M. (1983). "Microbiological and organic-chemical processes in the surface and mixed layers," in *Air–Sea Exchange of Gases and Particles*, eds P. S. Liss and W. G. N. Slinn (Hingham, MA: Reidel Publishers Co), 121–172.

Sieburth, J. M., Willis, P. J., Johnson, K. M., Burney, C. M., Lavoie, D. M., Hinga, K. R., et al. (1976). Dissolved organic-matter and heterotrophic microneuston in surface microlayers of north-atlantic. *Science* 194, 1415–1418.

Song, Y. K., Hong, S. H., Jang, M., Han, G. M., and Shim, W. J. (2015). Occurrence and distribution of microplastics in the sea surface microlayer in Jinhae Bay, South Korea. *Arch. Environ. Con. Tox.* 69, 279–287. doi: 10.1007/s00244-015-0209-9

Song, Y. K., Hong, S. H., Jang, M., Kang, J. H., Kwon, O. Y., Han, G. M., et al. (2014). Large accumulation of micro-sized synthetic polymer particles in the sea surface microlayer. *Environ. Sci. Technol.* 48, 9014–9021. doi: 10.1021/es501757s

Taylor, J. D., and Cunliffe, M. (2014). High-throughput sequencing reveals neustonic and planktonic eukaryote diversity in coastal waters. *J. Phycol.* 50, 960–965. doi: 10.1111/jpy.12228

Thornton, D. C. O. (2009). Spatiotemporal distribution of dissolved acidic polysaccharides (dAPS) in a tidal estuary. *Limnol. Oceanogr.* 54, 1449–1460. doi: 10.4319/lo.2009.54.5.1449

Thornton, D. C. O. (2014). Dissolved organic matter (DOM) release by phytoplankton in the contemporary and future ocean. *Eur. J. Phycol.* 49, 20–46. doi: 10.1080/09670262.2013.875596

van Pinxteren, M., Müller, C., Iinuma, Y., Stolle, C., and Herrmann, H. (2012). Chemical characterization of dissolved organic compounds from coastal sea surface microlayers (Baltic Sea, Germany). *Environ. Sci. Technol.* 46, 10455–10462. doi: 10.1021/es204492b

Verdugo, P. (2012). Marine Microgels. *Annu. Rev. Mar. Sci.* 4, 375–400. doi: 10.1146/annurev-marine-120709-142759

Wang, X., Sultana, C. M., Trueblood, J., Hill, T. C. J., Malfatti, F., Lee, C., et al. (2015). Microbial control of sea spray aerosol composition: a tale of two blooms. *ACS Cent. Sci.* 1, 124–131. doi: 10.1021/acscentsci.5b00148

Wetz, M. S., Robbins, M. C., and Paerl, H. W. (2009). Transparent exopolymer particles (TEP) in a river-dominated estuary: spatial-temporal distributions and an assessment of controls upon TEP formation. *Estuar. Coast.* 32, 447–455. doi: 10.1007/s12237-009-9143-2

Wilson, T. W., Ladino, L. A., Alpert, P. A., Breckels, M. N., Brooks, I. M., Browse, J., et al. (2015). A marine biogenic source of atmospheric ice-nucleating particles. *Nature* 525, 234–238. doi: 10.1038/nature14986

Wurl, O. (2009). "Sampling and sample treatments," in *Practical Guidelines for the Analysis of Seawater,* ed O. Wurl (Boca Raton, FL: CRC Press), 1–32.

Wurl, O., and Holmes, M. (2008). The gelatinous nature of the sea-surface microlayer. *Mar. Chem.* 110, 89–97. doi: 10.5194/bg-8-121-2011

Wurl, O., Miller, L., Ruttgers, R., and Vagle, S. (2009). The distribution and fate of surface-active substances in the sea-surface microlayer and water column. *Mar. Chem.* 115, 1–9. doi: 10.1016/j.marchem.2009.04.007

Wurl, O., Wurl, E., Miller, L., Johnson, K., and Vagle, S. (2011). Formation and global distribution of sea-surface microlayers. *Biogeosciences* 8, 121–135. doi: 10.1016/j.marchem.2008.02.009

Zack, G. W., Rogers, W. E., and Latt, S. A. (1977). Automatic-measurement of sister chromatid exchange frequency. *J. Histochem. Cytochem.* 25, 741–753.

Zar, J. H. (1996). *Biostatistical Analysis*. Upper Saddle River, NJ: Prentice-Hall.

Zhang, Z., Liu, L., Liu, C., and Cai, W. (2003). Studies on the sea surface microlayer - II. The layer of sudden change of physical and chemical properties. J. *Colloid Interf. Sci.* 264, 148–159. doi: 10.1016/s0021-9797(03)00390-4

Conflict of Interest Statement: The authors declare that the research was conducted in the absence of any commercial or financial relationships that could be construed as a potential conflict of interest.

frontiers in Microbiology

ORIGINAL RESEARCH
published: 28 March 2017
doi: 10.3389/fmicb.2017.00507

Production and Reutilization of Fluorescent Dissolved Organic Matter by a Marine Bacterial Strain, *Alteromonas macleodii*

Shuji Goto[1], Yuya Tada[2,3], Koji Suzuki[1,2] and Youhei Yamashita[1,2]*

[1] Graduate School of Environmental Science, Hokkaido University, Sapporo, Japan, [2] Faculty of Environmental Earth Science, Hokkaido University, Sapporo, Japan, [3] Project Team for Research and Development of Next-generation Technology for Ocean Resources Exploration, Japan Agency for Marine-Earth Science and Technology, Yokosuka, Japan

The recalcitrant fraction of marine dissolved organic matter (DOM) plays an important role in carbon storage on the earth's surface. Bacterial production of recalcitrant DOM (RDOM) has been proposed as a carbon sequestration process. It is still unclear whether bacterial physiology can affect RDOM production. In this study, we conducted a batch culture using the marine bacterial isolate *Alteromonas macleodii*, a ubiquitous gammaproteobacterium, to evaluate the linkage between bacterial growth and DOM production. Glucose (1 mmol C L^{-1}) was used as the sole carbon source, and the bacterial number, the DOM concentration in terms of carbon, and the excitation–emission matrices (EEMs) of DOM were monitored during the 168-h incubation. The incubation period was partitioned into the exponential growth (0–24 h) and stationary phases (24–168 h) based on the growth curve. Although the DOM concentration decreased during the exponential growth phase due to glucose consumption, it remained stable during the stationary phase, corresponding to approximately 4% of the initial glucose in terms of carbon. Distinct fluorophores were not evident in the EEMs at the beginning of the incubation, but DOM produced by the strain exhibited five fluorescent peaks during exponential growth. Two fluorescent peaks were similar to protein-like fluorophores, while the others could be categorized as humic-like fluorophores. All fluorophores increased during the exponential growth phase. The tryptophan-like fluorophore decreased during the stationary phase, suggesting that the strain reused the large exopolymer. The tyrosine-like fluorophore seemed to be stable during the stationary phase, implying that the production of tyrosine-containing small peptides through the degradation of exopolymers was correlated with the reutilization of the tyrosine-like fluorophore. Two humic-like fluorophores that showed emission maxima at the longer wavelength (525 nm) increased during the stationary phase, while the other humic-like fluorophore, which had a shorter emission wavelength (400 nm) and was categorized as recalcitrant, was stable.

OPEN ACCESS

Edited by:
Tony Gutierrez, Heriot-Watt University, UK

Reviewed by:
Emma Jane Rochelle-Newall, Institut de Recherche pour le Développement, France
Mary I. Abercrombie, Florida Gulf Coast University, USA

***Correspondence:**
Shuji Goto
gotoshuji@ees.hokudai.ac.jp

Specialty section:
This article was submitted to Aquatic Microbiology, a section of the journal Frontiers in Microbiology

Received: *09 September 2016*
Accepted: *13 March 2017*
Published: *28 March 2017*

Citation:
Goto S, Tada Y, Suzuki K and Yamashita Y (2017) Production and Reutilization of Fluorescent Dissolved Organic Matter by a Marine Bacterial Strain, Alteromonas macleodii. Front. Microbiol. 8:507. doi: 10.3389/fmicb.2017.00507

These humic-like fluorophore behaviors during incubation indicated that the composition of bacterial humic-like fluorophores, which were unavailable to the strain, differed between growth phases. Our results suggest that bacterial physiology can affect RDOM production and accumulation in the ocean interior.

Keywords: microbial carbon pump, recalcitrant DOM, fluorescent DOM, *Alteromonas macleodii*, growth phase, EEMs

INTRODUCTION

Marine dissolved organic matter (DOM) is one of the largest reduced organic carbon pools on the earth's surface, indicating that it plays as important role of the total carbon pool in the ocean (Hedges, 1992; Hansell and Carlson, 1998; Hansell et al., 2009). The average residence time of bulk DOM in the ocean has been estimated at approximately 2000–6000 years by ^{14}C dating analysis (Bauer et al., 1992; Druffel et al., 1992; Beaupré,, 2015). Observations of the global distribution of dissolved organic carbon (DOC) concentration with a coupled physical/biogeochemical model also showed that a major fraction of marine DOM is recalcitrant to microbial degradation with a time scale of more than a century (Hansell et al., 2009). Some constituents of marine DOM, e.g., humic-like fluorescent DOM (FDOM) (Yamashita and Tanoue, 2008; Catalá et al., 2015), carboxyl-rich aliphatic materials (Hertkorn et al., 2006), and polyaromatic compounds (Dittmar and Paeng, 2009), have been considered to be recalcitrant DOM (RDOM). However, the chemical characteristics of RDOM have not been fully clarified. Such molecularly uncharacterizable features of RDOM preclude a comprehensive understanding of the source and production mechanism of marine RDOM.

The microbial carbon pump (MCP) has recently been proposed as a carbon sequestration process driven by bacterial RDOM generation (Jiao et al., 2010). The MCP concept was derived from the results of microbial incubation studies (Ogawa et al., 2001; Kramer and Herndl, 2004; Kawasaki and Benner, 2006; Lønborg et al., 2009; Shimotori et al., 2009; Koch et al., 2014). These studies observed that DOM, which was distinct from labile substrates (such as glucose and glutamate) for microbes, was present in 20-day to 2-year incubations of microbial communities obtained from seawater. The residual DOM has been considered to be microbially derived DOM, which could not be utilized by heterotrophic bacteria during incubation. Ultrahigh resolution Fourier transform ion cyclotron resonance mass spectrometry (FT-ICR-MS) has recently been applied to determine the molecular composition of DOM obtained from in vitro incubations of marine microbial community. The results showed that experimentally obtained microbial DOM was similar to marine RDOM in terms of the molecular composition (Koch et al., 2014; Lechtenfeld et al., 2015), although it has also been reported that most microbial DOM is distinct from marine RDOM (Osterholz et al., 2015).

The products of MCP have also been traced using fluorescence techniques, e.g., excitation–emission matrices (EEMs), during in vitro incubation of marine microbial communities with various substrates, e.g., simple substrate, such as glucose (Kramer and Herndl, 2004; Lønborg et al., 2009; Shimotori et al., 2009), marine DOM (Jørgensen et al., 2014), and humic substances (Aparicio et al., 2015). These studies found that humic-like fluorophores were produced by marine microbes, and microbial humic-like fluorophores were usually not degraded during incubation. Shimotori et al. (2009) conducted a 90-day incubation experiment using a coastal microbial community with glucose as substrate, and reported that the coastal bacterial community generated a humic-like fluorophore that was similar to marine RDOM in terms of fluorescence characteristics, molecular size, and photo-degradability. Recent studies also suggest that production rates of humic-like fluorophore by marine microbial communities depended on the quality of substrates (Jørgensen et al., 2014; Aparicio et al., 2015). Such substrate dependency of humic-like fluorophore production by microbial communities is possibly due to changes in bacterial physiology and/or responding species with different substrates.

It has been suggested that the microbial RDOM is produced through bacterial exudation (Jiao et al., 2010, 2014), indicating a potential relationship between bacterial physiology and RDOM production. However, the relationship of RDOM production with bacterial physiology has scarcely been discussed because incubation experiments for evaluating MCP have usually been conducted with natural microbial communities, which include a wide variety of microbes with various physiologies. The incubation of a bacterial isolate could allow the evaluation of bacterial physiological states, as well as bacterial growth phase; yet, only few studies have been conducted on this topic. The FT-ICR-MS-based exometabolomics analysis of *Pseudovibrio* sp. incubation showed that the composition of bacterial DOM was affected by the growth phase (Romano et al., 2014). In contrast, Gruber et al. (2006) suggested that *Pseudomonas chlororaphis* produced persistent DOM, mainly during the exponential growth phase. On the other hand, Eichinger et al. (2009) reported that DOC accumulated during the stationary phase in the incubation of *Alteromonas infernus*. At present, only a few studies have assessed the microbial production of RDOM using marine bacterial isolates, and therefore, knowledge of the relationship between RDOM production and bacterial physiology is still limited, even though it is possibly one of the key parameters shaping the size and composition of the marine DOM pool.

The objective of this study was to investigate the relationship between physiology in terms of growth phase and RDOM production through in vitro incubation of a model marine bacterial isolate with glucose as the sole substrate. *Alteromonas macleodii*, a ubiquitous gammaproteobacterium from the surface to the deep layer of tropical and temperate oceans (López-Pérez et al., 2012), was used as a model marine bacterial isolate in

this study. *Alteromonas* was reported to grow predominantly during diatom blooms in the western North Pacific Ocean (Tada et al., 2011). An *Alteromonas* sp., designated strain AltSIO, was isolated by the Scripps Institution of Oceanography from coastal seawater and found to share ∼99% 16S ribosomal DNA sequence similarity with *A. macleodii* (Pedler et al., 2014; Pedler Sherwood et al., 2015). AltSIO alone consumed the entire pool of labile DOC, defined as the quantity consumed by coastal microbial assemblages within 5 days (Pedler et al., 2014), and has the capacity to significantly alter marine DOM composition (Pedler Sherwood et al., 2015). These studies suggested that *A. macleodii* also might contribute to high consumption and alteration of labile DOM in the ocean's surface. In this study, the humic-like fluorophores determined by EEMs were used to evaluate bacterial RDOM, while protein-like fluorophores in EEMs were used to monitor the reuse of the bacterial exopolymer.

MATERIALS AND METHODS

Marine Bacterial Isolate Model

The strain *A. macleodii* ATCC 27126 was obtained from the Japan Collection of Microorganisms, RIKEN Bio Resource Center (Tsukuba, Ibaraki, Japan), and was used as a model marine bacterial isolate.

Prior to the present experimental setup, 100 μL frozen stock of *A. macleodii* was inoculated onto 100 mL artificial seawater-based Aquil medium (Price et al., 1989) supplemented with glucose (1 mmol C L^{-1}) at 25°C for 24 h. Then, the medium was transferred onto new Aquil medium and incubated under the same conditions as the pre-culture medium. After 24 h of incubation, the culture was used as inoculum for the present experiment.

Experimental Setup

Alteromonas macleodii was cultivated in modified organic carbon-free Aquil medium (Price et al., 1989) (**Table 1**). Anhydrous salts used for artificial seawater (NaCl, Na_2SO_4, KCl, KBr) were combusted at 450°C for 4 h. $NaH_2PO_4{\cdot}H_2O$ (10 μmol P L^{-1}) and $NaNO_3$ (161 μmol N L^{-1}) were added as major nutrients. The media for control and experimental treatments were prepared without and with glucose (1 mmol C L^{-1}) in each triplicate, respectively. The *A. macleodii* inoculum was added to the medium of each treatment condition at a 1:1000 dilution. Then, each treatment condition with *A. macleodii* inoculum was dispensed into acid-washed (1 M HCl) 250 mL polyethylene terephthalate bottles. The bottle was filled with 100 mL of culture medium, and thus, gas phase was maintained in the bottles to keep oxygen at a high enough level to catabolize all of the added glucose. Incubations of the experimental and control treatments were conducted in the dark and in an incubator (CN-40, Mitsubishi-Engineering Co.) in which the temperature was maintained at 25°C. To determine the bacterial abundance, DOC concentration and DOM optical property, triplicate bottles were sampled at 0, 6, 12, 18 24, 72, 120, and 168 h in the experimental treatment and at 0 and 168 hours in the control treatment.

TABLE 1 | Composition of modified Aquil medium.

	Compound	Final concentration (mol L^{-1})
Salts	NaCl	4.20×10^{-1}
	Na_2SO_4	2.88×10^{-2}
	KCl	9.39×10^{-3}
	$NaHCO_3$	2.38×10^{-3}
	KBr	8.40×10^{-4}
	H_2BO_3	4.85×10^{-5}
	NaF	7.15×10^{-5}
	$MgCl_2{\cdot}6H_2O$	5.46×10^{-2}
	$CaCl_2{\cdot}2H_2O$	1.05×10^{-2}
	$SrCl_2{\cdot}6H_2O$	6.38×10^{-5}
Trace metal	$FeCl_2{\cdot}6H_2O$	1.00×10^{-6}
	$ZnSO_4{\cdot}7H_2O$	7.97×10^{-8}
	$MnCl_2{\cdot}4H_2O$	1.21×10^{-7}
	$CoCl_2{\cdot}6H_2O$	5.03×10^{-8}
	$CuSO_4{\cdot}5H_2O$	1.96×10^{-8}
	$Na_2MoO_4{\cdot}2H_2O$	1.00×10^{-7}
	Na_2SeO_3	1.00×10^{-8}
Major nutrients	$NaHPO_4{\cdot}H_2O$	1.00×10^{-5}
	$NaNO_3$	1.61×10^{-4}

Bacterial Abundance

Bacterial cell density was measured with an EPICS flow cytometer (XL ADC system, Beckman Coulter) equipped with a 15 mW air-cooled laser exciting at 488 nm, according to the protocol of Tada and Suzuki (2016). Samples were fixed in paraformaldehyde [2% (vol/vol) final concentration] and preserved at –25°C. Just before analysis, samples were stained with SYBR Gold (SYBR Gold Nucleic Acid Gel Stain, Life technologies) at a final concentration of 10^{-4} commercial stock solution for at least 15 min. To calculate the flow rate, 2 μm fluorescent beads (Fluoresbrite YG Carboxylate Microspheres 2.00 μm, Polysciences, Inc.) were added to the flow samples. We used a low flow rate mode and analyzed the samples until twenty thousand particles were counted or the measurement time reached 5 minutes. The measured values were corrected by blank value subtraction; the blank was measured with artificial seawater filtered with 0.2-μm pore size cellulose membrane filters (DISMIC-25AS 0.20 μm, ADVANTEC).

DOC Concentrations and DOM Optical Properties

Samples for DOM analyses were filtered through pre-combusted (450°C, 3 h) glass fiber filters with a nominal pore size of 0.3 μm (GF75, Whatman) under gentle vacuum (<0.02 MPa) at each incubation time to remove particles, including *A. macleodii*. The filtrate was collected into a pre-combusted (450°C, 3 h) glass vial with teflon-lined cap and was preserved at –25°C until analysis.

The DOC concentration was determined by high-temperature catalytic oxidation with a total organic carbon analyzer (TOC-V CSH, Shimadzu). The DOC concentrations were calculated using the standard curve of potassium hydrogen phthalate solution, which was determined daily. The accuracy and consistency of the measured DOC concentrations were checked by a deep seawater

reference sample (Hansell Laboratory, University of Miami), which was assessed daily.

Excitation–emission matrix was measured using a fluorometer (FluoroMax-4, Horiba) according to the procedure of Tanaka et al. (2014). Samples were allowed to reach near room temperature before the EEM measurements were undertaken. Forty-one emission scans from 290 to 600 nm taken at 2-nm intervals were acquired for the excitation wavelengths between 250 and 450 nm at 5-nm intervals. The bandpass was set to 5 nm for both excitation and emission. The fluorescence spectra were scanned with a 0.25 s integration time and acquired in the S/R mode. Several post-acquisition steps were involved in the correction of the fluorescence spectra, including instrumental bias correction and corrections of inner filter effect using absorbance. Following this, the EEMs of Milli-Q water were subtracted from those of the samples, and fluorescence intensities in EEMs were converted to Raman Units (RU) with the peak areas of Raman scatter at 350 nm excitation (Lawaetz and Stedmon, 2009). RU can be converted to quinine sulfate units (QSU) by using the equation QSU = RU/0.0767 (Lawaetz and Stedmon, 2009). The absorbance spectrum of each sample for correction of inner filter effect was measured with a Shimadzu UV-1800 spectrophotometer in a 1-cm quartz cuvette according to Yamashita et al. (2013). Because nitrate has relatively high absorbance in the UV-B region (Catalá et al., 2016) at high concentrations (e.g., 161 μmol N L^{-1} in the medium), investigations of changes in the absorption spectrum associated with *A. macleodii* incubation were abandoned. The contour of EEMs was plotted by R (version 3.2.3) (R Development Core Team, 2015).

RESULTS

Growth of *A. macleodii* and Change in DOC Concentration

The abundance of *A. macleodii* increased exponentially during the first 24 h in the experimental treatment (**Figure 1A**). The cell density was 4.1×10^4 cells mL^{-1} at the initiation of incubation ($t = 0$) and increased up to $3.7 \pm 1.8 \times 10^6$ cells mL^{-1} after 24 h. The cell density then remained stable on a logarithmic scale until the end of the experiment (**Figure 1A**). Therefore, the periods of 0–24 h and 24–168 h were defined as the exponential growth and stationary phases, respectively. The average specific growth rate was 0.19 ± 0.10 h^{-1} during the exponential growth phase. In the control treatment, cell density increased approximately twofold during the incubation (from 3.4×10^4 cells mL^{-1} at the initiation of the incubation to $8.0 \pm 0.5 \times 10^4$ cells mL^{-1} at the end of the incubation), indicating that bacterial growth caused by the medium substrate and carbon storage in the cells of the inoculum was much lower than that caused by glucose in the experimental treatment.

The DOC concentration gradually decreased during the early part of the exponential growth phase (first 18-h) from 995 μmol C L^{-1} to 830 ± 28 μmol C L^{-1} (**Figure 1B**) and then drastically decreased to 58 ± 15 μmol C L^{-1} in the latter part of the exponential growth phase (18–24 h). There was a larger relative decrease in DOC concentration normalized by bacterial cell density between 18 and 24 h (0.29 mmol C $cell^{-1}$) than between 0 and 18 h (0.17 mmol C $cell^{-1}$), thus suggesting a substantial increase in *A. macleodii* cell volume between 18 and 24 h. The DOC concentration was almost constant (from 51 ± 4 μmol C L^{-1} to 89 ± 29 μmol C L^{-1}) over the stationary phase and was 51 ± 4 μmol C L^{-1} at the end of the experimental incubations (168 h).

The DOC concentrations in the control treatment were 1–2 orders of magnitude lower than those in the experimental treatment and were 7.6 μmol C L^{-1} and 9.6 ± 1.5 μmol C L^{-1} at the beginning and end of the incubation, respectively. The DOC concentrations detected in the control experiment were possibly derived from the medium and bacterial inoculum.

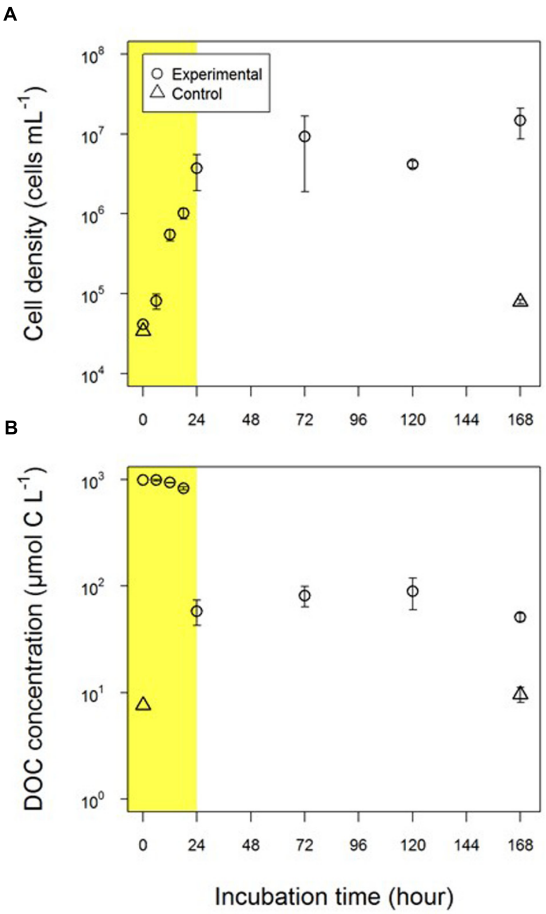

FIGURE 1 | Changes in (A) the abundance of *Alteromonas macleodii* (*A. macleodii*) and **(B)** the concentration of dissolved organic carbon (DOC). Circles and triangles represent the experimental and control treatments, respectively. Yellow shading indicates the exponential growth phase.

FDOM Derived from *A. macleodii*

Fluorescent peaks found in EEMs at the 24-h time point and the end of the experimental treatment are shown in **Figures 2B,D**, respectively. Because EEMs at the beginning of the experimental

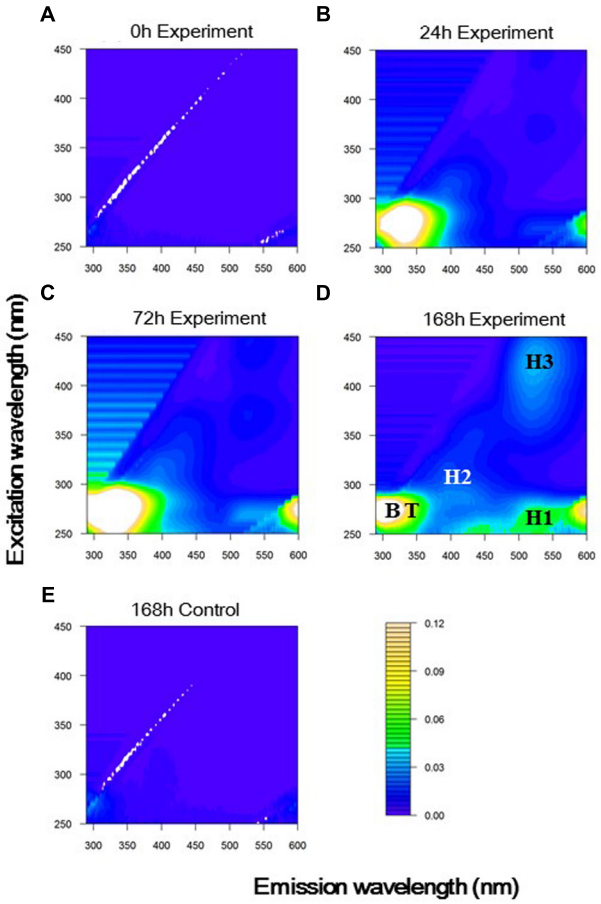

FIGURE 2 | Excitation-emission matrices (EEMs) based on the average of triplicate samples at (A) 0, **(B)** 24, **(C)** 72, and **(D)** 168 h in the experimental treatment, and at **(E)** 168 h in the control treatment. Peaks generated by *A. macleodii* were indicated with abbreviations: Tyrosine-like (B, Ex/Em = 275/300 nm); Tryptophan-like (T, Ex/Em = 275/330 nm); Humic-like 1 (H1, Ex/Em = 270/520 nm); Humic-like 2 (H2, Ex/Em = 315/400 nm); Humic-like 3 (H3, Ex/Em = 425/520 nm).

treatment (**Figure 2A**) and at the end of the control treatment (**Figure 2E**) did not show distinct fluorescent peaks, it can be concluded that fluorescent peaks found for the experimental treatment were derived from *A. macleodii* and not from the incubation medium or contamination during incubation.

Five fluorescent peaks were defined from EEMs obtained at the end of the experimental treatment (**Figure 2D** and **Table 2**). Two peaks were characterized as protein-like fluorescent peaks similar to the aromatic amino acids tyrosine and tryptophan (Coble, 1996; Mayer et al., 1999). From EEMs observed during the experimental treatment (**Figures 2B–D**), the excitation and emission wavelength (Ex/Em) of tyrosine-like and tryptophan-like peaks were defined to be 275/300 nm and 275/330 nm, respectively. Three peaks could be categorized to humic-like fluorophores. Two of them had emission maximum longer than 500 nm (H1: Ex/Em = 270/520 nm, H3: Ex/Em = 425/520 nm) and have usually been defined to be terrestrial humic-like FDOM in coastal environments (Stedmon and Markager, 2005). The combined fluorescence characteristics of H1 and H3 were similar to that found in the most abundant component in the humic acid fraction extracted from sediments/soils (He et al., 2006; Santín et al., 2009). The other humic-like fluorophore (H2: Ex/Em = 315/400 nm), which had a shorter emission wavelength than H1 and H3, was similar to traditionally defined marine/microbial humic-like FDOM (Coble, 1996, 2007) and was also similar to a fluorophore excreted by cultured phytoplankton (Romera-Castillo et al., 2010).

Changes in Fluorescence Intensity of Individual Peaks during *A. macleodii* Incubation

The fluorescence intensities of two protein-like peaks, namely tyrosine-like and tryptophan-like peaks, increased during the exponential growth phase, particularly during the period of 18–24 h (**Figure 3**), in which the DOC concentration drastically decreased (**Figure 1**). Tyrosine-like fluorescence intensity increased during the early part of the stationary phase (24–72 h, **Figure 3**; Student's *t*-test, $p < 0.05$) and was tended to decrease during the latter part of the stationary phase (72–168 h; Student's *t*-test, $p > 0.05$). Tryptophan-like fluorescence intensity decreased significantly during the latter part of the stationary phase (**Figure 3**; Student's *t*-test, $p < 0.05$).

Tyrosine-like and tryptophan-like fluorophores exhibited fluorescence peaks with an excitation wavelength of 275 nm (Coble, 2007). It is difficult to quantitatively evaluate changes in protein-like fluorescence intensities, because the emission spectra of tyrosine and tryptophan molecules overlap (Mayer et al., 1999; Lakowicz, 2006). Thus, in this study, the emission

TABLE 2 | Characteristics of fluorescent peaks produced by *A. macleodii*.

Excitation wavelength (nm)	Emission wavelength (nm)	Peak (abbreviation)	Description of previous study
275	300	Tyrosine-like (B)	Tyrosine[1] Low molecular weight peptide[2]
275	330	Tryptophan-like (T)	Tryptophan[1] High molecular weight peptide, protein molecule[2]
270	520	Humic-like 1 (H1)	Enriched in humic acid fraction[3,4]
315	400	Humic-like 2 (H2)	Marine autochthonic substance[5]
425	520	Humic-like 3 (H3)	Enriched in humic acid fraction[3,4]

[1]*Mayer et al. (1999);* [2]*Yamashita and Tanoue (2004);* [3]*He et al. (2006);* [4]*Santín et al. (2009);* [5]*Coble (1996).*

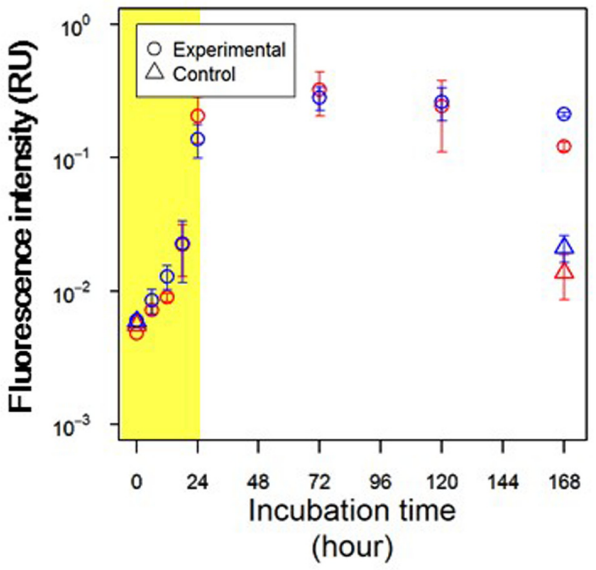

FIGURE 3 | Changes in fluorescence intensities of protein-like peak. Red and blue symbols indicate tyrosine-like peak (Ex/Em = 275/300 nm) and tryptophan-like peak (Ex/Em = 275/330 nm), respectively. Circles and triangles represent the experimental and control treatments, respectively. Yellow shading indicates the exponential growth phase.

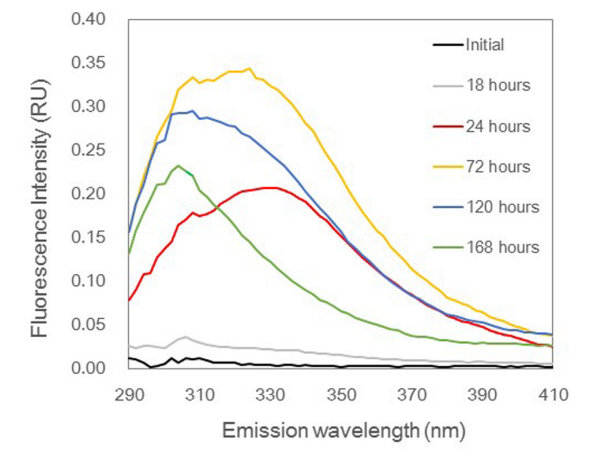

FIGURE 4 | Emission spectra at 275 nm excitation in the experimental treatment based on the average of triplicate samples. These spectra indicate changes of protein-like fluorophores. The color of each spectrum represents each incubation time.

spectrum at an excitation wavelength of 275 nm was used to evaluate the dominant protein-like fluorophore during *A. macleodii* incubation (**Figure 4**). The emission spectra were almost the same during 0–18 h, but the fluorescence intensities at wavelengths corresponding to protein-like fluorescence (approximately 290–370 nm) were slightly increased with incubation time (**Figures 3**, **4**). A single fluorophore peaked at 330 nm appeared in 24 h, indicating that tryptophan-like fluorophore was mainly produced during the exponential growth phase (**Figures 2B**, **4**). It seemed that two fluorophores peaked at 330 and 300 nm were the main components of the spectrum at 72 h, indicating that both tryptophan-like and tyrosine-like fluorophores were produced during the early part of the stationary phase (**Figures 2C**, **4**). Although fluorescence intensities corresponding to protein-like fluorophores decreased entirely during 72–168 h, the decrease in the tryptophan-like fluorophore (peak at 330 nm) was greater than that of the tyrosine-like fluorophore (peak at 300 nm) (**Figures 2D**, **4**). Furthermore, the tyrosine-like fluorophore became a major peak at 168 h. The fluorescence intensity at 300 nm should be composed of the peak maximum of tyrosine-like fluorophore and the peak edge of tryptophan-like fluorophore. Thus, changes in the shape of emission spectrum observed during 72–168 h imply that the tryptophan-like fluorophore decreased but the tyrosine-like fluorophore was relatively stable during the latter part of the stationary phase.

The fluorescence intensities of all humic-like fluorophores increased during the exponential growth phase (**Figure 5**). The changes in fluorescence intensity during the stationary phase varied among the humic-like fluorophores (**Figure 5**). Two humic-like fluorophores with emission maxima at longer wavelengths (H1 and H3) continuously increased throughout the stationary phase. In contrast, the other humic-like fluorophore (H2) was relatively stable during the stationary phase (Student's *t*-test, $p > 0.05$).

Fluorescence intensities of all fluorophores were comparable in the control and experimental treatments at the initiation of these treatments (**Figures 3**, **5**). In the control treatment, the fluorescence intensities of all humic-like fluorophores remained unchanged during the incubation (**Figure 5**). Although the fluorescence intensities of protein-like fluorophores in the control treatment increased several fold during the 168-h incubation, these intensities were 1 order of magnitude lower than those observed for the experimental treatment at the end of the incubation (**Figure 3**).

DISCUSSION

Changes in DOM Quantity and Quality with *A. macleodii* Growth

A. macleodii has been reported to be a ubiquitous gammaproteobacterium in temperate oceans (López-Pérez et al., 2012). The possibility that *A. macleodii* substantially contributes to the consumption and alteration of labile DOM in surface waters of marine environments has also been considered (Tada et al., 2011; Pedler et al., 2014; Pedler Sherwood et al., 2015). Glucose was used as a labile substrate for *A. macleodii* incubation in this study. Previous studies demonstrated that coastal microbial communities completely consumed glucose within 2 days of incubation (Ogawa et al., 2001; Kawasaki and Benner, 2006). The decrease in the DOC concentration was coupled with the increase in *A. macleodii* abundance, indicating that the decrease in the DOC concentration during

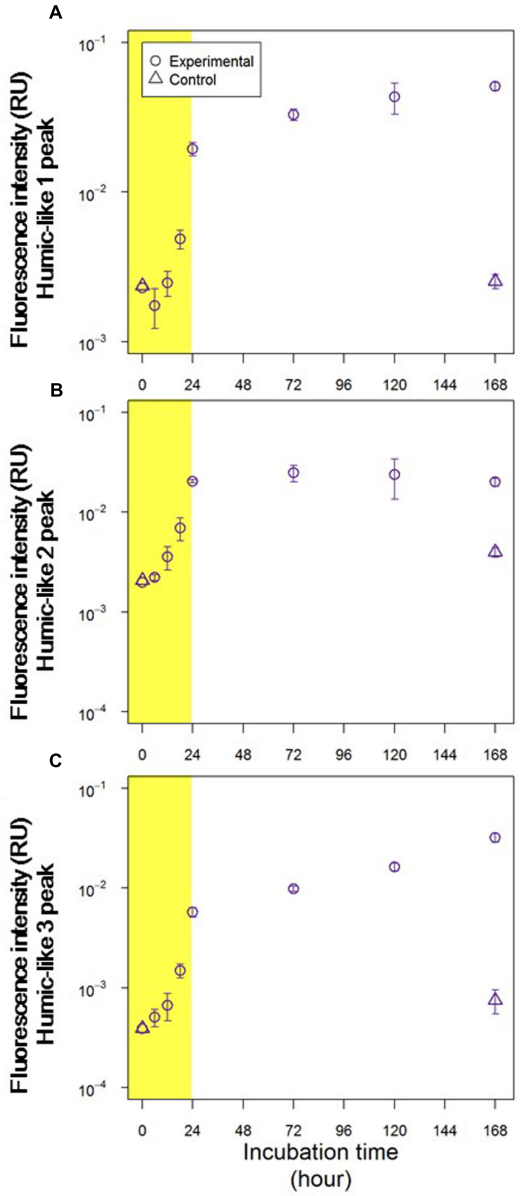

FIGURE 5 | Changes in fluorescence intensities of (A) humic-like 1 peak (Ex/Em = 270/520 nm), **(B)** humic-like 2 peak (Ex/Em = 315/400 nm) and **(C)** humic-like 3 peak (Ex/Em = 425/520 nm). Circles and triangles represent the experimental and control treatments, respectively. Yellow shading indicates the exponential growth phase.

the exponential growth phase should be due to the consumption of glucose by the bacterial strain. Assuming that the glucose was completely consumed within several days of incubation, residual DOC was produced by *A. macleodii*.

Protein molecules that contain both tryptophan and tyrosine molecules usually show only tryptophan fluorescence because of energy transfer (Lakowicz, 2006). A previous study analyzed the fluorescence properties of surface DOM in the Sagami Bay and showed that only tryptophan-like fluorescence was evident in high-molecular-weight fractions, whereas tyrosine-like fluorescence was dominant in low-molecular-weight fractions (Yamashita and Tanoue, 2004). Thus, changes in the composition of protein-like fluorophores with *A. macleodii* growth possibly reflected the changes in the relative molecular weight of peptides/proteins, which were released and reused by *A. macleodii*. Tryptophan-like fluorophore clearly appeared at 24 h in our experiment (**Figure 4**), implying that large polymers, such as protein molecules, were predominantly released during the exponential growth phase. The incubations contained not only tryptophan-like fluorophore but also tyrosine-like fluorophore, which both increased during 24–72 h (**Figure 4**). This result suggested that large polymers were still released but that part of these exopolymers were degraded to small peptides. The decrease in tryptophan-like fluorophore was predominant, but tyrosine-like fluorophore was relatively stable at the latter part of the stationary phase (72–168 h), suggesting that the production of small peptides due to the degradation of large exopolymers was correlated with the reutilization of tyrosine-like fluorophores.

The reutilization of exopolymer by *A. macleodii* was suggested in the stationary phase while two humic-like fluorophores continued to accumulate, implying that unavailable DOM were produced from available substrate. The DOC concentrations were relatively stable during the stationary phase, as mentioned above. These results suggested that major portions of DOM produced by *A. macleodii* are unavailable to these bacteria, although a minor fraction of this DOM is reusable by the strain. The remaining DOC concentration produced by *A. macleodii* was estimated to be 41 ± 4 μM C by subtracting the DOC concentration at the end of control treatment (9.6 ± 1.5 μM C; **Figure 1**) from that of experimental treatment (51 ± 4 μM C; **Figure 1**). This remnant DOC concentration corresponded to approximately 4% of the initial glucose used for the *A. macleodii* incubation. Notably, this estimation is comparable to the results obtained by previous studies that conducted incubations of bacterial isolates or microbial communities with glucose. Gruber et al. (2006) showed that 3% of initial glucose was converted to residual DOC by the bacterial isolate *P. chlororaphis* during 36 days of incubation. In addition, 3–6% of initial glucose was found to convert to molecularly uncharacterizable DOM in marine microbial communities, and occurred after 90-day to 2-year periods of incubation (Ogawa et al., 2001; Shimotori et al., 2009; Koch et al., 2014). Such consistency in the production efficiency of residual DOC (i.e., 3–6% of initial substrate) suggests that neither microbial community structure nor microbial growth affected the efficiency of MCP.

Humic-Like Fluorophores Produced by *A. macleodii*

The production of humic-like fluorophores has been observed in incubation experiments using marine microbial communities (Kramer and Herndl, 2004; Lønborg et al., 2009; Shimotori et al., 2009). This study demonstrated that humic-like fluorophores can be generated not only by microbial communities but also by single bacterial strains using simple substrates, such as glucose. This finding is consistent with those of Shimotori et al. (2012),

who found that humic-like fluorophores were generated during incubations of several bacterial isolates in Marine Broth culture medium.

A humic-like fluorophore (H2) produced by *A. macleodii* was similar to a previously defined marine microbial humic-like peak M (Coble, 1996, 2007). This fluorophore also corresponded to a fluorophore that was found to be microbial recalcitrant FDOM with the time scale of the thermohaline circulation (Yamashita and Tanoue, 2008). Fluorescent components similar to H2 were obtained through parallel factor analysis (PARAFAC) of FDOM from the open ocean and were found to be related to apparent oxygen utilization in the deep ocean (Jørgensen et al., 2011; Tanaka et al., 2014), implying that H2 produced by *A. macleodii* is possibly recalcitrant DOM. On the other hand, peak M was produced by phytoplankton isolates (Romera-Castillo et al., 2010) and consumed partially by bacterial communities (Romera-Castillo et al., 2011). These results suggest that the reactivity of the peak M-type fluorophore was dependent on its source; specifically, the fluorophore produced by heterotrophic bacteria is possibly recalcitrant, while that produced by phytoplankton includes a labile fraction.

The other two humic-like fluorophores (H1 and H3), which peaked at longer emission wavelengths than that of H2, continued to be produced by *A. macleodii* during both the stationary phase and the exponential growth phase. Shimotori et al. (2009) also observed a fluorophore peaked at >500 nm emission during the incubation of coastal microbial communities with glucose. On the other hand, there was a high presence of PARAFAC components that were similar to a combination of H1 and H3 in humic acid fractions extracted from soils and sediments (He et al., 2006; Santín et al., 2009). These PARAFAC components were also considered to be terrigenous FDOM (Stedmon and Markager, 2005; Singh et al., 2013). These results suggest that the fluorophore that peaked at a longer emission wavelength (>500 nm) might be ubiquitously produced by heterotrophic bacteria but is enriched in humic acid fractions from soils and sediments. Notably, in Shimotori's incubation studies (Shimotori et al., 2009), this fluorophore appeared in EEMs during the period of increasing bacterial abundance but disappeared from EEMs during the period of decreasing bacterial abundance. In the open ocean, this fluorophore is generally not present (Jørgensen et al., 2011; Tanaka et al., 2014). Thus, *A. macleodii* may be one of the key species that produces this fluorophore, and this fluorophore might be consumed by other microbes in natural environments.

Potential Relationship between Bacterial Growth and the Production of Humic-Like Fluorophore

The production rates of microbial humic-like fluorophore differ among substrates used in the incubation of marine bacterial communities (Jørgensen et al., 2014; Aparicio et al., 2015). For example, Aparicio et al. (2015) found that the production rates of marine humic-like fluorophore during the incubation of marine bacterial communities with Suwannee River humic acids were higher than those with glucose and acetate. Using different substrates for microbial community incubation reportedly cause changes in microbial community structure and/or bacterial physiology (Gómez-Consarnau et al., 2012). Therefore, in studies of bacterial communities, it is difficult to evaluate whether the factor regulating the production of humic-like fluorophores is bacterial species or physiology; in contrast, incubations using a bacterial isolate allow insight into the relationship between bacterial physiology and RDOM production.

The bacterial physiology was evaluated in terms of growth phases in this study. The quantity or quality of substrate is one of the critical factors in controlling bacterial growth (Jannasch and Egli, 1993). Therefore, the physiology of *A. macleodii* was likely altered by the change in substrate availability. The exponential growth phase of *A. macleodii* can be characterized as the period that the strain consumed glucose and produced various extracellular compounds, e.g., three humic-like fluorophores as well as a tryptophan-like fluorophore. The physiology of *A. macleodii* shifted to the stationary phase after the complete consumption of glucose, and the tryptophan-like fluorophore was consumed, but two humic-like fluorophores were produced. The results showed that the production mechanisms of humic-like fluorophores, which cannot be reused by the strain, are correlated with the physiology of *A. macleodii*. The humic-like fluorophore (H2) that is similar to recalcitrant microbial humic-like FDOM (Yamashita and Tanoue, 2008; Catalá et al., 2015) is only produced in the exponential phase, but other fluorophores (H1 and H3), which might be consumed by other microbes (Shimotori et al., 2009), are produced during both the exponential and the stationary phases of *A. macleodii*.

The relationship between bacterial growth and RDOM production that is apparent with *A. macleodii* was not consistent with the previous studies conducted by Gruber et al. (2006) and Eichinger et al. (2009). *A. macleodii* was found to produce extracellular humic-like fluorophores, which were unavailable to the strain during the exponential growth and the stationary phases. However, DOC produced by a different *Alteromonas* strain (*A. infernus*) was accumulated under conditions of carbon starvation of the isolate (i.e., the stationary phase in this study) during the incubation in which pyruvate was added every 48-hours as labile substrate (Eichinger et al., 2009). Specific compounds detected by mass spectrometry with electrospray ionization were produced in the exponential growth phase and remained at the end of *P. chlororaphis* incubation with glucose for 36 days, suggesting that recalcitrant compounds, which cannot be reused by the strain, were possibly produced during the exponential growth phase (Gruber et al., 2006). Although incubation conditions, such as temperature, the quality and quantity of substrate, and the composition of artificial seawater, varied among the studies, the results obtained by this study and the previous studies suggest that the physiology related to RDOM production might differ between bacterial species.

CONCLUSION AND REMARKS

The present study first evaluated the relationship between bacterial growth and the production of humic-like fluorophores during the incubation of a model bacterial isolate, *A. macleodii*,

with glucose as a substrate. The results of the experiment showed that *A. macleodii* produced three humic-like fluorophores; one is optically similar to recalcitrant microbial humic-like FDOM, while the other two might be consumed by other species of marine bacteria. The compositions of humic-like fluorophores produced by *A. macleodii* differed between the growth phases of the isolate, which might have been affected by the changes in available substrate from glucose to extracellular compounds (such as tryptophan-like fluorophore) released by the isolate.

On the basis of prior studies, variable recalcitrant characteristics are suggested by the humic-like fluorophores produced by *A. macleodii*, although these humic-like fluorophores appeared to be unavailable to the strain. To confirm the recalcitrant characteristics of DOM produced by bacterial isolates (e.g., humic-like fluorophores), the incubation of bacterial DOM with marine microbial communities is necessary. Isolate culture experiments with different incubation conditions (e.g., temperature, substrate quality and quantity) may provide a better understanding of the effect of bacterial physiology on RDOM production. Incubation studies using several species of bacterial isolates with the same conditions are also necessary to confirm whether the relationship between bacterial physiology and RDOM production differs among bacterial species. The cumulative results of such in vitro experiments will provide better insight into the relationship between bacterial physiology and RDOM production, and thus, such experiments will contribute to a better understanding of the factors that regulate the efficiency of MCP, which potentially shapes the pool size and composition of marine DOM.

AUTHOR CONTRIBUTIONS

All authors contributed to the design of the study. SG performed incubation experiment, sample measurements, and data analyses with help of YT, KS, and YY. SG wrote the initial draft of the manuscript and all authors contributed to its revision.

ACKNOWLEDGMENTS

This study was financially supported by the Grants-in-Aid (No. 24681002 and 24121003) from Japan Society for the Promotion of Science (JSPS) to YY, Grants-in-Aid (No. 13J04633 and 26740001) from JSPS to YT, and Grants-in-Aid (No. 24121004) from JSPS to KS.

REFERENCES

Aparicio, F. L., Nieto-Cid, M., Borrull, E., Romero, E., Stedmon, C. A., Sala, M. M., et al. (2015). Microbially-mediated fluorescent organic matter transformations in the deep ocean. Do the chemical precursors matter? *Front. Mar. Sci.* 2:106. doi: 10.3389/fmars.2015.00106

Bauer, J. E., Williams, P. M., and Druffel, E. R. M. (1992). 14C activity of dissolved organic carbon fractions in the north-central Pacific and Sargasso Sea. *Nature* 357, 667–670. doi: 10.1038/357667a0

Beaupré, S. R. (2015). "The carbon isotopic composition of marine DOC," in *Biogeochemistry of Marine Dissolved Organic Matter*, 2nd Edn, eds D. A. Hansell and C. A. Carlson (San Diego, CA: Academic Press), 481–508.

Catalá, T. S., Reche, I., Fuentes-Lema, A., Romera-Castillo, C., Nieto-Cid, M., Ortega-Retuerta, E., et al. (2015). Turnover time of fluorescent dissolved organic matter in the dark global ocean. *Nat. Commun.* 6:5986. doi: 10.1038/ncomms6986

Catalá, T. S., Reche, I., Ramón, C. L., López-Sanz, À., Álvarez, M., and Calvo, E. (2016). Chromophoric signatures of microbial by-products in the dark ocean. *Geophys. Res. Lett.* 43, 7639–7648. doi: 10.1002/2016GL069878

Coble, P. G. (1996). Characterization of marine and terrestrial DOM in seawater using excitation emission matrix spectroscopy. *Mar. Chem.* 51, 325–346. doi: 10.1016/0304-4203(95)00062-3

Coble, P. G. (2007). Marine optical biogeochemistry: the chemistry of ocean color. *Chem. Rev.* 107, 402–418. doi: 0.021/cr050350+

Dittmar, T., and Paeng, J. (2009). A heat-induced molecular signature in marine dissolved organic matter. *Nat. Geosci.* 2, 175–179. doi: 10.1038/ngeo440

Druffel, E. R. M., Williams, P. M., Bauer, J. E., and Ertel, J. R. (1992). Cycling of dissolved and particulate organic matter in the open ocean. *J. Geophys. Res.* 97, 15639–15659. doi: 10.1029/92JC01511

Eichinger, M., Kooijman, S. A. L. M., Sempere, R., Lefevre, D., Gregori, G., Charriere, B., et al. (2009). Consumption and release of dissolved organic carbon by marine bacteria in a pulsed-substrate environment: from experiments to modeling. *Aquat. Microb. Ecol.* 56, 41–54. doi: 10.3354/ame01312

Gómez-Consarnau, L., Lindh, M. V., Gasol, J. M., and Pinhassi, J. (2012). Structuring of bacterioplankton communities by specific dissolved organic carbon compounds. *Environ. Microbiol.* 14, 2361–2378. doi: 10.1111/j.1462-2920.2012.02804.x

Gruber, D. F., Simjouw, J.-P., Seitzinger, S. P., and Taghon, G. L. (2006). Dynamics and characterization of refractory dissolved organic matter produced by a pure bacterial culture in an experimental predator-prey system. *Appl. Environ. Microbiol.* 72, 4184–4191. doi: 10.1128/AEM.02882-05

Hansell, D. A., and Carlson, C. A. (1998). Deep-ocean gradients in the concentration of dissolved organic carbon. *Nature* 395, 263–266. doi: 10.1038/26200

Hansell, D. A., Carlson, C. A., Repeta, D. J., and Schlitzer, R. (2009). Dissolved organic matter in the ocean: a controversy stimulates new insights. *Oceanography* 22, 202–211. doi: 10.5670/oceanog.2009.109

He, Z., Ohno, T., Cade-Menum, B. J., Erich, M. S., and Honeycutt, C. W. (2006). Spectral and chemical characterization of phosphates associated with humic substances. *Soil Sci. Soc. Am. J.* 70, 1741–1751. doi: 10.2136/sssaj2006.0030

Hedges, J. I. (1992). Global biogeochemical cycles: progress and problems. *Mar. Chem.* 39, 67–93. doi: 10.1016/0304-4203(92)90096-S

Hertkorn, N., Benner, R., Frommberger, M., Schmitt-Kopplin, P., Witt, M., Kaiser, K., et al. (2006). Characterization of a major refractory component of marine dissolved organic matter. *Geochim. Cosmochim. Acta* 70, 2990–3010. doi: 10.1016/j.gca.2006.03.021

Jannasch, H. W., and Egli, T. (1993). Microbial growth kinetics: a historical perspective. *Antonie Van Leeuwenhoek* 63, 213–224. doi: 10.1007/BF00871219

Jiao, N., Herndl, G. J., Hansell, D. A., Benner, R., Kattner, G., Wilhelm, S. W., et al. (2010). Microbial production of recalcitrant dissolved organic matter: long-term carbon storage in the global ocean. *Nat. Rev. Microbiol.* 8, 593–599. doi: 10.1038/nrmicro2386

Jiao, N., Robinson, C., Azam, F., Thomas, H., Baltar, F., Dang, H., et al. (2014). Mechanisms of microbial carbon sequestration in the ocean–future research directions. *Biogeosciences* 11, 5285–5306. doi: 10.5194/bg-11-5565-2014

Jørgensen, L., Stedmon, C. A., Granskog, M. A., and Middelboe, M. (2014). Tracing the long-term microbial production of recalcitrant fluorescent dissolved organic matter in seawater. *Geophys. Res. Lett.* 41, 2481–2488. doi: 10.1002/2014GL059428

Jørgensen, L., Stedmon, C. A., Kragh, T., Markager, S., Middelboe, M., and Søndergaard, M. (2011). Global trends in the fluorescence characteristics and distribution of marine dissolved organic matter. *Mar. Chem.* 126, 139–148. doi: 10.1016/j.marchem.2011.05.002

Kawasaki, N., and Benner, R. (2006). Bacterial release of dissolved organic matter during cell growth and decline: molecular origin and composition. *Limnol. Oceanogr.* 51, 2170–2180. doi: 10.4319/lo.2006.51.5.2170

Koch, B. P., Kattner, G., Witt, M., and Passow, U. (2014). Molecular insights into the microbial formation of marine dissolved organic matter: recalcitrant or labile? *Biogeosciences* 11, 4173–4190. doi: 10.5194/bg-11-4173-2014

Kramer, G. D., and Herndl, G. J. (2004). Photo- and bioreactivity of chromophoric dissolved organic matter produced by marine bacterioplankton. *Aquat. Microb. Ecol.* 36, 239–246. doi: 10.3354/ame036239

Lakowicz, J. R. (2006). *Principles of Fluorescence Spectroscopy*, 3rd Edn. New York, NY: Springer. doi: 0.007/978-0-387-46312-4

Lawaetz, A. J., and Stedmon, C. A. (2009). Fluorescence intensity calibration using the Raman scatter peak of water. *Appl. Spectrosc.* 63, 936–940. doi: 10.1366/000370209788964548

Lechtenfeld, O. J., Hertkorn, N., Shen, Y., Witt, M., and Benner, R. (2015). Marine sequestration of carbon in bacterial metabolites. *Nat. Commun.* 6:6711. doi: 10.1038/ncomms7711

Lønborg, C., Álvarez-Salgado, X. A., Davidson, K., and Miller, A. E. J. (2009). Production of bioavailable and refractory dissolved organic matter by coastal heterotrophic microbial populations. *Estuar. Coast. Shelf Sci.* 82, 682–688. doi: 10.1016/j.ecss.2009.02.026

López-Pérez, M., Gonzaga, A., Martin-Cuadrado, A.-B., Onyshchenko, O., Ghavidel, A., Ghai, R., et al. (2012). Genomes of surface isolates of *Alteromonas macleodii*: the life of a widespread marine opportunistic copiotroph. *Sci. Rep.* 2:696. doi: 10.1038/srep00696

Mayer, L. M., Schick, L. L., and Loder, T. C. (1999). Dissolved protein fluorescence in two Maine estuaries. *Mar. Chem.* 64, 171–179. doi: 10.1016/S0304-4203(98)00072-3

Ogawa, H., Amagai, Y., Koike, I., Kaiser, K., and Benner, R. (2001). Production of refractory dissolved organic matter by bacteria. *Science* 292, 917–920. doi: 10.1126/science.1057627

Osterholz, H., Niggemann, J., Giebel, H.-A., Simon, M., and Dittmar, T. (2015). Inefficient microbial production of refractory dissolved organic matter in the ocean. *Nat. Commun.* 6:7422. doi: 10.1038/ncomms8422

Pedler, B. E., Aluwihare, L. I., and Azam, F. (2014). Single bacterial strain capable of significant contribution to carbon cycling in the surface ocean. *Proc. Natl. Acad. Sci. U.S.A.* 111, 7202–7207. doi: 10.1073/pnas.1401887111

Pedler Sherwood, B., Shaffer, E. A., Reyes, K., Longnecker, K., Aluwihare, L. I., and Azam, F. (2015). Metabolic characterization of a model heterotrophic bacterium capable of significant chemical alteration of marine dissolved organic matter. *Mar. Chem.* 177, 357–365. doi: 10.1016/j.marchem.2015.06.027

Price, N. M., Harrison, G. I., Hering, J. G., Hudson, R. J., Nirel, P. M. V., Palenik, B., et al. (1989). Preparation and chemistry of the artificial algal culture medium Aquil. *Biol. Oceanogr.* 6, 443–461. doi: 10.1080/01965581.1988.10749544

R Development Core Team (2015). *R: A Language and Environment for Statistical Computing*. Vienna: R Foundation for Statistical Computing.

Romano, S., Dittmar, T., Bondarev, V., Weber, R. J. M., Viant, M. R., and Schulz-Vogt, H. N. (2014). Exo-metabolome of *Pseudovibrio* sp. FO-BEG1 analyzed by ultra-high resolution mass spectrometry and the effect of phosphate limitation. *PLoS ONE* 9:e96038. doi: 10.1371/journal.pone.0096038

Romera-Castillo, C., Sarmento, H., Álvarez-Salgado, X. A., Gasol, J. M., and Marrasé, C. (2011). Net production and consumption of fluorescent colored dissolved organic matter by natural bacterial assemblages growing on marine phytoplankton exudates. *Appl. Environ. Microbiol.* 77, 7490–7498. doi: 10.1128/AEM.00200-11

Romera-Castillo, C., Sarmento, H., Alvarez-Salgado, X. A., Gasol, J. M., and Marraséa, C. (2010). Production of chromophoric dissolved organic matter by marine phytoplankton. *Limnol. Oceanogr.* 55, 446–454. doi: 10.4319/lo.2010.55.1.0446

Santín, C., Yamashita, Y., Otero, X. L., Álvarez, M. Á., and Jaffé, R. (2009). Characterizing humic substances from estuarine soils and sediments by excitation-emission matrix spectroscopy and parallel factor analysis. *Biogeochemistry* 96, 131–147. doi: 10.1007/s10533-009-9349-1

Shimotori, K., Omori, Y., and Hama, T. (2009). Bacterial production of marine humuc-like fluorescent dissolver organic matter and its biogeochemical importance. *Aquat. Microb. Ecol.* 58, 55–66. doi: 10.3354/ame01350

Shimotori, K., Watanabe, K., and Hama, T. (2012). Fluorescence characteristics of humic-like fluorescent dissolved organic matter produced by various taxa of marine bacteria. *Aquat. Microb. Ecol.* 65, 249–260. doi: 10.3354/ame01552

Singh, S., Inambar, S., and Scott, D. (2013). Comparison of two PARAFAC models of dissolved organic matter fluorescence for a mid-Atlantic forested watershed in the USA. *J. Ecosyst.* 2013:e532424. doi: 10.1155/2013/532424

Stedmon, C. A., and Markager, S. (2005). Resolving the variability in dissolved organic matter fluorescence in a temperate estuary and its catchment using PARAFAC analysis. *Limnol. Oceanogr.* 50, 686–697. doi: 10.4319/lo.2005.50.2.0686

Tada, Y., and Suzuki, K. (2016). Changes in the community structure of free-living heterotrophic bacteria in the open tropical Pacific Ocean in response to microalgal lysate-derived dissolved organic matter. *FEMS Microbiol. Ecol.* 92, fiw099. doi: 10.1093/femsec/fiw099

Tada, Y., Taniguchi, A., Nagao, I., Miki, T., Uematsu, M., Tsuda, A., et al. (2011). Differing growth responses of major phylogenetic groups of marine bacteria to natural phytoplankton blooms in the western North Pacific Ocean. *Appl. Environ. Microbiol.* 77, 4055–4065. doi: 10.1128/AEM.02952-10

Tanaka, K., Kuma, K., Hamasaki, K., and Yamashita, Y. (2014). Accumulation of humuc-like fluorescent dissolved organic matter in the Japan Sea. *Sci. Rep.* 4:5292. doi: 10.1038/srep05292

Yamashita, Y., Nosaka, Y., Suzuki, K., Ogawa, H., Takahashi, K., and Saito, H. (2013). Photobleaching as a factor controlling spectral characteristics of chromophoric dissolved organic matter in open ocean. *Biogeosciences* 10, 7207–7217. doi: 10.5194/bg-10-7207-2013

Yamashita, Y., and Tanoue, E. (2004). Chemical characteristics of amino acid-containing dissolved organic matter in seawater. *Org. Geochem.* 35, 679–692. doi: 10.1016/j.orggeochem.2004.02.007

Yamashita, Y., and Tanoue, E. (2008). Production of bio-refractory fluorescent dissolved organic matter in the ocean interior. *Nat. Geosci.* 1, 579–582. doi: 10.1038/ngeo279

Conflict of Interest Statement: The authors declare that the research was conducted in the absence of any commercial or financial relationships that could be construed as a potential conflict of interest.

frontiers in Microbiology

ORIGINAL RESEARCH
published: 27 February 2017
doi: 10.3389/fmicb.2017.00245

Different Types of Diatom-Derived Extracellular Polymeric Substances Drive Changes in Heterotrophic Bacterial Communities from Intertidal Sediments

Julio Bohórquez[1,2], Terry J. McGenity[2], Sokratis Papaspyrou[3], Emilio García-Robledo[1,4], Alfonso Corzo[1] and Graham J. C. Underwood[2]*

[1] Department of Biology, Faculty of Marine and Environmental Science, University of Cádiz, Puerto Real, Spain, [2] School of Biological Sciences, University of Essex, Colchester, UK, [3] Departamento de Biomedicina, Biotecnología y Salud Publica, Universidad de Cádiz, Puerto Real, Spain, [4] Microbiology Section, Department of Biosciences, University of Aarhus, Aarhus, Denmark

OPEN ACCESS

Edited by:
Uta Passow, University of California, Santa Barbara, USA

Reviewed by:
Lucas Stal, Royal Netherlands Institute for Sea Research (NWO), Netherlands
Hélène Montanié, University of La Rochelle, France

***Correspondence:**
Julio Bohórquez
julio.bohorquez@uca.es

Specialty section:
This article was submitted to Aquatic Microbiology, a section of the journal Frontiers in Microbiology

Received: *05 October 2016*
Accepted: *06 February 2017*
Published: *27 February 2017*

Citation:
Bohórquez J, McGenity TJ, Papaspyrou S, García-Robledo E, Corzo A and Underwood GJC (2017) Different Types of Diatom-Derived Extracellular Polymeric Substances Drive Changes in Heterotrophic Bacterial Communities from Intertidal Sediments. Front. Microbiol. 8:245. doi: 10.3389/fmicb.2017.00245

Intertidal areas support extensive diatom-rich biofilms. Such microphytobenthic (MPB) diatoms exude large quantities of extracellular polymeric substances (EPS) comprising polysaccharides, glycoproteins and other biopolymers, which represent a substantial carbon pool. However, degradation rates of different EPS components, and how they shape heterotrophic communities in sediments, are not well understood. An aerobic mudflat-sediment slurry experiment was performed in the dark with two different EPS carbon sources from a diatom-dominated biofilm: colloidal EPS (cEPS) and the more complex hot-bicarbonate-extracted EPS. Degradation rate constants determined over 9 days for three sediment fractions [dissolved organic carbon (DOC), total carbohydrates (TCHO), and (cEPS)] were generally higher in the colloidal-EPS slurries (0.105–0.123 d^{-1}) compared with the hot-bicarbonate-extracted-EPS slurries (0.060–0.096 d^{-1}). Addition of hot-bicarbonate-EPS resulted in large increases in dissolved nitrogen and phosphorous by the end of the experiment, indicating that the more complex EPS is an important source of regenerated inorganic nutrients. Microbial biomass increased ∼4–6-fold over 9 days, and pyrosequencing of bacterial 16S rRNA genes revealed that the addition of both types of EPS greatly altered the bacterial community composition (from 0 to 9 days) compared to a control with no added EPS. Bacteroidetes (especially *Tenacibaculum*) and Verrucomicrobia increased significantly in relative abundance in both the hot-bicarbonate-EPS and colloidal-EPS treatments. These differential effects of EPS fractions on carbon-loss rates, nutrient regeneration and microbial community assembly improve our understanding of coastal-sediment carbon cycling and demonstrate the importance of diverse microbiota in processing this abundant pool of organic carbon.

Keywords: EPS, microphytobenthos, intertidal sediment, nutrient regeneration, G-model, degradation rate, microbial community, pyrosequencing

INTRODUCTION

Microphytobenthic communities inhabiting intertidal sediments, such as salt marshes and mudflats, exhibit high rates of primary production (Underwood et al., 2005) and are able to influence carbon and nitrogen fluxes in shallow-water systems (Perkins et al., 2001; Thornton et al., 2002; McKew et al., 2013). Benthic diatoms are the major autotrophic microphytobenthic group in fine (cohesive) intertidal sediments, and can contribute up to 50% of the autochthonous carbon fixation in some ecosystems (Underwood et al., 2005). This productivity contributes to the ecosystem service and carbon and nitrogen cycling provision of coastal habitats (Beaumont et al., 2014; Luisetti et al., 2014). Benthic diatoms inhabit the first few millimeters of the sediment and exude extracellular polymeric substances (EPS), which play important ecological roles including motility of the pennate diatoms (Underwood and Paterson, 2003; Hanlon et al., 2006) and protection of cells from desiccation and salinity stress (Steele et al., 2014). In addition, EPS are used by bacteria, meio- and macrofauna as carbon and energy sources (Middelburg et al., 2000; Haynes et al., 2007; Bellinger et al., 2009) and contribute to sediment stability (Underwood and Paterson, 2003; Ubertini et al., 2015).

Diatom EPS include a wide range of different organic macromolecules, primarily polysaccharides (up to 90%: Underwood et al., 2010), but also glycoproteins and lesser amounts of lipids, nucleic acids and proteins (Hoagland et al., 1993; Underwood and Paterson, 2003; Hofmann et al., 2009). EPS is operationally described as material that precipitates in polar solvents (Decho, 1990), and can be separated by extraction procedures, for example. colloidal EPS (EPS_{coll}), water-soluble polymeric material isolated from colloidal aqueous extracts, and hot-bicarbonate extracted EPS (EPS_{HB}), higher molecular weight (HMW) and more insoluble compounds such as tightly bound and capsular EPS, solubilized using hot bicarbonate extraction protocols (Bellinger et al., 2005; Aslam et al., 2016). These labile and bound EPS fractions differ in biochemical composition, and in the seasonal changes of their chemical composition (Pierre et al., 2014; Passarelli et al., 2015).

Carbohydrate content varies between 40 and 90% of the EPS-carbon within diatom-rich biofilms (Underwood and Smith, 1998; Underwood and Paterson, 2003). The response of the heterotrophic bacterial community to this carbon source depends on its biochemistry, with bacteria having to deploy extracellular enzymes to transform the more complex EPS molecules into smaller monomers and oligosaccharides prior to uptake (Hofmann et al., 2009; Thornton et al., 2010; Arnosti, 2011). Previous slurry experiments have shown rapid utilization, within hours, of low-molecular-weight compounds, followed by a slower rate of degradation of more complex EPS by particular groups of bacteria (Haynes et al., 2007; Hofmann et al., 2009). The diversity of EPS composition results in a great variety of bacteria being involved in their degradation (Bacteroidetes, together with Alpha-, Beta- and Gammaproteobacteria, including *Acinetobacter*) (Elifantz et al., 2005; Haynes et al., 2007; McKew et al., 2013; Taylor et al., 2013; Passarelli et al., 2015). Coupling between diatom-derived EPS and bacterial community composition has been demonstrated (Taylor et al., 2013; Miyatake et al., 2014); nevertheless, still little is known about the loss processes affecting EPS budgets in intertidal sediments, and in particular on the differential degradation of the range of EPS produced within biofilms (McKew et al., 2013).

In order to better understand the effect of EPS composition on its turnover, we performed a microcosm experiment using slurries from intertidal diatom-dominated sediment enriched with two different carbon sources: colloidal EPS (EPS_{coll}), and more tightly-bound, extracellular components of the capsular EPS associated with the surface of the diatom frustules (EPS_{HB}), extracted from natural MPB biofilms. Our hypothesis was that due to the differences in structural complexity, the degradation rate of EPS_{coll} would be faster than for EPS_{HB}, and that the dominant groups of bacteria would change in relation to their preference and ability to respond to the different EPS components. Since EPS, in addition to carbohydrates, contain a certain amount of proteins, glycoproteins and phospholipids (Hoagland et al., 1993; Underwood and Paterson, 2003; Hofmann et al., 2009), we hypothesized that EPS degradation might be a (previously unknown) source of regenerated nutrients (N and P) in marine sediments.

In order to test these hypotheses, we compared changes in EPS-enriched slurries of: (1) concentrations of Dissolved Organic Carbon (DOC), which contains mainly carbohydrate and also amino acids and other low-molecular-weight organic carbon compounds; (2) concentrations of Total Carbohydrates (TCHO), which includes all dissolved and particulate carbohydrate and also structural polysaccharides; (3) concentrations of cEPS, (4) changes in the concentrations of inorganic nutrients, and (5) biomass and bacterial community assemblages based on DNA assays.

MATERIALS AND METHODS

Sampling Site and Extraction of Carbohydrates Fractions

Surface sediment (top 2 mm depth) was collected in October 2012 from a tidal mudflat near Alresford creek (Colne Estuary) (51°50′14.9″N, 0°59′35.2″E) (UK), where abundant diatom-dominated biofilms were present. Sediment was frozen at −20°C for 12 h and freeze-dried overnight. Two different operational EPS fractions (Underwood and Paterson, 2003) were extracted (multiple extractions of 5 g of sediment) from the freeze-dried sediments, following a sequential extraction procedure. First, the colloidal EPS fraction (EPS_{coll}) of water-soluble carbohydrate fractions was obtained (Decho, 1990). Then, after a hot-water extraction (to remove intracellular carbohydrates), a hot-bicarbonate (HB) solubilization step was performed (addition of 0.5 M $NaHCO_3$ solution at 95°C for 1 h) to obtain a fraction containing gelatinous extracellular polysaccharides termed EPS_{HB} (Bellinger et al., 2005).

The supernatant containing either EPS_{coll} or EPS_{HB} was precipitated in ethanol (70% final concentration) overnight at 4°C, then centrifuged at room temperature (3,000 × g, 15 min), the supernatant discarded and the resultant EPS pellets from

the parallel extractions pooled and resuspended in 400 mL of deionized water. The EPS_{coll} and EPS_{HB} extracts were dialyzed at room temperature overnight through an 8 kDa dialysis tubing against ultrapure water (18.2 MΩ cm, Milli-Q) with moderate stirring, to reach a final salinity <1‰. Subsamples of EPS_{coll} and EPS_{HB} extracts were measured spectrophotometrically (485 nm) after a phenol-sulfuric acid assay reaction (Dubois et al., 1956) as described by Hanlon et al. (2006). Carbohydrate concentration was quantified ($\mu g\ mL^{-1}$) as glucose equivalents (later transformed to $\mu mol\ C\ L^{-1}$) using a *D*-glucose standard curve. The final EPS_{coll} and EPS_{HB} extracts (215 mg C L^{-1}) were kept in the dark at 4°C, and subsamples used for amendment of sediment slurry experiments.

Experimental Microcosms

Fresh sediment (top 2 mm) from the same location as that used for the EPS extraction was sampled on 3rd December 2012 and used to make the sediment slurries within 1 day. Five different slurry treatments were prepared each in triplicate 100 mL conical flasks: (1) $+EPS_{coll}$ treatment consisted of 18.5 mL EPS_{coll} extract, 61.5 mL artificial sea water (salinity 35) and 200 mg wet weight estuarine sediment (containing ∼120 μg DOC, McKew et al., 2013). As a result, the slurry had a total volume of 80 mL with a salinity of 27 and a dissolved carbon concentration of 51.5 mg C L^{-1}; (2) the $+EPS_{HB}$ treatment was established using an identical setup but with the addition of Hot-Bicarbonate-extracted EPS instead of EPS_{coll} extract having the same final carbon concentration; (3) NoSed-EPS_{coll} and (4) NoSed-EPS_{HB} controls had the same amount of the relevant EPS extract and artificial sea water as before but with no sediment added to check for abiotic loss; and (5) NoAdd-EPS control contained sediment and artificial sea water but no additional carbon source to check for changes in bacterial composition that are not a consequence of growing on the added EPS.

The flasks were placed on a rocking platform (100 r. p. m.) at 16°C in the dark to avoid an increase of carbon content as result of primary production. Samples were taken every 3 days for a total of 9 days.

Organic Carbon and Carbohydrates

At each sampling time, subsamples of slurries (8 mL) were taken from each flask to measure organic carbon and carbohydrates in three inter-related fractions. Aliquots of 2.5 mL were filtered through pre-combusted GF/F filters, then diluted 10-fold with Milli-Q water to measure DOC on a Shimadzu TOC-VCSH Analyzer. An aliquot of slurry (4.5 mL) was centrifuged (3,000 × g, 15 min), after mixing by vortexing to remove the sediment particles and obtain a supernatant containing the colloidal material. The resultant supernatant was used to obtain the cEPS by precipitation in ethanol (70% final concentration). The remaining non-filtered 1 mL aliquot was used to measure TCHO. This fraction includes dissolved and colloidal carbohydrates as well as HW and HB fractions. Both cEPS and TCHO were quantified using the phenol-sulfuric acid assay as mentioned previously.

To quantitatively assess the degradability of the different organic fractions in the treatments, time course changes of the three carbon fractions, DOC, TCHO, and cEPS, were modeled in two ways. First, in order to facilitate comparison with other studies where only lineal degradation rates were provided, a linear degradation model according to Equation (1):

$$G_t = G_o - b \cdot t \quad (1)$$

Secondly, the so-called one-G model of organic matter degradation (Berner, 1964) was implemented using the following exponential equation:

$$G_t = G_o^{-kt} \quad (2)$$

where, G_t is the concentration of the organic fraction at time t, G_o is the initial concentration, b is the lineal degradation rate ($\mu mol\ C_{org}\ L^{-1}\ d^{-1}$) and k is the degradation constant in d^{-1} units.

Inorganic Nutrients

A portion of slurry (8 ml for days 0 and 9, and 4 ml for days 3 and 6) was transferred to a 15 ml Falcon tube, centrifuged at 3,000 × g for 10 min, the supernatant was filtered using pre-combusted GF/F filters, and frozen immediately at −20°C, and later used to measure dissolved inorganic nutrients. Nitrate (NO_3^-), nitrite (NO_2^-) and ammonium (NH_4^+), phosphate (PO_4^{3-}) and silicate (SiO_4^{4-}) were measured on a Seal Analytical AA3 HR Nutrient Autoanalyzer following the protocols described by Grasshoff et al. (1983).

To quantitatively assess the net rate of inorganic nutrient regeneration, time course changes in nutrients were fitted to a linear equation, where the slope represents the net regeneration rate. With some nutrients and in some treatments the use of a positive exponential model improved the correlation coefficients but we used a linear model in all cases to facilitate comparison.

Bacterial Community Analysis

DNA Extraction and Microbial Biomass Estimation

The pellet obtained after centrifuging the slurry for nutrients analysis was retained and frozen at −20°C until DNA extraction. DNA was extracted from sediment pellets using a bead-beating phenol-chloroform-isoamyl alcohol method as described previously (McKew et al., 2011).

Small aliquots (1 μL) of extracted total DNA were diluted and used as a proxy to estimate the total biomass of the microbial community with a NanoDrop® 3,300 fluorospectrometer, with replicates ($n = 3$) stained using Quant-iT™ PicoGreen® dsDNA reagent and measured on the basis of absorbance at 260 nm. The DNA extraction and subsequent quantification method applied here is used comparatively as a general biomass growth indicator, as it does not distinguish between the major groups (Bacteria, Archaea, Eukarya) or between intracellular DNA (from live and dead intact cells) and extracellular DNA (actively released or originating from lysed cells) (Torti et al., 2015).

PCR Amplification of Bacterial 16S rRNA Genes

PCR amplifications were carried out using bacterial primers 341GC-F (CGCCCGCCGCGCGCGGCGGGCGGGGCG

GGGGCACGGGGGGCCTACGGGAGGCAGCAG) and 534-R (ATTACCGCGGCTGCTGG) (Muyzer et al., 1993) for denaturing gradient gel electrophoresis (DGGE) analysis. All PCR amplifications were performed using a GeneAmp PCR system 9700 thermocycler (Applied Biosystems) as described by Folwell et al. (2016). Thermocycling consisted of 95°C for 5 min followed by 32 cycles of 95°C for 5 s, 55°C for 30 s, 72°C for 30 s, with a final elongation of 72°C for 7 min.

DGGE

DGGE analysis of bacterial 16S rRNA gene amplicons was performed using the Bio-Rad D Code system as described by Muyzer et al. (1993), running for 16 h on a gradient of 40–60%, and stained with silver nitrate (Acuña Alvarez et al., 2009).

454 Pyrosequencing

The composition of the bacterial communities was assessed from 16S rRNA genes libraries constructed from the DNA extracts of selected samples (+EPS_{coll} treatment replicates at day 0 as representative of the starting community, and replicates of +EPS_{coll}, +EPS_{HB}, and NoAdd-EPS treatments at day 9; Supplementary Table S1) using ROCHE 454 pyrosequencing technology at the NERC Molecular Genetic Facility at the University of Liverpool as described previously (McKew et al., 2011). The analytical procedure described by Folwell et al. (2016) was used. In brief, any sequences <150 bp in read length, containing errors or with low-quality scores, were removed from analysis. The remaining reads were clustered into operational taxonomic units (OTUs) at 95% similarity level and assigned to a taxonomic group using RDP classifier algorithm (Wang et al., 2007).

Statistical Analysis

All analyses were performed with three replicates for each sampling time. Differences in carbohydrate fractions and inorganic nutrients over time and with respect to treatments were tested by two-way repeated measures analysis of variance (factor time and factor treatment) (ANOVA) follow by Student Newman-Kewls multiple comparison tests when significant differences were found. Differences between degradation rates for DOC, TCHO, and cEPS calculated with both the linear degradation model and the one-G model (with data previously linearized by a *Ln* transform) were tested by comparison of slope by analysis of covariance (ANCOVA). Analyses were performed using the software PAST v 3.10 (Hammer et al., 2001).

Concentration of DNA was *Ln* transformed and fitted to a linear model where slopes represented the net growth. Differences between treatments +EPS_{coll} and +EPS_{HB} were tested by comparison of slopes by ANCOVA.

Changes in the community composition with treatment and over time were analyzed by permutational analysis of variance (PERMANOVA) (Anderson, 2001) on a Bray Curtis similarity resemblance matrix on data normalized by the total number of good reads in each sample. A total of 10,000 unrestricted permutations was set in all tests. When the number of permutations was small (<100), *p*-values were obtained through Monte Carlo random draw from the asymptotic permutation distribution (Anderson and Robinson, 2003). Community data patterns were then represented non-metric Multi-Dimensional Scaling (MDS) using a Bray-Curtis similarity index. Pearson

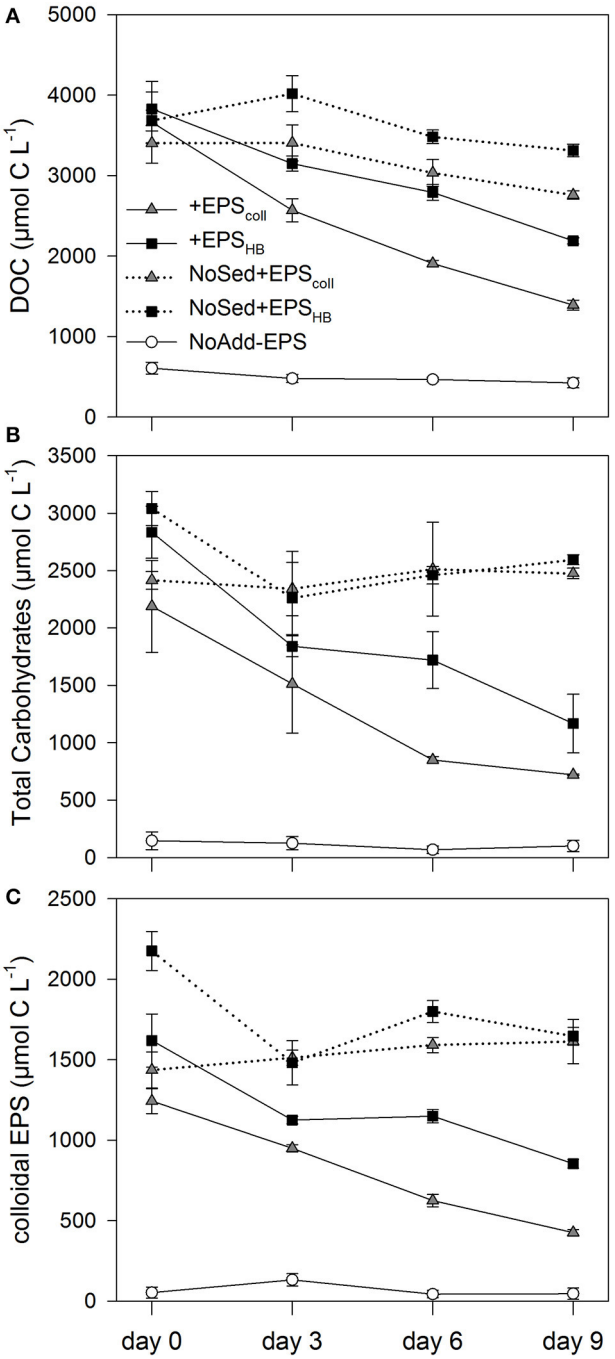

FIGURE 1 | Concentrations of the three carbohydrate fractions measured: Dissolved Organic Carbon (DOC) (A), Total Carbohydrates **(B)** and colloidal EPS **(C)**, in estuarine sediment slurries (200 mg from the top 2 mm, 80 mL artificial sea water (ASW) over 9 days) for the treatments +EPS_{coll}, +EPS_{HB}, NoAdd-EPS and the controls (no sediment added), NoSed+EPS_{coll} and NoSed+EPS_{HB} represented with dotted lines. Values are means ($n = 3$) ± standard error (SE), expressed as µmol C L^{-1} of slurry.

correlation biplots of *log* $(x + 1)$ transformed variables were drawn onto the MDS axes to examine their relationship with observed community patterns. All statistical analyses were run using the programs PRIMER 6.0 and PERMANOVA+ (PRIMER-e).

To test significant differences in taxonomic profiles of bacterial community at day 9 from the $+EPS_{coll}$, $+EPS_{HB}$, and NoAdd-EPS treatments, both at Class and at OTU level, we used Whelch's *t*-test implementation of STAMP v2 1.3 package (Parks and Beiko, 2010; Parks et al., 2014) with default parameters except that parameters for filtering out were: $p > 0.05$; difference between proportions < 0.2 or differences between ratios < 1.5.

Sequence Accession

Raw pyrosequences of amplified bacterial 16S rRNA genes from all the samples can be extracted from the European Nucleotide Archive (ENA) under accession number PRJEB15429. Supplementary Table S1 provides the information required to identify the relationship between sample and sequences.

RESULTS

Changes in Organic Carbon and Carbohydrate Fractions

The addition of EPS resulted in significantly higher DOC concentrations (between 3,600 and 3,800 μmol C L^{-1} on day 0, corresponding to 1.44 and 1.52 mmol C g^{-1} Wet Weight (WW) sediment, respectively) in all four EPS-addition treatments compared with the NoAdd-EPS control (DOC concentration 608 ± 74 μmol C L^{-1} or 0.24 mmol C g^{-1} WW sediment on day 0) (**Figure 1A**; Student-Newman-Keuls (SNK test), $p < 0.05$). Similarly, the TCHO concentration and cEPS concentration at day 0 (0.8–1.1 mmol C g^{-1} WW sediment and 0.5–0.6 mmol C g^{-1} WW sediment, respectively) were 15–19-fold and 20–30-fold higher, respectively, in EPS-supplemented microcosms compared with the NoAdd-EPS control (**Figures 1B,C**). The concentrations of DOC, TCHO and cEPS decreased significantly throughout the 9-day experiment in the treatments that had both added EPS and sediment inocula ($+EPS_{coll}$, $+EPS_{HB}$) (**Figures 1A–C**). However, there were no significant changes in any of the organic carbon fractions in the NoSed+EPS_{coll}, NoSed+EPS_{HB}, and NoAdd-EPS controls during the experiment (**Figures 1A–C**).

The value of *k* for the three different carbon fractions (DOC, TCHO, and cEPS) did not differ significantly within treatments, $+EPS_{coll}$ and $+EPS_{HB}$ (**Table 1**). However, values of *k* for DOC and cEPS fractions in the $+EPS_{coll}$ treatment were significantly higher than those calculated for $+EPS_{HB}$ treatment. Values of *k* for the TCHO fraction between $+EPS_{coll}$ and $+EPS_{HB}$ treatments were not statistically different (**Table 1**). The linear degradation rates of cEPS in both $+EPS_{coll}$ and $+EPS_{HB}$ treatments were significantly lower than those of DOC and TCHO ($p < 0.05$, ANCOVA).

The lower value of *k* for the three carbon fractions in the $+EPS_{HB}$ treatment indicated a lower degradability that must be based in chemical differences between these fractions derived from the EPS_{coll} or the EPS_{HB} enrichments. To address possible changes in the overall chemical composition in the added organic fractions, EPS_{coll} or the EPS_{HB}, we calculated the TCHO:DOC, cEPS:DOC, and cEPS:TCHO mass ratios in both enrichments (Supplementary Figure S1). These ratios were similar at day 0 for both enrichments, with observed differences not statistically significant. In general, both TCHO:DOC and cEPS:DOC remained constant or gradually decreased during the experiment in both enrichments. On the contrary cEPS:TCHO ratio in the EPS_{HB} enrichment increased significantly (linear correlation; $r^2 = 0.9664$; $p < 0.02$) with time, suggesting a lower relative degradability of cEPS material within the $+EPS_{HB}$ enrichment.

Changes of Dissolved Inorganic Nutrients

The EPS_{coll} and EPS_{HB} fractions added to the enrichments and the sediment inoculum contributed to the initial concentration of dissolved inorganic nutrients measured in the different treatments. These concentrations of nutrients, directly added with the EPS and sediment inoculum, were relatively low for all investigated nutrients at day 0 ($NO_3^- + NO_2^- < 6.5$ μmol L^{-1}, $NH_4^+ < 18.8$ μmol L^{-1}, $PO_4^{3-} < 31.0$ μmol L^{-1}, and $SiO_4^{4-} < 2.3$ μmol L^{-1}). The general trend was an increase of all nutrients in all treatments with time (**Figure 2**). This increase over time is necessarily the result of the net regeneration of inorganic nutrients from the mineralization of the EPS fractions and/or the organic matter introduced with the sediment inoculum.

Concentrations of Dissolved Inorganic Nitrogen (DIN, the sum of nitrate, nitrite and ammonium concentrations) increased steeply with time in $+EPS_{HB}$ treatment(24.6 μmol L^{-1} day^{-1}), while the regeneration rates were significantly lower (SNK test, $p < 0.05$) in the rest of the treatments (1.5–6.5 μmol L^{-1} day^{-1}). There were no significant differences in DIN regeneration rates between $+EPS_{coll}$ and NoAdd-EPS treatments that were 6.5 and 5.5 μmol L^{-1} day^{-1}, respectively (**Figure 2A**). The mineralization of the EPS_{HB} fraction was a major source of DIN regeneration, initially in the form of NH_4^+ and later in the form of $NO_3^- + NO_2^-$ (NO_x^-) (Supplementary Figure S2). The importance of the net regeneration of ammonium and NO_x^- shifted during the experiment as shown by changes in NO_x^-: NH_4^+ ratio, which increased from about 0.15 at day 3 up to 3.3 at day 9. The regeneration rate of NH_4^+ at the beginning of the experiment was similar in both $+EPS_{HB}$ treatment and the $+EPS_{HB}$ control without sediment (8.6–9.6 μmol L^{-1} day^{-1}) and considerably higher than in the other treatments (1.8–3.3 μmol L^{-1} day^{-1}). This emphasizes the strong difference between EPS_{HB} and EPS_{coll} regarding their potential as sources of regenerated inorganic nitrogen.

The EPS_{HB} fraction was a major source of regenerated dissolved phosphate, since its concentration increased in both treatments with added EPS_{HB} ($+EPS_{HB}$ and NoSed+EPS_{HB}) at a similar rate (4.9–5.9 μmol L^{-1} day^{-1}) up to the day 6 (**Figure 2B**). Dissolved phosphate decreased significantly between days 6 and 9 in the $+EPS_{HB}$ treatment (SNK, $p < 0.05$) but not in the NoSed+EPS_{HB} control. On the contrary, phosphate changed little or even decreased during the experiment in treatments with EPS_{coll} or sediment only.

TABLE 1 | Comparison of degradation constant (*k*) calculated using the one-G model for degradation of organic matter (Berner, 1964) or the lineal degradation constant (*b*) for the three carbon fractions measured [Dissolved Organic Carbon (DOC), Total Carbohydrates (TCHO) and colloidal EPS (cEPS)] in the $+EPS_{coll}$ and $+EPS_{HB}$ treatments during the 9-day period (± standard error of *k* and *b*).

Fraction	$+EPS_{coll}$		$+EPS_{HB}$	
	k (d^{-1})	*b* (mg C_{org} g^{-1} sed. WW d^{-1})	*k* (d^{-1})	*b* (mg C_{org} g^{-1} sed. WW d^{-1})
Dissolved Organic Carbon (DOC)	$0.105^{a} \pm 0.01$	1.19 ± 0.18	$0.060^{b} \pm 0.005$	$0.84^{a} \pm 0.08$
Total Carbohydrates (TCHO)	$0.123^{a} \pm 0.02$	$0.81^{a,b} \pm 0.19$	$0.096^{a,b} \pm 0.02$	$0.68^{a} \pm 0.16$
Colloidal EPS (cEPS)	$0.121^{a} \pm 0.007$	$0.44^{b} \pm 0.03$	$0.062^{b} \pm 0.01$	$0.36^{b} \pm 0.07$

The determination coefficients were significant for both the exponential and the lineal fitting ($p < 0.05$, $n = 12$). Differences in k or b were compared by ANCOVA between organic fractions (DOC, TCHO and cEPS) within the same treatment ($+EPS_{coll}$ or $+EPS_{HB}$), and between treatments for the same organic fraction. The same superscript letter (a,b) means absence of statistically significant differences among the corresponding values of k or b ($p < 0.05$).

Silicate concentrations increased with time, particularly from day 3 onwards in all of the treatments with added sediment, $+EPS_{coll}$, $+EPS_{HB}$, and NoAdd-EPS treatments (**Figure 2C**). The regeneration of silicate was positively affected by the sediment inoculum, since it was higher in all the treatments with sediment (0.7–1.28 μmol L^{-1} day^{-1}) compared with NoSed+EPS_{coll} and NoSed+EPS_{HB} controls lacking sediment inoculum, 0.16 and 0.41 μmol L^{-1} day^{-1}, respectively. This likely indicates that the sediment inoculum was the source of regenerated silicate during the experiment and not the added EPS.

Changes in DNA Concentration of Sediment Slurries

Extracted DNA concentration was used as a proxy for microbial biomass (**Figure 3**). At the beginning of the experiment, there were no significant differences between DNA concentrations in the $+EPS_{coll}$, $+EPS_{HB}$, and NoAdd-EPS treatments (**Figure 3**). DNA concentration increased significantly (by around 400%) in the $+EPS_{coll}$, and $+EPS_{HB}$ treatments by the end of the experiment (SNK, $p < 0.05$). In the NoAdd-EPS sediment-only control DNA concentration decreased by day 9 compared to day 0, with concentrations significantly lower than in the organic-carbon-amended treatments ($+EPS_{coll}$ and $+EPS_{HB}$) (SNK, $p < 0.001$). Microbial biomass exhibited exponential-like growth in the treatments $+EPS_{coll}$ and $+EPS_{HB}$ ($r^2 = 0.84$ and $r^2 = 0.56$, respectively), and no significant differences were observed between these two treatments.

Changes in the Bacterial Community Composition

Denaturing gradient gel electrophoresis (DGGE) of partial bacterial 16S rRNA genes (Supplementary Figure S3) showed consistency in the banding patterns between replicate treatments at day 9, and showed that the day-0 communities were identical regardless of treatment, justifying the use of the day-0 $+EPS_{coll}$ treatment only in subsequent pyrosequence analysis. By day-9 the bacterial community composition had changed from day-0 even in the NoAdd-EPS control, and at day-9 there were distinct differences in bacterial community composition between the treatments $+EPS_{coll}$, $+EPS_{HB}$, and NoAdd-EPS.

In order to quantify the changes in bacterial community composition and identify key taxa putatively involved in EPS degradation, pyrosequencing of 16S rRNA genes was performed on $+EPS_{coll}$, $+EPS_{HB}$ and NoAdd-EPS treatments after 9 days, and from a representative day-0 sample, $+EPS_{coll}$. Multidimensional scaling analysis revealed statistically significant temporal- and treatment-related changes (**Figure 4**). The bacterial communities from day-9 $+EPS_{coll}$ and $+EPS_{HB}$ treatments were different from both the NoAdd-EPS treatment at day 9 and the starting community ($p < 0.05$) (**Figure 4**). After 9 days, the NoAdd-EPS community was more similar to the starting community than those with added EPS. Also, there was a significant difference ($p < 0.05$) in the bacterial community composition between the $+EPS_{coll}$ and $+EPS_{HB}$ treatments at day 9.

The only phyla that were significantly enriched at day-9 in the $+EPS_{coll}$ treatment compared with the NoAdd-EPS control were the Bacteroidetes (∼2-fold more abundant) and Verrucomicrobia (∼5-fold more abundant; data not shown). These enrichments were specifically within the Sphingobacteria (Bacteroidetes), two classes from Verrucomicrobia (Verrucomicrobiae and Opitutae) and one class of Planctomycetes (Phycisphaerae), which were all significantly more abundant in the $+EPS_{coll}$ treatment (**Figure 5A**; see figure for statistical criteria). At the level of operational taxonomic units clustering at 95% similarity (OTU_{95}), OTU-2960, from the genus *Tenacibaculum* in the phylum Bacteroidetes, had the biggest additive increase in the treatment $+EPS_{coll}$ (12% relative abundance) compared with NoAdd-EPS (5%; **Figure 5B**). The Verrucomicrobia OTU-9279 increased most in relative abundance, constituting 3% of the community in treatment $+EPS_{coll}$ while in the NoAdd-EPS control it was absent (**Figure 5B**).

Bacteroidetes and Verrucomicrobia were also significantly enriched at day-9 in the $+EPS_{HB}$ treatment compared with the NoAdd-EPS control (∼2.5-fold and ∼6-fold more abundant respectively; data not shown). At the subphylum level, only Flavobacteria and Sphingobacteria from the Bacteroidetes were enriched significantly (**Figure 6A**). As with the $+EPS_{coll}$ treatment, there was a big increase in OTU-2960 from the genus *Tenacibaculum* (phylum Bacteroidetes) comprising 20% of the relative abundance (**Figure 6B**). OTU-7700, with 100% identity to *Algoriphagus yeomjeoni* from the phylum Bacteroidetes and OTU-2464 from the gammaproteobacterial

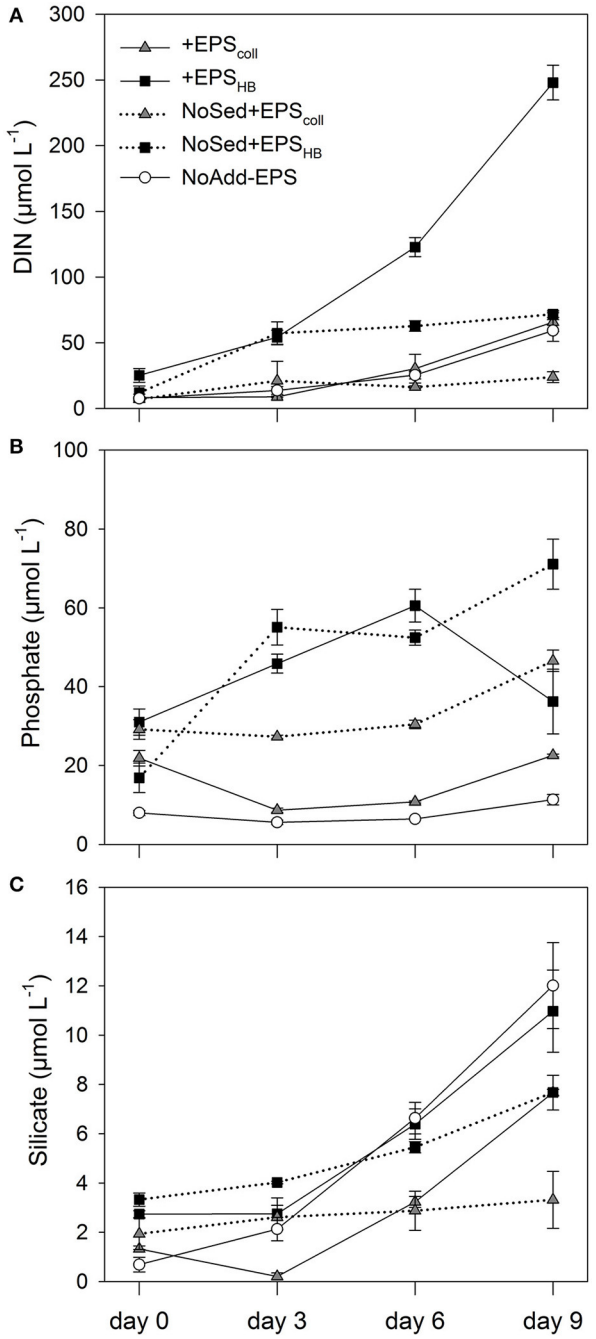

FIGURE 2 | Concentrations of different inorganic nutrients measured: Nitrate, Nitrite and Ammonium expressed as Dissolved Inorganic Nitrogen (DIN) (A), Phosphate **(B)**, and Silicate **(C)** in estuarine sediment slurries (200 mg from the top 2 mm, 80 mL artificial sea water (ASW) over 9 days) for the treatments +EPS$_{coll}$, +EPS$_{HB}$, NoAdd-EPS and the controls (no sediment added), NoSed+EPS$_{coll}$ and NoSed+EPS$_{HB}$ represented with dotted lines. Values are means ($n = 3$) ± standard error (SE), expressed as µmol L^{-1} of slurry.

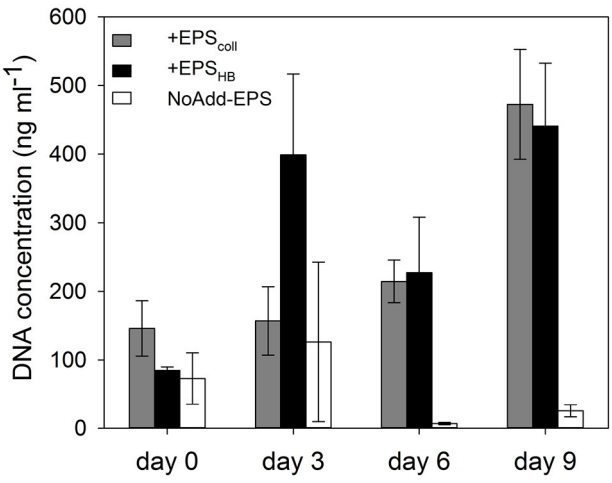

FIGURE 3 | DNA concentration (as a proxy for biomass) in estuarine sediment slurries for the treatments +EPS$_{coll}$, +EPS$_{HB}$, and NoAdd-EPS, expressed as ng mL^{-1} of slurry.

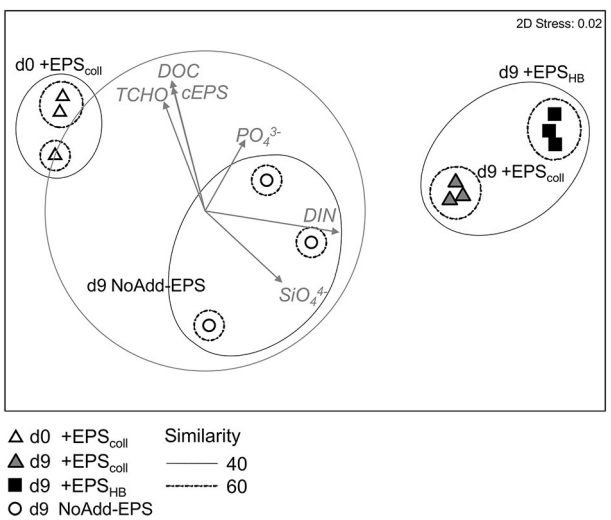

FIGURE 4 | Non-metric Multi-Dimensional Scaling ordination plot based on Bray Curtis similarity of relative abundance data of the bacterial community from the different treatments +EPS$_{coll}$, +EPS$_{HB}$, and NoAdd-EPS at day 9. Samples of +EPS$_{coll}$ treatment at day 0 are used as initial samples for the rest of treatments (stress: 0.02). Points represent centroids of replicate samples. Groups at 40 and 60% similarity are shown after applying a group average clustering. The vector overlay shows the environmental variables with correlation >0.5. Arrows indicate direction and relative magnitude of influence.

genus *Amphritea*, both had the biggest relative increase after EPS$_{HB}$ addition, and comprised ∼3% of the day-9 +EPS$_{HB}$ community (**Figure 6B**).

Bacterial communities from +EPS$_{coll}$ and +EPS$_{HB}$ treatments were 52% similar but significantly different (**Figure 4**, $p < 0.05$). There were no phylum-level significant differences in abundance between these two treatments. However, the addition of EPS$_{coll}$ stimulated significant increases in Opitutae from the phylum Verrucomicrobia and in Deltaproteobacteria as the only identified classes compared to EPS$_{HB}$-amended treatment (+EPS$_{HB}$ treatment)

(Supplementary Figure S4A). Three aforementioned OTUs belonging to the genera *Tenacibaculum*, *Amphritea,* and *Algoriphagus* were significantly relatively more abundant in $+EPS_{HB}$, whereas a range of OTUs from diverse phyla was relatively more abundant in $+EPS_{coll}$ (Supplementary Figure S4B).

Relationship between the Bacterial Community Composition and Environmental Variables

Pearson correlation biplots drawn on the MDS showed that DIN correlated strongly with the horizontal axis, separating the day 9 bacterial communities of $+EPS_{coll}$ and $+EPS_{HB}$ treatments from the initial samples. cEPS and the rest of the organic carbon source related variables (TCHO; DOC) had a high correlation with the second axis, which separates both $+EPS_{coll}$ and $+EPS_{HB}$ treatments from NoAdd-EPS treatment.

DISCUSSION

Degradation of Colloidal EPS by Heterotrophic Bacteria

The degradation of organic matter is a chemically and microbiologically complex process because organic matter is typically a mixture of organic compounds with different relative degradability (Hedges and Oades, 1997; Burdige, 2007; Arndt et al., 2013). Microbial degradation involves the extracellular breakdown of HMW polymers to LMW oligosaccharides and monomers (Goto et al., 2001; Hofmann et al., 2009), which can be readily incorporated by bacterial cells, with the initial polymer hydrolysis generally being the rate-limiting step (Meyer-Reil, 1990; Kristensen and Holmer, 2001). In our experiment, addition of EPS stimulated the degradation of the organic fractions (DOC, TCHO, and cEPS) in both $+EPS_{coll}$ and $+EPS_{HB}$ treatments (**Figure 1**). Ratios of cEPS:DOC and TCHO:DOC decreased consistently in both treatments, which might indicate a preferential degradation of cEPS and TCHO compared to DOC. On the other hand, the difference in the time evolution of cEPS:TCHO ratios between treatments suggests a lower degradability of cEPS from the hot-bicarbonate fraction. Typically, most slurry studies have found that the hot-bicarbonate carbohydrate fraction is more refractory that the cEPS fraction in oxic conditions (**Table 2**).

Organic matter degradation in marine sediments usually follows an exponential decay with time described by the G-models family (Berner, 1964; Arndt et al., 2013). Only a few studies have applied this model in EPS-related studies. Oakes et al. (2010) studying the degradation rates of several monosaccharide pools applied a 2-G model which assumes that the pool of organic matter consists of two fractions that degrade exponentially at different rates and included a non-reactive fraction as well. Three fractions in each monosaccharide pool were detected: (1) a highly labile fraction accounting for the largest part (65–87%) of each monosaccharide pool, with high exponential decay rates (k) (0.81–4.38 d^{-1}); (2) a more refractory fraction (7–18% of each monosaccharide pool), whose k was one or two order of magnitude lower (0.01–0.07 d^{-1}); and (3) a non-reactive fraction (6–23% of each monosaccharide pool) (**Table 2**). The presence of a second most refractory component was evident in the degradation kinetics of various sediment-extracted carbohydrate fractions both in oxic and anoxic conditions in a 25-day slurry experiment (McKew et al., 2013). Although the loss of TCHO and cEPS over time in our experiment could suggest the existence of a second more refractory component (especially in the $+EPS_{HB}$ treatment), testing for the inclusion of such a component in the model did not provide a significantly better fit (results not shown). It is probable that the time scale of our experiment was too short to detect the existence of more than one pool in the degradation kinetics of every fraction.

The exponential decay rates in our experiment (**Table 1**) fall between those of the highly reactive fraction and the less reactive fraction of Oakes et al. (2010) for specific monosaccharides. However, the exponential decay rates from the current study for specific carbohydrates and more complex or less unambiguously defined carbohydrate-related fractions, like TCHO and EPS, extracted from microbenthic algae (this study, Goto et al., 2001; Oakes et al., 2010), span two orders of magnitude (**Table 2**). Interestingly, these rates are higher and less variable than the wider range of reported k-values (10^{-11}–10^{-2} d^{-1}) for the degradation of bulk organic matter in different marine sediments (Arndt et al., 2013). This indicates the general lability of diatom-biofilm EPS in comparison to detritus derived from other sources, and highlights its importance in structuring heterotrophic communities (Hofmann et al., 2009; Taylor et al., 2013). However, comparison of degradation rate constants between different experiments or different environments must be done with caution since the degradability of organic matter depends on the interaction of its chemical composition and the particular environmental conditions where degradation takes place (Mayer, 1995; McKew et al., 2013).

EPS Degradation and Inorganic Nutrient Regeneration

Nutrient concentrations detected on day 0 were higher in all treatments with added EPS compared to the control. Although the sediment inoculum added may have represented a small source of inorganic nutrients to the slurries, it seems that both EPS-extraction methods recover some dissolved inorganic nutrients from the sediment plus microphytobenthic biofilm samples, a source of nutrients not previously accounted for (**Figure 2**). The extraction protocol of both EPS fractions involves freezing the sediment sample, which is known to break algal and bacterial cells releasing relatively large amounts of intracellular dissolved inorganic nutrients (García-Robledo et al., 2010, 2016; Stief et al., 2013; Yamaguchi et al., 2015). Although, there were no significant differences on day 0 between nutrients in the $+EPS_{coll}$ and $+EPS_{HB}$ treatments, the hot-bicarbonate method extracted an organic matter pool that was particularly rich in organic N and P (**Figure 2**, Supplementary Figure S2). Increases in dissolved inorganic nutrients during the experiment were more pronounced and rapid with added EPS_{HB} than for $+EPS_{coll}$, and

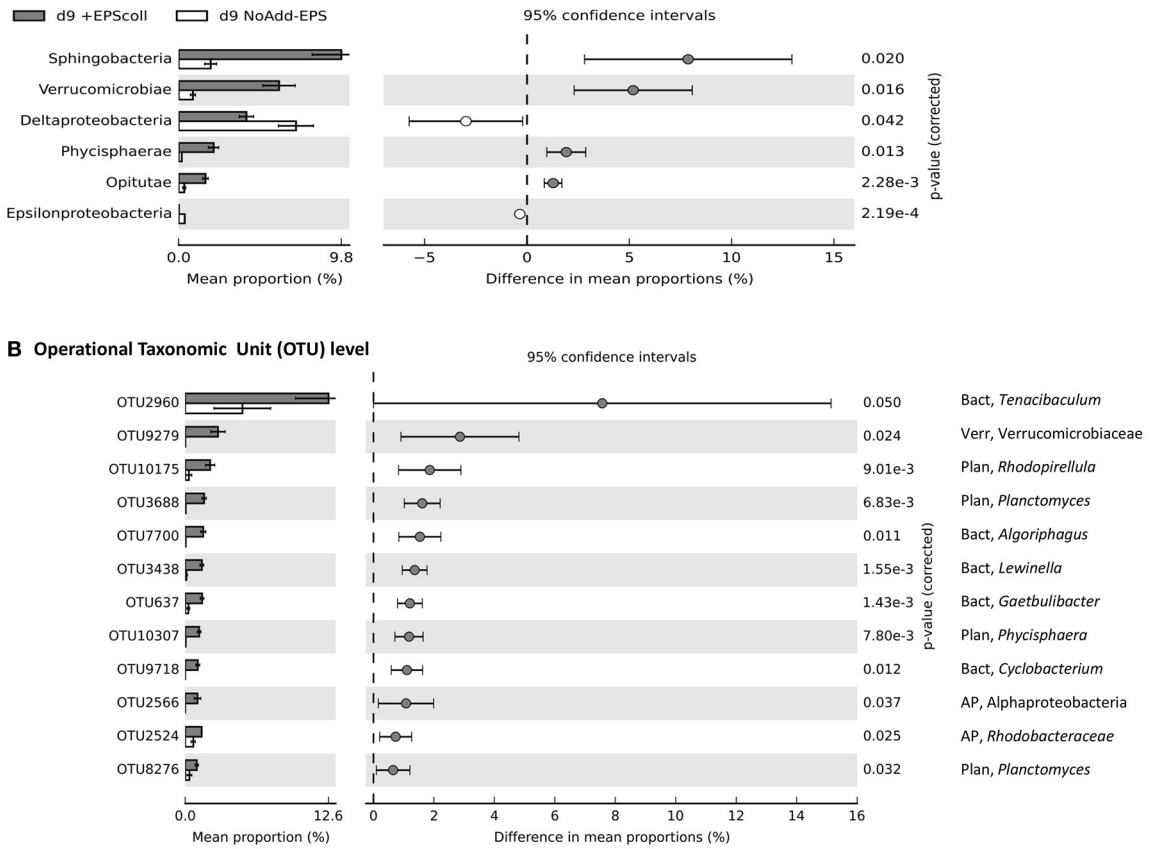

FIGURE 5 | Comparison of bacterial community profiles in +EPS$_{coll}$ vs. NoAdd-EPS by day 9 both at the levels of subphylum (class) (A) and Operational Taxonomic Unit (OTU) defined at >95% similarity **(B)**. Analysis was performed using STAMP (Parks and Beiko, 2010; Parks et al., 2014) with default parameters except that parameters for filtering out were: $p > 0.05$; difference between proportions <0.2 or difference between ratios <1.5. Data were sorted according to effect size. Note the differences in the scale of the x axes. The only phyla that were significantly enriched at day-9 in EPS$_{coll}$ treatment compared with the NoAdd-EPS control were the Bacteroidetes (~2-fold more abundant) and Verrucomicrobia (~5-fold more abundant; data not shown). The information to the right of the *p*-values is the identity of the OTU, whereby the phylum is indicated to the left of the comma (AP, Alphaprotebacteria; Bact, Bacteroidetes; Plan, Planctomycetes; Verr, Verrucomicrobia), and the lowest taxonomic level to which the OTU can be confidently assigned is indicated to the right of the comma. A total of 23 bacterial taxa was significantly enriched in +EPS$_{coll}$ treatment compared with NoAdd-EPS treatment but only the top 12 is shown.

represent the mineralization of nutrients associated to organic compounds included in the EPS$_{HB}$ fraction. EPS$_{HB}$ is one of the more abundant and heterogeneous fractions (Chiovitti et al., 2003) the extraction procedure of which not only recovers the extracellular carbohydrates but also uronic acids, proteins, glycoproteins, and phospholipids tightly bound to the mucilage of the diatom frustules (Underwood et al., 1995; Wustman et al., 1997).

The regeneration rate of NH_4^+ was similar in both treatments with EPS$_{HB}$, with and without sediment, suggesting a wider distribution of this trait such that the presence of the sediment microbial community plays a minor role in this process. On the contrary, further transformation of NH_4^+ to NO_2^- and NO_3^-, detected in the +EPS$_{HB}$ treatment, particularly toward the end the experiment (**Figure 2A**, Supplementary Figure S2B), can be only explained by an increase of nitrification rates due to the growth of a community of nitrifiers introduced with the sediment inoculum, that was absent in the control without sediment. Nitrifying bacteria were indeed present in our samples (e.g., *Nitrospira*, which oxidizes nitrite to nitrate, and the ammonia-oxidizing genus *Nitrosospira*), albeit in low relative abundance (~0.01%) in the +EPS$_{HB}$ treatment.

EPS$_{HB}$ was also an important source of regenerated PO_4^{3-}. The initial stoichiometry between NH_4^+ and PO_4^{3-} regeneration rates was about 1.7 in both EPS$_{HB}$ treatments, considerably richer in P than typical microphytobenthic biomass (Hillebrand and Sommer, 1999). MPB biofilm EPS$_{HB}$ extractions do frequently include some ribose, indicating some DNA/RNA contamination (Bellinger et al., 2005, 2009), which may be the source of the phosphate. The decrease of NH_4^+ and PO_4^{3-} from day 6 to 9 in the +EPS$_{HB}$ treatment might be explained by higher microbial consumption rate at the end of the experiment. Nonetheless, growth of the microbial community, as estimated from the increase in DNA over 9 days, was similar in both

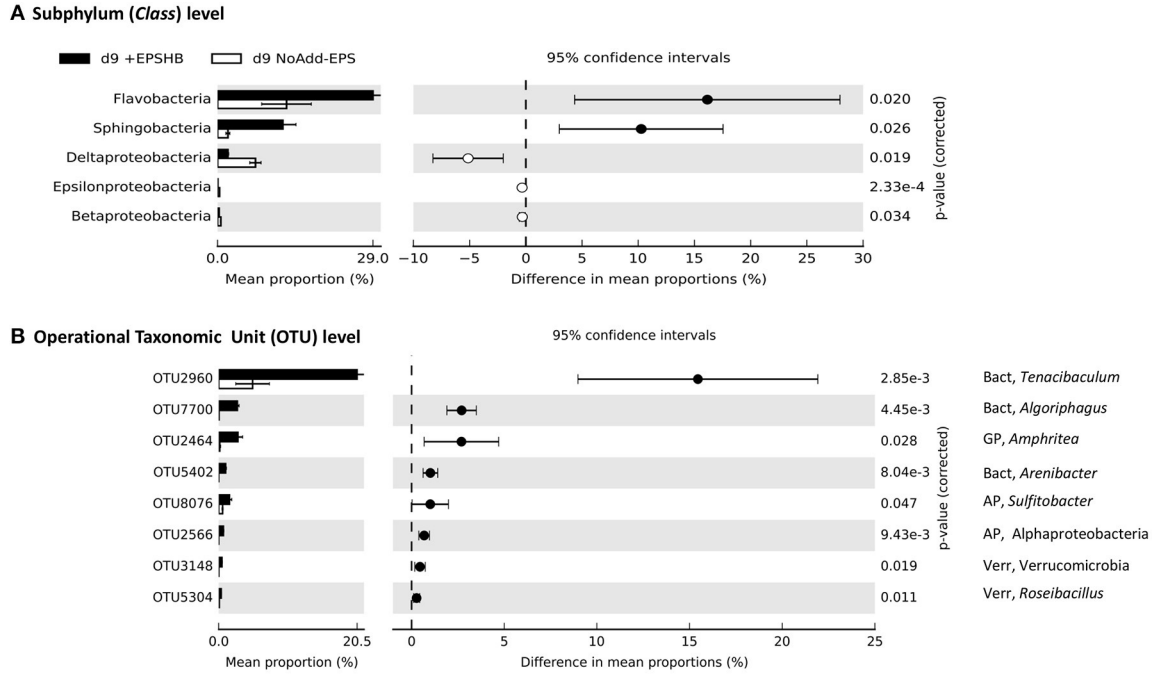

FIGURE 6 | Comparison of bacterial community profiles in +EPS$_{HB}$ vs. NoAdd-EPS by day 9 both at the levels of subphylum (class) (A) and Operational Taxonomic Unit (OTU) defined at >95% similarity **(B)**. Analysis was performed using STAMP (Parks and Beiko, 2010; Parks et al., 2014) with default parameters except that parameters for filtering out were: $p > 0.05$; difference between proportions <0.2 or difference between ratios <1.5. Data were sorted according to effect size. Note the differences in the scale of the x axes. The only phyla that were significantly enriched at day-9 in EPS$_{HB}$ treatment compared with the NoAdd-EPS control were the Bacteroidetes (~2.5-fold more abundant) and Verrucomicrobia (~6-fold more abundant; data not shown). The information to the right of the *p*-values is the identity of the OTU, whereby the phylum is indicated to the left of the comma (AP, Alphaprotebacteria; Bact, Bacteroidetes; GP, Gammaproteobacteria; Verr, Verrucomicrobia), and the lowest taxonomic level to which the OTU can be confidently assigned is indicated to the right of the comma. A total of eight bacterial taxa were significantly enriched in +EPS$_{HB}$ treatment compared with NoAdd-EPS treatment.

+EPS$_{HB}$ and +EPS$_{coll}$ treatments. Therefore, even the lower amount of regenerated nutrient released from the EPS$_{coll}$ fraction was enough to support the microbial demand for N and P.

The regeneration rate of silicate was 3–4 times higher in the treatments with sediment-inoculum added compared to the controls without sediment inoculum (**Figure 2C**). Most likely the increase in silicate is mainly due to its regeneration from a particulate pool bound to sediment particles. Even in the absence of any added EPS, in the NoAdd-EPS treatment (with sediment), the regeneration of silicate was similar to that of the +EPS$_{HB}$ treatment with sediment. Therefore, EPS seems to play a minor role in the recycling of silicate in marine sediments in contrast to what we have shown for N and P.

EPS-Induced Changes in the Bacterial Community Composition

Incubation of sediment slurries with both types of EPS resulted in a significant increase in microbial biomass by the end of the experiment using total DNA concentration as a proxy (**Figure 3**; Haynes et al., 2007). It also led to a significant shift in community composition, both temporally and as direct result of EPS addition (**Figure 4**). Given that EPS was the differentially added component, constituting a high proportion of the available DOC, and that its degradation was ongoing at day 9, the selectively enriched and actively growing microbial community at this time would contain a high proportion of active EPS-degraders. However, the dominance of such bacterial taxa is also the net result of the growth at the expense of the added EPS sources and any losses by grazing and viral lysis (Våge et al., 2013; Thingstad et al., 2014), which might have increased due to the increased inorganic nutrient content in the slurries (Miki and Jacquet, 2010). The relative similarity of many of the taxa comprising the bacterial communities in the +EPS$_{coll}$ and +EPS$_{HB}$ treatments indicate that most EPS-degrading bacteria readily consume a wide range of diatom-derived EPS (Taylor et al., 2013). Nevertheless, the significant difference overall between communities fed with EPS$_{coll}$ and EPS$_{HB}$ indicates that there are a number of specialist bacteria that preferentially use a particular fraction.

Several bacterial phyla, namely Bacteroidetes, Verrucomicrobia and Planctomycetes, increased their presence in the +EPS$_{coll}$ compared with the NoAdd-EPS treatment, and were thus probably involved in EPS$_{coll}$ biodegradation (**Figure 5A**). Verrucomicrobia is a phylum that is widely distributed, but rarely dominant (Freitas et al., 2012; Yilmaz et al., 2016). As there are few cultivated representatives of this

TABLE 2 | Comparison of degradation rates for different carbon fractions from previous published studies.

Publication	Added DOM/EPS	Fraction measured	Starting Conc.	Rate of degradation (units: § = μg gluc. g^{-1} DW d^{-1}; φ = μg g^{-1} DW biofilm h^{-1}; ¤ = μg gluc. g^{-1} WW h^{-1}; † = μg C g^{-1} DW d^{-1})	
Goto et al., 2001				^{14}C-labeled MPB community	
	^{14}C-EDOC	^{14}C-EDOC	NP*	k (d^{-1}): 0.616	
	^{14}C-EDTA-OC	^{14}C-EDTA-OC	NP*	k (d^{-1}): 0.916	
	^{14}C-EPS_{coll}	^{14}C-EPS_{coll}	NP*	k (d^{-1}): 0.616	
Haynes et al., 2007[b]	CHO_{coll}	EPS_{coll} (μg gluc. g^{-1} DW)	233.8	0–2 d: −81 §	4–10 d: +50 §
		CHO_{HB} (μg gluc. g^{-1} DW)	336.5	NP	
	EPS_{coll}	EPS_{coll} (μg gluc. g^{-1} DW)	383.2	0–2 d: −140 §	4–10 d: +224.8 §
		CHO_{HB} (μg gluc. g^{-1} DW)	482.7	NP	
Hofmann et al., 2009[c]	CHO_{coll}	EPS_{coll} (μg gluc. mL^{-1} slurry)	10.2	0–4 h: +15 ¤	4–24 h: −3.5 ¤
	EPS_{coll}	EPS_{coll} (μg gluc. mL^{-1} slurry)	27.7	0–4 h: −81 ¤	4–24 h: +0.85 ¤
Bellinger et al., 2009[d]	None**	Control treat			
		CHO_{HB} (μg g^{-1} DW biofilm)	1,625	4–12 h: +16.37 φ	
		13C-enriched treat			
		CHO_{HB} (μg g^{-1} DW biofilm)	1,300	4–12 h: +3.8 φ	12–48 h: −3.9 φ
Oakes et al., 2010[a]	None**			First order decay rate (2-G model)	
		Mannose (mmol C m^{-2})	24.8	k_1 (d^{-1}): 4.38 ± 1.02	k_2 (d^{-1}): 0.01 ± 0.01
		Fucose (mmol C m^{-2})	49.2	k_1 (d^{-1}): 1.5 ± 0.29	k_2 (d^{-1}): 0.05 ± 0.01
		Rhamnose (mmol C m^{-2})	80	k_1 (d^{-1}): 0.81 ± 0.18	k_2 (d^{-1}): 0.03 ± 0.01
		Galactose (mmol C m^{-2})	105	k_1 (d^{-1}): 1.27 ± 0.25	k_2 (d^{-1}): 0.03 ± 0.01
		Glucose (mmol C m^{-2})	113	k_1 (d^{-1}): 1.38 ± 0.25	k_2 (d^{-1}): 0.04 ± 0.01
		Xylose (mmol C m^{-2})	34.2	k_1 (d^{-1}): 1.43 ± 0.34	k_2 (d^{-1}): 0.02 ± 0.02
McKew et al., 2013[e]	None	DOC (μg C g^{-1} DW)	565	Aer. 0–10 d: −44 †	Aer. 10–25 d: +6 †
				Anaer. 0–10 d: −36 †	Anaer. 10–25 d: +7 †
		CHO_{HB} (μg C g^{-1} DW)	488	Aer. 0–10 d: +12 †	Aer. 10–25 d: −8.8 †
				Anaer. 0–10 d: −6 †	Anaer. 10–25 d: +1 †
		TCHO (μg C g^{-1} DW)	2,894	Aer. 0–10 d: −99 †	Aer. 10–25 d: +9.8 †
				Anaer. 0–10 d: −100 †	Anaer. 0–10 d: +3.6 †
Taylor et al., 2013[f]	^{13}C-labeled EPS	CHO_{coll} (ug gluc. g^{-1} WW)	89.85	0–30 h: +0.07¤	30–72 h: −1.06 ¤
		EPS_{coll} (ug gluc. g^{-1} WW)	47.75	0–30 h: −0.7 ¤	30–72 h: −0.2 ¤
		DOC in CHO_{coll} (ug gluc. g^{-1} WW)	402.23	0–72 h: −3.4 ¤	
		DOC in EPS_{coll} (ug gluc. g^{-1} WW)	49.98	0–72 h: −0.5 ¤	
	^{12}C-unlabeled EPS	CHO_{coll} (ug gluc. g^{-1} WW)	92.75	0–30 h: +0.39 ¤	30–72 h: −1.2 ¤
		EPS_{coll} (ug gluc. g^{-1} WW)	48.27	0–30 h: −1.03 ¤	
		DOC in CHO_{coll} (ug gluc. g^{-1} WW)	394.2	0–72 h: −2.9¤	
		DOC in EPS_{coll} (ug gluc. g^{-1} WW)	41.22	0–72 h: −0.24 ¤	

(Continued)

TABLE 2 | Continued

Publication	Added DOM/EPS	Fraction measured	Starting Conc.	Rate of degradation (units: § = μg gluc. g^{-1} DW d^{-1}; φ = μg g^{-1} DW biofilm h^{-1}; ¤ = μg gluc. g^{-1} WW h^{-1}; † = μg C g^{-1} DW d^{-1})
Miyatake et al., 2014[g]	None**	TCHO (μmol C g^{-1} DW)	27.1	NSC (27.04 μmol C g^{-1} DW; max. of 29.5 at 72 h)
		CHO_{coll} (μmol C g^{-1} DW)	3.6	0–72 h: −0.04 (μmol C g^{-1} DW h^{-1}; incr. of 1.9 at 120 h)
		EDTA-CHO (μmol C g^{-1} DW)	0.85	NSC (0.99 μmol C g^{-1} DW; min. of 0.3 at 72 h)

Rates were calculated using the data presented in the paper in the form of tables or graphs, when not provided by the authors. In the final column, showing the rates of degradation, sub-columns are used to indicate the rates with different treatments as indicated. In order to avoid confusion, rates are presented in the units given in the original publication. Symbols + and – preceding the degradation rates indicate accumulation or loss, respectively. Abbreviations and details of the microbial community involved in the degradation of the added carbon source are provided in the footnote.

**Although starting concentrations were not provided, calculations for degradation rates were estimated using the percentage of added substrates mineralized. **In these experiments no additional organic carbon source was added; sediment DOC/EPS was labeled using $NaH^{13}CO_3$.*

Details about the microbial community composition and EPS-induced changes are as follows:

[a]Microbial community was not studied.

[b]Increases in Bacteroidetes and Alphaproteobacteria, especially Acinetobacter (and in particular in the cEPS-enrichment).

[c]Isolation of Variovorax sp. as the main EPS-degrader (Betaproteobacteria).

[d]Gram-negative bacteria incorporated diatom-derived carbon faster than Gram-positive bacteria.

[e]Aerobic slurries had a high relative abundance of Gammaproteobacteria and a big increase in Verrucomicrobia, while in the anaerobic slurries Deltaproteobacteria were dominant (especially Desulfobacteraceae and Desulfobulbaceae).

[f]Alphaproteobacteria and Gammaproteobacteria increased in the slurry with added ^{13}C-diatom derived EPS.

[g]The bacterial community was dominated by Gammaproteobacteria (21%), and to a lesser extent by Bacteroidetes (8%) and Deltaproteobacteria (7%).

Abbreviations of DOM/EPS sources are: DOM, Dissolved Organic Matter; EPS, Extracellular Polymeric Substances; ^{14}C-EDOC, ^{14}C-labeled Extracellular Dissolved Organic Carbon; ^{14}C-EDTA-OC, ^{14}C-labeled EDTA-extracted Organic Carbon; ^{14}C-EPS_{coll}, ^{14}C-labeled colloidal EPS; CHO_{coll}, colloidal Carbohydrates; CHO_{HB}, Hot-Bicarbonate-extracted Carbohydrates; DOC, Dissolved Organic Carbon; TCHO, Total Carbohydrates; EDTA-CHO, EDTA-extracted Carbohydrates. Other abbreviations are: NP, Non-provided; NSC, No significant changes.

group, we have a poor understanding of its ecophysiology, but evidence is emerging that many species of Verrucomicrobia consume algal EPS and other biopolymers (Martinez-Garcia et al., 2012; Cardman et al., 2014; Landa et al., 2014; Orsi et al., 2016). McKew et al. (2013) showed that, in a mudflat enrichment, Verrucomicrobia had the biggest proportional increase (∼6-fold) when incubated aerobically with cEPS, but were ∼40% less abundant when grown anaerobically. In addition, PiCrust analysis suggests that Verrucomicrobia have a similar range and number of extracellular enzymes for breaking down complex polymers as do the Bacteroidetes, a recognized major biopolymer-degrading group (Yilmaz et al., 2016). Specifically, a metagenome from the marine *Candidatus* Spartobacteria baltica was rich in glycoside hydrolases (Herlemann et al., 2013). Thus, a picture is emerging that aerobic biopolymer degradation is a key trait of many Verrucomicrobia. Verrucomicrobia were also significantly enriched in the presence of EPS_{HB}, suggesting that they are able to degrade complex polymers. Two OTUs had a marginal increase in abundance in the presence of EPS_{HB}, one of which was related to *Roseibacillus*, species of which have been isolated from brown algae and also from marine water and sediments (Yoon et al., 2008), which may further indicate interactions with photosynthetic organisms.

The phylum Bacteroidetes was significantly more abundant when incubated with EPS_{HB} and with EPS_{coll}. Unlike the Verrucomicrobia, the Bacteroidetes are well known for their capacity to degrade biopolymers, including EPS (Haynes et al., 2007; McKew et al., 2013). Many OTUs from diverse classes of Bacteroidetes were selectively enriched (**Figures 5B**, **6B**), two of which were enriched under both EPS additions, but had a higher relative abundance with EPS_{HB}. One of these, from the genus *Tenacibaculum*, constituted 12% of the community with EPS_{coll} and 20% with EPS_{HB}, and has been shown to possess enzymes able to degrade a great range of organic compounds from a wide range of marine habitats including tidal flat sediments (Suzuki et al., 2001; Frette et al., 2004; Choi et al., 2006; Jung et al., 2006). The second Bacteroidetes OTU, 2-fold more abundant in EPS_{HB} than EPS_{coll}, was from the genus *Algoriphagus*, which is able to degrade an array of different compounds as carbon and energy sources (e.g., D-glucose, D-galactose, sucrose) (Yoon et al., 2005; Alegado et al., 2013). This genus is normally found in diverse marine habitats, such as seawater, tidal mudflats, and salterns, and also associated with algae (Nedashkovskaya et al., 2004) or cyanobacterial mats (Bowman et al., 2003). Such features indicate that *Algoriphagus* species might be considered as specialist EPS/carbohydrate degraders.

Similarly to Verrucomicrobia, certain taxa within the phylum Planctomycetes are emerging as important biopolymer-degrading microbes (Wang et al., 2015; Yilmaz et al., 2016). They generally are enriched in marine snow (Fuchsman et al., 2012), are associated with macroalgae (Lage and Bondoso, 2011), and increase in abundance in coastal diatom blooms (Morris et al., 2006), suggesting that they may be able to utilize the released algal organic carbon. Here, Planctomycetes (class Phycisphaerae) was more abundant when grown on EPS_{coll}

compared to NoAdd-EPS, with three OTUs specifically enriched (**Figure 5**), but not when incubated with EPS_{HB} compared to NoAdd-EPS (**Figure 6**). One of the most EPS_{coll}-enriched OTUs was from the genus *Rhodopirellula*. *Rhodopirellula baltica* degrades carbohydrates in marine environments (Gade et al., 2005) and genome sequencing revealed its ability to degrade algal-derived sulfated polysaccharides (Glöckner et al., 2003; Wegner et al., 2013). However, in contrast to the current finding, previous studies performed in the Colne estuary using different approaches did not detect this Planctomycetes as a specialist EPS degrader (Hofmann et al., 2009; McKew et al., 2013; Taylor et al., 2013), thus further work is needed to clarify the role of this phylum in intertidal systems.

The relative similarity of many taxa in the $+EPS_{coll}$ and $+EPS_{HB}$ treatments could indicate that there is a general capability of utilizing EPS, in accordance with previous studies. Miyatake et al. (2014), for example, showed that of the bacterial taxa targeted all incorporated diatom-derived material. For the Colne, previous studies showed only small changes in overall bacterial community composition in response to added EPS using different approaches (Hanlon et al., 2006; Haynes et al., 2007; Bellinger et al., 2009). Taylor et al. (2013) demonstrated that a diverse range of bacterial taxa were enriched when exposed to cEPS, including highly enriched Alphaproteobacteria and Gammaproteobacteria, but of different lower-order taxa to those found here. Although our results cannot preclude uptake of EPS by a wide range of bacteria, which express this capacity depending on the particular environmental conditions or composition of EPS, the results of the present experiment show clear and consistent changes in the abundance of several taxa when incubated with added EPS. This is consistent with other studies (Hanlon et al., 2006; Haynes et al., 2007; Taylor et al., 2013) and demonstrates some specialization for degradation of different types of EPS (EPS_{coll} and EPS_{HB}).

CONCLUSIONS

EPS constitute a large fraction of the available carbon and energy in marine sediments and wherever phototrophic microbes abound (Underwood et al., 2005; Bellinger et al., 2009). Here, we have shown that fractions of EPS with different structural complexity (operationally termed colloidal and hot-bicarbonate extracted) were degraded, at higher rates compared with those reported previously (**Table 2**), contributing to the transfer of organic C from microphytobenthos to heterotrophic bacteria. The comparison of degradation rate constants for the different organic fractions studied here, using a one-G exponential decay model, confirmed that DOC and cEPS fractions from the $+EPS_{HB}$ treatment are more refractory than their counterpart fraction in the $+EPS_{coll}$ treatment (**Table 1**) in accordance with most studies, where higher molecular weight, complex compounds have a lower degradability (**Table 2**). In addition, our results indicate that EPS, particularly the EPS_{HB} fraction, contain large amounts of N and P that may be released during EPS degradation at rates high enough to support microbial growth in slurries. The relevance of the EPS_{HB} fraction as a source of regenerated nutrient, mainly N and P, for the sediment microbial community *in situ* and the observed differences with respect to EPS_{coll} fraction require further investigation. The addition of different diatom-derived EPS also induced the enrichment of different bacterial taxa, indicating the existence of some specialization for degradation of different types of EPS. Given the widespread use of high-throughput amplicon sequencing, programs are being developed to infer microbial functions based on phylogeny. However, such approaches must be grounded on solid experimental evidence as presented here, considering the complex interactions of EPS degradation in sediments (Bellinger et al., 2009; McKew et al., 2013; Taylor et al., 2013). Further investigation is required to understand how changes in nutrient regeneration and EPS degradation rates and the differential enrichment of distinct taxa affect EPS budgets in intertidal sediments *in situ,* in relation to changes in the relative composition of EPS during a tidal or seasonal cycle.

AUTHOR CONTRIBUTIONS

All the authors designed the experiment. JB carried out the experiment and analyzed the samples. All authors analyzed and interpreted the data and wrote the manuscript.

FUNDING

The research was funded by Projects CTM-2009-10736, CTM2013-43857-R (Ministry of Economy and Competitiveness, Spain), and P11-RNM-7199 (Andalusian Regional Government). JB was funded by a FPI Grant (BES-2010-035711) from the Ministry of Economy and Competitiveness, Spain. GU and TM were funded by a NERC grant NE/K001914/1 (Data Synthesis and Management of Marine and Coastal Carbon).

ACKNOWLEDGMENTS

We thank Farid Benyahia, Tania Cresswell-Maynard, and John W. Green for their outstanding technical support at the University of Essex, Dr. Alex Dumbrell for bioinformatics support and Dave R. Clark for assistance with sequence submission.

SUPPLEMENTARY MATERIAL

The Supplementary Material for this article can be found online at: http://journal.frontiersin.org/article/10.3389/fmicb.2017.00245/full#supplementary-material

REFERENCES

Acuña Alvarez, L., Exton, D. A., Timmis, K. N., Suggett, D. J., and McGenity, T. J. (2009). Characterization of marine isoprene-degrading communities. *Environ. Microbiol.* 11, 3280–3291. doi: 10.1111/j.1462-2920.2009.02069.x

Alegado, R. A., Brown, L. W., Cao, S., Dermenjian, R. K., Zuzow, R., Fairclough, S. R., et al. (2013). *Algoriphagus machipongonensis* sp. nov., co-isolated with a colonial choanoflagellate. *Int. J. Syst. Evol. Microbiol.* 63, 163–168. doi: 10.1099/ijs.0.038646-0

Anderson, M. J. (2001). A new method for non-parametric multivariate analyses of variance in ecology. *Austral. Ecol.* 26, 32–46. doi: 10.1111/j.1442-9993.2001.01070.pp.x

Anderson, M. J., and Robinson, J. (2003). Generalized discriminant analysis based on distances. *Aust. N.Z. J. Stat.* 45, 301–338. doi: 10.1111/1467-842X.00285

Arndt, S., Jørgensen, B. B., LaRowe, D. E., Middelburg, J. J., Pancost, R. D., and Regnier, P. (2013). Quantifying the degradation of organic matter in marine sediments: a review and synthesis. *Earth Sci. Rev.* 123, 53–86. doi: 10.1016/j.earscirev.2013.02.008

Arnosti, C. (2011). Microbial extracellular enzymes in the marine carbon cycle. *Ann. Rev. Mar. Sci.* 3, 401–425. doi: 10.1146/annurev-marine-120709-142731

Aslam, S. N., Michel, C., Niemi, A., and Underwood, G. J. C. (2016). Patterns and drivers of carbohydrate budgets in ice algal assemblages from first year Arctic sea ice. *Limnol. Oceanogr.* 61, 919–937. doi: 10.1002/lno.10260

Beaumont, N. J., Jones, L., Garbutt, A., Hansom, J. D., and Toberman, M. (2014). The value of carbon sequestration and storage in coastal habitats. *Estuar. Coast. Shelf Sci.* 137, 32–40. doi: 10.1016/j.ecss.2013.11.022

Bellinger, B. J., Abdullahi, A. S., Gretz, M. R., and Underwood, G. J. C. (2005). Biofilm polymers: relationship between carbohydrate biopolymers from estuarine mudflats and unialgal cultures of benthic diatoms. *Aquat. Microb. Ecol.* 38, 169–180. doi: 10.3354/ame038169

Bellinger, B. J., Underwood, G. J. C., Ziegler, S. E., and Gretz, M. R. (2009). Significance of diatom-derived polymers in carbon flow dynamics within estuarine biofilms determined through isotopic enrichment. *Aquat. Microb. Ecol.* 55, 169–187. doi: 10.3354/ame01287

Berner, R. A. (1964). An idealized model of dissolved sulfate distribution in recent sediments. *Geochim. Cosmochim. Acta* 28, 1497–1503. doi: 10.1016/0016-7037(64)90164-4

Bowman, J. P., Nichols, C. M., and Gibson, J. A. E. (2003). *Algoriphagus ratkowskyi* gen. nov., sp. nov., *Brumimicrobium glaciale* gen. nov., sp. nov., *Cryomorpha ignava* gen. nov., sp. nov. and *Crocinitomix catalasitica* gen. nov., sp. nov., novel flavobacteria isolated from various polar habitats. *Int. J. Syst. Evol. Microbiol.* 53, 1343–1355. doi: 10.1099/ijs.0.02553-0

Burdige, D. J. (2007). The preservation of organic matter in marine sediments: controls, mechanisms and an imbalance in sediment organic carbon budgets? *Chem. Rev.* 107, 467–485. doi: 10.1021/cr050347q

Cardman, Z., Arnosti, C., Durbin, A., Ziervogel, K., Cox, C., Steen, A. D., et al. (2014). Verrucomicrobia are candidates for polysaccharide-degrading bacterioplankton in an arctic fjord of Svalbard. *Appl. Environ. Microbiol.* 80, 3749–3756. doi: 10.1128/AEM.00899-14

Chiovitti, A., Higgins, M. J., Harper, R. E., and Wetherbee, R. (2003). The complex polysaccharides of the raphid diatom Pinnularia viridis (Bacilliariophyceae). *J. Phycol.* 39, 543–554. doi: 10.1046/j.1529-8817.2003.02162.x

Choi, D. H., Kim, Y.-G., Hwang, C. Y., Yi, H., Chun, J., and Cho, B. C. (2006). *Tenacibaculum litoreum* sp. nov., isolated from tidal flat sediment. *Int. J. Syst. Evol. Microbiol.* 56, 635–664. doi: 10.1099/ijs.0.64044-0

Decho, A. W. (1990). Microbial exopolymer secretions in ocean environments: their role(s) in food webs and marine processes. *Oceanogr. Mar. Biol. Ann. Rev.* 28, 73–153.

Dubois, M., Gilles, K. A., Hamilton, J. K., Rebers, P. A., and Smith, F. (1956). Colorimetric method for determination of sugars and related substances. *Anal. Chem.* 28, 350–356. doi: 10.1021/ac60111a017

Elifantz, H., Malmstrom, R. R., Cottrel, M. T., and Kirchman, D. L. (2005). Assimilation of polysaccharides and glucose by major bacterial groups in the Delaware Estuary. *Appl. Environ. Microbiol.* 71, 7799–7805. doi: 10.1128/AEM.71.12.7799-7805.2005

Folwell, B. D., McGenity, T. J., and Whitby, C. (2016). Biofilm and planktonic bacterial and fungal communities transforming high-molecular-weight polycyclic aromatic hydrocarbons. *Appl. Environ. Microbiol.* 82, 2288–2299. doi: 10.1128/AEM.03713-15

Freitas, S., Hatosy, S., Fuhrman, J. A., Huse, S. M., Welch, D. B., Sogin, M. L., et al. (2012). Global distribution and diversity of marine Verrucomicrobia. *ISME J.* 6, 1499–1505. doi: 10.1038/ismej.2012.3

Frette, L., Jørgensen, N. O. G., Irming, H., and Kroer, N. (2004). *Tenacibaculum skagerrakense* sp. nov., a marine bacterium isolated from the pelagic zone in Skagerrak, Denmark. *Int. J. Syst. Evol. Microbiol.* 54, 519–524. doi: 10.1099/ijs.0.02398-0

Fuchsman, C. A., Staley, J. T., Oakley, B. B., Kirkpatrick, J. B., and Murray, J. W. (2012). Free-living and aggregate-associated Planctomycetes in the Black Sea. *FEMS Microbiol. Ecol.* 80, 402–416. doi: 10.1111/j.1574-6941.2012.01306.x

Gade, D., Gobom, J., and Rabus, R. (2005). Proteomic analysis of carbohydrate catabolism and regulation in the marine bacterium *Rhodopirellula baltica*. *Proteomics* 5, 3672–3683. doi: 10.1002/pmic.200401200

García-Robledo, E., Bohórquez, J., Corzo, A., Jiménez-Arias, J. L., and Papaspyrou, S. (2016). Dynamics of inorganic nutrients in intertidal sediments: porewater, exchangeable and intracellular pools. *Front. Microbiol.* 7:761. doi: 10.3389/fmicb.2016.00761

García-Robledo, E., Corzo, A., Papaspyrou, S., Jiménez-Arias, J. L., and Villahermosa, D. (2010). Freeze-lysable inorganic nutrients in intertidal sediments: dependence on microphytobenthos abundance. *Mar. Ecol. Prog. Ser.* 403, 155–163. doi: 10.3354/meps08470

Glöckner, F. O., Kube, M., Bauer, M., Teeling, H., Lombardot, T., Ludwig, W., et al. (2003). Complete genome sequencing of the marine planctomycete Pirellula sp. Strain 1. *Proc. Natl. Acad. Sci. U.S.A.* 100, 8298–8303. doi: 10.1073/pnas.1431443100

Goto, N., Mitamura, O., and Terai, H. (2001). Biodegradation of photosynthetically produced extracellular organic carbon from intertidal benthic algae. *J. Exp. Mar. Biol. Ecol.* 257, 73–86. doi: 10.1016/S0022-0981(00)00329-4

Grasshoff, K., Ehrhardt, M., and KremLing, K. (1983). *Methods of Seawater Analysis, 2nd Edn.* Weinheim: Verlag Chemie.

Hammer, Ø., Harper, D. A. T., and Ryan, P. D. (2001). Past: paleontological statistics software package for education and data analysis. *Palaeontol. Electr.* 4:9. Available online at: http://palaeo-electronica.org/2001_1/past/issue1_01.htm

Hanlon, A. R. M., Bellinger, B., Haynes, K., Xiao, G., Hofmann, T. A., Gretz, M. R., et al. (2006). Dynamics of extracellular polymeric substance (EPS) production and loss in an estuarine, diatom-dominated, microalgal biofilm over a tidal emersion-immersion period. *Limnol. Oceanogr.* 51, 79–93. doi: 10.4319/lo.2006.51.1.0079

Haynes, K., Hofmann, T. A., Smith, C. J., Ball, A. S., Underwood, G. J. C., and Osborn, A. M. (2007). Diatom-derived carbohydrates as factors affecting bacterial community composition in estuarine sediments. *Appl. Environ. Microbiol.* 73, 6112–6124. doi: 10.1128/AEM.00551-07

Hedges, J. I., and Oades, J. M. (1997). Comparative organic geochemistries of soils and marine sediments. *Org. Geochem.* 27, 319–361. doi: 10.1016/S0146-6380(97)00056-9

Herlemann, D. P. R., Lundin, D., Labrenz, M., Jürgens, K., Zheng, Z., Aspeborg, H., et al. (2013). Metagenomic *de novo* assembly of an aquatic representative of the verrucomicrobial class Spartobacteria. *mBio* 4:e00569-12. doi: 10.1128/mbio.00569-12

Hillebrand, H., and Sommer, U. (1999). The nutrient stoichiometry of benthic microalgal growth: redfield proportions are optimal. *Limnol. Oceanogr.* 44, 440–446. doi: 10.4319/lo.1999.44.2.0440

Hoagland, K. D., Rosowsky, J. R., Gretz, M. R., and Reomer, S. C. (1993). Diatom extracellular polymeric substances: function, fine structure, chemistry, chemistry and physiology. *J. Phycol.* 29, 537–556. doi: 10.1111/j.0022-3646.1993.00537.x

Hofmann, T., Hanlon, A. R. M., Taylor, J. D., Ball, A. S., Osborn, A. M., and Underwood, G. J. C. (2009). Dynamics and compositional changes in extracellular carbohydrates in estuarine sediments during degradation. *Mar. Ecol. Prog. Ser.* 379, 45–58. doi: 10.3354/meps07875

Jung, S.-Y., Oh, T.-K., and Yoon, J.-H. (2006). *Tenacibaculum aestuarii* sp. nov., isolated from a tidal flat sediment in Korea. *Int. J. Syst. Evol. Microbiol.* 56, 1577–1581. doi: 10.1099/ijs.0.64302-0

Kristensen, E., and Holmer, M. (2001). Decomposition of plant materials in marine sediment exposed to different electron acceptors (O_2, NO_3^{2-}, and SO_4^{2-}), with

emphasis on substrate origin, degradation kinetics, and the role of bioturbation. *Geochim. Cosmochim. Acta* 65, 419–433. doi: 10.1016/S0016-7037(00)00532-9

Lage, O. M., and Bondoso, J. (2011). Planctomycetes diversity associated with macroalgae. *FEMS Microbiol. Ecol.* 78, 366–375. doi: 10.1111/j.1574-6941.2011.01168.x

Landa, M., Cottrell, M. T., Kirchman, D. L., Kaiser, K., Medeiros, P. M., Tremblay, L., et al. (2014). Phylogenetic and structural response of heterotrophic bacteria to dissolved organic matter of different chemical composition in a continuous culture study. *Environ. Microbiol.* 16, 1668–1681. doi: 10.1111/1462-2920.12242

Luisetti, T., Turner, R. K., Jickells, T., Andrews, J., Elliott, M., Schaafsma, M., et al. (2014). Coastal Zone Ecosystem Services: from science to values and decision making; a case study. *Sci. Total Environ.* 493, 682–693. doi: 10.1016/j.scitotenv.2014.05.099

Martinez-Garcia, M., Brazel, D. M., Swan, B. K., Arnosti, C., Chain, P. S., Reitenga, K. G., et al. (2012). Capturing single cell genomes of active polysaccharide degraders: an unexpected contribution of verrucomicrobia. *PLoS ONE* 7:e35314. doi: 10.1371/journal.pone.0035314

Mayer, L. M. (1995). Sedimentary organic matter preservation: an assessment and speculative synthesis–a comment. *Mar. Chem.* 49, 123–126. doi: 10.1016/0304-4203(95)00011-F

McKew, B. A., Dumbrell, A. J., Taylor, J. D., McGenity, T. J., and Underwood, G. C. J. (2013). Differences between aerobic and anaerobic degradation of microphytobenthic biofilm-derived organic matter within intertidal sediments. *FEMS Microbiol. Ecol.* 84, 495–509. doi: 10.1111/1574-6941.12077

McKew, B. A., Taylor, J. D., McGenity, T. J., and Underwood, G. J. C. (2011). Resistance and resilience of benthic biofilm communities from a temperate saltmarsh to desiccation and rewetting. *ISME J.* 5, 30–41. doi: 10.1038/ismej.2010.91

Meyer-Reil, L.-A. (1990). Microorganisms in marine sediments: considerations concerning activity measurements. *Arch. Hydrobiol.* 34, 1–6.

Middelburg, J. J., Barranguet, C., Boschker, H. T. S., Herman, P. M. J., Moens, T., and Heip, C. H. R. (2000). The fate of intertidal microphytobenthos carbon: an in situ ^{13}C-labeling study. *Limnol. Oceanogr.* 45, 1224–1234. doi: 10.4319/lo.2000.45.6.1224

Miki, T., and Jacquet, S. (2010). Indirect interaction in the microbial world: specificities and similarities to plant-insect systems. *Popul. Ecol.* 52, 475–483. doi: 10.1007/s10144-010-0235-4

Miyatake, T., Moerdijk-Poortvliet, T. C. W., Stal, L. J., and Boschker, H. T. S. (2014). Tracing carbon flow from microphytobenthos to major bacterial groups in an intertidal marine sediment by using an *in situ* 13C pulse-chase method. *Limnol. Oceanogr.* 59, 1275–1287. doi: 10.4319/lo.2014.59.4.1275

Morris, R. M., Longnecker, K., and Giovannoni, S. J. (2006). Pirellula and OM43 are among the dominant lineages identified in an Oregon coast diatom bloom. *Environ. Microbiol.* 8, 1361–1370. doi: 10.1111/j.1462-2920.2006.01029.x

Muyzer, G., Dewaal, E. C., and Uitterlinden, A. G. (1993). Profiling of complex microbial-populations by denaturing gradient gel-electrophoresis analysis of polymerase chain reaction-amplified genes-coding for 16S rRNA. *Appl. Environ. Microbiol.* 59, 695–700.

Nedashkovskaya, O. I., Vancanneyt, M., Van Trappen, S., Vandemeulebroecke, K., Lysenko, A. M., Rohde, M., et al. (2004). Description of *Algoriphagus aquimarinus* sp. nov., *Algoriphagus chordae* sp. nov. and *Algoriphagus winogradskyi* sp. nov., from sea water and algae, transfer of Hongiella halophila Yi and Chun 2004 to the genus Algoriphagus as Algoriphagus halophilus comb. nov. and emended descriptions of the genera Algoriphagus Bowman et al. 2003 and Hongiella Yi and Chun 2004. *Int. J. Syst. Evol. Microbiol.* 54, 1757–1764. doi: 10.1099/ijs.0.02915-0

Oakes, J. M., Eyre, B. D., Middelburg, J. J., and Boschker, H. T. S. (2010). Composition, production, and loss of carbohydrates in subtropical shallow subtidal sandy sediments: rapid processing and long-term retention revealed by 13C-labeling. *Limnol. Oceanogr.* 55, 2126–2138. doi: 10.4319/lo.2010.55.5.2126

Orsi, W. D., Smith, J. M., Liu, S., Liu, Z., Sakamoto, C. M., Wilken, S., et al. (2016). Diverse, uncultivated bacteria and archaea underlying the cycling of dissolved protein in the ocean. *ISME J.* 10, 2158–2173. doi: 10.1038/ismej.2016.20

Parks, D. H., and Beiko, R. G. (2010). Identifying biologically relevant differences between metagenomic communities. *Bioinformatics* 26, 715–721. doi: 10.1093/bioinformatics/btq041

Parks, D. H., Tyson, G. W., Hugenholtz, P., and Beiko, R. G. (2014). STAMP: statistical analysis of taxonomic and functional profiles. *Bioinformatics* 30, 3123–3124. doi: 10.1093/bioinformatics/btu494

Passarelli, C., Meziane, T., Thiney, N., Boeuf, D., Jesus, B., Ruivo, M., et al. (2015). Seasonal variations of the composition of microbial biofilms in sandy tidal flats: focus of fatty acids, pigments and exopolymers. *Estuar. Coast. Shelf Sci.* 153, 29–37. doi: 10.1016/j.ecss.2014.11.013

Perkins, R. G., Underwood, G. J. C., Brotas, V., Snow, G., Jesus, B., and Ribeiro, L. (2001). Responses of microphytobenthos to light: primary production and carbohydrate allocation over an emersion period. *Mar. Ecol. Prog. Ser.* 223, 101–112. doi: 10.3354/meps223101

Pierre, G., Zhao, J. M., Orvain, F., Dupuy, C., Klein, G., Graber, M., et al. (2014). Seasonal dynamics of extracellular polymeric substances (EPS) in surface sediments of a diatom-dominated intertidal mudflat (Marennes-Oléron, France). *J. Sea Res.* 92, 26–35. doi: 10.1016/j.seares.2013.07.018

Steele, D. J., Franklin, D. J., and Underwood, G. J. C. (2014). Protection of cells from salinity stress by extracellular polymeric substances in diatom biofilms. *Biofouling* 30, 987–998. doi: 10.1080/08927014.2014.960859

Stief, P., Kamp, A., and De Beer, D. (2013). Role of diatoms in the spatial-temporal distribution of intracellular nitrate in intertidal sediments. *PLoS ONE* 8:e73257. doi: 10.1371/journal.pone.0073257

Suzuki, M., Nakagawa, Y., Harayama, S., and Yamamoto, S. (2001). Phylogenetic analysis and taxonomic study of marine Cytophaga-like bacteria: proposal for *Tenacibaculum* gen. nov. with *Tenacibaculum maritimum* comb. nov. and *Tenacibaculum ovolyticum* comb. nov., and description of *Tenacibaculum mesophilum* sp. nov. and *Tenacibaculum amylolyticum* sp. nov. *Int. J. Syst. Evol. Microbiol.* 51, 1639–1652. doi: 10.1099/00207713-51-5-1639

Taylor, J. D., McKew, B. A., Kuhl, A., McGenity, T. J., and Underwood, G. J. C. (2013). Microphytobenthic extracellular polymeric substances (EPS) in intertidal sediments fuel both generalist and specialist EPS-degrading bacteria. *Limnol. Oceanogr.* 58, 1463–1480. doi: 10.4319/lo.2013.58.4.1463

Thingstad, T. F., Våge, S., Storesund, J. E., Sandaa, R-A., and Giske, J. (2014). A theoretical analysis of how strain-specific viruses can control microbial species diversity. *Proc. Natl. Acad. Sci. U.S.A.* 111, 7813–7818. doi: 10.1073/pnas.1400909111

Thornton, D. C. O., Dong, F., Underwood, G. J. C., and Nedwell, D. B. (2002). Factors affecting microphytobenthic biomass, species composition and production in the Colne estuary (UK). *Aquat. Microb. Ecol.* 27, 285–300. doi: 10.3354/ame027285

Thornton, D. C. O., Kopac, S. M., and Long, R. A. (2010). Production and enzymatic hydrolysis of carbohydrates in intertidal sediment. *Aquat. Microb. Ecol.* 60, 109–125. doi: 10.3354/ame01403

Torti, A., Lever, M. A., and Jørgensen, B. B. (2015). Origin, dynamics, and implications of extracellular DNA pools in maine sediments. *Mar. Genomics* 24, 185–196. doi: 10.1016/j.margen.2015.08.007

Ubertini, M., Lefebre, S., Rakotomalala, C., and Orvain, F. (2015). Impact of sediment grain-size and biofilm age on Epipelic micrphytobenthos resuspension. *J. Exp. Mar. Biol. Ecol.* 467, 52–64. doi: 10.1016/j.jembe.2015.02.007

Underwood, G. J. C., Fietz, S., Papadimitriou, S., Thomas, D. N., and Dieckmann, G. S. (2010). Distribution and composition of dissolved extracellular polymeric substances (EPS) in Antarctic sea ice. *Mar. Ecol. Prog. Ser.* 404, 1–19. doi: 10.3354/meps08557

Underwood, G. J. C., and Paterson, D. M. (2003). The importance of extracellular carbohydrate production by marine epipelic diatoms. *Adv. Bot. Res.* 40, 183–240. doi: 10.1016/S0065-2296(05)40005-1

Underwood, G. J. C., Paterson, D. M., and Parkes, R. J. (1995). The measurement of microbial carbohydrates exopolymers from intertidal sediments. *Limnol. Oceanogr.* 40, 1243–1253. doi: 10.4319/lo.1995.40.7.1243

Underwood, G. J. C., Perkins, R. G., Consalvey, M. C., Hanlon, A. R. M., Oxborough, K., Baker, N. R., et al. (2005). Patterns in microphytobenthic primary productivity: species-specific variation in migratory rhythms and photosynthetic efficiency in mixed-species biofilms. *Limnol. Oceanogr.* 50, 755–767. doi: 10.4319/lo.2005.50.3.0755

Underwood, G. J. C., and Smith, D. J. (1998). Predicting Epipelic diatom exopolymer concentrations in intertidal sediments from sediment chlorophyll a. *Microb. Ecol.* 35, 116–125. doi: 10.1007/s002489900066

Våge, S., Storesund, J. E., and Thingstad, T. F. (2013). SAR11 viruses and defensive host strains. *Nature* 499, E3–E4. doi: 10.1038/nature12387

Wang, Q., Garrity, G. M., Tiedje, J. M., and Cole, J. R. (2007). Naïve Bayesian classifier for rapid assignment of rRNA sequences into the new bacterial taxonomy. *Appl. Environ. Microbiol.* 73, 5261–5267. doi: 10.1128/AEM.00062-07

Wang, X., Sharp, C. E., Jones, G. M., Grasby, S. E., Brady, A. L., and Dunfield, P. F. (2015). Stable-Isotope-Probing identifies uncultured Planctomycetes as primary degraders of a complex heteropolysaccharide in soil. *Appl. Environ. Microbiol.* 81, 4607–4615. doi: 10.1128/AEM.00055-15

Wegner, C. E., Richter-Heitmann, T., Klindworth, A., Klockow, C., Richter, M., Achstetter, T, et al. (2013). Expression of sulfatases genes in *Rhodopirellula baltica* and the diversity of sulfatases in the genus *Rhodopirellula*. *Mar. Genomics* 9, 51–61. doi: 10.1016/j.margen.2012.12.001

Wustman, B. A., Gretz, M. R., and Hoagland, K. D. (1997). Extracellular matrix assembly in diatoms (Bacilliariophyceae) I. A model of adhesives based on chemical characterization and localization of polysaccharides from the marine diatom Achnanthes longipes and other diatoms. *Plant Physiol.* 113, 1059–1069. doi: 10.1104/pp.113.4.1059

Yamaguchi, A., Umezawa, Y., Wada, M., and Sayama, M. (2015). Potential contribution of microalgal intracellular phosphorus to phosphorus distribution in tidal flat sediments during winter. *Plankton. Benthos. Res.* 10, 1–10. doi: 10.3800/pbr.10.1

Yilmaz, P., Yarza, P., Rapp, J. Z., and Glöckner, F. O. (2016). Expanding the world of marine bacterial and archaeal clades. *Front. Microbiol.* 6:1524. doi: 10.3389/fmicb.2015.01524

Yoon, J. H., Kang, S. J., Jung, S. Y., Lee, C. H., and Oh, T. K. (2005). *Algoriphagus yeomjeoni* sp. nov., isolated from a marine solar saltern of the Yellow Sea, Korea. *Int. J. Syst. Evol. Microbiol.* 55, 865–870. doi: 10.1099/ijs.0.63479-0

Yoon, J., Matsuo, Y., Adachi, K., Nozawa, M., Matsuda, S., Kasai, H., et al. (2008). Description of *Persicirhabdus sediminis* gen. nov., sp. nov., *Roseibacillus ishigakijimensis* gen. nov., sp. nov., *Roseibacillus ponti* sp. nov., *Roseibacillus persicicus* sp. nov., *Luteolibacter pohnpeiensis* gen. nov., sp. nov. and *Luteolibacter algae* sp. nov., six marine members of the phylum 'Verrucomicrobia', and emended descriptions of the class Verrucomicrobiae, the order Verrucomicrobiales and the family Verrucomicrobiaceae. *Int. J. Syst. Evol. Microbiol.* 58, 998–1007. doi: 10.1099/ijs.0.65520-0

Conflict of Interest Statement: The authors declare that the research was conducted in the absence of any commercial or financial relationships that could be construed as a potential conflict of interest.

Advantages of publishing in Frontiers

OPEN ACCESS
Articles are free to read for greatest visibility and readership

FAST PUBLICATION
Around 90 days from submission to decision

HIGH QUALITY PEER-REVIEW
Rigorous, collaborative, and constructive peer-review

TRANSPARENT PEER-REVIEW
Editors and reviewers acknowledged by name on published articles

Frontiers
Avenue du Tribunal-Fédéral 34
1005 Lausanne | Switzerland

Visit us: www.frontiersin.org
Contact us: info@frontiersin.org | +41 21 510 17 00

REPRODUCIBILITY OF RESEARCH
Support open data and methods to enhance research reproducibility

DIGITAL PUBLISHING
Articles designed for optimal readership across devices

FOLLOW US
@frontiersin

IMPACT METRICS
Advanced article metrics track visibility across digital media

EXTENSIVE PROMOTION
Marketing and promotion of impactful research

LOOP RESEARCH NETWORK
Our network increases your article's readership